https://doi.org/10.35662/unine-thesis-3033

Université de Neuchâtel

Very long chain ascarosides and their biogenesis in *Caenorhabditis elegans*

PhD thesis submitted to the Faculty of Science

Institute of Chemistry

University of Neuchâtel

For the degree of Doctor of Philosophy

By

Rocío de las Nieves Rivera Sánchez

Dissertation committee:

Prof. Stephan H. von Reuss, University of Neuchâtel, Thesis director

Prof. Bruno Therrien, University of Neuchâtel, Internal examiner

Prof. Chuanfu Dong, Beijing Normal University, External examiner

Defended on the 23rd of May 2023

unine
Université de Neuchâtel
Faculté des sciences

Rue Emile-Argand 11
CH-2000 Neuchâtel
doctorat.sciences@unine.ch

IMPRIMATUR POUR THESE DE DOCTORAT

La Faculté des sciences de l'Université de Neuchâtel autorise l'impression de la présente thèse soutenue par

Madame Rocío RIVERA SANCHEZ

Titre :

"Very long chain ascarosides and their biogenesis in *Caenorhabditis elegans*"

sur le rapport des membres du jury composé comme suit:

- Prof. Stephan von Reuss, directeur de thèse, Université de Neuchâtel, Suisse
- Prof. tit. Bruno Therrien, Université de Neuchâtel, Suisse
- Prof. ass. Chuanfu Dong, Beijing Normal University, Chine

Neuchâtel, le 25 mai 2023

Le Doyen, Prof. R. Bshary

Dedicated to my parents

1 Summary

In the first part of this thesis, a collection of very long chain alkyl ascarosides were synthesized based on the hypothesis that very long chain alkyl ascarosides might represent biosynthetic intermediates in the biosynthesis of short chain acyl ascarosides with signaling function in *C. elegans* and other nematodes. In addition, the corresponding [D_4]-labelled isotopomers were produced to serve as molecular probes for future biosynthetic studies. (2*R*,3*R*,5*R*,6*S*)-2-(henicosyloxy)-6-methyltetrahydro-2*H*-pyran-3,5-diol (**asc-ωC21-H**, **68a**), (2*S*,3*R*,5*R*,6*R*)-2-methyl-6-(((*R*)-pentacosan-2-yl)oxy)tetrahydro-2*H*-pyran-3,5-diol (**asc-C25-H**, **33a**), (2*S*,3*R*, 5*R*,6*R*)-2-methyl-6-(((*R*)-24-methylpentacosan-2-yl)oxy)tetrahydro-2*H*-pyran-3,5-diol (**asc-*i*C26-H**, **43a**), (2*R*,3*R*,5*R*,6*S*)-2-(((*R*)-hentriacontan-2-yl)oxy)-6-methyltetrahydro-2*H*-pyran-3,5-diol (**asc-C31-H**, **57a**) and their [D_4]-labelled isotopomers were prepared. Moreover, the corresponding acetyl-derivatives (2- and 4-monoacetyl, and 2,4-diacetyl) of the non-labelled ascarosides were synthesized. A total of sixteen very long chain alkyl ascarosides were obtained. Their mass spectrometric detection using different ionization techniques was evaluated, which highlighted GC-EIMS (of the corresponding TMS-derivatives) and LC-APCI-(-)-MS as the most suitable techniques. The conventional LC-MS ionization source ESI did not produce any detectable ion adducts for the highly lipophilic non-acetylated very long chain alkyl ascarosides, which might explain why these compounds have been missed in previous analyses of *C. elegans* and other nematodes. Comparison with authentic standards confirmed the structure assignment of **asc-ωC21-H** (**68a**), **asc-C25-H** (**33a**), and **asc-*i*C26-H** (**43a**), and facilitated the identification of additional acetyl-derivatives such as (2*S*,3*R*,5*R*,6*R*)-5-hydroxy-2-methyl-6-(((*R*)-pentacosan-2-yl)oxy)tetrahydro-2*H*-pyran-3-yl acetate (**4-Ac-asc-C25-H**, **81**), and (2*S*,3*R*,5*R*,6*R*)-5-hydroxy-2-methyl-6-(((*R*)-24-methylpentacosan-2-yl)oxy)tetrahydro 2*H*-pyran-3-yl acetate (**4-Ac-asc-*i*C26-H**, **82**) in *C. elegans*. The identification of representative alkyl ascarosides by comparison with authentic standards further enabled the assignment of two homologous alkyl ascaroside series with straight chain or *iso*-branched alkyl aglycones ranging from 23 to 32 carbons in several nematode species using APCI-(-)-MS, which demonstrates that very long chain alkyl ascarosides are highly conserved in nematodes. Furthermore, very long chain 2-hydroxyalkyl ascarosides (including their monoacetyl-derivatives) with 29-, 31-, and 33-carbon sidechains were identified in *C. elegans* eggs and worm bodies by APCI-(-)-MS. In addition, the biosynthesis of *iso*-branched **asc-*i*C26-H** (**43a**) and **4-Ac-asc-*i*C26-H** (**82**) in *C. elegans* was studied by incorporation experiments using an *E. coli* food source that is specifically enriched with a 1:1 mixture of [U-$^{13}C_6$]-/[U-$^{12}C_6$]-leucine or [U-$^{13}C_5$]-/[U-$^{12}C_5$]-valine, which demonstrated a L-leucine origin of the [U-$^{12}C_5$]-labelled *iso*-branched aglycones.

In the second part of this thesis, two (ω)-carboxy ascarosides, (*S*)-3-(((2*R*,3*R*,5*R*,6*S*)-3,5-dihydroxy-6-methyltetrahydro-2*H*-pyran-2-yl)oxy)-16-oxoheptadecanoic acid (**(ω-COOH)-asc-C16-MK**, **91**) and (*S*)-3-(((2*R*,3*R*,5*R*,6*S*)-3,5-dihydroxy-6-methyltetrahydro-2*H*-pyran-2-yl)oxy)octadecanedioic acid (**(ω-COOH)-asc-C17**, **92**) were successfully synthesized in order to confirm their putative identification as natural products and potential biosynthetic intermediates in ascaroside biosynthesis. Comparative analysis of the authentic standards and *the daf-22 exometabolome using* LC-MS and GC-MS (TMS-derivatives) techniques showed that **(ω-COOH)-asc-C16-MK** (**91**) and **(ω-COOH)-asc-C17** (**92**) cannot be confirmed as natural products in the *daf-22* mutant. Further experiments will be required to ascertain or refute the hypothesis that (ω)-carboxy ascarosides are biosynthetic intermediates in ascaroside biosynthesis.

In the third part of this thesis, odd numbered *iso*-fatty acids as building blocks derived from L-leucine (**14**) metabolism were evaluated as biosynthetic intermediates of *iso*-branched aglycones. For this purpose [D_6]-labelled isotopomers of *iso*-fatty acid were prepared as molecular probes. 11-Methyldodecanoic acid (*iso*C13, **16a**), 13-methyltetradecanoic acid (*iso*C15, **15a**) and 15-methylhexadecanoic acid (*iso*C17, **17a**), [D_6]-11-methyldodecanoic acid ([D_6]-*iso*C13, **16c**), [D_6]-13-methyltetradecanoic acid ([D_6]-*iso*C15, **15c**), and [D_6]-15-methylhexadecanoic acid ([D_6]-*iso*C17, **17c**) were synthetized. In parallel, the preparation of [D_4]-11-methyldodecanoic acid ([D_4]-*iso*C13, **16b**) and [D_4]-13-methyltetradecanoic acid ([D_4]-*iso*C15, **15b**) was developed, but their use as molecular probes was not tested in this thesis. Incorporation experiments of [D_6]-*iso*-fatty acid into *iso*-branched alkyl ascarosides using the *elo-5(gk208)* mutant reported to be defective in elongation of *iso*C13 (**16a**) to *iso*C15 (**15a**), giving no isotope enrichment with [D_6]-*iso*C13 (**16c**) and [D_6]-*iso*C15 (**15c**), whereas small [D_6]-enrichment of (2*S*, 3*R*,5*R*,6*R*)-2-methyl-6-(((*R*)-24-methylpentacosan-2-yl)oxy)tetrahydro-2*H*-pyran-3,5-diol (**asc-*i*C26-H**, **43a**) was observed with [D_6]-*iso*C17 (**17c**). The small level of [D_6]-enrichment demonstrated that other *elo-5* independent pathways for the biosynthesis of *iso*-branched ascarosides exist in *C. elegans*. Indeed, it was found that the *elo-5 (gk208)* loss of function mutant is not defective in *iso*-fatty acid elongation, in contrast to previous reports, and [D_6]-*iso*C13 (**16c**) and [D_6]-*iso*C15 (**15c**) were both incorporated into elongated [D_6]-*iso*-fatty acids, e.g., [D_6]-*iso*C15 (**15c**), [D_6]-*iso*C17 (**17c**), [D_6]-*iso*C19 (17-methyloctadecanoic acid). Thus, although *elo-5* is involved in *iso*-fatty acid biosynthesis, it is not essential for *iso*-fatty acid elongation, and it is conceivable that other enzymes such as *elo-6* might be able to complement for *elo-5* deficiency. *Iso*C15 (**15a**) is known to be an essential intermediate in *C. elegans'* sphingolipid biosynthesis. Incorporation of [D_6]-*iso*-fatty acids in *elo-5* worms showed no isotope enrichment with [D_6]-*iso*C13 (**16c**) or [D_6]-*iso*C15 (**15c**), whereas [D_6]-*iso*C17 (**17c**) gave almost exclusively [D_6]-labelled sphingolipids. Incorporation experiments with the *elo-5/daf-22* double mutant demonstrated that the incorporation of [D_6]-*iso*C17 (**17c**) requires the

DAF-22 enzyme for chain shortening of *iso*C17 (**17a**) into *iso*C15 (**15a**). In addition, the incorporation of [D_6]-labelled *iso*-fatty acid isotopomers as molecular probes demonstrated that other *iso*-branched glycolipids, such as 2-(9-methyldecanamido)ethyl ((2*S*,3*R*,4*S*,5*S*,6*R*)-3,4,5-trihydroxy-6-(hydroxymethyl)tetrahydro-2*H*-pyran-2-yl) phosphate (gnap-*iso*-11:0, **127**), are exclusively derived from chain shortening of *iso*C17 (**17a**). In conclusion, these results demonstrate that the use of [D_6]-labelled *iso*-fatty acids represents a powerful tool to study the *iso*-fatty acid metabolism in nematodes.

Keywords

C. elegans, nematodes, ascarosides, very long chain ascarosides, (ω)-carboxy ascarosides, alkyl ascarosides, β-oxidation, alkyl aglycone, fatty acids, *iso*-branched fatty acids, synthesis, lipid metabolism, biosynthesis, incorporation studies, molecular probes, isotopomers, sphingolipids.

2 Résumé

Dans la première partie de cette thèse, une série d'ascarosides d'alkyle à très longue chaîne a été synthétisée sur la base de l'hypothèse suivante : les ascarosides d'alkyle à très longue chaîne pourraient être des intermédiaires dans la biosynthèse des ascarosides d'acyle à chaîne courte et ainsi jouer un rôle de communication chez *C. elegans* et d'autres nématodes. De plus, les isotopomères marqués [D_4] correspondants ont été obtenus pour servir de sonde moléculaire lors de futures études de biosynthèse. En bref, le (2*R*,3*R*,5*R*,6*S*)-2-(henicosyloxy)-6-methyltetrahydro-2*H*-pyran-3,5-diol (**asc-ωC21-H**, **68a**), le (2*S*,3*R*,5*R*,6*R*)-2-methyl-6-(((*R*)-pentacosan-2-yl)oxy)tetrahydro-2*H*-pyran-3,5-diol (**asc-C25-H**, **33a**), le (2*S*,3*R*,5*R*,6*R*)-2-methyl-6-(((*R*)-24-methylpentacosan-2-yl)oxy)tetrahydro-2*H*-pyran-3,5-diol (**asc-*i*C26-H**, **43a**), le (2*R*,3*R*,5*R*,6*S*)-2-(((*R*)-hentriacontan-2-yl)oxy)-6-methyltetrahydro-2*H*-pyran-3,5-diol (**asc-C31-H**, **57a**) et leur isotopomères marqués au [D_4] ont été préparés. Au total, seize ascarosides d'alkyle à très longue chaîne ont été obtenus. L'analyse par spectrométrie de masse à l'aide de différentes techniques d'ionisation a permis de mettre en évidence que la GC-EIMS (des dérivés TMS correspondants) et la LC-APCI-(-)-MS sont les techniques les plus adaptées. L'ESI, source d'ionisation la plus largement utilisé en LC-MS ne permet pas la production d'adduit ionique détectable pour les ascarosides d'alkyle à très longue chaîne non acétylés hautement lipophiles, ce qui pourrait expliquer que ces composés n'ont pas pu être identifié lors d'analyses précédentes de *C. elegans* et d'autres nématodes. La comparaison avec des standards a permis de confirmer les structures : **asc-ωC21-H** (**68a**), **asc-C25-H** (**33a**), et **asc-*i*C26-H** (**43a**), et a facilité l'identification de dérivés acétylés supplémentaires tels que l' acétate de (2*S*,3*R*,5*R*,6*R*)-5-hydroxy-2-methyl-6-(((*R*)-pentacosan-2-yl)oxy)tetrahydro-2*H*-pyran-3-yl (**4-Ac-asc-C25-H**, **81**), et l'acétate de (2*S*,3*R*,5*R*,6*R*)-5-hydroxy-2-methyl-6-(((*R*)-24-methylpentacosan-2-yl)oxy)tetrahydro 2*H*-pyran-3-yl **4-Ac-asc-*i*C26-H**, **82**) chez *C. elegans*. La comparaison d'alkyl ascarosides représentatifs des grandes familles avec des standards a en outre permis l'identification par APCI-(-)-MS de deux séries d'alkyl ascarosides homologues avec des alkyl aglycones à chaîne non-ramifiée ou *iso* de 23 à 32 carbones chez plusieurs espèces de nématodes. La production d'ascarosides d'alkyle à très longue chaîne a donc prouvé être largement conservés chez les nématodes. Des ascarosides 2-hydroxyalkylés à très longue chaîne (y compris leurs dérivés mono-acétylés) avec des chaînes latérales à 29, 31 et 33 carbones ont pu être identifiés par APCI-(-)-MS dans les œufs et l'organisme entier de *C. elegans*. De plus, la biosynthèse chez *C. elegans* de composés ramifiées en *iso* : **asc-*i*C26-H** (**43a**) et de **4-Ac-asc-*i*C26-H** (**82**) a été étudiée par des expériences d'incorporation à l'aide d'*E. coli* comme source alimentaire spécifiquement enrichie avec un mélange 1:1 de [[U-$^{13}C_6$]-/[U-$^{12}C_6$]-leucine ou de [U-$^{13}C_5$]-/[U-$^{12}C_5$]-valine. Cette expérience a permis de démontrer que la L-leucine (**14**) est à la source d'aglycones ramifiés en *iso* marqués [U-$^{12}C_5$].

Dans la deuxième partie de cette thèse, deux (ω)-carboxy ascarosides, l'acide ((*S*)-3-(((2*R*, 3*R*,5*R*,6*S*)-3,5-dihydroxy-6-methyltetrahydro-2*H*-pyran-2-yl)oxy)-16-oxoheptadecanoïque (**(ω-COOH)-asc-C16-MK**, **91**) et l'acide (*S*)-3-(((2*R*,3*R*,5*R*,6*S*)-3,5-dihydroxy-6-methyltetrahydro-2*H*-pyran-2-yl)oxy)octadecanedioïque (**(ω-COOH)-asc-C17**, **92**) ont été synthétisés avec succès afin de confirmer leur future identification en tant que produits naturels et potentiel intermédiaires dans la biosynthèse des ascarosides. L'analyse par LC-MS et GC-MS (TMS-dérivés) des standards et de l'exométabolome issu de *daf-22* n'as pas permis de confirmer l'identification de **(ω-COOH)-asc-C16-MK** (**91**) et de **(ω-COOH)-asc-C17** (**92**) comme produit naturel chez le mutant *daf-22*. D'autres expériences seront nécessaires pour valider ou réfuter l'hypothèse selon laquelle les (ω)-carboxy ascarosides sont des intermédiaires dans la biosynthèse des ascarosides.

Dans la troisième partie de cette thèse, des acides gras au nombre impairs de carbone ramifiés en *iso* issus du métabolisme de la L-leucine (**14**) ont été évalués en tant qu'intermédiaires et bloc constitutif lors de la biosynthèse d'aglycones *iso*-ramifiés. Des isotopomères d'acide gras *iso*-ramifiés marqués au [D_6] ont été préparés afin d'être utilisé comme sonde moléculaire. L'acide 11-Methyldodecanoïque (*iso*C13, **16a**), l'acide 13-methyltetradecanoïque (*iso*C15, **15a**), l'acide 15-methylhexadecanoïque (*iso*C17, **17a**), l'acide [D_6]-11-methyldodecanoïque ([D_6]-*iso*C13, **16c**), l'acide [D_6]-13-methyltetradecanoïque ([D_6]-*iso*C15, **15c**), et l'acide [D_6]-15-methylhexadecanoïque ([D_6]-*iso*C17, **17c**) ont été synthétisé. En parallèle, la préparation de l'acide [D_4]-11-méthyldodécanoïque ([D_4]-*iso*C13, **16b**) et de l'acide [D_4]-13-méthyltétradécanoïque [D_4]-*iso*C15, **15b**) a été développée, mais leur utilisation comme sondes moléculaires n'a pas pu être testé dans cette thèse. Les expériences d'incorporation en utilisant le mutant *elo-5*(*gk208*) signalé comme étant défectueux dans l'élongation d'*iso*C13 (**16a**) à *iso*C15 (**15a**) de [D_6]-*iso*-acide gras dans des ascarosides d'alkyle *iso*-ramifiés ne montrent aucun enrichissement isotopique avec [D_6]-*iso*C13 (**16c**) et [D_6]-*iso*C15 (**15c**). Cependant, un enrichissement de faible teneur en [D_6] de (2*S*,3*R*,5*R*,6*R*)-2-methyl-6-(((*R*)-24-methylpentacosan-2-yl)oxy)tetrahydro-2*H*-pyran-3,5-diol (**asc-*i*C26-H**, **43a**) a été observé pour [D_6]-*iso*C17 (**17c**). Le faible niveau en [D_6] obtenu a démontré que d'autres voies de biosynthèse des ascarosides *iso*-ramifiés existent et sont indépendantes d'*elo-5* chez *C. elegans*. En effet et contrairement aux précédentes publications, il a été constaté que la perte de fonction du mutant *elo-5* (*gk208*) n'affecte pas l'allongement des *iso*-acides gras. Les composés [D_6]-*iso*C13 (**16c**) et [D_6]-*iso*C15 (**15c**) ont tous deux été incorporés dans des acides [D_6]-iso-gras allongés, par exemple, [D_6]-*iso*C15 (**15c**), [D_6]-*iso*C17 (**17c**), [D_6]-*iso*C19 (acide 17-méthyloctadécanoïque). Bien que *elo-5* soit impliqué dans la biosynthèse des *iso*-acides gras, il n'est pas essentiel pour l'élongation des *iso*-acides gras. Il est ainsi concevable que d'autres enzymes telles que *elo-6* puissent être en mesure de compléter le déficit en *elo-5*. Le produit *iso*C15 (**15a**) est connu pour être un intermédiaire essentiel dans la biosynthèse des sphingolipides de

C. elegans. L'incorporation de [D_6]- *iso*-acides gras dans le mutant *elo-5* n'a montré aucun enrichissement isotopique avec [D_6]-*iso*C13 (**16c**) ou [D_6]-*iso*C15 (**15c**), alors que [D_6]-*iso*C17 (**17c**) a produit presque exclusivement des Sphingolipides marqués au [D_6]. Des expériences d'incorporation avec le double mutant *elo-5*/*daf-22* ont démontré que l'incorporation de [D_6]-*iso*C17 (**17c**) requiert l'enzyme DAF-22 pour le rétrécissement de la chaîne d'*iso*C17 (**17a**) en *iso*C15 (**15a**). De plus, l'incorporation d'isotopomères d'acides gras marqués au [D_6] en tant que sondes moléculaires a démontré que d'autres glycolipides *iso*-ramifiés, tels que le ((2*S*,3*R*,4*S*,5*S*,6*R*)-3,4,5-trihydroxy-6-(hydroxymethyl)tetrahydro-2*H*-pyran-2-yl) phosphate de 2-(9-méthyldécanamido) éthyle (gnap-*iso*-11:0, **127**), proviennent exclusivement du rétrécissement de chaîne de l'*iso*C17 (**17a**). En conclusion, ces résultats démontrent que l'utilisation d'*iso*-acides gras marqués au [D_6] représente un outil puissant pour étudier leur métabolisme chez les nématodes.

Mots-clés

C. elegans, nématodes, ascarosides, ascarosides à très longue chaîne, (ω)-carboxy ascarosides, alkyl ascarosides, β-oxydation, alkyl aglycone, acides gras, acides gras isoramifiés, synthèse, métabolisme lipidique, biosynthèse, études d'incorporation, molécules sondes, isotopomères, sphingolipides.

3 Abbreviations list

A. suum	*Ascaris suum*
B. subtilis	*Bacillus subtilis*
BCAA	Branched-chain amino acids
C. elegans	*Caenorhabditis elegans*
DCM	Dichloromethane
DHP	3,4-Dihydropyran
DMSO	Dimethyl sulfoxide
E. coli	*Escherichia coli*
Et_3N	Triethylamine
Et_3SiH	Triethylsilane
EtOAc	Ethyl acetate
FA	Fatty acids
HMPA	Hexamethylphosphoramide
*iso*C13	11-Methyldodecanoic acid
*iso*C15	13-Methyltetradecanoic acid
*iso*C17	15-Methylhexadecanoic acid
MeOH	Methanol
mmBCFA	Monomethyl branched-chain fatty acids
MSTFA	*N*-methyl-*N*-(trimethylsilyl)trifluoroacetamide
n-BuLi	*n*-Butyllithium
NDMMs	Nematode-derived modular metabolites
$NHMe_2$	Dimethylamine
NMG	Nematode Growth Medium
OP50	Uracil-requiring B-type *E. coli*
P. pacificus	*Pristionchus pacificus*
PCC	Pyridinium chlorochromate
Pd/C	Palladium on carbon
PPh_3	Triphenylphosphine
S. maltophilia	*Stenotrophomonas maltophilia*
Sia_2BH	Disiamylborane
TBAB	Tetrabutylammonium bromide
TBAF	Tetrabutylammonium fluoride

TBSCl	*tert*-Butyldimethylsilyl chloride
tert-BuOK	Potassium *tert*-butoxide
THF	Tetrahydrofuran
TMS	Trimethylsilyl
TMSOTf	Trimethylsilyl trifluoromethanesulfonate
TsOH	*p*-Toluenesulfonic acid
VLCA	Very long chain ascaroside

4 Table of contents

5 Table of figures

6 Introduction

6.1 The model organism Caenorhabditis elegans

Nematodes, also called roundworms, constitute the most abundant group of multicellular organisms on earth. Their adaptability, their small size, a resistant cuticle, and a simple body plan enable them to be a dominant component of all trophic levels of the soil food web [(1) (2)]. They play an important role in soils as regulators of carbon, nutrient dynamics, and indicators of biological activities [(3)]. Furthermore, they are reported as parasites of plants, vertebrates, and insects [(1) (4)].

The bacterivorous nematode *Caenorhabditis elegans* (*C. elegans*) represents a powerful model organism in biology and medicine. This multicellular organism was the first to have its complete genome sequenced [(5)]. A 60 to 80% homology with human protein-coding genes was reported [(4)]. *C. elegans* has been used as a model organism in investigating complex human diseases like Alzheimer, Parkinson, diabetes, Duchenne muscular dystrophy, and cancer [(6)]. A small size (1-1.5 mm long), a short reproductive life cycle, a translucent body, a predetermined anatomy, easy cultivation, a small genome, availability of numerous deletion mutants, susceptibility to gene silencing by RNA-interferences, along with a well curated online database (www.wormbase.org) are characteristics that make *C. elegans* an attractive model organism [(7) (6)].

C. elegans is a self-fertilizing hermaphroditic species with rare males for facultative outcrossing. Its life cycle and lifespan depend on the growth temperature [(7)]. Indeed, under favorable conditions, its life cycle can take about three to five days to develop from the egg to an egg-laying adult, which lives another two to three weeks. Four larval stages (L1-L4) constitute the early development before reaching the reproductive adult (Figure 1-A). However, under unfavorable conditions, such as limited food availability, overcrowding, or high temperatures, *C. elegans* arrests at the L1 diapause and fails to further develop [(8)]. Furthermore, unfavorable conditions also induce an alternative non-feeding larval stage called dauer diapause (L3d). Dauer larvae can survive for several months by coordinating extensive changes throughout their morphology and metabolism that involve the suppression of aerobic respiration and food consumption. Moreover, when favorable conditions are encountered, dauer arrest is overcome and the worm proceeds to normal development via the L4 larvae to the adult stage [(9) (10)].

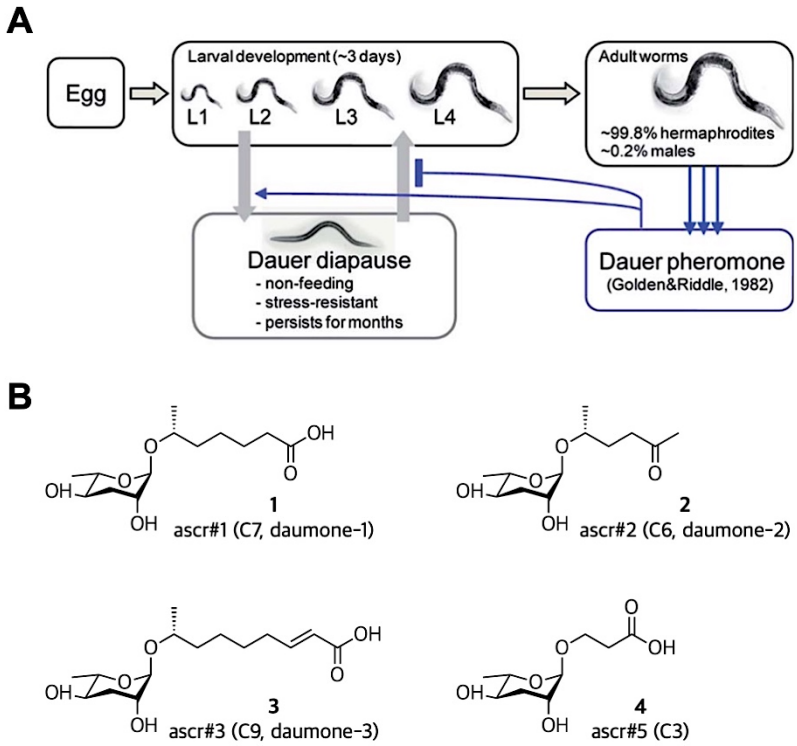

Figure 1. (A) Life cycle in *C. elegans*. (B) Ascarosides with potent dauer inducing activity [10].

Nematodes like *C. elegans* employ a set of small molecules to modulate the worm's development according to population density [11]. The first structural identification of these small molecules, or dauer pheromones, demonstrated that they are composed of L-α-3,6-dideoxymannose (L-ascarylose) attached to short chain fatty acids with 3 to 9 carbons (Figure 1-B) [10] [11] [12] [13] [12]. These short chain glycosides exhibit structural similarities with very long chain derivatives previously identified in *Ascaris* eggs called ascarosides since they are composed of an ascarylose unit linked to a sidechain [14].

6.2 Ascaroside signaling in nematodes

6.2.1 Ascarosides and dauer formation

Ascarosides are responsible for the formation of dauer larvae in *C. elegans*, the larval stage used for dispersal and long-term survival. To date, it is known that the developmental dauer diapause depends on the DAF-22 enzyme (peroxisomal β-ketoacyl-CoA thiolase), the TGF-β (transforming growth factor-β) pathway, and DAF-12 (a nuclear hormone receptor for dafachronic acid) [10] [13]. These dauer-inducing ascarosides are produced at low concentrations (nano- or micromolar) by the worms. For example, daumones ascr#1 (**1**), ascr#2 (**2**), ascr#3 (**3**), and ascr#5 (**4**) (Figure 1-B) were isolated by

activity-guided fractionation of worm culture media and shown to induce dauer formation at near physiological concentrations when employed individually [10].

Comparative metabolomics of *C. elegans* by NMR spectroscopy allowed the identification of additional dauer pheromone components [15]. These ascarosides exhibit supplementary moieties linked to the fatty acid-derived sidechain or the ascarylose unit (Figure 2). For example, one of the most potent dauer inducing ascarosides, ascr#8 (**5**), includes a *p*-aminobenzoic acid moiety linked via an amide bond with a seven-carbon α,β-unsaturated sidechain (Figure 2). Furthermore, mixtures of modular and simple ascarosides, e.g., ascr#3 (**3**), ascr#2 (**2**) ascr#8 (**5**), and ascr#4 (ascr#2 with a 2-glucoside), have been shown to act as potent male-specific attractants (Figure 1 & Figure 2). Ascarosides with indole carboxylate units linked to the ascarylose, icas#3 (**6**) and icas#9 (**7**) (Figure 2), have also been identified [16] [17]. The modular ascaroside icas#9 (**7**), for example, has been shown to play an important role in dauer formation as well as a potent aggregation pheromone at lower concentrations.

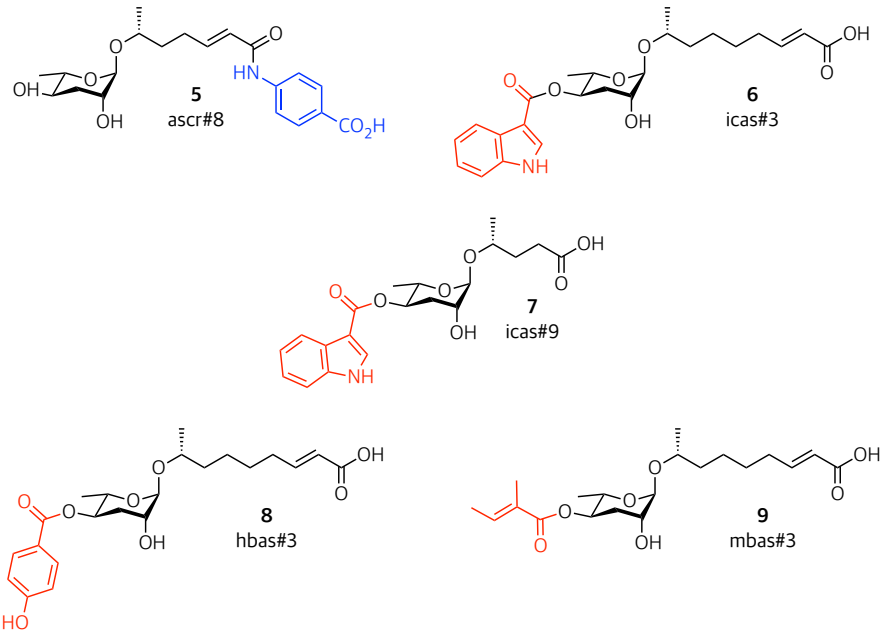

Figure 2. Examples of modular ascarosides involved in developmental regulation and behavioral phenotypes of *C. elegans*.

Modular ascarosides are involved in many aspects of nematode life history regulation, including development, lifespan, morphology, social communication, and interactions with other species [18]. Basic ascarosides are known to be highly conserved among nematodes [11]. Moreover, comparative analysis of the biological responses of modular ascarosides has shown that their functions are highly species-specific and thus represent the individual language of each species [10] [11].

6.2.2 Mass spectrometric detection of ascarosides

In recent years, many new ascaroside structures have been identified in *C. elegans* and other nematodes, resulting in a wide variety of nematode-derived ascarosides, as shown in Figure 3 [10] [18] [19]. To overcome the difficulties related to their small concentrations (pico- or nanomolar), several analytical techniques have been developed for the identification of ascarosides based on NMR, LC-MS and GC-MS methods [12] [14] [17] [20] [21] [22] [23].

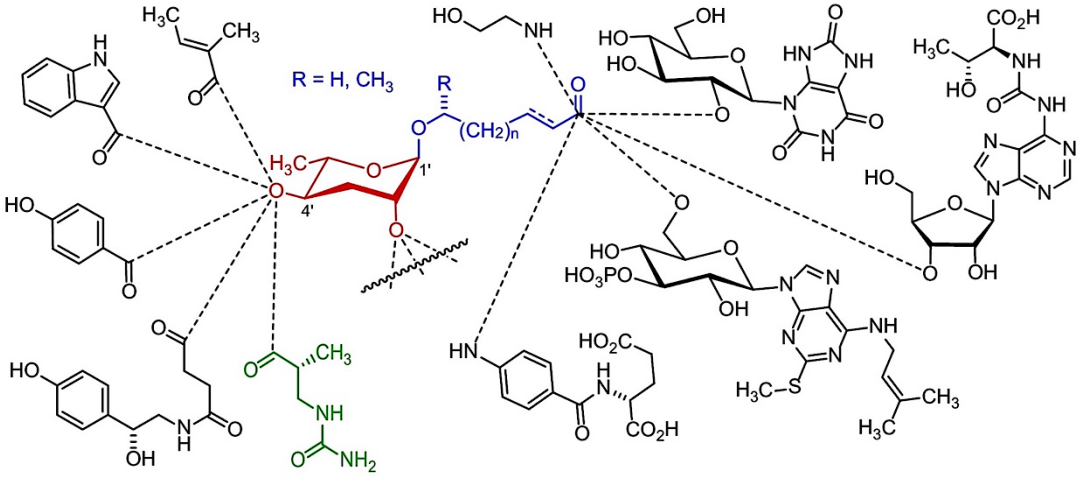

Figure 3. General scheme of modular ascarosides in nematodes [19].

Electrospray Ionization (ESI) as ion source for LC-MS analysis demonstrates effective detection of various types of short and medium chain ascarosides [17] [24] [25]. For example, the 4-(2-methylbutenoyl)- and 4-hydroxybenzoyl-substituted ascarosides, hbas#3 (**8**) and mbas#3 (**9**), respectively (Figure 2), were detected by MS/MS analyses of *C. elegans* metabolomes [17]. In most cases, ascarosides ionize as positively charged sodium adducts $[M+Na]^+$ and ammonium adducts $[M+NH_4]^+$ for ESI-(+) or by the loss of a proton $[M-H]^-$ in negative ionization mode [25]. LC-MS/MS screening for precursor ions of *m/z* 73 ($C_3H_5O_2$) in negative mode has been employed to detect a wide variety of known and previously unknown modular ascarosides [17] [21].

Ascarosides identified in *C. elegans*, *Pristionchus pacificus* (*P. pacificus*), *Panagrellus redivivus* (*P. redivivus*), *Heterorhabditis bacteriophora* (*H. bacteriophora*), and many other nematode species possess acyl (or 2-hydroxyalkyl) sidechains from 3 to 33 carbons [11] [14] [17] [26] [27]. Analysis of very long chain acyl ascarosides (VLCAs) by LC-ESI(+/-)-MS has been reported to have poor resolution due to their lipophilic sidechains. Therefore, GC-EIMS analysis of TMS-derivatives has been shown to provide good resolution and sensitivity for homologous series of highly lipophilic ascarosides [21]. Using this

technique, more than 200 acidic and non-acidic ascarosides with sidechains ranging from 3 to 33 carbons were detected. The characteristic ascarylose derived K1-fragment ion at *m/z* 130.1 $[C_6H_{14}OSi]^+$ (Figure 4) is used to screen for ascarylose containing compounds. Although no molecular ions are observed upon EIMS, the detection of sidechain-specific J1 and J2-fragment ions represents a powerful tool for structure assignment.

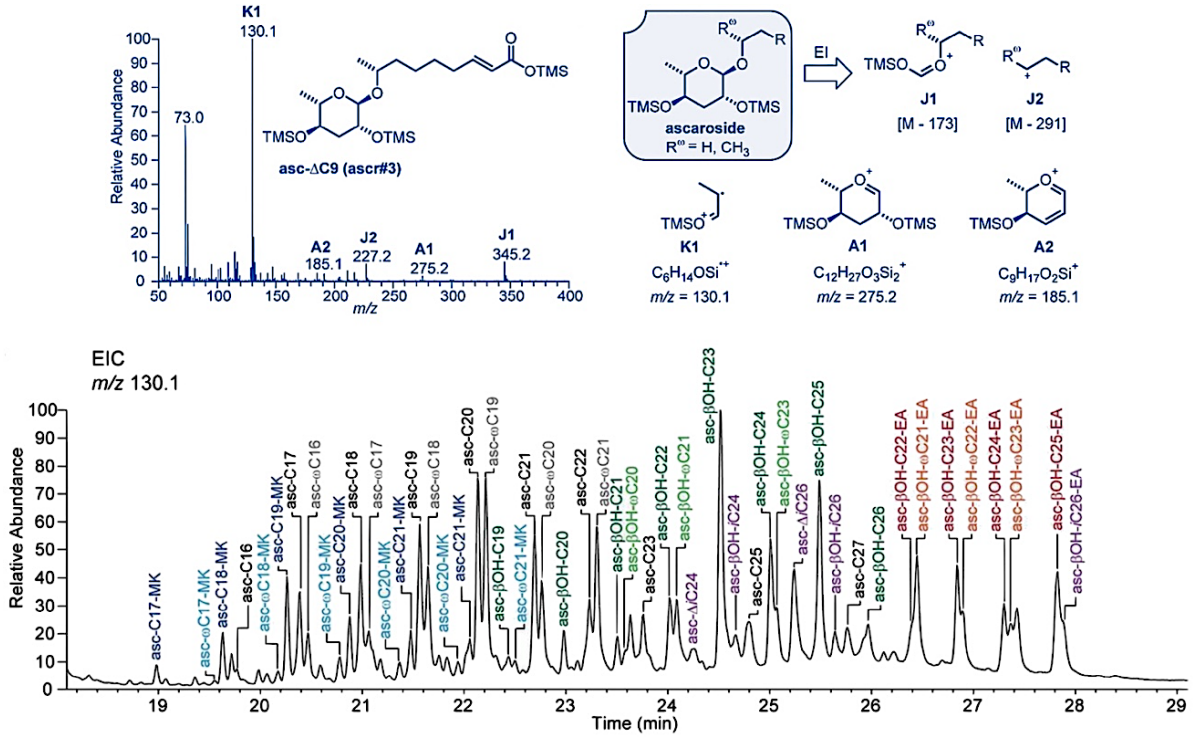

Figure 4. Identification of long and very long chain ascarosides with GC-EIMS analyses of ascaroside TMS-derivatives via screening for the K1-fragment. Modified figure from von Reuss *et al.* [21].

6.2.3 Biosynthesis of ascarosides

The use of MS/MS-based precursor ion screening of *C. elegans* metabolomes revealed that simple ascarosides are used as scaffolds for the formation of more complex modular derivatives. In addition, MS/MS-based precursor ion screening allowed the functional characterization of several genes involved in ascaroside biosynthesis.

In *C. elegans* and other nematodes, the ascaroside aglycones are derived from a primary metabolic pathway, which involves the peroxisomal β-oxidation cycle [13] [28] [29] [30] [31] [22]. The β-oxidation cycle utilizes the enzymes ACOX-1/2/3 (acyl-CoA oxidase), MAOC-1 (enoyl-CoA hydratase), DHS-28 ((3*R*)-hydroxyacyl-CoA dehydrogenase) and DAF-22 (peroxisomal β-ketoacyl-CoA thiolase) to shorten the ascaroside aglycone by two carbons per cycle (Figure 5).

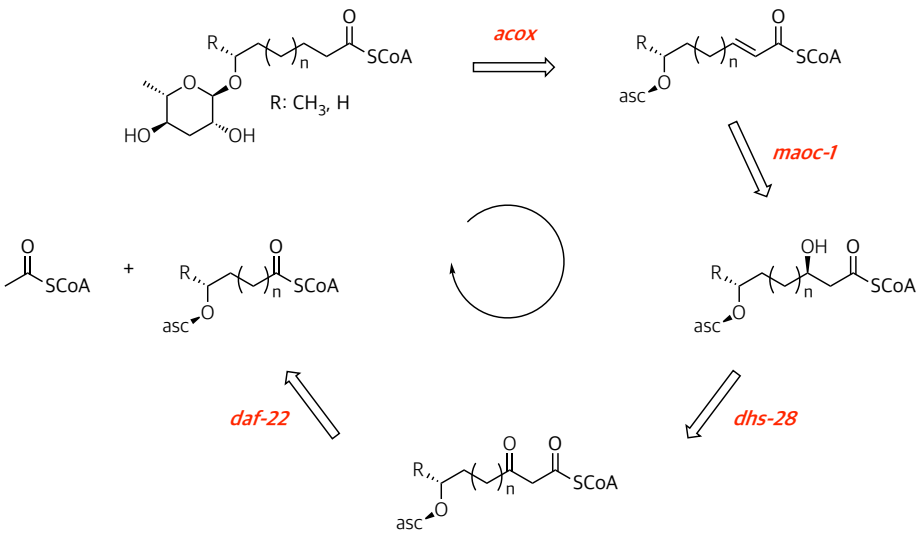

Figure 5. Peroxisomal β-oxidation cycle for ascaroside biosynthesis.

However, the origin of the building blocks involved in ascaroside biosynthesis is still unclear. The current proposal for a biosynthetic pathway assumes an origin of ascarosides from very long chain fatty acids (VLCFA) via their (ω)- and (ω-1)-hydroxylation. The ascarylose would be incorporated before entering the β-oxidation cycle to form very long chain ascarosides (VLCAs). These VLCAs would further generate short chain ascarosides, which could be linked to amino-acid-derived moieties and other building blocks to form the modular ascarosides (Figure 6) [17]. Indeed, ascaroside analyses of *C. elegans* and *P. pacificus* mutants defective in peroxisomal β-oxidation enzymes have shown a deficiency of short chain ascarosides and accumulation of ascarosides with long and very long sidechains (up to 33 carbons) [17] [21] [23] [25]. In addition, very long chain acyl ascarosides with very long methyl ketone and acyl ethanolamide sidechains were detected as shunt metabolites in the *C. elegans daf-22* mutant [23].

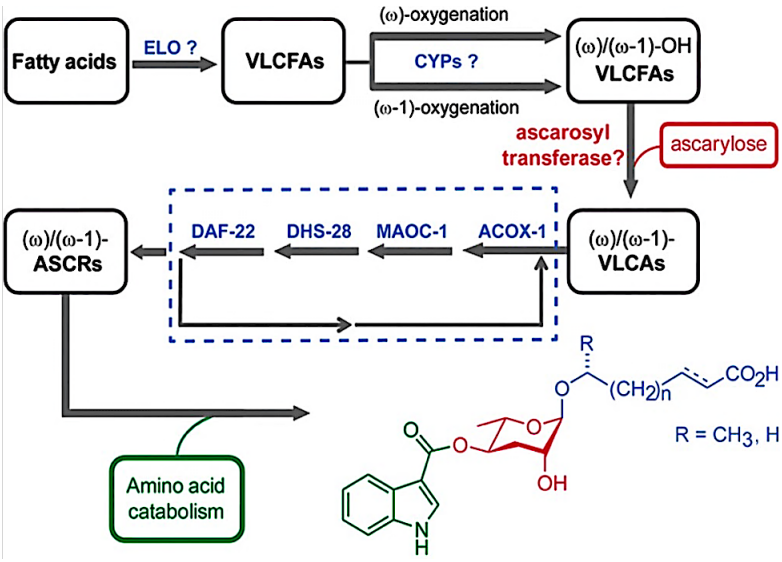

Figure 6. Ascarosides biosynthesis in *C. elegans* [17].

6.2.4 Very long chain ascarosides

Identification of very long chain alkyl chain ascarosides has been reported from several nematode species. For example, very long chain 2-hydroxyalkyl and alkyl ascarosides with side chains up to 35 carbons have been identified in the eggs of the parasitic *Ascaris* nematode as a protective lipid layer against environmental factors and toxic chemicals [14] (Figure 7). Similar structures with 2-hydroxyalkyl side chains of 29 to 33 carbons have also been reported for mixed populations of wildtype *C. elegans* [21] [32] [33] [34] [35].

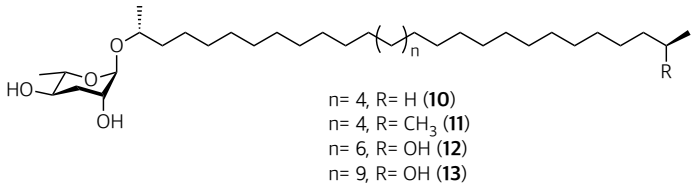

n= 4, R= H (**10**)
n= 4, R= CH_3 (**11**)
n= 6, R= OH (**12**)
n= 9, R= OH (**13**)

Figure 7. Structures of very long chain alkyl ascarosides found in *Ascaris* eggs.

The biosynthesis of VLCAs and their putative function as intermediates in the production of small chain ascarosides has not been investigated. Recent propositions by the von Reuss group have shown that (ω-1)- and (ω)-ascarosides have distinct biogenetic origins via different very long chain fatty acid precursors [24]. In contrast to previous proposal [17], this new model implies that fatty acid elongation and peroxisomal β-oxidation of (ω-1)- and (ω)-ascarosides utilize the unit at the terminal end of the sidechain as the starting point. Thus, (ω)-carboxy alkyl ascarosides could potentially act as intermediates of very long chain alkyl ascarosides, which are subsequently used as building blocks of acyl ascarosides. Moreover, the biosynthesis of (ω)-carboxy alkyl ascarosides would imply 3*S*-hydroxy alkyl acids as precursors. Preliminary HR-MS and MS^n analyses of the *daf-22* exometabolome revealed putative series of (ω)-carboxy acyl ascarosides (aglycones with C18-23 carbons) and (ω)-carboxy 2-oxoalkyl ascarosides (aglycones with C17-21 carbons) as potential biosynthetic intermediates.

To determine potential differences in the biosynthetic origins of (ω-1)- and (ω)-ascarosides, the exometabolome of *daf-22* mutants fed with [U-^{12}C]/[U-^{13}C]-*E. coli* was analyzed by GC-EI-MS. Based on these results, it was hypothesized that (ω-1)-ascarosides originate from *de novo* lipogenesis, whereas the (ω)-ascarosides originate from sidechain elongation of bacteria-derived C16 fatty acid. Since ascarosides with very long acyl chains were detected in *daf-22* exometabolomes, very long chain alkyl ascarosides were suggested as the starting point for their biosynthesis. Furthermore, the biosynthesis of (ω-1)-ascarosides with *iso*-branched sidechains (e.g., β-hydroxy-*iso*-acyl aglycones) was suggested to use *iso*-fatty acids as building blocks. In addition, (ω-1)-ascarosides with very long 2-hydroxyalkyl

side chains were found to be *daf-22* independent. Based on GC-MS data, the maximum length of the very long chain acyl ascarosides aglycones found in the *daf-22* exometabolome were determined as shown in Figure 8, supporting the assumption that these compounds are derived from distinct biosynthetic pathways.

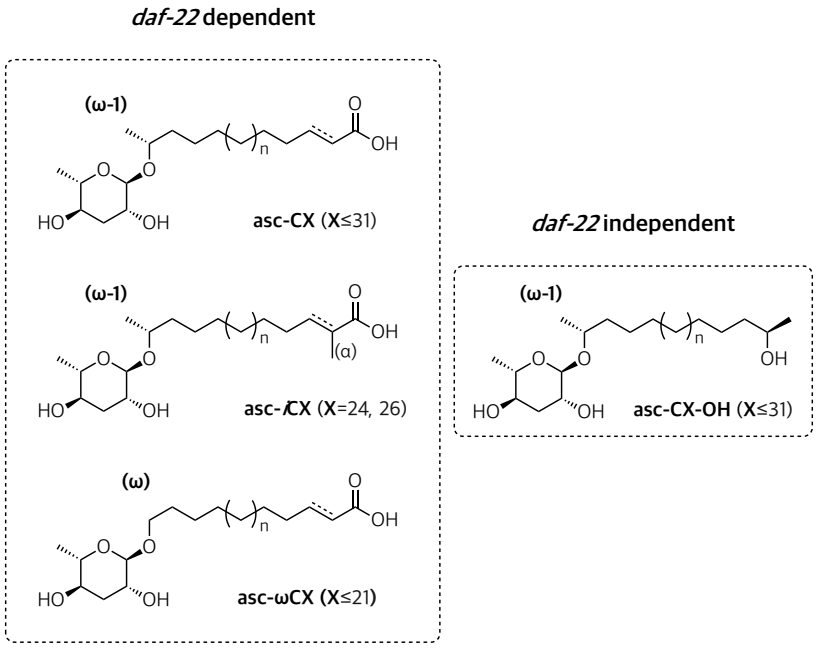

Figure 8. Maximum chain lengths of very long chain acyl ascaroside identified in the *daf-22* exometabolome.

6.2.5 Nomenclature

The large variety and complexity of homologous ascaroside structures results in complex and homologous names according to the IUPAC nomenclature. Therefore, trivial names such as daumone-1 or ascr#1 or C7 (**1**, Figure 1-B) were initially used [(12) (29)]. However, the continuous discovery of new types of ascaroside structures made these systems unsuitable. For example, the presence of multiple ascarosides with the same number of carbons in the sidechain makes naming systems based solely on the sidechain carbon number inconclusive.

The Schroeder group, in collaboration with WormBase, has introduced the Small Molecules Identifiers SMIDs (www.smid-db.org), consisting of 4-6 lowercase non-italicized letters referring to the general structural class of the compound, followed by a pound sign and a number, e.g., icas#9 (**7**) or hbas#3 (**8**) (Figure 2). This system has the advantage of being concise, simple, and producing a searchable entry for each compound, but it lacks most structural information.

In parallel, the Butcher group developed an ascaroside naming system that uses short-abbreviated codes containing structural information, such as the number of carbons in the sidechains, according to the following scheme: **head group-asc-(ω)(Δ)C#-terminus group** [25] (Figure 9). In this system, terminal sidechain attachment (instead of the standard (ω-1)-attachment) is indicated by the (ω) symbol, while unsaturation at α,β position is indicated by the (Δ) symbol. Corresponding abbreviations of head groups such as acetyl (Ac), indole-3-carbonyl (IC), 4-hydroxybenzoyl (HB), 2-(*E*)-methyl-2-butenoyl (MB), and octopamine succinyl (OS) are given. When necessary, the linkage of the head group in the ascarylose unit is indicated with the numbers 2- or 4- preceding the abbreviation. Furthermore, terminus groups such as *para*-aminobenzoic acid (PABA) and methyl ketone (MK) can be indicated.

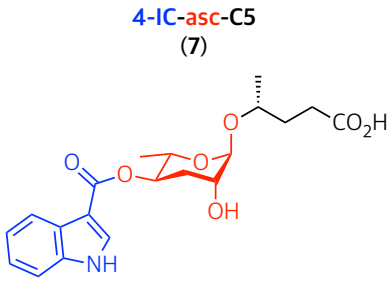

Figure 9. Renaming of icas#9 (**7**) according to the Butcher naming system.

Although names for complex compounds can become unpractically long with this system, it was used in this thesis for the nomenclature of ascarosides. The abbreviation "asc" (in lowercase letters) describes the ascarylose unit and "CX" the attached sidechain, where X corresponds to the number of carbons in the chain. In addition, the linkage of fatty acid-derived sidechains is represented by the symbol "(ω)". The "(ω-1)" linkage is not indicated but is assumed by default. *Iso*-branched sidechains with an α-methyl group are indicated by the lowercase acronym "*i*" before "CX". Ascarosides with sidechains ending in methyl ketone are indicated by "MK", while functional groups such as carboxylic acids are not further specified. Numbers referring to the position of the head group are defined first, followed by their abbreviation, for example: "4-Ac-asc" (Ac= acetyl group). Moreover, aglycones are designated "CX-H" for alkyl ascarosides, "CX-OH" for 2-hydroxyalkyl ascarosides, and "(ω-COOH)-asc-CX" for ω-carboxy ascarosides.

6.3 Lipid metabolism in *C. elegans*

Unlike most animals, the bacterivorous nematode *C. elegans* can synthesize a wide range of monomethyl and polyunsaturated fatty acids using acetyl-CoA or isovaleryl-CoA as precursors [36].

Furthermore, *C. elegans* can convert monounsaturated fatty acids into polyunsaturated fatty acids. *C. elegans* can biosynthesize monomethyl-branched chain fatty acids (mmBCFAs) *de novo*, their physiological role in the worm metabolism makes them of high interest. Specifically, the mmBCFA biosynthesis involves acetyl-CoA carboxylase (ACC), fatty acid synthase (FAS), the branched-chain ketoacid dehydrogenase complex (BCKDC), fatty acid synthase (FASN-1), fatty acyl elongase (ELO-5 and ELO-6), 3-ketoacyl-CoA reductase (LET-767), and acyl-CoA synthetase (ACS-19) [36] [37] [38] [39] [40]. Furthermore, the amino acid L-leucine (**14**) is known to be used as a precursor for the synthesis of the essential 13-methyltetradecanoic acid (*iso*C15, **15a**), which is accumulated in storage lipids, glycerophospholipids, and sphingolipids (Figure 10) [36] [37]. The production of *iso*C15 (**15a**) proceeds via the *iso*-branched fatty acid 11-methyldodecanoic acid (*iso*C13, **16a**) with the ELO-5/ELO-6 enzymes elongating *iso*C13 (**16a**) to *iso*C15 (**15a**) and 15-methylhexadecanoic acid (*iso*C17, **17a**) by condensation with one acetate group per cycle.

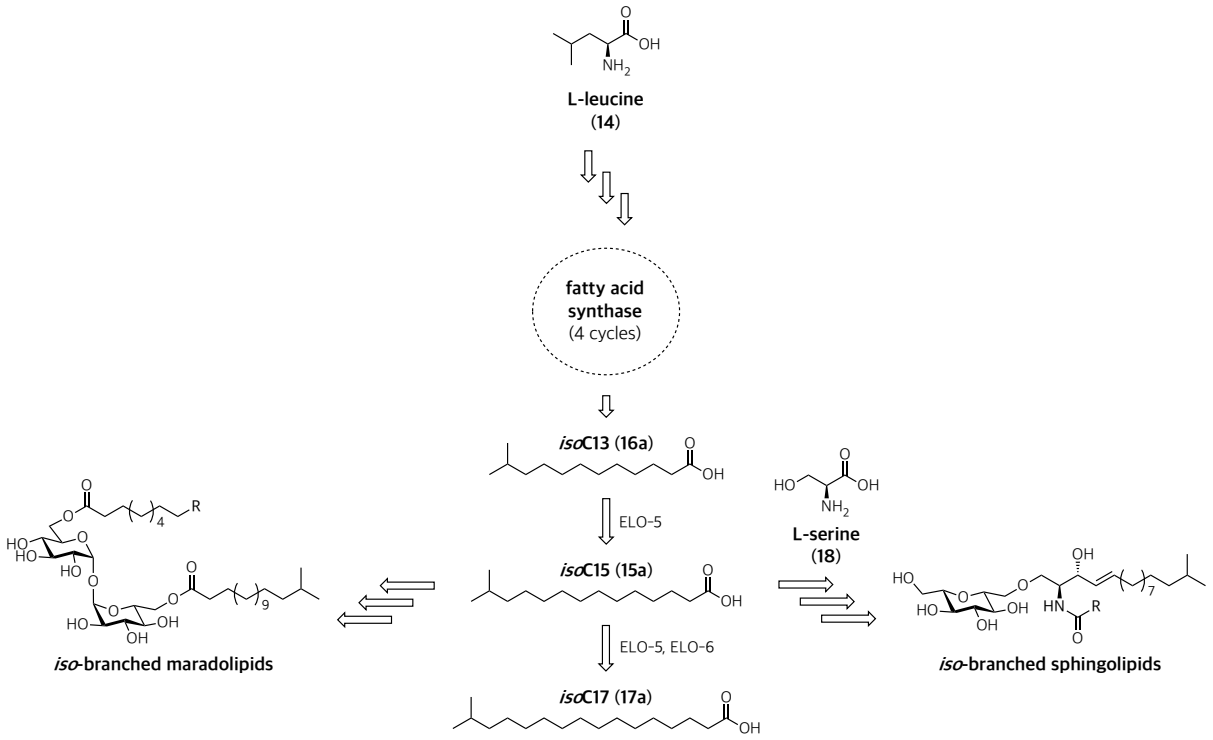

Figure 10. Pathway of de *iso*-fatty acid biosynthesis in *C. elegans* [41] [42] [43].

Iso-branched chain glycolipids in *C. elegans*, such as sphingolipids, are involved in the intestinal function of the worm [42], whereas maradolipids are involved in structuring the gut of the dauer larvae [44]. In general, sphingolipids and maradolipids with *iso*-branched fatty acids are derived from the *iso*-fatty acid precursor *iso*C15 (**15a**). In *iso*-branched sphingolipids, the C17 *iso*-branched sphingoid base unit (d17:*iso*-sphinganine) is the result of the condensation of *iso*C15 (**15a**) with the amino acid L-serine (**18**) [42] [45] [46] [47]. In dauer-specific maradolipids, the attachment of C15 *iso*-branched has not been

studied, but larger amounts of *iso*-branched chain fatty acids have been found in the *iso*-fatty acid moieties bound to the diacyltrehalose unit [43] [44] [48].

7 Aims of the project

7.1 Syntheses and detection of very long chain alkyl ascarosides in nematodes

Our current understanding regarding the biosynthetic origin of VLCAs and their role in ascaroside biosynthesis in nematodes is limited. Unpublished results by Dolke and von Reuss suggested that alkyl ascarosides act as potential intermediates of very long chain acyl ascarosides (ω)- and (ω-1)-linked. Based on the maximum lengths of the very long chain acyl ascarosides aglycones found on the *daf-22* exometabolome (Figure 8), three very long chain alkyl ascarosides are proposed as biosynthetic intermediates. The (ω)-ascaroside with a 21-carbon aglycone, which might act as a possible precursor of the longest (ω)-acyl ascaroside is obtained from the elongation of bacterial palmitic acid. The (ω-1)-ascaroside with a 31-carbon sidechain might be a precursor of very long chain acyl and 2-hydroxyalkyl ascarosides. The very long chain alkyl ascaroside (ω-1)-linked with an *iso*-branched aglycone of 26-carbons might be a possible precursor of α-methyl branched *iso*-acyl ascarosides.

The authors also reported, based on GC-EIMS analysis of *C. elegans* exometabolomes, two homologous series of very long chain alkyl ascarosides, one with an odd- and one with an even-numbered sidechain (Figure 11). The putative identification of these alkyl ascarosides was based on sidechain-specific fragments described in the literature (Figure 4). A comparison of the retention times of the odd- and even-numbered alkyl ascarosides showed that those with even-number aglycones elute earlier. As a result, it was proposed that the alkyl ascarosides with even-numbered aglycones were *iso*-branched and those with odd-numbered aglycones were straight chained. The hypothesis of *iso*-branched alkyl ascarosides acting as biosynthetic intermediates of α-methyl branched *iso*-acyl ascarosides (previously found in *daf-22*) is also supported by the mentioned propositions. Thus, the (ω-1)-ascaroside with a 25-carbon sidechain (**asc-C25-H**, Figure 11) could be suggested as a representation of an odd-numbered alkyl ascaroside. Consecutively, the (ω-1)-ascaroside with an *iso*-branched aglycone of 26-carbons could be suggested as an even-numbered (**asc-*i*C26-H**, Figure 11).

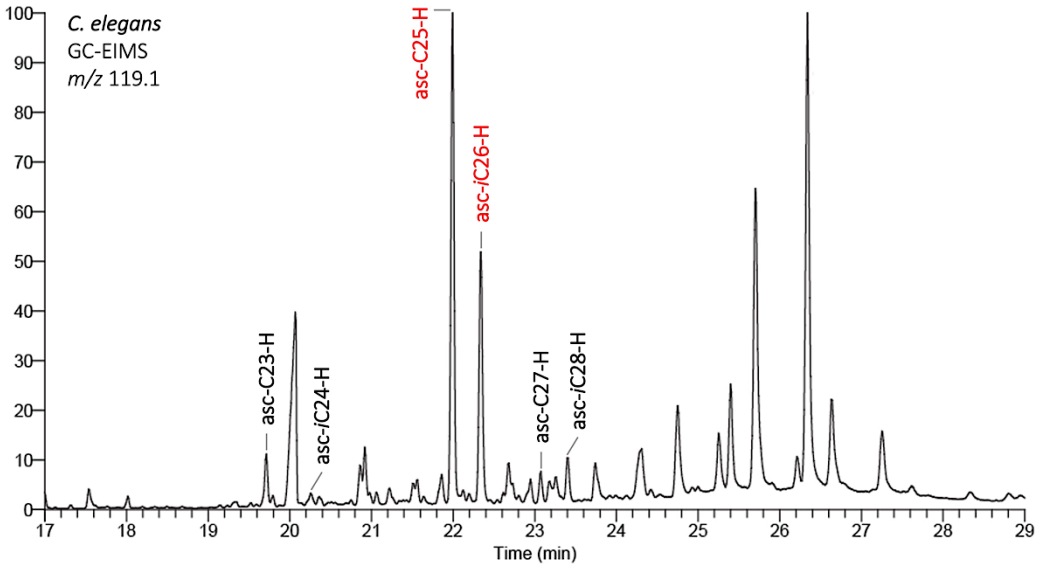

Figure 11. Detection of very long chain alkyl ascarosides in *C. elegans* exometabolomes.

To corroborate the mentioned hypotheses, the present study focused on the total synthesis and detection of the targeted very long chain alkyl ascarosides in *C. elegans* and other nematode species. The synthesis of these compounds and their biological characterization required the development of the following points:

- Preparation of novel ascarosides with very long alkyl aglycones. One (ω)-ascaroside with 21 carbons, two (ω-1)-ascarosides with 25 and 31 carbons, and one (ω-1)-linked *iso*-branched ascaroside with 26-carbons.

- Detection of the synthetic standards by LC-MS and/or GC-MS methods and their identification in *C. elegans* metabolomes.

- Detection of very long chain alkyl ascarosides in eggs and worms of the *C. elegans* wild type, as well as the lipidome of other nematode species.

7.2 Syntheses and detection of (ω)-carboxy ascarosides in *C. elegans*

Recent hypotheses predict the importance of (3*S*)-hydroxy alkyl acids for ascaroside biosynthesis, which implies (ω)-carboxy alkyl ascarosides as potential intermediates. HR-MS and MS^n analyses of a

daf-22 exometabolome revealed potential ascarosides with a high content of oxygen in the sidechains. Specifically, these putative derivatives include two homologous series of (ω)-carboxy ascarosides: (ω)-carboxy acyl ascarosides (sidechains from C18-23 carbons) and (ω)-carboxy 2-oxoalkyl ascarosides (sidechains from C17-21 carbons). Based on the high intensity of peaks corresponding to the (ω)-carboxy β-ketoalkyl ascaroside with an aglycone of 17 carbons and the (ω)-carboxy acyl ascaroside with a C18 sidechain, these products were selected as target compounds. Thus, the present study focused on the development of synthetic routes for the preparation of the mentioned (ω)-carboxy ascarosides and their use as synthetic standards for the screening of *C. elegans* metabolome extracts.

7.3 Lipid metabolism in nematodes

The importance of *iso*-fatty acids for sphingolipid biosynthesis in *C. elegans* has been previously demonstrated. Currents hypotheses from the von Reuss group suggested that the biosynthesis of *iso*-branched ascarosides (as well as other *iso*-branched metabolites in nematodes) could involve *iso*-branched fatty acids as precursors. Because the *iso*-fatty acids 11-methyldodecanoic acid (*iso*C13, **16a**), 13-methyltetradecanoic acid (*iso*C15, **15a**), and 15-methylhexadecanoic acid (*iso*C17, **17a**) have previously been considered as essential for the production of *iso*-branched metabolites in *C. elegans* (Figure 10), [D_6]-*iso*-fatty acid isotopomers were used as molecular probes to test this hypothesis. In consequence, the development of synthetic routes for the preparation of *iso*-fatty acid isotopomers is required, to facilitate their incorporation as dietary supplements in *C. elegans*.

8 Results

8.1 Very long chain alkyl ascarosides

A collection of four very long chain alkyl ascarosides representing putative biosynthetic intermediates for very long chain acyl ascarosides (Figure 11) were synthesized and used as authentic standards. The VLCAs series was also derivatized with different acetyl head groups to produce mono-acetylated and di-acetylated alkyl ascarosides. Synthetic routes were developed to obtain (ω-1)-linked ascarosides with odd-numbered sidechains (25 and 31 carbons) and one even-numbered (26 carbons) *iso*-branched sidechain. Furthermore, the (ω)-linked alkyl ascaroside with a sidechain of 21 carbons was synthesized. Stable isotopomers of the alkyl ascarosides were synthesized with aglycones [D_4]-labelled, at (ω-1)/(ω-2)-position for the (ω)-ascaroside or (ω-2)/(ω-3)-position for the (ω-1)-ascarosides, to serve as metabolic probes. This specific labelling pattern on the ascaroside sidechain will be required to determine the potential role of very long chain alkyl ascarosides as precursors of long and short chain acyl ascarosides. However, the present investigation only focused on their syntheses. Figure 12 provides a general overview of the very long chain alkyl ascarosides series synthesized.

A

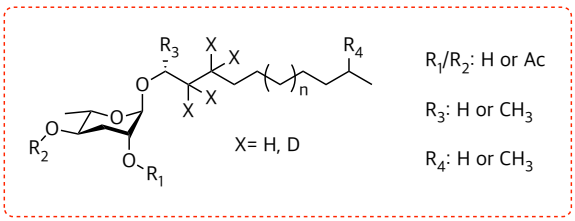

B

VLCAsc	n	X	R_1/R_2	R_3	R_4
asc-ωC21-H	12	H	H, H	H	H
asc-C25-H	15	H	H, H	CH_3	H
asc-*i*C26-H	15	H	H, H	CH_3	CH_3
asc-C31-H	21	H	H, H	CH_3	H

VLCAsc	n	X	R_1/R_2	R_3	R_4
[D_4]-asc-ωC21-H	12	D	H, H	H	H
[D_4]-asc-C25-H	15	D	H, H	CH_3	H
[D_4]-asc-*i*C26-H	15	D	H, H	CH_3	CH_3
[D_4]-asc-C31-H	21	D	H, H	CH_3	H

Figure 12. (A) General scheme of the very long alkyl chain ascaroside structures synthesized in this research. (B) Examples of non-acetylated very long alkyl chain ascarosides and their deuterium labelled isotopomers.

8.1.1 Synthesis of very long chain alkyl ascarosides

The synthesis of a short chain ascaroside like daumone (ascr#1, C7, **1**, Figure 1-B) was first reported by Jeong *et al.* [(12)]. These authors obtained ascr#1 (**1**) by glycosylation of two building blocks: a 2,4-

protected ascarylose (**19**) and the hydroxy sidechain (**20**) (Figure 13). The preparation of the ascarylose building block, 2,4-di-*O*-benzoyl ascarylose (**19**), was performed in eight steps using commercially available L-rhamnose (**21**). The (ω-1)-hydroxylated sidechain (**20**) was built from the commercially available (*R*)-(+)-propyleneoxide (**22**) by reacting with a short chain alkenyl Grignard reagent (**23**) using organocuprate catalysis with CuBr.

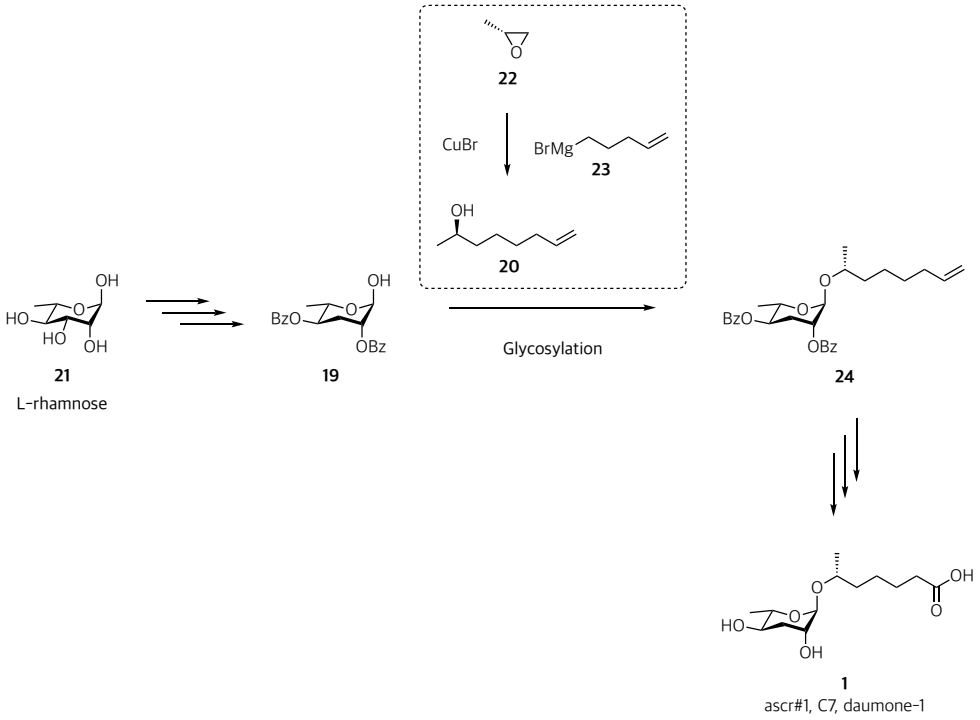

Figure 13. Synthesis of (*R*)-6-(((2*R*,3*R*,5*R*,6*S*)-3,5-dihydroxy-6-methyltetrahydro-2*H*-pyran-2-yl)oxy)heptanoic acid (**1**, ascr#1, C7) proposed by Jeong *et al.* [12].

Alternative syntheses of (ω-1)-ascarosides with short, medium, and long acyl sidechains (3 to 18 carbons) have been reported [17] [21] [24] [49] that follow a procedure similar to the one described by Jeong *et al.* [12]. The (*R*)-configured chiral center was introduced by reacting (*R*)-(+)-propyleneoxide (**22**) with the homologous alkenyl Grignard reagents, and the glycosylation employs the benzoyl ascarylose (**19**) and an alcohol as building blocks. Additional extension of the sidechains for the preparation of long chain ascarosides (up to 18 carbons), or the introduction of an acyl terminus in the sidechain, have been described to proceed by Grubbs metathesis. In general, the glycosylation has been reported by two methods: direct reaction of the building blocks with BF_3-Et_2O [12] [49] or initial preparation of an ascarosyl trichloroacetimidate intermediate further treated with an alcohol and trimethylsilyl trifluoromethanesulfonate [17] [21] [24]. For example, the (2*S*,3*R*,5*R*,6*R*)-2-methyl-6-((*R*)-non-8-en-2-yl)oxy)tetrahydro-2*H*-pyran-3,5-diyl dibenzoate (**25**) was reported to be synthesized from the 2,4-di-*O*-benzoyl ascarylose (**19**) with an (ω-1)-hydroxyalkene (Figure 14). The extension of the sidechain of

the alkenyl intermediate **25** with methyl undec-10-enoate (**26**) was achieved by Grubbs metathesis to furnish the acyl ester **27**. The compound **27** could be converted to a very long chain acyl ascarosides upon hydrogenation and deprotection (Figure 14).

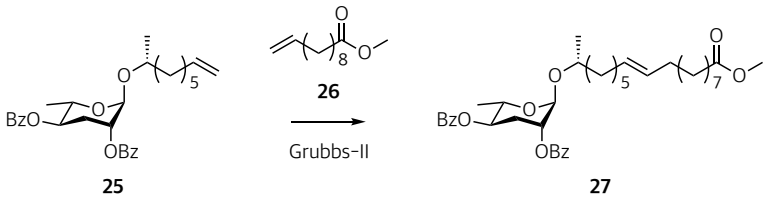

Figure 14. Example of olefin metathesis used for introduction of an acyl terminus in the sidechain [21].

Preparation of (ω)- and (ω-1)-ascarosides with long chain aglycones (up to 22 carbons) utilizing direct attachment of commercially available long chain alkyl alcohols has also been described [12] [17] [21] [50]. In particular, the synthesis of an (ω)-alkyl ascaroside with a 22-carbon sidechain was reported from the reaction of 2-tricosanol with 3,4-di-*O*-acetyl-L-rhamnal using BF_3-Et_2O [50]. The synthesis of a very long chain (ω-1)-linked alkyl ascaroside with a sidechain of 23 carbons has been attempted via the reaction of 3,4-di-*O*-acetyl-L-rhamnal and 2-hydroxytricosanol using BF_3-Et_2O, but no satisfactory reaction was achieved [50]. Thus, part of the present study focused on the syntheses of very long chain (ω-1)-hydroxy alkanes and their reactions with 2,4-di-*O*-benzoyl ascarylose (**19**). The synthesis of the ascarylose building block (**19**) and the methodology for glycosylation followed a previously reported procedure [24] with modifications. Moreover, the preparation of the aglycone building blocks required the development of new synthetic routes to generate the deuterium labelled very long chain alkyl ascaroside isotopomers shown in Figure 12. Previous routes for the synthesis of the aglycones by using (*R*)-(+)-propyleneoxide (**22**) for the (ω-1)-chiral center in (*R*)-configuration was not suitable for the isotopomers. Instead, (*R*)-3-butyn-2-ol was chosen as a chiral building block for the introduction of the (*R*)-chiral center, which enabled the introduction of the deuterium label via catalyzed deuterogenation with D_2. Using this method, even- and odd-numbered very long chain aglycones, [D_4]-labelled and unlabeled, were synthesized. Subsequently, very long chain alkyl ascarosides and their acetyl derivatives were prepared.

8.1.2 Syntheses and characterization of very long chain alkyl ascarosides

8.1.2.1 Synthesis of (2*R*,3*R*,5*R*,6*S*)-2-hydroxy-6-methyltetrahydro-2*H*-pyran-3,5-diyl dibenzoate (19)

The synthesis of (2*R*,3*R*,5*R*,6*S*)-2-hydroxy-6-methyltetrahydro-2*H*-pyran-3,5-diyl dibenzoate (**19**) was based on a previously reported procedure [24]. The synthesis of **19** was carried out in six-steps, starting with the benzoylation of the four hydroxyl groups of commercially available L-rhamnose (**21**) (Figure 15). The compound **28** was obtained as a mixture of the α:β anomers using an excess of benzoyl chloride in pyridine. The deprotection of the anomeric hydroxy group at the 1-position with dimethylamine in acetonitrile generates (3*R*,4*R*,5*S*,6*S*)-6-methyltetrahydro-2*H*-pyran-2,3,4,5-tetrayl tetrabenzoate (**29**) as anomeric mixture. In contrast with the previously reported purification procedure, the compound **29** was recrystallized from toluene with an 86% yield compared with the 79% reported. The lactone **30** was obtained by the oxidation of the 1-OH-position in **29** using pyridinium chlorochromate. In contrast with the original procedure, the crude product could be purified by simple filtration over a silica gel column with DCM as eluent. The selective elimination of a benzoate group from the 3-*O*-position was accomplished with triethylamine in $CHCl_3$ to yield (2*S*,3*R*)-2-methyl-6-oxo-3,6-dihydro-2*H*-pyran-3,5-diyl dibenzoate (**31**) with a 99% yield. At this stage, the lactone **31** was purified by column chromatography using a mixture of toluene and EtOAc to improve yields in the subsequent synthetic steps. For example, the following stereoselective hydrogenation of the compound **31** with H_2 and Pd/C as catalyst generated (2*S*,3*R*,5*R*)-2-methyl-6-oxotetrahydro-2*H*-pyran-3,5-diyl dibenzoate (**32**) with a 99% yield compared to the 68% reported. The final product (2*R*,3*R*,5*R*,6*S*)-2-hydroxy-6-methyltetrahydro-2*H*-pyran-3,5-diyl dibenzoate (**33**) was also synthesized with higher yields (90% yield vs. the 71% reported). This last step consisted in the selective reduction of the cyclic lactone in **19** using *in situ* generated disiamylborane prepared from 2-methyl-2-butene and BH_3-THF.

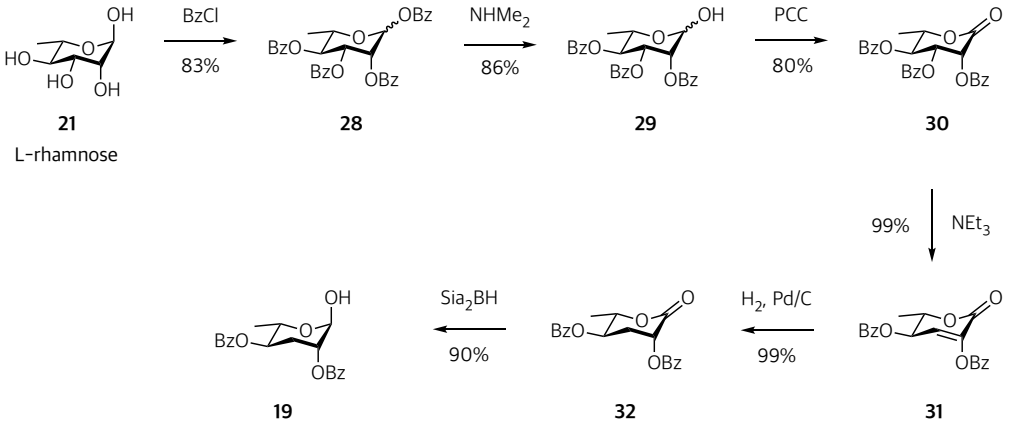

Figure 15. Synthetic route to (2*R*,3*R*,5*R*,6*S*)-2-hydroxy-6-methyltetrahydro-2*H*-pyran-3,5-diyl dibenzoate (**19**) from L-rhamnose (**21**).

8.1.2.2 Synthesis of (2*S*,3*R*,5*R*,6*R*)-2-methyl-6-((*R*)-pentacosan-2-yl)oxy)tetrahydro-2*H*-pyran-3,5-diol and [D_4]-(2*S*,3*R*,5*R*,6*R*)-2-methyl-6-((*R*)-pentacosan-2-yl)oxy)tetrahydro-2*H*-pyran-3,5-diol

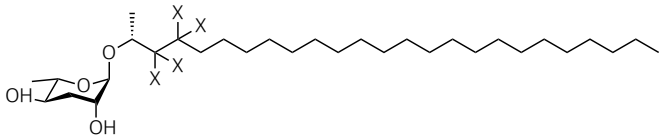

(2*S*,3*R*,5*R*,6*R*)-2-methyl-6-(((*R*)-pentacosan-2-yl)oxy)tetrahydro-2*H*-pyran-3,5-diol (X=H, **asc-C25-H**, **33a**)

[D_4]-(2*S*,3*R*,5*R*,6*R*)-2-methyl-6-(((*R*)-pentacosan-2-yl)oxy)tetrahydro-2*H*-pyran-3,5-diol (X=D, **[D_4]-asc-C25-H**, **33b**)

Figure 16. Structure of **asc-C25-H** (**33a**) and **[D_4]-asc-C25-H** (**33b**).

The syntheses of (2*S*,3*R*,5*R*,6*R*)-2-methyl-6-((*R*)-pentacosan-2-yl)oxy)tetrahydro-2*H*-pyran-3,5-diol (**asc-C25-H**, **33a**) and [D_4]-(2*S*,3*R*,5*R*,6*R*)-2-methyl-6-((*R*)-pentacosan-2-yl)oxy)tetrahydro-2*H*-pyran-3,5-diol (**[D_4]-asc-C25-H**, **33b**) (Figure 16) required the preparation of the very long chain fatty alcohols (*R*)-pentacosan-2-ol (**34a**) and [D_4]-(*R*)-pentacosan-2-ol (**34b**) as starting materials. Figure 17 summarizes the pathway performed for their synthesis. This route started with the preparation of 1-bromohenicosane (**35**) from commercially available henicosan-1-ol (**36**) using Br_2 and PPh_3. Subsequently, synthesis of the (*R*)-*tert*-butyldimethyl(pentacos-3-yn-2-yloxy)silane (**37**) proceeded by alkylation of lithiated (*R*)-(but-3-yn-2-yloxy)(*tert*-butyl)dimethylsilane (**38**) with the alkyl bromide **35**. The preparation of **37** first required the optimization of reaction conditions [51] [52] [53], which have subsequently been used for all the alkyne alkylations of this study. Best results were achieved by combining two separate mixtures, in which the first consists of the deprotonated alkyne **38** and the second contains the alky bromide **35** along with hexamethylphosphoramide. Therefore, the (*R*)-*tert*-butyldimethyl(pentacos-3-yn-2-yloxy)silane (**37**) was synthesized by combining a mixture of 1-bromohenicosane (**35**), and hexamethylphosphoramide with a mixture of (*R*)-(but-3-yn-2-yloxy)(*tert*-butyl)dimethylsilane (**37**) that has been treated with *n*-butyllithium.

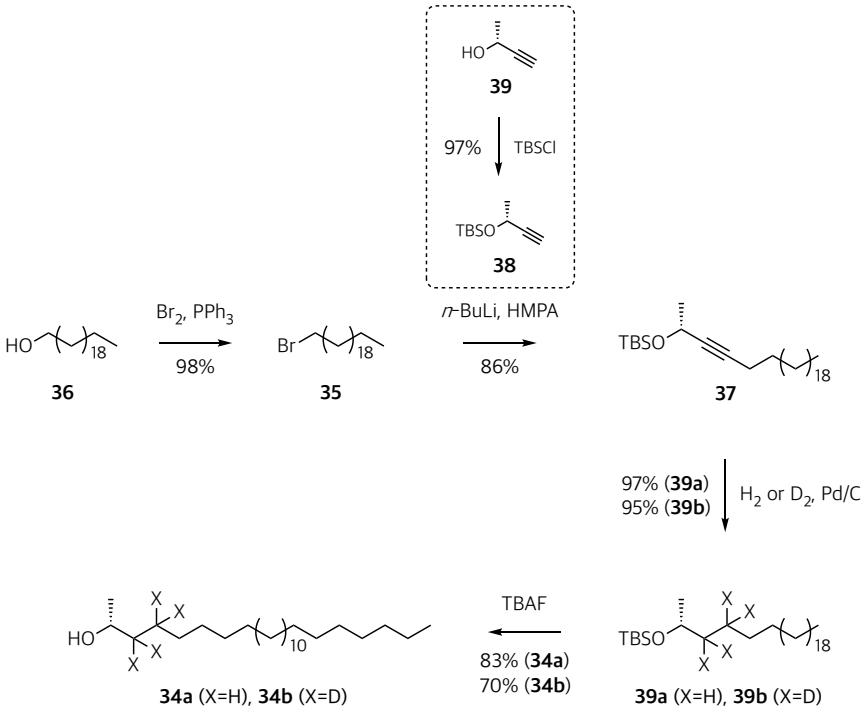

Figure 17. Synthesis of (*R*)-pentacosan-2-ol (**34a**) or [D_4]-(*R*)-pentacosan-2-ol (**34b**).

The alkylation step to obtain (*R*)-*tert*-butyldimethyl(pentacos-3-yn-2-yloxy)silane (**37**) was followed by 1D NMR and GC-MS analyses. Characteristic ^{1}H NMR signals for (*R*)-*tert*-butyldimethyl(pentacos-3-yn-2-yloxy)silane appeared at δ_H 1.40 ppm for the methyl group (1-CH_3), δ_H 4.53 ppm (qt, J=6.5, 1.9 Hz) for 2-H, δ_H 2.19 ppm (td, J=7.1, 1.9 Hz) for 5-CH_2 and δ_H 1.50 ppm (m) for 6-CH_2 (Figure 18). The presence of **37** was also confirmed by GC-MS, which showed a fragment ion at *m/z* 463.5 for $[M\text{-}CH_3]^+$.

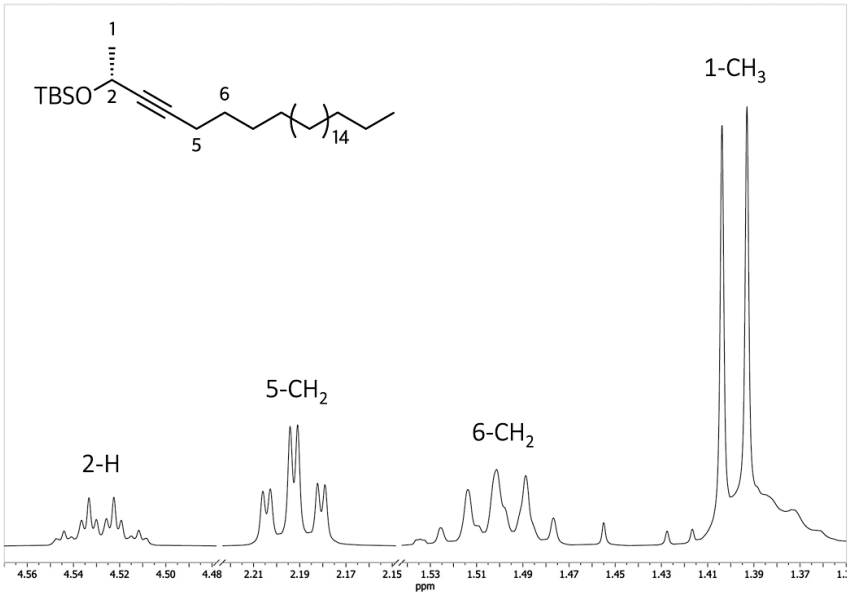

Figure 18. Sections of the ^{1}H NMR spectrum of the alkyne (*R*)-*tert*-butyldimethyl(pentacos-3-yn-2-yloxy)silane (**37**).

The reduction of the triple bond of (*R*)-*tert*-butyldimethyl(pentacos-3-yn-2-yloxy)silane (**37**) under atmospheric pressure with H_2 or D_2 and Pd/C as catalyst affords the (*R*)-*tert*-butyldimethyl(pentacosan-2-yloxy)silane (**39a**) and [D_4]-(*R*)-*tert*-butyldimethyl(pentacosan-2-yloxy)silane (**39b**), respectively. Consecutive *O*-desilylation of **39a** and **39b** with an excess of tetra-*n*-butylammonium fluoride solution generated the fatty alcohols (*R*)-pentacosan-2-ol (**34a**) and [D_4]-(*R*)-pentacosan-2-ol (**34b**). However, GC-MS analysis demonstrated that the synthesis of **34b** with Pd-catalyst generated a mixture of isotopomers. For future studies in which specific [D_X]-labelling (X=1,2,3…) will be required, the use of Wilkinson's catalyst for the deuterogenation process could be suggested [(54)].

The glycosylation of (*R*)-pentacosan-2-ol (**34a**) and [D_4]-(*R*)-pentacosan-2-ol (**34b**) with (2*R*,3*R*,5*R*,6*S*)-2-hydroxy-6-methyltetrahydro-2*H*-pyran-3,5-diyl dibenzoate (**19**) proceeds as shown in Figure 19. Initially, the preparation of the ascarosyl trichloroacetimidate intermediate **40** from the ascarylose building block **19** was required and performed as previously reported [(24)]. The preparation of this unstable intermediate was accomplished by the reaction of **19** with trichloroacetonitrile and 1,8-diazabicyclo[5.4.0]undec-7-ene. The instability of the product required immediate purification. Next, the ascarosyl trichloroacetimidate intermediate (**40**) was reacted with trimethylsilyl trifluoromethanesulfonate and the pre-synthesized fatty alcohols (*R*)-pentacosan-2-ol (**34a**) or [D_4]-(*R*)-pentacosan-2-ol (**34b**) to generate (2*R*,3*S*,5*S*,6*S*)-2-methyl-6-((*R*)-pentacosan-2-yl)oxy)tetrahydro-2*H*-pyran-3,5-diyl dibenzoate (**41a**) or [D_4]-(2*R*,3*S*,5*S*,6*S*)-2-methyl-6-((*R*)-pentacosan-2-yl)oxy)tetrahydro-2*H*-pyran-3,5-diyl dibenzoate (**41b**). Final cleavage of the benzoyl groups with concentrated NaOH solution generates the very long chain alkyl ascarosides (2*S*,3*R*,5*R*,6R)-2-methyl-6-((*R*)-pentacosan-2-yl)oxy)tetrahydro-2*H*-pyran-3,5-diol (**asc-C25-H**, **33a**) and [D_4]-(2*S*,3*R*,5*R*,6*R*)-2-methyl-6-((*R*)-pentacosan-2-yl)oxy)tetrahydro-2*H*-pyran-3,5-diol (**[D_4]-asc-C25-H**, **33b**) in 84% and 87% yield, respectively.

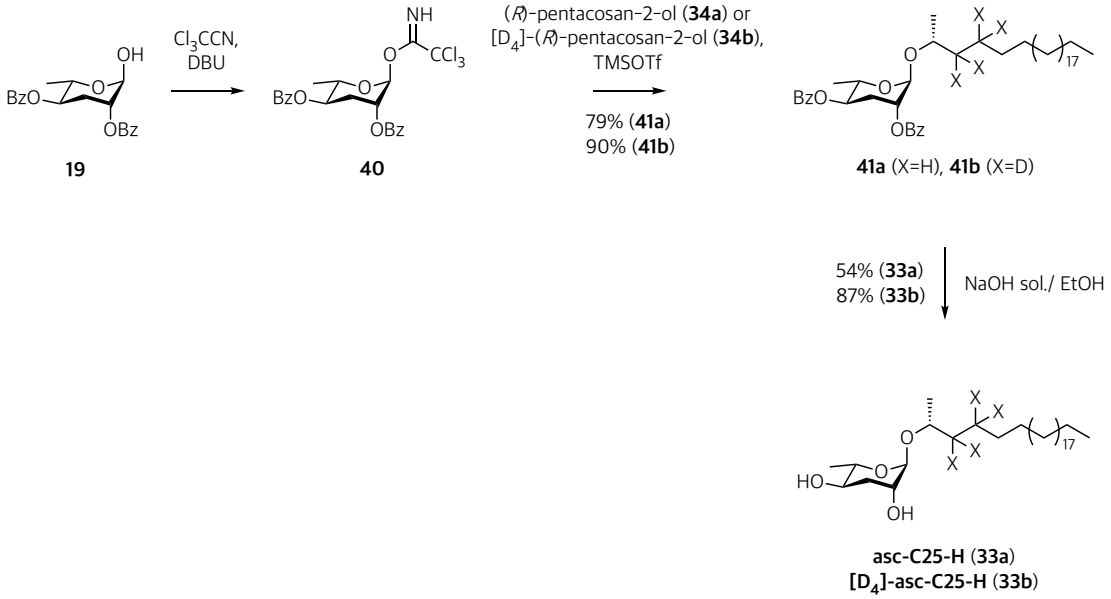

Figure 19. Synthesis of (2*S*,3*R*,5*R*,6*R*)-2-methyl-6-((*R*)-pentacosan-2-yl)oxy)tetrahydro-2*H*-pyran-3,5-diol (**asc-C25-H**, **33a**) or [D4]-(2*S*,3*R*,5*R*,6*R*)-2-methyl-6-((*R*)-pentacosan-2-yl)oxy)tetrahydro-2*H*-pyran-3,5-diol (**[D4]-asc-C25-H**, **33b**).

8.1.2.3 Synthesis of (2*S*,3*R*,5*R*,6*R*)-2-methyl-6-((*R*)-24-methylpentacosan-2-yl)oxy)tetrahydro-2*H*-pyran-3,5-diol and [D4]-(2*S*,3*R*,5*R*,6*R*)-2-methyl-6-((*R*)-24-methylpentacosan-2-yl)oxy)tetrahydro-2*H*-pyran-3,5-diol

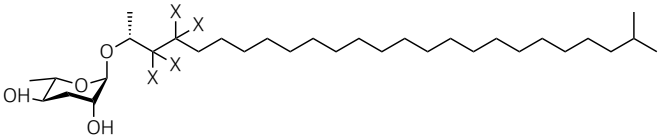

(2*S*,3*R*,5*R*,6*R*)-2-methyl-6-(((*R*)-24-methylpentacosan-2-yl)oxy)tetrahydro-2*H*-pyran-3,5-diol (X=H, **asc-*i*C26-H**, **43a**)

[D4]-(2*S*,3*R*,5*R*,6*R*)-2-methyl-6-(((*R*)-24-methylpentacosan-2-yl)oxy)tetrahydro-2*H*-pyran-3,5-diol (X=D, **[D4]-asc-*i*C26-H**, **43b**)

Figure 20. Structure of **asc-*i*C26-H** (**43a**) and **[D4]-asc-*i*C26-H** (**43b**).

The syntheses of the *iso*-branched alkyl ascarosides (2*S*,3*R*,5*R*,6*R*)-2-methyl-6-((*R*)-24-methylpentacosan-2-yl)oxy)tetrahydro-2*H*-pyran-3,5-diol (**asc-*i*C26-H**, **43a**) and [D4]-(2*S*,3*R*,5*R*,6*R*)-2-methyl-6-((*R*)-24-methylpentacosan-2-yl)oxy)tetrahydro-2*H*-pyran-3,5-diol (**[D4]-asc-*i*C26-H**, **43b**) (Figure 20) required the preparation of fatty alcohols with a terminal *iso*-branch with 26 carbons. The structural difference of the *iso*-branched chain required the adaptation and development of a particular synthetic pathway. The products (*R*)-24-methylpentacosan-2-ol (**44a**) and [D4]-(*R*)-24-methylpentacosan-2-ol (**44b**) were obtained in eight steps starting from commercially available pentadecanolide (**45**) (Figure 21). The alcohols 15-methylhexadecane-1,15-diol (**46a**) and 15-

methylhexadecan-1-ol (**47a**) were prepared as described by Williams *et al.* [55] with few modifications. The reaction of the lactone **45** with methylmagnesium bromide generates the diol **46a**, which was selectively reduced with $BF_3{\cdot}Et_2O$ and triethylsilane to afford **47a** in excellent yields (95-99%). The consecutive reaction of the alkyl alcohol **47a** with *N*-bromosuccinimide and PPh_3 afforded 1-bromo-15-methylhexadecane (**48**) [56]. In parallel, commercially available 5-bromopentan-1-ol (**49**) was protected with 3,4-dihydropyran to generate 2-((5-bromopentyl)oxy)tetrahydro-2*H*-pyran (**50**), which was coupled with the freshly prepared Grignard reagent **51**.

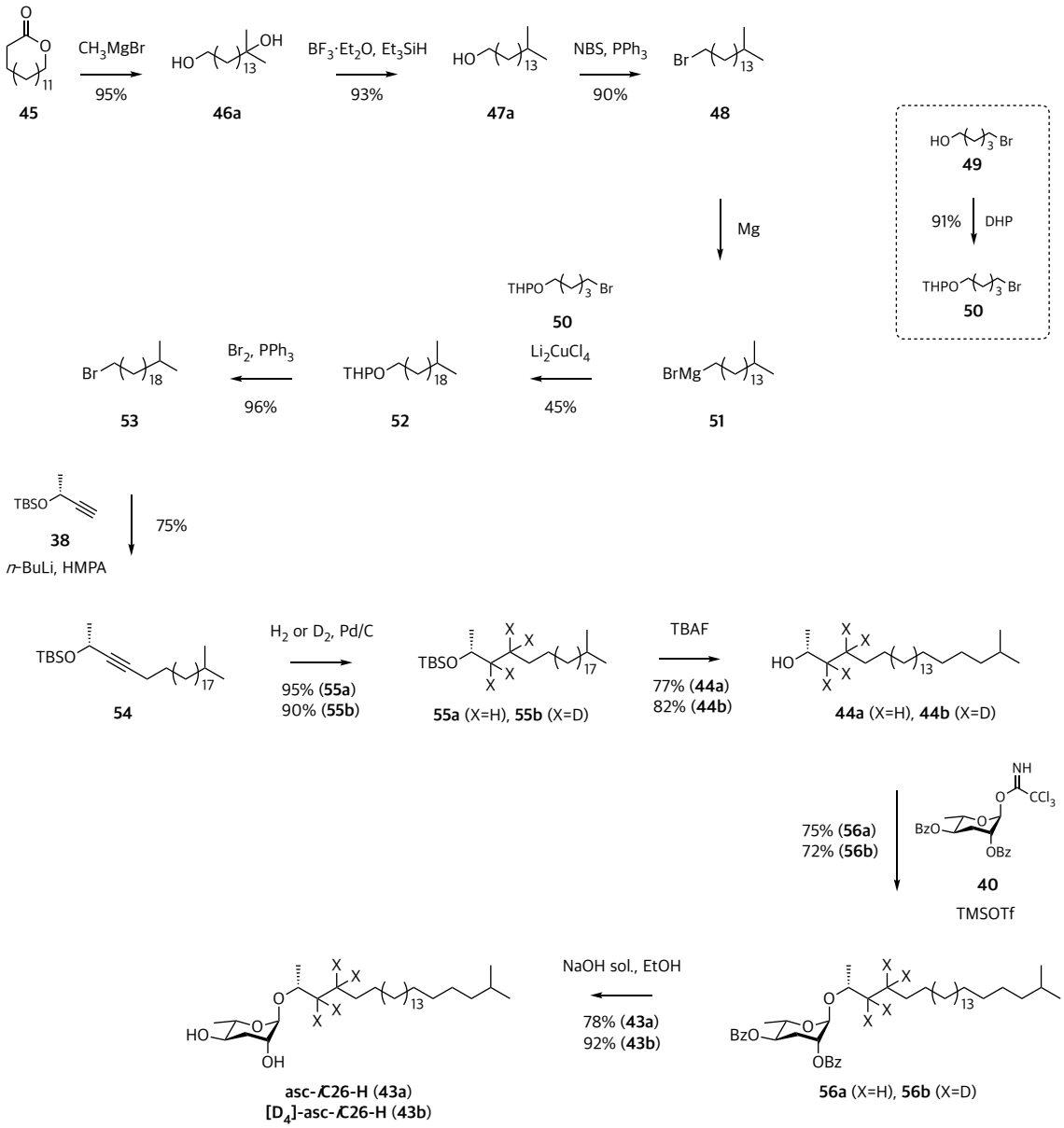

Figure 21. Synthesis of (2*S*,3*R*,5*R*,6*R*)-2-methyl-6-((*R*)-24-methylpentacosan-2-yl)oxy)tetrahydro-2*H*-pyran-3,5-diol (**asc-*i*C26-H**, **43a**) or [D_4]-(2*S*,3*R*,5*R*,6*R*)-2-methyl-6-((*R*)-24-methylpentacosan-2-yl)oxy)tetrahydro-2*H*-pyran-3,5-diol (**[D_4]-asc-*i*C26-H**, **43b**).

For the C-C coupling, the Grignard reagent could be prepared from both halides, 3-(bromomethyl)-2-methylpentadecane (**48**) or 2-((5-bromopentyl)oxy)tetrahydro-2*H*-pyran (**50**). However, synthesis with **48** achieved a better yield (45%). Therefore, the 2-((20-methylhenicosyl)oxy)tetrahydro-2*H*-pyran (**52**) was obtained by the cross-coupling between the compound **50** and the Grignard reagent **51**, catalyzed by dilithium tetrachlorocuprate [57]. The extension of the alkyl chain was a crucial step for this pathway. The structure of the compound **52** was confirmed by ^{1}H and ^{13}C NMR and GC-MS. For example, the EIMS spectrum in Figure 22 shows a signal at *m/z* 409.4 $[C_{27}H_{53}O_2]^+$ along with a fragment ion at *m/z* 85.1 $[C_5H_9O]^+$, which confirms the structure of **52**.

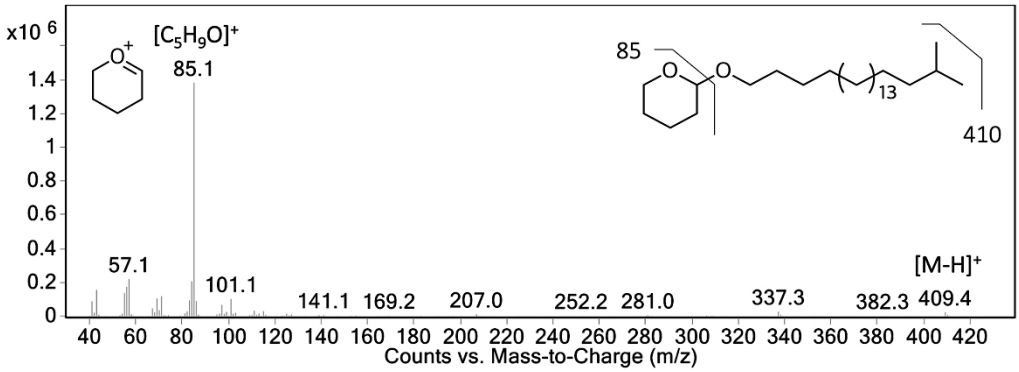

Figure 22. GC-MS spectrum of 2-((20-methylhenicosyl)oxy)tetrahydro-2*H*-pyran (**52**).

Subsequent reaction of the tetrahydropyranyl ether **52** with PPh_3 and Br_2 [58] gave the *iso*-alkyl bromide compound 1-bromo-20-methylhenicosane (**53**) in 96% yield. The very long chain alkyne (*R*)-*tert*-butyldimethyl((24-methylpentacos-3-yn-2-yl)oxy)silane (**54**) was synthesized in the same way as (*R*)-*tert*-butyldimethyl(pentacos-3-yn-2-yloxy)silane (**37**). The Reduction of the triple bond with H_2 or D_2 of compound **54** catalyzed with Pd/C affords (*R*)-*tert*-butyldimethyl((24-methylpentacosan-2-yl)oxy)silane (**55a**) or [D_4]-(*R*)-*tert*-butyldimethyl((24-methylpentacosan-2-yl)oxy)silane (**55b**), respectively. Final *O*-desilylation with an excess of tetra-*n*-butylammonium fluoride solution furnished the products (*R*)-24-methylpentacosan-2-ol (**44a**) and [D_4]-(*R*)-24-methylpentacosan-2-ol (**44b**). The synthesis of (2*S*,3*R*,5*R*,6*R*)-2-methyl-6-((*R*)-24-methylpentacosan-2-yl)oxy)tetrahydro-2*H*-pyran-3,5-diyl dibenzoate (**56a**) and [D_4]-(2*S*,3*R*,5*R*,6*R*)-2-methyl-6-((*R*)-24-methylpentacosan-2-yl)oxy)tetrahydro-2*H*-pyran-3,5-diyl dibenzoate (**56b**) consisted in the glycosylation of long chain aglycones with the (2*R*,3*S*,5*S*,6*R*)-2-methyl-6-(2,2,2-trichloro-1-iminoethoxy)tetrahydro-2*H*-pyran-3,5-diyl dibenzoate (**40**) intermediate. Cleavage of the benzoyl groups of **56a** and **56b** required an excess of concentrated NaOH solution to yield the *iso*-branched ascarosides (2*S*,3*R*,5*R*,6*R*)-2-methyl-6-((*R*)-24-methylpentacosan-2-yl)oxy)tetrahydro-2*H*-pyran-3,5-diol (**asc-*i*C26-H**, **43a**) and [D_4]-(2*S*,3*R*,5*R*,6*R*)-2-methyl-6-((*R*)-24-methylpentacosan-2-yl)oxy)tetrahydro-2*H*-pyran-3,5-diol (**[D_4]-asc-*i*C26-H**, **43b**).

8.1.2.4 Synthesis of (2*R*,3*R*,5*R*,6*S*)-2-((*R*)-hentriacontan-2-yl)oxy)-6-methyltetrahydro-2*H*-pyran-3,5-diol and [D_4]-(2*R*,3*R*,5*R*,6*S*)-2-((*R*)-hentriacontan-2-yl)oxy)-6-methyltetrahydro-2*H*-pyran-3,5-diol

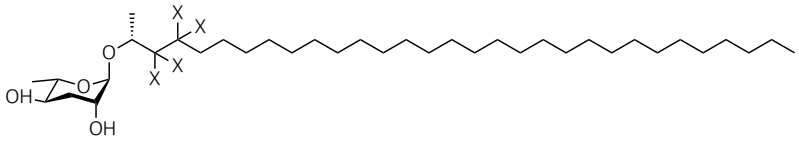

(2*R*,3*R*,5*R*,6*S*)-2-(((*R*)-hentriacontan-2-yl)oxy)-6-methyltetrahydro-2*H*-pyran-3,5-diol (X=H, **asc-C31-H**, **67a**)

[D_4]-(2*R*,3*R*,5*R*,6*S*)-2-(((*R*)-hentriacontan-2-yl)oxy)-6-methyltetrahydro-2*H*-pyran-3,5-diol (X=D, **[D_4]-asc-C31-H**, **67b**)

Figure 23. Structure of **asc-C31-H** (**57a**) and **[D_4]-asc-C31-H** (**57b**).

The syntheses of the very long chain ascarosides (2*R*,3*R*,5*R*,6*S*)-2-((*R*)-hentriacontan-2-yl)oxy)-6-methyltetrahydro-2*H*-pyran-3,5-diol (**asc-C31-H**, **57a**) and [D_4]-(2*R*,3*R*,5*R*,6*S*)-2-((*R*)-hentriacontan-2-yl)oxy)-6-methyltetrahydro-2*H*-pyran-3,5-diol (**[D_4]-asc-C31-H**, **57b**) (Figure 23) required the preparation of the 31-carbon aglycone moiety, which was obtained by using multiple alkyne alkylation steps. The preparation of the fatty alcohols (*R*)-hentriacontan-2-ol (**58a**) and [D_4]-(*R*)-hentriacontan-2-ol (**58b**) was accomplished by using 2-(undec-10-yn-1-yloxy)tetrahydro-2*H*-pyran (**59**) as starting material (Figure 24). The compound **60** was obtained by the reaction of undec-10-yn-1-ol (**61**) with 3,4-dihydropyran [(59)]. Subsequently, the alkylation of the lithiated alkyne **60** with 1-bromohexadecane (**62**) gave 2-(heptacos-10-yn-1-yloxy)tetrahydro-2*H*-pyran (**59**) as a precursor for the next step. Pd-catalyzed hydrogenation of the alkyne bond of **59** afforded the tetrahydropyranyl ether 2-(heptacosyloxy)tetrahydro-2*H*-pyran (**63**). Reaction of the ether **63** with an excess of PPh_3 and bromine produced 1-bromoheptacosane (**64**) in 98% yield, which was used for alkylation of lithiated (*R*)-(but-3-yn-2-yloxy)(*tert*-butyl)dimethylsilane (**38**) to afford (*R*)-*tert*-butyl(hentriacont-3-yn-2-yloxy)dimethylsilane (**65**). Pd/C catalyzed reduction of the alkyne **65** with H_2 or D_2 gave (*R*)-*tert*-butyl(61entriacontane-2-yloxy)dimethylsilane (**66a**) or [D_4]-(*R*)-*tert*-butyl(61entriacontane-2-yloxy)dimethylsilane (**66b**), respectively. Cleavage of the silyl-protecting group with an excess of tetrabutylammonium fluoride solution in THF gave the desired alkyl alcohols (*R*)-hentriacontan-2-ol (**58a**) and [D_4]-(*R*)-hentriacontan-2-ol (**58b**) with good yields (70%). Final glycosylation of fatty alcohols **58a** and **58b** with the 2,4-benzoyl ascarylose trichloroacetimidate **40** was achieved using the previously detailed procedure (see section 8.1.2.2). Subsequently, the ascarosides **67a** and **67b** were debenzoylated with concentrated NaOH solution to yield (2*R*,3*R*,5*R*,6*S*)-2-((*R*)-hentriacontan-2-yl)oxy)-6-methyltetrahydro-2*H*-pyran-3,5-diol (**asc-C31-H**, **57a**) and [D_4]-(2*R*,3*R*,5*R*,6*S*)-2-((*R*)-hentriacontan-2-yl)oxy)-6-methyltetrahydro-2*H*-pyran-3,5-diol (**[D_4]-asc-C31-H**, **57b**).

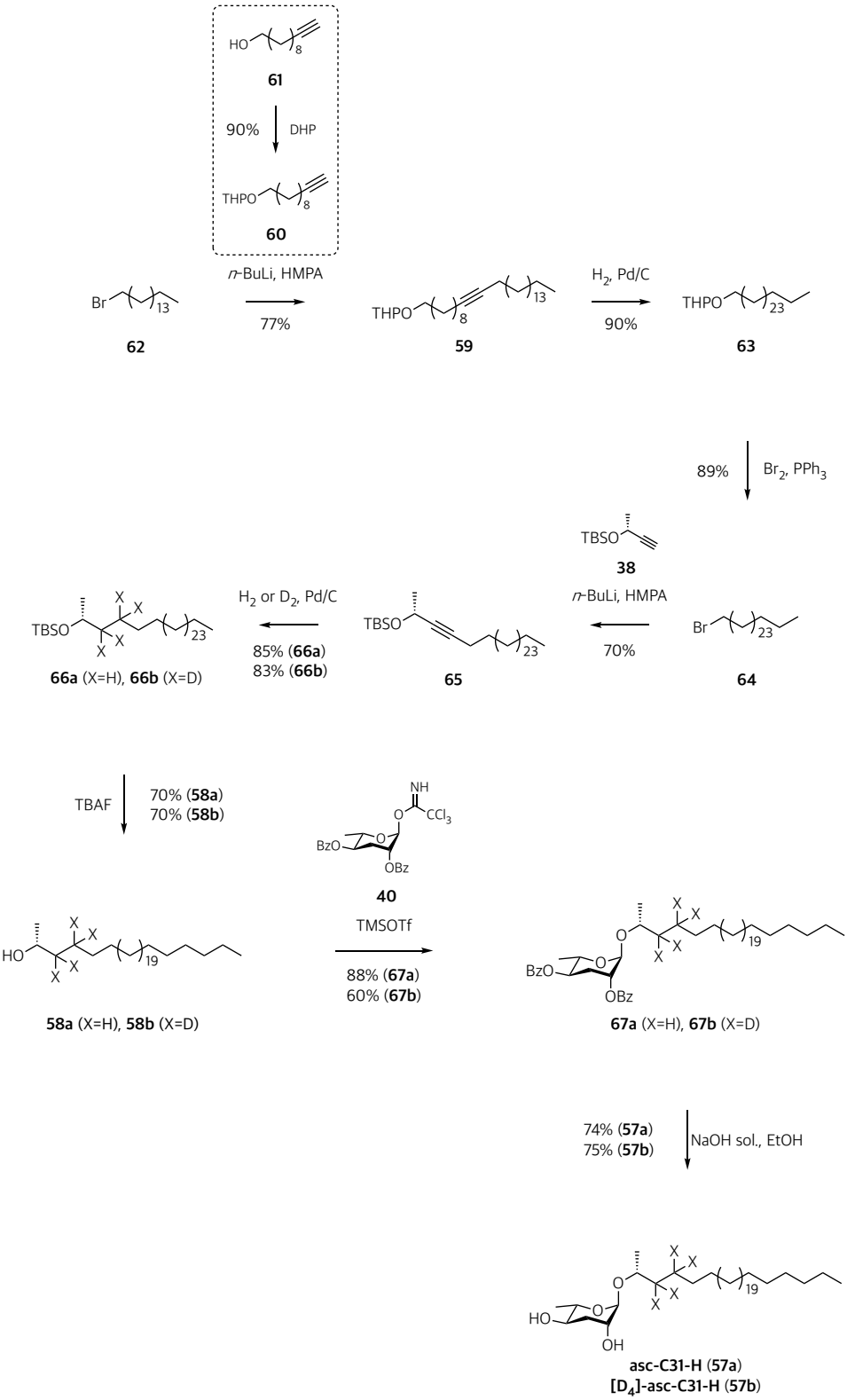

Figure 24. Synthesis of (2*R*,3*R*,5*R*,6*S*)-2-((*R*)-hentriacontan-2-yl)oxy)-6-methyltetrahydro-2*H*-pyran-3,5-diol (**asc-C31-H**, **57a**) or [D_4]-(2*R*,3*R*,5*R*,6*S*)-2-((*R*)-hentriacontan-2-yl)oxy)-6-methyltetrahydro-2*H*-pyran-3,5-diol (**[D_4]-asc-C31-H**, **57b**).

8.1.2.5 Synthesis of (2*S*,3*S*,5*S*,6*R*)-2-(henicosyloxy)-6-methyltetrahydro-2*H*-pyran-3,5-diol and [D_4]-(2*S*,3*S*,5*S*,6*R*)-2-(henicosyloxy)-6-methyltetrahydro-2*H*-pyran-3,5-diol

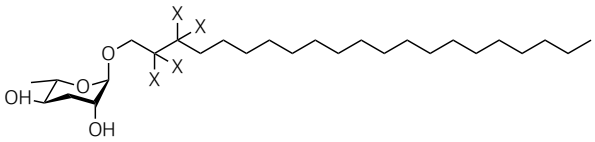

(2*S*,3*S*,5*S*,6*R*)-2-(henicosyloxy)-6-methyltetrahydro-2*H*-pyran-3,5-diol (X=H, **asc-ωC21-H**, **70a**)

[D_4]-(2*S*,3*S*,5*S*,6*R*)-2-(henicosyloxy)-6-methyltetrahydro-2*H*-pyran-3,5-diol (X=D, **[D_4]-asc-ωC21-H**, **70b**)

Figure 25. Structure of **asc-ωC21-H** (**68a**) and **[D_4]-asc-ωC21-H** (**68b**).

The synthesis of unlabeled (ω)-henicosanyl ascaroside (2*S*,3*S*,5*S*,6*R*)-2-(henicosyloxy)-6-methyltetrahydro-2*H*-pyran-3,5-diol (**asc-ωC21-H**, **68a**) was achieved by glycosylation of commercially available henicosan-1-ol (**69a**) with (2*S*,3*R*,5*R*,6*S*)-2-methyl-6-(2,2,2-trichloro-1-iminoethoxy)tetrahydro-2*H*-pyran-3,5-diyl dibenzoate (**40**) and further cleavage of the benzoyl groups (**70a**) with an excess of concentrated NaOH solution (Figure 26).

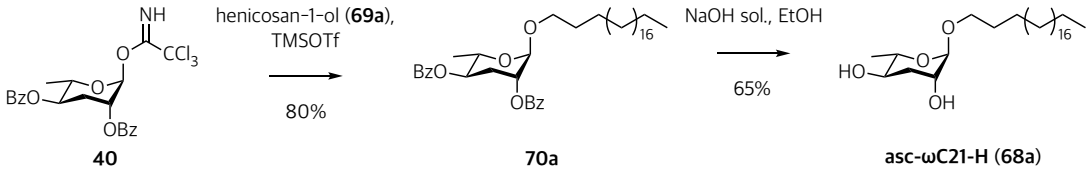

Figure 26. Synthesis of (2*S*,3*S*,5*S*,6*R*)-2-(henicosyloxy)-6-methyltetrahydro-2*H*-pyran-3,5-diol (**asc-ωC21-H**, **68a**).

The preparation of the deuterium labelled isotopomer [D_4]-(2*S*,3*S*,5*S*,6*R*)-2-(henicosyloxy)-6-methyltetrahydro-2*H*-pyran-3,5-diol (**[D_4]-asc-ωC21-H**, **68b**) required the development of a synthetic pathway for this specific aglycone. The synthesis of [D_4]-henicosan-1-ol (**69b**) (Figure 27) starts with commercially available prop-2-yn-1-ol (**71**) and *tert*-butyldimethylsilyl chloride for the protection of the hydroxy group and the generation of *tert*-butyldimethyl(prop-2-yn-1-yloxy)silane (**72**). The lithiated alkyne from **72** was further alkylated with 1-iodooctadecane (**73**) to obtain *tert*-butyl(henicos-2-yn-1-yloxy)dimethylsilane (**74**). Reduction of the triple bond of **74** with D_2 and Pd/C as catalyst, followed by the deprotection of [D_4]-*tert*-butyl(henicosyloxy)dimethylsilane (**75**) with an excess of tetra-*n*-butylammonium fluoride solution to yield the desired [D_4]-henicosan-1-ol (**69b**). Finally, the alcohol **70b** was glycosylated with the 2,4-benzoyl ascarylose trichloro acetimidate **40** to generate the benzoyl-ascaroside (**68b**), which was further deprotected with NaOH solution to obtain the [D_4]-(2*S*,3*S*,5*S*,6*R*)-2-(henicosyloxy)-6-methyltetrahydro-2*H*-pyran-3,5-diol (**[D_4]-asc-ωC21-H**, **70b**).

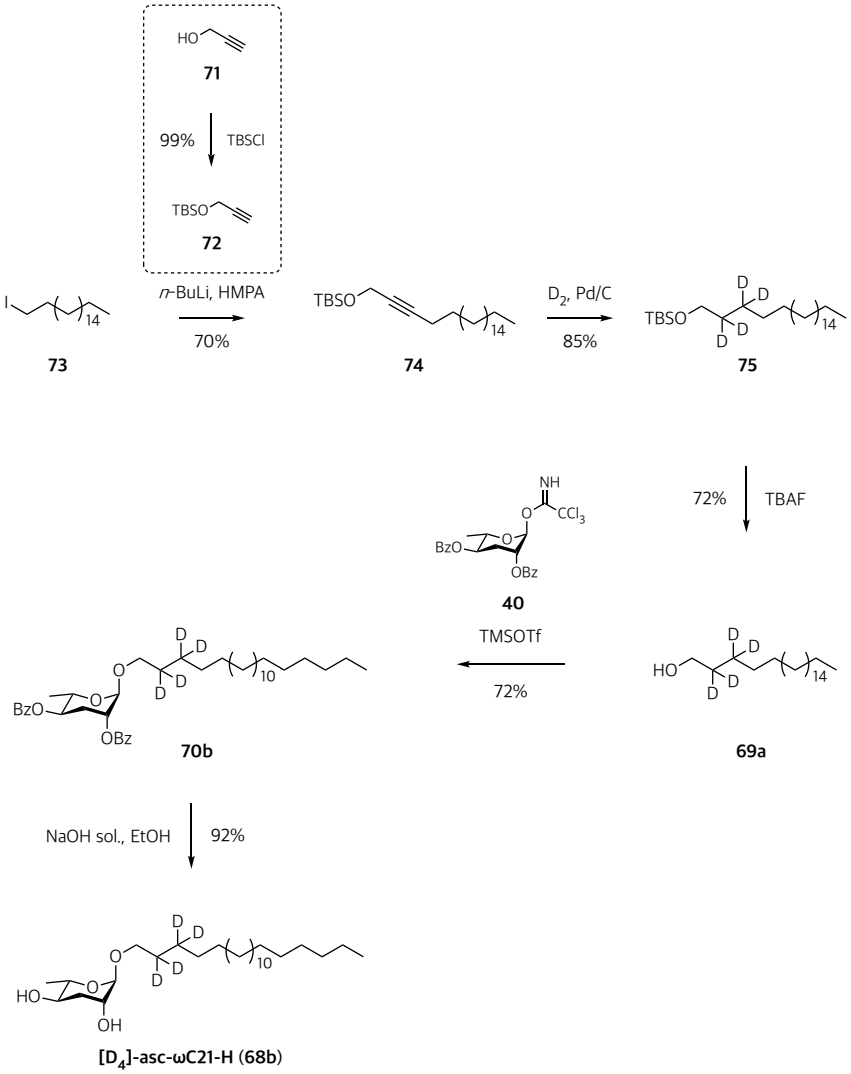

Figure 27. Synthesis of [D$_4$]-(2*S*,3*S*,5*S*,6*R*)-2-(henicosyloxy)-6-methyltetrahydro-2*H*-pyran-3,5-diol (**[D$_4$]-asc-ωC21-H**, **68b**).

8.1.2.6 Characterization of very long chain alkyl ascarosides

The previously described (ω)- and (ω-1)-alkyl ascarosides with sidechains of 21, 25, 26, and 31 carbons were characterized using 1D and 2D NMR, LC-MS, and GC-MS. NMR spectroscopy was employed to confirm key structural differences between ascarosides with (ω)- or (ω-1)-sidechains. Examples of characteristic signals observed in the ^{1}H NMR spectra of the four non-labelled alkyl ascarosides are shown in Figure 28. The ^{1}H NMR spectrum of the (ω)-linked (2*S*,3*S*,5*S*,6*R*)-2-(henicosyloxy)-6-methyltetrahydro-2*H*-pyran-3,5-diol (**asc-ωC21-H**, **68a**) displayed signals for the methylene protons at 3.43 ppm (2H, *dt*). Furthermore, in the spectra of **asc-ωC21-H** (**68a**) signals corresponding to methine protons located at the 1- and 2-positions of the ascarylose are shifted in comparison with the (ω-1)-ascarosides. In contrast, the ^{1}H NMR spectra of the (ω-1)-linked (2*S*,3*R*,5*R*,6*R*)-2-methyl-6-((*R*)-

pentacosan-2-yl)oxy)tetrahydro-2*H*-pyran-3,5-diol (**asc-C25-H**, **33a**), (2*S*,3*R*,5*R*,6*R*)-2-methyl-6-((*R*)-24-methylpentacosan-2-yl)oxy)tetrahydro-2*H*-pyran-3,5-diol (**asc-*i*C26-H**, **43a**) and (2*R*,3*R*,5*R*,6*S*)-2-((*R*)-hentriacontan-2-yl)oxy)-6-methyltetrahydro-2*H*-pyran-3,5-diol (**asc-C31-H**, **57a**) display signals for methyl protons corresponding to the ω-position at 1.12 ppm (3H, *d*, J=6.1 Hz). In addition, the signals corresponding to the anomeric proton at the 1-position of the ascarylose unit are shifted from 4.57 ppm (br *s*) in the ω-linked compound to 4.70 ppm in the (ω-1)-linked compounds.

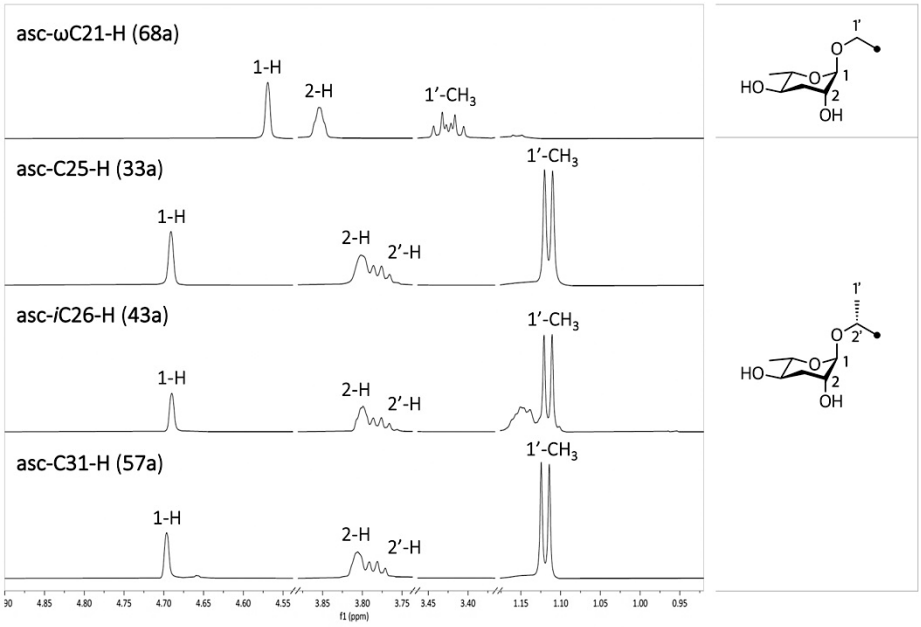

Figure 28. Comparison of ^{1}H NMR spectra of alkyl ascarosides showing signals corresponding to protons at the 1- and 2-positions of the sugar moiety and the ω-position of the sidechain.

GC-EIMS analyses of the synthesized very long chain alkyl ascarosides required TMS-derivatization with 2,2,2-trifluoro-*N*-methyl-*N*-(trimethylsilyl)acetamide (MSTFA). Previously reported analysis of EIMS fragmentation [(21) (60)] were used as templates for the characterization of the compounds. For example, TMS-derivatives of (2*S*,3*S*,5*S*,6*R*)-2-(henicosyloxy)-6-methyltetrahydro-2*H*-pyran-3,5-diol (**asc-ωC21-H**, **68a**) and (2*S*,3*R*,5*R*,6*R*)-2-methyl-6-((*R*)-pentacosan-2-yl)oxy)tetrahydro-2*H*-pyran-3,5-diol (**asc-C25-H**, **33a**) revealed signals corresponding to the ascarylose derived **K1**-fragment at *m/z* 130.1 $[C_6H_{14}Osi]^+$ and oxonium ion signals (**J1**) at [M-173] (Figure 29). **A1** fragment ions at *m/z* 275.2 corresponding to the ascarylose moiety $[C_{12}H_{27}O_3Si_2]^+$ were also obtained. Moreover, the **A2**-fragment at *m/z* 185.1 was observed as a minor signal but is not assigned in the MS spectrum shown in Figure 29. Contrasting to previously reported fragmentation for acyl ascarosides [(21)], the **J2**-fragment at [M-291]$^+$ could not be observed for the alkyl ascarosides. However, (ω-1)-alkyl ascarosides furnished a characteristic fragment ion signal at *m/z* 119.1 $[C_4H_{11}O_2Si]^+$ (**J3**) that could serve as a marker.

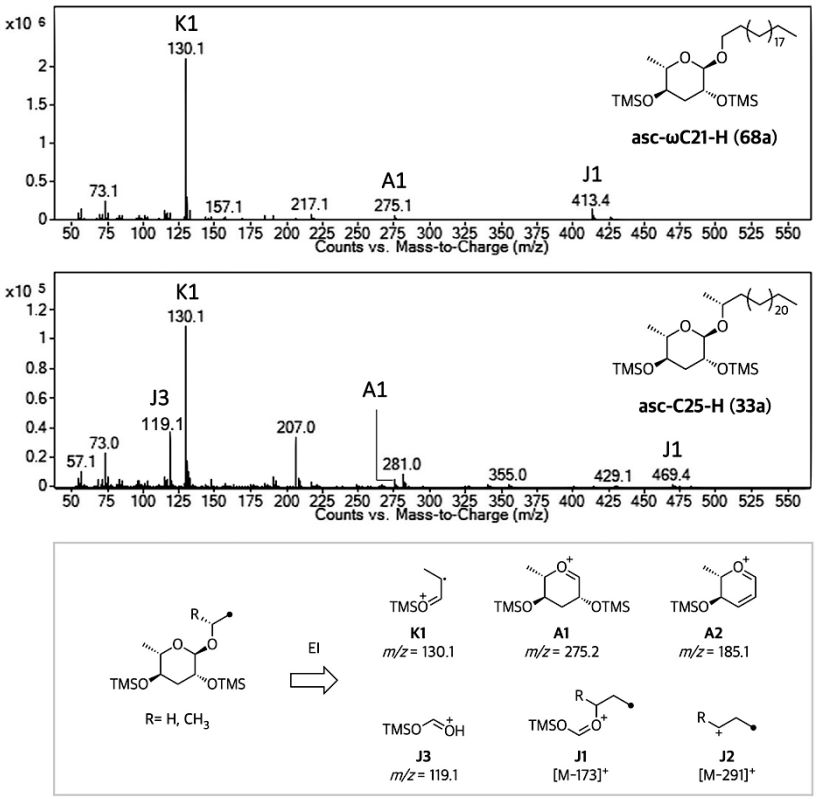

Figure 29. GC-MS spectra of TMS-derivatives of **asc-ωC21-H** (**68a**) and **asc-C25-H** (**33a**) showing the characteristic fragmentation of (ω)- and (ω-1)-ascarosides.

Finally, HPLC-MS analysis of the alkyl ascarosides has been used to investigate their characteristic ionization. Previous studies have reported the analysis of a wide range of acyl ascarosides with various head groups by ESI-(-) and ESI-(+)-MS [17] [22] [61]. However, ascarosides with very long 2-hydroxyalkyl sidechains up to 33 carbons have been reported to be better detected by GC-MS in comparison to LC-ESI-MS [21]. Two different ionization sources, Electrospray Ionization (ESI) and Atmospheric Pressure Chemical Ionization (APCI) in positive and negative modes, were used to characterize the synthetic very long chain alkyl ascarosides. LC-ESI-(+)-MS detected the VLCA series as ammonium adducts $[M+NH_4]^+$ but exhibited only poor ionization due to the very lipophilic sidechains. Furthermore, ESI-(-) failed to ionize the VLCAs as expected. Therefore, the poor ionization of standards with EIS-MS methods could explain why the alkyl ascarosides have not yet been detected in *C. elegans* and other related nematodes. Nevertheless, APCI in negative-ion mode with methanol as mobile phase at 80°C produced $[M+O_2]^-$ adducts of all synthetic VLCAs with excellent sensitivity. The use of APCI-MS as an ionization method for the analysis of VLCAs has not been reported. Table 1 provides the data of the synthetic very long chain alkyl ascarosides by LC-APCI-(-)-MS.

Table 1. LC-APCI-(-)-MS data of the very long chain alkyl ascaroside standards.

Ascaroside	Detected molecular formula	*m/z* $[M+O_2]^-$ (cal.)	*m/z* $[M+O_2]^-$ (obs.)	Retention time (min)
asc-ωC21-H (**68a**)	$C_{27}H_{54}O_6$	474.3926	474.3917	13.74
asc-C25-H (**33a**)	$C_{31}H_{62}O_6$	530.4552	530.4558	15.83
asc-*i*C26-H (**43a**)	$C_{32}H_{64}O_6$	544.4708	544.4702	16.15
asc-C31-H (**57a**)	$C_{37}H_{74}O_6$	614.5491	614.5477	18.29

8.1.2.7 Synthesis and characterization of diacetyl alkyl ascarosides

Using the synthetic alkyl ascarosides: (2*S*,3*S*,5*S*,6*R*)-2-(henicosyloxy)-6-methyltetrahydro-2*H*-pyran-3,5-diol (**asc-ωC21-H**, **68a**), (2*S*,3*R*,5*R*,6*R*)-2-methyl-6-(((*R*)-pentacosan-2-yl)oxy)tetrahydro-2*H*-pyran-3,5-diol (**asc-C25-H**, **33a**), (2*S*,3*R*,5*R*,6*R*)-2-methyl-6-(((*R*)-24-methylpentacosan-2-yl)oxy)tetrahydro-2*H*-pyran-3,5-diol (**asc-*i*C26-H**, **43a**) and (2*R*,3*R*,5*R*,6*S*)-2-(((*R*)-hentriacontan-2-yl)oxy)-6-methyltetrahydro-2*H*-pyran-3,5-diol (**asc-C31-H**, **57a**), acetyl derivatives were prepared to serve as authentic standards. The acetylation of the alkyl ascarosides employed an identical procedure for all the (ω)- and (ω-1)-linked components. The synthesis of the 2,4-diacetyl ascarosides started with the reaction of the very long chain alkyl ascarosides with an excess of 4-dimethylaminopyridine and acetic anhydride (Figure 30).

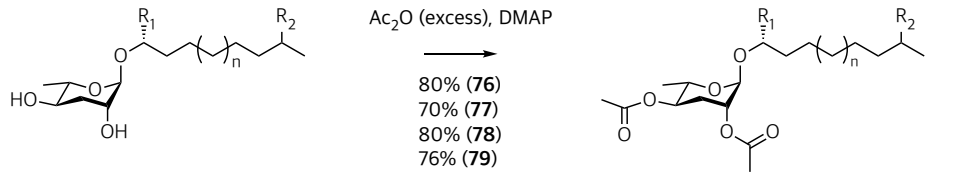

	n	R_1	R_2
asc-ωC21-H (68a)	14	H	H
asc-C25-H (33a)	17	CH_3	H
asc-*i*C26-H (43a)	18	CH_3	CH_3
asc-C31-H (57a)	23	CH_3	H

	n	R_1	R_2
Ac2-asc-ωC21-H (76)	14	H	H
Ac2-asc-C25-H (77)	17	CH_3	H
Ac2-asc-*i*C26-H (78)	18	CH_3	CH_3
Ac2-asc-C31-H (79)	23	CH_3	H

Figure 30. Synthesis of 2,4-diacetyl alkyl ascarosides: (2*R*,3*R*,5*R*,6*S*)-2-(henicosyloxy)-6-methyltetrahydro-2*H*-pyran-3,5-diyl diacetate (**Ac2-asc-ωC21-H**, **76**), (2*S*,3*R*,5*R*,6*R*)-2-methyl-6-(((*R*)-pentacosan-2-yl)oxy)tetrahydro-2*H*-pyran-3,5-diyl (**Ac2-asc-C25-H**, **77**), (2*S*,3*R*,5*R*,6*R*)-2-methyl-6-(((*R*)-24-methylpentacosan-2-yl)oxy)tetrahydro-2*H*-pyran-3,5-diyl diacetate (**Ac2-asc-*i*C26-H**, **78**) and

(2*R*,3*R*,5*R*,6*S*)-2-(((*R*)-hentriacontan-2-yl)oxy)-6-methyltetrahydro-2*H*-pyran-3,5-diyl diacetate (**Ac2-asc-C31-H**, **79**).

Products were characterized by a combination of 1D and 2D NMR spectroscopy, LC-MS, and GC-MS. Data obtained from GC-MS and LC-MS analyses are discussed below.

The GC-MS spectrum of (2*S*,3*R*,5*R*,6*R*)-2-methyl-6-(((*R*)-pentacosan-2-yl)oxy)tetrahydro-2*H*-pyran-3,5-diyl (**Ac2-asc-C25-H**, **77**) is used as an example for fragmentation of the diacetyl ascarosides (Figure 31). The MS spectrum displays an intense signal at *m/z* 215.1 (**A1**-fragment) corresponding to the oxonium ion $[C_{10}H_{15}O_5]^+$, as well as a signal at *m/z* 452.5 $[M\text{-}130]^{+\bullet}$ (**H1**-fragment) corresponding to the partial fragmentation of the sugar moiety. Furthermore, **H2**-fragments at $[M\text{-}231]^+$ were observed for (ω-1)-alkyl ascarosides but not for (ω)-alkyl ascarosides. In the example below, the fragment **H2** is shown at *m/z* 351.4 $[C_{25}H_{51}]^+$.

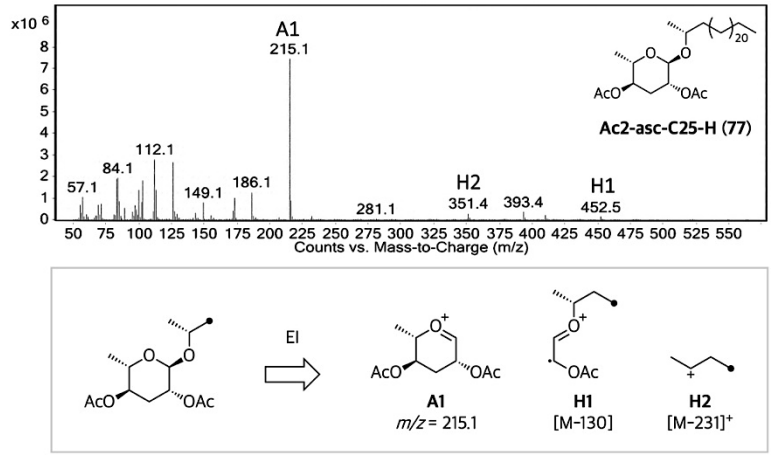

Figure 31. Assignments of EIMS fragment ions from the 2,4-diacetyl ascarosides with (2*S*,3*R*,5*R*,6*R*)-2-methyl-6-(((*R*)-pentacosan-2-yl)oxy)tetrahydro-2*H*-pyran-3,5-diyl (**Ac2-asc-C25-H**, **77**) as an example.

LC-MS screening of the 2,4-diacetyl ascarosides standards with LC-ESI-(+)-MS and LC-APCI-(-)-MS was possible. APCI was deemed the most sensitive technique. Data obtained for the 2,4-diacetyl ascarosides with the APCI-(-) ion source are compiled in Table 2.

Table 2. LC-APC(-)-MS data were achieved for the diacetyl ascarosides.

Ascaroside	Detected molecular formula	*m/z* $[M+O_2]^-$ (cal.)	*m/z* $[M+O_2]^-$ (obs.)	Retention time (min)
Ac2-asc-ωC21-H (**76**)	$C_{31}H_{58}O_8$	544.4572	544.4576	15.29
Ac2-asc-C25-H (**77**)	$C_{35}H_{66}O_8$	600.5198	600.5204	17.90
Ac2-asc-*i*C26-H (**78**)	$C_{36}H_{68}O_8$	614.5354	614.5349	18.29
Ac2-asc-C31-H (**79**)	$C_{41}H_{78}O_8$	684.6137	684.6144	20.88

8.1.2.8 Synthesis and characterization of monoacetyl alkyl ascarosides

Monoacetyl-ascarosides were prepared by two complementary methodologies: partial acetylation and partial deacetylation. Partial acetylation of the alkyl ascarosides (2*S*,3*S*,5*S*,6*R*)-2-(henicosyloxy)-6-methyltetrahydro-2*H*-pyran-3,5-diol (**asc-ωC21-H**, **68a**), (2*S*,3*R*,5*R*,6*R*)-2-methyl-6-(((*R*)-pentacosan-2-yl)oxy)tetrahydro-2*H*-pyran-3,5-diol (**asc-C25-H**, **33a**) and (2*S*,3*R*,5*R*,6*R*)-2-methyl-6-(((*R*)-24-methylpentacosan-2-yl)oxy)tetrahydro-2*H*-pyran-3,5-diol (**asc-*i*C26-H**, **43a**) were achieved by using near stoichiometric quantities of acetic anhydride (0.8 equivalents) and 4-dimethylaminopyridine (1.1 equivalents) (Figure 32). However, this methodology resulted in a mixture of unreacted starting material along with fully 2,4-diacetylated and 2- and 4-monoacetylated derivatives, of which the 4-acetylated compound was the major product.

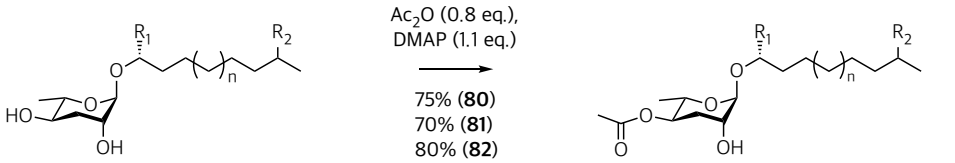

	n	R_1	R_2
asc-ωC21-H (68a)	14	H	H
asc-C25-H (33a)	17	CH_3	H
asc-*i*C26-H (43a)	18	CH_3	CH_3

	n	R_1	R_2
4-Ac-asc-ωC21-H (80)	14	H	H
4-Ac-asc-C25-H (81)	17	CH_3	H
4-Ac-asc-*i*C26-H (82)	18	CH_3	CH_3

Figure 32. Synthesis of the 4-acetyl alkyl ascarosides: (2*S*,3*R*,5*R*,6*R*)-6-(henicosyloxy)-5-hydroxy-2-methyltetrahydro-2*H*-pyran-3-yl acetate (**4-Ac-asc-ωC21-H**, **80**), (2*S*,3*R*,5*R*,6*R*)-5-hydroxy-2-methyl-6-(((*R*)-pentacosan-2-yl)oxy)tetrahydro-2*H*-pyran-3-yl acetate (**4-Ac-asc-C25-H**, **81**) and (2*S*,3*R*,5*R*,6*R*)-5-hydroxy-2-methyl-6-(((*R*)-24-methylpentacosan-2-yl)oxy)tetrahydro-2*H*-pyran-3-yl acetate (**4-Ac-asc-*i*C26-H**, **82**).

Comparative analyses of the ^{1}H NMR spectra of (2*S*,3*R*,5*R*,6*R*)-2-methyl-6-(((*R*)-pentacosan-2-yl)oxy)tetrahydro-2*H*-pyran-3,5-diol (**asc-C25-H**, **68a**), (2*S*,3*R*,5*R*,6*R*)-2-methyl-6-(((*R*)-pentacosan-2-yl)oxy)tetrahydro-2*H*-pyran-3,5-diyl diacetate (**Ac2-asc-C25-H**, **77**) and (2*S*, 3*R*,5*R*,6*R*)-5-hydroxy-2-methyl-6-(((*R*)-pentacosan-2-yl)oxy)tetrahydro-2*H*-pyran-3-yl acetate (**4-Ac-asc-C25-H**, **81**) enabled the assignment of 2- and 4-monoacetylated derivatives (Figure 33). Distinct signals for the anomeric 1-H could be observed. Considering the dominating signals for the CH-OAc methine proton with *ddd* multiplicity, the **4-Ac-asc-C25-H** (**81**) was identified as the dominant monoacetylated component in the mixture.

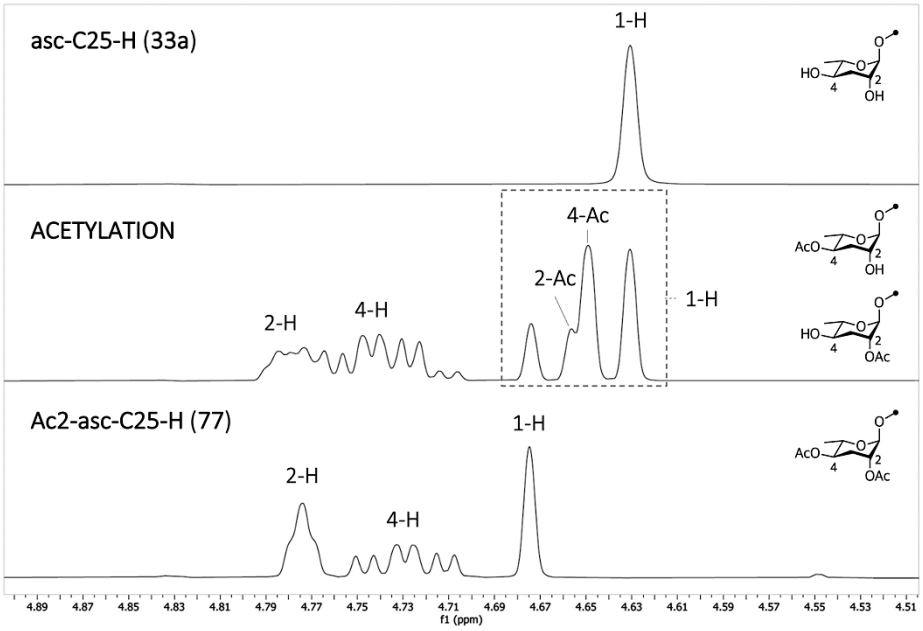

Figure 33. Comparative ^{1}H NMR analyses of **asc-C25-H** (**33a**), **Ac2-asc-C25-H** (**77**), and the mixture of partially acetylated components.

Since the acetylation generates a mixture of compounds, a different methodology for the synthesis of the monoacetyl-ascaroside with the sidechain of 31 carbons was explored. Partial deacetylation of fully acetylated (2*R*,3*R*,5*R*,6*S*)-2-(((*R*)-hentriacontan-2-yl)oxy)-6-methyltetrahydro-2*H*-pyran-3,5-diyl diacetate (**Ac2-asc-C31-H**, **79**) dissolved in DCM-MeOH (1:1) with sodium methoxide solution generated the 4-monoacetylated product (Figure 34). Although a mixture of compounds was obtained, the quantity of (2*S*,3*R*,5*R*,6*R*)-6-(((*R*)-hentriacontan-2-yl)oxy)-5-hydroxy-2-methyltetrahydro-2*H*-pyran-3-yl acetate (**4-Ac-asc-C31-H**, **83**) was considerably higher in comparison with the partial acetylation procedure.

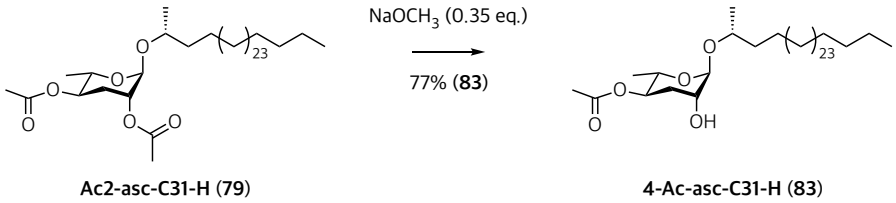

Figure 34. Synthesis of (2*S*,3*R*,5*R*,6*R*)-6-(((*R*)-hentriacontan-2-yl)oxy)-5-hydroxy-2-methyltetrahydro-2*H*-pyran-3-yl acetate (**4-Ac-asc-C31-H**, **83**) by partial deacetylation.

A comparison of the performance of the two reaction procedures based on the NMR data is shown in Figure 35. ^{1}H NMR spectra of synthetic mixtures obtained from partial acetylation and partial deacetylation of (2*S*,3*R*,5*R*,6*R*)-2-methyl-6-(((*R*)-pentacosan-2-yl)oxy)tetrahydro-2*H*-pyran-3,5-diol (**asc-C25-H**, **33a**) and (2*R*,3*R*,5*R*,6*S*)-2-(((*R*)-hentriacontan-2-yl)oxy)-6-methyltetrahydro-2*H*-pyran-3,5-diyl diacetate (**Ac2-asc-C31-H**, **79**) are presented. The signal of the anomeric 1-H corresponding to the 4-acetyl ascaroside is dominant in both mixtures, demonstrating that the axial 2-acetyl ester is preferably hydrolyzed. However, the partial deacetylation showed a higher preference for the 4-*O*-acetylated derivative in comparison to all the other products of the mixture.

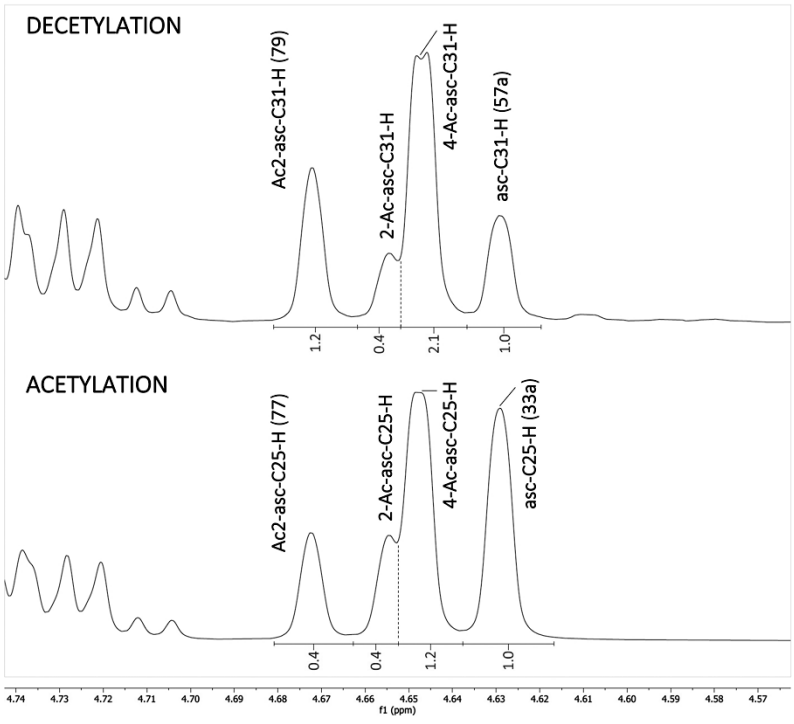

Figure 35. Comparative ^{1}H NMR analysis of partially acetylated ascarosides obtained by deacetylation or acetylation. Integrals are based on the anomeric 1-H of the ascarylose unit and normalized from the signals of the nonacetylated (**asc-C25-H**, **33a**) and (**asc-C31-H**, **57a**).

The chromatographic purification of the monoacetylated ascarosides was not attempted. The individual products were characterized within the mixtures by 1D and 2D NMR, LC-MS, and GC-MS. The NMR data of the monoacetyl-ascarosides is not going to be described in this section, but data from the GC-MS and LC-MS analyses are discussed below.

Due to the limited volatility of the monoacetyl alkyl ascarosides, their analyses by GC-MS required the preparation of TMS-derivatives. Specific fragmentation patterns depending on the position of the acetyl substituent (2- or 4-position) were observed, which are described in the examples shown in Figure 36. The (2*S*,3*R*,5*R*,6*R*)-5-hydroxy-2-methyl-6-(((*R*)-pentacosan-2-yl)oxy)tetrahydro-2*H*-pyran-3-yl acetate (**4-Ac-asc-C25-H**, **81**) and (2*R*, 3*R*,5*R*,6*S*)-5-hydroxy-6-methyl-2-(((*R*)-pentacosan-2-yl)oxy)tetrahydro-2*H*-pyran-3-yl acetate (**2-Ac-asc-C25-H**, **84**) share a common fragment ion corresponding to the ascarylose unit at *m/z* 245.1 (**A1**). Both alkyl ascarosides, 2- and 4-acetylated, show characteristic fragments at *m/z* $[M-173]^+$ (**J1**), *m/z* [M-291] (**J2**) and *m/z* 119.1 (**J3**) from the loss of the sugar unit. Furthermore, **2-Ac-asc-C25-H** (**84**) showed an intense **K1**-fragment ion at *m/z* 130.1 $[C_6H_{14}OSi]^+$, whereas **4-Ac-asc-C25-H** (**81**) displayed characteristic fragments at *m/z* 161.1 $[C_6H_{13}O_3Si]^+$ and *m/z* 185.1 $[C_9H_{17}O_2Si]^+$.

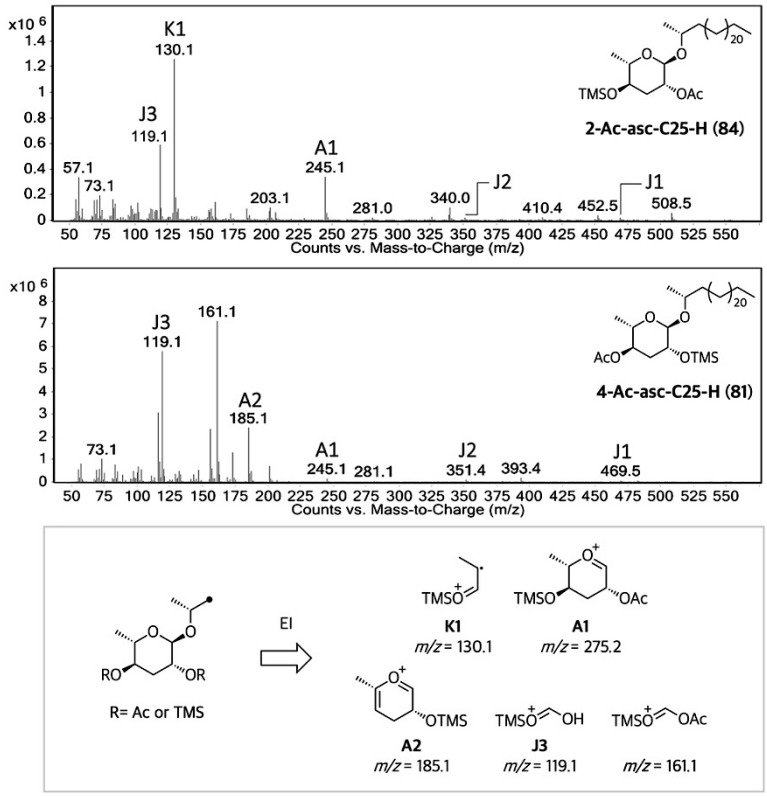

Figure 36. EIMS fragmentation observed for **2-Ac-asc-C25-H** (**84**) and **4-Ac-asc-C25-H** (**81**).

Furthermore, monoacetyl alkyl ascarosides were analyzed by LC-ESI-(+)-MS and LC-APCI-(-)-MS with satisfactory results. In Table 3, data for the identification of the monoacetyl-ascarosides by APCI(-)-MS are shown. These results are comparable to the nonacetylated alkyl ascarosides (Table 3) that only ionize by APCI-(-).

Table 3. LC-APC(-)-MS data for the monoacetyl alkyl ascarosides.

Ascaroside	Detected molecular formula	*m/z* $[M+O_2]^-$ (cal.)	*m/z* $[M+O_2]^-$ (obs.)	Retention time (min)
2-Ac-asc-ωC21-H (**84**)	$C_{29}H_{56}O_7$	516.4032	516.4016	14.62
4-Ac-asc-ωC21-H (**80**)	$C_{29}H_{56}O_7$	516.4032	516.4025	15.20
2-Ac-asc-C25-H	$C_{33}H_{64}O_7$	572.4658	572.4640	16.49
2-Ac-asc-*i*C26-H	$C_{34}H_{66}O_7$	586.4814	586.4818	16.79
4-Ac-asc-C25-H (**81**)	$C_{33}H_{64}O_7$	572.4658	572.4662	16.94
4-Ac-asc-*i*C26-H (**82**)	$C_{34}H_{66}O_7$	586.4814	586.4802	17.23
2-Ac-asc-C31-H	$C_{39}H_{76}O_7$	614.5491	ND	ND
4-Ac-asc-C31-H (**83**)	$C_{39}H_{76}O_7$	614.5491	614.5497	18.28

ND: not detected due to low concentration

8.1.1 Very long chain alkyl ascarosides in nematodes

8.1.1.1 Comparison of very long chain alkyl ascarosides standards with the *daf-22* exometabolome

The identification of targeted compounds in the *daf-22* exometabolome required the cultivation of worms in liquid cultures. The wide diversity and low concentration of very long chain ascarosides in the extracts required fractionation of the samples to enrich the target compounds and facilitate their detection. Consequently, the exometabolome was separated by Solid Phase Extraction (SPE) on reverse phase C18 cartridges using mixtures of water/methanol as eluent. Subsequently, very long chain alkyl ascarosides were detected by GC-EIMS and LC-APCI-(-)-MS analyses.

Comparatives GC-MS analysis of TMS-derivatives of *daf-22* SPE-fractions and the authentic standards enabled the identification of (2*S*,3*S*,5*S*,6*R*)-2-(henicosyloxy)-6-methyltetrahydro-2*H*-pyran-3,5-diol

(**asc-ωC21-H**, **68a**), (2*S*,3*R*,5*R*,6*R*)-2-methyl-6-(((*R*)-pentacosan-2-yl)oxy)tetrahydro-2*H*-pyran-3,5-diol (**asc-C25-H**, **33a**) and (2*S*,3*R*,5*R*,6*R*)-2-methyl-6-(((*R*)-24-methylpentacosan-2-yl)oxy)tetrahydro-2*H*-pyran-3,5-diol (**asc-*i*C26-H**, **43a**), as it was hypothesized by Dolke and von Reuss (Figure 11). In parallel and with the use of the authentic standards, (2*S*,3*R*,5*R*,6*R*)-5-hydroxy-2-methyl-6-(((*R*)-pentacosan-2-yl)oxy)tetrahydro-2*H*-pyran-3-yl acetate (**4-Ac-asc-C25-H**, **81**) and (2*S*,3*R*,5*R*,6*R*)-5-hydroxy-2-methyl-6-(((*R*)-24-methylpentacosan-2-yl)oxy)tetrahydro-2*H*-pyran-3-yl acetate (**4-Ac-asc-*i*C26-H**, **82**) were identified as well. However, (2*S*,3*R*,5*R*,6*R*)-6-(henicosyloxy)-5-hydroxy-2-methyltetrahydro-2*H*-pyran-3-yl acetate (**4-Ac-asc-ωC21-H**, **80**), (2*R*,3*R*,5*R*,6*S*)-2-(((*R*)-hentriacontan-2-yl)oxy)-6-methyltetrahydro-2*H*-pyran-3,5-diol (**asc-C31-H**, **57a**) and (2*S*,3*R*,5*R*,6*R*)-6-(((*R*)-hentriacontan-2-yl)oxy)-5-hydroxy-2-methyltetrahydro-2*H*-pyran-3-yl acetate (**4-Ac-asc-C31-H**, **83**), and their diacetyl-derivatives could not be detected in any of the enriched natural product fractions. An example of these results is illustrated in Figure 37. Identical MS spectra of the authentic standard (2*S*,3*R*,5*R*,6*R*)-5-hydroxy-2-methyl-6-(((*R*)-24-methylpentacosan-2-yl)oxy)tetrahydro-2*H*-pyran-3-yl acetate (**4-Ac-asc-*i*C26-H**, **82**) and the natural product confirmed the structural assignment.

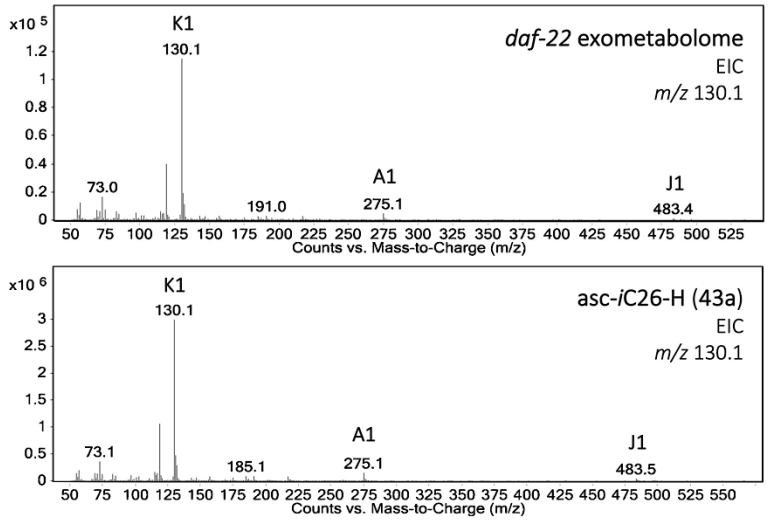

Figure 37. EIMS spectra of the synthetic standard **asc-*i*C26-H** (**43a**) and the natural product from *C. elegans*.

Figure 38 illustrates the results of the very long chain alkyl ascaroside identification by GC-MS. Comparative analyses of extracted ion chromatograms for *m/z* 130.1 $[C_6H_{14}OSi]^+$ and *m/z* 161.1 $[C_6H_{13}O_3Si]^+$ for non-acetylated and 4-acetyl ascarosides confirmed the presence of **asc-ωC21-H** (**68a**), **asc-C25-H** (**33a**), **asc-*i*C26-H** (**43a**), **4-Ac-asc-C25-H** (**81**), and **4-Ac-asc-*i*C26-H** (**82**) in the exometabolome extract. Furthermore, a homologous series of very long chain ascarosides, 4-acetylated and non-acetylated, could be identified in *daf-22* lipophilic fractions by EIMS screening.

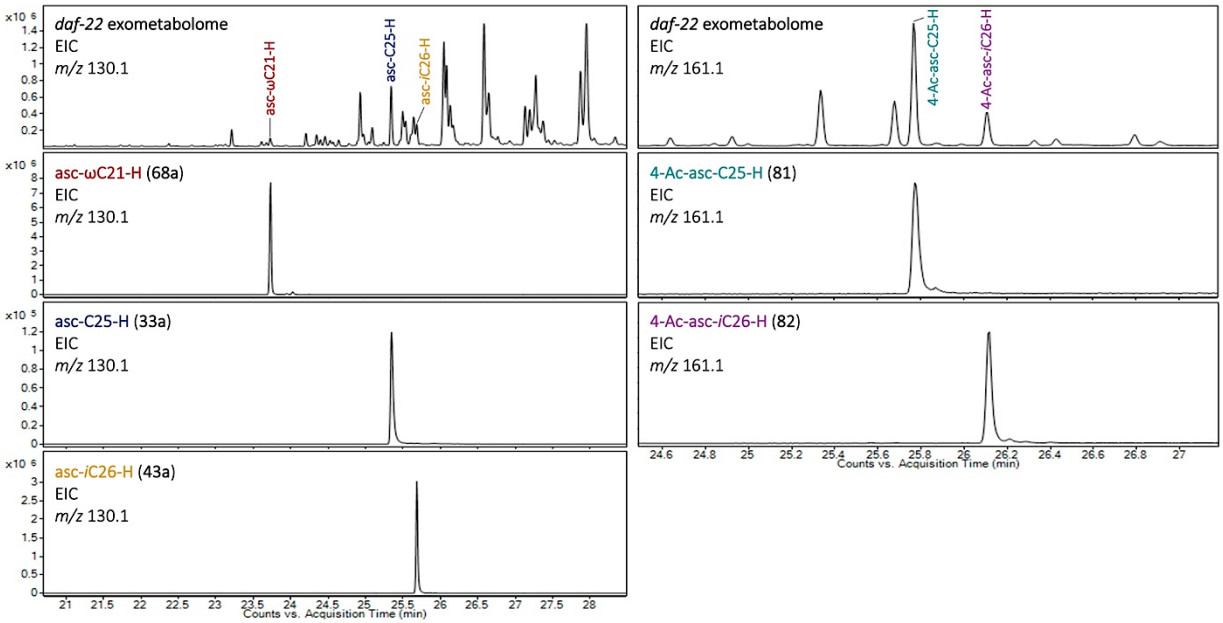

Figure 38. Identification of **asc-ωC21-H** (**68a**), **asc-C25-H** (**33a**), **asc-*i*C26-H** (**43a**), **4-Ac-asc-C25-H** (**81**), and **4-Ac-asc-*i*C26-H** (**82**) in the *daf-22* exometabolome by GC-MS analysis.

The authentic standards of **asc-ωC21-H** (**68a**), **asc-C25-H** (**33a**), **asc-*i*C26-H** (**43a**), **4-Ac-asc-C25-H** (**81**) and **4-Ac-asc-*i*C26-H** (**82**) were also used for identification of the natural products in the *daf-22* exometabolome by LC-APCI-(-)-MS. Moreover, the targeted screening for **asc-C31-H** (**57a**), **4-Ac-asc-ωC21-H** (**80**), **4-Ac-asc-C31-H** (**83**) and all diacetyl-derivatives in the exometabolome did not reveal any candidate peaks, as it was previously observed by GC-MS analysis. The comparison of LC-APCI-(-)-MS data between the natural products and the authentic standards is summarized in Figure 39.

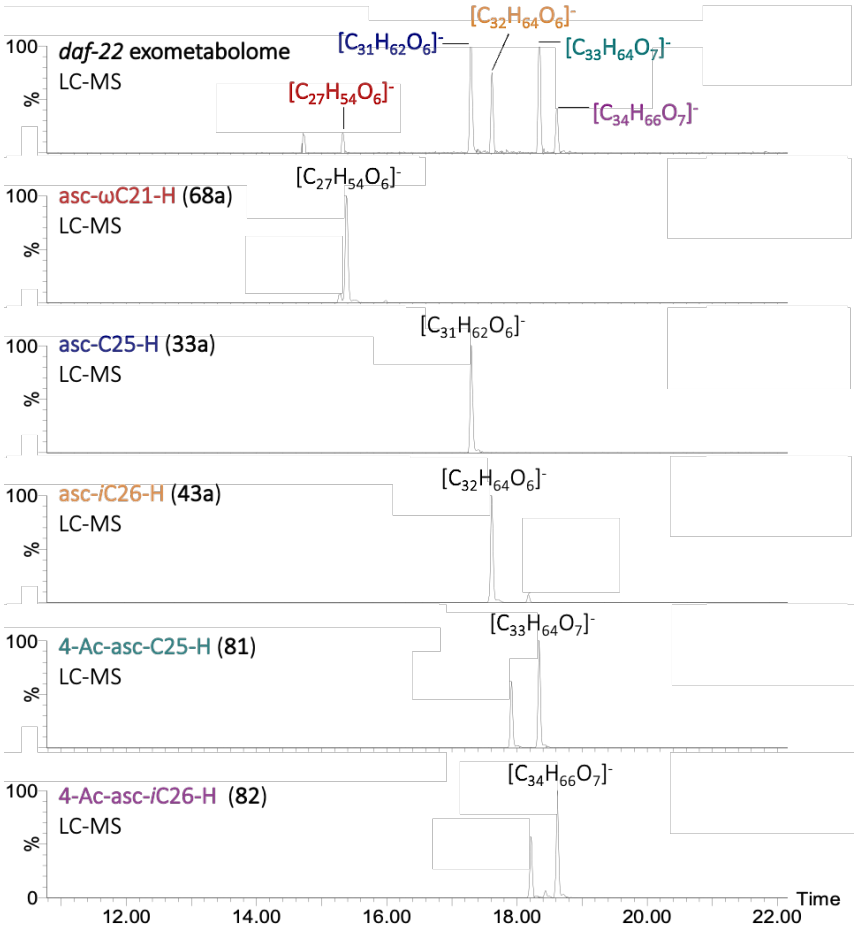

Figure 39. Identification of **asc-ωC21-H** (**68a**), **asc-C25-H** (**33a**), **asc-*i*C26-H** (**43a**), **4-Ac-asc-C25-H** (**81**), and **4-Ac-asc-*i*C26-H** (**82**) in the *C. elegans* exometabolome by LC-APCI-(-)-MS analysis.

8.1.1.2 Biosynthesis of *iso*-branched ascarosides in *C. elegans*

The *iso*-branched ascarosides (2*S*,3*R*,5*R*,6*R*)-2-methyl-6-(((*R*)-24-methylpentacosan-2-yl)oxy)tetrahydro-2*H*-pyran-3,5-diol (**asc-*i*C26-H**, **43a**) and (2*S*,3*R*,5*R*,6*R*)-5-hydroxy-2-methyl-6-(((*R*)-24-methylpentacosan-2-yl)oxy)tetrahydro-2*H*-pyran-3-yl acetate (**4-Ac-asc-*i*C26-H**, **82**) were unequivocally detected in the *daf-22* exometabolome. Based on these results, a hypothesis that involves *iso*-fatty acids as building blocks for the biosynthesis of *iso*-branched aglycones in *C. elegans* has been developed.

In bacteria, for example, the biosynthesis of monomethyl branched-chain fatty acids (mmBCFA) uses short-chain *iso*-acyl-CoA precursors, for which malonyl-CoA acts as the chain extender [62] [40]. The biosynthesis of odd-numbered mmBCFA like 13-methyltetradecanoic acid (*iso*C15, **15a**) and 15-methylhexadecanoic acid (*iso*C17, **17a**) is known to require isovaleric acid, which is derived from L-leucine (**14**, Figure 10). Moreover, the biosynthesis of odd-numbered *anteiso*-mmBCFA employs 2-

methylbutyric acid derived from L-isoleucine, and the biosynthesis of even-numbered *iso*-mmBCFA requires isobutyric acid with L-valine as a precursor [63]. In a similar way as in bacteria, the branched-chain amino acid (BCAA) degradation in *C. elegans* generates precursors for the mmBCFA biosynthesis [17] [40]. Therefore, the potential implication of *iso*-fatty acids in the biosynthesis of **asc-*i*C26-H** (**43a**) and **4-Ac-asc-*i*C26-H** (**82**) was investigated.

Auxotrophic *E. coli Δleu Δile Δval* mutant defective in the biosynthesis (*ΔilvD, ΔleuB, ΔavtA, ΔilvE*) and metabolism (*ΔavtA, ΔilvE*) of branched chain amino acids was grown in a medium containing either a 1:1 mixture of [U-^{13}C]- and [U-^{12}C]-isotopomers of L-leucine (**14**) or L-valine. With this bacterium, *daf-22* worms were cultivated for 6 days. The lipid fraction of worm bodies was extracted and analyzed by LC-ESI-(+)-MS. [$^{13}C_5$]-Enriched *iso*-alkyl ascarosides such as **asc-*i*C26-H** (**43a**) and **4-Ac-asc-*i*C26-H** (**82**) were detected upon feeding with [U-$^{13}C_6$]-leucine but not with [U-$^{13}C_5$]-valine. The occurrence of [$^{13}C_5$]-labelled *iso*-alkyl ascarosides and their 4-acetylated derivatives confirms that *iso*-branching depends on L-leucine (**14**) as a biosynthetic precursor. Figure 40 shows an example for the [$^{13}C_5$]-enrichment of **4-Ac-asc-*i*C26-H** (**82**) upon feeding with [U-$^{13}C_6$]-leucine, whereas no ^{13}C-enrichment was observed when [U-$^{13}C_5$]-valine was used.

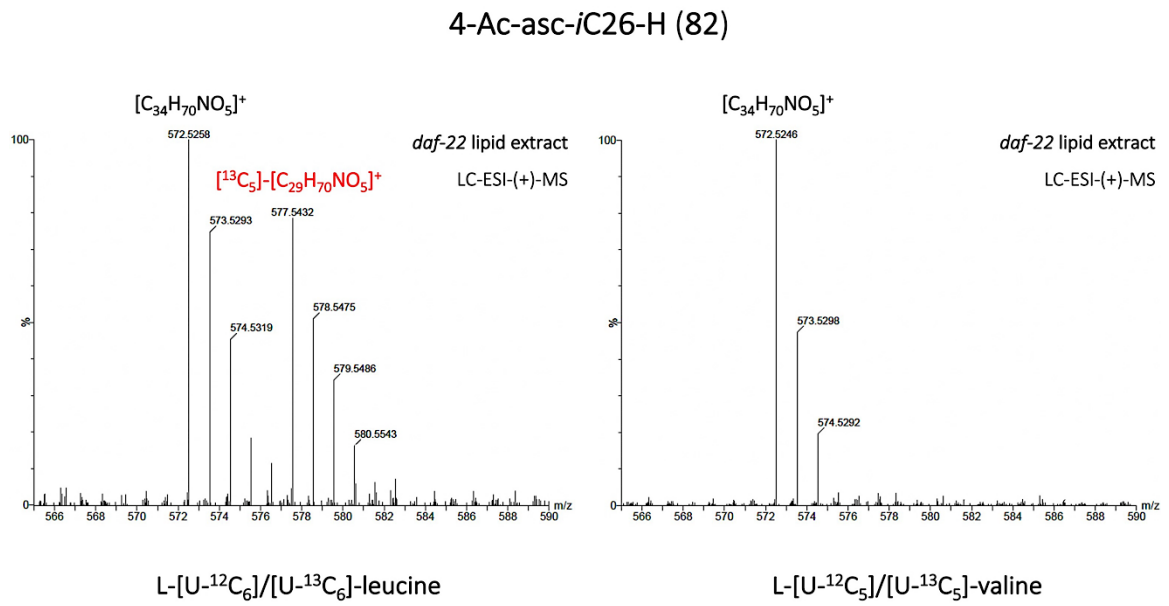

Figure 40. LC-ESI-(+)-MS of isotopic pattern of **4-Ac-asc-*i*C26-H** (**82**) from *daf-22* exometabolome extracts upon cultivation with *E. coli* enriched with a 1:1 mixture of [U-^{13}C] and [U-^{12}C] L-leucine or L-valine. $[M+NH_4]^+$ adducts are represented.

According to previous investigations, *C. elegans* produces mmBCFA *de novo* [24] [64]. Furthermore, it has been proven that the *C. elegans elo-5(gk208)* mutant carries a defect in the *elo-5* elongase gene

responsible for the elongation of 11-methyldodecanoic acid (*iso*C13, **16a**) to 13-methyltetradecanoic acid (*iso*C15, **15a**) and subsequently to 15-methylhexadecanoic acid (*iso*C17, **17a**) [36] [37]. However, the involvement of mmBCFAs as precursors for *iso*-alkyl ascarosides has not been demonstrated yet. To determine if the peroxisomal β-oxidation process acts in the production of *iso*-alkyl ascarosides with mmBCFAs as building blocks, the *C. elegans elo-5/daf-22* double mutant was used. Experiments with *elo-5/daf-22* used *B. subtilis* as a diet due to its capability to produce mmBCFA, such as *iso*C15 (**15a**) and *iso*C17 (**17a**). *Iso*-fatty acids in *B. subtilis* were [$^{13}C_5$]-labelled by growing the bacterium on [U-$^{13}C_6$] and [U-$^{12}C_6$] L-leucine, and unlabelled *B. subtilis* was used as a control. Lipid extracts were analyzed by LC-ESI-(+)-MS and [$^{13}C_5$]-enrichment was detected for ascarosides carrying *iso*-alkyl sidechains with 22, 24, 26 (**82**), or 28 carbons (Figure 41). These results are in agreement with a L-leucine-based biosynthesis of *daf-22* dependent *iso*-branched acyl ascarosides previously observed by the von Reuss group and support the assumption that *iso*-alkyl ascarosides might serve as precursors for the *iso*-acyl ascarosides, which accumulate in the *daf-22* exometabolome (Figure 8).

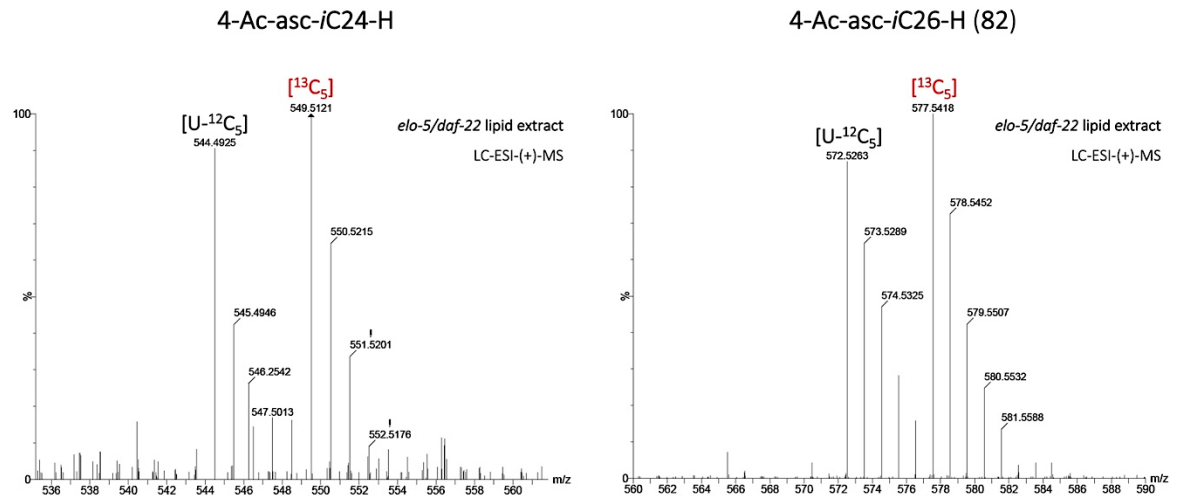

Figure 41. [$^{13}C_5$]-isotopomers of **4-Ac-asc-*i*C24-H** and **4-Ac-asc-*i*C26-H** (**82**) were observed in *elo-5/daf-22* double mutant fed with *B. subtilis* grown in a 1:1 mixture of [U-$^{13}C_6$] and [U-$^{12}C_6$] L-leucine. Adducts at $[M+NH_4]^+$ are represented.

Considering these results, two hypotheses can be made concerning the biosynthetic origin of *iso*-alkyl ascarosides in *C. elegans* (Figure 42). In the first scenario (pathway **A**), the worm employs L-leucine derived bacterial *iso*-fatty acids (*iso*C15, **15a**, or *iso*C17, **17a**) as precursors of the aglycone biosynthesis via *iso*-fatty acid elongation and subsequent linkage of the ascarylose unit to generate the *iso*-branched ascarosides. In the second scenario (pathway **B**), the worm biosynthesizes the *iso*-branched sidechain *de novo* via some L-leucine (**14**) derived metabolites of the diet that have not yet been identified. Therefore, experiments with *elo-5* worms defective in *iso*-fatty acid biosynthesis that were fed with

mixtures of *E. coli* and *iso*-fatty acid isotopomers are required to further clarify the biosynthetic origin of the *iso*-alkyl ascarosides (see chapter 8.3).

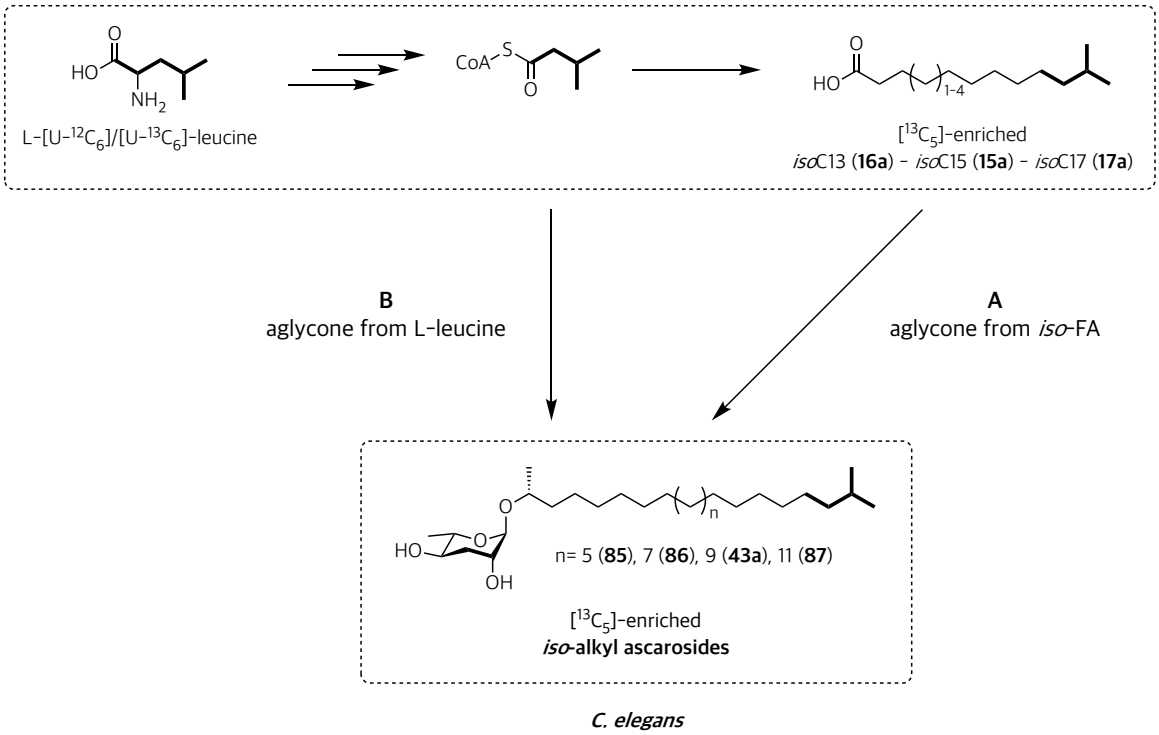

Figure 42. Propositions for the origin of the *iso*-branch aglycones of *iso*-alkyl ascarosides of *C. elegans*. **A**: incorporation of the *iso*-branched [$^{13}C_5$]-unit via odd-numbered bacterial *iso*-fatty acids. **B**: incorporation of the *iso*-branched [$^{13}C_5$]-unit from L-leucine into the *iso*-alkyl ascaroside by *de novo* biosynthesis.

8.1.1.3 Very long chain hydroxy alkyl ascarosides in *C. elegans* eggs and worms

Previous studies reported the identification of 2-hydroxyalkyl ascarosides such as (2*R*,3*R*,5*R*,6*S*)-2-(((2*R*,28*R*)-28-hydroxynonacosan-2-yl)oxy)-6-methyltetrahydro-2*H*-pyran-3,5-diol (**asc-C29-OH**, **88**), (2*R*,3*R*,5*R*,6*S*)-2-(((2*R*,30*R*)-30-hydroxyhentriacontan-2-yl)oxy)-6-methyltetrahydro-2*H*-pyran-3,5-diol (**asc-C31-OH**, **12**) and (2*R*,3*R*,5*R*,6*S*)-2-(((2*R*,32*R*)-32-hydroxytritriacontan-2-yl)oxy)-6-methyltetrahydro-2*H*-pyran-3,5-diol (**asc-C33-OH**, **89**) in *Ascaris* eggs and in mixed populations of *C. elegans* (Figure 43) [14] [21] [32] [33].

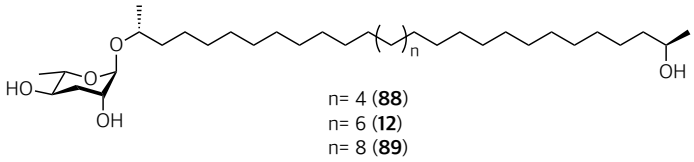

Figure 43. Examples of 2-hydroxyalkyl ascarosides found in *C. elegans* mixed populations and *Ascaris* eggs [14] [21] [32] [33].

Very long chain 2-hydroxyalkyl ascarosides in *C. elegans* have been reported to be *daf-22* independent [21], but additional information about their biosynthesis is still lacking. Based on the identification of very long chain 2-hydroxyalkyl ascarosides in *Ascaris* eggs, their presence in *C. elegans* eggs has often been assumed but never proven experimentally . Consequently, the identification of a homologous 2-hydroxyalkyl ascaroside series in *C. elegans* eggs and worm bodies by LC-MS is described in the present section. Because the synthetic standards of very long chain alkyl ascarosides had demonstrated excellent ionization by APCI-(-) showing $[M+O_2]^-$ adducts, the same ionization technique was used for the detection of very long chain 2-hydroxyalkyl ascarosides in nematode egg and body samples.

Mass spectrometry analysis of *Ascaris* extracts had revealed very long-chain 2-hydroxyalkyl ascarosides with acetyl and propionyl residues [34] [65], but the exact location of these acyl groups has never been reported. Nonetheless, 2D-NMR analysis of metabolite extracts of *C. elegans* revealed variable amounts of 4-acetylated derivatives of long chain 2-hydroxyalkyl ascarosides [15]. Based on the information described above, *C. elegans* egg and worm samples were screened for very long chain 2-hydroxyalkyl ascarosides and their monoacetyl derivatives (without making any structural assumption).

Prior to analysis, the *C. elegans* eggs and worms were isolated and extracted. Initial screens for very long chain alkyl ascarosides failed to confirm their presence (possibly due to very small amounts). However, $[M+O_2]^-$ adducts of the 2-hydroxyalkyl ascarosides with molecular formulas such as $C_{35}H_{70}O_5$ (**asc-C29-OH**, **88**), $C_{37}H_{74}O_5$ (**asc-C31-OH**, **12**), and $C_{39}H_{78}O_5$ (**asc-C33-OH**, **89**), and their mono-acetylated derivatives $C_{37}H_{72}O_6$ (**asc-C29-OAc**), $C_{39}H_{76}O_6$ (**asc-C31-OAc**), and $C_{41}H_{80}O_6$ (**asc-C33-OAc**) were identified (Figure 44).

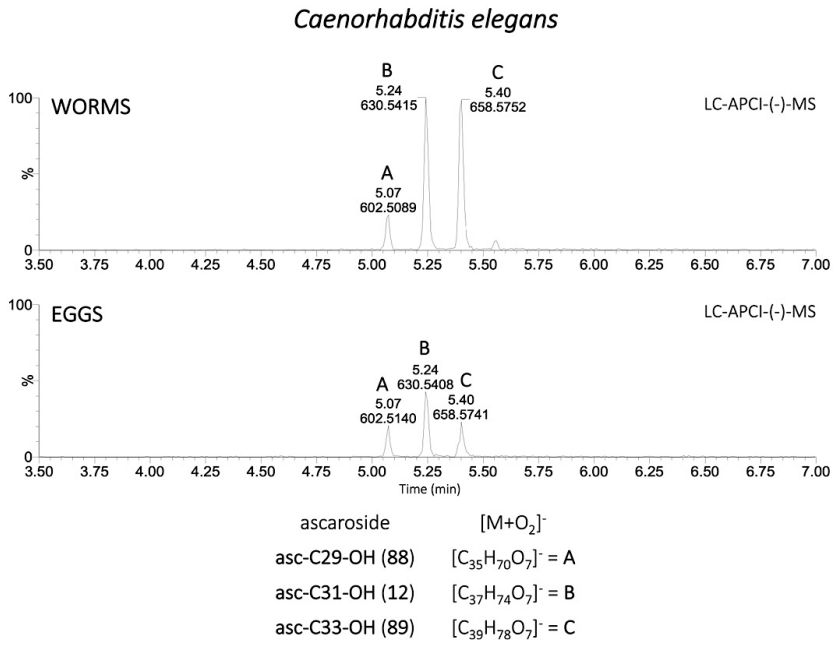

Figure 44. Identification of 2-hydroxyalkyl ascarosides in *C. elegans* worms and eggs by LC-APCI-(-)-MS. Adducts at $[M+O_2]^-$ are shown.

The relative composition of the identified 2-hydroxyalkyl ascarosides in extracts of *C. elegans* eggs and worm bodies was calculated based on chromatographic peak areas and is shown in Figure 45. Although the content of the targeted ascarosides was similar in both samples, their composition was different. For example, the content of the 2-hydroxyalkyl ascaroside **asc-C33-OH** shows higher values in the worm sample than in the egg sample. In contrast, quantities of **asc-C31-OH** are higher in eggs than in worms.

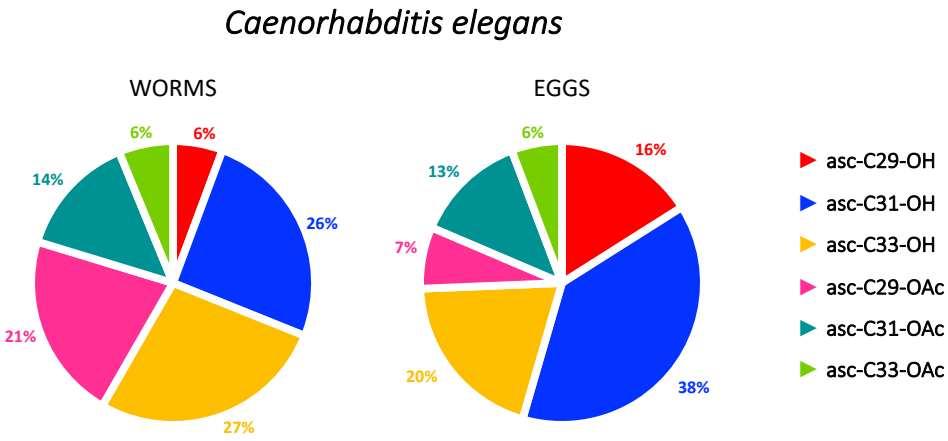

Figure 45. Proportion of 2-hydroxyalkyl ascarosides in *C. elegans* eggs and worms.

8.1.1.4 Very long chain alkyl ascarosides in different nematode species

Because LC-APCI-(-)-MS resulted in excellent ionization of the very long chain alkyl ascarosides in *C. elegans*, several very long chain alkyl ascarosides could be identified in different nematode species. Lipid extracts of the following nematode species and strains were used: *C. elegans* wildtype laboratory strain (N2), *C. elegans* Australian wildtype (AB1), *C. elegans* Hawaiian wildtype (CB4856), *C. brenneri* (PB2801), *C. remanei* (PB4641), *C. wallacei* (JU1904), *C. nigoni* (JU1422), *C. tropicalis* (JU1373) and *Ascaris lumbricoides*. Targeted analyses for the $[M+O_2]^-$ adducts corresponding to very long chain alkyl ascarosides exhibiting sidechains from 23 to 36 carbons revealed a diversity of homologous compounds. Homologous structures were assigned based on the authentic standards (2*R*,3*R*,5*R*,6*S*)-2-(henicosyloxy)-6-methyltetrahydro-2*H*-pyran-3,5-diol (**asc-ωC21-H**, **68a**), (2*S*,3*R*,5*R*,6*R*)-2-methyl-6-(((*R*)-pentacosan-2-yl)oxy)tetrahydro-2*H*-pyran-3,5-diol (**asc-C25-H**, **33a**), (2*S*,3*R*,5*R*,6*R*)-2-methyl-6-(((*R*)-24-methylpentacosan-2-yl)oxy)tetrahydro-2*H*-pyran-3,5-diol (**asc-*i*C26-H**, **43a**) and (2*R*,3*R*,5*R*,6*S*)-2-(((*R*)-hentriacontan-2-yl)oxy)-6-methyltetrahydro-2*H*-pyran-3,5-diol (**asc-C31-H**, **57a**). Results of the identification of very long chain alkyl ascarosides by LC-APCI(-)-MS from the mentioned nematodes are shown in Figure 46.

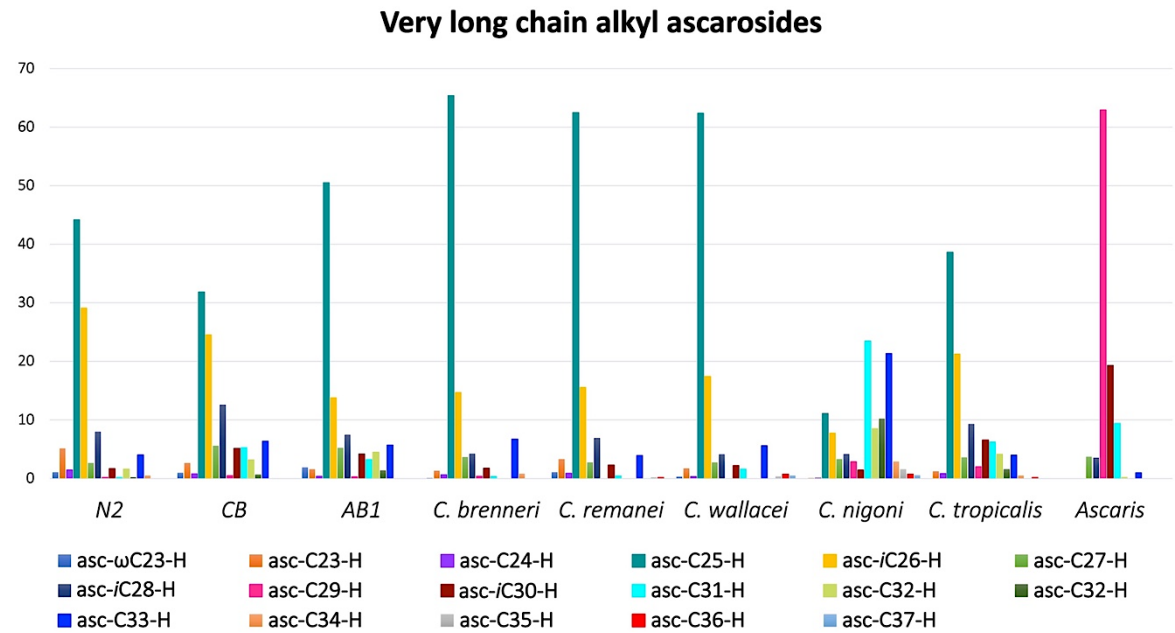

Figure 46. Identification of very long chain alkyl ascarosides in different nematode strains and species.

The major alkyl ascaroside identified from *C. elegans*, *C. brenneri*, *C. remanei*, *C. wallacei*, and *C. tropicalis* was (2*S*,3*R*,5*R*,6*R*)-2-methyl-6-(((*R*)-pentacosan-2-yl)oxy)tetrahydro-2*H*-pyran-3,5-diol (**asc-C25-H**, **33a**), whereas this component was not detected in *Ascaris*. In contrast, *Ascaris* biosynthesizes

high concentrations of (2*S*,3*R*,5*R*,6*R*)-2-methyl-6-(((*R*)-nonacosan-2-yl)oxy)tetrahydro-2*H*-pyran-3,5-diol (**asc-C29-H**) and (2*S*,3*R*,5*R*,6*R*)-2-methyl-6-(((*R*)-29-methyltriacontan-2-yl)oxy)tetrahydro-2*H*-pyran-3,5-diol (**asc-*i*C30-H**). The very long chain alkyl ascaroside **asc-C29-H** was absent in *C. elegans*, *C. brenneri*, *C. remanei*, and *C. wallacei*. Furthermore, the dominant very long chain *iso*-branched ascaroside in *C. elegans*, *C. elegans* Australian wildtype (AB1), *C. elegans* Hawaiian wildtype (CB4856), *C. brenneri*, *C. remanei*, *C. wallacei*, *C. nigoni* and *C. tropicalis* is (2*S*,3*R*,5*R*,6*R*)-2-methyl-6-(((*R*)-24-methylpentacosan-2-yl)oxy)tetrahydro-2*H*-pyran-3,5-diol (**asc-*i*C26-H**, **43a**). Moreover, the content of very long chain alkyl ascarosides in *C. nigoni* shows a different distribution form the others *Caenorhabditis* nematodes. For example, in *C. nigoni* (2*R*,3*R*,5*R*,6*S*)-2-(((*R*)-hentriacontan-2-yl)oxy)-6-methyltetrahydro-2*H*-pyran-3,5-diol (**asc-C31-H**, **57a**) and (2*S*,3*R*,5*R*,6*R*)-2-methyl-6-(((*R*)-tritriacontan-2-yl)oxy)tetrahydro-2*H*-pyran-3,5-diol (**asc-C33-H**) were identified as the major alkyl ascarosides, whereas these were observed as minor compounds in the other *Caenorhabditis* nematodes.

8.1.2 Conclusions

- Several (ω)- and (ω-1)-linked very long chain alkyl ascarosides with sidechains of 21, 25, 26, and 31 carbons, as well as their monoacetyl- and diacetyl-derivatives, were synthesized as authentic standards. In parallel, [D_4]-isotopomers with isotope labels at the (ω-1)/(ω-2)-position for the (ω)-ascaroside and (ω-2)/(ω-3)-position for the (ω-1)-ascarosides were prepared. This [D_4]-labelled very long alkyl chain ascarosides will be used to investigate the VLCA biosynthesis through incorporation studies. A total of sixteen different very long chain alkyl ascarosides structures were synthesized.

- Monoacetyl-derivatives of the very long alkyl chain ascarosides were obtained by partial acetylation of the alkyl ascarosides or deacetylation of the diacetyl alkyl ascarosides. Deacetylation was the most efficient way to obtain the desired 4-acetyl ascarosides.

- Characteristic GC-MS fragmentation of TMS-derivatives of acetyl alkyl ascarosides was observed. Ascarosides with acetyl groups at the 4-position of the ascarylose unit generate a characteristic marker ion *m/z* 161.1 $[C_6H_{13}O_3Si]^+$. Furthermore, ascarosides with acetyl groups at the 2-position of the ascarylose unit produce an intense **K1**-fragment ion at *m/z* 130.1 $[C_6H_{14}OSi]^+$. The signal of the **J2**-fragment at *m/z* [M-291] could be observed for 4- and 2,4-acetylated (ω)- and (ω-1)-ascarosides, whereas this signal was not observed for the non-acetylated ascarosides.

- Analysis of the acetylated and non-acetylated very long chain alkyl ascaroside standards by LC-APCI-(-)-MS provides $[M+O_2]^-$ adducts and represents an effective detection technique. Furthermore, the very long chain alkyl ascaroside standards could also be detected by LC-ESI-(+)-MS as ammonium adducts ($[M+NH_4]^+$), but with comparably lower sensitivity. As expected, the standard method to screen for acyl ascarosides, LC-ESI-MS in negative ion mode, failed to detect very long-chain alkyl ascaroside standards.

- Identification of (2*R*,3*R*,5*R*,6*S*)-2-(henicosyloxy)-6-methyltetrahydro-2*H*-pyran-3,5-diol (**asc-ωC21-H**, **68a**), (2*S*,3*R*,5*R*,6*R*)-2-methyl-6-(((*R*)-pentacosan-2-yl)oxy)tetrahydro-2*H*-pyran-3,5-diol (**asc-C25-H**, **33a**), (2*S*,3*R*,5*R*,6*R*)-2-methyl-6-(((*R*)-24-methylpentacosan-2-yl)oxy)tetrahydro-2*H*-pyran-3,5-diol (**asc-*i*C26-H**, **43a**), (2*S*,3*R*,5*R*,6*R*)-5-hydroxy-2-methyl-6-(((*R*)-pentacosan-2-yl)oxy)tetrahydro-2*H*-pyran-3-yl acetate (**4-Ac-asc-C25-H**, **81**) and (2*S*,3*R*,5*R*,6*R*)-5-hydroxy-2-methyl-6-(((*R*)-24-methylpentacosan-2-yl)oxy)tetrahydro 2*H*-pyran-3-yl acetate (**4-Ac-asc-*i*C26-H**, **82**) in *daf-22* exometabolome fractions was accomplished by comparative GC-MS and LC-APCI(-)-MS analyses of the natural samples with the synthetic standards.

- The biosynthesis of alkyl ascarosides with *iso*-branched sidechains depends on L-leucine (**14**) as the biosynthetic precursor. [$^{13}C_5$]-Incorporation upon feeding with L-[$^{13}C_6$]-leucine enriched *B. subtilis* by the mmBCFA biosynthesis deficient *C. elegans elo-5* mutant suggested the involvement of *iso*-fatty acid intermediates (*iso*C15, *iso*C17). At this stage, alternative pathways cannot be excluded.

- Identification of the 2-hydroxyalkyl ascarosides **asc-C29-OH**, **asc-C31-OH**, and **asc-C33-OH**, including their monoacetyl derivatives, in *C. elegans* eggs and worm bodies was achieved by LC-APCI-(-)-MS analysis. The content of these ascarosides differs in eggs and worm bodies of *C. elegans*, suggesting the accumulation of specific compounds in specific tissues.

- Very long chain alkyl ascarosides with sidechains varying from 23 to 32 carbons were characterized in *C. elegans* (N2), *C. elegans* Australian wildtype (AB1), *C. elegans* Hawaiian wildtype (CB4856), *C. brenneri* (PB2801), *C. remanei* (PB4641), *C. wallacei* (JU1904), *C. nigoni* (JU1422), *C. tropicalis* (JU1373), and *Ascaris lumbricoides* by LC-APCI-(-)-MS analysis, demonstrating that alkyl ascarosides are highly conserved among nematodes.

8.2 (ω)-Carboxy alkyl ascarosides as potential intermediates in ascaroside biosynthesis

Unpublished results from Dolke and von Reuss imply that fatty acid elongation upon lipogenesis and chain shortening by the β-oxidation cycle in *C. elegans* ascaroside biosynthesis operate from opposite sides of the aglycone [24] and that (ω)-carboxy alkyl ascarosides might be biosynthetic intermediates. HR-MS and MS^n analysis of lipophilic exometabolome fractions of *daf-22* revealed potential ascaroside intermediates with a high content of oxygen in the sidechains. Specifically, ESI-(+)-MS/MS screening shows a series of compounds that display neutral loss of 130 [$C_6H_{10}O_3$], 146 [$C_6H_{10}O_4$], 164 [$C_6H_{10}O_4$ and H_2O], and 224 amu [$C_6H_{10}O_4$ and H_2O and $C_2H_4O_2$]. In Figure 47 an example of the screening of a possible biosynthetic intermediate, (*S*)-3-(((2*R*,3*R*,5*R*,6*S*)-3,5-dihydroxy-6-methyltetrahydro-2*H*-pyran-2-yl)oxy)-17-oxooctadecanoic acid (**(ω-COOH)-asc-C17-MK**, **90**), can be observed. MS^2 fragmentation exhibited characteristic ion signals at *m/z* 313 and *m/z* 295 form the cleavage of the aglycone. Furthermore, MS^3 fragmentation shows the loss of the acetate group of the aglycone with a signal at *m/z* 267.

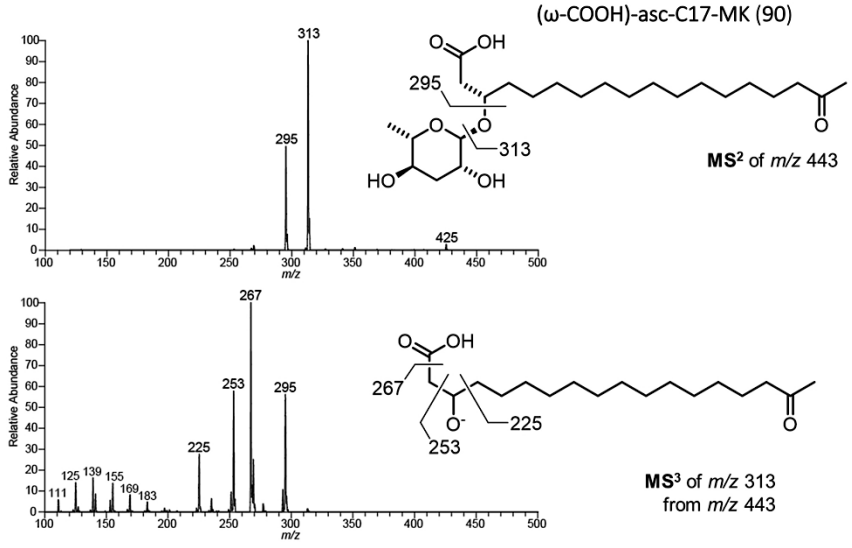

Figure 47. An example of the assignment of (ω)-carboxy β-ketoalkyl ascarosides in the *daf-22* exometabolome by ESI-(+)-MS^n analysis.

The fragmentation of putative derivatives revealed two homologous series of (ω)-carboxy ascarosides: (ω)-carboxy acyl ascaroside (sidechains from C18-23 carbons) and (ω)-carboxy 2-oxoalkyl ascarosides (sidechains from C17-21 carbons). Therefore, one representative for (ω)-carboxy β-ketoalkyl

ascaroside with a C17 sidechain and one for (ω)-carboxy acyl ascarosides with a C18 sidechain were selected for total synthesis (Figure 48).

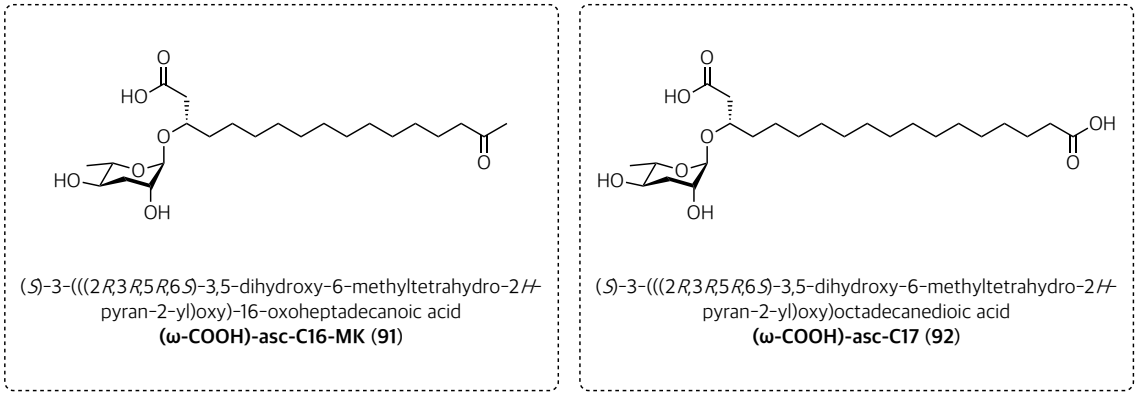

Figure 48. Representative (ω)-carboxy alkyl ascarosides as possible biosynthetic intermediates.

The preparation of the authentic standards (*S*)-3-(((2*R*,3*R*,5*R*,6*S*)-3,5-dihydroxy-6-methyltetrahydro-2*H*-pyran-2-yl)oxy)-16-oxoheptadecanoic acid (**(ω-COOH)-asc-C16-MK**, **91**) and (*S*)-3-(((2*R*,3*R*,5*R*,6*S*)-3,5-dihydroxy-6-methyltetrahydro-2*H*-pyran-2-yl)oxy)octadecanedioic acid (**(ω-COOH)-asc-C17**, **92**) proceeded similar to the syntheses of the very long chain alkyl ascarosides. The glycosylation of a (*R*)-3-hydroxypent-4-enoate ester with the freshly prepared 2,4-benzoyl ascarylose trichloroacetimidate (**40**) was used for the preparation of an (ω)-carboxy alkenyl-ascaroside intermediate. The sidechain of the alkenyl-ascaroside intermediate was further extended by Grubbs metathesis, as in Figure 14 [24].

8.2.1 Syntheses and characterization (ω)-carboxy alkyl ascarosides

8.2.1.1 Synthesis and characterization of (*S*)-3-(((2*R*,3*R*,5*R*,6*S*)-3,5-dihydroxy-6-methyltetrahydro-2*H*-pyran-2-yl)oxy)-16-oxoheptadecanoic acid

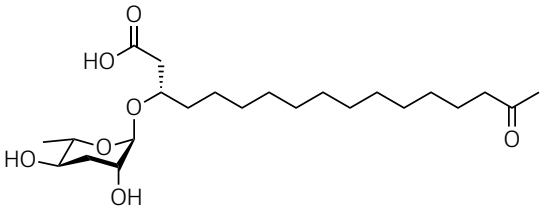

Figure 49. Structure of (*S*)-3-(((2*R*,3*R*,5*R*,6*S*)-3,5-dihydroxy-6-methyltetrahydro-2*H*-pyran-2-yl)oxy)-16-oxoheptadecanoic acid (**(ω-COOH)-asc-C16-MK**, **91**).

The synthesis of the carboxy-ascaroside (**(ω-COOH)-asc-C17-MK**, **91**) (Figure 49) required three different starting materials, such as (2*R*,3*R*,5*R*,6*S*)-2-hydroxy-6-methyltetrahydro-2*H*-pyran-3,5-diyl dibenzoate (**19**), a β-hydroxy pentenoate ester (*tert*-butyl (*R*)-3-hydroxypent-4-enoate, **93**) and a terminal alkenyl-ketone (13-tetradecene-2-one, **94**). Kinetic resolution of the commercially available racemic *tert*-butyl 3-hydroxypent-4-enoate (**95**) with Amano lipase PS (lipase PS-30) and vinyl acetate was employed for the synthesis of the enantiomerically pure *tert*-butyl (*R*)-3-hydroxypent-4-enoate (**93**) (Figure 50) [66]. Increasing the reaction time to 72 hours ensured a high enantiopurity of the unreacted (*R*)-3-hydroxy pentenoate ester **93**, which was separated by column chromatography.

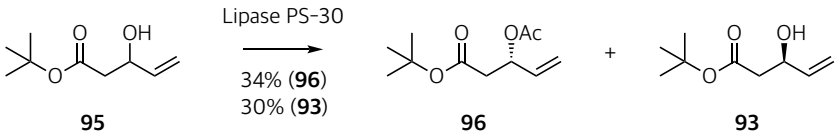

Figure 50. Kinetic resolution of racemic β-hydroxy esters.

Comparative ^{1}H NMR analysis of *tert*-butyl (*R*)-3-hydroxypent-4-enoate (**93**) and *tert*-butyl (*S*)-3-acetoxypent-4-enoate (**96**) confirmed the assignment of both isomers based on the methine proton signal of the alcohol **93** and the ester **96**, respectively at 4.49 ppm and 5.60 ppm (Figure 51).

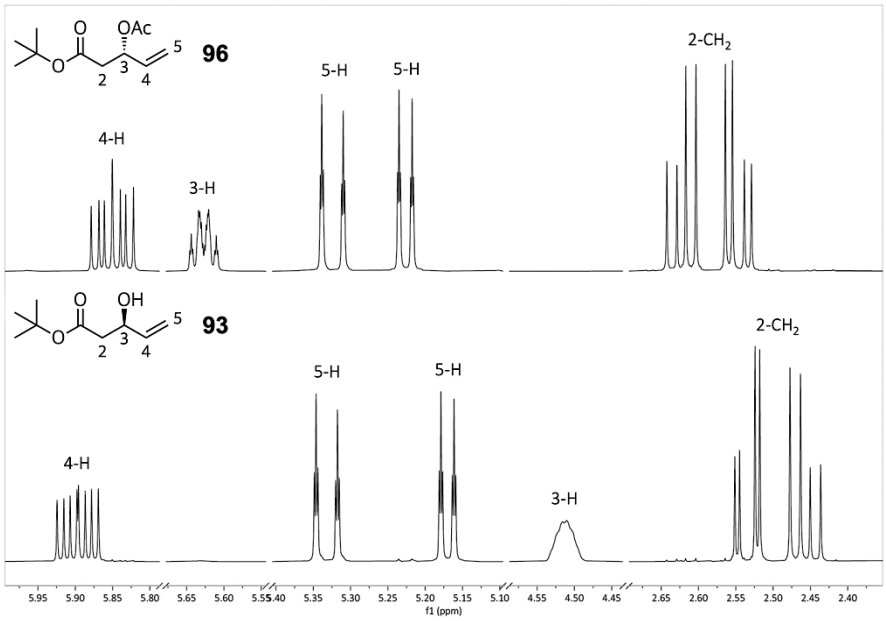

Figure 51. Sections of the ^{1}H NMR spectra of *tert*-butyl (*S*)-3-acetoxypent-4-enoate (**96**) and (*R*)-3-hydroxypent-4-enoate (**93**).

In parallel, 13-tetradecene-2-one (**94**) was synthesized by following a methodology reported by Ishmuratov *et al.* [67] with modifications (Figure 52). Initially, the commercially available 11-bromo-1-

undecene (**97**) and ethyl 3-oxobutanoate (**98**) were used for the preparation of ethyl 2-acetyltridec-12-enoate (**99**). Subsequently, and in contrast with the original procedure, an aqueous NaOH solution was used for the hydrolysis of the unsaturated ketone **99** to generate the 13-tetradecene-2-one (**94**) upon decarboxylation.

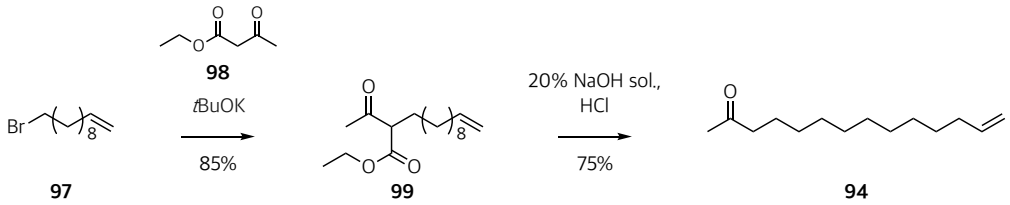

Figure 52. Synthesis of 13-tetradecene-2-one (**94**).

Identification of the product was confirmed by ^{1}H and ^{13}C NMR analyses. The ^{1}H spectrum of 13-tetradecene-2-one (**94**) (Figure 53) shows signals corresponding to the protons of the terminal vinyl group at 4.95, 5.02, and 5.82 ppm. Furthermore, a signal corresponding to the allylic protons in the 12-CH_2 position was observed at 2.06 ppm (*m*). The signal of the methylene protons adjacent to the carbonyl group (3-CH_2) appears at 2.44 ppm (*t*, J=7.5 Hz).

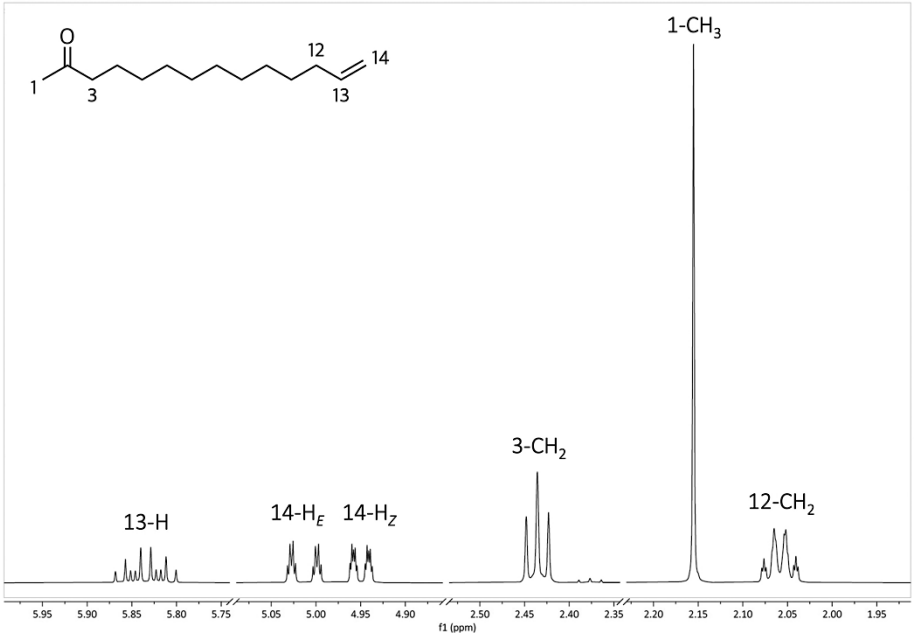

Figure 53. Sections of the ^{1}H spectrum of 13-tetradecene-2-one (**94**).

Glycosylation of the *tert*-butyl (*R*)-3-hydroxypent-4-enoate (**82**) with the 2,4-benzoyl ascarylose trichloroacetimidate (**40**) generated the (2*R*,3*R*,5*R*,6*S*)-2-(((*R*)-5-(*tert*-butoxy)-5-oxopent-1-en-3-yl)oxy)-6-methyltetrahydro-2*H*-pyran-3,5-diyl dibenzoate (**100**) intermediate, as shown in Figure 54.

Subsequent Grubbs metathesis with 13-tetradecene-2-one (**94**) and the alkenyl-ascaroside intermediate **100** gave the (2*R*,3*R*,5*R*,6*S*)-2-(((*R*,*E*)-1-(*tert*-butoxy)-1,16-dioxoheptadec-4-en-3-yl)oxy)-6-methyltetrahydro-2*H*-pyran-3,5-diyl dibenzoate (**101**). Reduction of the C-C double bond of **101** with H_2 catalyzed by Pd/C generated (2*R*,3*R*,5*R*,6*S*)-2-(((*S*)-1-(*tert*-butoxy)-1,16-dioxoheptadecan-3-yl)oxy)-6-methyltetrahydro-2*H*-pyran-3,5-diyl dibenzoate (**102**), which was deprotected with an excess of concentrated NaOH solution to obtain the (*S*)-3-(((2*R*,3*R*,5*R*,6*S*)-3,5-dihydroxy-6-methyltetrahydro-2*H*-pyran-2-yl)oxy)-16-oxoheptadecanoic acid (**(ω-COOH)-asc-C16-MK**, **91**).

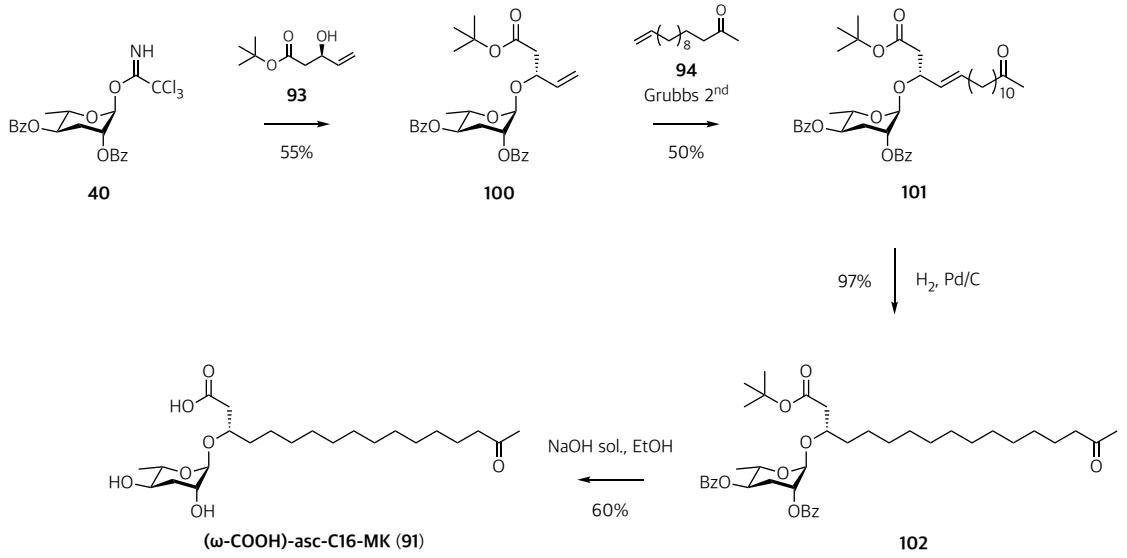

Figure 54. Synthesis of (*S*)-3-(((2*R*,3*R*,5*R*,6*S*)-3,5-dihydroxy-6-methyltetrahydro-2*H*-pyran-2-yl)oxy)-16-oxoheptadecanoic acid (**(ω-COOH)-asc-C16-MK**, **91**).

Characterization of the new compound (*S*)-3-(((2*R*,3*R*,5*R*,6*S*)-3,5-dihydroxy-6-methyltetrahydro-2*H*-pyran-2-yl)oxy)-16-oxoheptadecanoic acid (**(ω-COOH)-asc-C16-MK**, **91**) was performed by 1D and 2D NMR, GC-MS, and LC-MS. Due to the low volatility of **(ω-COOH)-asc-C16-MK** (**91**), its GC-MS analysis required the preparation of the corresponding TMS-derivative. The EIMS spectrum of this derivative displays characteristic fragments assigned accordingly to the nomenclature [21], including fragments corresponding to the ascarylose unit at *m/z* 130.1 (**K1**), 275.2 (**A1**) and 185.1 (**A2**) (Figure 55). Additionally, oxonium ion signals corresponding to the fragmentation of the sidechain at $[M-173]^+$ (**J1**), as well as the carbocation sidechain fragment **J2** at $[M-291]^+$ could be detected.

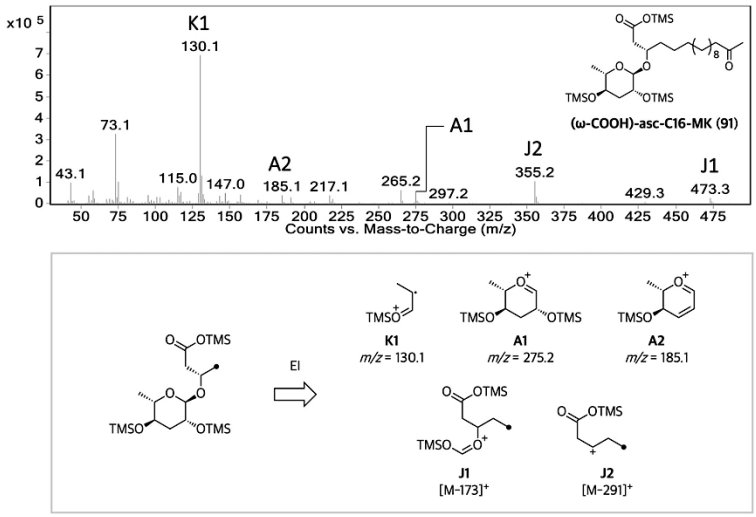

Figure 55. EIMS screening of (*S*)-3-(((2*R*,3*R*,5*R*,6*S*)-3,5-dihydroxy-6-methyltetrahydro-2*H*-pyran-2-yl)oxy)-16-oxoheptadecanoic acid (**(ω-COOH)-asc-C16-MK**, **91**).

Furthermore, HPLC-ESI-(+)-MS analysis of (*S*)-3-(((2*R*,3*R*,5*R*,6*S*)-3,5-dihydroxy-6-methyltetrahydro-2*H*-pyran-2-yl)oxy)-16-oxoheptadecanoic acid (**(ω-COOH)-asc-C16-MK**, **91**) showed a sodium adduct at *m/z* 453.2807 for $[C_{23}H_{42}NaO_7]^+$.

8.2.1.2 Synthesis and characterization of (*S*)-3-(((2*R*,3*R*,5*R*,6*S*)-3,5-dihydroxy-6-methyltetrahydro-2*H*-pyran-2-yl)oxy)octadecanedioic acid

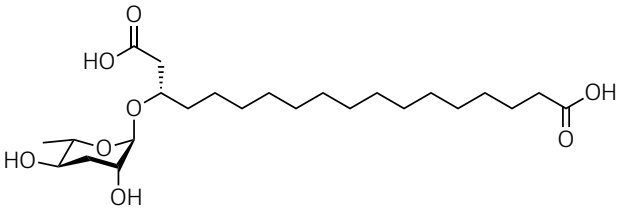

Figure 56. Structure of (*S*)-3-(((2*R*,3*R*,5*R*,6*S*)-3,5-dihydroxy-6-methyltetrahydro-2*H*-pyran-2-yl)oxy)octadecanedioic acid (**(ω-COOH)-asc-C17**, **92**).

Similar to what has been described for the synthesis of the (ω)-carboxy ascaroside (*S*)-3-(((2*R*,3*R*,5*R*,6*S*)-3,5-dihydroxy-6-methyltetrahydro-2*H*-pyran-2-yl)oxy)-16-oxoheptadecanoic acid (**(ω-COOH)-asc-C16-MK**, **91**), the preparation of (*S*)-3-(((2*R*,3*R*,5*R*,6*S*)-3,5-dihydroxy-6-methyltetrahydro-2H-pyran-2-yl)oxy)octadecanedioic acid (**(ω-COOH)-asc-C17**, **92**) (Figure 56) required three different starting materials, such as (2*R*,3*R*,5*R*,6*S*)-2-hydroxy-6-methyltetrahydro-2*H*-pyran-3,5-diyl dibenzoate (**40**), methyl pentadec-14-enoate (**103**) and *tert*-butyl (*R*)-3-hydroxypent-4-enoate (**93**). The pentadec-14-enoate (**103**) was synthesized in four steps from commercially available pentadecanolide (**45**, Figure

57). A procedure for the synthesis of a tail-end [^{11}C]-labelled palmitic acid ([ω-^{11}C]-palmitic acid) [68] with some modifications was used. The synthesis started with the opening of the pentadecanolide ring (**45**) with sodium methanolate to generate the methyl 15-hydroxypentadecanoate (**104**). Subsequently, the alcohol **104** was treated with PPh_3 and bromine to generate the methyl 15-bromopentadecanoate (**105**). The pentadec-14-enoic acid (**106**) resulted from the HBr elimination by treating **105** with an excess of potassium *tert*-butoxide. At this stage, the formation of the *tert*-butyl ester has been reported but could not be reproduced. Therefore, the resulting free pentadec-14-enoic acid (**106**) was readily converted to methyl pentadec-14-enoate (**103**) in a 75% yield using trimethylsilyldiazomethane [24].

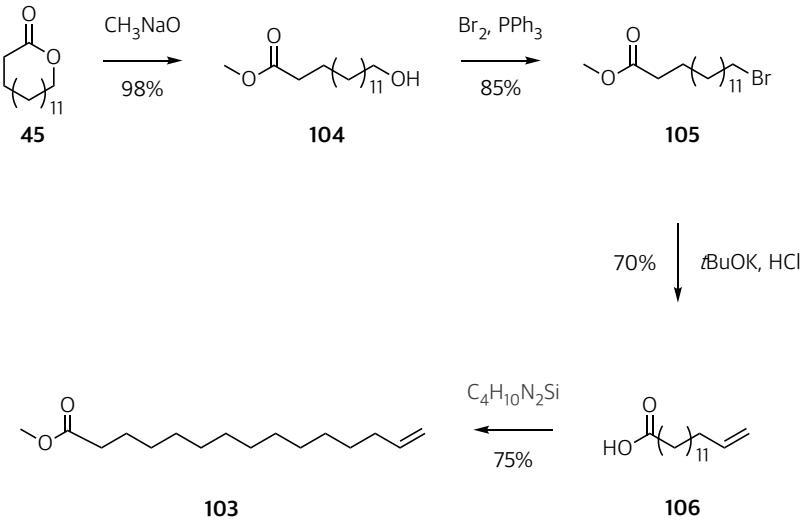

Figure 57. Synthesis of methyl pentadec-14-enoate (**103**).

The characterization of methyl pentadec-14-enoate (**103**) was performed by ^{1}H NMR (Figure 58). Multiplet signals corresponding to the protons of the terminal vinyl group were observed at 4.95, 5.01, and 5.83 ppm. Furthermore, a characteristic singlet signal corresponding to the methyl ester at 3.67 ppm was observed. A triplet signal (J=7.6 Hz) for the protons adjacent to the carbonyl group (2.32 ppm), as well as the allylic methylene protons adjacent to the double bond (*m*, 2.05 ppm) could be assigned.

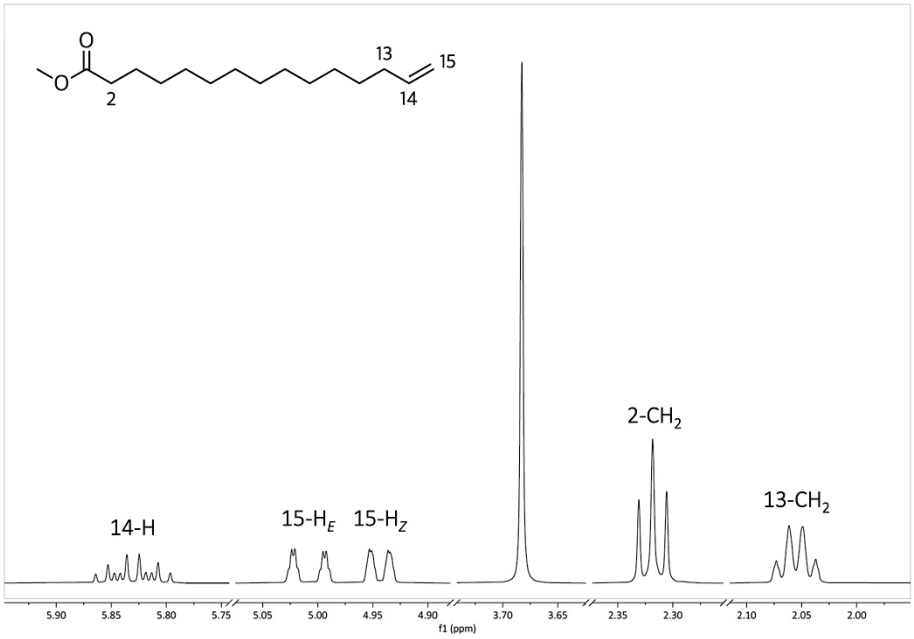

Figure 58. Sections of the ^{1}H spectrum of methyl pentadec-14-enoate (**103**).

The synthesis of the (*S*)-3-(((2*R*,3*R*,5*R*,6*S*)-3,5-dihydroxy-6-methyltetrahydro-2*H*-pyran-2-yl)oxy)octadecanedioic acid (**(ω-COOH)-asc-C17**, **92**) required the preparation of the alkenyl ascaroside intermediate **100** by the glycosylation of *tert*-butyl (*R*)-3-hydroxypent-4-enoate (**93**) with the 2,4-benzoyl ascarylose trichloroacetimidate (**40**) (Figure 54). Nevertheless, at this stage, the intermediate (2*R*,3*R*,5*R*,6*S*)-2-(((*R*)-5-(*tert*-butoxy)-5-oxopent-1-en-3-yl)oxy)-6-methyltetrahydro-2*H*-pyran-3,5-diyl dibenzoate (**100**) could not be produced (Figure 59). Therefore, the resulting free acid (*R*)-3-(((2*R*,3*R*,5*R*,6*S*)-3,5-bis(benzoyloxy)-6-methyltetrahydro-2*H*-pyran-2-yl)oxy)pent-4-enoic acid (**107**) was readily converted with trimethylsilyldiazomethane to (2*R*,3*R*,5*R*,6*S*)-2-(((*R*)-5-methoxy-5-oxopent-1-en-3-yl)oxy)-6-methyltetrahydro-2*H*-pyran-3,5-diyl dibenzoate (**108**). Subsequently, the metathesis of methyl pentadec-14-enoate (**103**) with the intermediate alkenyl ascaroside **108** generated the dimethyl (*R*,*E*)-3-(((2*R*,3*R*,5*R*,6*S*)-3,5-bis(benzoyloxy)-6-methyltetrahydro-2*H*-pyran-2-yl)oxy)octadec-4-enedioate (**109**), which was treated with H_2 and Pd/C as catalyst to yield the 2,4-benzoyl ascaroside **110**. Finally, deprotection with an excess of concentrated NaOH solution gave **(ω-COOH)-asc-C17** (**92**) as the desired product.

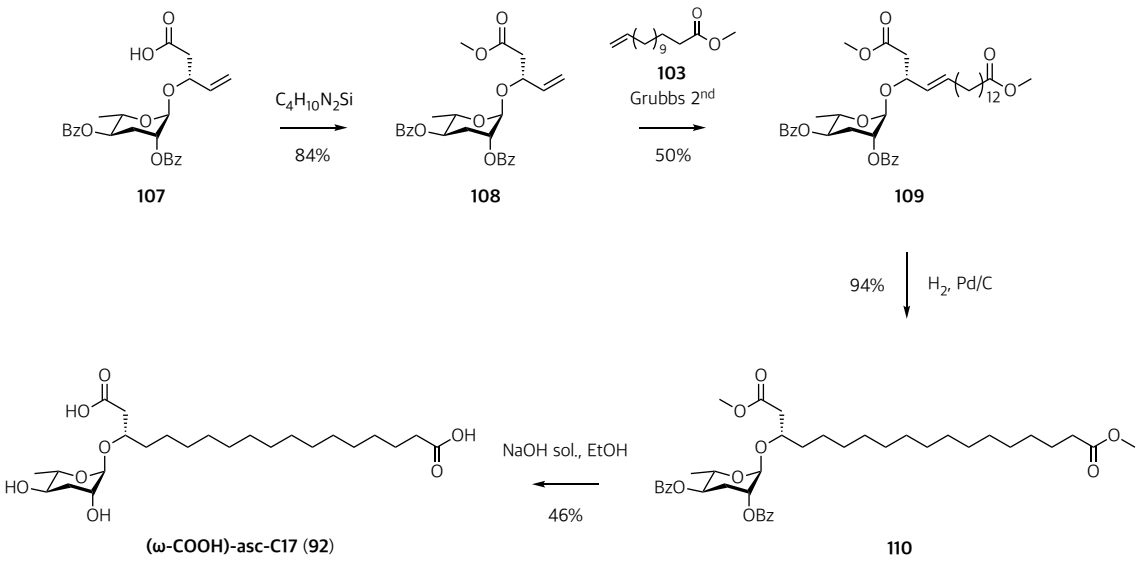

Figure 59. Synthesis of (*S*)-3-(((2*R*,3*R*,5*R*,6*S*)-3,5-dihydroxy-6-methyltetrahydro-2*H*-pyran-2-yl)oxy)octadecanedioic acid (**(ω-COOH)-asc-C17**, **92**).

The GC-MS analysis of (*S*)-3-(((2*R*,3*R*,5*R*,6*S*)-3,5-dihydroxy-6-methyltetrahydro-2*H*-pyran-2-yl)oxy)octadecanedioic acid (**(ω-COOH)-asc-C17**, **92**) is shown in Figure 60. The fragmentation of the TMS-derivative was based on the previously reported nomenclature [21]. Ascarylose derived fragments at *m/z* 130.1 (**K1**), 275.2 (**A1**) and 185.1 (**A2**), and an oxonium ion signal at $[M-173]^+$ (**J1**) were observed along with a characteristic signal corresponding to the **J2**-fragment at $[M-291]^+$.

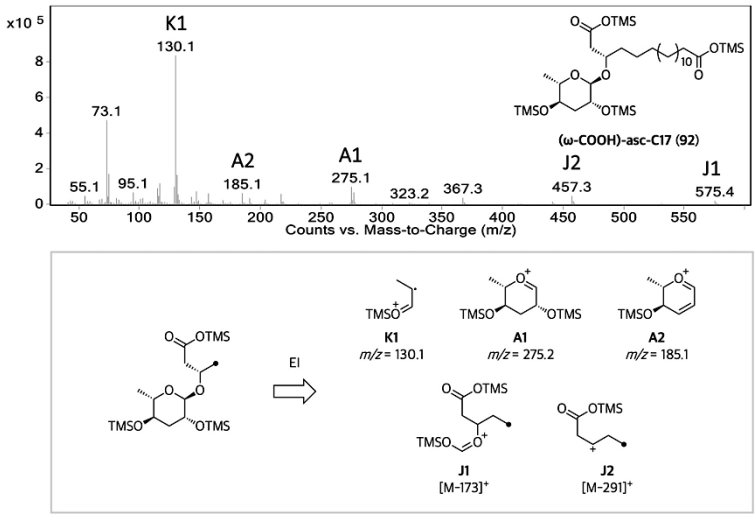

Figure 60. EIMS fragmentation of **(ω-COOH)-asc-C17** (**92**).

Finally, structural confirmation of the (*S*)-3-(((2*R*,3*R*,5*R*,6*S*)-3,5-dihydroxy-6-methyltetrahydro-2*H*-pyran-2-yl)oxy)octadecanedioic acid (**(ω-COOH)-asc-C17**, **92**) structure was derived from HPLC-ESI(+)-MS analysis, which showed a molecular ion adduct at *m/z* 483.2931 for $[C_{24}H_{44}NaO_8]^+$.

8.2.2 Comparison of (ω)-carboxy alkyl ascarosides with the *daf-22* exometabolome

Comparative analyses of SPE fractions of the *C. elegans daf-22* exometabolome and the synthetic (ω)-carboxy ascaroside standards, (*S*)-3-(((2*R*,3*R*,5*R*,6*S*)-3,5-dihydroxy-6-methyltetrahydro-2*H*-pyran-2-yl)oxy)-16-oxoheptadecanoic acid (**(ω-COOH)-asc-C16-MK**, **91**) and (*S*)-3-(((2*R*,3*R*,5*R*,6*S*)-3,5-dihydroxy-6-methyltetrahydro-2*H*-pyran-2-yl)oxy)octadecanedioic acid (**(ω-COOH)-asc-C17**, **92**), were performed by LC-MS and GC-MS.

TMS-derivatives of the authentic standards and the *daf-22* fractions were analyzed by GC-MS, which demonstrated that **(ω-COOH)-asc-C16-MK** (**91**) is not present in the *C. elegans* metabolome. However, a peak that corresponds to **(ω-COOH)-asc-C17** (**92**) was observed in the *daf-22* RP-C18-fraction eluted with 80% of MeOH. In Figure 61, extracted ion traces for the characteristic **J2**-fragment at $[M-291]^+$ show peaks with identical retention times for a natural product in the *daf-22* exometabolome and the authentic **(ω-COOH)-asc-C17** (**92**) standard .

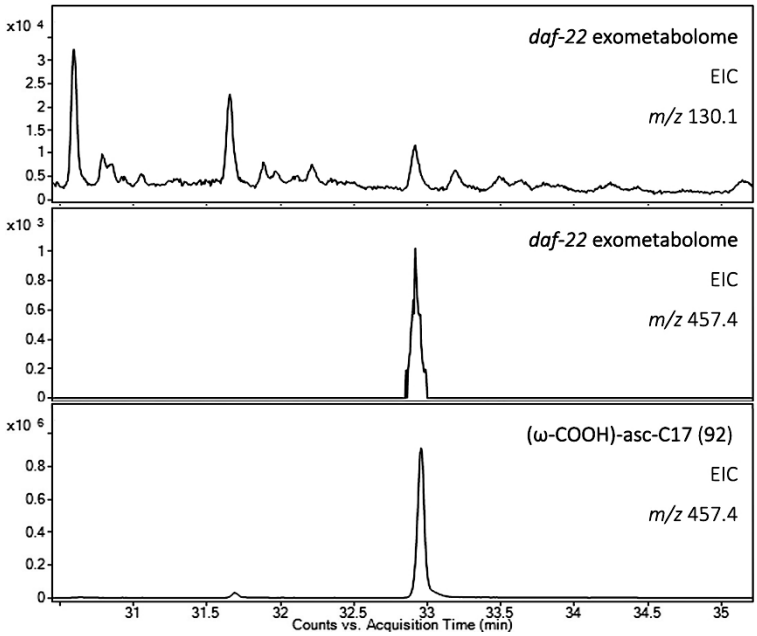

Figure 61. Comparison of EIMS screening of the *daf-22* exometabolome and the authentic standard **(ω-COOH)-asc-C17** (**92**).

Furthermore, GC-MS fragmentation of the TMS-derivatives of the authentic standard (*S*)-3-(((2*R*,3*R*,5*R*,6*S*)-3,5-dihydroxy-6-methyltetrahydro-2*H*-pyran-2-yl)oxy)octadecanedioic acid (**(ω-COOH)-asc-C17**, **92**) and the natural compound were compared (Figure 62). Both spectra exhibited signals corresponding to the loss of the ascarylose unit at *m/z* 185.1 (**A2**) and 275.2 (**A1**) as well as fragment ion signals corresponding to the sidechain at *m/z* 457.3 (**J2**) and 575.4 (**J1**).

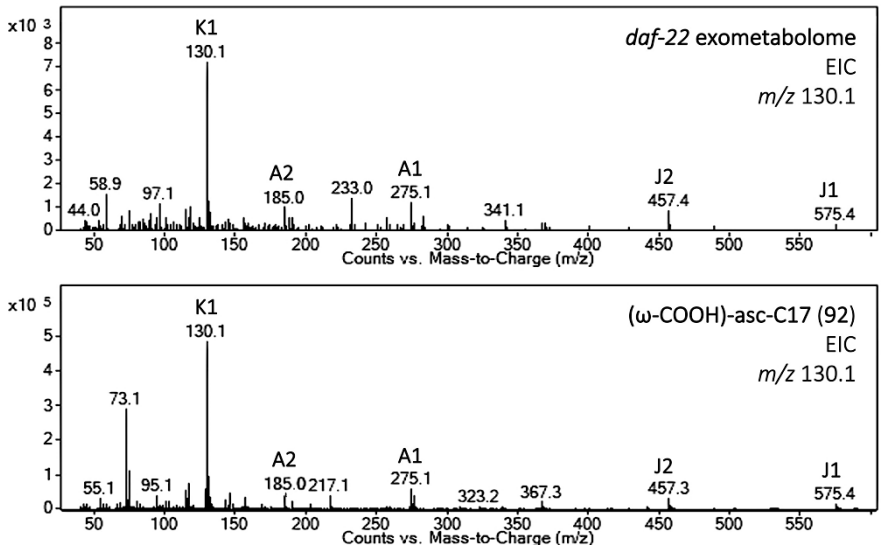

Figure 62. Comparative analyses of the EIMS spectra of the authentic standard **(ω-COOH)-asc-C17** (**92**) and its suspected natural equivalent in the *daf-22* exometabolome.

However, data collected by HPLC-HR-ESI-(+)-MS analysis using the authentic standard **(ω-COOH)-asc-C17** (**92**) and the *daf-22* exometabolome samples failed to confirm its presence as a natural product. Therefore, the (*S*)-3-(((2*R*,3*R*,5*R*,6*S*)-3,5-dihydroxy-6-methyltetrahydro-2*H*-pyran-2-yl)oxy)-16-oxoheptadecanoic acid (**(ω-COOH)-asc-C17**, **92**) cannot be confirmed as an intermediate in the biosynthesis of ascarosides.

8.2.3 Conclusions

- Two (ω-COOH)-ascarosides (*S*)-3-(((2*R*,3*R*,5*R*,6*S*)-3,5-dihydroxy-6-methyltetrahydro-2*H*-pyran-2-yl)oxy)-16-oxoheptadecanoic acid (**(ω-COOH)-asc-C16-MK**, **91**) and (*S*)-3-(((2*R*,3*R*,5*R*,6*S*)-3,5-dihydroxy-6-methyltetrahydro-2*H*-pyran-2-yl)oxy)octadecanedioic acid (**(ω-COOH)-asc-C17**, **92**) were synthesized using a new procedure based on Grubbs metathesis.

- Both (ω)-carboxy acyl ascarosides, **(ω-COOH)-asc-C16-MK** (**91**) and **(ω-COOH)-asc-C17** (**92**), could not be detected in the *daf-22* exometabolome. Therefore, their participation as intermediates in ascaroside biosynthesis cannot be confirmed.

8.3 Lipid metabolism in C. elegans

To determine if the biosynthesis of *iso*-branched alkyl ascarosides employs *iso*-fatty acids as biosynthetic intermediates, incorporation experiments with stable isotope labelled *iso*-fatty acids in the diet of *C. elegans elo-5* and *elo-5/daf-22* mutants were performed. Syntheses of the fatty acids 11-methyldodecanoic acid (*iso*C13, **16a**), 13-methyltetradecanoic acid (*iso*C15, **15a**), 15-methylhexadecanoic acid (*iso*C17, **17a**), [D_6]-11-methyldodecanoic acid ([D_6]-*iso*C13, **16c**), [D_6]-13-methyltetradecanoic acid ([D_6]-*iso*C15, **15c**) and [D_6]-15-methylhexadecanoic acid ([D_6]-*iso*C17, **17c**) were required for these experiments. Based on reported studies that used *iso*C13 (**16a**), *iso*C15 (**15a**) and *iso*C17 (**17a**) as dietary supplements for *elo-5* mutants [37] [69] [70] [39], incorporation experiments using the *iso*-fatty acid isotopomers were developed. Optimization of the incorporation conditions with the *iso*-fatty acid isotopomers was required.

8.3.1 Synthetic proposal of labelled and unlabeled *iso*-branched fatty acids

The incorporation experiments with *iso*-fatty acid isotopomers required the synthesis of *iso*-branched fatty acids with chains of 13, 15, and 17 carbons. Richardson *et al.* [55] have reported a viable synthetic pathway for the syntheses of 11-methyldodecanoic acid (*iso*C13, **16a**) and 15-methylhexadecanoic acid (*iso*C17, **17a**), which served as models for this research. Moreover, they had reported a synthetic procedure for the preparation of 13-methyltetradecanoic acid (*iso*C15, **15a**). The large number of total steps were not attractive for our approaches.

Two different routes were performed for *iso*C13 (**16a**) and *iso*C15 (**15a**), in which deuterium isotope labels could be incorporated at the methyl groups as [D_6] or at the sidechain as [D_4]. The metabolic studies carried out in this investigation required deuterium labels at the methyl groups of the *iso*-fatty acid. However, additional synthetic routes were developed for future studies. Furthermore, the syntheses of *iso*C13 (**16a**) and *iso*C15 (**15a**) were accomplished in two different ways. In summary, Figure 63 shows the *iso*-fatty acids synthesized by each route. Route 1 gave *iso*C13 (**16a**), *iso*C15 (**15a**), and their [D_4]-isotopomers using identical procedures but different starting materials. Route 2 was used for the synthesis of *iso*C13 (**16a**) and [D_6]-*iso*C13 and served as the starting point for the synthesis of the products obtained via route 3. Finally, route 4 was used to generate the fatty acids *iso*C17 (**17a**) and [D_6]-*iso*C17.

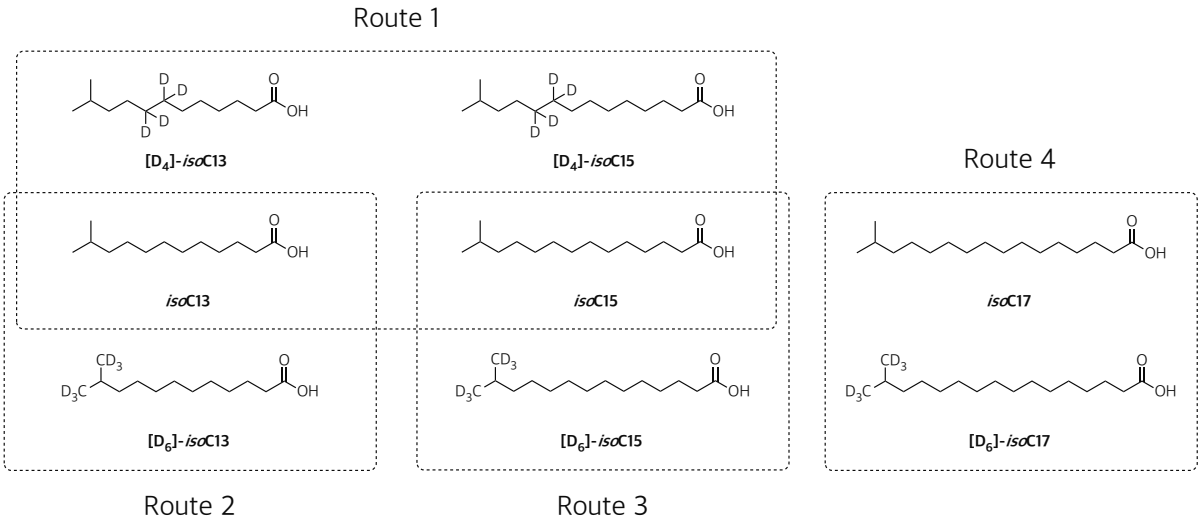

Figure 63. Classification of *iso*-fatty acid by synthetic routes.

8.3.2 Syntheses and characterization of *iso*-fatty acids

8.3.2.1 Syntheses of 11-methyldodecanoic acid, [D_4]-11-methyldodecanoic acid, 13-methyltetradecanoic acid and [D_4]-13-methyltetradecanoic acid (route 1).

The *iso*-fatty acids 11-methyldodecanoic acid (*iso*C13, **16a**), [D_4]-11-methyldodecanoic acid ([D_4]-*iso*C13, **16b**), 13-methyltetradecanoic acid (*iso*C15, **15a**) and [D_4]-13-methyltetradecanoic acid ([D_4]-*iso*C15, **15b**) were synthesized as shown in Figure 64. The preparation of all products started with commercially available 5-methylhex-1-yne (**111**). Depending on the *iso*-fatty acid chain length, 2-((6-bromohexyl)oxy)tetrahydro-2*H*-pyran (**112**) or 2-((8-bromooctyl)oxy)tetrahydro-2*H*-pyran (**113**) were utilized for initial alkyne alkylation. Deprotection of the tetrahydropyranyl ethers (**114** or **115**) with *p*-toluenesulfonic acid in methanol gave the alcohols 11-methyldodec-7-yn-1-ol (**116**) or 13-methyltetradec-9-yn-1-ol (**117**). Subsequent hydrogenation or deuterogenation of the alkynes with Pd/C as catalyst under atmospheric pressure provided the *iso*-branched hydroxy alkanes 11-methyldodecan-1-ol (**118a**), [D_4]-11-methyldodecan-1-ol (**118b**), 13-methyltetradecan-1-ol (**119a**) and [D_4]-13-methyltetradecan-1-ol (**119b**). Finally, oxidation of the alcohols with potassium permanganate [55] generated the fatty acids *iso*C13 (**16a**), *iso*C15 (**15a**) and their [D_4]-isotopomers (**16b** or **15b**).

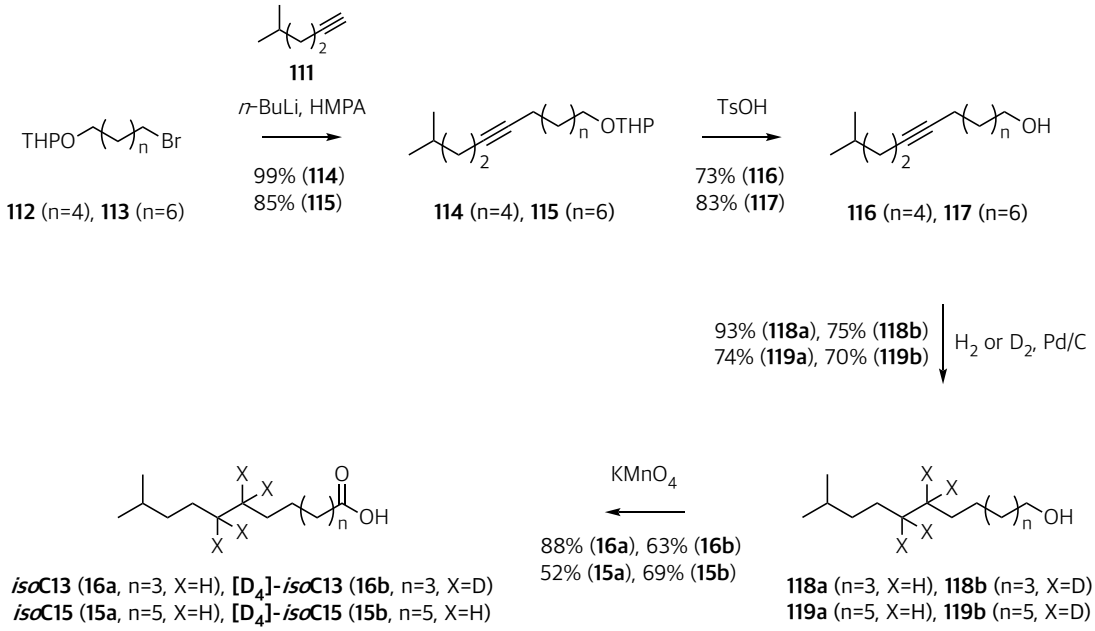

Figure 64. General synthetic scheme (route 1) illustrating the synthesis of *iso*C13 (**16a**), [D_4]-*iso*C13 (**16b**), *iso*C15 (**15b**) and [D_4]-*iso*C15 (**15b**).

8.3.2.2 Synthesis of 11-methyldodecanoic acid and [D_6]-11-methyldodecanoic acid (route 2).

The synthesis of 11-methyldodecanoic acid (*iso*C13, **16a**) and [D_6]-11-methyldodecanoic acid ([D_6]-*iso*C13, **16c**) (Figure 65) started with the reaction of methyl undec-10-enoate (**120**) with CH_3MgI or CD_3MgI to generate the 2-methyldodec-11-en-2-ol (**121a**) or [D_6]-2-methyldodec-11-en-2-ol (**121c**), respectively. Reduction with $BF_3{\cdot}Et_2O$ and triethylsilane gave the *iso*-branched alkenes, 11-methyldodec-1-ene (**122a**) or [D_6]-11-methyldodec-1-ene (**122c**), in 68-84% yields. Subsequent hydroboration-oxidation of the alkenes [71] generated the alcohols 11-methyldodecan-1-ol (**123a**) and [D_6]-11-methyldodecan-1-ol (**123c**), which were oxidized with $KMnO_4$/TBAB to produce the *iso*-fatty acids *iso*C13 (**16a**) and [D_6]-*iso*C13 (**16c**) in 81% and 91% yields, respectively.

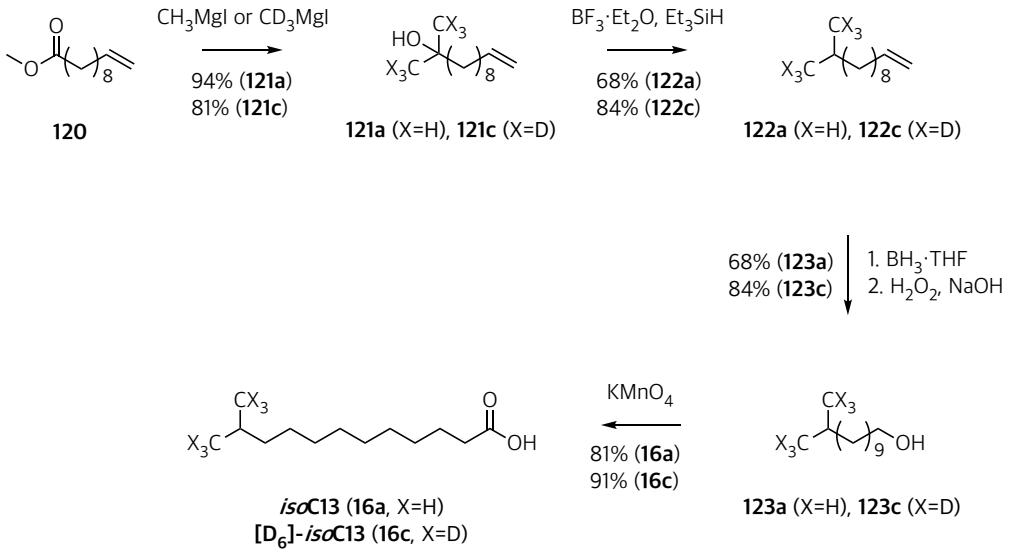

Figure 65. Synthetic pathway of *iso*C13 (**16a**) or [D_6]-*iso*C13 (**16c**) (route 2).

8.3.2.3 Synthesis of 13-methyltetradecanoic acid and [D_6]-13-methyltetradecanoic acid (route 3)

The synthesis of 13-methyltetradecanoic acid (*iso*C15, **15a**) and [D_6]-13-methyltetradecanoic acid ([D_6]-*iso*C15, **15c**) started with the reaction of 11-methyldodecan-1-ol (**123a**) or [D_6]-11-methyldodecan-1-ol (**123c**) with Br_2 and PPh_3 as shown in Figure 66. After formation of 1-bromo-11-methyldodecane (**124a**) or [D_6]-1-bromo-11-methyldodecane (**124c**), cross-coupling with an excess of vinylmagnesium bromide catalyzed by dilithium tetrachlorocuprate(II) afforded the *iso*-alkenes 13-methyltetradec-1-ene (**125a**) and [D_6]-13-methyltetradec-1-ene (**125c**) in moderate yields (60-64%). Hydroboration-oxidation of the alkenes **125a** and **125c** generated the alcohols 13-methyltetradecan-1-ol (**126a**) and [D_6]-13-methyltetradecan-1-ol (**126c**). Subsequent oxidation of the alcohols **126a** and **126c** with $KMnO_4$/TBAB, generated *iso*C15 (**15a**) and [D_6]-*iso*C15 (**15c**).

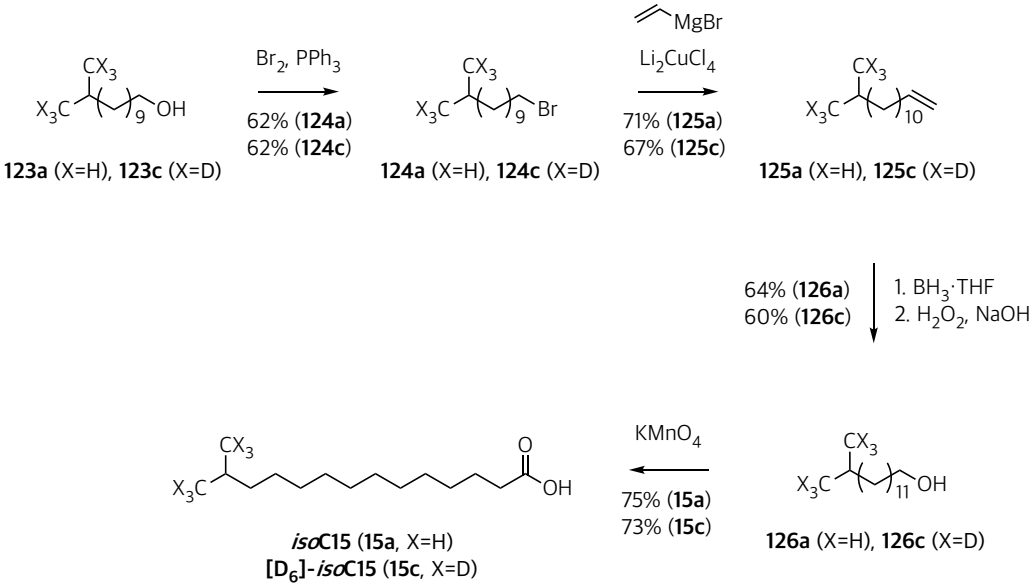

Figure 66. Synthetic pathway of *iso*C15 (**15a**) or [D_6]-*iso*C15 (**15c**) (route 3).

8.3.2.4 Synthesis of 15-methylhexadecanoic acid and [D_6]-15-methylhexadecanoic acid (route 4)

The syntheses of 15-methylhexadecanoic acid (*iso*C17, **17a**) and [D_6]-15-methylhexadecanoic acid ([D_6]-*iso*C17, **17c**) were based on the previously reported methodology of Richardson and Williams [55] with modifications (Figure 67). As described in section 8.1.2.3, commercially available pentadecanolide (**45**) was used as the starting material to produce 15-methylhexadecane-1,15-diol (**46a**). The synthesis of [D_6]-15-methylhexadecan-1-ol (**46c**) employed pentadecanolide (**45**) as well, but with CD_3MgI as the Grignard reagent. Subsequent preparation of 15-methylhexadecane-1,15-diol (**47a**) and [D_6]-15-methylhexadecan-1-ol (**47c**) required the reduction of the diols **46a** and **46c** with $BF_3{\cdot}Et_2O$ and triethylsilane. Thus, final oxidation of the alcohols **47a** and **47c** with $KMnO_4$/TBAB gave the products *iso*C17 (**17a**) and [D_6]-*iso*C17 (**17c**) in yields of 90 to 95%.

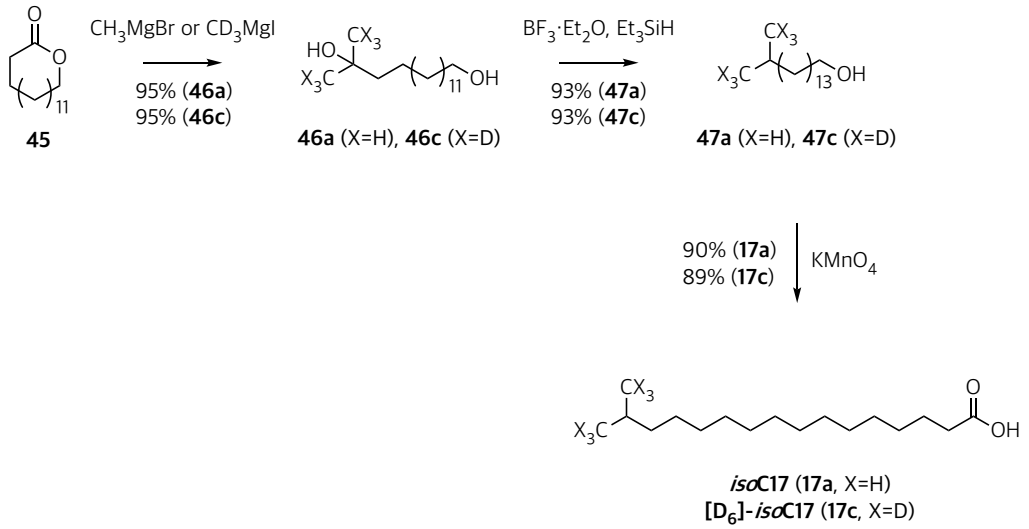

Figure 67. Synthesis of *iso*C17 (**17a**) or [D_6]-*iso*C17 (**17c**).

8.3.2.5 Characterization of *iso*-fatty acids

The characterization of the labelled and non-labelled *iso*-fatty acids with 13, 15, and 17 carbons was done by 1D NMR and GC-MS. For example, the ^{1}H NMR spectra of 15-methylhexadecanoic acid (*iso*C17, **17a**) and [D_6]-15-methylhexadecanoic acid ([D_6]-*iso*C17, **17c**) are shown in Figure 68. For *iso*C17 (**17a**) a referential doublet signal corresponding with the methyl groups at δ_H 0.86 ppm (J=6.7 Hz) could be observed, whereas for [D_6]-*iso*C17 (**17c**) this signal was not present. In both spectra, a signal corresponding to the multiple methylene protons of the alkyl chain at δ_H 1.25 ppm is shown as a multiplet. Furthermore, characteristic signals appeared at δ_H 1.63 ppm for 3-CH_2 (*m*), δ_H 2.35 ppm for 2-CH_2 (*t*, J=7.5 Hz) and δ_H 1.52 ppm for 15-H appearing as a multiplet for *iso*C17 (**17a**), and [D_6]-*iso*C17 (**17c**) at 1.48 ppm.

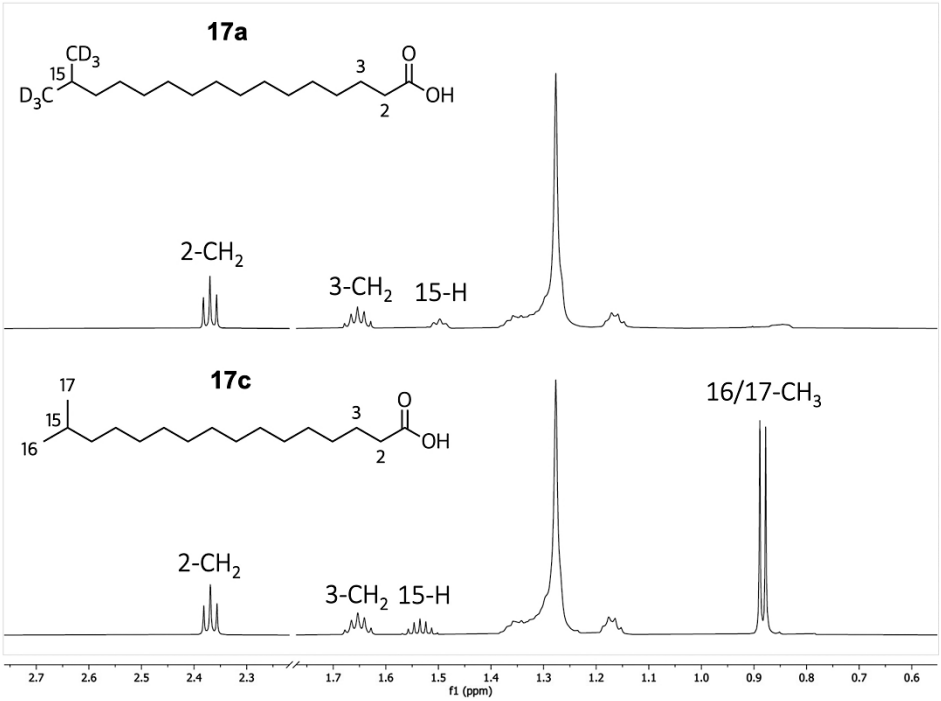

Figure 68. Comparison of the ^{1}H spectra of *iso*C17 (**17a**) and [D_6]-*iso*C17 (**17c**).

Structural confirmation of the *iso*-fatty acids was also provided by GC-MS. The molecular ions of the *iso*-fatty acids were compared as illustrated in Figure 69. Spectra of 13-methyltetradecanoic acid (*iso*C15, **15a**), [D_4]-13-methyltetradecanoic acid ([D_4]-*iso*C15, **15b**) and [D_6]-13-methyltetradecanoic acid ([D_6]-*iso*C15, **15c**) are used as examples. All the [D_4]-labelled *iso*-fatty acids were shown to consist of mixtures of isotopomers due to the introduction of the labels with Pd as catalyst. Moreover, comparison of the molecular ions of the *iso*-fatty acids and their respective [D_6]-isotopomers confirmed the selective deuterogenation of the methyl groups.

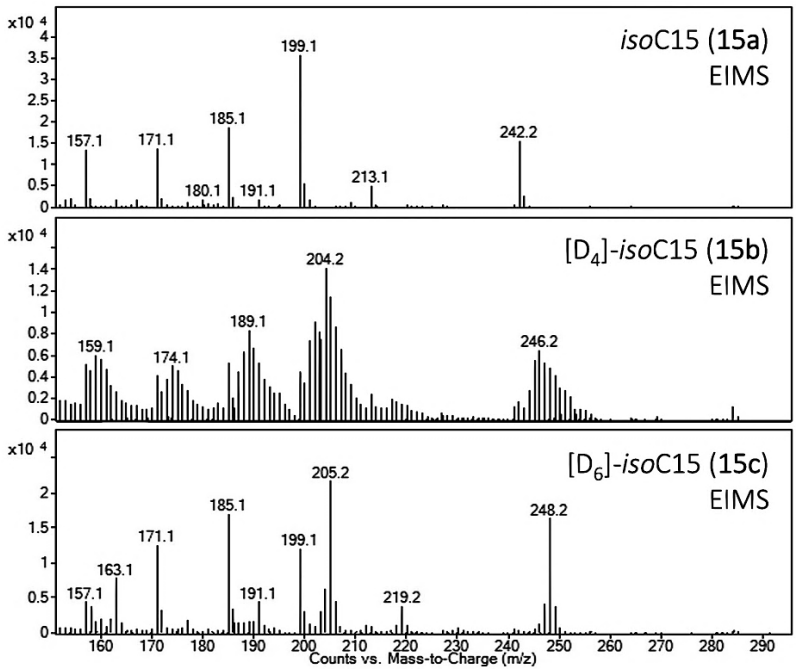

Figure 69. GC-MS spectra of the *iso*-fatty acids *iso*C15 (**15a**), [D_4]-*iso*C15 (**15b**), and [D_6]-*iso*C15 (**15c**).

8.3.3 Iso-fatty acids as dietary supplements for *elo-5* and *elo-5/daf-22* worms

Application of the *iso*-fatty acid isotopomers as dietary supplements for the cultivation of *elo-5* and *elo-5/daf-22* worms required optimization of the incorporation conditions. The best conditions were obtained by using a dietary mixture of 50 µL of *iso*-fatty acid solution (10 mM in ethanol) per 450 µL of *E. coli* OP50 for each uniformly seeded 6 cm NGM-agar plate. All the incorporation experiments were performed in triplicates at 23 °C.

Initial feeding experiments on NGM-agar plates with 11-methyldodecanoic acid (*iso*C13, **16a**), 13-methyltetradecanoic acid (*iso*C15, **15a**), and 15-methylhexadecanoic acid (*iso*C17, **17a**) were performed to verify nematode growth with the external fatty acid supplement. The development of *elo-5* worms with *iso*C17 (**17a**) supplements was faster and reached higher population densities. It was observed that the number of nematodes per plate depends on the supplied fatty acid and follows the order *iso*C17 (**17a**) > *iso*C15 (**15a**) > *iso*C13 (**16a**). Furthermore, it was noticed that *elo-5* worms arrested in L1 diapause when the dietary supplement was consumed, and that without any *iso*-fatty acid supplement *elo-5* was unable to develop. The double mutants *elo-5/daf-22* exhibited identical developmental limitations but also required longer times (1 or 2 days of difference) to reach the same population density.

Incorporation of non-labelled *iso*-fatty acids shows results that are consistent with previous reports [37]. As expected, there was no difference between unlabelled and [D_6]-labelled *iso*-fatty acids as supplements. Figure 70 shows a summary of the development of *elo-5* and *elo-5/daf-22* mutants supplemented with [D_6]-*iso*-fatty acids. Culture growth depends on the labelled *iso*-fatty acid supplement by following the order [D_6]-15-methylhexadecanoic acid ([D_6]-*iso*C17, **17c**) > [D_6]-13-methyltetradecanoic acid ([D_6]-*iso*C15, **15c**) > [D_6]-11-methyldodecanoic acid ([D_6]-*iso*C13, **16c**). Moreover, it was found that without any [D_6]-*iso*-fatty acid supplementation the worms could not develop. The double mutant *elo-5/daf-22* achieved the same population density as *elo-5* in an additional 1 or 2 days.

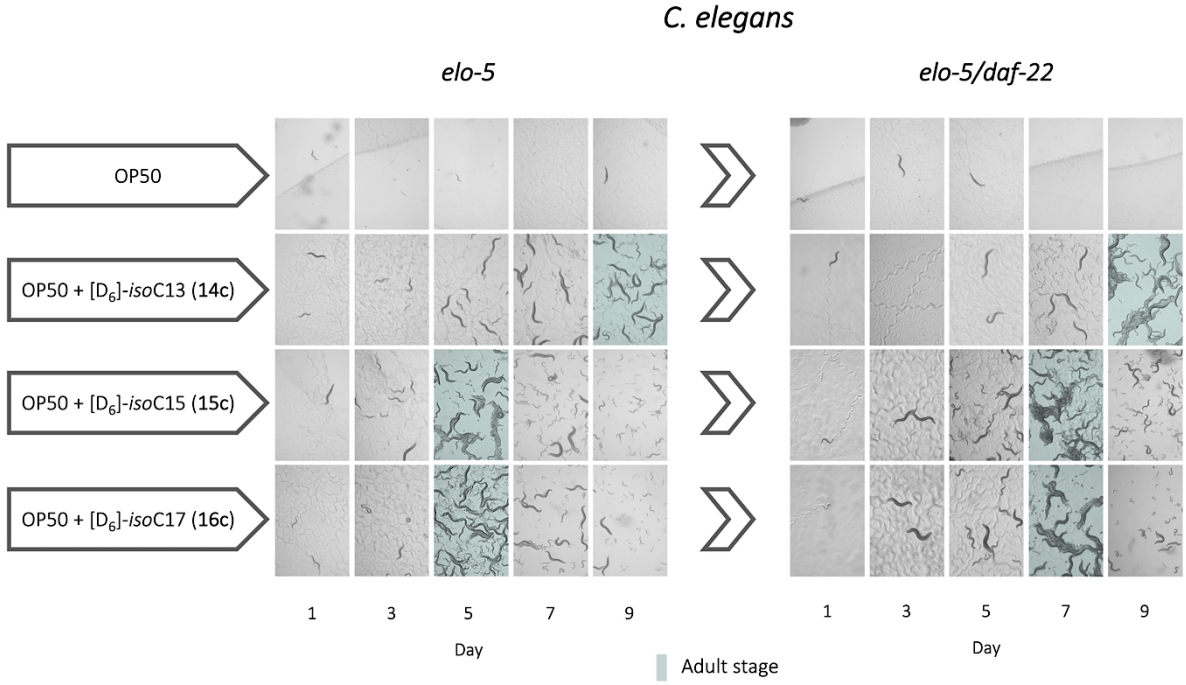

Figure 70. Monitoring the development of *elo-5* and *elo-5/daf-22* with [D_6]-*iso*-fatty acids as dietary supplements.

8.3.3.1 Incorporation studies of *iso*-fatty acids in *elo-5* and *elo-5/daf-22* worms

In section 8.1.1.2 it was described that the biosynthesis of *iso*-branched ascarosides depends on L-leucine (**14**) as a biosynthetic precursor. Furthermore, it was hypothesized that L-leucine (**14**) could incorporate into essential *iso*-fatty acids such as 13-methyltetradecanoic acid (*iso*C15, **15a**) and 15-methylhexadecanoic acid (*iso*C17, **17a**), and that these could act as building blocks in the biosynthesis of *iso*-branched aglycones. To probe this proposal, incorporation experiments with *elo-5* worms fed with the *iso*-fatty acids or their [D_6]-isotopomers along with the *E. coli* bacterium were developed.

In *C. elegans*, the ELO-5 elongase has been reported to play a role in the production of *iso*C15 (**15a**) and *iso*C17 (**17a**) from *iso*C13 (**16a**) [37] [45] [72]. Therefore, incorporation of the [D_6]-enrichment into the ascaroside *iso*-branch aglycone by using [D_6]-11-methyldodecanoic acid ([D_6]-*iso*C13, **16c**), [D_6]-13-methyltetradecanoic acid ([D_6]-*iso*C15, **15c**) and [D_6]-15-methylhexadecanoic acid ([D_6]-*iso*C17, **17c**), as dietary supplements was analyzed. Cultivation of worms with the same non-labelled *iso*-fatty acids was used as a control. Nematode cultures supplied with mixtures of OP50, and *iso*-fatty acid were cultivated until the worm's reached adulthood. Nematodes were collected, lyophilized, and extracted with methyl *tert*-butyl ether (MTBE) prior to analysis by LC-MS. APCI-(-)-MS source was used to screen the *iso*-alkyl ascarosides for [D_6]-enriched as an indication for incorporation of [D_6]-*iso*-fatty acids.

The analytical results show that no [D_6]-enrichment was observed in any of the *iso*-branched alkyl ascarosides when [D_6]-*iso*C13 (**16c**) and [D_6]-*iso*C15 (**15c**) were used as dietary supplements. However, when [D_6]-*iso*C17 (**17c**) was employed, small levels of [D_6]-enriched *iso*-alkyl ascarosides were observed. For example, [D_6]-enrichment of (2*S*,3*R*,5*R*,6*R*)-2-methyl-6-(((*R*)-24-methylpentacosan-2-yl)oxy)tetrahydro-2*H*-pyran-3,5-diol (**asc-*i*C26-H**, **43a**) demonstrated that the *iso*-fatty acid [D_6]-*iso*C17 (**17c**) can serve as a precursor for the *iso*-branched aglycone (Figure 71). Nevertheless, the very low level of incorporation further shows that the supplemented [D_6]-*iso*C17 (**17c**) was not the dominant source of the *iso*-alkyl aglycones.

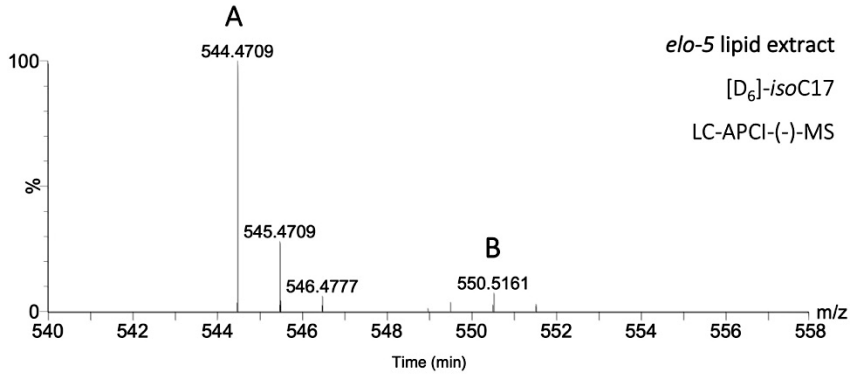

ascaroside	$[M+O_2]^-$
asc-*i*C26-H (43a)	$[C_{32}H_{64}O_6]^-$ = A
[D_6]-asc-*i*C26-H	[D_6]-$[C_{32}H_{64}O_6]^-$ = B

Figure 71. APCI-(-)-MS spectrum of **asc-*i*C26-H** (**43a**) obtained from the lipid extract of *elo-5* worms cultured with [D_6]-15-methylhexadecanoic acid ([D_6]-*iso*C17, **17c**).

Investigation of the free fatty acid composition of *elo-5* worms cultured with 11-methyldodecanoic acid (*iso*C13, **16a**), 13-methyltetradecanoic acid (*iso*C15, **15a**) and 15-methylhexadecanoic acid

(*iso*C17, **17a**) demonstrated that the *elo-5*(gk208) loss of function mutant is not fully defective in *iso*-fatty acid biosynthesis, in contrast with literature reports [36] [37] [40] (Figure 72). When *iso*C13 (**16a**) was used as a dietary supplement small amounts of *iso*C13 (**16a**), *iso*C15 (**15a**), *iso*C17 (**17a**), and *iso*C19 (17-methyloctadecanoic acid) were found. Furthermore, supplementation of *elo-5* worms with *iso*C15 (**15a**) shows a moderate content of *iso*C15 (**15a**) and a higher content of *iso*C17 (**17a**). When *iso*C17 (**17a**) was incorporated, reduction of *iso*C15 (**15a**), *iso*C17 (**17a**), and *iso*C19 (17-methyloctadecanoic acid) was observed in the *elo-5* extracts, suggesting chain shortening via the β-oxidation cycle.

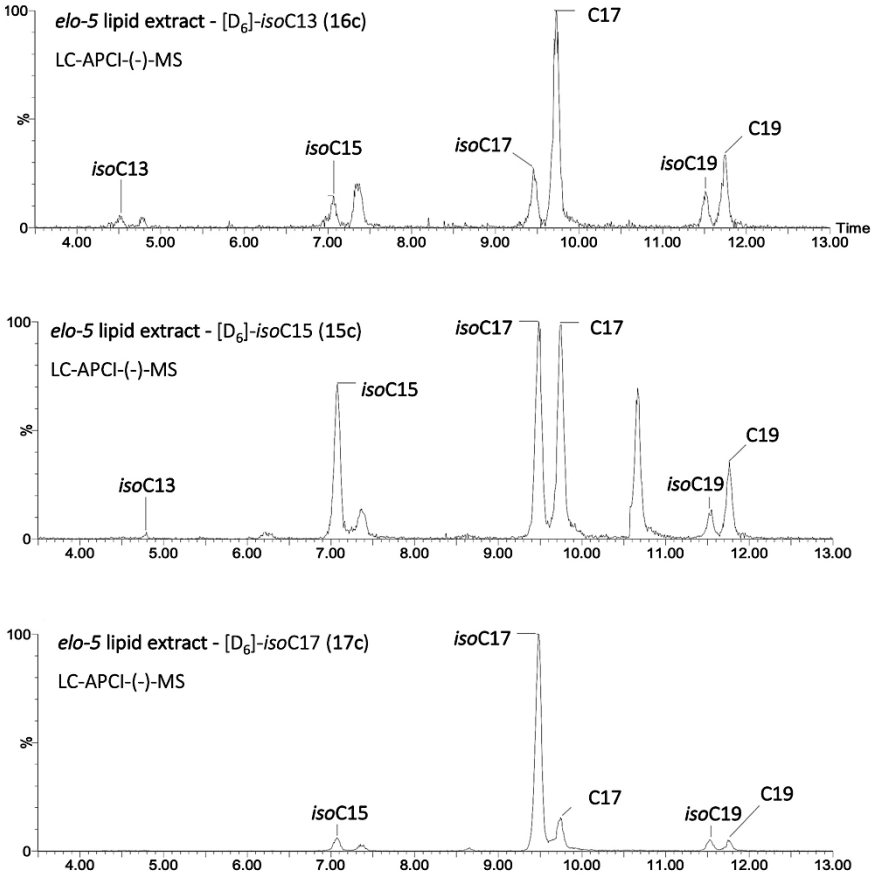

Figure 72. *Iso*-fatty acid content of *elo-5* lipid extracts after using *iso*-fatty acids as dietary supplements.

Having shown that incorporation of supplemented *iso*-fatty acids is not the dominant source for the *iso*-alkyl aglycone in ascarosides, potential [D_6]-enrichment of sphingolipids was evaluated. Sphingolipids in *C. elegans* possess a C17 *iso*-branched sphingoid bases (d17:*iso*-sphinganine) [46] [47] [42] [45], which provides characteristic fragment ions that can be used for targeted screens. Based on this fragmentation, ESI-(+)-MS^2 screening of sphingolipids (Figure 73) provides peaks derived from the neutral loss of *N*-acyls groups as ketene at *m/z* 238.3 ($[C_{16}H_{32}N]^+$), 250.3 ($[C_{17}H_{32}N]^+$) and 268.3 ($[C_{17}H_{34}NO]^+$) [45]. Nevertheless, the HR-MS/MS analysis of the *C. elegans* sphingolipids in this research

uses only the most intense fragment ion at *m/z* 250.3 ($[C_{17}H_{32}N]^+$) along with the mass of its [D_6]-isotopomer at *m/z* 256.3 ($[C_{17}H_{26}D_6N]^+$) for detection.

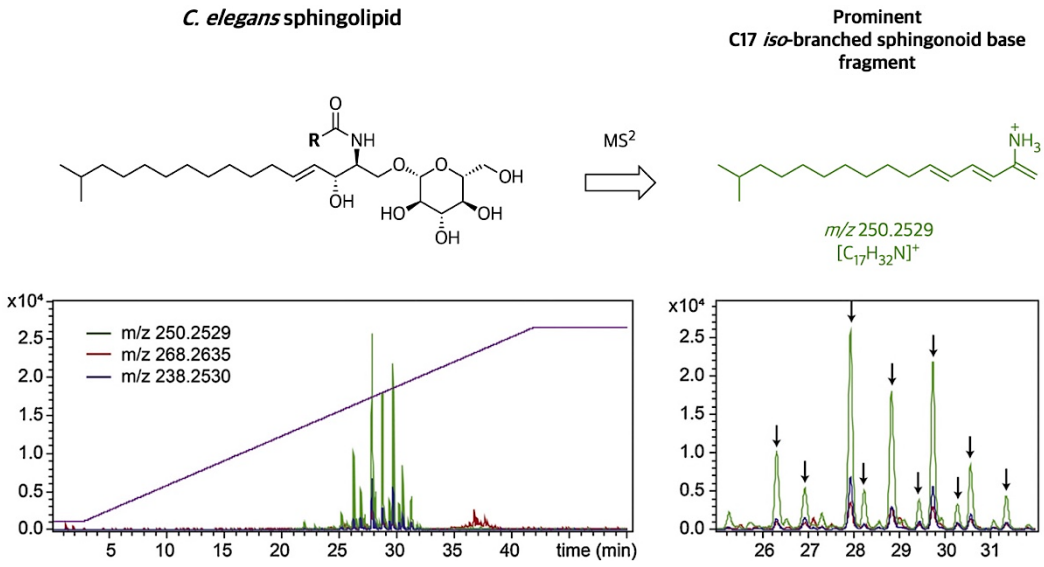

Figure 73. Common MS^2 fragmentation of C17 *iso*-branched sphingoid bases in *C. elegans* [45].

In LC-ESI-(+)-MS/MS analyses of *elo-5* lipid extracts supplemented with [D_6]-*iso*C13 (**16c**) and [D_6]-*iso*C15 (**15c**), the screening for the fragment ion $[C_{17}H_{26}D_6N]^+$ at *m/z* 256.3 did not show any [D_6]-enrichment of sphingolipids. Although *iso*C15 (**15a**) has been established as a biosynthetic intermediate in sphingoid biosynthesis. However, cultures supplemented with [D_6]-*iso*C17 (**17c**) show exclusively [D_6]-enriched sphingolipids (Figure 74). Characteristic fragment ions at *m/z* 250.3 ($[C_{17}H_{32}N]^+$) and 256.3 ($[C_{17}H_{26}D_6N]^+$) were observed when *iso*C17 (**17a**) and [D_6]-*iso*C17 (**17c**) were used as supplements, respectively.

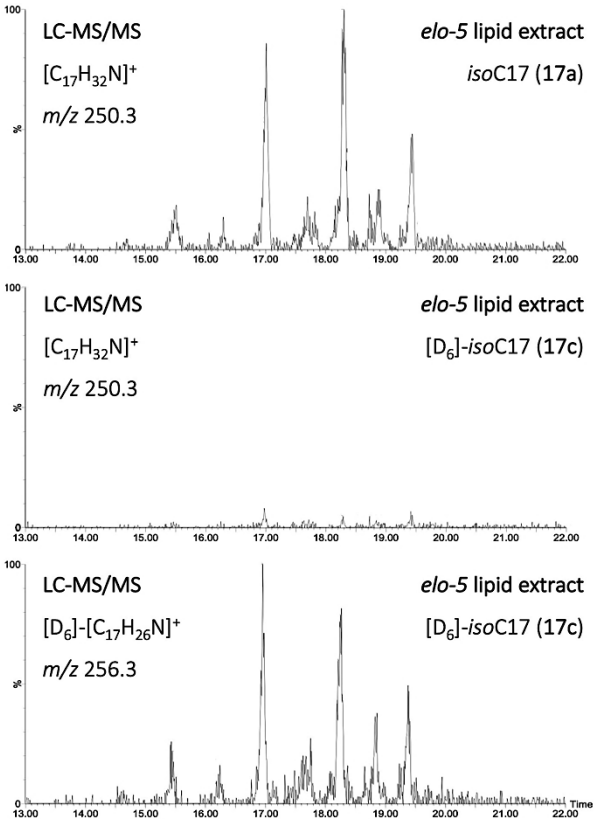

Figure 74. ESI(+)-MS/MS screening for sphingolipids using *m/z* 250.3 ($[C_{17}H_{32}N]^+$) and 256.3 ($[C_{17}H_{26}D_6N]^+$) in *elo-5* cultures supplemented with *iso*C17 (**17a**) and [D_6]-*iso*C17 (**17c**).

Based on previous investigations [46] [73], *iso*-branched sphingolipids in *C. elegans* are derived from the condensation of 13-methyltetradecanoic acid (*iso*C15, **15a**) and L-serine (**18**, Figure 10). Consequently, the lipid analysis performed here shows that in the *elo-5* mutant, the supplemented *iso*C17 (**17a**) is shortened to *iso*C15 (**15a**) for its incorporation into sphingolipids. To determine if the *iso*-sphingolipid production in *C. elegans* involves β-oxidation by the β-ketoacyl-CoA thiolase (*daf-22*), incorporation of [D_6]-*iso*C17 (**17c**) in the *elo-5/daf-22* double mutant was analyzed by LC-ESI-(+)-MS. Lipid extracts from liquid cultures grown with [D_6]-*iso*C17 (**17c**) show no [D_6]-enrichment of sphingolipids (Figure 75). Therefore, it was concluded that the incorporation of *iso*C17 (**17a**) into sphingolipids requires the DAF-22 enzyme and proceeds via peroxisomal β-oxidation of *iso*C17 (**17a**) to *iso*C15 (**15a**) as a known precursor of sphingolipids.

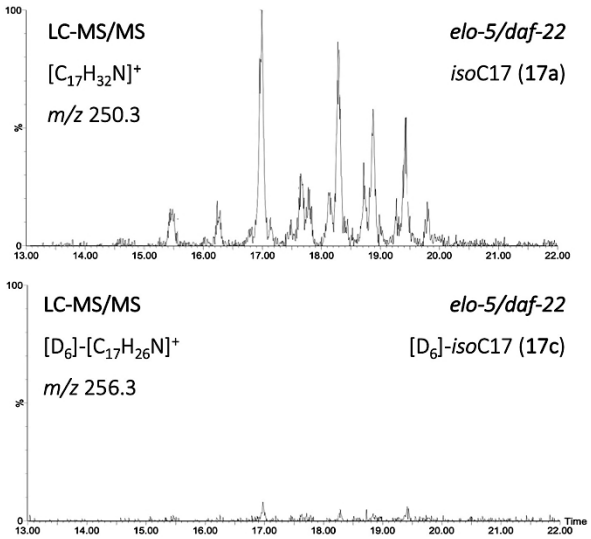

Figure 75. ESI(+)-MS/MS screening for sphingolipids using *m/z* 250.3 ($[C_{17}H_{32}N]^+$) and 256.3 ($[C_{17}H_{26}D_6N]^+$) in *elo-5/daf-22* cultures supplemented with *iso*C17 (**17a**) and $[D_6]$-*iso*C17 (**17c**).

The lipid metabolism studies performed during this research revealed interesting results summarized in Figure 76. In brief, 15-methylhexadecanoic acid (*iso*C17, **17a**) represents a poor precursor for *iso*-alkyl ascarosides. The *elo-5* loss of function mutant is not defective in the elongation of *iso*-fatty acids, in contrast to previous reports [36] [37] [40]. Supplements of 11-methyldodecanoic acid (*iso*C13, **16a**) and 13-methyltetradecanoic acid (*iso*C15, **15a**) are poor precursors for the biosynthesis of *iso*-fatty acids, whereas *iso*C17 (**17a**) has been demonstrated to be a better precursor for the biosynthesis of *iso*-fatty acids such as *iso*C15 (**15a**), *iso*C17 (**17a**) and 17-methyloctadecanoic acid (*iso*C19). Incorporation of *iso*C17 (**17a**) into sphingolipids proceeds via peroxisomal β-oxidation.

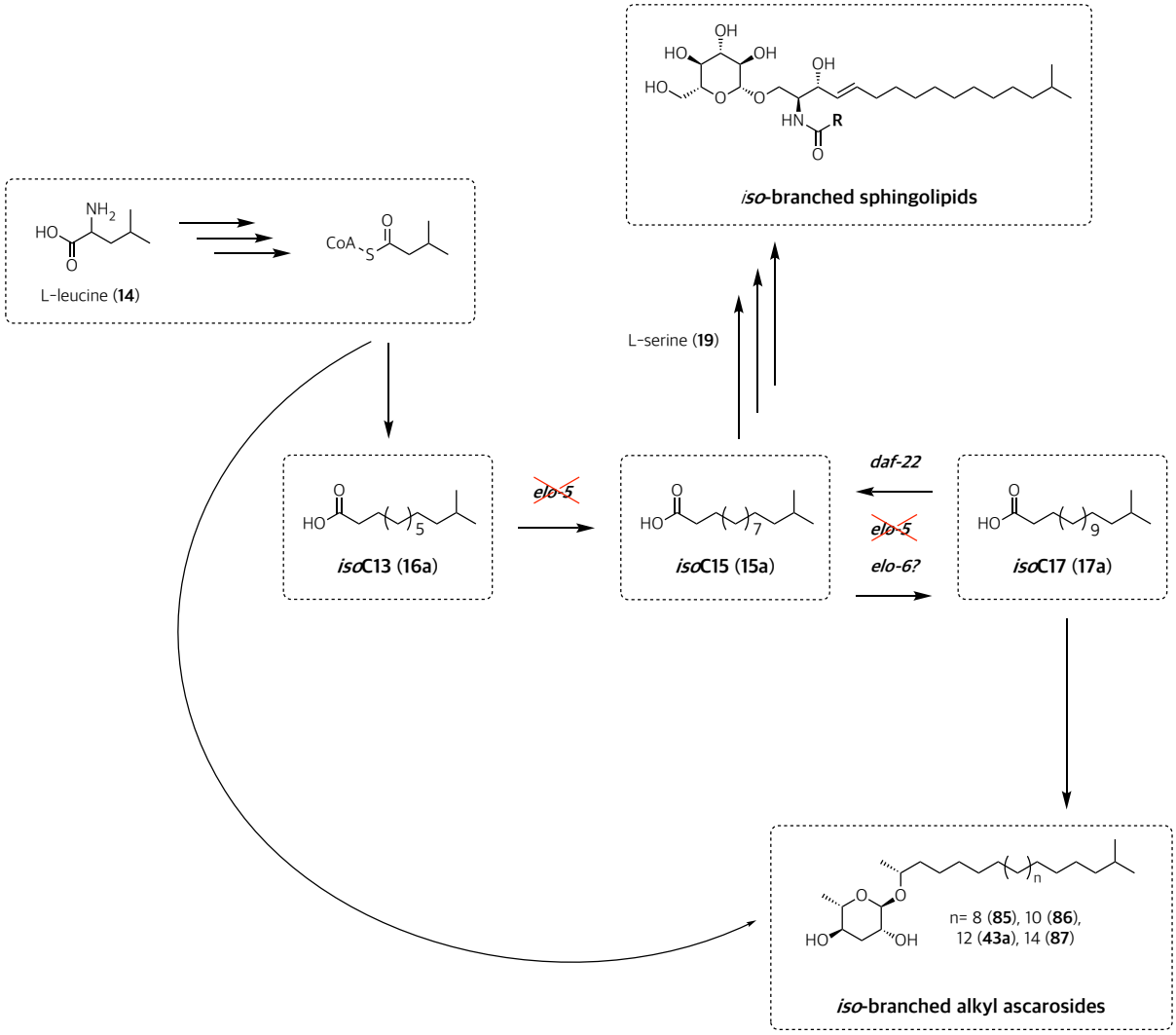

Figure 76. Summary of the results observed with the *iso*-fatty acid incorporation experiments in *C. elegans*. Examples of the *iso*-branched structures of the alkyl ascaroside and sphingolipid are referential.

8.3.3.2 [D_6]-15-methylhexadecanoic acid and the identification of 2-(9-methyldecanamido)ethyl ((2*S*,3*R*,4*S*,5*S*,6*R*)-3,4,5-trihydroxy-6-(hydroxymethyl)tetrahydro-2*H*-pyran-2-yl) phosphate

[D_6]-15-methylhexadecanoic acid ([D_6]-*iso*C17, **17c**) has proven to be a good precursor for *iso*-fatty acid derived metabolites in *C. elegans*. **17c** was also employed for the study of the biosynthesis of branched-chain *N*-isoacyl ethanolamine derivatives characterized in various *Caenorhabditis* species. The (2*S*,3*R*,4*S*,5*S*,6*R*)-3,4,5-trihydroxy-6-(hydroxymethyl)tetrahydro-2*H*-pyran-2-yl hydrogen (2-(9-methyldecanamido)ethyl)phosphonate (gnap-*iso*-11:0, **127**) (Figure 77) was identified in previous studies focusing on nematode derived modular metabolome (NDMMs) by Dr. Siva Bandi. Aiming to

detect its biosynthetic origin, a feeding experiment was performed in which the *C. brenneri* nematode was fed with an *E. coli Δleu Δile Δval* mutant grown in a 1:1 mixture of L-[U-$^{13}C_6$]-leucine and L-[U-$^{12}C_6$]-leucine. The [$^{13}C_5$]-incorporation into gnap-*iso*-11:0 (**127**) demonstrated that *iso*-fatty acids are involved in its biosynthesis (Figure 78-A). Feeding experiments with the *C. elegans elo-5* (gk208) loss of function mutant supplemented with either *iso*C17 (**17a**) or [D_6]-*iso*C17 (**17c**) were performed to confirm its pathway (Figure 78-B and C). Since the relative amounts of the target compound in the metabolome were very small, liquid cultures of *elo-5* were required to obtain larger quantities. The same 1:9 dietary mixture of *iso*C17 (**17a**) or [D_6]-*iso*C17 (**17a**) solution (10 mM) per *E. coli* OP50 was used as part of the culture medium. Nematodes were cultivated in triplicate in 100 mL of S-medium at 180 rpm and 20 °C. After 12 days, the worms were centrifuged and the exometabolomes were frozen at -20 °C and lyophilized. LC-ESI-(-)-MS analyses of the extracts revealed signals at *m/z* 470.2161 corresponding to the mass of gnap-*iso*-11:0 (**127**) upon feeding with *iso*C17 (**17a**), whereas feeding with [D_6]-*iso*C17 (**17c**) furnished exclusively [D_6]-gnap-*iso*-11:0 with *m/z* 476.2537. Therefore, it was demonstrated that gnap-*iso*-11:0 (**127**) is exclusively derived from chain shortening of *iso*C17 (**17a**) and not from direct synthesis of *iso*-C11:0. Moreover, these results demonstrated that the use of [D_6]-labelled *iso*-fatty acids represents a powerful tool to study the *iso*-fatty acid metabolism in *C. elegans* and other *Caenorhabditis* species.

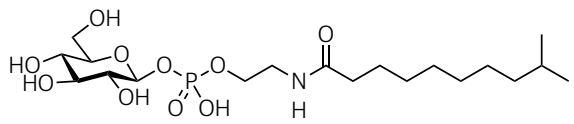

gnap-*iso*-11:0 (**127**)

(2*S*,3*R*,4*S*,5*S*,6*R*)-3,4,5-trihydroxy-6-(hydroxymethyl)tetrahydro-2*H*-pyran-2-yl hydrogen (2-(9-methyldecanamido)ethyl)phosphonate

Figure 77. β-glucosyl *N*-acyl phosphoethanolamine (gnap-*iso*-11:0, **127**).

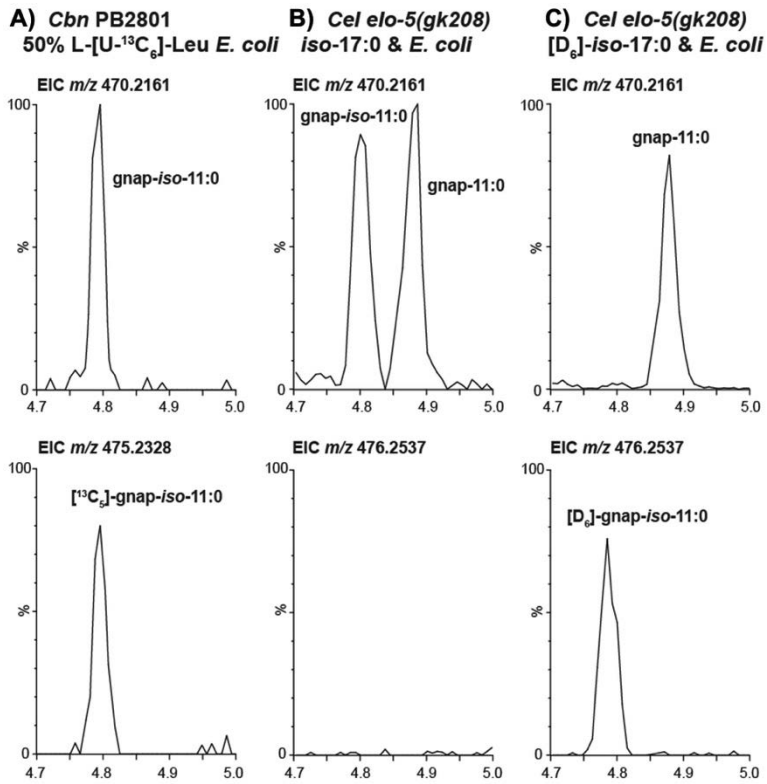

Figure 78. Comparative analysis of extracted ion traces of the exometabolomes of *C. brenneri* and *C. elegans elo-5* show [$^{13}C_5$]-enrichment upon incorporation of L-[$^{13}C_6$]-leucine, and [D_6]-enrichment upon incorporation of [D_6]-*iso*C17 (**17c**).

8.3.4 Conclusions

- Three *iso*-fatty acids and their stable isotope labelled [D_4] or [D_6] isotopomers were synthesized: 11-methyldodecanoic acid (*iso*C13, **16a**), 13-methyltetradecanoic acid (*iso*C15, **15a**) and 15-methylhexadecanoic acid (*iso*C17, **17a**), as well as their [D_6]-isotopomers: [D_6]-11-methyldodecanoic acid ([D_6]-*iso*C13, **16c**), [D_6]-13-methyltetradecanoic acid ([D_6]-*iso*C15, **15c**) and [D_6]-15-methylhexadecanoic acid ([D_6]-*iso*C17, **17c**), and the supplementary [D_4]-11-methyldodecanoic acid ([D_4]-*iso*C13, **16b**) and [D_4]-13-methyltetradecanoic acid (D_4]-*iso*C15, **15b**).

- *Iso*-fatty acids have been used as dietary supplements for the study of lipid metabolism in *C. elegans*. Feeding experiments with incorporation of *iso*C13 (**16a**), *iso*C15 (**15a**), *iso*C17 (**17a**), [D_6]-*iso*C13 (**16c**), [D_6]-*iso*C15 (**15c**) and [D_6]-*iso*C17 (**17c**) in *elo-5* and *elo-5/daf-22* worms were performed.

- Analysis of incorporation experiments demonstrated that the ELO-5 enzyme is not essential for *iso*-fatty acid production in *C. elegans*.

- The fatty acid *iso*C17 (**17a**) is a poor precursor for the biosynthesis of *iso*-alkyl ascarosides in *C. elegans*.

- Exogenous *iso*C17 (**17a**) is incorporated into sphingolipids via β-oxidation by *daf-22*.

- The incorporation of [D_6]-*iso*C17 (**17c**) in *elo-5* demonstrated that (2*S*,3*R*,4*S*,5*S*,6*R*)-3,4,5-trihydroxy-6-(hydroxymethyl)tetrahydro-2*H*-pyran-2-yl hydrogen (2-(9-methyldecanamido)ethyl)phosphonate (gnap-*iso*-11:0, **127**) is exclusively derived from chain shortening of *iso*C17 and not from direct synthesis of *iso*-C11:0.

- Incorporation experiments with [D_6]-*iso*-fatty acid isotopomers as molecular probes represent a powerful tool to study the *iso*-fatty acid metabolism in *C. elegans*.

9 Conclusions and outlook

The model organism *Caenorhabditis elegans* uses ascarosides to modulate its development according to population density. Modular ascarosides play a crucial role in the worm's lifespan, being highly species-specific and representing the individual language of each species. The biosynthesis of ascarosides in *C. elegans* indicates that very long chain fatty acids and ascarylose act as biosynthetic precursors. Nevertheless, the origin of the building blocks involved in ascaroside aglycone biosynthesis has remained unclear up to date. Recent studies from Dolke and von Reuss revealed that the biosynthesis of ascarosides might involve 3-hydroxy fatty acids as precursors of very long chain alkyl ascaroside intermediates. In contrast to previous proposals, fatty acid elongation upon lipogenesis and chain shortening via the peroxisomal β-oxidation cycle are believed to operate from opposite sides of the aglycones. Therefore, (ω)-carboxy alkyl ascarosides might act as biosynthetic intermediates of very long chain alkyl ascarosides, which are subsequently oxidized to furnish of the very long chain acyl ascarosides as precursors for the peroxisomal β-oxidation cycle. Furthermore, it was proposed that ascarosides with *iso*-branched aglycones could use *iso*-fatty acids as precursors. Thus, the present research aimed to confirm these hypotheses by identification of the putative biosynthetic intermediates, as well as incorporation experiments with stable isotope labelled compounds.

The detection of very long chain alkyl ascarosides in *C. elegans daf-22* (based on authentic standards) supports the hypothesis that suggests their potential function as precursors of acyl ascarosides. Moreover, the assumption of (ω)-carboxy ascarosides as biosynthetic intermediates is supported by the identification of very long chain alkyl ascarosides in *C. elegans daf-22*, although the structural assignment of putative (ω)-carboxy ascarosides could not be confirmed. In parallel, the detection of very long chain alkyl ascarosides series in several nematode species demonstrates that alkyl ascarosides are *daf-22* independent. These results were obtained by using LC-APCI-(-)-MS and GC-EIMS as analytical techniques. Electron ionization (EI) induced fragmentation of TMS-derivatized acyl ascarosides reported in the literature coincided with the fragmentation exhibited for the very long chain alkyl ascarosides, which exhibit a characteristic marker at *m/z* 119.1 ($[C_4H_{11}O_2Si]^+$). In addition, a marker ion at *m/z* 161.1 ($[C_6H_{13}O_3Si]^+$) for 4-acetylated ascarosides was detected during the systematic analysis of the authentic standards. LC-APCI-(-)-MS represents a particularly efficient technique for the detection of the very long chain alkyl ascarosides, whereas poor ionization was observed when using ESI-MS methods due to the lipophilic characteristics of the very long chain. The poor ionization of very long chain alkyl ascarosides with ESI-MS methods could explain why these widely distributed alkyl ascarosides have never been detected in *C. elegans* and other nematodes before (apart from *Ascaris*

sp.). Therefore, a reanalysis of the *daf-22* exo- and endometabolome will be required to detect additional putative biosynthetic intermediates in ascaroside biosynthesis. Additional screening for (ω)-carboxy ascarosides and other derivatives is suggested. They might potentially be isolated and identified by NMR spectroscopic techniques. In a more general way, the use of APCI-(-) is strongly advised to reanalyze various nematode exo- and endometabolome, tissues, and eggs to screen for very long chain alkyl ascarosides.

The study of the origin of *iso*-branch aglycones in ascarosides involved the use of *iso*-fatty acid isotopomers as molecular probes, in which it was found that incorporation experiments with [D_6]-*iso*-fatty acids represented a powerful tool to study the *iso*-fatty acid metabolism in *C. elegans*. For example, the *iso*-branched *iso*C17 has been shown to represent a precursor for the biosynthesis of *iso*-alkyl ascarosides in *C. elegans*, but other *elo-5* independent pathways are dominating. Moreover, and in contrast to previous reports, it was found that the ELO-5 enzyme is not essential for the elongation of *iso*-fatty acids in *C. elegans*. Instead, the homologous series of odd-numbered *iso*-fatty acid series (*iso*C13, *iso*C15, and *iso*C17) was identified in the *elo-5(gk208)* loss of function mutant.

On the point of view of the synthesis, it was observed that the preparation of monoacetyl derivatives provided mixtures of 2- and 4-acetyl alkyl ascarosides upon partial acetylation or partial hydrolysis. However, partial hydrolysis of the 2,4-diacetyl ascaroside furnished larger quantities of the desired 4-monoacetyl derivative. Furthermore, an optimized procedure for alkyne alkylation was developed for the synthesis of highly lipophilic alkyl chains, but the preparation of non-alkyl chains, such as those with acyl groups, cannot be accomplished with this procedure.

Finally, for future investigations focused on ascaroside biosynthesis, the application of the [D_4]-labelled very long chain alkyl ascaroside isotopomers as molecular probes in feeding experiments with *daf-22* mutants is suggested. This incorporation could confirm their role as biosynthetic intermediates in ascaroside biosynthesis. The identification of very long chain alkyl ascarosides in *C. elegans* will enable the screening of mutants for defects in alkyl ascaroside biosynthesis and thereby help to decipher the biosynthetic pathway that connects lipogenesis and ascaroside signaling in nematodes.

10 Materials and methods

10.1 Chemicals and analytical instrumentation

Commercial reagents were employed without purification, and dry solvents were commercially purchased. Column chromatographic separations were performed with silica gel SiO_2 60Å (6 mm pore sieve) from Carl-Roth. Thin layer chromatography (TLC) was carried out using 0.20 mm silica gel 60 F254 on alumina backed plates from Macherey-Nagel. Visualization of the compounds on plates used UV light (254 nm) or staining with potassium permanganate solution (3 g $KMnO_4$, 20 g K_2CO_3, 5 mL 1 M NaOH, 300 mL H_2O) and/or thymol solution (1 g thymol, 100 mL EtOH, 5 mL H_2SO_4 conc.) followed by heating.

10.1.1 NMR spectroscopy

NMR spectra of synthetic products were recorded in $CDCl_3$ at 400 MHz for ^1H and 100 MHz for ^{13}C using a Bruker Avance II 400 instrument equipped with a 5 mm BBFO probe (NPAC, UniNE) or/and at 600 MHz for ^1H and 151 MHz for ^{13}C using a Bruker Avance Neo Ascend 600 MHz equipped with a 5 mm BB1 probe (BBI H-BB-D-05 Z) NPAC, UniNE. Residual solvent signals at 7.26 ppm for ^1H and at 77.16 ppm for ^{13}C were used as internal references. Two-dimensional homonuclear double quantum filtered (*dqf*)-COSY spectra were recorded employing phase cycling for coherence selection. ^{13}C NMR data were obtained from broadband decoupled ^{13}C $\{^1H\}$ or HSQC and HMBC spectra. Chemical shifts (δ) are expressed in parts per million (ppm) and coupling constants (J) in hertz (Hz). Spectra were zero-filled prior to Fourier transformation, phased, and baseline corrected. Processing and analyses were performed using the Mnova NMR software package (v.14.2.0, MestReLab Research S.L., Spain).

10.1.2 Gas chromatography-electron ionization-mass spectrometry (GC-EIMS).

GC-MS analysis of natural and synthetic samples was performed using a GC 7890B coupled to MSD 5977 (Agilent). Chromatographic separations were achieved using a Zebron ZB-5 Guardian column (15 m, 0.25 mm ID, 0.25 µm film thickness with 10 m guardian end) with helium as the carrier gas at a flow rate of 1 mL/min. A temperature program starting at 130 °C for 5 min, followed by a linear gradient of +10 °C/min with to 350 °C. A total volume of 1 µL was injected using a 10:1 split ratio and an injector

temperature of 250 °C. 70 eV mass spectra were acquired from *m/z* 35-650 amu. Data were processed with MassHunter GC/MS Acquisition B.07.02.1938 08-Sep-2014, Agilent Technologies, Inc.

10.1.3 TMS-derivatization

TMS-derivatization of ascarosides was performed as described by von Reuss *et al.* [21]. 10 µL of 0.1 mg/mL solution were placed in a vial, and the solvent was removed. To the residue were added 10 µL of *N*-methyl-*N*-(trimethylsilyl)trifluoroacetamide (MSTFA) and the resulting mixture was heated at 60 °C for 40 min. The mixture was diluted with 20 µL of dry DCM before analysis.

10.1.4 Liquid chromatography electrospray ionization (LC-ESI(+/-)-MS) and atmospheric pressure chemical ionization (LC-APCI(+/-)-MS) mass spectrometric

Analyses of very long chain ascarosides, ω-carboxy ascarosides and nematode extracts were performed using an Acquity ultra-high-pressure liquid chromatography (UHPLC) system coupled to a Synapt G2 QTOF mass spectrometer (Waters, Milford, MA, USA) controlled by MassLynx 4.1. The separation was performed on a Waters Acquity BEH C18 column (100 × 2.1 mm i.d., 1.7 µm particle size) thermostated at 80 °C using a linear gradient from 60 to 100% in 20 min and at 100% for 6 min. When ESI was used as probe, mobile phases consisted of water containing 0.1% of ammonium formate 10 mM (solvent A) and acetonitrile containing 0.1% of ammonium formate 10 mM (solvent). When APCI was used as probe, mobile phases consisted of water (solvent A) and methanol (solvent B). Mass spectra were acquired from 50 Da to 1200 Da. Data were analyzed with the MassLynx software (Waters, Milford, MA, USA).

10.2 Organisms and nematodes culturing

Lipid analyses were performed using *C. elegans* wildtype (N2) and *elo-5*(*gk208*) strain VC410 from the *Caenorhabditis elegans* Genetics Center (CGC) and *elo-5(gk208)/daf-22(oh693)* double mutant from the wildtype strain of PB4641. The strains and species: *C. elegans* (N2), (AB1), (CB4856), *C. brenneri* (PB2801), *C. remanei* (PB4641), *C. wallacei* (JU1904), *C. nigoni* (JU1422), *C. tropicalis* (JU1373) and *Ascaris lumbricoides* (from WARD'S Science preserved) were used for metabolic studies. For maintenance, the nematodes were cultivated at 15 °C on 6 cm NGM-agar plates. Pure *Escherichia coli* OP50 was used as a food source for the maintenance and study of worms without mutations. However, the diet for *elo-5* and *elo-5/daf-22* worms required a mixture of *E. coli* OP50 and a 10 mM solution of

synthetic *iso*-fatty acid (9:1) for metabolic studies and pure *Bacillus subtilis ilvB2 leuA169* (GB7044) for conservation. Furthermore, preparation of [U-^{13}C]-labelled *E. coli* and L-[U-$^{13}C_6$]-leucine or L-[U-$^{12}C_5$]-valine enriched *E. coli* was performed for metabolic studies. The preparation of bacteria and solutions was performed as reported in the literature [55] [24].

10.2.1 *Iso*-fatty acid depleted *C. elegans elo-5*

C. elegans elo-5 mutants maintained on *Stenotrophomonas maltophilia* were bleached and the released eggs were placed and grown on seeded NGM-plates with a 1:9 mixture of 10 mM *iso*-fatty acid solution and *E. coli* OP50 at 23 °C. After 3 to 5 days, depending on the worm's development, the young adults were transferred to a fresh plate. Subsequent cultivation of the worms for a minimum of 2 generations was necessary before the bleaching was repeated to generate the final axenic culture. Axenic worms were transferred for a minimum of 4 generations using the same fatty acid supplement, before large scale cultivation for further analyses. To confirm the successful removal of *S. maltophilia*, axenic *elo-5* worms were transferred to plates with OP50 as a food source, in which L1 arrested worms would show after 3 to 5 days. Subsequent transfer of L1 to a new OP50 plate without *iso*-fatty acid supplement was done to ensure their axenic state.

10.2.2 *Iso*-fatty acid incorporation and lipid analysis

10.2.2.1 *Iso*-fatty acid supplemented plates

NGM-agar plates supplemented with the *iso*-fatty acids: 11-methyldodecanoic acid (*iso*C13, **14a**), [D_6]-11-methyldodecanoic acid ([D_6]-*iso*C13, **14c**), 13-methyltetradecanoic acid (*iso*C15, **15a**), [D_6]-13-methyltetradecanoic acid ([D_6]-*iso*C15, **15c**), 15-methylhexadecanoic acid (*iso*C17, **16a**), and [D_6]-15-methylhexadecanoic acid ([D_6]-*iso*C17, **16c**), were prepared for the development of *elo-5* and *elo-5/daf-22* worms. The dietary mixtures were prepared with overnight OP50 culture and a 10 mM *iso*-fatty acid solution in a 9:1 ratio. For example, the preparation of *iso*C17 plates required the mixing of 1 mL of 2.7 mg/mL *iso*C17 (**16a**) solution and 9 mL of OP50 prior to seeding the plates. Each 6 cm plate was supplied with 500 µL of the dietary mixture, dried with the lids on, and stored at 4 °C.

10.2.2.2 Lipid extraction from *iso*-fatty acid supplemented plates

Adult worms grown on 20 small plates (6 cm) seeded with *iso*-fatty acid and OP50 at 23 °C were collected in M9-Buffer. Centrifugation of the mixture for 8 minutes (4696xg) at 5 °C gave worm pellets, which were washed three times with M9-buffer. The liquid phase was removed, the pellets froze at -20 °C and lyophilized. Lipids were extracted (74) from 10 mg of worm pellet using methyl *tert*-butyl methyl ether (MTBE) with vigorous stirring and consecutive sonication for 30 minutes at 0 °C. After addition of 0.5 mL H_2O the mixture was again sonicated for 15 minutes. Centrifugation of the mixture for 15 minutes at 4 °C and 4696xg allowed to separate the pellets from the supernatant. Consecutive re-extractions (2 times) of the aqueous phase with 1.7 mL MTBE and sonication during 15 minutes at room temperature furnished a lipid extract. Combination of the organic phases and evaporation of the solvent gave an oily residue, which was dissolved in ACN-*i*PrOH-H_2O (65:30:5 mL, v/v/v) to get a final concentration of 100 mg dry worms/mL, which was analyzed by LC-MS.

10.2.3 Incorporation of 15-methylhexadecanoic or [D_6]-15-methylhexadecanoic acid for liquid cultures and lipid analysis

10.2.3.1 Liquid cultures

Nematodes grown at 23 °C on six small NGM-plates (6 cm) seeded with a 1:9 mixture of *iso*C17(**16a**)/[D_6]-*iso*C17(**16c**) (10mM) and OP50, were collected in the minimum quantity of S-medium (9 mL) and used as inoculums for liquid cultures. The worms were grown in 100 mL of S-medium at 180 rpm and 20 °C. Concentrated OP50 bacterial pellets (from an overnight culture in LB-medium) were supplemented with 100 µL of a 10 mM solution of *iso*-fatty acid in EtOH, mixed with the minimum quantity of S-medium and used as food from day 1 until day 5. The cultures were grown for a total of 11 days.

10.2.3.2 Lipid extraction from liquid cultures

After 11 days of growth, liquid cultures were individually separated by centrifugation (4696xg during 15 minutes at 4 °C). The supernatant media was frozen at -20 °C, lyophilized, and extracted twice for 12 hours each with 100 mL of MeOH. The combined extracts were filtered, concentrated to dryness (40 °C) and reconstituted with 2 mL of MeOH. From this last solution 50 µL diluted in 50 µL of MeOH was used for LC-MS analysis. The experiments were performed in triplicates.

10.2.3.3 SPE-fractionation of exometabolome extracts

Concentrated exometabolome extracts were fractionated by solid phase extraction (SPE) on 5 g reverse phase C18 cartridges (CHROMABOND). The elution of the fractions employed a stepwise gradient of methanol in water (0 to 100% in 10% steps, v/v) to afford 10 fractions of 20 ml each. The fractions were concentrated to dryness under reduced pressure, reconstituted in methanol, and analyzed by HPLC-ESI-HR-MS/MS.

10.3 Chemical Syntheses

10.3.1 Synthesis of ascarylose

10.3.1.1 (3*R*,4*R*,5*S*,6*S*)-6-methyltetrahydro-2*H*-pyran-2,3,4,5-tetrayl tetrabenzoate (28)

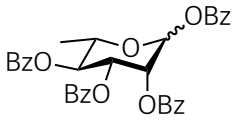

A mixture of 15.3 g of L-rhamnose (**21**) monohydrate (93.17 mmol) with 200 mL of dry pyridine and 60 mL benzoyl chloride (0.52 mol) reacted for 2 hours at 0 °C and at the same temperature. The mixture was warmed to room temperature and stirred overnight. Quenching of the reaction required 30 mL of water and subsequent extraction of the product with DCM. The organic phase was washed several times (4 to 6 times) with portions of 10 M HCl solution followed by saturated $NaHCO_3$ solution (3 times) and dried over anhydrous $MgSO_4$. After concentration at a reduced pressure, 44.8 g (77.16 mol) of white product were obtained (83% yield). The (3*R*,4*R*,5*S*,6*S*)-6-methyltetrahydro-2*H*-pyran-2,3,4,5-tetrayl tetrabenzoate (**28**) was used for the next step without additional purification. **α:** ^{1}H NMR (600 MHz, $CDCl_3$): δ 1.48 (d, J=6.2 Hz, 3H), 4.35 (dq, J=10.0 Hz, J=6.2 Hz, 1H), 5.73 (m, 1H), 5.86 (dd, J=3.4 Hz, J=2.0 Hz, 1H), 6.07 (dd, J=2.8 Hz, J=1.3 Hz, 1H), 6.55 (d, J=1.9 Hz, 1H), 7.24 - 8.20 (m, 20H). ^{13}C NMR (151 MHz, $CDCl_3$): δ 17.9, 69.5, 69.9, 70.0, 71.3, 91.5, 128.5 (2C), 128.6 (2C), 128.7 (2C), 128.8 (3C), 128.9 (3C), 129.0 (2C), 129.9 (2C), 130.0 (2C), 130.2 (2C), 130.3 (2C), 164.2, 165.5, 165.8, 165.9. **β:** ^{1}H NMR (600 MHz, $CDCl_3$): δ 1.39 (d, J=6.2 Hz, 3H), 4.09 (m, 1H), 5.72 (m, 1H), 6.07 (dd, J=2.8 Hz, J=1.2 Hz, 1H), 6.35 (d, J=1.2 Hz, 1H), 7.24 - 8.20 (m, 20H). ^{13}C NMR (151 MHz, $CDCl_3$): δ 17.9, 69.8, 71.3, 71.6, 72.0, 91.3, 128.5 (2C), 128.6 (2C), 128.7 (2C), 128.8 (3C), 129.9 (3C), 130.0 (2C), 130.2 (2C), 130.3 (2C), 133.5 (2C), 133.6 (2C), 133.7, 133.9, 164.4, 165.6, 165.8, 165.9.

10.3.1.2 (3*R*,4*R*,5*S*,6*S*)-2-hydroxy-6-methyltetrahydro-2*H*-pyran-3,4,5-triyl tribenzoate (29)

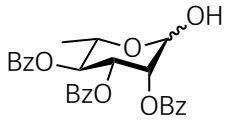

44.8 g of (3*R*,4*R*,5*S*,6*S*)-6-methyltetrahydro-2*H*-pyran-2,3,4,5-tetrayl tetrabenzoate (**28**) (77.16 mmol) were dissolved in 50 mL ACN and treated under vigorous stirring with 60 mL of 2 M dimethylamine solution in THF (0.12 mol). After monitoring the reaction by TLC, the solution was concentrated under reduced pressure, and the product **29** was recrystallized with toluene to afford 31.6 g (66.35 mmol) of a white lustrous solid (86% yield). ^{1}H NMR (600 MHz, $CDCl_3$): δ 1.36 (d, 6.2 Hz, 3H), 4.46 (dq, J=9.6 Hz, J=6.2Hz, 1H), 5.46 (dd, J=3.9 Hz, J=1.7 Hz, 1H), 5.69 (d, J=10.0 Hz, 1H), 5.71 (dd, 3.4, J=1.80 Hz, 1H), 5.92 (dd, J=10.2 Hz, J=3.4 Hz, 1H), 7.26 (t, J=7.8 Hz, 2H), 7.40 (m, 3H), 7.51 (m, 3H), 7.61 (ddd, J=7.5 Hz, J=1.3 Hz, 1H), 7.83 (dd, J=8.4 Hz, J=1.3 Hz, 2H), 7.98 (dd, J=8.4 Hz, J=1.3 Hz, 2H), 8.11 (dd, J=8.4 Hz, J=1.3 Hz, 2H). ^{13}C NMR (151 MHz, $CDCl_3$): δ 17.9, 66.9, 69.7, 71.3, 72.0, 92.4, 128.4 (2C), 128.6 (2C), 128.7 (2C), 129.3, 129.4, 129.5, 129.8 (2C), 129.9 (2C), 130.3 (2C), 133.2, 133.5, 133.6, 165.7, 165.8, 166.0.

10.3.1.3 (2*S*,3*S*,4*R*,5*R*)-2-methyl-6-oxotetrahydro-2*H*-pyran-3,4,5-triyl tribenzoate (30)

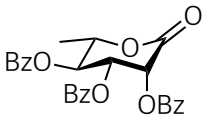

To a solution of 31.4 g of pyridinium chlorochromate (145.64 mol) in 100 mL of DCM were added 10 g of dried molecular sieves (4Å). After 30 min of stirring, a solution of 17.4 g of (3*R*,4*R*,5*S*,6*S*)-2-hydroxy-6-methyltetrahydro-2*H*-pyran-3,4,5-triyl tribenzoate (**29**) (36.51 mmol) in 100 mL of DCM was added and allowed to react overnight under N_2. Consecutive addition of 100 mL of Et_2O completed the reaction after an extra 20 min. Removal of the molecular sieves by filtration proceed with evaporation of the solvents. The remaining solid was again dissolved in DCM and quickly filtrated by a silica column to yield the (2*S*,3*S*,4*R*,5*R*)-2-methyl-6-oxotetrahydro-2*H*-pyran-3,4,5-triyl tribenzoate (**30**) as a white solid (13.8 g, 29.08 mmol, 80% yield). The product was used without additional purification. ^{1}H NMR (600 MHz, $CDCl_3$): δ 1.62 (d, J=6.3 Hz, 3H), 4.86 (dq, J=8.3 Hz, J=6.4 Hz, 1H), 5.33 (dd, J=8.3 Hz, J=1.6 Hz, 1H), 6.01 (dd, J=3.9 Hz, J=1.6 Hz, 1H), 6.23 (d, J=3.9 Hz, 1H), 7.36 (dd, J=8.2 Hz, J=7.6Hz, 2H), 7.49 (m, 4H), 7.53 (1H, m), 7.63 (m, 2H), 7.96 (dd, J=8.3 Hz, J=1.3 Hz, 2H), 8.08 (ddd, J=8.3 Hz, J=2.1 Hz, J=1.2

Hz, 4H). ^{13}C NMR (151 MHz, $CDCl_3$): δ 19.3, 67.6, 71.8, 74.4, 74.9, 128.5, 128.6 (2C), 128.7, 128.8 (2C), 128.9 (2C), 130.1 (2C), 130.2 (2C), 130.3 (2C), 133.9, 134.0, 134.2, 164.9, 165.0, 165.2, 165.8.

10.3.1.4 (2*S*,3*R*)-2-methyl-6-oxo-3,6-dihydro-2*H*-pyran-3,5-diyl dibenzoate (31)

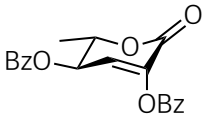

13.5 g of (2*S*,3*S*,4*R*,5*R*)-2-methyl-6-oxotetrahydro-2*H*-pyran-3,4,5-triyl tribenzoate (**30**) (28.45 mmol) was dissolved in 100 mL of DCM and treated with 104 mL of Et_3N. After 20 hours of stirring, the mixture was carefully washed with 3 M HCl solution, and the organic phase was dried over anhydrous $MgSO_4$. Removal of the solvent afforded a solid, which was purified by column chromatography on silica using 9:1 toluene-EtOAc. Concentration under reduced pressure gave the (2*S*,3*R*)-2-methyl-6-oxo-3,6-dihydro-2*H*-pyran-3,5-diyl dibenzoate (**31**) as a white solid (9.9 g, 28.10 mmol, 99% yield). ^{1}H NMR (600 MHz, $CDCl_3$): δ 1.65 (d, J=6.7 Hz, 3H), 4.96 (qdd, J=6.7 Hz, J=4.7 Hz, J=0.7 Hz, 1H), 5.70 (dd, J=4.7 Hz, 1H), 6.71 (dd, J=4.7 Hz, J=0.7 Hz, 1H), 7.48 (m, 5H), 7.62 (m, 2H), 8.07 (dd, J=7.2 Hz, J=1.3 Hz, 2H), 8.12 (d, J=8.1 Hz, 3H). ^{13}C NMR (151 MHz, $CDCl_3$): δ 18.5, 68.7, 77.5, 125.7, 128.6, 128.8 (2C), 128.9 (2C), 130.1, 130.3, 130.6, 133.9, 134.0, 134.4, 140.9, 158.1, 164.4, 165.6, 171.6.

10.3.1.5 (2*S*,3*R*,5*R*)-2-methyl-6-oxotetrahydro-2*H*-pyran-3,5-diyl dibenzoate (32)

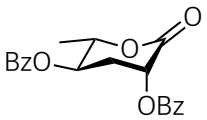

In 100 mL of EtOAc were dissolved 9.9 g (28.1 mmol) of the lactone **31** and 10% mol of Pd/C were added with vigorous stirring. Subsequent hydrogenation of the solution for 16 hours was followed by the partial removal of the solvent and consecutive filtration over silica by column to remove the catalyst. Concentration under reduced pressure afforded the (2*S*,3*R*,5*R*)-2-methyl-6-oxotetrahydro-2*H*-pyran-3,5-diyl dibenzoate (**32**) as a white solid in 99% yield (9.8 g, 27.65 mmol). ^{1}H NMR (600 MHz, $CDCl_3$): δ 1.59 (d, J=6.5 Hz, 3H), 2.58 (ddd, J=14.2 Hz, J=7.4 Hz, J=3.6 Hz, 1H), 2.71 (ddd, J=14.2 Hz, J=12.1 Hz, J=6.2 Hz, 1H), 4.82 (dq, J=6.3 Hz, J=6.2 Hz, 1H), 5.28 (td, J=6.1 Hz, J=3.6 Hz, 1H), 5.90 (dd, J=12.2 Hz, J=7.4 Hz, 1H), 7.48 (m, 4H), 7.61 (m, 2H), 8.05 (dd, J=8.2 Hz, J=1.2 Hz, 2H), 8.10 (m, 2H). ^{13}C

NMR (151 MHz, $CDCl_3$): δ 19.3, 30.2, 65.0, 70.5, 128.6 (2C), 128.7 (2C), 129.0, 129.1, 129.9 (2C), 130.2 (2C), 130.3, 133.8, 133.9, 165.5, 168.0.

10.3.1.6 (2*R*,3*R*,5*R*,6*S*)-2-hydroxy-6-methyltetrahydro-2*H*-pyran-3,5-diyl dibenzoate (19)

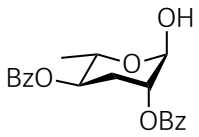

23.4 mL of 2-methyl-2-butene (221.2 mmol) were carefully added to 110.6 mL of 1 M BH_3-THF solution (110.6 mmol) at 0 °C. After 2 hours of stirring, the cold bath was removed, and a solution of the lactone **32** (9.8 g, 27.65 mmol) dissolved in 82 mL of dry THF was added. The resultant mixture reacted for 20 h at room temperature. Subsequent quenching of the reaction proceeded by adding 41 mL of water and after 30 min, 41 mL of 35% H_2O_2 at 0 °C. Once the pH of the solution was rectified (pH=7-8) the solvent was evaporated, and the crude product was purified by column chromatography with 6:4 hexane-EtOAc. Concentration at reduced pressure gave 8.8 g (24.69 mmol) of (2*R*,3*R*,5*R*,6*S*)-2-hydroxy-6-methyltetrahydro-2*H*-pyran-3,5-diyl dibenzoate (**19**) as a white lustrous solid in 90% yield. ^{1}H NMR (600 MHz, $CDCl_3$): δ1.30 (d, J=6.3 Hz, 3H), 2.29 (ddd, J=13.8 Hz, J=11.2 Hz, J=3.2 Hz, 1H), 2.42 (ddd, J=13.8 Hz, J=3.6 Hz, 1H), 4.37 (dq, J=9.7 Hz, J=6.2 Hz, 1H), 5.20 (ddd, J=11.0 Hz, J=9.8 Hz, J=4.7 Hz, 1H), 5.26 (m, 1H), 5.29 (brs, 1H), 7.48 (m, 6H), 7.60 (m, 2H), 8.04 (dd, J=8.3 Hz, J=1.3 Hz, 2H), 8.12 (m, 2H). ^{13}C NMR (151 MHz, $CDCl_3$): δ 18.0, 29.2, 67.0, 70.7, 70.9, 91.2, 128.6 (4C), 129.7 (3C), 130.0 (3C), 133.4, 133.5, 165.8, 166.0.

10.3.2 Kinetic resolution of tert-butyl 3-hydroxypent-4-enoate (95)

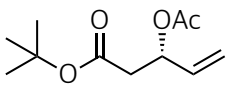

96

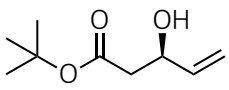

93

A stirred solution of 2.0 g of racemic *tert*-butyl 3-hydroxypent-4-enoate (**95**, 11.6 mmol) in 100 mL of pentane was treated with 5.4 mL of vinyl acetate (58.6 mmol), 1.4 g of Amano lipase PS and 2.0 g of molecular sieve 4Å. The mixture was refluxed at 35 °C for 72 h. The solution was filtrated, and the solvent was carefully removed. The products were separated by column chromatography with hexane-EtOAc (9:1) to yield tert-butyl (*S*)-3-acetoxypent-4-enoate (**96**, 847 mg, 3.95 mmol, 34% yield) and ***tert*-butyl (*R*)-3-hydroxypent-4-enoate** (**93**, 598 mg, 3.47 mmol, 30% yield) as transparent oils. ^{1}H NMR of

96 (600 MHz, $CDCl_3$): δ 1.44 (s, 9H), 2.05 (s, 3H), 2.52 (dd, J = 15.3, 5.7 Hz, 1H), 2.60 (dd, J = 15.3, 8.2 Hz, 1H), 5.20 (dd, J=10.5 Hz, J=1.1 Hz, 1H), 5.30 (dd, J=17.2 Hz, J=1.2 Hz, 1H), 5.60 (m, 1H), 5.83 (ddd, J=17.0 Hz, J=10.5 Hz, J=6.2 Hz, 1H). ^{1}H NMR of **93** (600 MHz, $CDCl_3$): δ 1.46 (s, 9H), 2.43 (dd, J=16.2 Hz, J=8.4 Hz, 1H), 2.51 (dd, J=16.2 Hz, J=3.8 Hz, 1H), 3.11 (bs, OH), 4.49 (m, 1H), 5.14 (dd, J=10.5 Hz, J=1.4 Hz, 1H), 5.31 (dd, J=17.2, 1.5 Hz, 1H), 5.87 (ddd, J=17.2 Hz, J=10.5 Hz, J=5.5 Hz, 1H).

10.3.3 Syntheses of alkyl aglycones

10.3.3.1 General procedure for bromoalkanes

To a stirred solution of alkyl alcohol (or tetrahydropyranyl alkane) (1 eq.) in dry DCM at 0 °C was added PPh_3 (2 eq.) and subsequently in portions Br_2 (or NBS) (2 eq.). After 2 hours, the reaction was quenched and washed by adding concentrated solutions of $Na_2S_2O_3$ (for Br_2) or $NaHCO_3$ (for NBS). The aqueous layer was removed, and the organic solvent was evaporated. The resulting mixtures were purified by column chromatography with hexane-EtOAc mixtures. Evaporation under reduced pressure of the organic solvent achieved the bromoalkanes.

10.3.3.2 General procedure for protection of alcohols with *tert*-butyldimethylsilyl chloride

To a stirred solution of alkyl alcohol (1 eq.) and imidazole (1.5 eq.) in dry THF was added *tert*-butyl(chloro)dimethylsilane (1.4 eq.) at 0 °C. After 2 hours, the mixture was quenched with H_2O, and the crude product was extracted with Et_2O. The organic layer was washed with brine, dried over Na_2SO_4, and concentrated under reduced pressure. The mixtures were purified by column chromatography using gradients of pentane-EtOAc to give the products as transparent oils.

10.3.3.3 General procedure for remotion of *tert*-butyldimethylsilyl group

Under N_2 a stirred solution of protected alcohol (1eq.) in dry THF was added an excess of a 1 M tetrabutylammonium fluoride solution (10 eq.). After 16 hours, the solvent was evaporated, and the crude product was purified by column chromatography using gradients of hexane-EtOAc. After the removal of the solvents the alkyl alcohols were obtained.

10.3.3.4 General procedure for deuterogenation/hydrogenation

A solution of 1 eq. of unsaturated compound, in hexane or EtOAc, was treated with 10% mol of Pd/C in a H_2 or D_2 atmosphere overnight. After the reaction was complete, the catalyst was removed by filtration of the product through a silica column.

10.3.3.5 General procedure for protection of alcohols with 3,4-dihydropyran

A stirred solution of 1 eq. of alkyl alcohol in dry DCM at 0 °C was treated with 3,4-dihydro-2*H*-pyran (1 eq.) and *p*-toluenesulfonic acid (0.3 eq.). The mixture was warmed to room temperature, and after 16 hours the reaction was quenched with saturated $NaHCO_3$ solution. The organic phase was washed with water and brine and dried under $MgSO_4$. The resulting products were purified by column chromatography using gradients of hexane-EtOAc as eluent and concentrated under reduced pressure.

10.3.3.6 General procedure for alkylation of alkynes

Under N_2, a solution of alkyne (1 eq.) in dry THF at -30 °C was treated with 2.5 M *n*-BuLi in hexane (1.5 eq.) and allowed to react for 1 hour. Separately under N_2, a solution of haloalkane (1 eq.) in dry THF was mixed with HMPA (6 eq.) at 0 °C. After 30 minutes, the subsequent haloalkane solution was added to the lithiated alkyne while keeping the cold bath at -30 °C. The resulting mixture was stirred overnight at room temperature. The reaction was quenched with water, extracted with diethyl ether, dried over $MgSO_4$, and concentrated under reduced pressure. Purification by column chromatography of the crude mixtures with hexane-EtOAc gave the products.

10.3.3.7 General procedure for *O*-methylation of hydroxyl groups

A solution of reactant (1 eq.) dissolved in a 1:1 mixture of toluene-MeOH was treated dropwise with a solution of 2 M $TMSCHN_2$ (1.9 eq.) in hexane. After stirring for 1 hour, the excess of reagent was neutralized with acetic acid. Evaporation of the solvents under reduced pressure was followed by filtration of the crude product in Et_2O over a short silica column. Column chromatography with gradients of hexane-EtOAc as eluents afforded the final products.

10.3.3.8 General procedure for the formation of tertiary alcohols with Grignard reagents

Under nitrogen, a stirred solution of carboxylate ester (1 eq.) in dry THF (1 g/mL) at 0 °C was added to the Grignard reagent (3 eq.) in solution. After 16 hours, the mixture was cooled to 0 °C and the reaction

was quenched with concentrated acetic acid until the formed solid was dissolved. Water was added to the mixture, and the product was extracted with DCM. The organic phase was washed with brine, dried over $MgSO_4$, and concentrated under reduced pressure. The crude product was purified by column chromatography with mixtures of hexane-EtOAc/Et_2O.

10.3.3.9 General procedure of selective reduction of tertiary alcohols

Under nitrogen, to a solution of tertiary alcohol (1 eq.) in dry DCM (1 g/mL) at 0 °C was added $BF_3 \cdot Et_2O$ (2 eq.) and triethylsilane (2 eq.). The cooling was removed, and the mixture was stirred for 1 hour at room temperature. The reaction was quenched with an ice-water solution, and the product was extracted with DCM. The organic phase was washed with saturated $NaHCO_3$ solution, dried over $MgSO_4$, and concentrated under reduced pressure. The crude product was purified by column chromatography with mixtures of hexane-EtOAc.

10.3.3.10 1-Bromohenicosane (35)

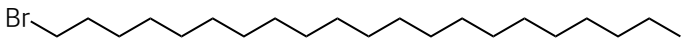

Procedure 10.3.3.1; 1.1 g 1-heneicosanol (**36**, 3.51 mmol), 1.8 g PPh_3 (7.02 mmol), 0.3 mL Br_2 (7.02 mmol), hexane as eluent. 1-Bromohenicosane (**35**): 1.2 g transparent oil (3.20 mmol), 98% yield. ^{1}H NMR (600 MHz, $CDCl_3$): δ 0.88 (t, J=7.0 Hz, 3H), 1.24 - 1.32 (m, 34H), 1.38 - 1.46 (m, 2H), 1.85 (m, 2H), 3.41 (t, J=6.9 Hz, 2H). ^{13}C NMR (151 MHz, $CDCl_3$): δ 14.3, 22.9, 28.4, 28.9, 29.5, 29.6, 29.7, 29.9 (11C), 32.1, 33.0, 34.2.

10.3.3.11 (*R*)-(but-3-yn-2-yloxy)(*tert*-butyl)dimethylsilane (38)

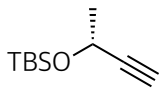

Procedure 10.3.3.2; 2.2 mL (*R*)-3-butyn-2-ol (**39**, 27.93 mmol), 2.9 g imidazole (41.89 mmol), 5.9 g TBSCl (39.10 mmol), 30 mL dry THF, pentane as eluent. (*R*)-(but-3-yn-2-yloxy)(*tert*-butyl)dimethylsilane (**38**): 5.3 g of light oil (28.7 mmol) in 97% yield. ^{1}H NMR (600 MHz, $CDCl_3$): δ 0.04 - 0.18 (m, 6H), 0.81 - 1.05 (m, 9H), 1.44 (d, J=6.5 Hz, 3H), 2.39 (d, J=2.1 Hz, 1H), 4.53 (qd, J=6.5 Hz, J=2.0 Hz, 1H). ^{13}C NMR (151 MHz, $CDCl_3$): δ -4.9, -4.5, 25.5, 25.8, 59.0, 71.3, 86.6.

10.3.3.12 (*R*)-*tert*-butyldimethyl(pentacos-3-yn-2-yloxy)silane (37)

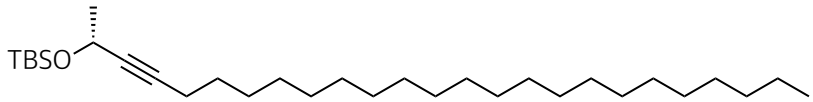

Procedure 10.3.3.6; 123 mg (*R*)-(but-3-yn-2-yloxy)(*tert*-butyl)dimethylsilane (**38**, 1.75 mmol), 660 mg 1-bromohenicosane (**35**, 1.75 mmol), 1.9 mL HMPA (10.5 mmol), 1.1 mL 2.5 M *n*-BuLi (2.63 mmol), 9:1 hexane-EtOAc as eluent. (*R*)-*tert*-butyldimethyl(pentacos-3-yn-2-yloxy)silane (**37**): 439 mg (0.92 mmol), 86% yield. ^{1}H NMR (600 MHz, $CDCl_3$): δ 0.12 - 0.16 (m, 6H), 0.88 - 0.96 (m, 12H), 1.24 - 1.32 (m, 36H), 1.40 (d, J=6.5 Hz, 3H), 1.44 - 1.55 (m, 2H), 2.19 (td, J=7.1 Hz, J=1.9 Hz, 2H), 4.53 (qt, J=6.5 Hz, J=1.9 Hz, 1H). ^{13}C NMR (151 MHz, $CDCl_3$): δ -4.7, -4.4, 14.3, 18.4, 18.8, 22.8, 25.9, 26.0, 28.8, 29.0, 29.3, 29.5, 29.8 (15C), 32.1, 59.4, 82.9, 83.9. EIMS (70 eV) 463.5 $[M\text{-}CH_3]^+$, calculated for $C_{31}H_{62}OSi$ *m/z* 478.5.

10.3.3.13 (*R*)-*tert*-butyldimethyl(pentacosan-2-yloxy)silane (39a)

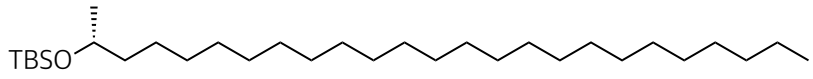

Procedure 10.3.3.4; 143 mg (*R*)-*tert*-butyldimethyl(pentacos-3-yn-2-yloxy)silane (**37**, 0.30 mmol), H_2, 5 mL hexane. (*R*)-*tert*-butyldimethyl(pentacosan-2-yloxy)silane (**39a**): 140 mg (0.29 mmol), 97% yield. ^{1}H NMR (600 MHz, $CDCl_3$): δ -0.06 - -0.04 (m, 3H), 0.05 - 0.10 (m, 3H), 0.87 - 0.93 (m, 12H), 1.28 (m, 42H), 1.30 - 1.38 (m, 3H), 1.36 - 1.50 (m, 2H), 3.76 - 3.82 (m, 1H). ^{13}C NMR (151 MHz, $CDCl_3$): δ -4.7, -4.4, 14.1, 22.7, 25.9 (2C), 29.4, 29.6 (21C), 31.9, 39.8, 68.7. EIMS (70 eV) 467.5 $[M\text{-}CH_3]^+$, calculated for $C_{31}H_{66}OSi$ *m/z* 482.5.

10.3.3.14 [D_4]-(*R*)-*tert*-butyldimethyl(pentacosan-2-yloxy)silane (39b)

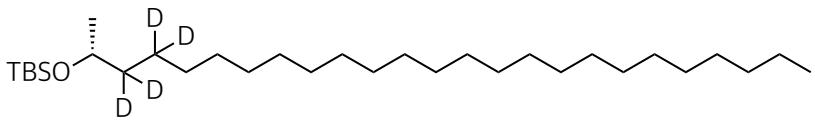

Procedure 10.3.3.4; 166 mg (*R*)-*tert*-butyldimethyl(pentacos-3-yn-2-yloxy)silane (**37**, 0.34 mmol), D_2, 5 mL hexane. [D_4]-(*R*)-*tert*-butyldimethyl(pentacosan-2-yloxy)silane (**39b**): 157 mg (0.32 mmol), 95% yield. ^{1}H NMR (600 MHz, $CDCl_3$): δ -0.06 - -0.02 (m, 3H), 0.06 - 0.09 (m, 3H), 0.86 - 0.93 (m, 12H), 1.14 (d, J=6.1 Hz, 3H), 1.17 - 1.48 (m, 40H), 3.76 - 3.82 (m, 1H). ^{13}C NMR (151 MHz, $CDCl_3$): δ -4.6, -4.3, 14.3,

22.9, 26.0, 29.5, 29.8 (21C), 32.1, 68.8. EIMS (70 eV) 471.5 $[M\text{-}CH_3]^+$, calculated for $C_{31}H_{62}D_4OSi$ *m/z* 486.5.

10.3.3.15 (*R*)-pentacosan-2-ol (34a)

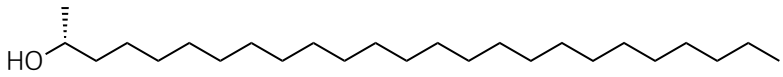

Procedure 10.3.3.3; 140 mg (*R*)-*Tert*-butyldimethyl(pentacosan-2-yloxy)silane (**39a**, 0.29 mmol), 0.5 mL dry THF, 2.9 mL 1 M TBAF (2.90 mmol), 9:1 hexane-EtOAc as eluent. (*R*)-pentacosan-2-ol (**34a**): 89 mg as a white solid (0.24 mmol) in 83% yield. ^{1}H NMR (600 MHz, $CDCl_3$): δ 0.88 (t, J=7.0 Hz, 3H), 1.19 (d, J=6.2 Hz, 3H), 1.25 - 1.28 (m, 42H), 1.42 (m, 2H), 3.79 (m, 1H). ^{13}C NMR (151 MHz, $CDCl_3$): δ 14.3, 22.9, 23.6, 25.9, 29.5, 29.8 (3C), 29.9 (13C), 32.1, 39.4, 68.4. EIMS (70 eV) 350.4 $[M\text{-}H_2O]^+$, calculated for $C_{25}H_{52}O$ *m/z* 368.4.

10.3.3.16 [D_4]-(*R*)-pentacosan-2-ol (34b)

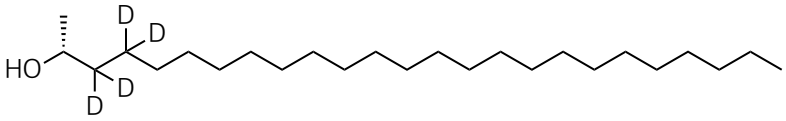

Procedure 10.3.3.3; 157 mg [D_6]-(*R*)-*tert*-butyldimethyl(pentacosan-2-yloxy)silane (**39b**, 0.32 mmol), 0.5 mL dry THF (6.17 mmol), 3.2 mL 1 M TBAF (3.20 mmol), 9:1 hexane-EtOAc as eluent. [D_4]-(*R*)-pentacosan-2-ol (**34a**): 84 mg white solid (0.23 mmol), 70% yield. ^{1}H NMR (600 MHz, $CDCl_3$): δ 0.88 (t, J=7.0 Hz, 3H), 1.18 (d, J=6.2 Hz, 3H), 1.25 - 1.28 (m, 40H), 3.76 (m, 1H). ^{13}C NMR (151 MHz, $CDCl_3$): δ 14.3, 22.9, 23.6, 25.9, 29.5, 29.9 (15C), 32.1, 39.5, 68.4.

10.3.3.17 15-Methylhexadecane-1,15-diol (46a)

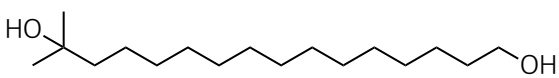

Procedure 10.3.3.8; 5.0 g pentadecanolide (**45**, 20.80 mmol), 20.8 mL CH_3MgI 3 M (62.40 mmol), 9:1 hexane-EtOAc as eluent. 15-Methylhexadecane-1,15-diol (**46a**): 5.4 g lustrous white solid (19.81 mmol), 95% yield. ^{1}H NMR (600 MHz, $CDCl_3$): δ 1.21 (s, 6H), 1.25 - 1.42 (m, 23H), 1.44 - 1.48 (m, 2H),

1.54 - 1.60 (m, 2H), 3.64 (t, J=6.7 Hz, 2H). ^{13}C NMR (151 MHz, $CDCl_3$): δ 24.5, 25.9, 29.4 (2C), 29.6, 29.8 (7C), 30.3, 32.9, 44.1, 63.2, 71.2.

10.3.3.18 15-Methylhexadecan-1-ol (47a)

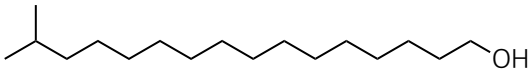

Procedure 10.3.3.9; 5.4 g 15-methylhexadecane-1,15-diol (**46a**, 21.05 mmol), 5.2 mL $BF_3{\cdot}Et_2O$ (42.10 mmol), 6.7 mL Et_3SiH (42.10 mmol), 9:1 hexane-EtOAc as eluent. 15-Methylhexadecan-1-ol (**47a**): 5.1 g white solid (19.99 mmol), 93% yield. ^{1}H NMR (600 MHz, $CDCl_3$): δ 0.86 (d, J=6.6 Hz, 6H), 1.15 (m, 1H), 1.23 - 1.48 (m, 21H), 1.48 - 1.61 (m, 4H), 3.64 (t, J=6.6 Hz, 2H). ^{13}C NMR (151 MHz, $CDCl_3$): δ 22.8 (2C), 25.9, 29.5, 29.8 (8C), 29.9, 30.1, 32.9, 39.2, 63.2.

10.3.3.19 1-Bromo-15-methylhexadecane (48)

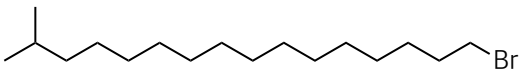

Procedure 10.3.3.1; 3.7 g 15-methylhexadecan-1-ol **47a** (14.42 mmol), 7.6 g PPh_3 (28.84 mmol), 5.1 g NBS (28.84 mmol), hexane as eluent. 1-Bromo-15-methylhexadecane (**48**): 4.1 g transparent oil (12.83 mmol), 90% yield. ^{1}H NMR (600 MHz, $CDCl_3$): δ 0.87 (d, J=6.6 Hz, 6H), 1.13 - 1.28 (m, 2H), 1.26 - 1.31 (m, 20H), 1.40 - 1.45 (m, 2H), 1.49 - 1.54 (m, 1H), 1.85 (tt, J=14.7 Hz, J=14.1 Hz, J=8.1 Hz, J=7.1 Hz, 2H), 3.41 (t, J=6.9 Hz, 2H). ^{13}C NMR (151 MHz, $CDCl_3$): δ 22.8 (2C), 27.6, 28.1, 28.4, 29.0, 29.6, 29.7, 29.8 (5C), 30.1, 33.0, 34.1, 39.2.

10.3.3.20 2-((5-Bromopentyl)oxy)tetrahydro-2*H*-pyran (50)

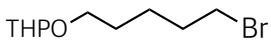

Procedure 10.3.3.5; 3.5 g 5-bromo-1-pentanol (**49**, 20.91 mmol), 20 mL dry DCM, 1.8 mL DHP (20.91 mmol), 1.1 g PTSA (6.27 mmol), 10:1 hexane-EtOAc as eluent. 2-((5-Bromopentyl)oxy)tetrahydro-2*H*-pyran (**50**): 4.8 g yellow oil (19.10 mmol), 91% yield. ^{1}H NMR (600 MHz, $CDCl_3$): δ 1.50 - 1.66 (m, 9H), 1.69 - 1.74 (m, 1H), 1.82 (td, J=8.9 Hz, J=4.1 Hz, 1H), 1.90 (dt, J=14.4 Hz, J=6.9 Hz, 2H), 3.38 - 3.44 (m, 3H), 3.49 - 3.52 (m, 1H), 3.75 (dt, J=9.7 Hz, J=6.7 Hz, J=6.6 Hz, 1H), 3.86 (ddd, J=11.1 Hz, J=7.7 Hz, J=3.1

Hz, 1H), 4.57 (dd, J=4.4 Hz, J=3.0 Hz, 1H). ^{13}C NMR (151 MHz, $CDCl_3$): δ 19.8, 25.1, 25.6, 29.0, 30.9, 32.8, 33.9, 62.5, 67.3, 99.0.

10.3.3.21 (15-Methylhexadecyl)magnesium bromide (51)

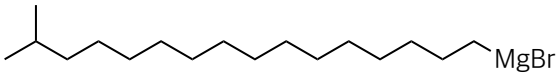

Under N_2, 0.3 g of dried Mg turnings (4.17 mmol) were mixed with 3 mL of dry THF. To this mixture was added with low stirring 0.5 g of 1-bromo-15-methylhexadecane (**48**, 1.56 mmol) dissolved in 5 mL of dry THF. After 20 minutes, the stirring was increased, and the mixture was heated for 3 hours at 80 °C. The 5-methylhexadecyl)magnesium bromide (**51**) in solution was cooled to room temperature, separated from the excess of Mg turnings, and used directly.

10.3.3.22 2-((20-Methylhenicosyl)oxy)tetrahydro-2*H*-pyran (52)

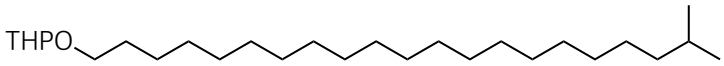

Under N_2, the freshly prepared 15-methylhexadecyl)magnesium bromide (**51**) solution was added to 2-((5-bromopentyl)oxy)tetrahydro-2*H*-pyran **50** (1.1 g, 4.17 mmol) in 3 mL of dry THF. Subsequently, 14.5 mL of 0.1 M Li_2CuCl_4 (1.45 mmol) were slowly added with vigorous stirring. After 16 hours, the reaction was quenched with saturated NH_4Cl solution. The crude product was extracted with Et_2O, and the organic phase was washed with H_2O and brine and dried under $MgSO_4$. Purification by column chromatography with 9:1 hexane-EtOAc gave 771 mg of 2-((20-methylhenicosyl)oxy)tetrahydro-2*H*-pyran (**52**) (1.88 mmol) as a yellow oily-solid (45% yield). ^{1}H NMR (600 MHz, $CDCl_3$): δ 0.89 (d, J=6.6 Hz, 6H), 1.14 - 1.20 (m, 2H), 1.28 (m, 32H), 1.49 - 1.65 (m, 7H), 1.70 - 1.77 (m, 1H), 1.81 - 1.90 (m, 1H), 3.37 - 3.44 (m, 1H), 3.49 - 3.56 (m, 1H), 3.71 - 3.78 (m, 1H), 3.86 - 3.93 (m, 1H), 4.57 - 4.58 (m, 1H). ^{13}C NMR (151 MHz, $CDCl_3$): δ 19.9, 22.8 (2C), 25.7, 26.4, 27.6, 28.1, 29.7, 29.9 (13C), 30.1, 31.0, 39.2, 62.5, 67.9, 99.0. EIMS (70 eV) 409.4 $[M-H]^+$, calculated for $C_{27}H_{54}O_2$ *m/z* 410.4.

10.3.3.23 1-Bromo-20-methylhenicosane (53)

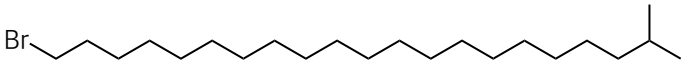

Procedure 10.3.3.1; 771 mg of 2-((20-methylhenicosyl)oxy)tetrahydro-2*H*-pyran (**52**, 1.88 mmol), 986 mg PPh_3 (3.76 mmol), 601 mg Br_2 (3.76 mmol), hexane as eluent. 1-Bromo-20-methylhenicosane (**53**): 703 mg white lustrous solid (1.80 mmol), 96% yield. ^{1}H NMR (600 MHz, $CDCl_3$): δ 0.86 (d, J=6.6 Hz, 6H), 1.14 - 1.21 (m, 2H), 1.28 (m, 29H), 1.40 -1.48 (m, 2H), 1.49 - 1.58 (m, 2H), 1.87 (tt, J=14.6 Hz, J=7.0 Hz, 2H), 3.41 (t, J=6.9 Hz, 2H). ^{13}C NMR (151 MHz, $CDCl_3$): δ 22.8 (2C), 27.6, 28.1, 28.3, 28.9, 29.6, 29.7, 29.9 (10C), 30.0, 33.0, 34.2, 39.2.

10.3.3.24 (*R*)-*tert*-butyldimethyl((24-methylpentacos-3-yn-2-yl)oxy)silane (54)

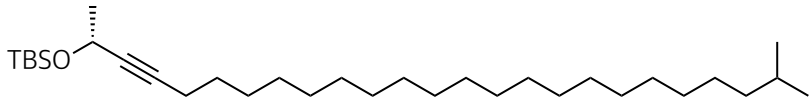

Procedure 10.3.3.6; 332 mg (*R*)-(but-3-yn-2-yloxy)(*tert*-butyl)dimethylsilane (**38**, 1.80 mmol), 703 mg 1-bromo-20-methylhenicosane (**53**, 1.80 mmol), 1.9 mL HMPA (10.80 mmol), 1.8 mL 2.5 M *n*-BuLi (2.70 mmol), 10:1 hexane-EtOAc as eluent. (*R*)-*tert*-butyldimethyl((24-methylpentacos-3-yn-2-yl)oxy)silane (**54**): 665 mg transparent oil (1.35 mmol), 75% yield. ^{1}H NMR (600 MHz, $CDCl_3$): δ 0.11 (d, J=6.1 Hz, 6H), 0.86 (d, J=6.6 Hz, 6H), 0.90 (s, 9H), 1.13 - 1.16 (m, 2H), 1.25 (m, 32H), 1.37 (d, J=6.5 Hz, 3H), 1.45 - 1.53 (m, 3H), 2.17 (td, J=7.1 Hz, J=2.0 Hz, 2H), 4.50 (qt, J=6.5 Hz, J=1.9 Hz, 1H). ^{13}C NMR (151 MHz, $CDCl_3$): δ -4.7, -4.4, 18.4, 18.8, 22.8 (2C), 25.9, 26.0 (3C), 27.6, 28.1, 28.8, 29.0, 29.3, 29.7, 29.9 (11C), 30.1, 39.2, 59.4, 82.9, 83.9.

10.3.3.25 (*R*)-*tert*-butyldimethyl((24-methylpentacosan-2-yl)oxy)silane (55a)

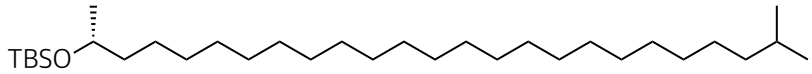

Procedure 10.3.3.4; 115 mg (*R*)-*tert*-butyldimethyl((24-methylpentacos-3-yn-2-yl)oxy)silane (**54**, 0.23 mmol), H_2, 5 mL hexane. (*R*)-*tert*-butyldimethyl((24-methylpentacosan-2-yl)oxy)silane (**55a**): 108 mg (0.22 mmol), 95% yield. ^{1}H NMR (600 MHz, $CDCl_3$): δ 0.04 (m, 6H), 0.86 (d, J=6.6 Hz, 6H), 0.89 (s, 9H), 1.11 (d, J=6.0 Hz, 3H), 1.14 (m, 2H), 1.22 - 1.39 (m, 39H), 1.42 (m, 1H), 1.51 (m, 1H), 3.76 (m, 1H). ^{13}C NMR (151 MHz, $CDCl_3$): δ -4.5, -4.3, 22.8 (2C), 24.0, 26.0, 26.1 (3C), 27.6, 28.1, 29.8, 29.9 (16C), 30.1, 39.2, 39.9, 68.8.

10.3.3.26 [D_4]-(*R*)-*tert*-butyldimethyl((24-methylpentacosan-2-yl)oxy)silane (55b)

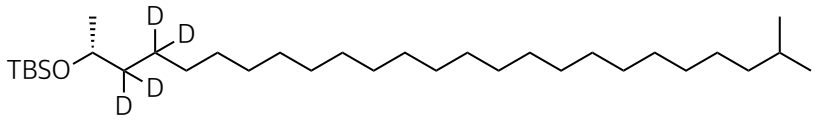

Procedure 10.3.3.4; 160 mg (*R*)-*tert*-butyldimethyl((24-methylpentacos-3-yn-2-yl)oxy)silane (**54**, 0.32 mmol), D_2, 5 mL hexane. [D_4]-(*R*)-*tert*-butyldimethyl((24-methylpentacosan-2-yl)oxy)silane (**55b**): 144 mg (0.29 mmol), 90% yield. ^{1}H NMR (600 MHz, $CDCl_3$): δ 0.07 (m, 6H), 0.88 (d, J=6.6 Hz, 6H), 0.91 (m, 9H), 1.13 (d, J=6.1 Hz, 3H), 1.17 (m, 2H), 1.28 (m, 32H), 1.35 (m, 2H), 1.53 (h, J=6.7 Hz, 1H), 3.76 (m, 1H). ^{13}C NMR (151 MHz, $CDCl_3$): δ -4.6, -4.3, 18.3, 22.8 (2C), 26.1 (3C), 27.6, 28.1, 29.7, 29.8 (15C), 29.9, 30.1, 39.2, 68.8.

10.3.3.27 (*R*)-24-Methylpentacosan-2-ol (44a)

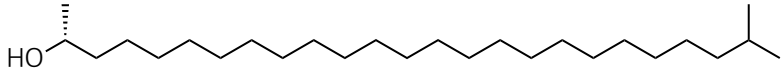

Procedure 10.3.3.3; 108 mg (*R*)-*tert*-butyldimethyl((24-methylpentacosan-2-yl)oxy)silane (**55a**, 0.22 mmol), 0.5 mL dry THF, 2.2 mL 1 M TBAF (2.2 mmol), 10:1 hexane-EtOAc as eluent. (*R*)-24-methylpentacosan-2-ol (**44a**): 65 mg white solid (0.17 mmol) in 77% yield. ^{1}H NMR (600 MHz, $CDCl_3$): δ 0.88 (d, J=6.6 Hz, 6H), 1.14 (m, 2H), 1.1921 (d, J=6.2 Hz, 3H), 1.25 - 1.31 (m, 39H), 1.37 - 1.48 (m, 2H), 1.51 (m, 1H), 3.81 (m, 1H). ^{13}C NMR (151 MHz, $CDCl_3$): δ 22.8, 23.6, 25.9, 27.6, 28.1, 29.5, 29.8 (4C), 29.9 (12C), 30.1, 39.2, 39.5, 68.4. EIMS (70 eV) 364.4 $[M\text{-}H_2O]^+$, calculated for $C_{26}H_{54}O$ *m/z* 382.4.

10.3.3.28 [D_4]-(*R*)-24-methylpentacosan-2-ol (44b)

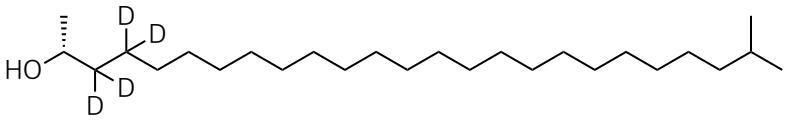

Procedure 10.3.3.3; 144 mg (*R*)-*tert*-butyldimethyl((24-methylpentacosan-2-yl-3,3,4,4-d_4)oxy)silane (**55b**, 0.29 mmol), 0.7 mL dry THF, 2.9 mL 1 M TBAF (2.9 mmol), 10:1 hexane-EtOAc as eluent. [D_4]-(*R*)-24-methylpentacosan-2-ol (**44b**): 92 mg white solid (0.24 mmol), 82% yield. ^{1}H NMR (600 MHz, $CDCl_3$): δ 0.86 (d, J=6.6 Hz, 6H), 1.15 (m, 3H), 1.25 (m, 38H), 1.51 (m, 2H), 3.76 (m, 1H). ^{13}C NMR (151 MHz, $CDCl_3$): δ 22.8, 26.1, 27.6, 28.1, 29.5, 29.9 (17C), 30.1, 39.2, 68.7.

10.3.3.29 2-(Undec-10-yn-1-yloxy)tetrahydro-2*H*-pyran (60)

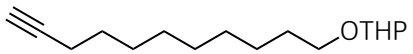

Procedure 10.3.3.5; 2.5 g 10-undecyn-1-ol (**61**, 14.68 mmol), 15 mL dry DCM, 1.3 mL DHP (14.68 mmol), 0.8 g PTSA (4.40 mmol), hexane as eluent. 2-(Undec-10-yn-1-yloxy)tetrahydro-2*H*-pyran (**60**): 3.3 g transparent oil (13.01 mmol), 90% yield. ^{1}H NMR (600 MHz, $CDCl_3$): δ 1.27 - 1.32 (m, 10H), 1.34 - 1.42 (m, 2H), 1.54 - 1.66 (m, 4H), 1.67- 1.74 (m, 2H), 2.35 (s, 1H), 3.37 (dt, J=9.6 Hz, J=6.7 Hz, 1H), 3.72 (dt, J=9.6 Hz, J=6.9 Hz, 1H), 3.86 (ddd, J=11.1 Hz, J=7.7 Hz, J=3.1 Hz, 1H), 4.56 (dd, J=4.4 Hz, J=3.0 Hz, 1H). ^{13}C NMR (151 MHz, $CDCl_3$): δ 18.5, 19.8, 25.7, 28.6, 28.8, 29.2, 29.6 (3C), 29.9, 30.9, 62.5, 67.8, 68.2, 84.9, 99.0.

10.3.3.30 2-(Heptacos-10-yn-1-yloxy)tetrahydro-2*H*-pyran (59)

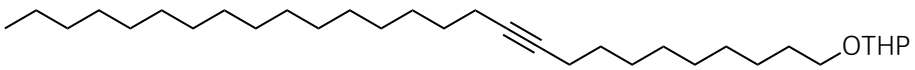

Procedure 10.3.3.6; 1.0 g 2-(undec-10-yn-1-yloxy)tetrahydro-2*H*-pyran (**60**, 3.9 mmol), 1.2 g 1-bromohexadecane (**62**, 3.9 mmol), 4.4 mL HMPA (23.6 mmol), 2.4 mL 2.5 M *n*-BuLi (5.9 mmol), 20:1 hexane-EtOAc as eluent. 2-(Heptacos-10-yn-1-yloxy)tetrahydro-2*H*-pyran (**59**): 1.5 g transparent oil (3.1 mmol), 77% yield. ^{1}H NMR (600 MHz, $CDCl_3$): δ 0.88 (t, J=7.0 Hz, 3H), 1.25 (m, 14H), 1.29 (t, J=6.2 Hz, 12H), 1.31 - 1.40 (m, 9H), 1.41 - 1.64 (m, 12H), 1.71 (ddt, J=12.4 Hz, J=8.7 Hz, J=3.0 Hz, 1H), 1.79 - 1.87 (m, 1H), 2.10 - 2.16 (m, 3H), 3.38 (dt, J=9.6 Hz, J=6.7 Hz, 1H), 3.50 (ddt, J=10.9 Hz, J=5.1 Hz, J=2.5 Hz, 1H), 3.73 (dt, J=9.6 Hz, J=6.9 Hz, 1H), 3.87 (ddd, J=11.1 Hz, J=7.6 Hz, J=3.1 Hz, 1H), 4.57 (dd, J=4.4 Hz, J=3.0 Hz, 1H). ^{13}C NMR (151 MHz, $CDCl_3$): δ 14.3, 18.9, 19.9, 22.8, 25.7, 26.4, 29.0 (2C), 29.3 (3C), 29.5, 29.6, 29.7, 29.8 (10C), 29.9, 30.9, 32.1, 62.5, 67.8, 80.3, 80.4, 99.0.

10.3.3.31 2-(Heptacosyloxy)tetrahydro-2*H*-pyran (63)

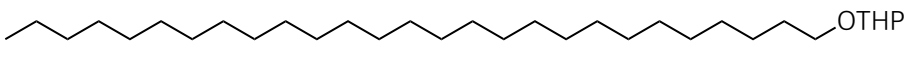

Procedure 10.3.3.4; 1.5 g 2-(heptacos-10-yn-1-yloxy)tetrahydro-2*H*-pyran (**59**, 3.1 mmol), H_2, 10 mL hexane. 2-(Heptacosyloxy)tetrahydro-2*H*-pyran (**63**): 1.4 g (2.9 mmol), 90% yield. ^{1}H NMR (600 MHz, $CDCl_3$): δ 0.88 (t, J=7.0 Hz, 3H), 1.25 (m, 35H), 1.26 - 1.30 (m, 4H), 1.28 - 1.38 (m, 9H), 1.48 - 1.58 (m,

4H), 1.71 (m, 4H), 3.38 (dt, J=9.6 Hz, J=6.7 Hz, 1H), 3.50 (ddt, J=10.9 Hz, J=5.1 Hz, J=2.5 Hz, 1H), 3.73 (dt, J=9.6 Hz, J=6.9 Hz, 1H), 3.87 (ddd, J=11.1 Hz, J=7.7 Hz, J=3.2 Hz, 1H), 4.57 (dd, J=4.4 Hz, J=3.0 Hz, 1H). ^{13}C NMR (151 MHz, $CDCl_3$): δ 14.3, 19.9, 22.9, 25.7, 26.4, 29.5, 29.7, 29.8 (19C), 29.9, 30.9, 32.1, 62.5, 67.9, 99.0. EIMS (70 eV) 479.5 $[M-H]^+$, calculated for $C_{32}H_{64}O_2$ *m/z* 480.5.

10.3.3.32 1-Bromoheptacosane (64)

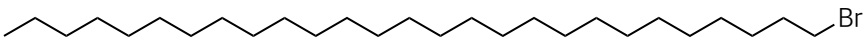

Procedure 10.3.3.1; 1.4 g 2-(Heptacosyloxy)tetrahydro-2*H*-pyran (**63**, 2.9 mmol), 1.5 g PPh_3 (5.8 mmol), 0.3 mL Br_2 (5.8 mmol), hexane as eluent. 1-Bromoheptacosane (**64**): 1.2 g white solid (2.6 mmol), 89% yield. ^{1}H NMR (600 MHz, $CDCl_3$): δ 0.88 (t, J=7.0 Hz, 3H), 1.25 - 1.31 (m, 46H), 1.42 (m, 2H), 1.86 (tt, J=7.0 Hz, J=6.9 Hz, 2H), 3.41 (t, J=6.9 Hz, 2H). ^{13}C NMR (151 MHz, $CDCl_3$): δ 14.3, 22.8, 28.3, 28.9, 29.5, 29.6, 29.7 (17C), 29.8, 32.1, 33.0, 34.2.

10.3.3.33 (*R*)-*tert*-butyl(hentriacont-3-yn-2-yloxy)dimethylsilane (65)

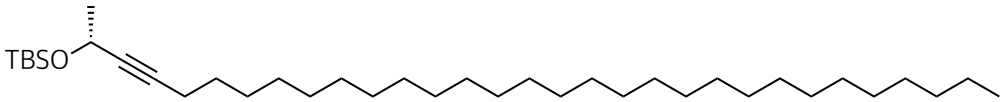

Procedure 10.3.3.6; 208 mg (*R*)-(But-3-yn-2-yloxy)(*tert*-butyl)dimethylsilane (**38**, 1.13 mmol), 518 g 1-bromoheptacosane (**64**, 1.13 mmol), 1.2 mL HMPA (6.78 mmol), 0.7 mL 2.5 M *n*-BuLi (1.70 mmol), 9:1 hexane-EtOAc as eluent. (*R*)-*tert*-butyl(hentriacont-3-yn-2-yloxy)dimethylsilane (**65**): 445 mg yellow oily-solid (0.79 mmol), 70% yield. ^{1}H NMR (600 MHz, $CDCl_3$): δ 0.12 (d, J=6.0 Hz, 6H), 0.92 (s, 9H), 1.22 - 1.33 (m, 49H), 1.38 (d, J=6.5 Hz, 3H), 1.48 (m, 2H), 2.17 (td, J=7.1 Hz, J=1.8 Hz, 2H), 4.50 (q, J=6.4 Hz, 1H). ^{13}C NMR (151 MHz, $CDCl_3$): δ -4.7, -4.5, 14.3, 18.8, 22.9, 25.9, 26.0, 28.8, 29.0, 29.1, 29.3, 29.8, 29.9(21C), 32.1, 59.4, 82.9, 83.9. EIMS (70 eV) 547.6 $[M-CH_3]^+$, calculated for $C_{37}H_{74}OSi$ *m/z* 562.6.

10.3.3.34 (*R*)-*tert*-butyl(hentriacontan-2-yloxy)dimethylsilane (66a)

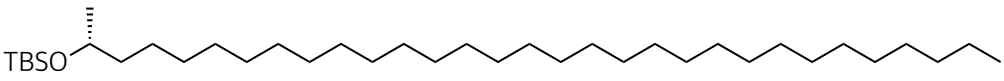

Procedure 10.3.3.3; 182 mg (*R*)-*tert*-butyl(hentriacont-3-yn-2-yloxy)dimethylsilane (**65**, 0.32 mmol), H_2, 5 mL hexane. (*R*)-*tert*-butyl(hentriacontan-2-yloxy)dimethylsilane (**66a**): 154 mg (0.27 mmol), 85% yield. ^{1}H NMR (600 MHz, $CDCl_3$): δ 0.07 (m, 6H), 0.88 (t, J=6.7 Hz, 3H), 0.90 (s, 9H), 1.11 (d, J=6.1 Hz, 3H), 1.24 - 1.32 (m, 50H), 1.37 (m, 2H), 3.77 (m, 1H). ^{13}C NMR (151 MHz, $CDCl_3$): δ -4.5, -4.2, 14.3, 22.9, 24.0, 25.8, 26.0, 29.4, 29.6, 29.7 (25C), 32.1, 39.9, 68.8.

10.3.3.35 [D_4]-(*R*)-*tert*-butyl(hentriacontan-2-yloxy)dimethylsilane (66b)

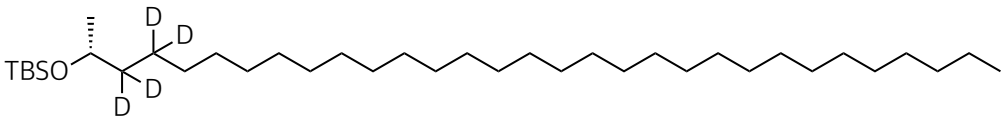

Procedure 10.3.3.3; 217 mg (*R*)-*Tert*-butyl(hentriacont-3-yn-2-yloxy)dimethylsilane (**65**, 0.38 mmol), D_2, 5 mL hexane. [D_4]-(*R*)-*tert*-butyl(hentriacontan-2-yloxy)dimethylsilane (**66b**): 180 mg (0.32 mmol), 83% yield. ^{1}H NMR (600 MHz, $CDCl_3$): δ 0.07 (m, 6H), 0.89 (d, J=2.9 Hz, 3H), 0.91 (s, 9H), 1.13 (d, J=6.1 Hz, 3H), 1.28 (m, 50H), 3.78 (q, J=5.9 Hz, 1H). ^{13}C NMR (151 MHz, $CDCl_3$): -4.5, -4.2, 14.3, 18.3, 22.9, 26.1 (3C), 29.6, 29.9 (24C), 32.1, 68.8.

10.3.3.36 (*R*)-Hentriacontan-2-ol (58a)

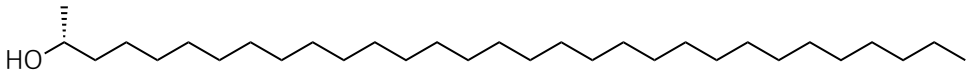

Procedure 10.3.3.3; 154 mg (*R*)-*tert*-butyl(hentriacontan-2-yloxy)dimethylsilane (**66a**, 0.27 mmol), 1 mL dry THF, 2.7 mL 1 M TBAF (2.70 mmol), 6:4 hexane-EtOAc as eluent. (*R*)-Hentriacontan-2-ol (**58a**): 85 mg white solid (0.19 mmol), 70% yield. ^{1}H NMR (600 MHz, $CDCl_3$): δ 0.88 (t, J=3.5 Hz, 3H), 1.11 (d, J=6.2 Hz, 3H), 1.22 - 1.32 (m, 55H), 1.35 - 1.52 (m, 2H), 3.74 - 3.82 (m, 1H). ^{13}C NMR (151 MHz, $CDCl_3$): δ 14.3, 22.9, 23.6, 25.9, 26.1, 29.5, 29.8 (23), 32.1, 39.5, 68.4. EIMS (70 eV) *m/z* 434.5 [M-H_2O]$^+$, calculated for $C_{31}H_{64}O$ *m/z* 452.5.

10.3.3.37 [D_4]-(*R*)-hentriacontan-2-ol (58b)

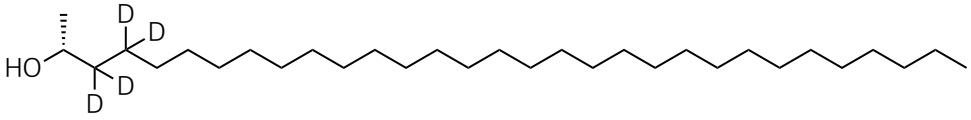

Procedure 10.3.3.3; 180 mg (*R*)-*tert*-butyl((hentriacontan-2-yl-3,3,4,4-d_4)oxy)dimethylsilane (**66b**, 0.32 mmol), 1 mL dry THF, 3.2 mL 1 M TBAF (3.20 mmol), 6:4 hexane-EtOAc as eluent. [D_4]-(*R*)-hentriacontan-2-ol (**58b**): 102 mg white solid (0.22 mmol), 70% yield. ^{1}H NMR (600 MHz, $CDCl_3$): δ 0.87 - 0.89 (m, 3H), 1.18 (d, J=6.2 Hz, 3H), 1.22 - 1.35 (m, 53H), 3.78 - 3.85 (m, 1H). ^{13}C NMR (151 MHz, $CDCl_3$): δ 14.3, 22.9, 23.6, 29.5, 29.8, 29.9 (22C), 32.1, 68.3.

10.3.3.38 *Tert*-butyldimethyl(prop-2-yn-1-yloxy)silane (72)

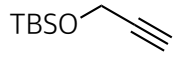

Procedure 10.3.3.2; 1.4 g prop-2-yn-ol (**71**, 24.96 mmol), 2.5 g imidazole (37.44 mmol), 5.3 g TBSCl (34.94 mmol), 10 mL dry THF, pentane as eluent. *Tert*-butyldimethyl(prop-2-yn-1-yloxy)silane (**72**): 4.2 g (24.66 mmol) of light oil, 99% yield. ^{1}H NMR (600 MHz, $CDCl_3$): δ 0.03 - 0.07 (m, 3H), 0.08 - 0.11 (m, 3H), 0.83 - 0.97 (m, 9H), 3.72 (t, J=2.6 Hz, 1H), 4.28 (d, J=2.5 Hz, 2H). ^{13}C NMR (151 MHz, $CDCl_3$): δ -5.1 (2C), 18.4, 25.9 (3C), 51.6, 73.0, 82.5.

10.3.3.39 *Tert*-butyl(henicos-2-yn-1-yloxy)dimethylsilane (74)

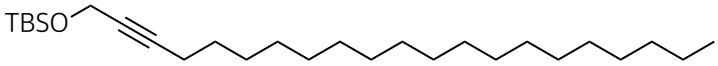

Procedure 10.3.3.6; 0.4 g *tert*-butyldimethyl(prop-2-yn-1-yloxy)silane (**72**, 2.62 mmol), 1.0 g 1-iodooctadecane (**73**, 2.62 mmol), 2.7 mL HMPA (15.72 mmol), 1.6 mL 2.5 M *n*-BuLi (3.93 mmol), 9:1 hexane-EtOAc as eluent. *Tert*-butyl(henicos-2-yn-1-yloxy)dimethylsilane (**74**): 775 mg yellow oily-solid (1.83 mmol), 70% yield. ^{1}H NMR (600 MHz, $CDCl_3$): δ 0.12 (m, 6H), 0.88 (t, J=7.0 Hz, 3H), 0.91 (s, 9H), 1.24 - 1.27 (m, 25H), 1.27 - 1.39 (m, 9H), 1.46 - 1.52 (m, 2H), 2.19 (ddd, J=7.1 Hz, J=7.1 Hz, J=2.2 Hz, 2H), 4.32 (s, 1H). ^{13}C NMR (151 MHz, $CDCl_3$): δ -4.9 (2C), 14.3, 18.9, 22.9 (2C), 26.0 (3C), 28.8, 29.0, 29.3, 29.5, 29.7, 29.8, 29.9 (8C), 32.1, 52.2, 78.8, 85.7. EIMS (70 eV) *m/z* 407.4 [M-CH_3]$^+$, calculated for $C_{27}H_{54}OSi$ *m/z* 422.4.

10.3.3.40 [D_4]-*tert*-butyl(henicosyloxy)dimethylsilane (75)

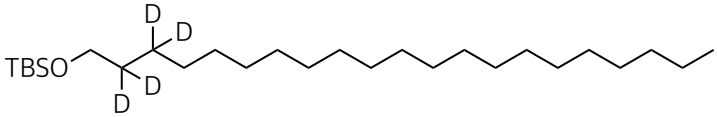

Procedure 10.3.3.3; 202 mg *tert*-butyl(henicos-2-yn-1-yloxy)dimethylsilane (**74**, 0.48 mmol), D_2, 4 mL hexane. [D_4]-*tert*-butyl(henicosyloxy)dimethylsilane (**75**): 176 mg (0.41 mmol), 85% yield. ^{1}H NMR (600 MHz, $CDCl_3$): δ 0.12 (m, 6H), 0.88 (t, J=7.0 Hz, 3H), 0.90 (s, 9H), 1.24 - 1.27 (m, 42H), 1.27 - 1.34 (m, 9H), 1.48 (dd, J=12.1 Hz, J=6.9 Hz, 1H), 1.93 - 2.03 (m, 2H), 3.58 (s, 1H). ^{13}C NMR (151 MHz, $CDCl_3$): δ -5.2, -5.1, 14.3, 18.5, 22.9, 25.8, 26.2 (3C), 29.5, 29.8 (12C), 29.9, 32.1, 63.4.

10.3.3.41 [D_4]-henicosan-1-ol (68a)

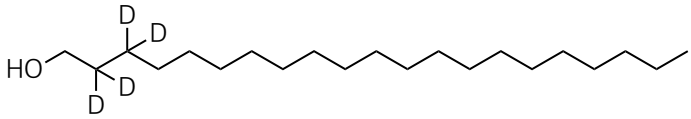

Procedure 10.3.3.3; 176 mg [D_4]-*tert*-butyl(henicosyloxy)dimethylsilane (**75**, 0.41 mmol), 1 mL dry THF, 4.1 mL 1 M TBAF (4.10 mmol), 6:4 hexane-EtOAc as eluent. [D_4]-henicosan-1-ol (**69a**): 93 mg white solid (0.29 mmol), 72% yield. ^{1}H NMR (600 MHz, $CDCl_3$): δ 0.88 (t, J=7.0 Hz, 3H), 1.24 - 1.26 (m, 20H), 1.28 - 1.33 (m, 11H), 1.58 (m, 2H), 1.91 - 1.98 (m, 2H), 3.62 (s, 2H). ^{13}C NMR (151 MHz, $CDCl_3$): δ 14.3, 22.8, 29.3, 29.5, 29.7, 29.8, 29.9 (11C), 32.1, 63.1.

10.3.3.42 Ethyl 2-acetyltridec-12-enoate (99)

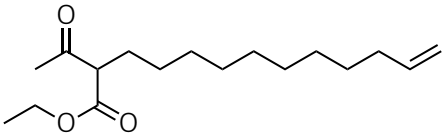

A stirred solution of sodium methanolate (from dissolving 0.1 g of sodium, 4.35 mmol) in 4 mL of EtOH) was cooled to 0 °C and treated with 0.6 g of ethyl 3-oxobutanoate (**98**, 4.61 mmol). After 1 hour at room temperature, 0.9 mL of 11-bromo-1-undecene (**97**, 4.09 mmol) dissolved in 3 mL of EtOH were added. The mixture was treated under reflux overnight. The solvent was removed under reduced pressure, and the residue was distributed between Et_2O and water. The organic layer was collected, dried over $MgSO_4$, and concentrated under reduced pressure. Purification by column chromatography with a gradient of pentane-Et_2O (0-100%) gave the ethyl 2-acetyltridec-12-enoate (**99**) as a yellow oil (982 mg, 3.47 mmol, 85% yield). ^{1}H NMR (600 MHz, $CDCl_3$): 1.25 (m, 4H), 1.27 (t, J=6.3 Hz, 3H), 1.30 - 1.45 (m, 10H), 1.78 - 1.90 (m, 2H), 1.98 - 2.07 (m, 3H), 2.22 (s, 2H), 3.35 - 3.42 (m, 1H), 4.19 (qd, J=7.1 Hz, J=1.3 Hz, 2H), 4.93 (ddt, J=10.2 Hz, J=2.3 Hz, J=1.2 Hz, 1H), 4.99 (dq, J=17.1 Hz, J=1.6 Hz, 1H), 5.81 (ddt, J=16.9 Hz, J=10.2 Hz, J=6.7 Hz, 1H). ^{13}C NMR (151 MHz, $CDCl_3$): δ 14.2, 27.5, 28.3, 28.8, 29.0, 29.2,

29.4 (2C), 29.5 (2C), 33.9, 60.1, 61.4, 114.2, 139.4, 170.1, 203.6. EIMS (70 eV) *m/z* 250.2 $[M\text{-}H_2O]^+$, calculated for $C_{16}H_{28}O_3$ *m/z* 268.2.

10.3.3.43 Tetradec-13-en-2-one (94)

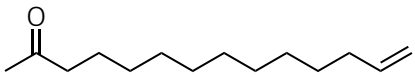

A mixture of 982 mg of ethyl 2-acetyltridec-12-enoate (**99**, 3.47 mmol) and 15 mL of 20% NaOH solution (0.50 mol) was stirred at 50 °C for 2 hours. The mixture was cooled to 0 °C and treated with concentrated HCl until pH≈2. The cold bath was removed, and the resulting mixture was refluxed at 80 °C for 5 h. The crude product was extracted with EtOAc, the organic phase was washed with water, dried over $MgSO_4$, and concentrated under reduced pressure. The tetradec-13-en-2-one (**94**) was purified by column chromatography with 9:1 hexane-EtOAc as eluent to afford a yellow oil (548 mg, 2.60 mmol, 75% yield). ^{1}H NMR (600 MHz, $CDCl_3$): δ 1.27 - 1.30 (m, 12H), 1.33 - 1.42 (m, 2H), 1.56 - 1.61 (m, 2H), 2.02 - 2.09 (m, 2H), 2.16 (s, 3H), 2.44 (t, J=7.5 Hz, 2H), 4.95 (ddt, J=10.2 Hz, J=2.3 Hz, J=1.2 Hz, 1H), 4.99 - 5.04 (m, 1H), 5.79 - 5.88 (m, 1H). ^{13}C NMR (151 MHz, $CDCl_3$): δ 24.0, 29.1, 29.3 (2C), 29.5 (2C), 29.6 (2C), 29.7, 30.0, 34.0, 44.0, 114.2, 139.4, 209.5.

10.3.3.44 Methyl 15-hydroxypentadecanoate (104)

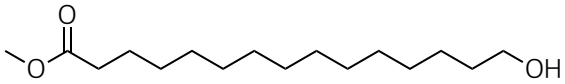

A stirred solution of 1.7 g of sodium methoxide (49.95 mmol) in 50 mL of MeOH was treated with 1.5 g of pentadecanolide (**45**, 6.24 mmol). The mixture was refluxed at 80 °C for 5 hours and quenched with 50 mL of 2 M HCl followed by 50 mL of water. The crude product was extracted with EtOAc. The organic phase was washed with brine, dried over Na_2SO_4, and concentrated under reduced pressure to yield the methyl 15-hydroxypentadecanoate (**104**) as a white solid (1.7 g, 6.11 mmol, 98% yield). The product was used without additional purification. ^{1}H NMR (600 MHz, $CDCl_3$): δ 1.23 - 1.40 (m, 21H), 1.54 - 1.66 (m, 4H), 2.32 (t, J=7.7 Hz, 2H), 3.66 (t, J=6.7 Hz, 2H), 3.68 (s, 3H). ^{13}C NMR (151 MHz, $CDCl_3$): δ 25.1, 25.8, 29.3, 29.4, 29.7 (7C), 32.9, 34.2, 51.6, 63.2, 174.5.

10.3.3.45 Methyl 15-bromopentadecanoate (105)

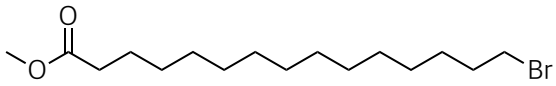

Procedure 10.3.3.1; 1.7 g methyl 15-hydroxypentadecanoate (**104**, 6.11 mmol), 3.2 g PPh_3 (12.22 mmol), 2.0 g Br_2 (12.22 mmol), 20:1 hexane-EtOAc as eluent. Methyl 15-bromopentadecanoate (**105**): 1.7 g white solid (5.07 mmol), 85% yield. ^{1}H NMR (600 MHz, $CDCl_3$): δ 1.25 - 1.35 (m, 16H), 1.38 - 1.46 (m, 4H), 1.58 - 1.66 (m, 2H), 1.86 (dt, J=14.5 Hz, J=7.0 Hz, 2H), 2.30 (t, J=7.6 Hz, 2H), 3.40 (t, J=6.9 Hz, 2H), 3.66 (s, 3H). ^{13}C NMR (151 MHz, $CDCl_3$): δ 25.1, 28.3, 28.9, 29.0, 29.3, 29.4, 29.6, 29.7 (4C), 33.0, 34.2, 34.3, 51.6, 174.5.

10.3.3.46 Pentadec-14-enoic acid (106)

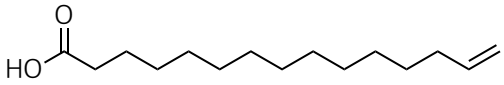

A stirred solution of 1.7 g of methyl 15-bromopentadecanoate (**105**, 5.07 mmol) in 20 mL of dry DCM was treated with 5.6 g of *tert*-BuOK (49.91 mmol) at room temperature. After 16 hours, the solution was neutralized with 10 M HCl, and the crude product was extracted with DCM. The organic phase was washed with water, dried over Na_2SO_4, and concentrated under reduced pressure. The residue was purified by column chromatography with 9:1 hexane-EtOAc as eluent to afford the pentadec-14-enoic acid (**106**) as a white solid (853 mg, 3.55 mmol, 70% yield). ^{1}H NMR (600 MHz, $CDCl_3$): δ 1.24 - 1.47 (m, 19H), 1.61 - 1.69 (m, 2H), 2.03 - 2.09 (m, 2H), 2.37 (t, J=7.5 Hz, 2H), 4.92 - 4.97 (m, 1H), 4.98 - 5.04 (m, 1H), 5.79 - 5.88 (m, 1H). ^{13}C NMR (151 MHz, $CDCl_3$): δ 24.8, 29.1, 29.2, 29.3, 29.4, 29.6, 29.7 (3C), 29.8, 34.0 (2C), 114.2, 139.4, 179.3. EIMS (70 eV) *m/z* 222.2 $[M\text{-}H_20]^+$, calculated for $C_{15}H_{28}O_2$ *m/z* 240.2.

10.3.3.47 Methyl pentadec-14-enoate (103)

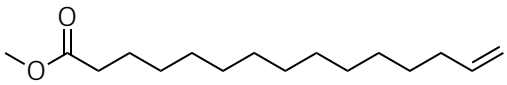

Procedure 10.3.3.7; 853 mg pentadec-14-enoic acid (**106**, 3.55 mmol), 8 mL 1:1 MeOH-Toluene, 3.4 mL 2 M $TMSCHN_2$ (6.75 mmol), 9:1 hexane-EtOAc as eluent. Methyl pentadec-14-enoate (**103**): 677 mg colorless oil (2.66 mmol), 75% yield. ^{1}H NMR (600 MHz, $CDCl_3$): δ 1.22 - 1.35 (m, 15H), 1.35 - 1.48

(m, 2H), 1.59 - 1.70 (m, 3H), 2.02 - 2.09 (m, 2H), 2.32 (t, J=7.6 Hz, 2H), 3.66 (s, 3H), 4.92 - 4.97 (m, 1H), 4.97 - 5.04 (m, 1H), 5.78 - 5.88 (m, 1H). ^{13}C NMR (151 MHz, $CDCl_3$): δ 25.1, 29.1, 29.3 (2C), 29.4, 29.6, 29.7 (3C), 29.8, 34.0, 34.3, 51.6, 114.2, 139.4, 174.5.

10.3.4 Syntheses of ascarosides

10.3.4.1 General procedure for Grubbs metathesis

Under N_2, to a solution of alkenyl ascaroside (1 eq.) in dry DCM (10 mg/mL), was added the alkenyl-ketone or alkenyl-ester (1.2 eq.) dissolved in the minimum quantity of dry DCM, followed by the addition of the Grubbs 2nd generation catalyst (0.3 eq.). The mixture was refluxed at 45 °C overnight. The reaction was terminated by the evaporation of the solvent under reduced pressure, and the crude products were purified by column chromatography with a mixture of 9:1 hexane-EtOAc as eluent.

10.3.4.2 General procedure for glycosylation

Under nitrogen, a stirred solution of (2*R*,3*R*,5*R*,6*S*)-2-hydroxy-6-methyltetrahydro-2*H*-pyran-3,5-diyl dibenzoate (**19**, 1.1 eq.) dissolved in dry DCM (10 mg/mL) was treated with CCl_3CN (3 eq.) and 1,8-diazabicyclo[5.4.0]undec-7-ene (15% mol). After 30 minutes, the solvent was removed, and the 2,4-benzoyl ascarylose trichloro acetimidate (**40**) was purified by column chromatography with a mixture of 6:4 hexane-EtOAc. The 2,4-benzoyl ascarylose trichloro acetimidate was concentrated under reduced pressure and directly used for the next step. Under N_2, a solution of 2,4-benzoyl ascarylose trichloro acetimidate dissolved in dry DCM was treated with a solution of alkyl alcohol or alkenyl alcohol (1 eq.) dissolved in the minimum volume of dry DCM at 0°C and activated by the addition of TMSOTf (0.1 eq.). The reaction was stirred at room temperature overnight for the preparation of the very long chain alkyl ascaroside or stirred for two hours for the preparation of the (ω)-carboxy ascaroside. Subsequently, the synthesis of the very long chain alkyl ascaroside was terminated by removing the solvent under reduced pressure, whereas the synthesis of the (ω)-carboxy ascaroside was neutralized with $NaHCO_3$ saturated solution. The crude product was purified by column chromatography with a mixture of 9:1 hexane-EtOAc as eluent, and the very long chain or (ω)-carboxy ascaroside resulted as a white solid.

10.3.4.3 General procedure of ester hydrolysis

A stirred solution of benzoyl-ascaroside (1 eq.) in EtOH was treated with an excess of NaOH (6 eq.) solution. After 30 minutes, the mixture was neutralized with acetic acid and the product was extracted with EtOAc. The organic phase was dried over $MgSO_4$, and the solvent was removed under reduced pressure. The crude products were washed with pentane and purified by column chromatography. The very long chain and (ω)-carboxy ascarosides were obtained as white solids.

10.3.4.4 General procedure of acetylation of very long chain alkyl ascarosides

A solution of very long chain alkyl ascaroside (1 eq.) in dry DCM (5 mg/mL) was treated with a 0.1 M DMAP solution in DCM (1.1 eq.), and acetic acid anhydride (0.8-4.0 eq.). After stirring overnight, the reaction was terminated by the removal of the solvent under reduced pressure. The crude product was dissolved in EtOAc and washed with water. Subsequent filtration over a short silica column gave the monoacetyl/diacetyl ascarosides as white oily solids.

10.3.4.5 Procedure of deacetylation of very long chain alkyl ascarosides

A solution of 1 eq. of 2,4-diacetyl ascaroside in a 1:1 mixture of DCM/MeOH (5 mg/mL) was treated with 0.5 eq. of 1M CH_3ONa solution. After 1.5 hours, the solvents were removed under reduced pressure. The product was filtered through a short silica column with EtOAc and concentrated to yield a white oily solid.

10.3.4.6 [D_4]-(2*R*,3*R*,5*R*,6*S*)-2-(henicosyloxy)-6-methyltetrahydro-2*H*-pyran-3,5-diyl dibenzoate (70b)

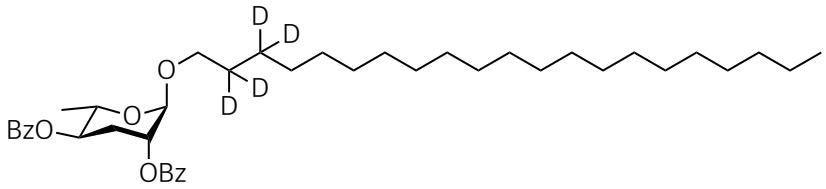

Procedure 10.3.4.2; 93 mg [D_4]-henicosan-1-ol (**69b**, 0.29 mmol), 114 mg benzoyl ascarylose **19** (0.32 mmol). [D_4]-(2*R*,3*R*,5*R*,6*S*)-2-(henicosyloxy)-6-methyltetrahydro-2*H*-pyran-3,5-diyl dibenzoate (**70b**): 150 mg (0.23 mmol), 79% yield. ^{1}H NMR (600 MHz, $CDCl_3$): δ 0.88 (t, J=6.9 Hz, 3H), 1.26 (m, 35H), 1.30 (d, J=6.2 Hz, 3H), 2.22 (ddd, J=14.0 Hz, J=11.5 Hz, J=3.1 Hz, 1H), 2.42 (dt, J=13.3 Hz, J=3.7 Hz, 1H), 3.51 (dd, J=15.9 Hz, J=8.3 Hz, 1H), 3.75 (d, J=9.6 Hz, 1H), 4.08 (dd, J=9.8 Hz, J=6.3 Hz, 1H), 5.18 (ddd, J=11.2

Hz, J=9.8 Hz, J=4.7 Hz, 1H), 5.21 (m, 1H), 7.46 (m, 4H), 7.58 (m, 2H), 8.04 (d, J=7.3 Hz, 2H), 8.11 (d, J=7.3 Hz, 2H).

10.3.4.7 [D_4]-(2*S*,3*S*,5*S*,6*R*)-2-(henicosyloxy)-6-methyltetrahydro-2*H*-pyran-3,5-diol ([D_4]-asc-ωC21-H, 68b)

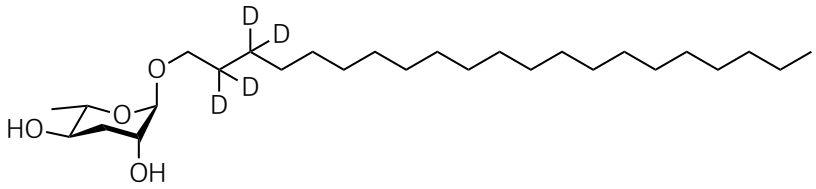

Procedure 10.3.4.3; 66 mg [D_4]-(2*R*,3*R*,5*R*,6*S*)-2-(henicosyloxy)-6-methyltetrahydro-2*H*-pyran-3,5-diyl dibenzoate (**70b**, 0.10 mmol). [D_4]-(2*S*,3*S*,5*S*,6*R*)-2-(henicosyloxy)-6-methyltetrahydro-2*H*-pyran-3,5-diol (**[D_4]-asc-ωC21-H**, **68b**): 36 mg (0.08 mmol), 81% yield. ^{1}H NMR (600 MHz, $CDCl_3$): δ 0.88 (t, J=7.0 Hz, 3H), 1.25 (m, 37H), 1.29 (d, J=6.1 Hz, 3H), 1.84 (ddd, J=11.1 Hz, J=3.8 Hz, J=3.0 Hz, 1H), 2.07 (ddd, J=13.0 Hz, J=3.8 Hz, J=3.8 Hz, 1H), 3.42 (m, 1H), 3.60 (m, 1H), 3.67 (m, 1H), 3.86 (m, 1H), 4.57 (m, 1H).

10.3.4.8 (2*R*,3*R*,5*R*,6*S*)-2-(henicosyloxy)-6-methyltetrahydro-2*H*-pyran-3,5-diyl dibenzoate (70a)

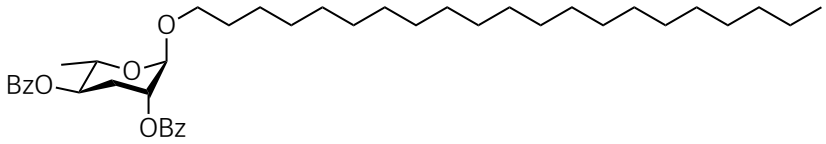

Procedure 10.3.4.2; 127 mg heneicosanol (**69a**, 0.41 mmol), 160 mg benzoyl ascarylose **19** (0.45 mmol). (2*R*,3*R*,5*R*,6*S*)-2-(henicosyloxy)-6-methyltetrahydro-2*H*-pyran-3,5-diyl dibenzoate (**70a**): 213 mg (0.33 mmol), 80% yield. ^{1}H NMR (600 MHz, $CDCl_3$): δ 0.88 (t, J=7.0 Hz, 3H), 1.22 - 1.36 (m, 34H), 1.40 (m, 4H), 1.68 (m, 2H), 2.22 (ddd, J=13.8 Hz, J=11.4 Hz, J=3.1 Hz, 1H), 2.42 (ddd, J=13.5 Hz, J=3.7 Hz, J=3.7 Hz, 2H), 3.51 (ddd, J=9.6 Hz, J=6.6 Hz, J=6.6 Hz, 1H), 3.76 (ddd, J=9.6 Hz, J=6.8 Hz, J=6.8 Hz, 1H), 4.07 (dq, J=10.3 Hz, J=6.5 Hz, 1H), 4.83 (m, 1H), 5.18 (ddd, J=11.3 Hz, J=9.9 Hz, J=4.7 Hz, 1H), 5.21 (m, 1H), 7.47 (m, 4H), 7.56 - 7.62 (m, 2H), 8.04 (dd, J=8.3 Hz, J=1.2 Hz, 2H), 8.12 (dd, J=8.3 Hz, J=1.2 Hz, 2H).

10.3.4.9 [D_4]-(2*R*,3*S*,5*S*,6*S*)-2-methyl-6-(((*R*)-pentacosan-2-yl)oxy)tetrahydro-2*H*-pyran-3,5-diyl dibenzoate (41b)

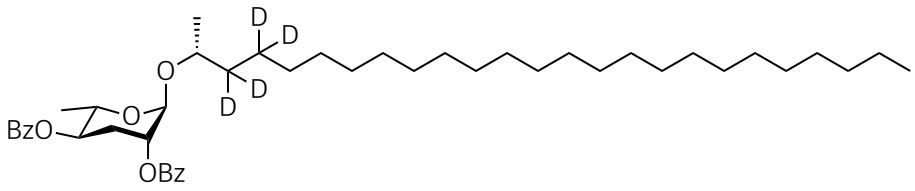

Procedure 10.3.4.2; 64 mg [D_4]-(*R*)-pentacosan-2-ol (**34b**, 0.17 mmol), 68 mg benzoyl ascarylose **19** (0.19 mmol). [D_4]-(2*R*,3*S*,5*S*,6*S*)-2-methyl-6-(((*R*)-pentacosan-2-yl)oxy)tetrahydro-2*H*-pyran-3,5-diyl dibenzoate (**41b**): 109 mg (0.15 mmol), 90% yield. ^{1}H NMR (600 MHz, $CDCl_3$): δ 0.88 (t, J=7.0 Hz, 3H), 1.19 (d, J=6.1 Hz, 3H), , 1.25 (m, 30H), 1.40 - 1.56 (m, 8H), 1.51 (dt, J=18.7 Hz, J=6.2 Hz, 1H), 2.22 (ddd, J=13.9 Hz, J=11.5 Hz, J=3.1 Hz, 1H), 2.41 (dt, J=13.4 Hz, J=3.8 Hz, 1H), 3.84 (h, J=6.1 Hz, 1H), 4.13 (dq, J=9.9 Hz, J=6.0 Hz, 1H), 4.98 (m, 1H), 5.17 (m, 1H), 5.20 (ddd, J=11.2 Hz, J=10.0 Hz, J=4.7 Hz, 1H), 7.47 (m, 4H), 7.58 (m, 2H), 8.06 (dd, J=8.4 Hz, J=1.4 Hz, 2H), 8.14 (dd, J = 8.5 Hz, J=1.5 Hz, 2H).

10.3.4.10 [D_4]-(2*S*,3*R*,5*R*,6*R*)-2-methyl-6-(((*R*)-pentacosan-2-yl)oxy)tetrahydro-2*H*-pyran-3,5-diol ([D_4]-asc-C25-H, 33b)

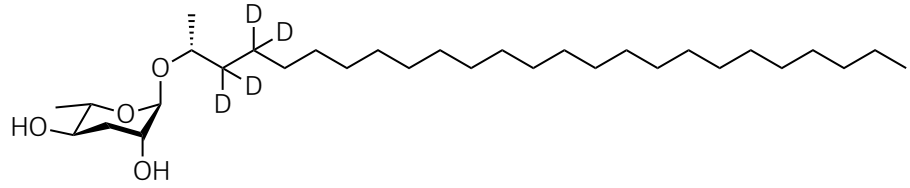

Procedure 10.3.4.3; 55 mg [D_4]-(2*R*,3*S*,5*S*,6*S*)-2-methyl-6-(((*R*)-pentacosan-2-yl)oxy)tetrahydro-2*H*-pyran-3,5-diyl dibenzoate (**41b**, 0.08 mmol). [D_4]-(2*S*,3*R*,5*R*,6*R*)-2-methyl-6-(((*R*)-pentacosan-2-yl)oxy)tetrahydro-2*H*-pyran-3,5-diol (**[D_4]-asc-C25-H**, **33b**): 34 mg (0.07 mmol), 87% yield. ^{1}H NMR (600 MHz, $CDCl_3$): δ 0.88 (t, J=7.0 Hz, 3H), 1.11 (d, J=6.1 Hz, 3H), 1.22 (s, 3H), 1.20 - 1.26 (m, 26H), 1.27 (d, J=6.2 Hz, 3H), 1.27 - 1.45 (m, 12H), 1.84 (ddd, J=13.0 Hz, J=11.2 Hz, J=3.0 Hz, 1H), 2.06 (ddd, J=13.0 Hz, J=3.9 Hz, J=3.2 Hz, 1H), 3.59 (ddd, J=11.1 Hz, J=9.3 Hz, J=4.6 Hz, 1H), 3.69 (q, J=9.2 Hz, 1H), 3.77 (m, 1H), 3.80 (m, 1H), 4.69 (m, 1H).

10.3.4.11 (2*R*,3*S*,5*S*,6*S*)-2-methyl-6-(((*R*)-pentacosan-2-yl)oxy)tetrahydro-2*H*-pyran-3,5-diyl dibenzoate (41a)

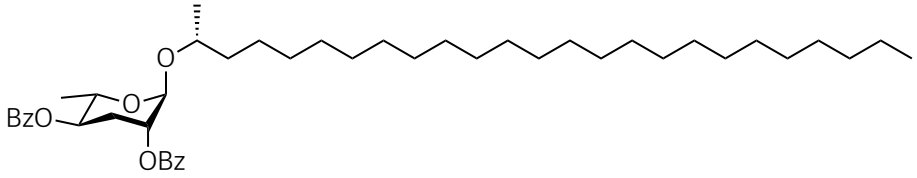

Procedure 10.3.4.2; 91 mg (*R*)-pentacosan-2-ol (**34a**, 0.25 mmol), 99 mg benzoyl ascarylose **19** (0.28 mmol). (2*S*,3*R*,5*R*,6R)-2-methyl-6-(((*R*)-pentacosan-2-yl)oxy)tetrahydro-2*H*-pyran-3,5-diol (**asc-C25-H**, **41a**): 140 mg (0.20 mmol), 79% yield. ^{1}H NMR (600 MHz, $CDCl_3$): δ 0.88 (t, J=6.7 Hz, 3H), 1.19 (d, J=6.1 Hz, 3H), 1.23 - 1.27 (m, 28H), 1.28 (d, J=6.3 Hz, 3H), 1.29 - 1.47 (m, 10H), 1.65 (m, 2H), 2.22 (ddd, J=13.8 Hz, J=11.5 Hz, J=3.1 Hz, 1H), 2.42 (ddd, J=13.4 Hz, J=3.8 Hz, J=3.2 Hz, 1H), 3.85 (q, J=6.2 Hz, 1H), 4.13 (dq, J=9.9 Hz, J=6.6 Hz, 1H), 4.96 (m, 1H), 5.15 (m, 2H), 5.19 (ddd, J=11.2 Hz, J=10.0 Hz, J=4.7 Hz, 1H), 7.46 (m, 4H), 7.58 (m, 3H), 8.04 (dd, J=8.4 Hz, J=1.3 Hz, 2H), 8.11 (dd, J=8.4 Hz, J=1.3 Hz, 2H).

10.3.4.12 [D_4]-(2*S*,3*R*,5*R*,6*R*)-2-methyl-6-(((*R*)-24-methylpentacosan-2-yl)oxy)tetrahydro-2*H*-pyran-3,5-diyl dibenzoate (56b)

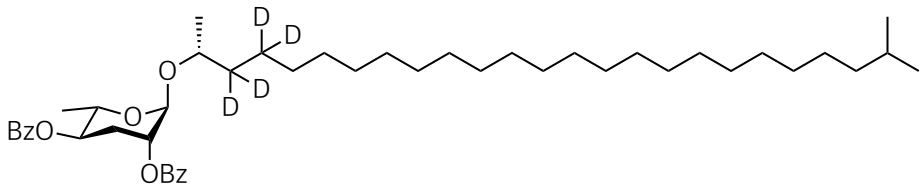

Procedure 10.3.4.2; 115 mg [D_4]-(*R*)-24-methylpentacosan-2-ol (**44b**, 0.30 mmol), 117 mg benzoyl ascarylose **19** (0.33 mmol). [D_4]-(2*S*,3*R*,5*R*,6*R*)-2-methyl-6-(((*R*)-24-methylpentacosan-2-yl)oxy)tetrahydro-2*H*-pyran-3,5-diyl dibenzoate (**56b**): 156 mg (0.22 mmol), 72% yield. ^{1}H NMR (600 MHz, $CDCl_3$): δ 0.86 (d, J=6.6 Hz, 6H), 1.15 (q, J=6.7 Hz, 2H), 1.19 (d, J=6.1 Hz, 3H), 1.25 (m, 37H), 1.28 (d, J=6.3 Hz, 3H), 1.33 (d, J=10.9 Hz, 4H), 1.51 (dhept, J=13.2 Hz, J=6.7 Hz, 1H), 2.22 (ddd, J=13.7 Hz, J=11.5 Hz, J=3.1 Hz, 1H), 2.42 (dt, J=13.5 Hz, J=3.6 Hz, 1H), 3.84 (q, J=6.1 Hz, 1H), 4.09 - 4.16 (m, 1H), 4.95 (s, 1H), 5.13 - 5.22 (m, 2H), 7.41 - 7.51 (m, 4H), 7.58 (ddd, J=8.7 Hz, J=5.6 Hz, J=2.9 Hz, J=1.4 Hz, 2H), 8.01 - 8.07 (m, 2H), 8.12 (dt, J=8.4 Hz, J=1.5 Hz, 2H).

10.3.4.13 [D_4]-(2*S*,3*R*,5*R*,6*R*)-2-methyl-6-(((*R*)-24-methylpentacosan-2-yl)oxy)tetrahydro-2*H*-pyran-3,5-diol ([D_4]-asc-*i*C26-H, 43b)

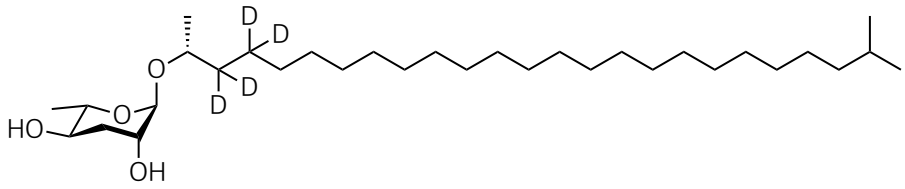

Procedure 10.3.4.3; 98 mg [D_4]-(2*S*,3*R*,5*R*,6*R*)-2-methyl-6-(((*R*)-24-methylpentacosan-2-yl)oxy)tetrahydro-2*H*-pyran-3,5-diyl dibenzoate (**56b**, 0.14 mmol). [D_4]-(2*S*,3*R*,5*R*,6*R*)-2-methyl-6-(((*R*)-24-methylpentacosan-2-yl)oxy)tetrahydro-2*H*-pyran-3,5-diol (**[D_4]-asc-*i*C26-H**, **43b**): 66 mg (0.13 mmol), 93% yield. ^{1}H NMR (600 MHz, $CDCl_3$): δ 0.86 (d, J=6.7 Hz, 6H), 1.11 (d, J=6.4 Hz, 3H), 1.25 (m, 25H), 1.27 (d, J=6.3 Hz, 3H), 1.30 - 1.40 (m, 1H), 1.51 (dhept, J=13.3 Hz, J=6.6 Hz, 1H), 1.83 (m, 1H), 2.05 (dt, J=12.9 Hz, J=3.8 Hz, 1H), 3.58 (m, 1H), 3.68 (m, 1H), 3.76 (q, J=6.1 Hz, 1H), 3.80 (s, 1H), 4.68 (s, 1H).

10.3.4.14 (2*S*,3*R*,5*R*,6*R*)-2-methyl-6-(((*R*)-24-methylpentacosan-2-yl)oxy)tetrahydro-2*H*-pyran-3,5-diyl dibenzoate (56a)

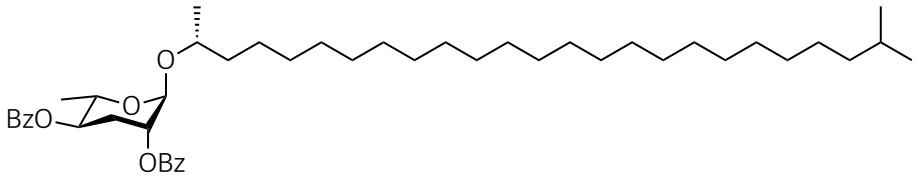

Procedure 10.3.4.2; 134 mg (*R*)-24-methylpentacosan-2-ol (**44a**, 0.35 mmol), 139 mg benzoyl ascarylose **19** (0.39 mmol). (2*S*,3*R*,5*R*,6*R*)-2-methyl-6-(((*R*)-24-methylpentacosan-2-yl)oxy)tetrahydro-2*H*-pyran-3,5-diyl dibenzoate (**56a**): 189 mg (0.26 mmol), 75% yield. ^{1}H NMR (600 MHz, $CDCl_3$): δ 0.86 (d, J=6.6 Hz, 6H), 1.12 - 1.17 (m, 4H), 1.19 (d, J=6.1 Hz, 3H), 1.25 - 26 (m, 38H), 1.28 (d, J=6.3 Hz, 3H), 1.33 - 1.36 (m, 5H), 1.45 - 1.55 (m, 4H), 1.65 (ddt, J=12.0 Hz, J=7.9 Hz, J=4.9 Hz, 1H), 2.21 (ddd, J=13.8 Hz, J=11.5 Hz, J=3.1 Hz, 1H), 2.41 (dt, J=13.4 Hz, J=3.7 Hz, 1H), 3.85 (q, J=6.2 Hz, 1H), 4.13 (dq, 1H), 4.95 (s, 1H), 5.13 - 5.16 (m, 1H), 5.18 (td, J=11.3 Hz, J=4.7 Hz, 1H), 7.46 (p, J=7.7 Hz, 4H), 7.54 - 7.61 (m, 2H), 8.04 (dd, J=8.3 Hz, J=1.2 Hz, 2H), 8.11 (dd, J=8.2 Hz, J=1.1 Hz, 2H).

10.3.4.15 [D_4]-(2*R*,3*R*,5*R*,6*S*)-2-(((*R*)-hentriacontan-2-yl)oxy)-6-methyltetrahydro-2*H*-pyran-3,5-diyl dibenzoate (67b)

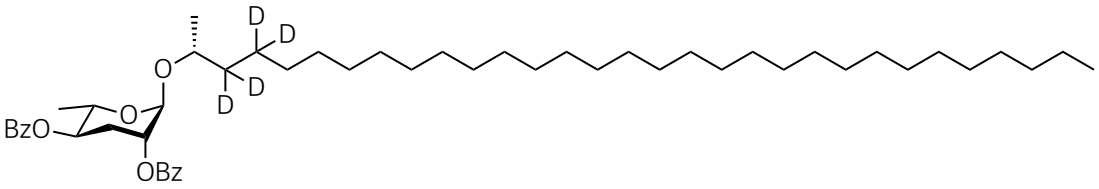

Procedure 10.3.4.2; 35 mg [D_4]-(*R*)-hentriacontan-2-ol (**58b**, 0.08 mmol), 32 mg benzoyl ascarylose **19** (0.09 mmol). [D_4]-(2*R*,3*R*,5*R*,6*S*)-2-(((*R*)-hentriacontan-2-yl)oxy)-6-methyltetrahydro-2*H*-pyran-3,5-diyl dibenzoate (**67b**): 38 mg (0.05 mmol), 62% yield. ^{1}H NMR (600 MHz, $CDCl_3$): δ 0.88 (t, J=7.0 Hz, 3H), 1.19 (d, J=6.1 Hz, 3H), 1.26 (m, 37H), 1.29 (d, J=6.2 Hz, 3H), 1.31 - 1.54 (m, 7H), 1.55 - 1.66 (m, 2H), 2.22 (ddd, J=13.9 Hz, J=11.5 Hz, J=3.1 Hz, 1H), 2.42 (ddd, J=13.4 Hz, J=4.2 Hz, J=3.8 Hz, 1H), 3.85 (m, 1H), 4.13 (m, 1H), 4.96 (m, 1H), 5.15 (m, 2H), 5.19 (td, J=11.2 Hz, J=4.6 Hz, 1H), 7.46 (m, 4H), 7.58 (m, 2H), 8.04 (m, 2H), 8.12 (m, 2H).

10.3.4.16 [D_4]-(2*R*,3*R*,5*R*,6*S*)-2-(((*R*)-hentriacontan-2-yl)oxy)-6-methyltetrahydro-2*H*-pyran-3,5-diol ([D_4]-asc-C31-H, 57b)

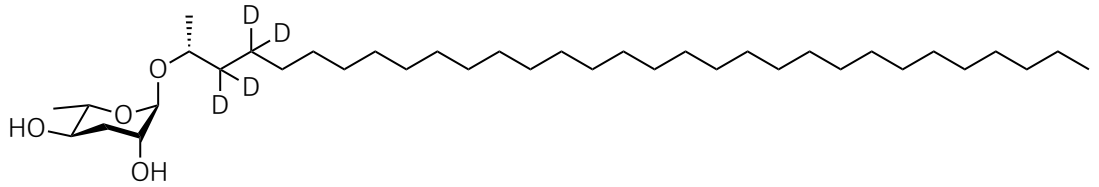

Procedure 10.3.4.3; 34 mg [D_4]-(2*R*,3*R*,5*R*,6*S*)-2-(((*R*)-hentriacontan-2-yl)oxy)-6-methyltetrahydro-2*H*-pyran-3,5-diyl dibenzoate (**67b**, 0.04 mmol). [D_4]-(2*R*,3*R*,5*R*,6*S*)-2-(((*R*)-hentriacontan-2-yl)oxy)-6-methyltetrahydro-2*H*-pyran-3,5-diol (**[D_4]-asc-C31-H**, **57b**): 17 mg (0.03 mmol), 75% yield. ^{1}H NMR (600 MHz, $CDCl_3$): δ 0.88 (t, J=7.0 Hz, 3H), 1.12 (d, J=6.1 Hz, 3H), 1.13 - 1.19 (m, 1H), 1.25 (m, 40H), 1.29 (d, J=10.0 Hz, 1H), 1.45 - 1.70 (m, 1H), 1.84 - 1.88 (m, 1H), 2.07 (ddd, J=13.0 Hz, J=4.0 Hz, J=3.8 Hz, 1H), 3.59 (dd, J=10.3 Hz, J=9.5 Hz, J=4.5 Hz, 1H), 3.77 (m, 1H), 3.81 (m, H), 4.69 (m, 1H).

10.3.4.17 (2*R*,3*R*,5*R*,6*S*)-2-(((*R*)-hentriacontan-2-yl)oxy)-6-methyltetrahydro-2*H*-pyran-3,5-diyl dibenzoate (67a)

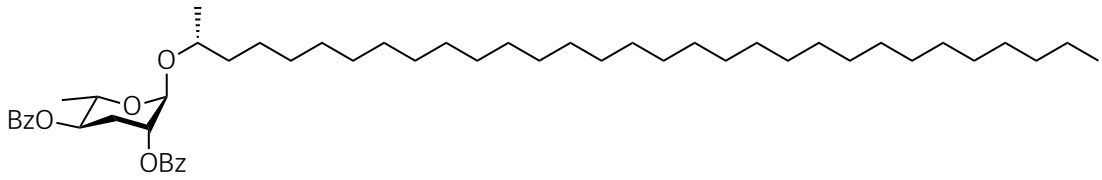

Procedure 10.3.4.2; 36 mg (*R*)-hentriacontan-2-ol (**58a**, 0.08 mmol), 32 mg benzoyl ascarylose **19** (0.09 mmol). (2*R*,3*R*,5*R*,6*S*)-2-(((*R*)-hentriacontan-2-yl)oxy)-6-methyltetrahydro-2*H*-pyran-3,5-diyl dibenzoate (**67a**): 56 mg (0.07 mmol), 88% yield. ^{1}H NMR (600 MHz, $CDCl_3$): δ 0.88 (t, J=7.0 Hz, 3H), 1.19 (d, J=6.1 Hz, 3H), 1.25 (m, 48H), 1.28 (d, J=6.2 Hz, 3H), 1.31 - 1.35 (m, 4H), 1.37 - 1.54 (m, 4H), 1.59 - 1.68 (m, 2H), 2.22 (ddd, J=13.9 Hz, J=11.6 Hz, J=3.1 Hz, 1H), 2.41 (ddd, J=13.4 Hz, J=3.8 Hz, J=3.8 Hz, 1H), 4.13 (dq, 1H), 3.83 - 3.87 (m, 1H), 4.95 - 4.96 (m, 1H), 5.14 - 5.16 (m, 1H), 5.18 (ddd, J=11.1 Hz, J=11.1 Hz, J=4.6 Hz, 1H), 7.46 (m, J=7.8 Hz, 4H), 7.55 - 7.66 (m, 2H), 8.02 - 8.06 (m, 2H), 8.09 - 8.14 (m, 2H).

10.3.4.18 (2*R*,3*R*,5*R*,6*S*)-2-(((*R*)-5-(tert-butoxy)-5-oxopent-1-en-3-yl)oxy)-6-methyltetrahydro-2*H*-pyran-3,5-diyl dibenzoate (100)

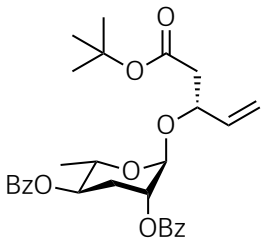

Procedure 10.3.4.2: 81 mg *tert*-butyl (*R*)-3-hydroxypent-4-enoate (**93**, 0.47 mmol), 185 mg benzoyl ascarylose **19** (0.52 mmol). (2*R*,3*R*,5*R*,6*S*)-2-(((*R*)-5-(tert-butoxy)-5-oxopent-1-en-3-yl)oxy)-6-methyltetrahydro-2*H*-pyran-3,5-diyl dibenzoate (**100**): 132 mg (0.26 mmol), 55% yield. ^{1}H NMR (600 MHz, $CDCl_3$): δ 1.30 (d, J=6.3 Hz, 3H), 1.33 - 1.44 (m, 1H), 2.04 (s, 9H), 2.29 (ddd, J=13.9 Hz, J=11.3 Hz, J=3.1 Hz, 2H), 2.43 (dt, J=13.6 Hz, J=3.9 Hz, 2H), 4.12 (q, J=7.1 Hz, 1H), 4.33 (dt, J=12.5 Hz, J=6.2 Hz, 1H), 5.12 - 5.23 (m, 1H), 5.23 - 5.33 (m, 3H), 5.37 (m, 1H), 5.87 (m, 1H), 7.46 (m, 4H), 7.59 (m, 3H), 7.98 - 8.15 (m, 4H).

10.3.4.19 (2*R*,3*R*,5*R*,6*S*)-2-(((*R*)-5-methoxy-5-oxopent-1-en-3-yl)oxy)-6-methyltetrahydro-2*H*-pyran-3,5-diyl dibenzoate (108)

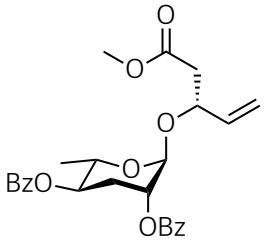

Procedure 10.3.4.2: 172 mg (*R*)-3-(((2*R*,3*R*,5*R*,6*S*)-3,5-bis(benzoyloxy)-6-methyltetrahydro-2*H*-pyran-2-yl)oxy)pent-4-enoic acid (**107**, 0.38 mmol). (2*R*,3*R*,5*R*,6*S*)-2-(((*R*)-5-methoxy-5-oxopent-1-en-3-yl)oxy)-6-methyltetrahydro-2*H*-pyran-3,5-diyl dibenzoate (**108**): 149 mg (0.32 mmol), 84% yield. ^{1}H NMR (600 MHz, $CDCl_3$): δ 1.23 (d, J=6.3 Hz, 3H), 2.17 (ddd, J=13.9 Hz, J=11.4 Hz, J=3.1 Hz, 1H), 2.40 (ddd, J=13.5 Hz, J=3.7 Hz, J=3.7 Hz, 1H), 2.58 (dd, J=15.4 Hz, J=5.2 Hz, 1H), 2.73 (dd, J=15.4 Hz, J=8.4 Hz, 1H), 3.73 (s, 3H), 4.10 (dq, J=10.0 Hz, J=6.2 Hz, 1H), 4.56 - 4.62 (m, 1H), 5.00 (s, 1H), 5.13 - 5.20 (m, 2H), 5.22 (d, J=10.4 Hz, 1H), 5.35 (d, J=17.2 Hz, 1H), 5.95 (ddd, J=17.5 Hz, J=10.4 Hz, J=7.3 Hz, 1H), 7.46 (q, J=7.8 Hz, 3H), 7.55 - 7.66 (m, 3H), 8.03 (dd, J=8.2 Hz, J=1.1 Hz, 2H), 8.10 (dd, J=8.2 Hz, J=1.1 Hz, 2H).

10.3.4.20 (2*R*,3*R*,5*R*,6*S*)-2-(((*R*,*E*)-1-(*tert*-butoxy)-1,16-dioxoheptadec-4-en-3-yl)oxy)-6-methyl tetrahydro-2*H*-pyran-3,5-diyl dibenzoate (101)

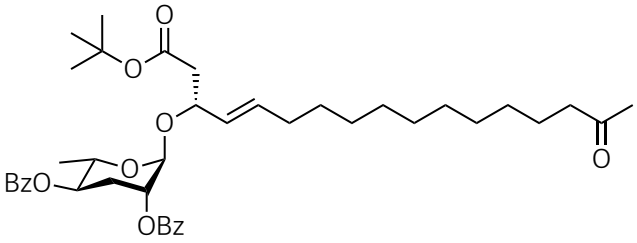

Procedure 10.3.4.1: 37 mg (2*R*,3*R*,5*R*,6*S*)-2-(((*R*)-5-(tert-butoxy)-5-oxopent-1-en-3-yl)oxy)-6-methyltetrahydro-2*H*-pyran-3,5-diyl dibenzoate (**100**, 0.072 mmol), 17 mg tetradec-13-en-2-one (**94**, 0.08 mmol). (2*R*,3*R*,5*R*,6*S*)-2-(((*R*,*E*)-1-(*tert*-butoxy)-1,16-dioxoheptadec-4-en-3-yl)oxy)-6-methyltetrahydro-2*H*-pyran-3,5-diyl dibenzoate (**101**): 25 mg (0.036 mmol), 50% yield. ^{1}H NMR (600 MHz, $CDCl_3$): δ 1.22 (d, J=6.2 Hz, 3H), 1.25 - 1.29 (m, 9H), 1.31 – 1.43 (m, 3H), 1.45 (s, 9H), 1.54 (m, 2H), 2.04 (dq, J=13.6 Hz, J=6.5 Hz, 3H), 2.12 (s, 3H), 2.18 (ddd, J=13.8 Hz, J=9.4 Hz, J=3.0 Hz, 2H), 2.35 - 2.39 (m, 1H), 2.40 (s, 1H), 2.41 - 2.47 (m, 1H), 2.62 (dd, J=15.0 Hz, J=8.1 Hz, 1H), 4.07 - 4.15 (m, 1H), 4.49

(td, J=8.0 Hz, J=5.8 Hz, 1H), 4.98 (s, 1H), 5.11 - 5.19 (m, 3H), 5.50 - 5.55 (m, 1H), 5.76 (dt, J=15.1 Hz, 6.7 Hz, 1H), 7.45 (td, J=7.7 Hz, J=5.0 Hz, 4H), 7.58 (t, J=7.4 Hz, 2H), 7.97 - 8.05 (m, 2H), 8.07 - 8.12 (m, 2H).

10.3.4.21 (2*R*,3*R*,5*R*,6*S*)-2-(((*S*)-1-(*tert*-butoxy)-1,16-dioxoheptadecan-3-yl)oxy)-6-methyltetrahydro-2*H*-pyran-3,5-diyl dibenzoate (102)

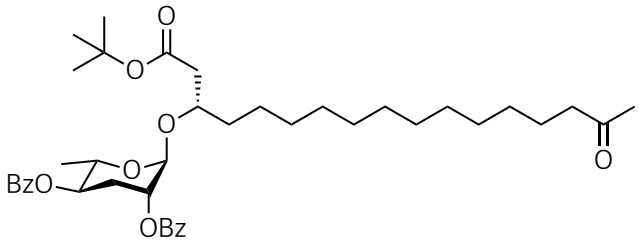

Procedure 10.3.3.4: 25 mg (2*R*,3*R*,5*R*,6*S*)-2-(((*R*,*E*)-1-(*tert*-butoxy)-1,16-dioxoheptadec-4-en-3-yl)oxy)-6-methyltetrahydro-2*H*-pyran-3,5-diyl dibenzoate (**101**, 0.036 mmol). (2*R*,3*R*,5*R*,6*S*)-2-(((*S*)-1-(*tert*-butoxy)-1,16-dioxoheptadecan-3-yl)oxy)-6-methyltetrahydro-2*H*-pyran-3,5-diyl dibenzoate (**102**): 24 mg (0.035 mmol), 97% yield. ^{1}H NMR (600 MHz, $CDCl_3$): δ 1.25 (m, 9H), 1.28 (d, J=6.3 Hz, 3H), 1.30 - 1.44 (m, 9H), 1.45 (s, 9H), 1.52 – 1.58 (m, 3H), 1.59 - 1.75 (m, 4H), 2.12 (s, 2H), 2.18 (ddd, J=13.9 Hz, J=11.5 Hz, J=3.0 Hz, 1H), 2.37 - 2.46 (m, 4H), 2.53 (dd, J=15.2 Hz, J=6.9 Hz, 1H), 4.09 - 4.13 (m, 1H), 4.15 (dq, J=9.9 Hz, J=6.1 Hz, 1H), 4.96 - 4.99 (m, 1H), 5.12 - 5.14 (m, 1H), 5.16 (ddd, J=11.2 Hz, J=10.0 Hz, J=4.6 Hz, 1H), 7.41 - 7.49 (m, 4H), 7.55 - 7.61 (m, 2H), 8.03 (dd, J=8.3 Hz, J=1.2 Hz, 2H), 8.10 (dd, J=8.3 Hz, J=1.2 Hz, 2H).

10.3.4.22 Dimethyl (*R*,*E*)-3-(((2*R*,3*R*,5*R*,6*S*)-3,5-bis(benzoyloxy)-6-methyltetrahydro-2*H*-pyran-2-yl)oxy)150ctadic-4-enedioate (109)

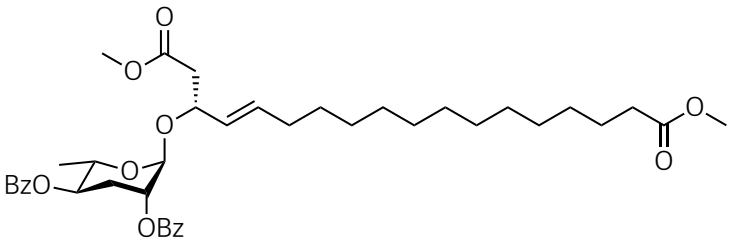

Procedure 10.3.4.1: 39 mg (2*R*,3*R*,5*R*,6*S*)-2-(((*R*)-5-methoxy-5-oxopent-1-en-3-yl)oxy)-6-methyltetrahydro-2*H*-pyran-3,5-diyl dibenzoate (**108**, 0.08 mmol), 32 mg methyl pentadec-14-enoate (**103**, 0.13 mmol). Dimethyl (*R*,*E*)-3-(((2*R*,3*R*,5*R*,6*S*)-3,5-bis(benzoyloxy)-6-methyltetrahydro-2*H*-pyran-2-yl)oxy)octadec-4-enedioate (**109**): 25 mg (0.04 mmol), 50% yield. ^{1}H NMR (600 MHz, $CDCl_3$): δ 1.19 -

1.28 (m, 22H), 1.30 (d, J=6.3 Hz, 3H), 1.32 - 1.40 (m, 4H), 1.45 - 1.47 (m, 2H), 1.56 - 1.64 (m, 2H), 2.05 (m, 2H), 2.17 (m, 2H), 2.26 - 2.32 (m, 1H), 2.40 (ddd, J=17.1 Hz, J=8.2 Hz, J=3.1 Hz, 1H), 2.58 (dd, J=15.5 Hz, J=5.3 Hz, 1H), 2.73 (ddd, J=15.2 Hz, J=11.0 Hz, 8.4 Hz, 2H), 3.48 (m, 1H), 3.66 (s, 3H), 3.73 (s, 3H), 4.10 (dq, J=11.0 Hz, J=5.5 Hz, 2H), 4.57 (m, 1H), 5.18 (m, 1H), 5.27 (m, 1H), 5.36 (d, J=17.2 Hz, 2H), 5.95 (ddd, J=17.5 Hz, J=10.4 Hz, J=7.3 Hz, 1H), 7.37 - 7.52 (m, 3H), 7.50 - 7.66 (m, 3H), 7.95 - 8.21 (m, 4H).

10.3.4.23 Dimethyl (*S*)-3-(((2*R*,3*R*,5*R*,6*S*)-3,5-bis(benzoyloxy)-6-methyltetrahydro-2*H*-pyran-2-yl)oxy)octadecanedioate (110)

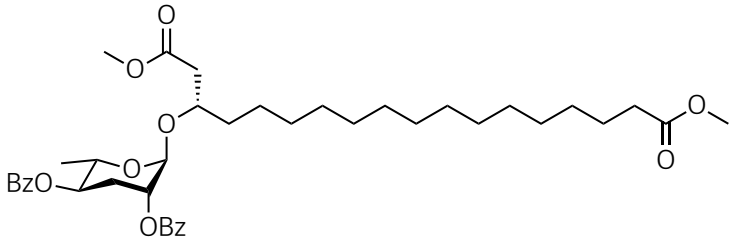

Procedure 10.3.3.4: 25 mg dimethyl (*R*,*E*)-3-(((2*R*,3*R*,5*R*,6*S*)-3,5-bis(benzoyloxy)-6-methyltetrahydro-2*H*-pyran-2-yl)oxy)octadec-4-enedioate (**109**, 0.036 mmol). Dimethyl (*S*)-3-(((2*R*,3*R*,5*R*,6*S*)-3,5-bis(benzoyloxy)-6-methyltetrahydro-2*H*-pyran-2-yl)oxy)octadecanedioate (**110**): 24 mg (0.034 mmol), 94% yield. ^{1}H NMR (600 MHz, $CDCl_3$): δ 1.15 - 1.27 (m, 3H), 1.28 (d, J=6.4 Hz, 3H), 1.30 - 1.49 (m, 4H), 1.67 (ddd, J=48.9 Hz, J=22.5 Hz, J=15.1 Hz, 7.7 Hz, 3H), 2.18 (tt, J=14.5 Hz, J=3.2 Hz, 1H), 2.24 - 2.33 (m, 1H), 2.42 (ddt, J=17.0 Hz, J=13.8 Hz, J=3.9 Hz, 1H), 2.54 (dd, J=15.3 Hz, J=5.4 Hz, 1H), 2.61 (ddd, J=15.2, 7.3, 2.9 Hz, 1H), 3.66 (s, 3H), 3.72 (s, 3H), 4.06 - 4.15 (m, 1H), 4.13 - 4.20 (m, 1H), 5.11 (d, J=3.2 Hz, 1H), 5.18 (td, J=10.7 Hz, J=4.6 Hz, 1H), 7.46 (m, J=7.4 Hz, 4H), 7.58 (t, J=7.0 Hz, 2H), 8.04 (d, J=7.6 Hz, 2H), 8.11 (dd, J=8.1 Hz, J=3.5 Hz, 2H).

10.3.4.24 (2*S*,3*S*,5*S*,6*R*)-2-(henicosyloxy)-6-methyltetrahydro-2*H*-pyran-3,5-diol (asc-ωC21-H, 68a)

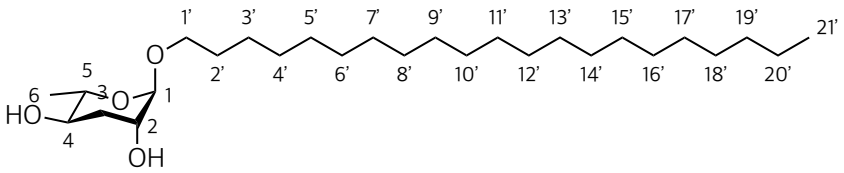

Procedure 10.3.4.3; 37 mg (2*R*,3*S*,5*S*,6*S*)-2-methyl-6-(((*R*)-pentacosan-2-yl)oxy)tetrahydro-2*H*-pyran-3,5-diyl dibenzoate (**70a**, 0.06 mmol). (2*S*,3*S*,5*S*,6*R*)-2-(henicosyloxy)-6-methyltetrahydro-2*H*-pyran-3,5-diol (**asc-ωC21-H**, **68a**): 17 mg (0.04 mmol), 65% yield.

Table 4. NMR data of (2*S*,3*S*,5*S*,6*R*)-2-(henicosyloxy)-6-methyltetrahydro-2*H*-pyran-3,5-diol (**asc-ωC21-H**, **68a**). ^{1}H (600 MHz), ^{13}C (151 MHz).

Position	δ ^{13}C (ppm)	δ ^{1}H (ppm)	multiplicity	^{1}H-^{1}H coupling (Hz)
1	99.1	4.57	br s	
2	69.7	3.65	m	
3	35.4	1.84 (ax)	ddd	$J_{3(ax),3(eq)}$=13.2 $J_{3(ax),4}$=11.0 $J_{3(ax),2}$=3.0
		2.07 (eq)	ddd	$J_{3(eq),3(ax)}$=13.2 $J_{3(eq),2}$=3.9 $J_{3(eq),4}$=3.4
4	69.0	3.85	m	
5	68.4	3.59	dq	$J_{5,4}$=10.6 $J_{5,6}$=6.0
6	17.8	1.29	d	$J_{6,5}$=6.0
1'	67.8	3.69 (a)	dt	$J_{1',1'}$=9.7 $J_{1',2'}$=6.8
		3.43 (b)	dt	$J_{1',1'}$=9.7 $J_{1',2'}$=6.5
2'	29.6	1.58	m	
3'	26.3	1.34	m	
4'	29.7	1.28	m	
5' - 18'	29.9	1.28	m	
19'	32.1	1.28	m	
20'	22.8	1.28	m	
21'	14.3	0.88	t	$J_{20',21'}$=7.0

10.3.4.25 (2*S*,3*R*,5*R*,6*R*)-6-(henicosyloxy)-5-hydroxy-2-methyltetrahydro-2*H*-pyran-3-yl acetate (4-Ac-asc-ωC21-H, 80)

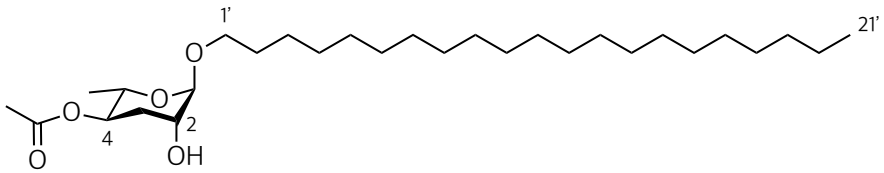

Procedure 10.3.4.5: 5 mg (2*S*,3*S*,5*S*,6*R*)-2-(henicosyloxy)-6-methyltetrahydro-2*H*-pyran-3,5-diol (**asc-ωC21-H**, **68a**, 0.01 mmol). (2*S*,3*R*,5*R*,6*R*)-6-(henicosyloxy)-5-hydroxy-2-methyltetrahydro-2*H*-pyran-3-yl acetate (**4-Ac-asc-ωC21-H**, **80**): 4.2 mg (0.009 mmol), 87% yield.

Table 5. NMR data of (2*S*,3*R*,5*R*,6*R*)-6-(henicosyloxy)-5-hydroxy-2-methyltetrahydro-2*H*-pyran-3-yl acetate (**4-Ac-asc-ωC21-H**, **80**), product in a mixture. ^{1}H (600 MHz), ^{13}C (151 MHz).

Position	δ ^{13}C (ppm)	δ ^{1}H (ppm)	multiplicity	^{1}H-^{1}H coupling (Hz)
1	99.1	4.57	br s	
2	68.4	3.86	m	
3	32.1	1.90 (ax)	ddd	$J_{3(ax),3(eq)}$=13.4 $J_{3(ax),4}$=10.7 $J_{3(ax),2}$=3.0
		2.11 (eq)	ddd	$J_{3(eq),3(ax)}$=13.4 $J_{3(eq),2}$=8.5 $J_{3(eq),4}$=4.5
4	69.7	4.81	ddd	$J_{4,3(ax)}$=10.7 $J_{4,5}$=9.3 $J_{4,3(eq)}$=4.6
5	67.8	3.83	m	
6	17.8	1.19	m	
1'	68.4	3.69 (a)	m	
		3.43 (b)	m	
2'	29.6	1.60	m	
3'	26.3	1.36	m	
4'	29.7	1.28	m	

5' - 18'	29.9	1.28	m	
19'	31.9	1.28	m	
20'	22.9	1.28	m	
21'	14.3	0.88	t	$J_{20',21'}$=7.0
4-$OCOCH_3$	170.3			
4-$OCOCH_3$	21.4	2.05	s	

10.3.4.26 (2*R*,3*R*,5*R*,6*S*)-2-(henicosyloxy)-6-methyltetrahydro-2*H*-pyran-3,5-diyl diacetate (Ac2-asc-ωC21-H, 76)

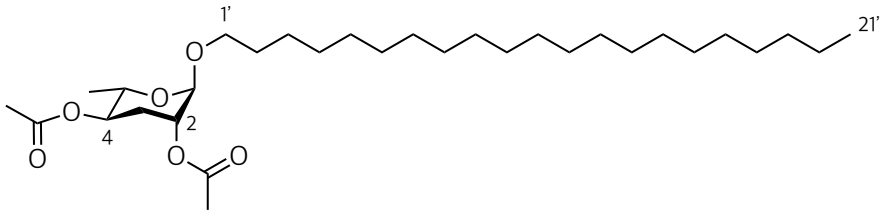

Procedure 10.3.4.4: 5 mg (2*S*,3*S*,5*S*,6*R*)-2-(henicosyloxy)-6-methyltetrahydro-2*H*-pyran-3,5-diol (**asc-ωC21-H**, **68a**, 0.01 mmol). (2*R*,3*R*,5*R*,6*S*)-2-(henicosyloxy)-6-methyltetrahydro-2*H*-pyran-3,5-diyl diacetate (**Ac2-asc-ωC21-H**, **76**): 4.4 mg (0.008 mmol), 80% yield.

Table 6. NMR data of (2*R*,3*R*,5*R*,6*S*)-2-(henicosyloxy)-6-methyltetrahydro-2*H*-pyran-3,5-diyl diacetate (**Ac2-asc-ωC21-H**, **76**). ^{1}H (600 MHz), ^{13}C (151 MHz).

Position	δ ^{13}C (ppm)	δ ^{1}H (ppm)	multiplicity	^{1}H-^{1}H coupling (Hz)
1	96.4	4.90	br s	
2	70.2	4.61	m	
3	29.6	1.95 (ax)	ddd	$J_{3(ax),3(eq)}$= 13.8 $J_{3(ax),4}$=11.4 $J_{3(ax),2}$=3.2
		2.11 (eq)	m	
4	70.0	4.79	ddd	$J_{4,3(ax)}$= 11.3 $J_{4,5}$=10.0 $J4,3_{(eq)}$= 4.6
5	66.6	3.82	dq	$J_{5,4}$=10.0 $J_{5,6}$=6.2

6	17.8	1.19	d	$J_{6,5}$=6.2
1'	67.9	3.66 (a) 3.42 (b)	dt dt	$J_{1'(a),1'(b)}$=9.6 $J_{1'(a),2'}$=6.6 $J_{1'(b),1'(a)}$=9.6 $J_{1'(b),2'}$=6.5
2'	29.5	1.60	m	
3'	26.3	1.36	m	
4'	29.8	1.28	m	
5' - 18'	29.9	1.28	m	
19'	32.1	1.28	m	
20'	22.8	1.28	m	
21'	14.3	0.88	t	$J_{20',21'}$=6.9
2-$OCOCH_3$	170.5			
2-$OCOCH_3$	21.3	2.05	s	
4-$OCOCH_3$	170.2			
4-$OCOCH_3$	21.4	2.11	s	

10.3.4.27 (2*S*,3*R*,5*R*,6*R*)-2-methyl-6-(((*R*)-pentacosan-2-yl)oxy)tetrahydro-2*H*-pyran-3,5-diol (asc-C25-H, 33a)

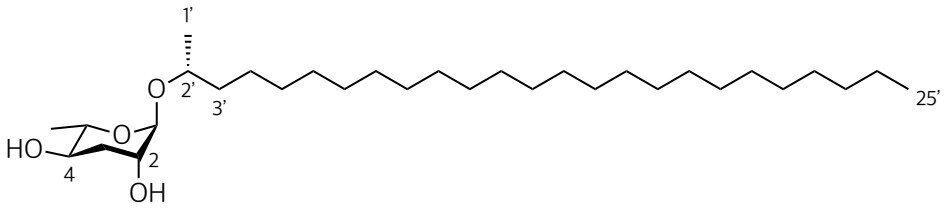

Procedure 10.3.4.3; 91 mg (2*R*,3*S*,5*S*,6*S*)-2-methyl-6-(((*R*)-pentacosan-2-yl)oxy)tetrahydro-2*H*-pyran-3,5-diyl dibenzoate (**41a**, 0.13 mmol). (2*S*,3*R*,5*R*,6*R*)-2-methyl-6-(((*R*)-pentacosan-2-yl)oxy)tetrahydro-2*H*-pyran-3,5-diol (**asc-C25-H**, **33a**): 37 mg (0.07 mmol), 54% yield.

Table 7. NMR data of (2*S*,3*R*,5*R*,6*R*)-2-methyl-6-(((*R*)-pentacosan-2-yl)oxy)tetrahydro-2*H*-pyran-3,5-diol (**asc-C25-H**, **33a**). ^{1}H (600 MHz), ^{13}C (151 MHz).

Position	δ ^{13}C (ppm)	δ ^{1}H (ppm)	multiplicity	^{1}H-^{1}H coupling (Hz)
1	96.2	4.70	br s	
2	69.5	3.81	m	
3	35.4	1.84 (ax)	ddd	$J_{3(ax),3(eq)}$=13.7 $J_{3(ax),4}$=11.2 $J_{3(ax),2}$=3.0
		2.07 (eq)	ddd	$J_{3(eq),3(ax)}$=13.6 $J_{3(eq),2}$=4.8 $J_{3(eq),4}$=4.5
4	68.4	3.59	ddd	$J_{4,3(ax)}$=11.2 $J_{4,5}$=9.3 $J_{4,3(eq)}$=4.5
5	69.9	3.69	dq	$J_{5,4}$=9,2 $J_{5,6}$=6.2
6	17.8	1.27	d	$J_{6,5}$=6.3
1'	19.1	1.12	d	$J_{1',2'}$=6.1
2'	71.8	3.79	m	
3'	37.4	1.58 (a)	m	
		1.44 (b)	m	
4'- 21'	29.9	1.28	m	
22'	32.1	1.28	m	
23'	22.9	1.28	m	
24'	22.7	1.28	m	
25'	14.3	0.88	t	$J_{'24,25'}$=6.9

10.3.4.28 (2*S*,3*R*,5*R*,6*R*)-5-hydroxy-2-methyl-6-(((*R*)-pentacosan-2-yl)oxy)tetrahydro-2*H*-pyran-3-yl acetate (4-Ac-asc-C25-H, 81)

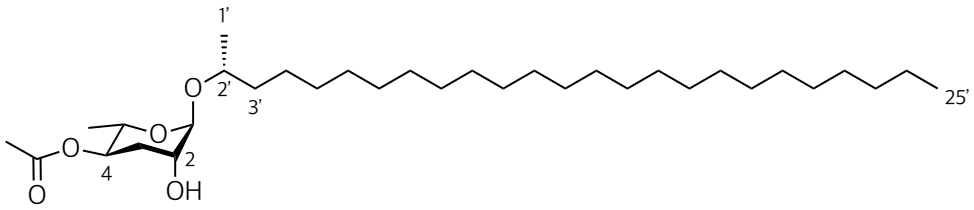

Procedure 10.3.4.5: 5 mg (2*S*,3*R*,5*R*,6*R*)-2-methyl-6-(((*R*)-pentacosan-2-yl)oxy)tetrahydro-2*H*-pyran-3,5-diol (**asc-C25-H**, **33a**, 0.01 mmol). (2*S*,3*R*,5*R*,6*R*)-5-hydroxy-2-methyl-6-(((*R*)-pentacosan-2-yl)oxy)tetrahydro-2*H*-pyran-3-yl acetate (**4-Ac-asc-C25-H**, **81**): 4.2 mg (0.008 mmol), 79% yield.

Table 8. NMR data of (2*S*,3*R*,5*R*,6*R*)-5-hydroxy-2-methyl-6-(((*R*)-pentacosan-2-yl)oxy)tetrahydro-2*H*-pyran-3-yl acetate (**4-Ac-asc-C25-H**, **81**), product in a mixture. ^{1}H (600 MHz), ^{13}C (151 MHz).

Position	δ ^{13}C (ppm)	δ ^{1}H (ppm)	multiplicity	^{1}H-^{1}H coupling (Hz)
1	96.2	4.71	br s	
2	67.2	3.88	m	
3	32.1	1.91 (ax) 2.11 (eq)	m m	
4	68.4	4.69	m	
5	69.9	3.69	dq	$J_{5,4}$=9.2 $J_{5,6}$=6.2
6	17.8	1.28	d	$J_{6,5}$=6.2
1'	19.2	1.13	d	$J_{1',2'}$=6.1
2'	71.8	3.78	m	
3'	29.5	1.60	m	
4'	26.3	1.36	m	
5'	29.7	1.28	m	
6' - 22'	29.9	1.28	m	
23'	31.9	1.28	m	
24'	22.9	1.28	m	
25'	14.3	0.88	t	$J_{'24,25'}$=6.9
4-$OCOCH_3$	170.3			
4-$OCOCH_3$	21.3	2.06	s	

10.3.4.29 (2*S*,3*R*,5*R*,6*R*)-2-methyl-6-(((*R*)-pentacosan-2-yl)oxy)tetrahydro-2*H*-pyran-3,5-diyl (Ac2-asc-C25-H, 77)

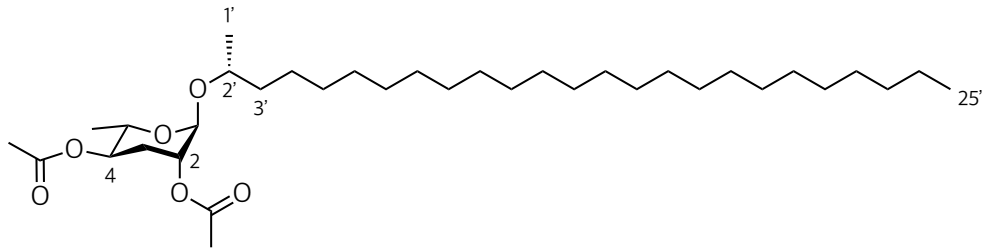

Procedure 10.3.4.4: 5 mg (2*S*,3*R*,5*R*,6*R*)-2-methyl-6-(((*R*)-pentacosan-2-yl)oxy)tetrahydro-2*H*-pyran-3,5-diol (**asc-C25-H**, **33a**, 0.01 mmol). (2*S*,3*R*,5*R*,6*R*)-2-methyl-6-(((*R*)-pentacosan-2-yl)oxy)tetrahydro-2*H*-pyran-3,5-diyl (**Ac2-asc-C25-H**, **77**): 4.1 mg (0.007 mmol), 70% yield.

Table 9. NMR data of (2*S*,3*R*,5*R*,6*R*)-2-methyl-6-(((*R*)-pentacosan-2-yl)oxy)tetrahydro-2*H*-pyran-3,5-diyl (**Ac2-asc-C25-H**, **77**). ^{1}H (600 MHz), ^{13}C (151 MHz).

Position	δ ^{13}C (ppm)	δ ^{1}H (ppm)	multiplicity	^{1}H-^{1}H coupling (Hz)
1	93.8	4.74	br s	
2	70.8	4.84	m	
3	32.1	1.94 (ax)	ddd	$J_{3(ax),3(eq)}$= 13.7 $J_{3(ax),4}$=11.4 $J_{3(ax),2}$=3.2
		2.10 (eq)	m	
4	70.1	4.79	ddd	$J_{4,3(ax)}$= 11.3 $J_{4,5}$=10.0 $J_{4,3(eq)}$= 4.7
5	66.8	3.87	dq	$J_{5,4}$=9.9 $J_{5,6}$=6.4
6	17.8	1.28	d	$J_{6,5}$=6.3
1'	19.2	1.12	d	$J_{1',2'}$=6.1
2'	72.5	3.76	m	
3'	29.5	1.60	m	
4'	26.3	1.36	m	
5'	29.7	1.28	m	

6' - 22'	29.9	1.28	m	
23'	31.9	1.28	m	
24'	22.9	1.28	m	
25'	14.3	0.88	t	$J_{24',25'}$=7.0
2-$OCOCH_3$	170.5			
2-$OCOCH_3$	21.3	2.06	s	
4-$OCOCH_3$	170.3			
4-$OCOCH_3$	21.4	2.11	s	

10.3.4.30 (2*S*,3*R*,5*R*,6*R*)-2-methyl-6-(((*R*)-24-methylpentacosan-2-yl)oxy)tetrahydro-2*H*-pyran-3,5-diol (asc-*i*C26-H, 43a)

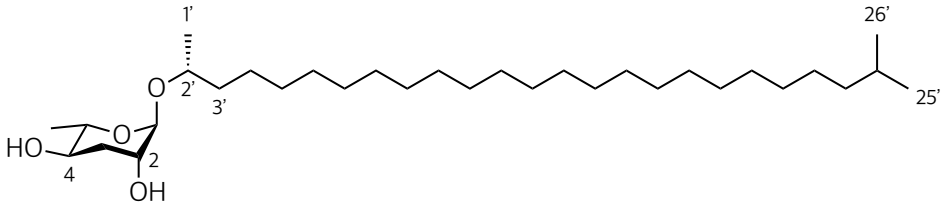

Procedure 10.3.4.3; 119 mg (2*S*,3*R*,5*R*,6*R*)-2-methyl-6-(((*R*)-24-methylpentacosan-2-yl)oxy)tetrahydro-2*H*-pyran-3,5-diyl dibenzoate (**56a**, 0.165 mmol). (2*S*,3*R*,5*R*,6*R*)-2-methyl-6-(((*R*)-24-methylpentacosan-2-yl)oxy)tetrahydro-2*H*-pyran-3,5-diol (**asc-*i*C26-H**, **43a**): 68 mg (0.13 mmol), 78% yield.

Table 10. NMR data of (2*S*,3*R*,5*R*,6*R*)-2-methyl-6-(((*R*)-24-methylpentacosan-2-yl)oxy)tetrahydro-2*H*-pyran-3,5-diol (**asc-*i*C26-H**, **43a**). ^{1}H (600 MHz), ^{13}C (151 MHz).

Position	δ ^{13}C (ppm)	δ ^{1}H (ppm)	multiplicity	^{1}H-^{1}H coupling (Hz)
1	96.2	4.69	br s	
2	69.5	3.80	m	
3	32.1	1.92 (ax) 2.11 (eq)	m m	
4	68.3	3.58	ddd	$J_{4,3(ax)}$=11.4 $J_{4,5}$=9.6 $J_{4,3(eq)}$=4.5
5	69.9	3.69	dq	$J_{5,4}$=9,1

				$J_{5,6}$=6.2
6	17.8	1.28	d	$J_{6,5}$=6.3
1'	19.1	1.12	d	$J_{1',2'}$=6.1
2'	71.9	3.78	m	
3'	37.4	1.54	m	
4'	25.9	1.41	m	
5'	29.8	1.28	m	
6' - 21'	29.9	1.28	m	
22'	27.6	1.38	m	
23'	39.2	1.15	m	
24'	28.1	1.50	m	
25'/26'	22.8	0.86	d	$J_{25',24'}$=6.6

10.3.4.31 (2*S*,3*R*,5*R*,6*R*)-5-hydroxy-2-methyl-6-(((*R*)-24-methylpentacosan-2-yl)oxy) tetrahydro-2*H*-pyran-3-yl acetate (4-Ac-asc-*i*C26-H, 82)

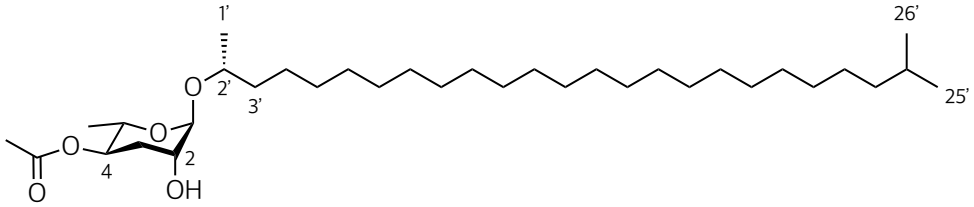

Procedure 10.3.4.4: 5 mg (2*S*,3*R*,5*R*,6*R*)-2-methyl-6-(((*R*)-24-methylpentacosan-2-yl)oxy)tetrahydro-2*H*-pyran-3,5-diol (**asc-*i*C26-H**, **43a**, 0.009 mmol). 2*S*,3*R*,5*R*,6*R*)-5-hydroxy-2-methyl-6-(((*R*)-24-methylpentacosan-2-yl)oxy)tetrahydro-2*H*-pyran-3-yl acetate (**4-Ac-asc-*i*C26-H**, **82**): 4.1 mg (0.007 mmol), 77% yield.

Table 11. NMR data of (2*S*,3*R*,5*R*,6*R*)-5-hydroxy-2-methyl-6-(((*R*)-24-methylpentacosan-2-yl)oxy)tetrahydro-2*H*-pyran-3-yl acetate (**4-Ac-asc-*i*C26-H**, **82**), product in a mixture. ^{1}H (600 MHz), ^{13}C (151 MHz).

Position	δ ^{13}C (ppm)	δ ^{1}H (ppm)	multiplicity	^{1}H-^{1}H coupling (Hz)
1	96.3	4.73	br s	
2	69.9	3.78	m	
3	32.1	1.92 (ax)	m	

		2.11 (eq)	m	
4	70.3	4.79	ddd	$J_{4,3(ax)}$=11.4 $J_{4,5}$=9.6 $J_{4,3(eq)}$=4.5
5	69.9	3.69	dq	$J_{5,4}$=9.5 $J_{5,6}$=6.2
6	17.8	1.28	d	$J_{6,5}$=6.3
1'	19.2	1.12	d	$J_{1',2'}$=6.1
2'	72.5	3.76	m	
3'	37.2	1.54	m	
4'	25.9	1.41	m	
5'	29.7	1.28	m	
6' - 21'	29.9	1.28	m	
22'	25.9	1.38	m	
23'	39.2	1.15	m	
24'	28.1	1.52	m	
25'/26'	22.8	0.86	d	$J_{25',24'}$=6.6
4-$OCOCH_3$	170.3			
4-$OCOCH_3$	21.3	2.06	s	

10.3.4.32 (2*S*,3*R*,5*R*,6*R*)-2-methyl-6-(((*R*)-24-methylpentacosan-2-yl)oxy)tetrahydro-2*H*-pyran-3,5-diyl diacetate (Ac2-asc-*i*C26-H, 78)

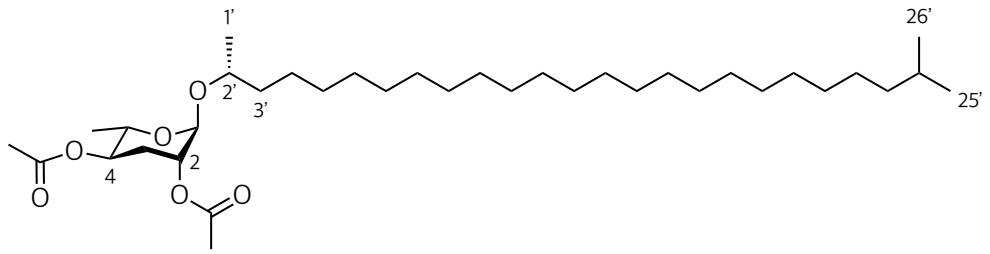

Procedure 10.3.4.5: 5 mg (2*S*,3*R*,5*R*,6*R*)-2-methyl-6-(((*R*)-24-methylpentacosan-2-yl)oxy)tetrahydro-2*H*-pyran-3,5-diol (**asc-*i*C26-H**, **43a**, 0.01 mmol). (2*S*,3*R*,5*R*,6*R*)-2-methyl-6-(((*R*)-24-methylpentacosan-2-yl)oxy)tetrahydro-2*H*-pyran-3,5-diyl diacetate (**Ac2-asc-*i*C26-H**, **78**): 4.7 mg (0.008 mmol), 80% yield.

Table 12. NMR data of (2*S*,3*R*,5*R*,6*R*)-2-methyl-6-(((*R*)-24-methylpentacosan-2-yl)oxy)tetrahydro-2*H*-pyran-3,5-diyl diacetate (**Ac2-asc-*i*C26-H**, **78**). ^{1}H (600 MHz), ^{13}C (151 MHz).

Position	δ ^{13}C (ppm)	δ ^{1}H (ppm)	multiplicity	^{1}H-^{1}H coupling (Hz)
1	93.8	4.74	br s	
2	70.8	4.84	m	
3	29.6	1.94 (ax)	ddd	$J_{3(ax),3(eq)}$= 13.7 $J_{3(ax),4}$=11.5 $J_{3(ax),2}$=3.2
		2.11 (eq)	m	
4	70.1	4.80	ddd	$J_{4,3(ax)}$= 11.2 $J_{4,5}$=10.1 $J_{4,3(eq)}$= 4.7
5	66.8	3.88	dq	$J_{5,4}$=10.0 $J_{5,6}$=6.3
6	17.8	1.19	d	$J_{6,5}$=6.3
1'	19.2	1.12	d	$J_{1',2'}$=6.1
2'	72.5	3.76	m	
3'	37.3	1.54	m	
4'	25.9	1.41	m	
5'	29.7	1.28	m	
6'- 21'	29.9	1.28	m	
22'	25.9	1.38	m	
23'	39.2	1.15	m	
24'	28.1	1.52	m	
25'/26'	22.8	0.86	d	$J_{25',24'}$=6.6
2-$OCOCH_3$	170.5			
2-$OCOCH_3$	21.3	2.06	s	
4-$OCOCH_3$	170.3			
4-$OCOCH_3$	21.4	2.11	s	

10.3.4.1 (2*R*,3*R*,5*R*,6*S*)-2-(((*R*)-hentriacontan-2-yl)oxy)-6-methyltetrahydro-2*H*-pyran-3,5-diol (asc-C31-H, 57a)

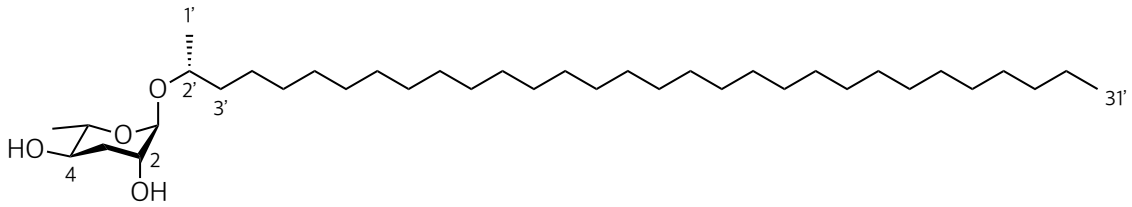

Procedure 10.3.4.3; 57 mg (2*R*,3*R*,5*R*,6*S*)-2-(((*R*)-hentriacontan-2-yl)oxy)-6-methyltetrahydro-2*H*-pyran-3,5-diyl dibenzoate (**67a**, 0.072 mmol). (2*R*,3*R*,5*R*,6*S*)-2-(((*R*)-hentriacontan-2-yl)oxy)-6-methyltetrahydro-2*H*-pyran-3,5-diol (**asc-C31-H**, **57a**): 31 mg (0.053 mmol), 74% yield.

Table 13. NMR data of (2*R*,3*R*,5*R*,6*S*)-2-(((*R*)-hentriacontan-2-yl)oxy)-6-methyltetrahydro-2*H*-pyran-3,5-diol (**asc-C31-H**, **57a**). ^{1}H (600 MHz), ^{13}C (151 MHz).

Position	δ ^{13}C (ppm)	δ ^{1}H (ppm)	multiplicity	^{1}H-^{1}H coupling (Hz)
1	96.2	4.70	br s	
2	69.5	3.81	m	
3	35.4	1.84 (ax)	ddd	$J_{3(ax),3(eq)}$=13.5 $J_{3(ax),4}$= 11.2 $J_{3(ax),2}$= 3.0
		2.07 (eq)	ddd	$J_{3(eq),3(ax)}$=13.6 $J_{3(eq),2}$= 4.8 $J_{3(eq),4}$= 4.5
4	68.4	3.59	ddd	$J_{4,3(ax)}$=11.1 $J_{4,5}$=9.3 $J_{4,3(eq)}$=4.5
5	69.9	3.69	dq	$J_{5,4}$=9.2 $J_{5,6}$=6.2
6	17.8	1.27	d	$J_{6,5}$=6.2
1'	19.1	1.12	d	$J_{1',2'}$=6.1
2'	71.8	3.78	m	
3'	37.4	1.54	m	
4'	25.9	1.41	m	

5'	29.8	1.25	m	
6'- 21'	29.9	1.25	m	
22'	29.5	1.25	m	
29'	31.9	1.25	m	
30'	22.8	1.22	m	
31'	14.3	0.88	t	$J_{31',30'}$=7.0

10.3.4.2 (2*S*,3*R*,5*R*,6*R*)-6-(((*R*)-hentriacontan-2-yl)oxy)-5-hydroxy-2-methyltetrahydro-2*H*-pyran-3-yl acetate (4-Ac-asc-C31-H, 83)

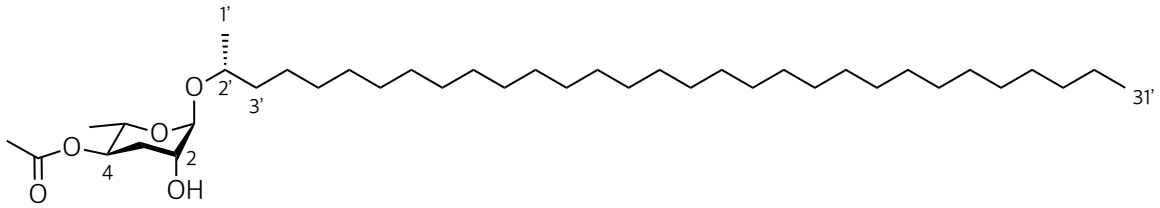

Procedure 10.3.4.5: 4 mg (2*R*,3*R*,5*R*,6*S*)-2-(((*R*)-hentriacontan-2-yl)oxy)-6-methyltetrahydro-2*H*-pyran-3,5-diyl diacetate (**Ac2-asc-C31-H**, **79**, 0.0065 mmol). (2*S*,3*R*,5*R*,6*R*)-6-(((*R*)-hentriacontan-2-yl)oxy)-5-hydroxy-2-methyltetrahydro-2*H*-pyran-3-yl acetate (**4-Ac-asc-C31-H**, **83**): 3 mg (0.005 mmol), 77% yield.

Table 14. NMR data of (2*S*,3*R*,5*R*,6*R*)-6-(((*R*)-hentriacontan-2-yl)oxy)-5-hydroxy-2-methyltetrahydro-2*H*-pyran-3-yl acetate (**4-Ac-asc-C31-H**, **83**), product in a mixture. ^{1}H (600 MHz), ^{13}C (151 MHz).

Position	δ ^{13}C (ppm)	δ ^{1}H (ppm)	multiplicity	^{1}H-^{1}H coupling (Hz)
1	93.7	4.73	br s	
2	68.3	3.79	m	
3	32.1	1.91 (ax)	ddd	$J_{3(ax),3(eq)}$=13.5 $J_{3(ax),4}$=11.2 $J_{3(ax),2}$=3.0
		2.12 (eq)	m	
4	70.8	4.84	m	
5	66.8	3.69	dq	$J_{5,4}$=9.2 $J_{5,6}$=6.2
6	17.8	1.27	d	$J_{6,5}$=6.2

1'	19.2	1.12	d	$J_{1',2'}$=6.1
2'	72.1	3.78	m	
3'	37.3	1.54	m	
4'	25.9	1.41	m	
5'	29.5	1.25	m	
6'- 21'	29.9	1.25	m	
22'	29.4	1.25	m	
29'	32.1	1.25	m	
30'	22.9	1.22	m	
31'	14.3	0.88	t	$J_{31',30'}$=7.0
4-$OCOCH_3$	170.3			
4-$OCOCH_3$	21.3	2.11	s	

10.3.4.3 (2*R*,3*R*,5*R*,6*S*)-2-(((*R*)-hentriacontan-2-yl)oxy)-6-methyltetrahydro-2*H*-pyran-3,5-diyl diacetate (Ac2-asc-C31-H, 79)

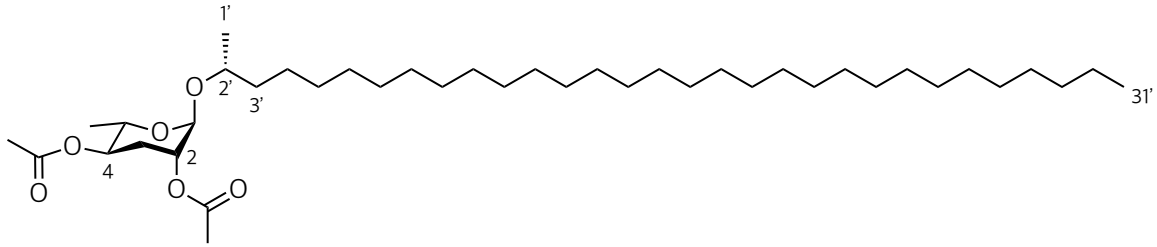

Procedure 10.3.4.4: 1 mg (2*R*,3*R*,5*R*,6*S*)-2-(((*R*)-hentriacontan-2-yl)oxy)-6-methyltetrahydro-2*H*-pyran-3,5-diol (**asc-C31-H**, **57a**, 0.0017mmol). (2*R*,3*R*,5*R*,6*S*)-2-(((*R*)-hentriacontan-2-yl)oxy)-6-methyltetrahydro-2*H*-pyran-3,5-diyl diacetate (**Ac2-asc-C31-H**, **79**): 1 mg (0.0013 mmol), 76% yield.

Table 15. NMR data of (2*R*,3*R*,5*R*,6*S*)-2-(((*R*)-hentriacontan-2-yl)oxy)-6-methyltetrahydro-2*H*-pyran-3,5-diyl diacetate (**Ac2-asc-C31-H**, **79**). ^{1}H (600 MHz), ^{13}C (151 MHz).

Position	δ ^{13}C (ppm)	δ ^{1}H (ppm)	multiplicity	^{1}H-^{1}H coupling (Hz)
1	93.7	4.74	br s	
2	70.0	4.84	ddd	$J_{2,1}$=3.1 $J_{2,3(ax)}$=3.0 $J_{2,3(eq)}$=1.5

3	29.6	1.91 (ax) 2.12 (eq)	ddd m	$J_{3(ax),3(eq)}$=13.5 $J_{3(ax),4}$=11.2 $J_{3(ax),2}$=3.0
4	70.8	4.79	ddd	$J_{4,3(ax)}$=11.4 $J_{4,5}$=9.9 $J_{4,3(eq)}$=4.7
5	66.8	3.87	dq	$J_{5,4}$=10.0 $J_{5,6}$=6.3
6	17.8	1.17	d	$J_{6,5}$=6.3
1'	19.2	1.12	d	$J_{1',2'}$=6.1
2'	72.5	3.76	m	
3'	37.2	1.54	m	
4'	25.9	1.41	m	
5'	29.7	1.25	m	
6'- 27'	29.9	1.25	m	
28'	29.5	1.25	m	
29'	32.1	1.25	m	
30'	22.8	1.22	m	
31'	14.3	0.88	t	$J_{31',30'}$=7.0
2-$OCOCH_3$	170.5			
2-$OCOCH_3$	21.3	2.06	s	
4-$OCOCH_3$	170.3			
4-$OCOCH_3$	21.4	2.11	s	

10.3.4.1 (*S*)-3-(((2*R*,3*R*,5*R*,6*S*)-3,5-dihydroxy-6-methyltetrahydro-2*H*-pyran-2-yl)oxy)-16-oxoheptadecanoic acid ((ω-COOH)-asc-C16-MK, 91)

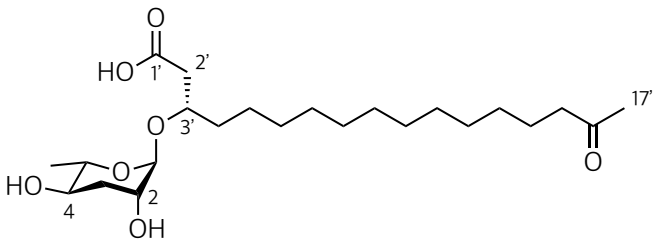

Procedure 10.3.4.3: 36 mg (2*R*,3*R*,5*R*,6*S*)-2-(((*S*)-1-(*tert*-butoxy)-1,16-dioxoheptadecan-3-yl)oxy)-6-methyltetrahydro-2*H*-pyran-3,5-diyl dibenzoate (**102**, 0.05 mmol). (*S*)-3-(((2*R*,3*R*,5*R*,6*S*)-3,5-dihydroxy-6-methyltetrahydro-2*H*-pyran-2-yl)oxy)-16-oxoheptadecanoic acid (**(ω-COOH)-asc-C16-MK**, **91**): 12 mg (0.03 mmol), 60% yield.

Table 16. NMR data of (*S*)-3-(((2*R*,3*R*,5*R*,6*S*)-3,5-dihydroxy-6-methyltetrahydro-2*H*-pyran-2-yl)oxy)-16-oxoheptadecanoic acid (**(ω-COOH)-asc-C16-MK**, **91**). ^{1}H (600 MHz), ^{13}C (151 MHz).

Position	δ ^{13}C (ppm)	δ ^{1}H (ppm)	multiplicity	^{1}H-^{1}H coupling (Hz)
1	99.3	4.71	br s	
2	69.1	3.79	ddd	$J_{2,1}$=3.1 $J_{2,3(ax)}$=3.0 $J_{2,3(eq)}$=1.5
3	35.1	1.84 (ax)	ddd	$J_{3(ax),3(eq)}$=13.5 $J_{3(ax),4}$=11.2 $J_{3(ax),2}$=3.0
		2.03 (eq)	m	
4	68.5	3.61	ddd	$J_{4,3(ax)}$=11.4 $J_{4,5}$=9.9 $J_{4,3(eq)}$= 4.7
5	70.6	3.73	dq	$J_{5,4}$=10.0 $J_{5,6}$=6.3
6	17.7	1.17	d	$J_{6,5}$=6.3
1'	171.1			
2'	41.0	2.40	m	
3'	75.8	4.03	m	
4'	35.3	1.61	m	
5'	25.4	1.35	m	
6'- 13'	29.7	1.27	m	
14'	24.0	1.55	m	
15'	44.0	2.42	m	
16'	209.6			
17'	29.6	2.13	s	

10.3.4.2 (*S*)-3-(((2*R*,3*R*,5*R*,6*S*)-3,5-dihydroxy-6-methyltetrahydro-2*H*-pyran-2-yl)oxy)octadecane dioic acid ((ω-COOH)-asc-C17, 92)

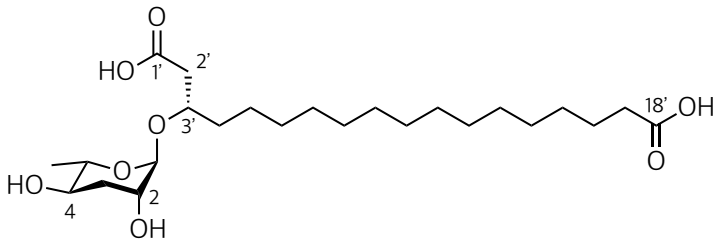

Procedure 10.3.4.3: 9 mg dimethyl (*S*)-3-(((2*R*,3*R*,5*R*,6*S*)-3,5-bis(benzoyloxy)-6-methyltetrahydro-2*H*-pyran-2-yl)oxy)octadecanedioate (**110**, 0.013 mmol). (*S*)-3-(((2*R*,3*R*,5*R*,6*S*)-3,5-dihydroxy-6-methyltetrahydro-2H-pyran-2-yl)oxy)octadecanedioic acid (**(ω-COOH)-asc-C17**, **92**): 2.6 mg (0.006 mmol), 46% yield.

Table 17. NMR data of (*S*)-3-(((2*R*,3*R*,5*R*,6*S*)-3,5-dihydroxy-6-methyltetrahydro-2*H*-pyran-2-yl)oxy)octadecanedioic acid (**(ω-COOH)-asc-C17**, **92**). ^{1}H (600 MHz), ^{13}C (151 MHz).

Position	δ ^{13}C (ppm)	δ ^{1}H (ppm)	multiplicity	^{1}H-^{1}H coupling (Hz)
1	98.1	4.72	br s	
2	68.8	3.82	m	
3	34.9	1.83 (ax)	ddd	$J_{3(ax),3(eq)}$=13.5 $J_{3(ax),4}$=11.2 $J_{3(ax),2}$=3.0
		2.03 (eq)	m	
4	68.1	3.63	ddd	$J_{4,3(ax)}$=11.4 $J_{4,5}$=9.9 $J_{4,3(eq)}$= 4.7
5	70.4	3.73	dq	$J_{5,4}$=10.0 $J_{5,6}$=6.2
6	17.5	1.28	d	$J_{6,5}$=6.3
1'	176.1			
2'	40.4	2.44	m	
3'	73.9	4.09	m	
4'	34.6	1.65	m	

5'	25.4	1.38	m
6' - 15'	29.7	1.28	m
16'	24.3	1.66	m
17'	43.6	2.42	m
18'	178.6		

10.3.5 Syntheses of *iso*-fatty acids

10.3.5.1 General procedure for cleavage of the tetrahydropyranyl group

A stirred solution of tetrahydropyranyl ether (1 eq.) in MeOH was treated with 0.1 eq. TsOH. After reacting overnight, the reaction was quenched with a saturated $NaHCO_3$ solution, the product was extracted with Et_2O, dried over $MgSO_4$, and concentrated under reduced pressure. Purification of the product was followed by column chromatography with hexane-EtOAc as eluent.

10.3.5.2 General procedure for oxidation of primary alcohols

A stirred solution of alkyl alcohol (1 eq.) in DCM was treated with TBAB (1 eq.), $KMnO_4$ (4 eq.), acetic acid (4 eq.) and water (20 g/mL) and refluxed at 60 °C for 16 hours. The pH of the reaction was monitored, and additional HCl added (if required). The reaction was cooled to 0 °C and portions of Na_2SO_3 were carefully added until the brown solid disappeared. The organic layer was separated, combined with subsequent DCM extractions, and dried under $MgSO_4$. The solvent was removed under reduced pressure, and the resulting solid was purified by column chromatography with hexane-EtOAc as eluent. The products were obtained as a lustrous solid.

10.3.5.3 General procedure for preparation of alcohols from alkenes

A stirred solution of alkene (1 eq.) in dry THF was treated with BH_3·THF (1.2 eq.) at 0 °C. After 2 hours, a minimum amount of H_2O was added until the bubbling disappeared, and the resulting mixture was stirred for 20 min. Subsequently, the mixture was cooled to 0° C and equal portions of 30% H_2O_2 and 3 M NaOH (1:1) were carefully added. The mixture was stirred for an extra 30 minutes, and the crude product was extracted with Et_2O. The organic phase was dried over Na_2SO_4, the solvent was removed under reduced pressure, and the crude product was purified by column chromatography using hexane-Et_2O as eluent.

10.3.5.4 General procedure for the chain extension with vinylmagnesium bromide

Under argon, a stirred solution of alkyl halide (1 eq.) in dry THF was treated with 1 M vinylmagnesium bromide (3 eq.). The mixture was cooled to 0°C, and 0.1 M Li_2CuCl_4 solution (0.2 eq.) was added drop by drop. After 16 hours, the reaction was quenched with a saturated NH_4Cl solution. The crude product was extracted with hexane, and the organic phase was dried over $MgSO_4$ and concentrated under reduced pressure. The product was filtrated through a short silica column to afford a transparent oil.

10.3.5.5 2-((11-Methyldodec-7-yn-1-yl)oxy)tetrahydro-2*H*-pyran (114)

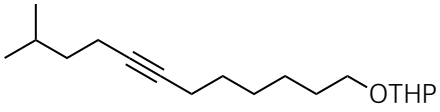

Procedure 10.3.3.6 (section 10.3.3); 0.7 mL 5-methylhex-1-yne (**111**, 4.98 mmol), 1.1 mL 2-((6-bromohexyl)oxy)tetrahydro-2*H*-pyran (**112**, 4.98 mmol), 5.4 mL HMPA (29.88 mmol), 2.9 mL 2.5 M *n*-BuLi (7.47 mol), 9:1 hexane-EtOAc as eluent. 2-((11-Methyldodec-7-yn-1-yl)oxy)tetrahydro-2*H*-pyran (**114**): 1.38 g (4.92 mmol), 99% yield. ^{1}H NMR (600 MHz, $CDCl_3$): δ 0.88 (d, J=6.6 Hz, 6H), 1.33 - 1.92 (m, 17H), 2.11 - 2.21 (m, 4H), 3.38 - 3.45 (m, 1H), 3.49 - 3.55 (m, 1H), 3.72 - 3.79 (m, 1H), 3.86 - 3.92 (m, 1H), 4.59 (t, J=3.0 Hz, 1H). ^{13}C NMR (151 MHz, $CDCl_3$): δ 16.9, 18.9, 19.9, 22.4 (2C), 25.7, 26.0, 27.3, 28.8, 29.3, 29.8, 30.9, 38.3, 62.5, 67.6, 80.1, 80.5, 99.0.

10.3.5.6 2-((13-Methyltetradec-9-yn-1-yl)oxy)tetrahydro-2*H*-pyran (115)

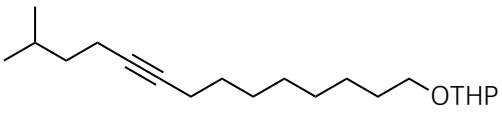

Procedure 10.3.3.6 (section 10.3.3); 0.8 mL 6-methylhept-1-yne (**111**, 5.54 mmol), 1.4 mL 2-((8-bromooctyl)oxy)tetrahydro-2*H*-pyran (**113**, 5.54 mol), 5.8 mL HMPA (33.24 mol), 2.4 mL 2.5 M *n*-BuLi (6.09 mol), 9:1 hexane-EtOAc as eluent. 2-((13-Methyltetradec-9-yn-1-yl)oxy)tetrahydro-2*H*-pyran (**115**): 1.45 g (4.70 mmol), 85% yield. ^{1}H NMR (600 MHz, $CDCl_3$): δ 0.88 (d, J=6.6 Hz, 6H), 1.26 - 1.90 (m, 21H), 2.12 - 2.20 (m, 4H), 3.36 - 3.45 (m, 1H), 3.48 - 3.59 (m, 1H), 3.71 - 3.78 (m, 1H), 3.86 - 3.92 (m, 1H), 4.57 (t, J=3.7 Hz, 1H). ^{13}C NMR (151 MHz, $CDCl_3$): δ 16.9, 18.9, 19.9, 22.4 (2C), 25.7, 26.4, 27.3, 29.0, 29.3 (2C), 29.5, 29.9, 30.9, 38.3, 62.5, 67.8, 80.2, 80.4, 99.0.

10.3.5.7 11-Methyldodec-7-yn-1-ol (116)

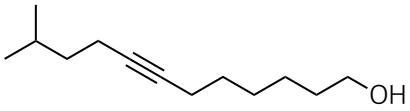

Procedure 10.3.5.1; 1.1 g 2-((8-bromooctyl)oxy)tetrahydro-2*H*-pyran (**114**, 3.92 mmol), 67 mg TsOH (0.39 mmol), 9:1 hexane-EtOAc as eluent. 11-Methyldodec-7-yn-1-ol (**116**): 566 mg yellow oil (2.88 mmol), 73% yield. ^{1}H NMR (600 MHz, CDCl^{3}): δ 0.89 (d, J=6.6 Hz, 6H), 1.35 - 1.68 (m, 11H), 2.13 - 2.16 (m, 4H), 3.65 (t, J=5.8 Hz, 2H). ^{13}C NMR (151 MHz, $CDCl_3$): δ 16.9, 18.8, 22.3 (2C), 25.4, 27.3, 28.7, 29.2, 32.8, 38.3, 63.1, 80.0, 80.5.

10.3.5.8 13-Methyltetradec-9-yn-1-ol (117)

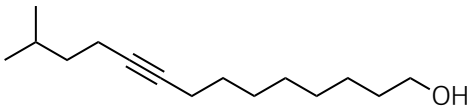

Procedure 10.3.5.1; 0.5 g 2-((13-methyltetradec-9-yn-1-yl)oxy)tetrahydro-2H-pyran (**115**, 1.62 mmol), 28 mg TsOH (0.16 mmol), 9:1 hexane-EtOAc as eluent. 13-Methyltetradec-9-yn-1-ol (**117**): 304 mg yellow oil (1.35 mmol), 83% yield. ^{1}H NMR (600 MHz, $CDCl_3$): δ 0.88 (d, J=6.9 Hz, 6H), 1.25 - 1.43 (m, 10H), 1.45 - 1.53 (m, 2H), 1.55 - 1.58 (m, 2H), 1.67 (m, 1H), 2.12 - 2.15 (m, 4H), 3.64 (t, J=6.8 Hz, 2H). ^{13}C NMR (151 MHz, $CDCl_3$): δ 16.9, 18.9, 22.4 (2C), 25.8, 27.3, 28.9, 29.3 (2C), 29.5, 32.9, 38.3, 63.2, 80.2, 80.4.

10.3.5.9 11-Methyldodecan-1-ol (118a)

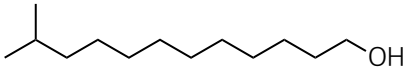

Procedure 10.3.3.4 (section 10.3.3); 304 mg 11-methyldodec-7-yn-1-ol (**116**, 1.35 mmol), H_2, 10 mL hexane. 11-Methyldodecan-1-ol (**118a**): 253 mg white oily solid (1.26 mmol), 93% yield. ^{1}H NMR (600 MHz, $CDCl_3$): δ 0.88 (d, J=6.6 Hz, 6H), 1.13 - 1.20 (m, 2H), 1.22 - 1.42 (m, 12H), 1.50 - 1.59 (m, 5H), 3.65 (t, J=6.6 Hz, 2H). ^{13}C NMR (151 MHz, $CDCl_3$): δ 22.8 (2C), 25.9, 27.6, 28.1, 29.6, 29.8 (2C), 29.9, 30.1, 33.0, 39.2, 63.3.

10.3.5.10 [D_4]-11-methyldodecan-1-ol (118b)

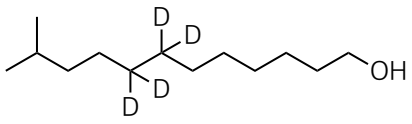

Procedure 10.3.3.4 (section 10.3.3); 800 mg 11-methyldodec-7-yn-1-ol (**116**, (3.55 mmol), D_2, 10 mL hexane. [D_4]-11-methyldodecan-1-ol (**118b**): 545 mg white oily solid (2.67 mmol), 75% yield. ^{1}H NMR (600 MHz, $CDCl_3$): δ 0.88 (d, J=6.7 Hz, 6H), 1.13 - 1.18 (m, 2H), 1.20 - 1.40 (m, 8H), 1.47 - 1.58 (m, 5H), 3.64 (t, J=6.7 Hz, 2H). ^{13}C NMR (151 MHz, $CDCl_3$): δ 22.8 (2C), 25.7, 28.1, 29.8 (4C), 33.0, 39.2, 63.2.

10.3.5.11 13-Methyltetradecan-1-ol (119a)

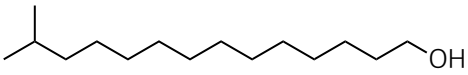

Procedure 10.3.3.4 (section 10.3.3); 1.1 g 13-methyltetradec-9-yn-1-ol (**117**, 4.90 mmol), H_2, 10 mL hexane. 13-Methyltetradecan-1-ol (**119a**): 832 mg white oily solid (3.64 mmol), 74% yield. ^{1}H NMR (600 MHz, $CDCl_3$): δ 0.88 (d, J=6.6 Hz, 6H), 1.14 - 1.20 (m, 2H), 1.22 - 1.42 (m, 16H), 1.49 - 1.63 (m, 5H), 3.66 (t, J=6.6 Hz, 2H). ^{13}C NMR (151 MHz, $CDCl_3$): δ 22.8 (2C), 25.9, 27.6, 28.1, 29.6, 29.7, 29.8 (3C), 29.9, 30.1, 32.9, 39.2, 63.2.

10.3.5.12 [D_4]-13-methyltetradecan-1-ol (119b)

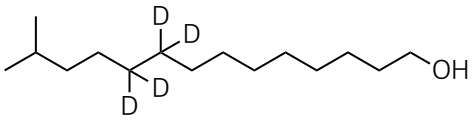

Procedure 10.3.3.4 (section 10.3.3); 1.2 g 13-methyltetradec-9-yn-1-ol (**117**, 5.35 mmol), D_2, 10 mL hexane. [D_4]-13-methyltetradecan-1-ol (**119b**): 873 g white oily solid (3.76 mmol), 70% yield. ^{1}H NMR (600 MHz, $CDCl_3$): δ 0.88 (d, J=6.7 Hz, 6H), 1.12 - 1.20 (m, 2H), 1.19 - 1.41 (m, 12H), 1.49 - 1.58 (m, 5H), 3.64 (t, J=6.7 Hz, 2H). ^{13}C NMR (151 MHz, $CDCl_3$): δ 22.8 (2C), 25.9, 28.1, 29.8 (5C), 33.0, 39.2, 63.2.

10.3.5.13 11-Methyldodecanoic acid (*iso*C13, 16a), from route 1

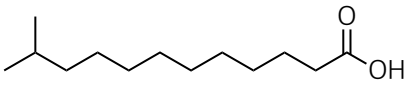

Procedure 10.3.5.2; 700 mg 11-methyldodecan-1-ol (**118a**, 3.49 mmol), 1.1 g TBAB (3.49 mmol), 2.2 g $KMnO_4$ (13.96 mmol). 11-Methyldodecanoic acid (*iso*C13, **16a**): 659 mg white oily-solid (3.08 mmol), 88% yield. ^{1}H NMR (600 MHz, $CDCl_3$): δ 0.87 (d, J=6.7 Hz, 6H), 1.13 - 1.20 (m, 2H), 1.22 - 1.40 (m, 12H), 1.53 (m, J=13.3 Hz, J=6.8 Hz, 1H), 1.65 (tt, J=14.7 Hz, J=7.2 Hz, 2H), 2.36 (t, J=7.5 Hz, 2H). ^{13}C NMR (151 MHz, $CDCl_3$): δ 22.8 (2C), 24.8, 27.6, 28.1, 29.2, 29.4, 29.6, 29.8, 30.0, 34.2, 39.2, 180.4. EIMS (70 eV) *m/z* 214.2 $[C_{13}H_{26}O_2]^+$, calculated for $C_{13}H_{26}O_2$ *m/z* 214.2.

10.3.5.14 [D_4]-11-methyldodecanoic acid ([D_4]-*iso*C13, 16b), from route 1

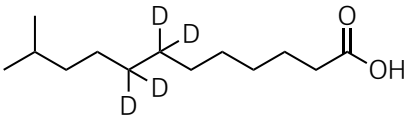

Procedure 10.3.5.2; 808 mg [D_4]-11-methyldodecan-1-ol (**118b**, 3.95 mmol), 1.3 g TBAB (3.95 mmol), 2.5 g $KMnO_4$ (15.80 mmol). [D_4]-11-methyldodecanoic acid ([D_4]-*iso*C13, **16b**): 545 mg white oily solid (2.50 mmol), 63% yield. ^{1}H NMR (600 MHz, $CDCl_3$): δ 0.86 (d, J=6.7 Hz, 6H), 1.11 - 1.20 (m, 2H), 1.20 - 1.40 (m, 8H), 1.53 (m, J=13.4 Hz, J=13.0 Hz, J=6.7 Hz, 1H), 1.65 (tt, J=15.0 Hz, J=7.6 Hz, 2H), 2.37 (t, J=7.6 Hz, 2H). ^{13}C NMR (151 MHz, $CDCl_3$): δ 22.8 (2C), 24.8, 27.6, 28.1, 29.2 (3C), 34.2, 39.2, 180.4. EIMS (70 eV) *m/z* 218.2 $[C_{13}H_{22}D_4O_2]^+$, calculated for $C_{13}H_{22}D_4O_2$ *m/z* 218.2.

10.3.5.15 13-Methyltetradecanoic acid (*iso*C15, 15a), from route 1

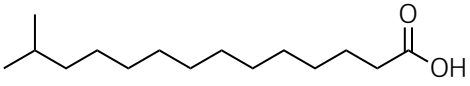

Procedure 10.3.5.2; 585 mg 13-methyltetradecan-1-ol (**119a**, 2.56 mmol), 0.8 g TBAB (3.95 mmol), 1.6 g $KMnO_4$ (10.24 mmol). 13-Methyltetradecanoic acid (*iso*C15, **15a**): 326 mg white solid (1.34 mmol), 52% yield. ^{1}H NMR (600 MHz, $CDCl_3$): δ 0.86 (d, J=6.7 Hz, 6H), 1.12 - 1.18 (m, 2H), 1.20 - 1.39 (m, 16H), 1.51 (m, J=13.3 Hz, J=6.7 Hz, 1H), 1.63 (tt, J=15.2 Hz, J=14.5 Hz, 7.4 Hz, 2H), 2.35 (t, J=7.5 Hz, 2H). ^{13}C

NMR (151 MHz, $CDCl_3$): δ 22.8 (2C), 24.8, 27.5, 28.1, 29.2, 29.4, 29.5, 29.8 (2C), 29.9, 30.1, 34.3, 39.2, 179.8. EIMS (70 eV) *m/z* 242.2 $[C_{15}H_{30}O_2]^+$, calculated for $C_{15}H_{30}O_2$ *m/z* 242.2.

10.3.5.16 [D_4]-13-Methyltetradecanoic acid ([D_4]-*iso*C15, 15b), from route 1

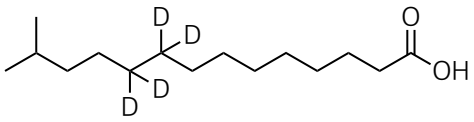

Procedure 10.3.5.2; 510 mg [D_4]-13-methyltetradecan-1-ol (**119b**, 2.19 mmol), 0.7 g TBAB (2.19 mmol), 1.4 g $KMnO_4$ (8.76 mmol). [D_4]-13-Methyltetradecanoic acid ([D_4]-*iso*C15, **15b**) 372 mg white solid (1.51 mmol), 69% yield. ^{1}H NMR (600 MHz, $CDCl_3$): δ 0.86 (d, J=6.7 Hz, 6H), 1.11 - 1.17 (m, 2H), 1.18 - 1.38 (m, 12H), 1.51 (m, J=13.5 Hz, J=6.8 Hz, 1H), 1.63 (tt, J=15.0 Hz, J=7.5 Hz, 2H), 2.35 (t, J=7.6 Hz, 2H). ^{13}C NMR (151 MHz, $CDCl_3$): δ 22.8 (2C), 24.9, 28.2, 29.5 (6C), 34.2, 39.2, 180.3. EIMS (70 eV) *m/z* 246.2 $[C_{15}H_{26}D_4O_2]^+$, calculated for $C_{15}H_{26}D_4O_2$ *m/z* 246.2.

10.3.5.17 2-Methyldodec-11-en-2-ol (121a)

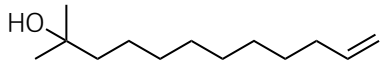

Procedure 10.3.3.8 (section 10.3.3); 7.1 g methyl 10-undecenoate (**120**, 35.80 mmol), 35.8 mL 3 M CH_3MgI (107.40 mmol). 2-Methyldodec-11-en-2-ol (**121a**): 6.6 g yellow oil (33.65 mmol), 94% yield. ^{1}H NMR (600 MHz, $CDCl_3$): δ 1.21 (m, 6H), 1.26 - 1.44 (m, 12H), 1.45 - 1.51 (m, 2H), 2.03 - 2.10 (m, 2H), 4.95 (ddt, J=10.2 Hz, J=2.4 Hz, J=1.3 Hz, 1H), 5.01 (ddt, J=18.8 Hz, J=15.6 Hz, J=1.7 Hz, 1H), 5.80 (ddt, J=16.9 Hz, J=10.2 Hz, J=6.7 Hz, 1H). ^{13}C NMR (151 MHz, $CDCl_3$): δ 24.5, 29.1, 29.3, 29.4, 29.6, 29.7, 30.3, 33.9, 44.1, 71.2, 114.2, 139.4.

10.3.5.18 [D_6]-2-methyldodec-11-en-2-ol (121c)

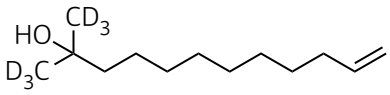

Procedure 10.3.3.8 (section 10.3.3); 6.1 g methyl 10-undecenoate (**120**, 30.75 mmol), 30.8 mL 3 M CD_3MgI (92.25 mmol). [D_6]-2-methyldodec-11-en-2-ol (**121c**): 5.1 g yellow oil (24.95 mmol), 81% yield.

^{1}H NMR (600 MHz, $CDCl_3$): δ 1.29 (d, J=3.9 Hz, 12H), 1.45 (m, 2H), 2.02 - 2.10 (m, 2H), 4.95 (ddt, J=10.2 Hz, J=2.3 Hz, J=1.2 Hz, 1H), 5.01 (ddt, J=18.8 Hz, J=1.7 Hz, J=0.1 Hz, 1H), 5.83 (ddt, J=16.9 Hz, J=10.2 Hz, J=6.7 Hz, 1H). ^{13}C NMR (151 MHz, $CDCl_3$): δ 24.4, 29.1, 29.3, 29.6, 29.7, 30.3, 33.4, 44.0, 70.9, 114.2, 139.4.

10.3.5.19 11-Methyldodec-1-ene (122a)

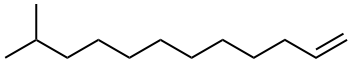

Procedure 10.3.3.9 (section 10.3.3); 6.6 g 2-methyldodec-11-en-2-ol (**121a**, 33.65 mmol), 8.3 mL $BF_3{\cdot}Et_2O$ (67.30 mmol), 10.7 mL Et_3SiH (67.3 mmol), hexane as eluent. 11-Methyldodec-1-ene (**122a**): 5.2 g transparent oil (28.51 mmol), 85% yield. ^{1}H NMR (600 MHz, $CDCl_3$): δ 0.87 (d, J=6.7 Hz, 6H), 1.14 - 1.21 (m, 2H), 1.23 - 1.36 (m, 11H), 1.36 - 1.45 (m, 2H), 1.54 (m, J = 13.4 Hz, J=6.7 Hz, 1H), 2.03 - 2.10 (m, 2H), 4.95 (ddt, J=13.5 Hz, J=11.4 Hz, J=1.3 Hz, 1H), 5.00 (m, 1H), 5.84 (ddt, J=16.9 Hz, J=10.2 Hz, J=6.7 Hz, 1H). ^{13}C NMR (151 MHz, $CDCl_3$): δ 22.8 (2C), 27.6, 28.1, 29.1, 29.3, 29.7, 29.8, 30.1, 34.0, 39.2, 114.2, 139.4.

10.3.5.20 [D_6]-11-methyldodec-1-ene (122c)

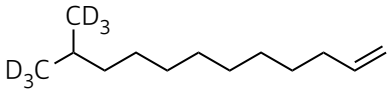

Procedure 10.3.3.9 (section 10.3.3); 5.1 g [D_6]-2-methyldodec-11-en-2-ol (**121c**, 24.95 mmol), 6.2 mL $BF_3{\cdot}Et_2O$ (49.90 mmol), 7.9 mL Et_3SiH (49.90 mmol), hexane as eluent. [D_6]-11-methyldodec-1-ene (**122c**): 3.2 g transparent oil (16.99 mmol), 68% yield. ^{1}H NMR (600 MHz, CDCl3): δ 1.15 (q, J=7.0 Hz, 2H), 1.21 - 1.34 (m, 11H), 1.38 (p, J=7.2 Hz, 2H), 2.01 - 2.08 (m, 2H), 4.93 (ddt, J=11.3 Hz, J=6.9 Hz, J=1.3 Hz, 1H), 5.00 (ddt, J=15.4 Hz, J=3.7 Hz, J=1.7 Hz, 1H), 5.82 (ddt, J=16.9 Hz, 10.2 Hz, J=6.7 Hz, 1H). ^{13}C NMR (151 MHz, $CDCl_3$): δ 27.6 (2C), 29.1, 29.3, 29.7, 29.8, 30.1, 34.0, 39.1, 114.2, 139.4.

10.3.5.21 11-Methyldodecan-1-ol (123a)

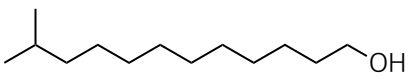

Procedure 10.3.5.3; 2.0 g 11-methyldodec-1-ene (**122a**, 10.96 mmol), 13.2 mL 1 M BH_3·THF (13.15 mmol). 11-Methyldodecan-1-ol (**123a**): 1.8 g light yellow oil (8.92 mmol), 81% yield. ^{1}H NMR (600 MHz, $CDCl_3$): δ 0.86 (d, J=6.6 Hz, 6H), 1.11 - 1.17 (m, 2H), 1.20 - 1.36 (m, 16H), 1.45 - 1.59 (m, 5H), 3.63 (t, J=6.7 Hz, 2H). ^{13}C NMR (151 MHz, $CDCl_3$): δ 22.8 (2C), 25.9, 27.6, 28.1, 29.6, 29.8 (3C), 30.1, 33.0, 39.1, 63.2.

10.3.5.22 [D_6]-11-methyldodecan-1-ol (123c)

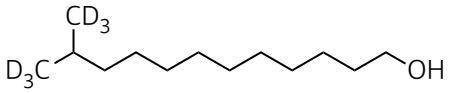

Procedure 10.3.5.3; 1.9 g [D_6]-11-methyldodec-1-ene (**122c**, 10.08 mmol), 12.1 mL 1 M BH_3·THF (12.10 mol). [D_6]-11-methyldodecan-1-ol (**123c**): 1.9 g light yellow oil (9.21 mmol), 91% yield. ^{1}H NMR (600 MHz, $CDCl_3$): δ 1.11 - 1.18 (m, 2H), 1.22 - 1.40 (m, 14H), 1.47 - 1.52 (m, 1H), 1.54 - 1.61 (m, 2H), 3.66 (t, J=6.7 Hz, 2H). ^{13}C NMR (151 MHz, $CDCl_3$): δ 25.9, 27.6 (2C), 29.6, 29.8 (2C), 29.9, 30.1, 33.0, 39.1, 63.2.

10.3.5.23 11-Methyldodecanoic acid (*iso*C13, 16a), from route 2

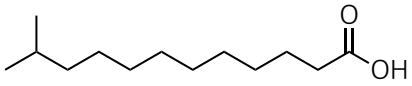

Procedure 10.3.5.2; 260 mg 11-methyldodecan-1-ol (**123a**, 1.30 mmol), 419 mg TBAB (1.30 mmol), 822 mg $KMnO_4$ (5.20 mmol). 11-Methyldodecanoic acid (*iso*C13, **16a**): 251 mg white oily-solid (1.17 mmol), 90% yield. ^{1}H NMR (600 MHz, $CDCl_3$): δ 0.86 (d, J=6.8 Hz, 6H), 1.11 - 1.18 (m, 2H), 1.19 - 1.38(m, 12H), 1.51 (m, 1H), 1.63 (tt, J=14.6 Hz, J=7.3 Hz, 2H), 2.35 (t, J=7.5 Hz, 2H). ^{13}C NMR (151 MHz, $CDCl_3$): δ 22.8 (2C), 24.8, 27.6, 28.1, 29.2, 29.4, 29.6, 29.8, 30.0, 34.2, 39.2, 180.4. EIMS (70 eV) *m/z* 214.2 $[C_{13}H_{26}O_2]^{+\bullet}$, calculated for $C_{13}H_{26}O_2$ *m/z* 214.2.

10.3.5.24 [D_6]-11-methyldodecanoic acid ([D_6]-*iso*C13, 16c), from route 2

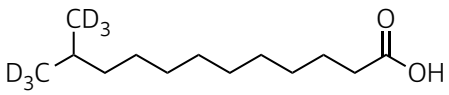

Procedure 10.3.5.2; 0.7 g 11-methyldodecan-1-ol (**123a**, 3.40 mmol), 1.1 g TBAB (3.40 mmol), 2.1 g $KMnO_4$ (13.6 mmol). [D_6]-11-methyldodecanoic acid ([D_6]-*iso*C13, **16c**): 649 mg white oily solid (2.94 mmol), 86% yield. ^{1}H NMR (600 MHz, $CDCl_3$): δ 1.12 - 1.19 (m, 2H), 1.21 - 1.42 (m, 12H), 1.50 (m, 1H), 1.65 (tt, J=14.6 Hz, J=7.3 Hz, 2H), 2.37 (t, J=7.5 Hz, 2H). ^{13}C NMR (151 MHz, $CDCl_3$): δ 24.8, 27.6, 29.2, 29.4, 29.6, 29.7, 29.8 (2C), 29.9, 34.1, 39.2, 180.3. EIMS (70 eV) *m/z* 220.2 $[C_{13}H_{20}D_6O_2]^{+\bullet}$, calculated for $C_{13}H_{20}D_6O_2$ *m/z* 220.2.

10.3.5.25 1-Bromo-11-methyldodecane (124a)

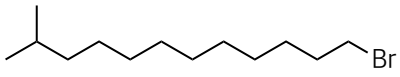

Procedure 10.3.3.1 (section 10.3.3); 2.2 g 11-methyldodecan-1-ol (**123a**, 10.98 mmol), 1.1 mL Br_2 (21.96 mmol), 5.8 g PPh_3 (21.96 mmol), hexane as eluent. 1-Bromo-11-methyldodecane (**124a**): 1.8 g transparent oil (6.84 mmol), 62% yield. ^{1}H NMR (600 MHz, $CDCl_3$): δ 0.87 (d, J=6.6 Hz, 6H), 1.12 - 1.18 (m, 2H), 1.21 - 1.36 (m, 12H), 1.38 - 1.46 (m, 2H), 1.47 - 1.55 (m, 1H), 1.82 - 1.90 (m, 2H), 3.41 (t, J=6.9 Hz, 2H). ^{13}C NMR (151 MHz, $CDCl_3$): δ 22.8 (2C), 27.6, 28.1, 28.3, 28.9, 29.6, 29.7, 29.8, 30.1, 33.0, 34.2, 39.2.

10.3.5.26 [D_6]-1-bromo-11-methyldodecane (124c)

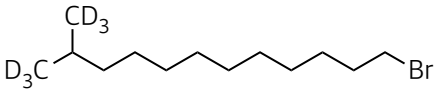

Procedure 10.3.3.1 (section 10.3.3); 1.2 g [D_6]-11-methyldodecan-1-ol (**123c**, 5.81 mmol), 0.6 mL Br_2 (11.62 mmol), 3.1 g PPh_3 (11.62 mmol), hexane as eluent. [D_6]-1-bromo-11-methyldodecane (**124c**): 969 mg transparent oil (3.60 mmol), 62% yield. ^{1}H NMR (600 MHz, $CDCl_3$): δ 1.11 - 1.18 (m, 2H), 1.23 - 1.32 (m, 12H), 1.38 - 1.46 (m, 2H), 1.48 (m, 1H), 1.86 (tt, J=14.2, 7.0 Hz, 2H), 3.41 (t, J=6.9 Hz, 2H). ^{13}C NMR (151 MHz, $CDCl_3$): δ 27.5, 28.3, 28.9, 29.6, 29.7, 29.8, 30.1, 33.0, 34.2, 39.1.

10.3.5.27 13-Methyltetradec-1-ene (125a)

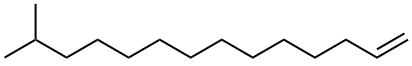

Procedure 10.3.5.4; 701 mg 1-bromo-11-methyldodecane (**124a**, 2.66 mmol), 8.0 mL 1 M vinylmagnesium bromide (7.98 mmol). 13-Methyltetradec-1-ene (**125a**): 400 mg transparent light oil (1.90 mmol), 71% yield. ^{1}H NMR (600 MHz, $CDCl_3$): δ 0.86 (d, J=6.6 Hz, 6H), 1.12 - 1.18 (m, 2H), 1.26 (m, 16H), 1.47 - 1.56 (m, 1H), 2.01 - 2.08 (m, 2H), 4.93 (ddt, J=10.2 Hz, J=2.3 Hz, J=1.3 Hz, 1H), 4.99 (ddt, J=13.5 Hz, J=3.7 Hz, J=1.6 Hz, 1H), 5.82 (ddt, J=16.9 Hz, J=10.2 Hz, J=6.7 Hz, 1H). ^{13}C NMR (151 MHz, $CDCl_3$): δ 22.8 (2C), 27.6, 28.1, 29.1, 29.5, 29.8 (2C), 29.9 (2C), 30.1, 34.0, 39.2, 114.2, 139.4.

10.3.5.28 [D_6]-13-methyltetradec-1-ene (125c)

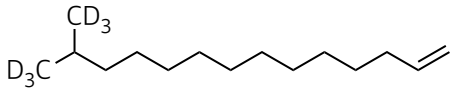

Procedure 10.3.5.4; 815 mg [D_6]-1-bromo-11-methyldodecane (**124c**, 3.03 mmol), 9.1 mL 1 M vinylmagnesium bromide (9.09 mmol). [D_6]-13-methyltetradec-1-ene (**125c**): 438 mg transparent light oil (2.02 mmol), 67% yield. ^{1}H NMR (600 MHz, $CDCl_3$): δ 1.12 -1.16 (m, 2H), 1.20 - 1.33 (m, 14H), 1.34 - 1.42 (m, 2H), 1.48 (t, J=7.0 Hz, 1H), 2.01 - 2.08 (m, 2H), 4.93 (ddt, J=10.2 Hz, J=2.4 Hz, J=1.3 Hz, 1H), 5.00 (ddt, J=13.6 Hz, J=3.8 Hz, J=2.0 Hz, J=1.5 Hz, 1H), 5.82 (ddt, J=16.9 Hz, J=10.2 Hz, J=6.7 Hz, 1H). ^{13}C NMR (151 MHz, $CDCl_3$): δ 27.5 (2C), 29.0, 29.1, 29.3, 29.7, 29.8 (2C), 30.1, 34.0, 39.1, 114.2, 139.4.

10.3.5.29 13-Methyltetradecan-1-ol (126a)

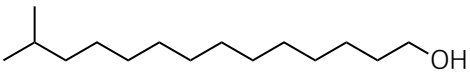

Procedure 10.3.5.3; 400 mg 13-methyltetradec-1-ene (**125a**, 1.90 mmol), 2.3 mL 1 M BH_3·THF (2.28 mmol). 13-Methyltetradecan-1-ol (**126a**): 276 mg white oily solid (1.21 mmol), 64% yield. ^{1}H NMR (600 MHz, $CDCl_3$): δ 0.86 (d, J=6.7 Hz, 6H), 1.11 - 1.16 (m, 2H), 1.26 (m, 16H), 1.47 - 1.60 (m, 5H), 3.66 (t, J=6.7 Hz, 2H). ^{13}C NMR (151 MHz, $CDCl_3$): δ 22.8 (2C), 25.9, 27.6, 28.1, 29.6, 29.8 (3C), 29.9 (2C), 30.1, 30.5, 32.9, 39.2, 63.4.

10.3.5.30 [D_6]-13-methyltetradecan-1-ol (126c)

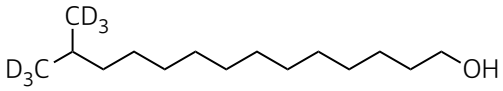

Procedure 10.3.5.3; 437 mg [D_6]-13-methyltetradec-1-ene (**125c**, 2.02 mmol), 2.4 mL 1 M BH_3·THF (2.42 mmol). [D_6]-13-methyltetradecan-1-ol (**126c**): 283 mg white oily solid (1.21 mmol), 60% yield. ^{1}H NMR (600 MHz, $CDCl_3$): δ 1.12 - 1.16 (m, 2H), 1.25 (m, 17H), 1.44 - 1.50 (m, 2H), 1.51 - 1.58 (m, 2H), 3.64 (t, J=6.7 Hz, 2H). ^{13}C NMR (151 MHz, $CDCl_3$): δ 25.9, 27.6 (2C), 29.3, 29.6, 29.8, 29.9 (3C), 30.1, 33.0, 39.1, 63.2.

10.3.5.31 13-Methyltetradecanoic acid (*iso*C15, 15a), from route 2

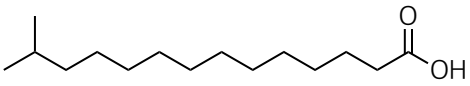

Procedure 10.3.5.2; 276 mg 13-methyltetradecan-1-ol (**126a**, 1.21 mmol), 386 mg TBAB (1.21 mmol), 764 mg $KMnO_4$ (4.84 mmol). 13-Methyltetradecanoic acid (*iso*C15, **15a**): 221 mg white solid (0.91 mmol), 75% yield. ^{1}H NMR (600 MHz, $CDCl_3$): δ 0.86 (d, J=6.7 Hz, 6H), 1.12 - 1.18 (m, 2H), 1.26 (m, 17H), 1.51 (m, 1H), 1.63 (m, 1H), 2.35 (t, J=7.5 Hz, 2H). ^{13}C NMR (151 MHz, $CDCl_3$): δ 22.8 (2C), 24.8, 27.6, 28.1, 29.2, 29.6 (2C), 29.8 (2C), 29.9, 30.1, 34.1, 39.2, 179.8. EIMS (70 eV) *m/z* 242.2 $[C_{15}H_{30}O_2]^{+\bullet}$, calculated for $C_{15}H_{30}O_2$ *m/z* 242.2.

10.3.5.32 [D_6]-13-methyltetradecanoic acid ([D_6]-*iso*C15, 15c), from route 2

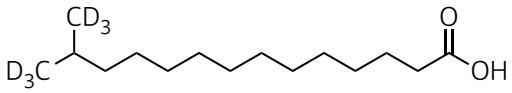

Procedure 10.3.5.2; 536 mg [D_6]-13-methyltetradecan-1-ol (**126c**, 2.29 mmol), 738 mg TBAB (2.29 mmol), 1.4 g $KMnO_4$ (9.16 mmol). [D_6]-13-methyltetradecanoic acid ([D_6]-*iso*C15, **15c**): 419 mg white solid (1.67 mmol), 73% yield. ^{1}H NMR (600 MHz, $CDCl_3$): δ 1.12 - 1.20 (m, 2H), 1.22 - 1.40 (m, 16H), 1.50 (m, 1H), 1.65 (tt, J=14.8 Hz, J=7.4 Hz, 2H), 2.37 (t, J=7.5 Hz, 2H). ^{13}C NMR (151 MHz, $CDCl_3$): δ 24.8, 27.6 (2C), 29.2, 29.4, 29.6, 29.8 (2C), 29.9, 30.2, 34.2, 39.1, 180.1. EIMS (70 eV) *m/z* 248.2 $[C_{15}H_{24}D_6O_2]^{+\bullet}$, calculated for $C_{15}H_{24}D_6O_2$ *m/z* 248.3.

10.3.5.33 [D_6]-15-methylhexadecan-1-ol (46c)

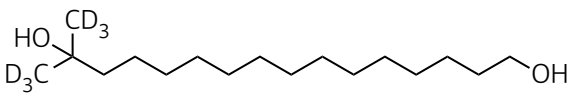

Procedure 10.3.3.8 (section 10.3.3); 2.4 g pentadecanolide (**45**, 9.98 mmol), 30 mL 1 M CD_3MgI (29.94 mmol), 9:1 hexane-EtOAc as eluent. [D_6]-15-methylhexadecan-1-ol (**46c**): 2.6 g lustrous white solid (9.48 mmol), 95% yield. ^{1}H NMR (600 MHz, $CDCl_3$): δ 1.23 - 1.38 (m, 23H), 1.43 - 1.47 (m, 2H), 1.54 - 1.60 (m, 2H), 3.64 (t, J=6.6 Hz, 2H). ^{13}C NMR (151 MHz, $CDCl_3$): δ 24.5, 25.9, 29.6, 29.7, 29.8 (5C), 30.3, 32.9, 44.0, 63.2, 71.0.

10.3.5.34 [D_6]-15-methylhexadecan-1-ol (47c)

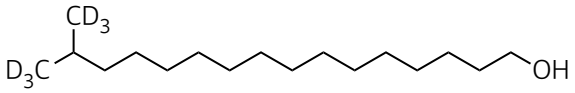

Procedure 10.3.3.9 (section 10.3.3); 2.6 g [D_6]-15-methylhexadecan-1-ol (**46c**, 9.48 mmol), 2.3 mL $BF_3{\cdot}Et_2O$ (18.96 mmol), 3.0 mL Et_3SiH (18.96 mmol), 9:1 hexane-EtOAc as eluent. [D_6]-15-methylhexadecan-1-ol (**47c**): 2.3 g white solid (8.81 mmol), 93% yield. ^{1}H NMR (600 MHz, $CDCl_3$): δ 1.12 - 1.17 (m, 2H), 1.22 - 1.38 (m, 23H), 1.48 (m, 1H), 1.54 - 1.60 (m, 2H), 3.64 (t, J=6.7 Hz, 2H). ^{13}C NMR (151 MHz, $CDCl_3$): δ 25.9, 27.5 (2C), 29.6, 29.8 (5C), 29.9 (2C), 30.1, 33.0, 39.1, 63.2.

10.3.5.35 15-Methylhexadecanoic acid (*iso*C17, 17a)

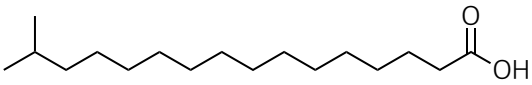

Procedure 10.3.5.2; 1.8 g 15-methylhexadecane-1,15-diol (**47a**, 7.02 mmol), 2.3 g TBAB (7.02 mmol), 4.4 g $KMnO_4$ (28.08 mmol). 15-Methylhexadecanoic acid (*iso*C17, **17a**): 1.7 g bright white solid (6.32 mmol), 90% yield. ^{1}H NMR (600 MHz, $CDCl_3$): δ 0.86 (d, J=6.7 Hz, 6H), 1.14 (m, 2H), 1.25 (m, 20H), 1.52 (m, 1H), 1.63 (m, 2H), 2.35 (t, J=7.5 Hz, 2H). ^{13}C NMR (151 MHz, $CDCl_3$): δ 22.8 (2C), 24.8, 27.6, 28.1, 29.2, 29.4, 29.6, 29.8(4C), 29.9, 30.1, 34.2, 39.2, 180.3. EIMS (70 eV) *m/z* 270.2 $[C_{17}H_{34}O_2]^{+\bullet}$, calculated for $C_{17}H_{34}O_2$ *m/z* 270.3.

10.3.5.36 [D_6]-15-methylhexadecanoic acid ([D_6]-*iso*C17, 17c)

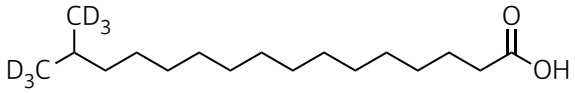

Procedure 10.3.5.2; 1.8 g [D_6]-15-methylhexadecan-1-ol (**47c**, 6.86 mmol), 2.2 g TBAB (6.86 mmol), 4.3 g $KMnO_4$ (27.44 mmol). [D_6]-15-methylhexadecanoic acid ([D_6]-*iso*C17, **17c**): 1.7 g bright white solid (6.11 mmol), 89% yield. ^{1}H NMR (600 MHz, $CDCl_3$): δ 1.13 (m, 2H), 1.25 (m, 21H), 1.48 (m, 1H), 1.63 (m, 2H), 2.35 (t, J=7.5 Hz, 2H). ^{13}C NMR (151 MHz, $CDCl_3$): δ 24.8, 27.6 (2C), 29.2, 29.4, 29.6, 29.8 (4C), 29.9, 30.1, 34.2, 39.1, 180.1. EIMS (70 eV) *m/z* 276.2 $[C_{17}H_{28}D_6O_2]^{+\bullet}$, calculated for $C_{17}H_{28}D_6O_2$ *m/z* 276.3.

12 References

1. **A. Coghlan** (2005), *Nematode genome evolution.* WormBook, pp. 1-15.

2. **A. Shatilovich, A. Tchesunov, T. Neretina, I. Grabarnik, S. Gubin, T. Vishnivetskaya, T. Onstott, E. Rivkina** (2018), *Viable nematodes from late pleistocene permafrost of the Kolyma river Lowland.* Dokl. Biol. Sci., Vol. 480, pp. 100-102.

3. **J. van den Hoogen, T. Ward Crowther** (2019), *Soil nematode abundance and functional group composition at a global scale.* Nature, Vol. 572, pp. 194-198.

4. **D. Weinstein, S. Allen, M. Lau, M. Erasmus, K. Asalone, K. Walters-Conte, G. Deikus, R. Sebra, G. Borgonie, E. van Heerden, T. Onstott, J. Bracht** (2019), *The genome of a subterrestrial nematode reveals adaptations to heat.* Nat. Commun., Vol. 10.

5. **Consortium, C. elegans Sequencing** (1998), *Genome sequence of the nematode C. elegans: a platform for investigating biology.* Science., Vol. 282, pp. 2012-2018.

6. **L. O'Reilly, C. Luke, D. Perlmutter, G. Silverman, S. Pak** (2014), *C. elegans in high-throughput drug discovery.* Adv. Drug Deliv. Rev., Vol. 20, pp. 247-253.

7. **O. Sin, H. Michels, E. Nollen** (2014), *Genetic screens in Caenorhabditis elegans models for neurodegenerative diseases.* BBA, Vol. 1842, pp. 1951-1959.

8. **N. Fielenbach, A. Antebi** (2008), *C. elegans dauer formation and the molecular basis of plasticity.* Genes Dev., Vol. 22, pp. 2149-2165.

9. **R. Cassada, R. Russell** (1975), *The dauerlarva, a post-embryonic developmental variant of the nematode Caenorhabditis elegans.* Dev. Biol., Vol. 46, pp. 326-342.

10. **F. Schroeder, S. von Reuss** (2015), *Combinatorial chemistry in nematodes: modular assembly of primary metabolism-derived building blocks.* Nat. Prod. Rep., Vol. 32, pp. 994-1006.

11. **A. Choe, S. von Reuss, D. Kogan, R. Gasser, E. Platzer, F. Schroeder, P. Sternberg** (2012), *Ascaroside signaling is widely conserved among nematodes.* Curr. Biol., Vol. 22, pp. 772-780.

12. **P. Jeong, M. Jung, Y. Yim, H. Kim, M. Park, E. Hong, W. Lee, Y. Hwan Kim, K. Kim, Y. Paik** (2005), *Chemical structure and biological activity of the Caenorhabditis elegans dauer-inducing pheromone.* Nature, Vol. 433, pp. 541-545.

13. **J. Golden, D. Riddle** (1985), *A gene affecting production of the Caenorhabditis elegans dauer-inducing pheromone.* Mo. Gen. Genet., Vol. 198, pp. 534-536.

14. **J. Bartley, E. Bennett, P. Darben** (1996), *Structure of the ascarosides from Ascaris suum.* J. Nat. Prod., Vol. 59, pp. 921-926.

15. **C. Pungaliya, J. Srinivasan, B. Fox, R. Malik, A. Ludewig, P. Sternberg, F. Schroeder** (2009), *A shortcut to identifying small molecule signals that regulate behavior and development in Caenorhabditis elegans.* PNAS, Vol. 106, pp. 7708-7713.

16. **J. Srinivasan, S. von Reuss, N. Bose, A. Zaslaver, P. Mahanti, M. Ho, O. O'Doherty, A. Edison, P. Sternberg, F. Schroeder** (2012), *A modular library of small molecule signals regulates social behaviors in Caenorhabditis elegans.* PLoS Biology, Vol. 10, p. e1001237.

17. **S. von Reuss, N. Bose, J. Srinivasan, J. Yim, J. Judkins, P. Sternberg, F. Schroeder** (2012), *Comparative metabolomics reveals biogenesis of ascarosides, a modular library of small-molecule signals in C. elegans.* J. Am. Chem. Soc., Vol. 134, pp. 1817-1824.

18. **Y. Zhang, M. Sanchez-Ayala, P. Sternberg, J. Srinivasan, F. Schroeder** (2017), *Improved synthesis for modular ascarosides uncovers biological activity.* Org. Lett., Vol. 19, pp. 2837-2840.

19. **H. Le, C. Wrobel, S. Cohen, J. Yu, H. Park, M. Helf, B. Curtis, J. Kruempel, P. Rodrigues, P. Hu, P. Sternberg, F. Schroeder** (2020), *Modular metabolite assembly in Caenorhabditis elegans depends on carboxylesterases and formation of lysosome-related organelles.* Elife., Vol. 9, p. e61886.

20. **A. Ludewig, F. Schroeder** (2013), *Ascaroside signaling in C. elegans.* WormBook., pp. 1-22.

21. **S. von Reuss, F. Dolke, C. Dong** (2017), *Ascaroside profiling of Caenorhabditis elegans using GC-EIMS.* Anal. Chem., Vol. 89, pp. 10570-10577.

22. **X. Zhang, L. Feng, S. Chinta, P. Singh, Y. Wang, J. Nunnery, R. Butcher** (2015), *Acyl-CoA oxidase complexes control the chemical message produced by Caenorhabditis elegans.* PNAS, Vol. 112, pp. 3955-3960.

23. **Y. Izrayelit, S. Robinette, N. Bose, S. von Reuss, F. Schroeder** (2013), *2D NMR-based metabolomics uncovers interactions between conserved biochemical pathways in the model organism Caenorhabditis elegans.* ACS Chem. Biol., Vol. 8, pp. 314-319.

24. **F. Dolke** (2016), *Synthesis of structurally diverse ascarosides from Caenorhabditis species and the role of very long chain fatty acids in the ascaroside biosynthesis.* University of Jena, Jena. Thesis.

25. **X. Zhang, J. Noguez, Y. Zhou, R. Butcher** (2013), *Analysis of ascarosides from Caenorhabditis elegans using Mass Spectrometry and NMR spectroscopy.* Methods Mol. Biol., Vol. 1068, pp. 71-92.

26. **N. Bose, A. Ogawa, S. von Reuss, J. Yim, E. Ragsdale, R. Sommer, F. Schroeder** (2012), *Complex Small-Molecule Architectures Regulate Phenotypic Plasticity in a Nematode.* Angew. Chem., Vol. 51, pp. 12438-12443.

27. **C. Dong, C. Weadick, V. Truffault, R. Sommer** (2020), *Convergent evolution of small molecule pheromones in Pristionchus nematodes.* ELife, Vol. 9, p. e55687.

28. **R. Butcher, J. Ragains, E. Kim, J. Clardy** (2008), *A potent dauer pheromone component in Caenorhabditis elegans that acts synergistically with other components.* PNAS, Vol. 105, pp. 14288-14292.

29. **J. Srinivasan, F. Kaplan, R. Ajredini, C. Zachariah, H. Alborn, P. Teal, R. Malik, A. Edison, P. Sternberg, F. Schroeder** (2008), *A blend of small molecules regulates both mating and development in Caenorhabditis elegans.* Nature, Vol. 454, pp. 1115-1118.

30. **R. Butcher, J. Ragain, W. Li, G. Ruvkun, J. Clardy, H. Mak** (2009), *Biosynthesis of the Caenorhabditis elegans dauer pheromone.* PNAS, Vol. 106, pp. 1875-1879.

31. **H. Joo, K. Kim, Y. Yim, Y. Jin, H. Kim, Mu. Kim, Y. Paik** (2010)**,** *Contribution of the peroxisomal acox gene to the dynamic balance of daumone production in Caenorhabditis elegans.* JBC, Vol. 285, pp. 29319-29325.

32. **V. Zagoriy, V. Matyash, T. Kurzchalia** (2010), *Long-chain O-ascarosyl-alkanediols are constitutive components of Caenorhabditis elegans but do not inducedauer larva formation.* Chem. Biodivers., Vol. 7, pp. 2016-2022.

33. **S. Olson, G. Greenan, A. Desai, T. Müller-Reichert, K. Oegem** (2012), *Hierarchical assembly of the eggshell and permeability barrier in C. elegans.* J. Cell Biol., 2012, Vol. 198, pp. 731-748.

34. **G. Tarr, H. Schnoes** (1973), *Structures of ascaroside aglycones.* Arch. Biochem., Vol. 158, pp. 288-296.

35. **G. Tarr, D. Fairbairn** (1973), *Ascarosides of the ovaries and eggs of Ascaris lumbricoides (nematoda*), Lipids., Vol. 8, pp. 7-16.

36. **M. Kniazeva, Q. Crawford, M. Seiber, C. Wang, M. Han** (2004), *Monomethyl branched-chain fatty acids play an essential role in Caenorhabditis elegans development.* PLoS Biology, Vol. 2, p. e257.

37. **M. Kniazeva, T. Euler, M. Han** (2008), *A branched-chain fatty acid is involved in post-embryonic growth control in parallel to the insulin receptor pathway and its biosynthesis is feedbackregulated in C. elegans.* Genes & Development, Vol. 22, pp. 2102-2110.

38. **E. Entchev, D. Schwudke, V. Zagoriy, V. Matyash, A. Bogdanova, B. Habermann, L. Zhu, A. Shevchenko, T. Kurzchalia** (2008), *LET-767 is required for the production of bbranched chain and long chain fatty acids in Caenorhabditis elegans.* J. Biol. Chem., Vol. 283, pp. 17550-17560.

39. **M. Kniazeva, H. Zhu, A. Sewell, M. Han** (2015), *A lipid-TORC1 pathway promotes neuronal development and foraging behavior under both fed and fasted conditions in C. elegans.* Dev. Cell, Vol. 33, pp. 260-271.

40. **F. Jia, M. Cui, M. Than, M. Han** (2016), *Developmental defects of Caenorhabditis elegans lacking branched-chain α-ketoacid dehydrogenase are mainly caused by monomethyl branched-chain fatty acid deficiency.* J. Biol. Chem., Vol. 291, pp. 2967-2973.

41. **J. Watts, M. Ristow** (2017), *Lipid and carbohydrate metabolism in Caenorhabditis elegans.* Genetics, Vol. 207, pp. 413-446.

42. **J. Thomas Hannich, D. Mellal, S. Feng, A. Zumbuehl, H. Riezman** (2017), *Structure and conserved function of iso-branched sphingoid bases from the nematode Caenorhabditis elegans.* Chem. Sci., Vol. 8, pp. 3676-3686.

43. **M. Witting, U. Schmidt, H. Knölker** (2021), *UHPLC-IM-Q-ToFMS analysis of maradolipids, found exclusively in Caenorhabditis elegans dauer larvae.* Anal. Bioanal. Chem., Vol. 413, pp. 2091-2102.

44. **S. Penkov, F. Mende, V. Zagoriy, C. Erkut, R. Martin, U. Pässler, K. Schuhmann, D. Schwudke, M. Gruner, J. Mäntler, T. Reichert-Müller, A. Shevchenko, H. Knölker, T. Kurzchalia** (2010), *Maradolipids: diacyltrehalose glycolipids specific to dauer larva in Caenorhabditis elegans.* Angew. Chem. Int. Ed. Engl., Vol. 122, pp. 9430-9435.

45. **V. Hänel, C. Pendleton, M. Witting** (2019), *The sphingolipidome of the model organism Caenorhabditis elegans.* Chem. Phys. Lipids., Vol. 222, pp. 15-22.

46. **D. Chitwood, W. Lusby, M. Thompson, J. Kochansky, O. Howarth** (1995), *The glycosylceramides of the nematode Caenorhabditis elegans contain an unusual, branched-chain sphingoid base.* Lipids, Vol. 30, pp. 567-573.

47. **S. Gerdt, G. Lochnit, R. Dennis, R. Geyer** (1997), *Isolation and structural analysis of three neutral glycosphingolipids from a mixed population of Caenorhabditis elegans (Nematoda: Rhabditida).* Glycobiology, Vol. 7, pp. 265-275.

48. **V. Sarpe, S. Kulkarni** (2011), *Synthesis of maradolipid.* J. Org. Chem., Vol. 76, pp. 6866-6870.

49. **K. Hollister, E. Conner, X. Zhang, M. Spell, G. Bernard, P. Patel, A. de Carvalho, R. Butcher, and J. Ragains** (2013), *Ascaroside activity in Caenorhabditis elegans is highly dependent on chemical structure.*. Bioorg Med Chem., Vol. 21, pp. 5754-5769.

50. **J. Joly, F. Roze, S. Banas, F. Quilès** (2010), *Synthesis and Raman spectra of 3-deoxy-a-L-rhamnosides as model sugars of the Ascaris egg shell.* Tetrahedron Lett., Vol. 51, pp. 3161-3250.

51. **K. Mori, T. Ohtaki, H. Ohrui, D. Berkebile, D. Carlson** (2004), *Synthesis of the four stereoisomers of 6-acetoxy-19-methylnonacosane, the most potent component of the female sex pheromone of the new world screwworm fly, with special emphasis on partial racemization in the course of catalytic hydrogenation.* Eur. J. Org. Chem., Vol. 5, pp. 1089-1096.

52. **K. Mori** (2011), *Protective group-free syntheses of (±)-frontalin, (±)-endo-brevicomin, (±)-exo-brevicomin, and (±)-3,4-dehydro-exo-brevicomin: racemic pheromones with a 6,8-dioxabicyclo[3.2.1]octane ring.* Biosci. Biotechnol. Biochem., Vol. 75, pp. 976–981.

53. **R. Weaving, E. Roulland, C. Monneret, J. Florent** (2003), *A rapid access to chiral alkylidene cyclopentenone prostaglandins involving ring-closing metathesis reaction.* Tetrahedron Lett., Vol. 44, pp. 2579–2581.

54. **G. Reader** (1977), *Isotopically labelled fatty acids. CA1078865A,* Canada.

55. **M. Richardson, S. Williams** (2013), *A practical synthesis of long-chain iso-fatty acids (iso-C12–C19) and related natural products.* Beilstein J. Org. Chem., Vol. 9, pp. 1807-1812.

56. **I. Mohammada, J. Muna, A. Onorato, M. Morton, A. Saleh, M. Smith** (2017), *The influence of distal substitution on the base-induced isomerization of long-chain terminal alkynes.* Tetrahedron Lett., Vol. 58, pp. 4162-4165.

57. **Y. Masuda, M. Yoshida, K. Mori** (2002), *Synthesis of (2S,2R,3S,4R)-2-(2-Hydroxy-21-methyldocosanoylamino)- 1,3,4-pentadecanetriol, the ceramide sex pheromone of the female hair crab, Erimacrus isenbeckii.* Biosci. Biotechnol. Biochem., Vol. 66, pp. 1531-1537.

58. **P. Sonnet** (1976), *Direct conversion of an alcohol tetrahydropyranyl ether to a bromide, chloride, methyl ether, nitrile or trifluoroacetate.* Synth. Commun., Vol. 6, pp. 21-26.

59. **S. Drescher, K. Helmis, A. Langner, B. Dobner** (2010), *Synthesis of novel symmetrical, single-chain, diacetylene-modified bolaamphiphiles with different alkyl chain lengths.* Monatsh. Chem., Vol. 141, pp. 339-349.

60. **N. Chizhov, O. Kochetkov** (1966), *Mass Spectrometry of carbohydrate derivatives.* Adv. Carb. Chem., Vol. 21, pp. 39-93.

61. **A. Artyukhin, J. Yim, J. Srinivasan, Y. Izrayelit, N. Bose, S. von Reuss, Y. Jo, J. Jordan, L. Baugh, M. Cheong, P. Sternberg, L. Avery, F. Schroeder** (2013), *Succinylated octopamine ascarosides and a new pathway of biogenic amine metabolism in Caenorhabditis elegans.* J. Biol. Chem., Vol. 288, pp. 18778-18783.

62. **T. Kaneda** (1991), *Iso- and anteiso-fatty acids in bacteria: biosynthesis, function and taxonomic significance.* Annu. Rev. Microbiol., Vol. 55, pp. 288-302.

63. **M. Mansilla, L. Cybulski, D. Albanesi, D. de Mendoza.** (2004), *Control of membrane lipid fluidity by molecular thermosensors.* J. Bacteriol. Res., Vol. 186, pp. 6681-6688.

64. **C. Perez, M. Van Gilst** (2008), *A 13C isotope labeling strategy reveals the influence of insulin signaling on lipogenesis in C. elegans.* Cell Metab., Vol. 8, pp. 266-74.

65. **D. Fairbairn, P. Jezyk** (1967), *Ascarosides and ascaroside esters in Ascaris lumbricoides (nematoda).* CBP, Vol. 23, pp. 691-705.

66. **A. Lorente, F. Albericio, M. Álvarez** (2014), *Selective formation of a Z-trisubstituted double bond using a 1-(tert-butyl)tetrazolyl sulfone.* J. Org. Chem., Vol. 79, pp. 10648-10654.

67. **G. Ishmuratov, M. Yakovleva, R. Kharisov, O. Botsman, O. Izibairov, A. Mannapov, G. Tolstikov** (2001), *Synthesis of the honey-bee attractant 13-hydroxy-2-oxotridecane.* Chem. Nat. Compd., Vol. 37, pp. 165-166.

68. **E. Hostetler, S. Fallis, T. McCarthy, M. Welch J. Katzenellenbogen** (1998), *Improved methods for the synthesis of [ω-11C]palmitic acid.* J. Org. Chem., Vol. 63, pp. 1348-1351.

69. **H. Zhu, H. Shen, A. Sewell, M. Kniazeva, M. Han** (2013), *A novel sphingolipid-TORC1 pathway critically promotes postembryonic development in Caenorhabditis elegans.* Elife., Vol. 2, p. e00429.

70. **H. Zhu, A. Sewell, M. Han** (2015), *Intestinal apical polarity mediates regulation of TORC1 by glucosylceramide in C. elegans* Genes Dev., Vol. 29, pp. 1218-1223.

71. **E. Burkhardt, K. Matos** (2006), *Boron reagents in process chemistry: excellent tools for selective reductions.* Chem. Rev., Vol. 106, pp. 2617-2650.

72. **J. Zhang, Y. Hu, Y. Wang, L. Fu, X. Xu, C. Li, J. Xu, C. Li, L. Zhang, R. Yang, X. Jiang, Y. Wu, Pi. Liu, X. Zou, B. Liang** (2021), *mmBCFA C17iso ensures endoplasmic reticulum integrity for lipid droplet growth.* J. Cell Biol., Vol. 220, p. e202102122.

73. **H. Zhang, N. Abraham, L. Khan, D. Hall, J. Fleming, V. Göbel** (2011), *Apicobasal domain identities of expanding tubular membranes depend on glycosphingolipid biosynthesis.* Nat. Cell Bio., Vol. 13, pp. 1189-1201.

74. **V. Matyash, G. Liebisch, T. Kurzchalia, A. Shevchenko, D. Schwudke** (2008), *Lipid extraction by methyl-tert-butyl ether for high-throughput lipidomics.* J. Lipid Res., Vol. 49, pp. 1137-1146.

13 Supporting information

13.1 NMR spectra

13.1.1 (3*R*,4*R*,5*S*,6*S*)-6-methyltetrahydro-2*H*-pyran-2,3,4,5-tetrayl tetrabenzoate (28)

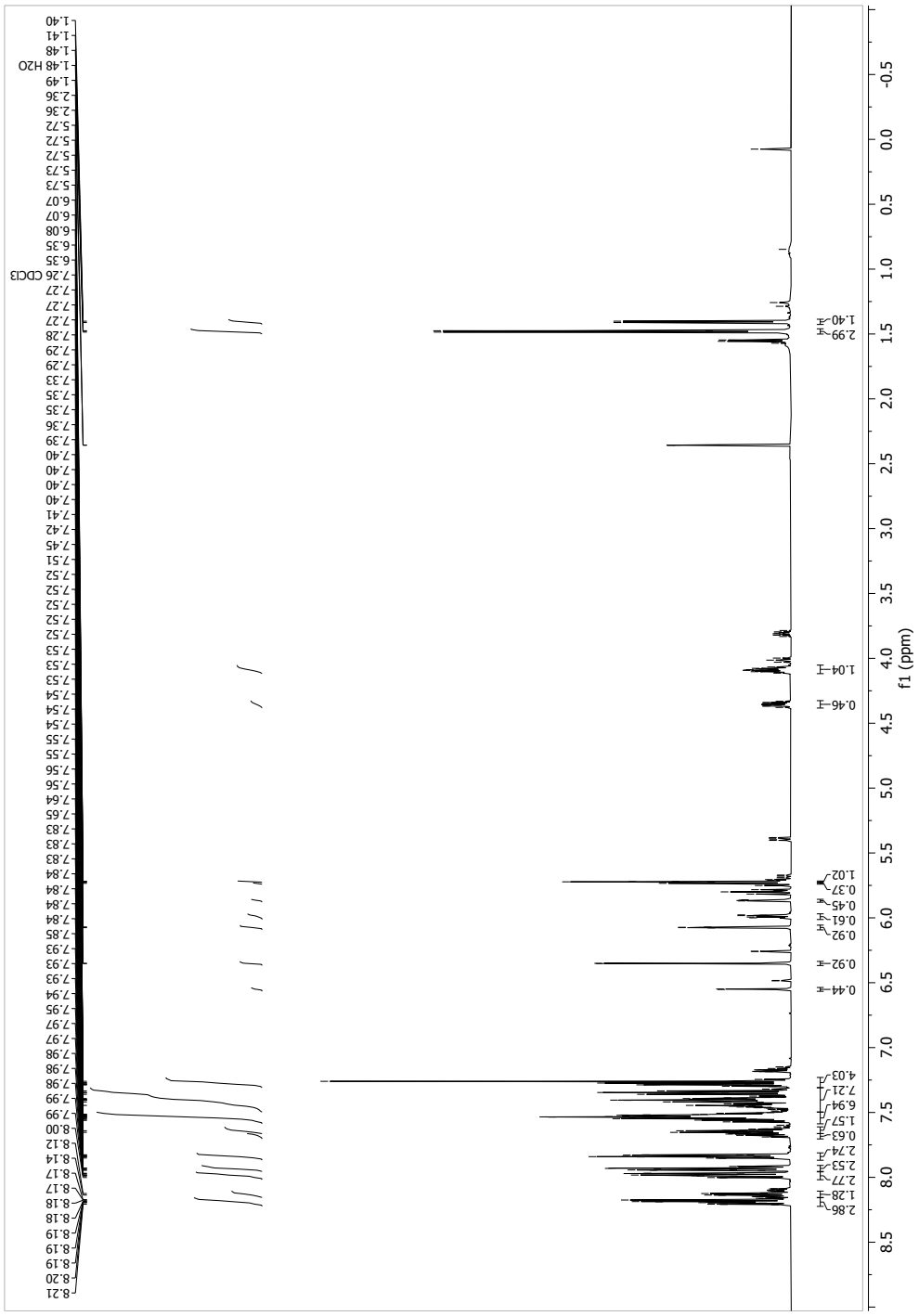

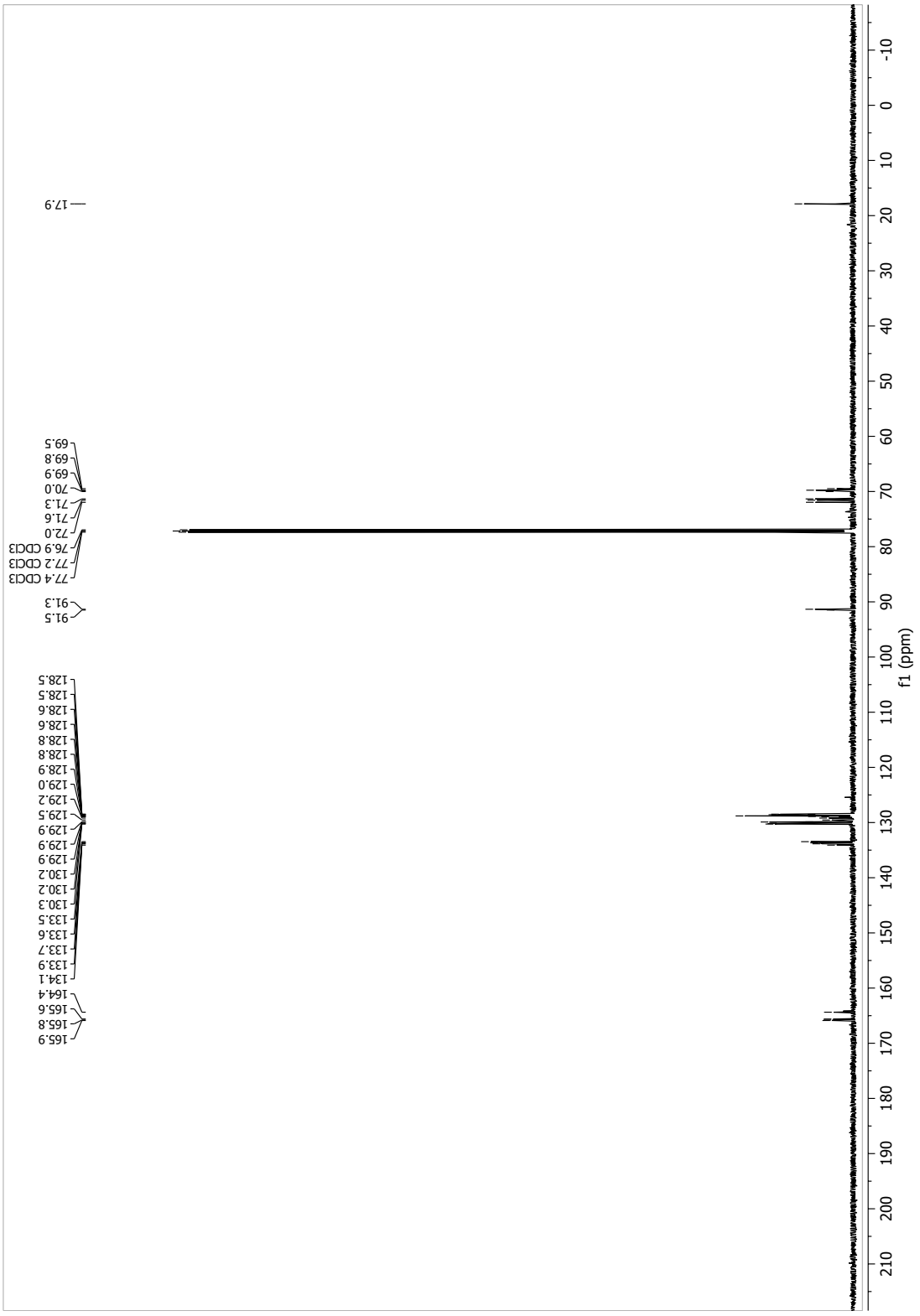
165.9
165.8
165.6
164.4
134.1
133.9
133.7
133.6
133.5
130.3
130.2
129.9
129.9
129.9
129.5
129.2
129.0
128.9
128.8
128.8
128.6
128.6
128.5
128.5
91.5
91.3
77.4 CDCl3
77.2 CDCl3
76.9 CDCl3
72.0
71.6
71.3
70.0
69.9
69.8
69.5
17.9
f1 (ppm)

13.1.2 (3*R*,4*R*,5*S*,6*S*)-2-hydroxy-6-methyltetrahydro-2*H*-pyran-3,4,5-triyl tribenzoate (29)

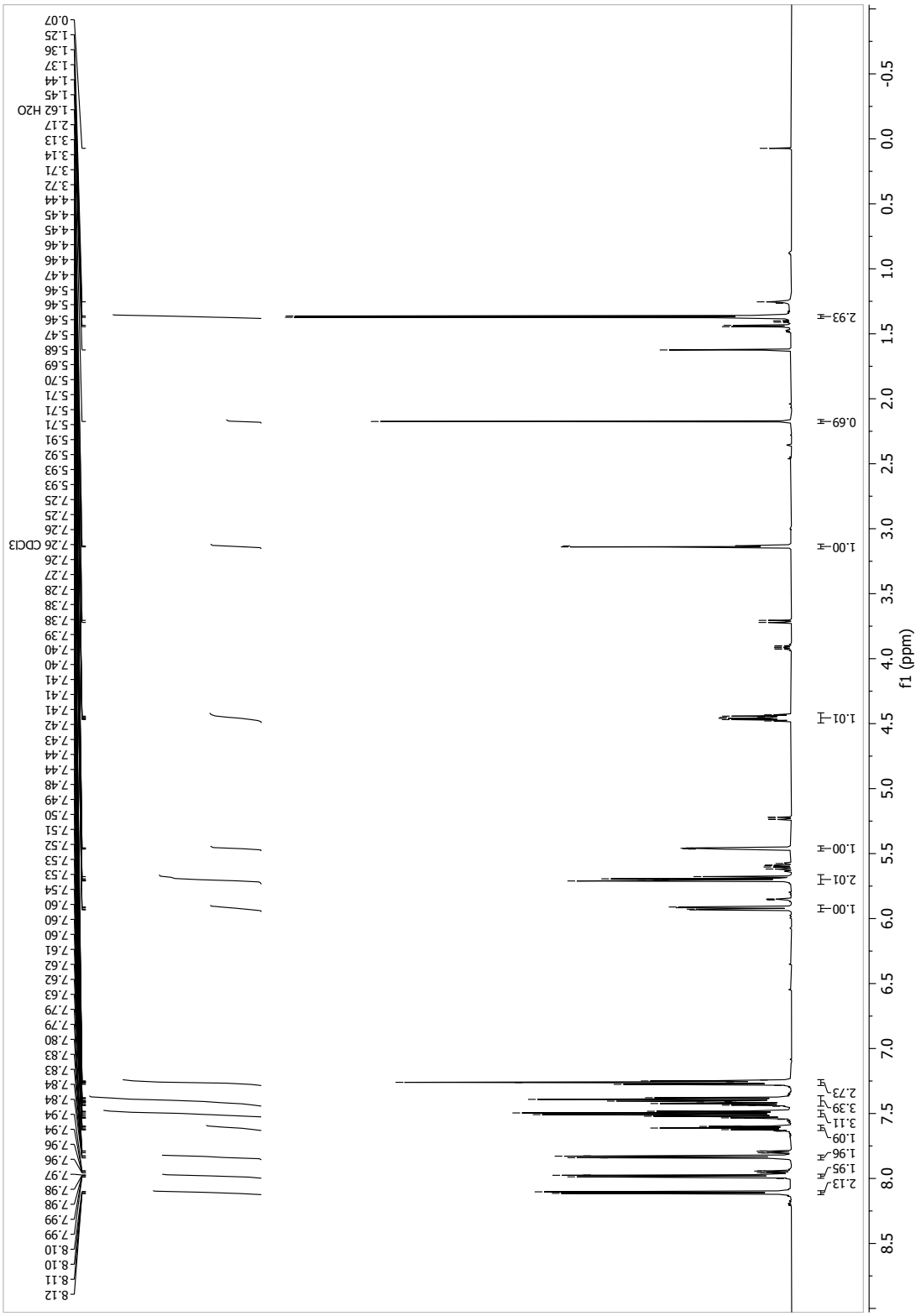

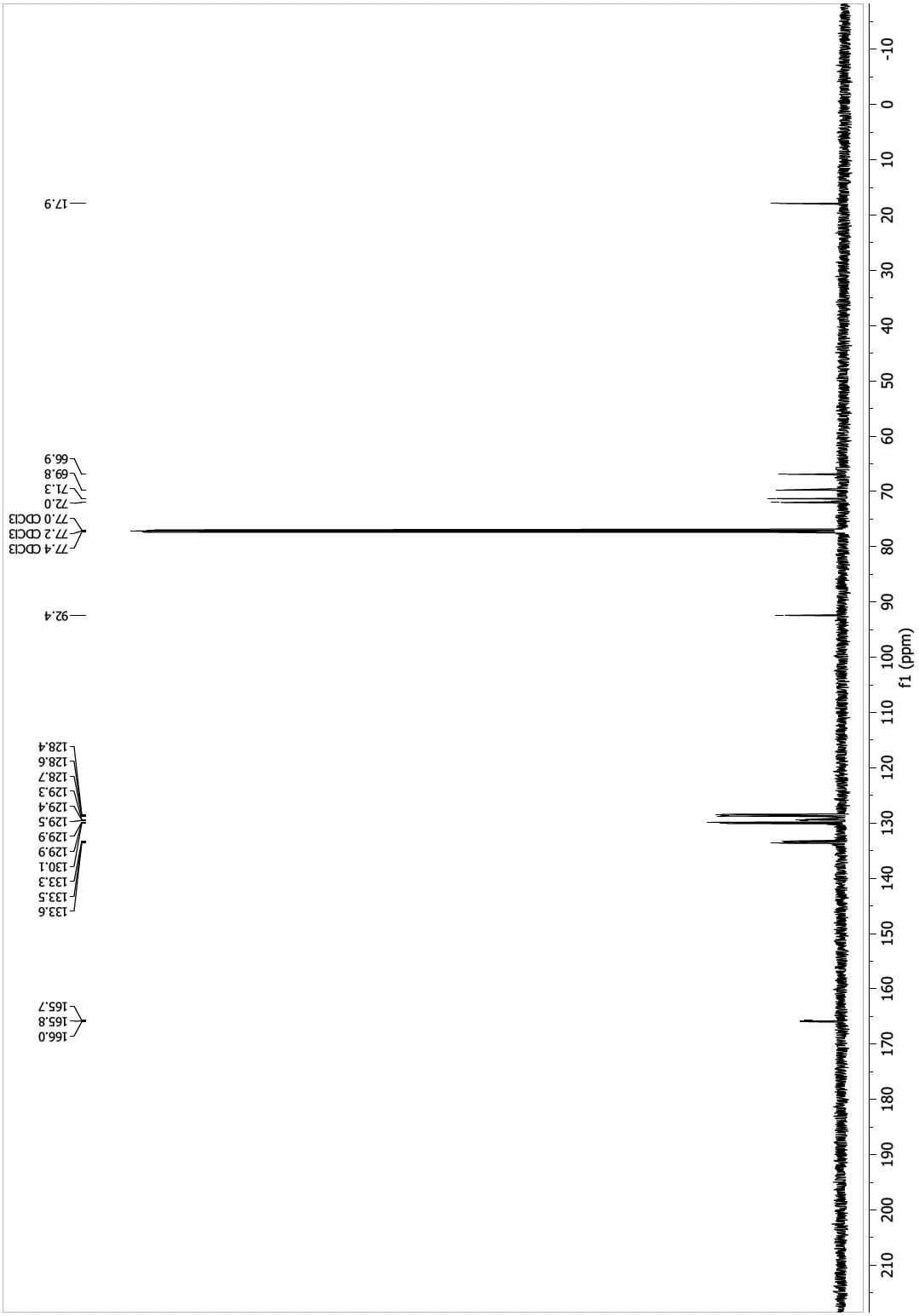
166.0
165.8
165.7
133.6
133.5
133.3
130.1
129.9
129.9
129.5
129.4
129.3
128.7
128.6
128.4
92.4
77.4 CDCl3
77.2 CDCl3
77.0 CDCl3
72.0
71.3
69.8
66.9
17.9
f1 (ppm)

13.1.4 (2*S*,3*S*,4*R*,5*R*)-2-methyl-6-oxotetrahydro-2*H*-pyran-3,4,5-triyl tribenzoate (30)

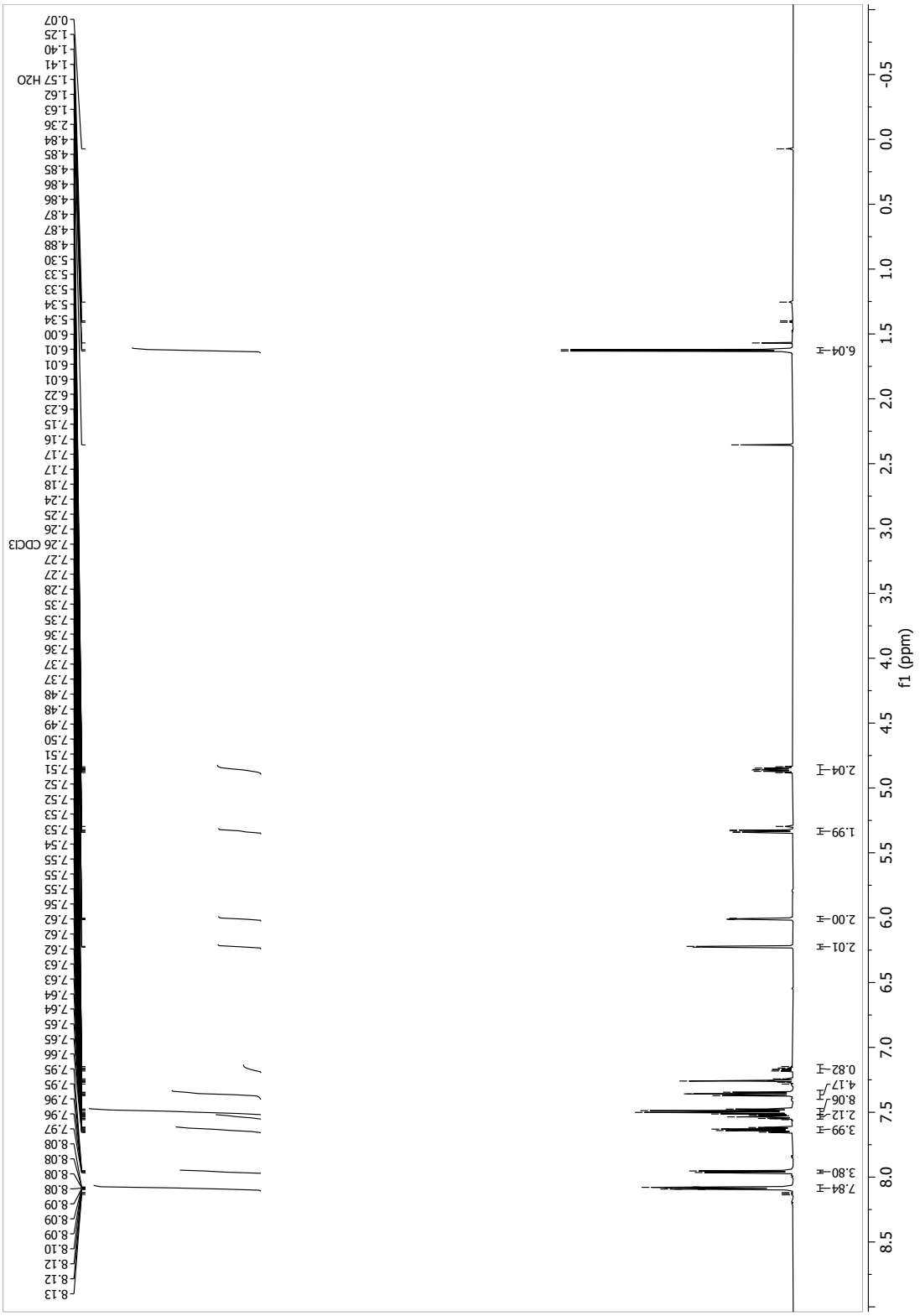

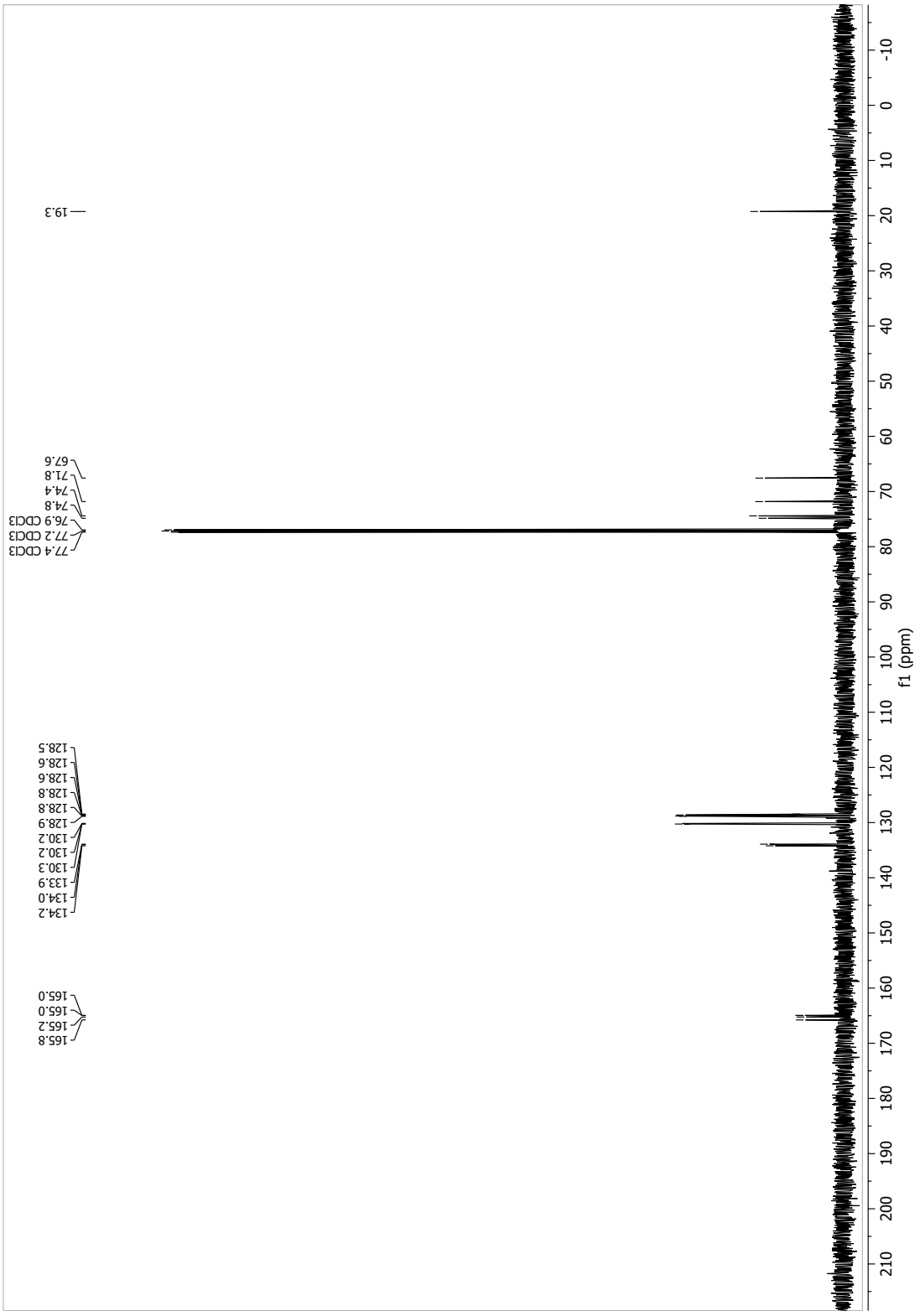
165.8
165.0
165.2
165.0
134.2
134.0
133.9
130.3
130.2
130.2
128.9
128.8
128.8
128.6
128.6
128.5
77.4 CDCl3
77.2 CDCl3
76.9 CDCl3
74.8
74.4
71.8
67.6
19.3
f1 (ppm)

13.1.5 (2*S*,3*R*)-2-methyl-6-oxo-3,6-dihydro-2*H*-pyran-3,5-diyl dibenzoate (31)

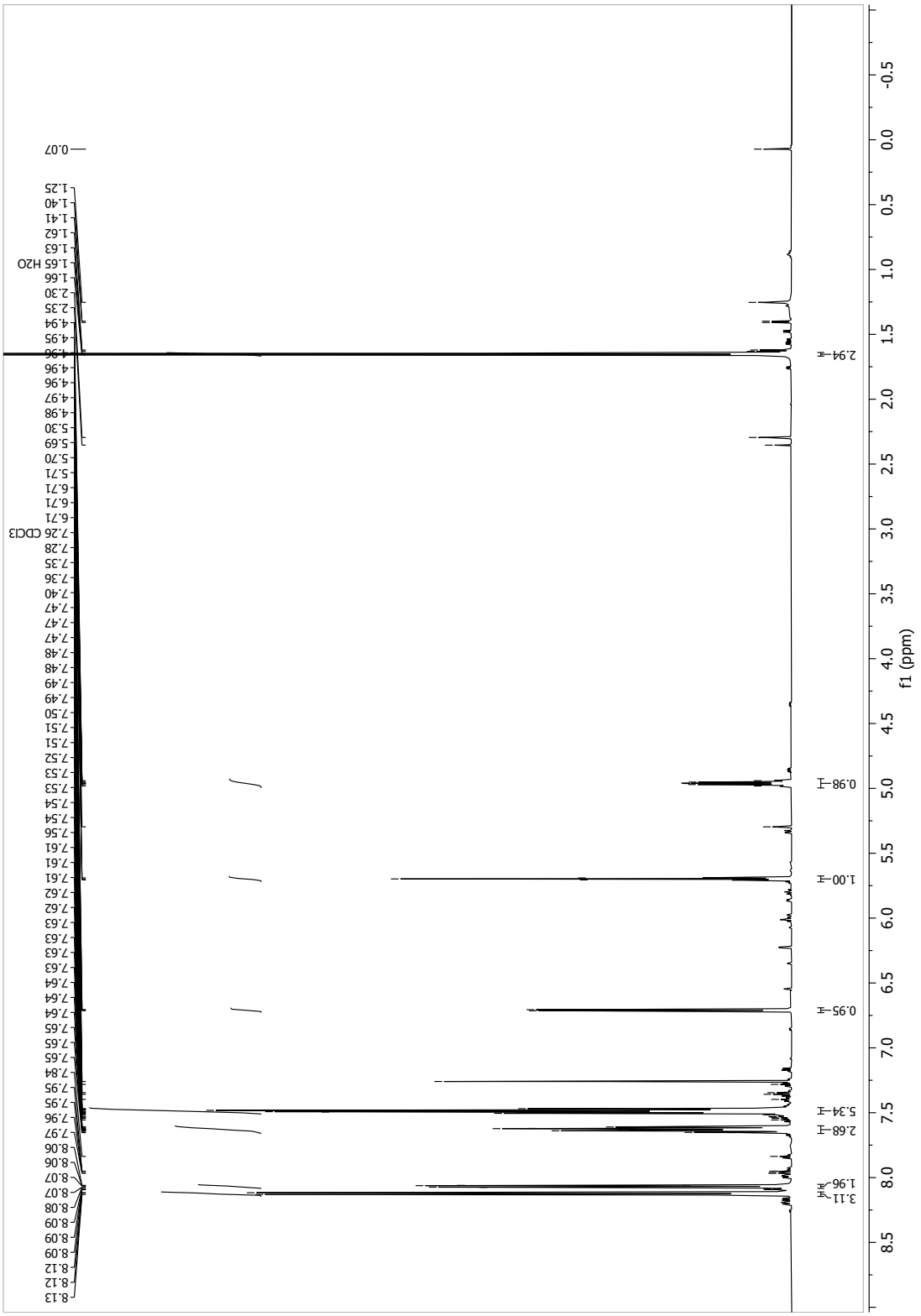

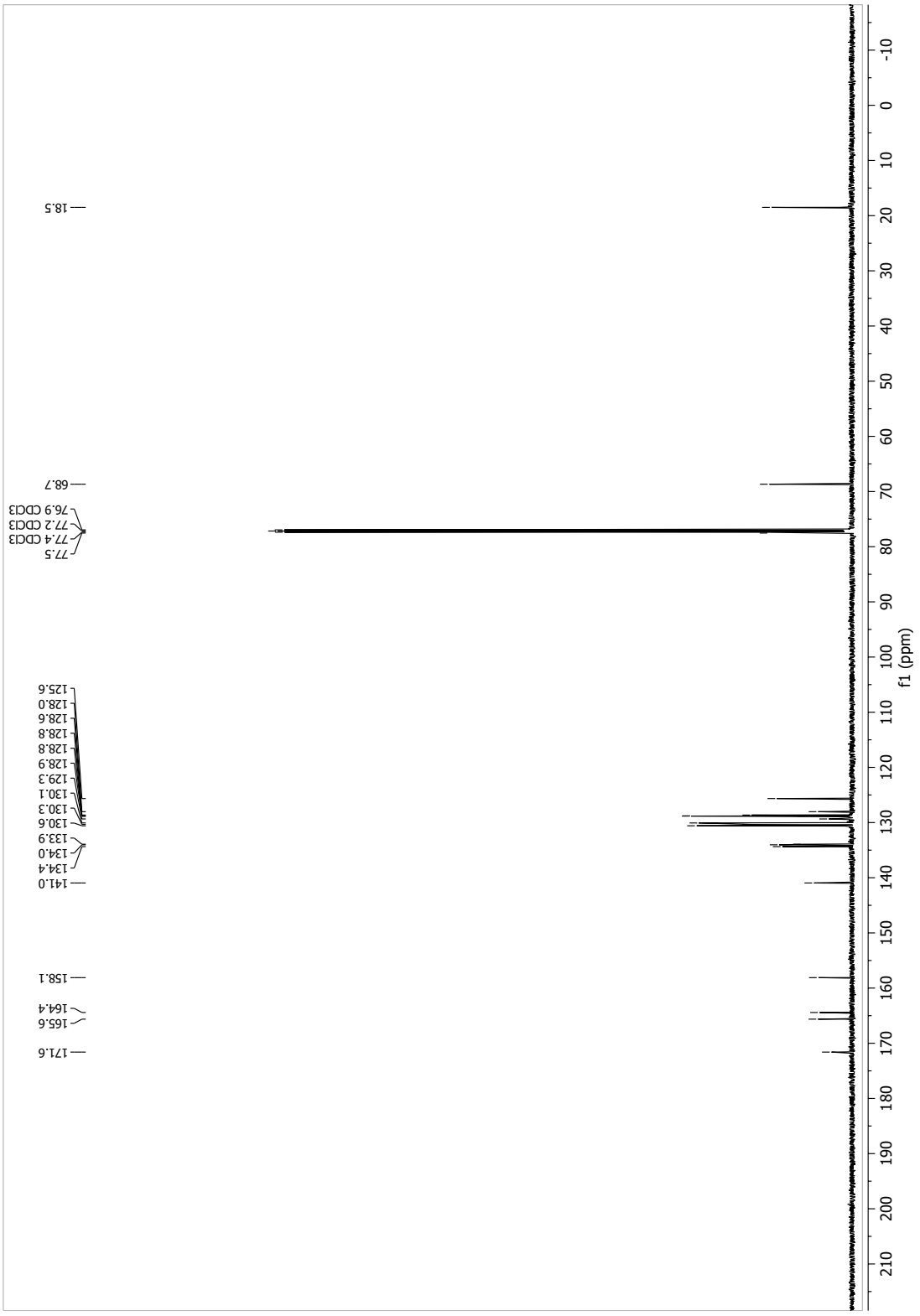
18.5
68.7
77.5
77.4 CDCl3
77.2 CDCl3
76.9 CDCl3
125.6
128.0
128.6
128.8
128.8
128.9
129.3
130.1
130.3
130.6
133.9
134.0
134.4
141.0
158.1
164.4
165.6
171.6
f1 (ppm)

13.1.6 (2*S*,3*R*,5*R*)-2-methyl-6-oxotetrahydro-2*H*-pyran-3,5-diyl dibenzoate (32)

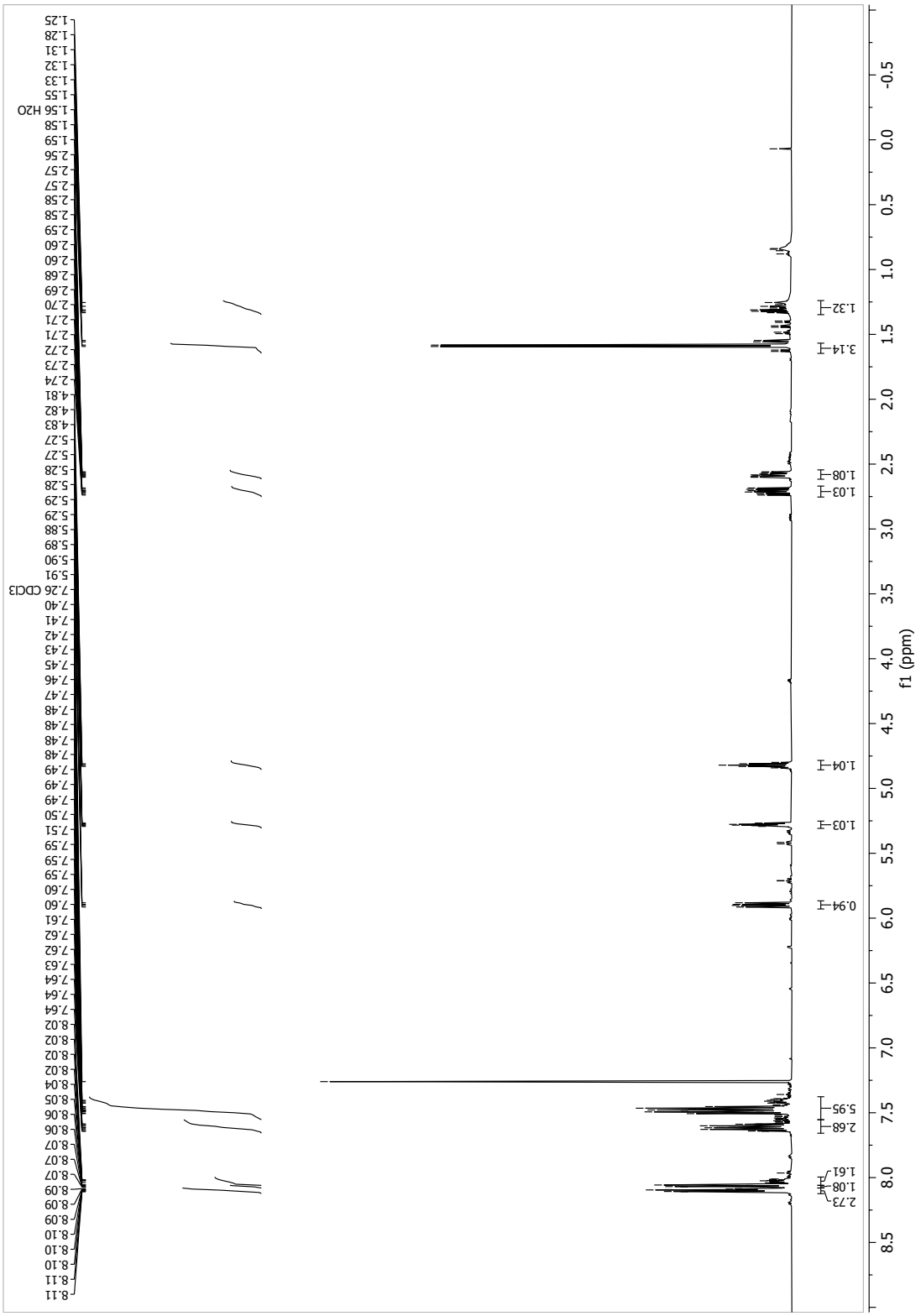

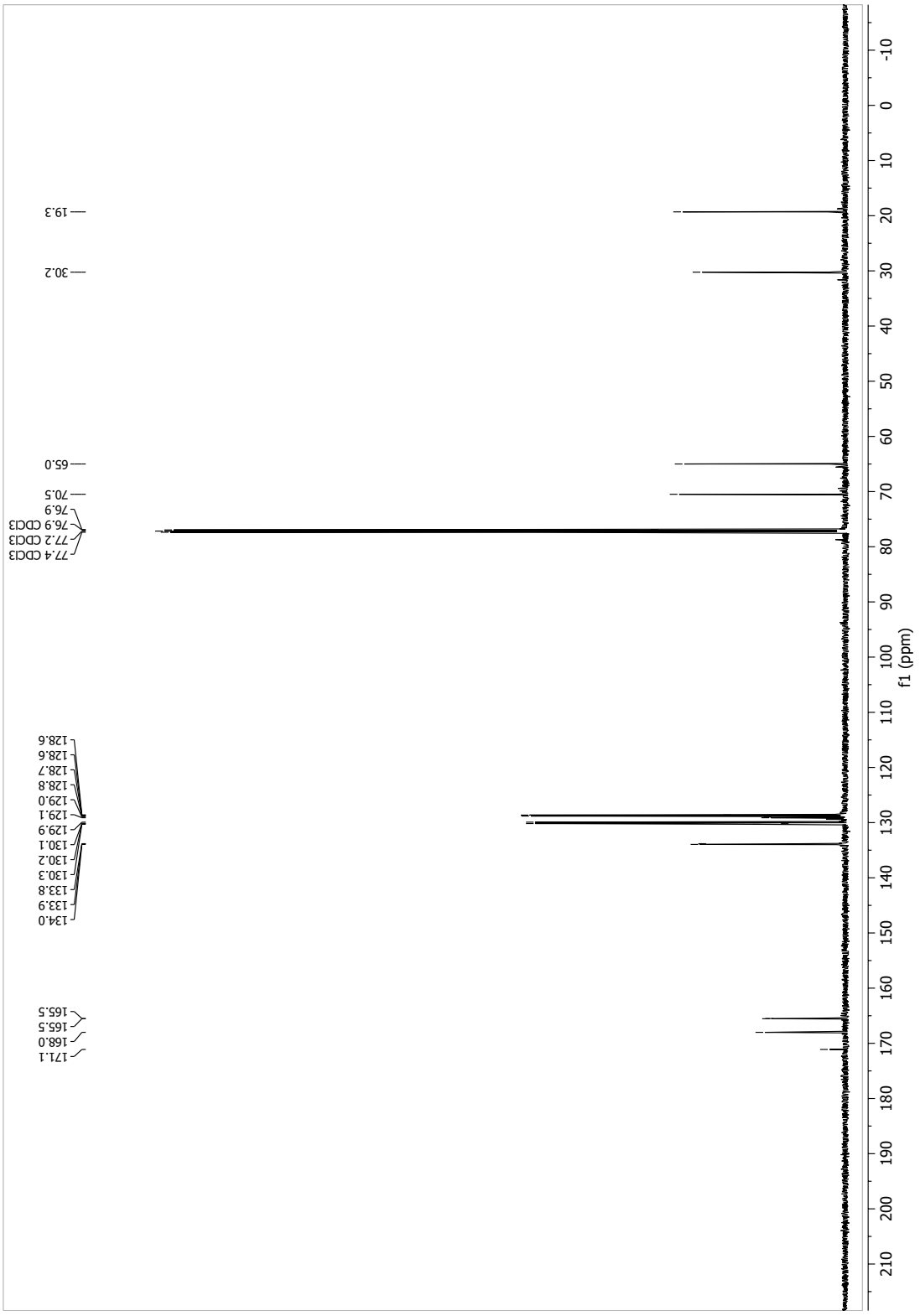
171.1
168.0
165.5
165.5
134.0
133.9
133.8
130.3
130.2
130.1
129.9
129.1
129.0
128.8
128.7
128.6
128.6
77.4 CDCl3
77.2 CDCl3
76.9 CDCl3
76.9
70.5
65.0
30.2
19.3
f1 (ppm)

13.1.7 (2*R*,3*R*,5*R*,6*S*)-2-hydroxy-6-methyltetrahydro-2*H*-pyran-3,5-diyl dibenzoate (19)

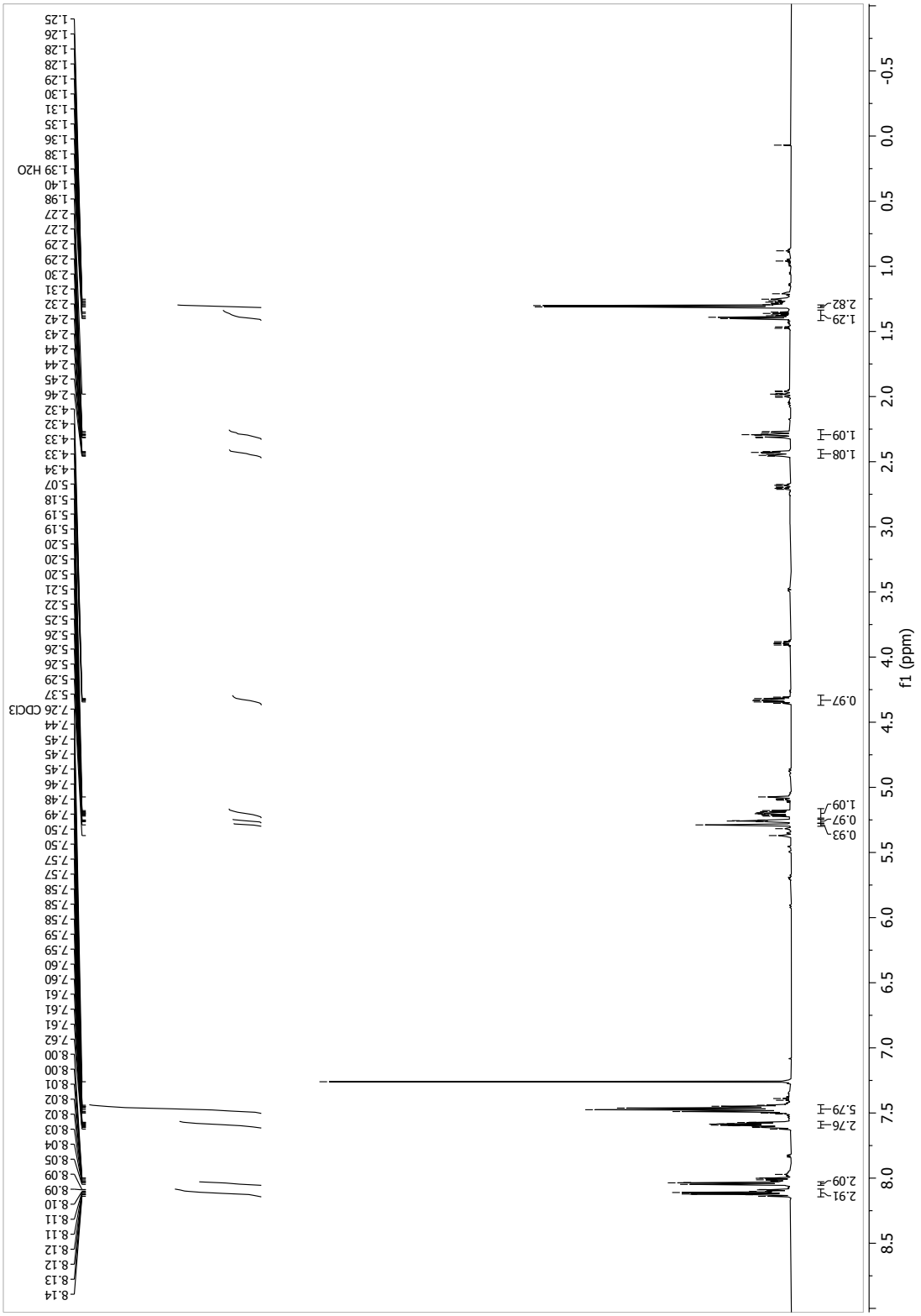

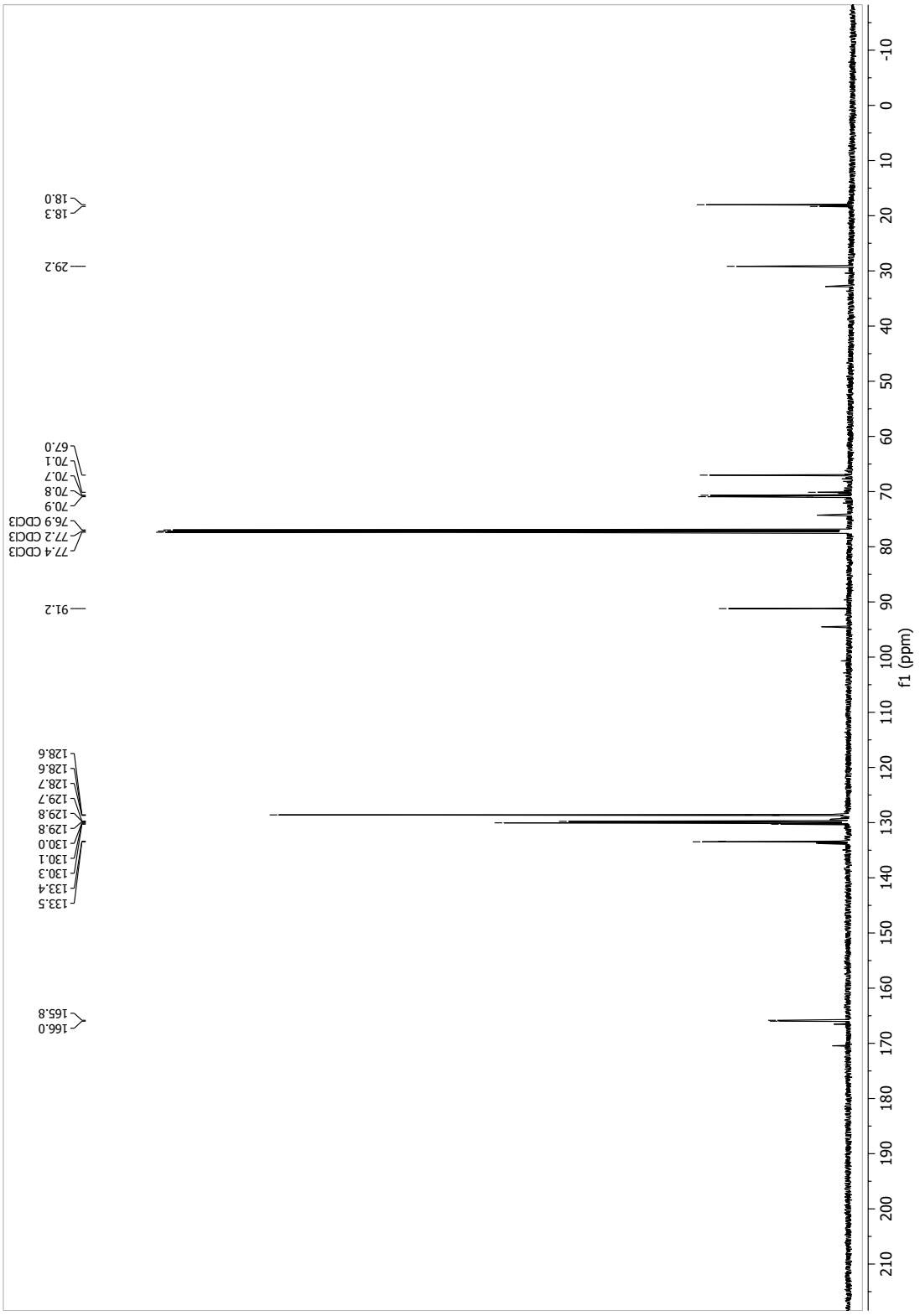
166.0
165.8
133.5
133.4
130.3
130.1
130.0
129.8
129.8
129.7
128.7
128.6
128.6
91.2
77.4 CDCl3
77.2 CDCl3
76.9 CDCl3
70.9
70.8
70.7
70.1
67.0
29.2
18.3
18.0
f1 (ppm)

13.1.8 *Tert*-butyl (*S*)-3-acetoxypent-4-enoate (96)

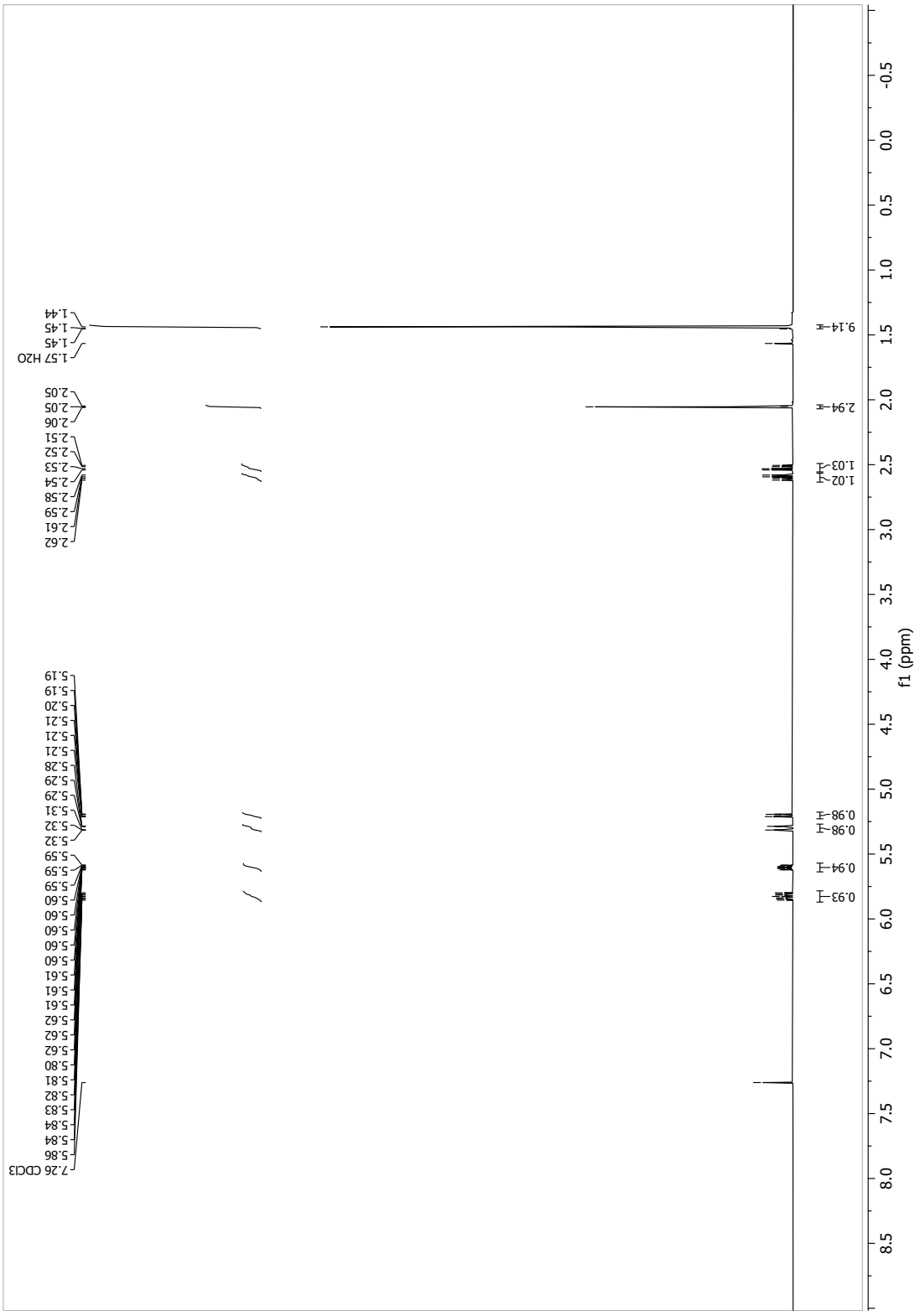

13.1.9 *Tert*-butyl (*R*)-3-hydroxypent-4-enoate (93)

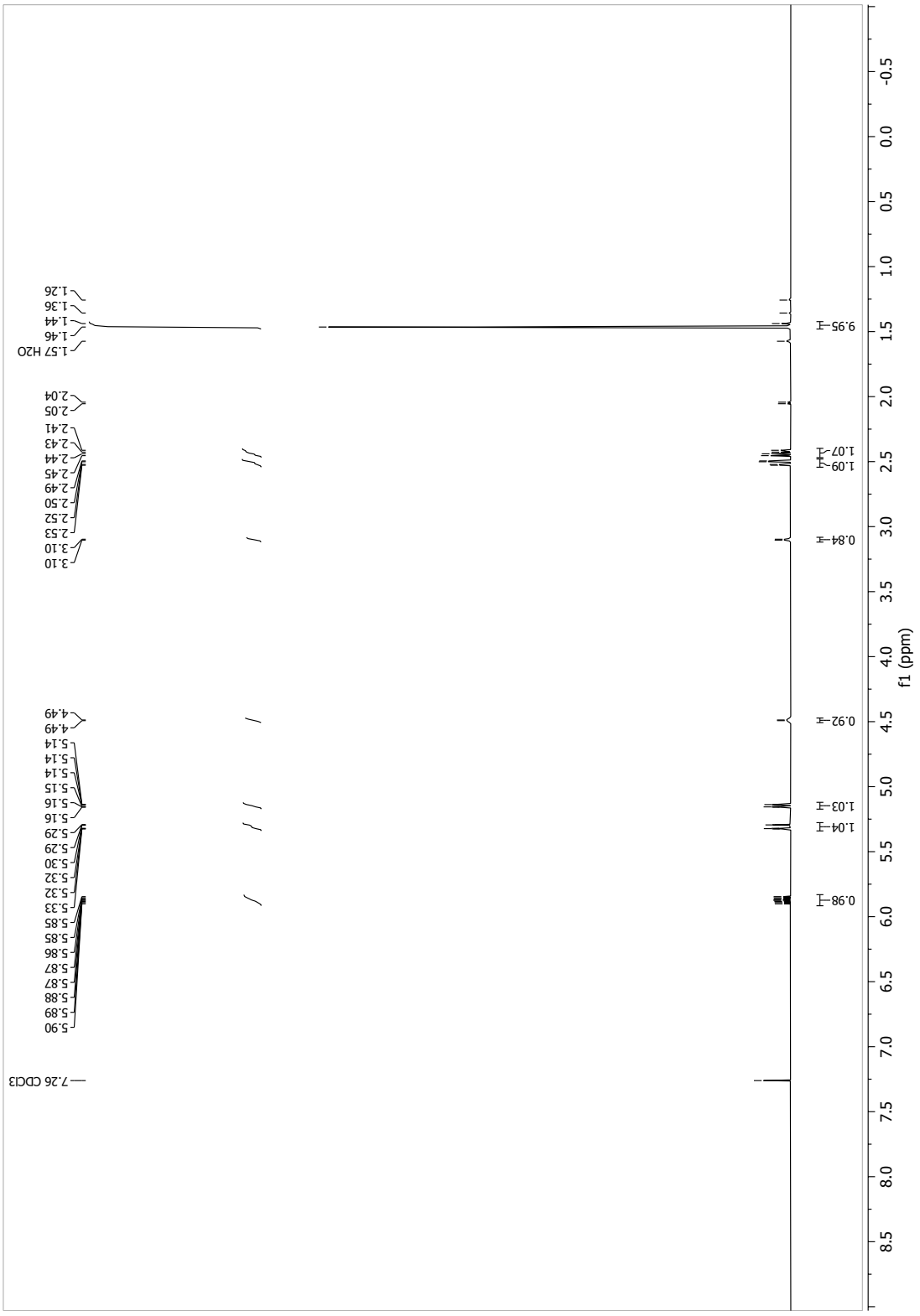

13.1.10 1-Bromohenicosane (35)

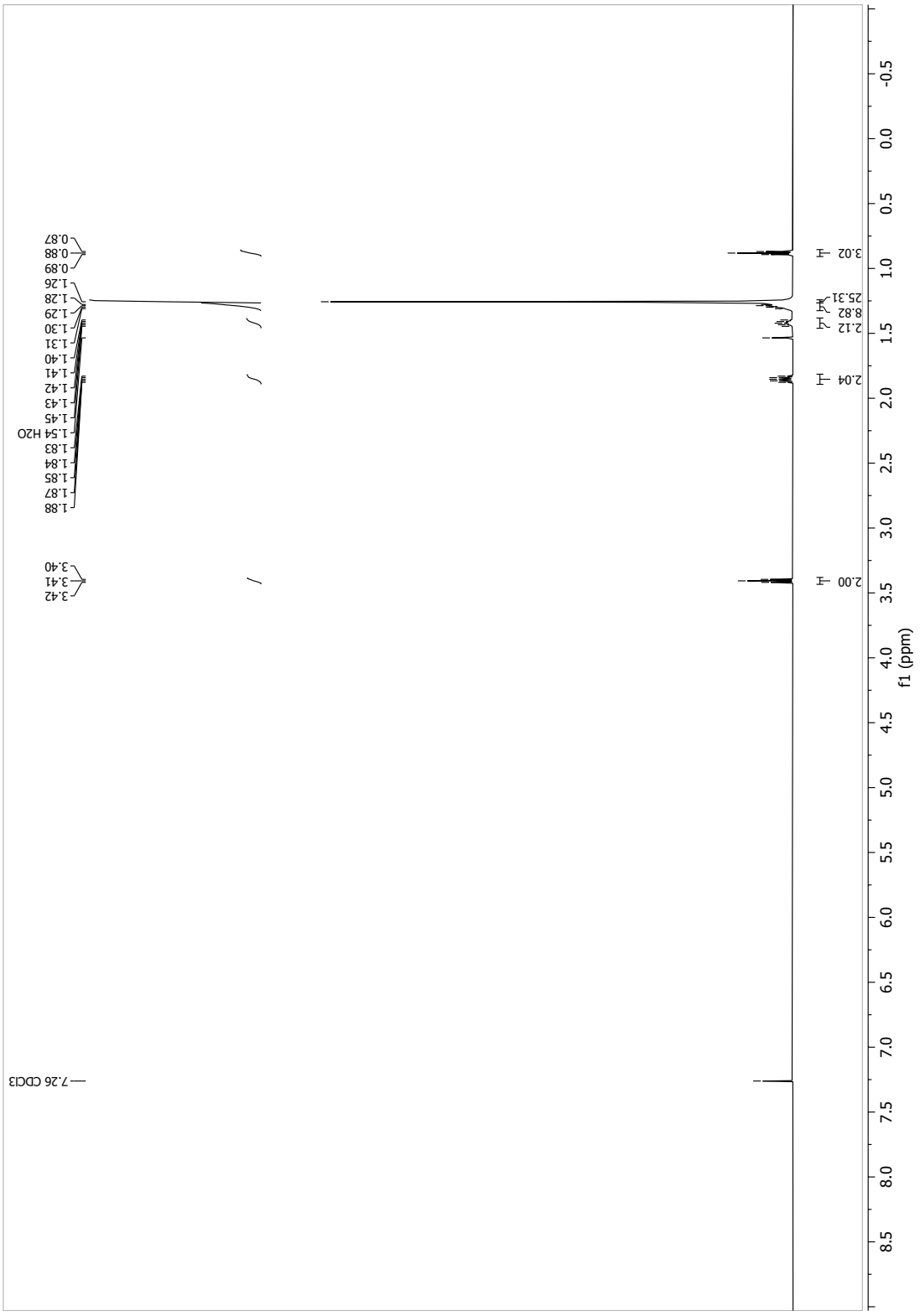

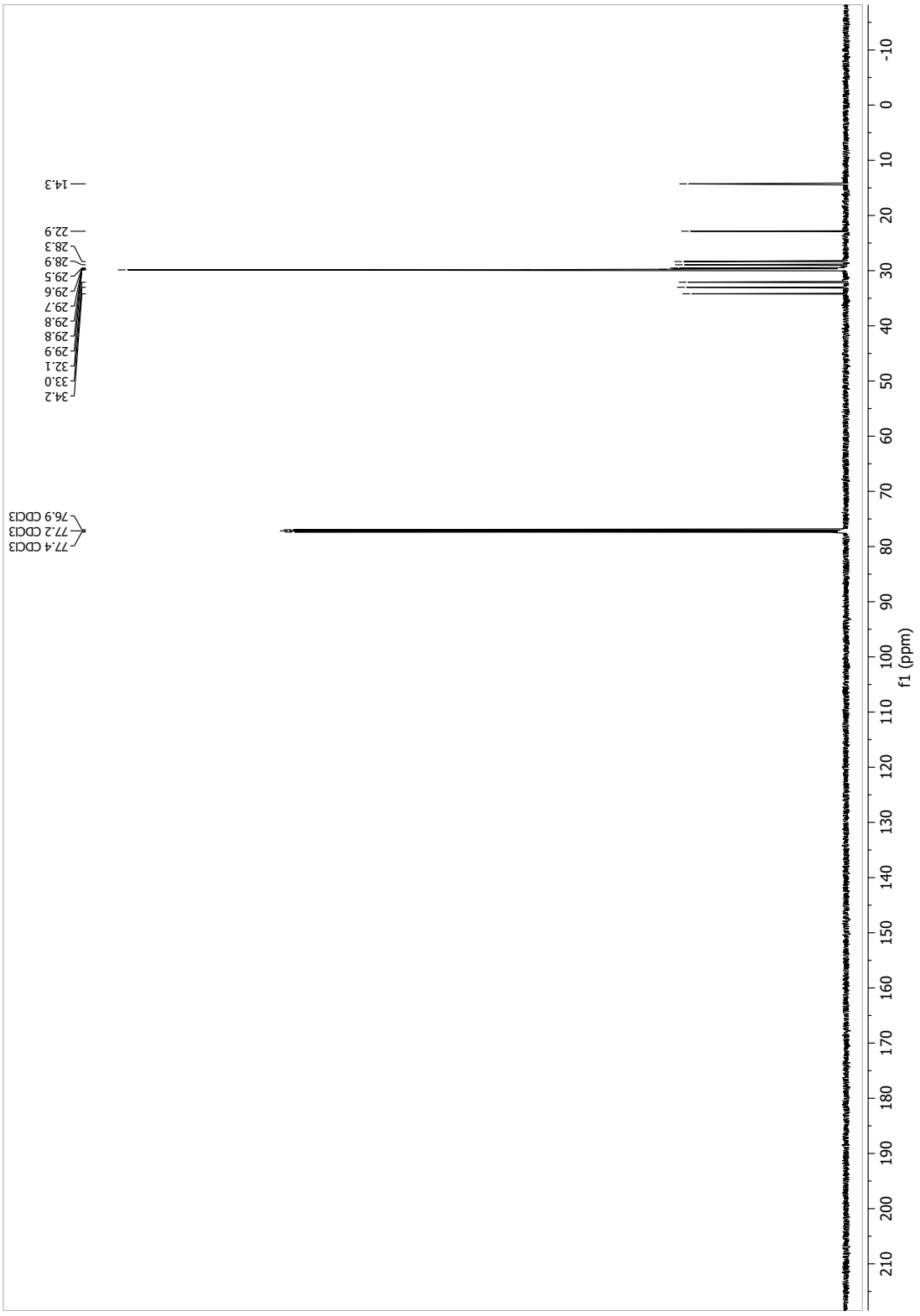
14.3
22.9
28.3
28.9
29.5
29.6
29.7
29.8
29.8
29.9
32.1
33.0
34.2
77.4 CDCl3
77.2 CDCl3
76.9 CDCl3
f1 (ppm)

13.1.11 (*R*)-(but-3-yn-2-yloxy)(*tert*-butyl)dimethylsilane (38)

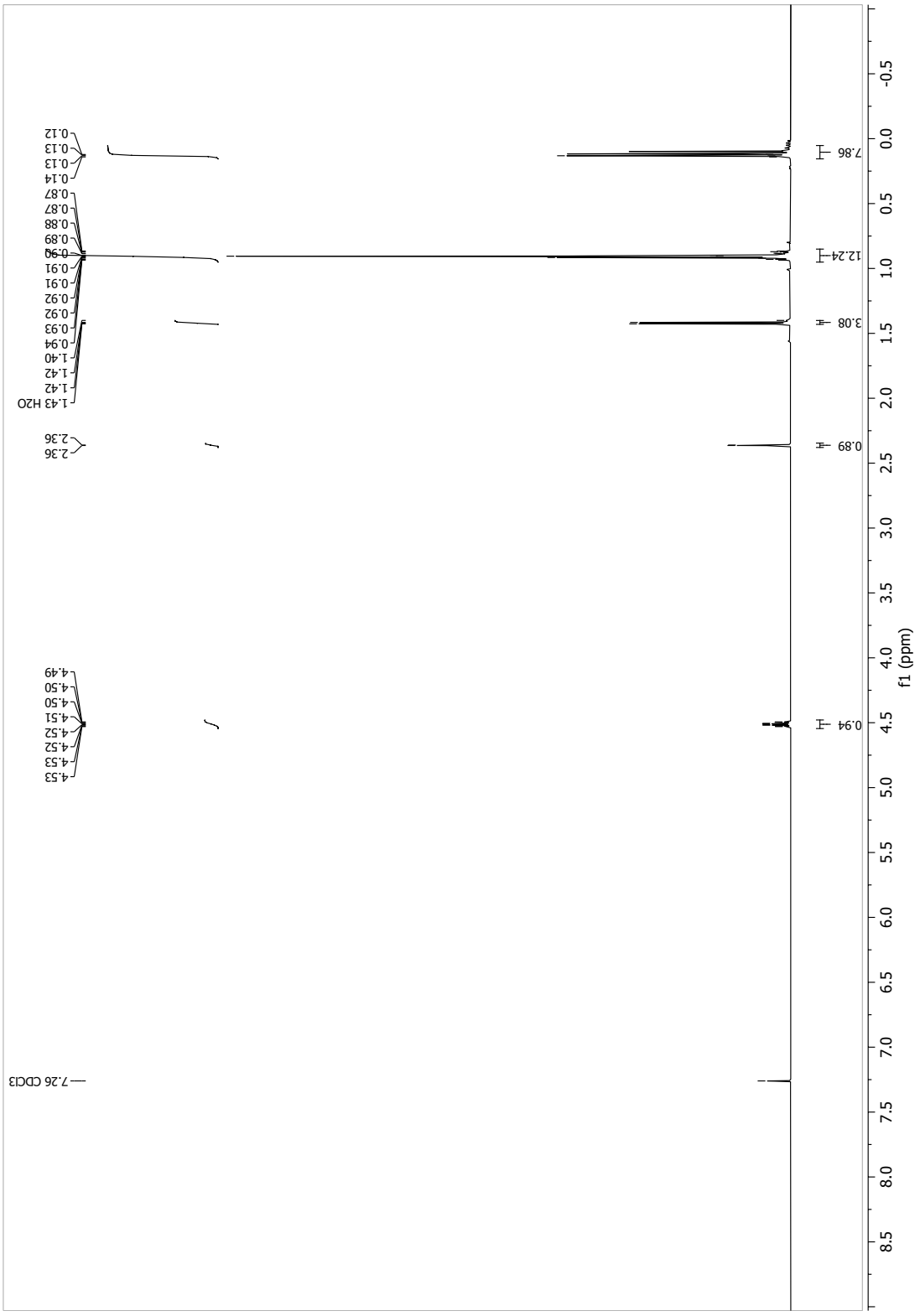

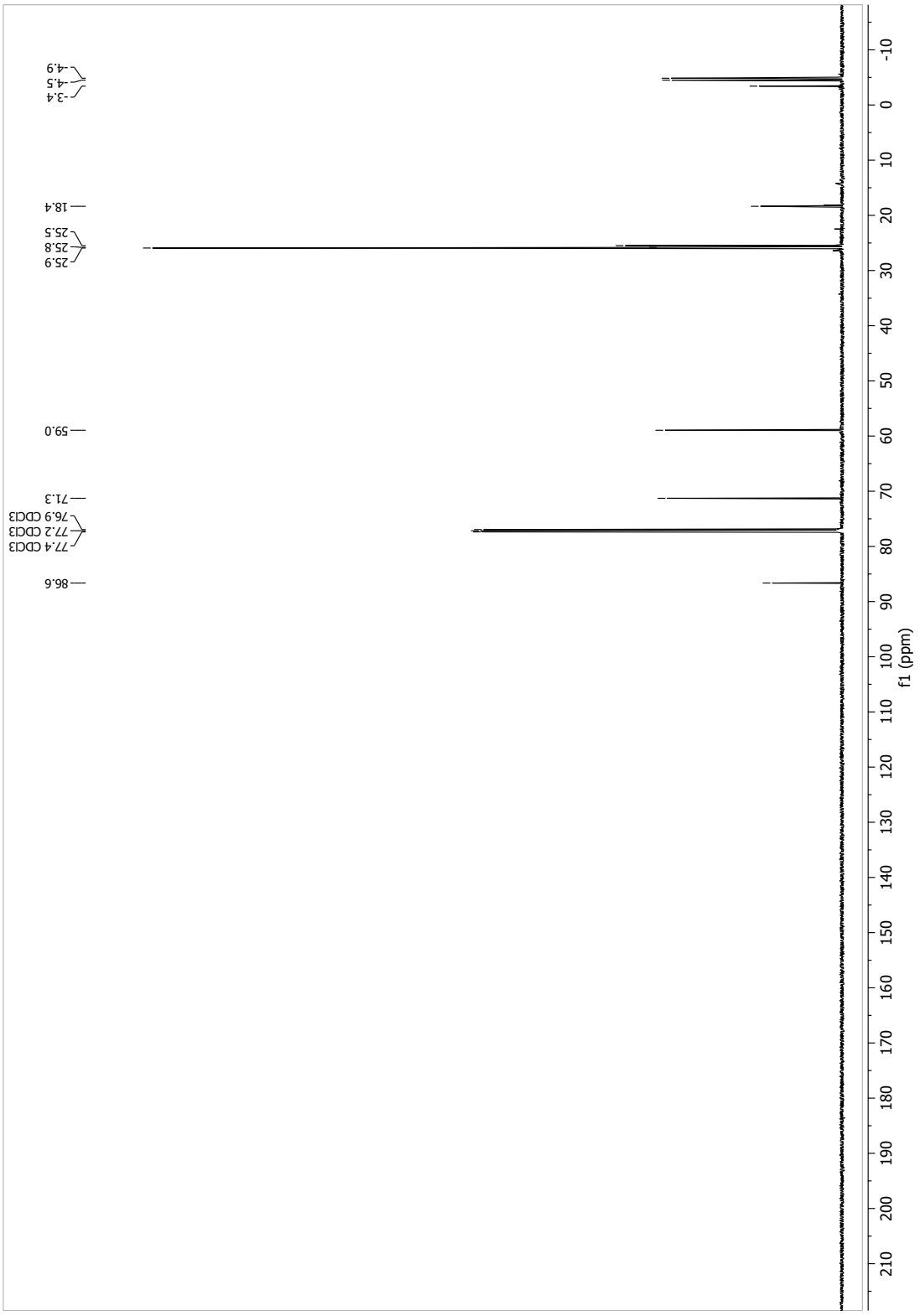
-4.9
-4.5
-3.4
18.4
25.9
25.8
25.5
59.0
71.3
76.9 CDCl3
77.2 CDCl3
77.4 CDCl3
86.6
f1 (ppm)

13.1.12 (*R*)-*tert*-butyldimethyl(pentacos-3-yn-2-yloxy)silane (37)

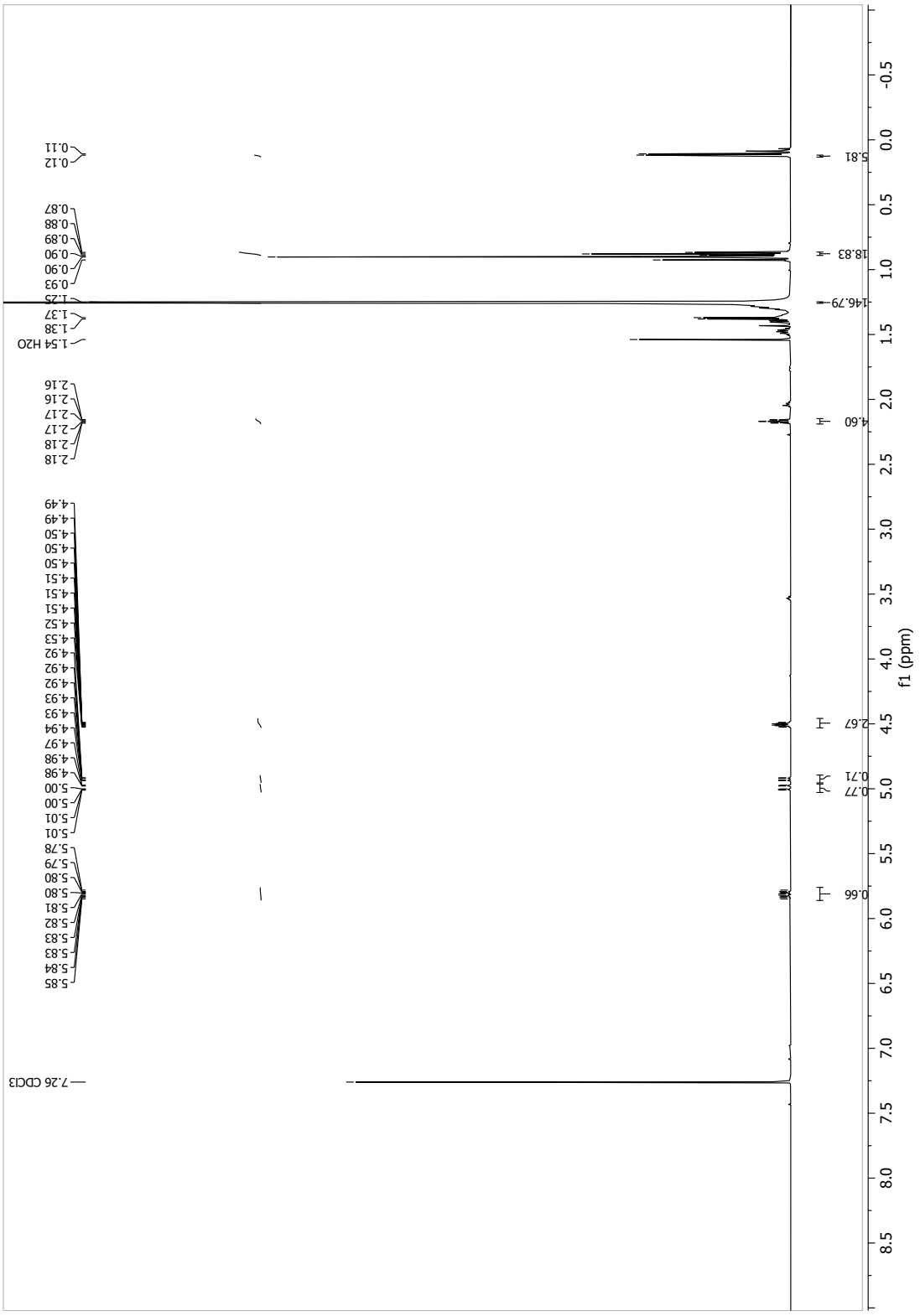

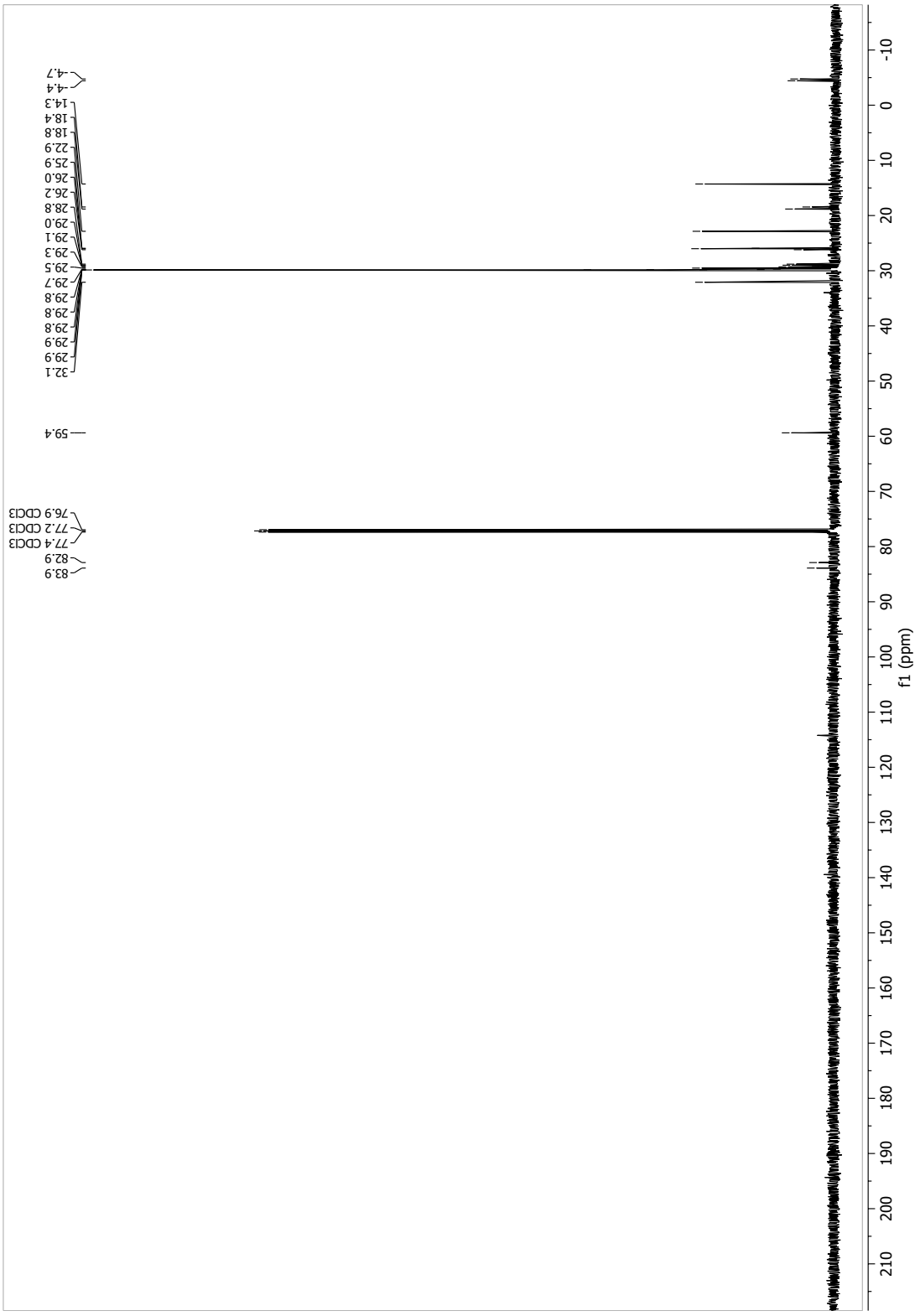
83.9
82.9
77.4 CDCl3
77.2 CDCl3
76.9 CDCl3
59.4
32.1
29.9
29.9
29.8
29.8
29.8
29.7
29.5
29.3
29.1
29.0
28.8
26.2
26.0
25.9
22.9
18.8
18.4
14.3
-4.4
-4.7
f1 (ppm)

13.1.14 (*R*)-*tert*-butyldimethyl(pentacosan-2-yloxy)silane (39a)

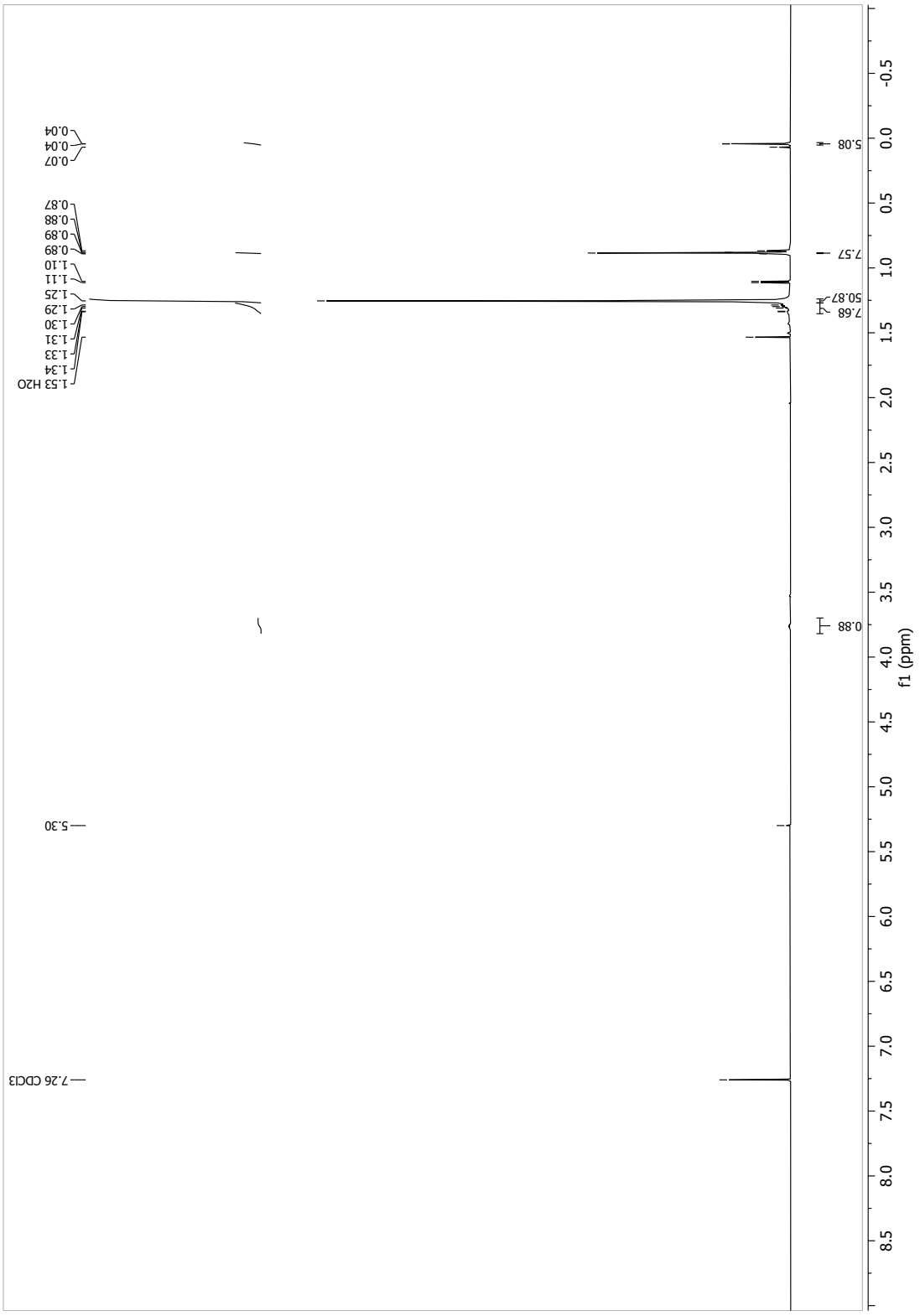

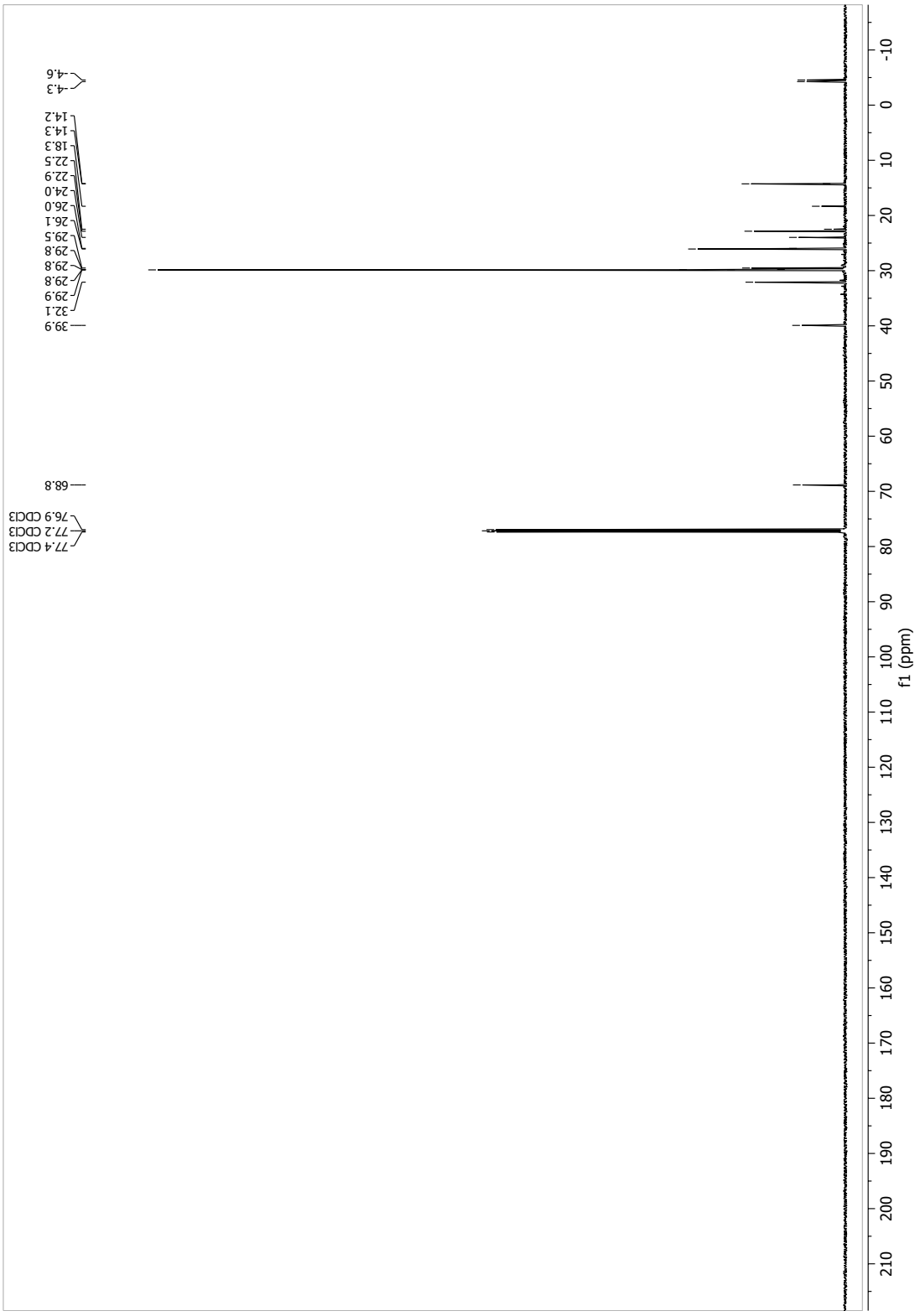
77.4 CDCl3
77.2 CDCl3
76.9 CDCl3
68.8
39.9
32.1
29.9
29.8
29.8
29.8
29.5
26.1
26.0
24.0
22.9
22.5
18.3
14.3
14.2
-4.3
-4.6
f1 (ppm)

13.1.16 [D_4]-(*R*)-*tert*-butyldimethyl(pentacosan-2-yloxy)silane (39b)

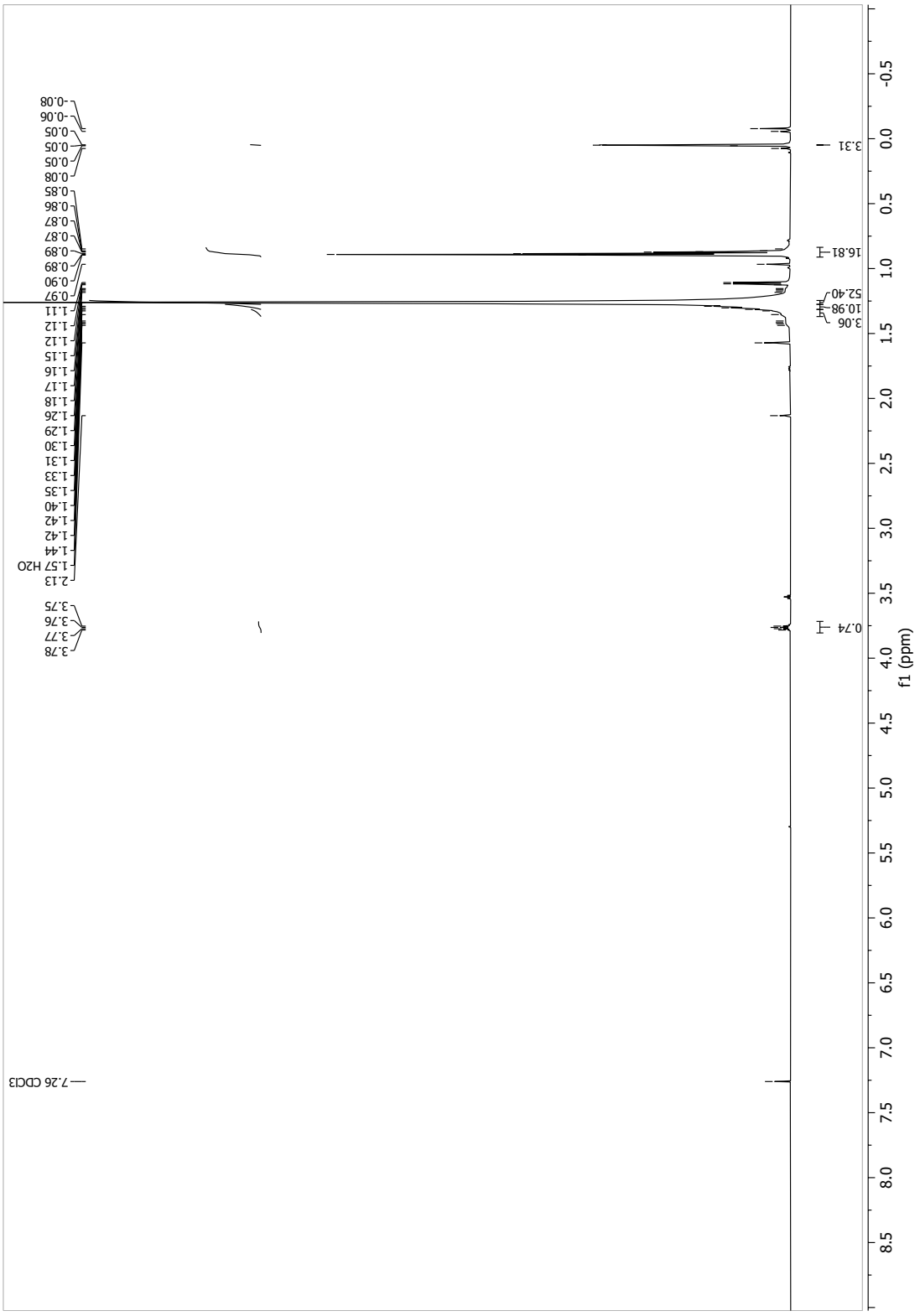

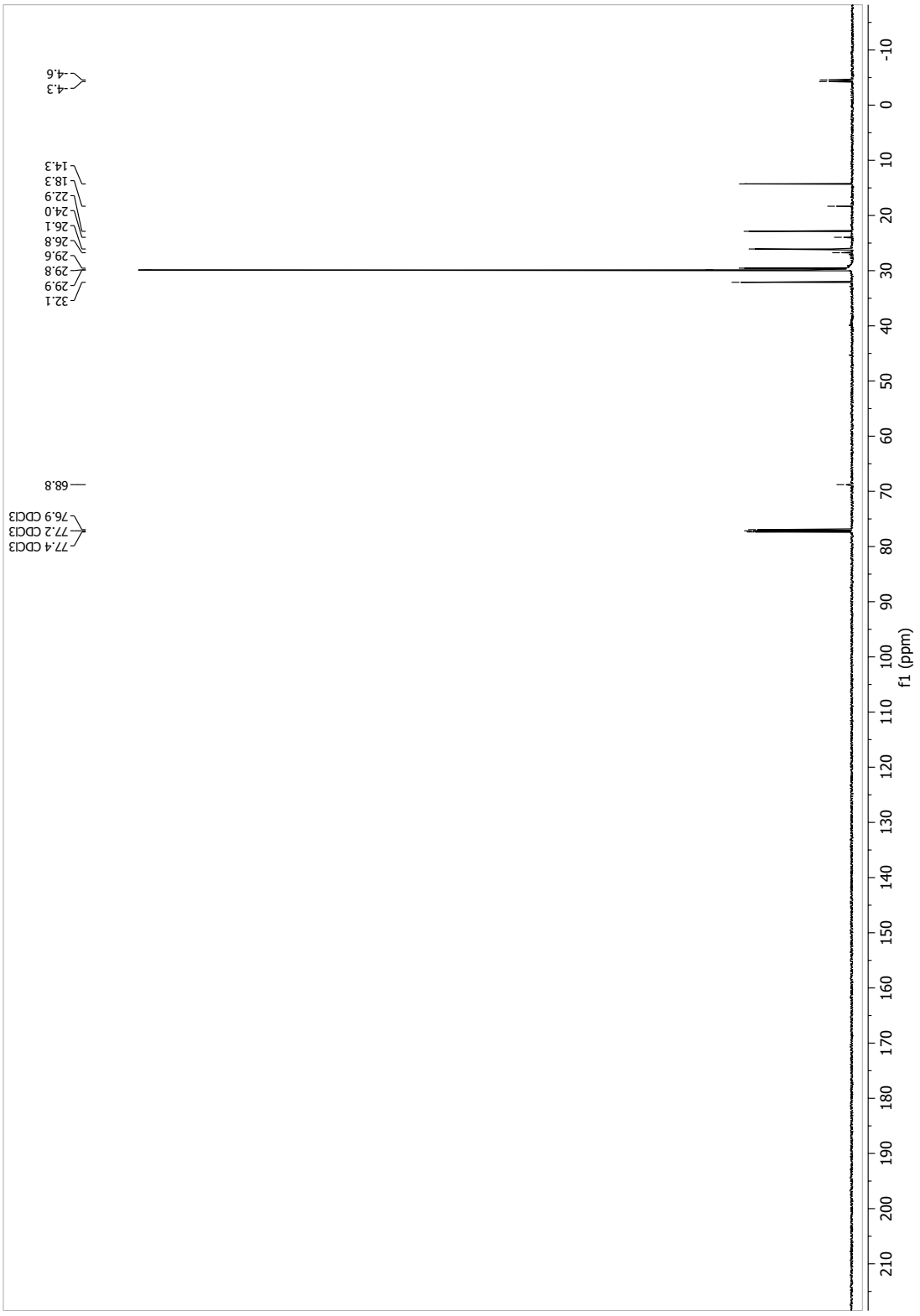
77.4 CDCl3
77.2 CDCl3
76.9 CDCl3
68.8
32.1
29.9
29.8
29.6
26.8
26.1
24.0
22.9
18.3
14.3
-4.3
-4.6
f1 (ppm)

13.1.18 (*R*)-pentacosan-2-ol (34a)

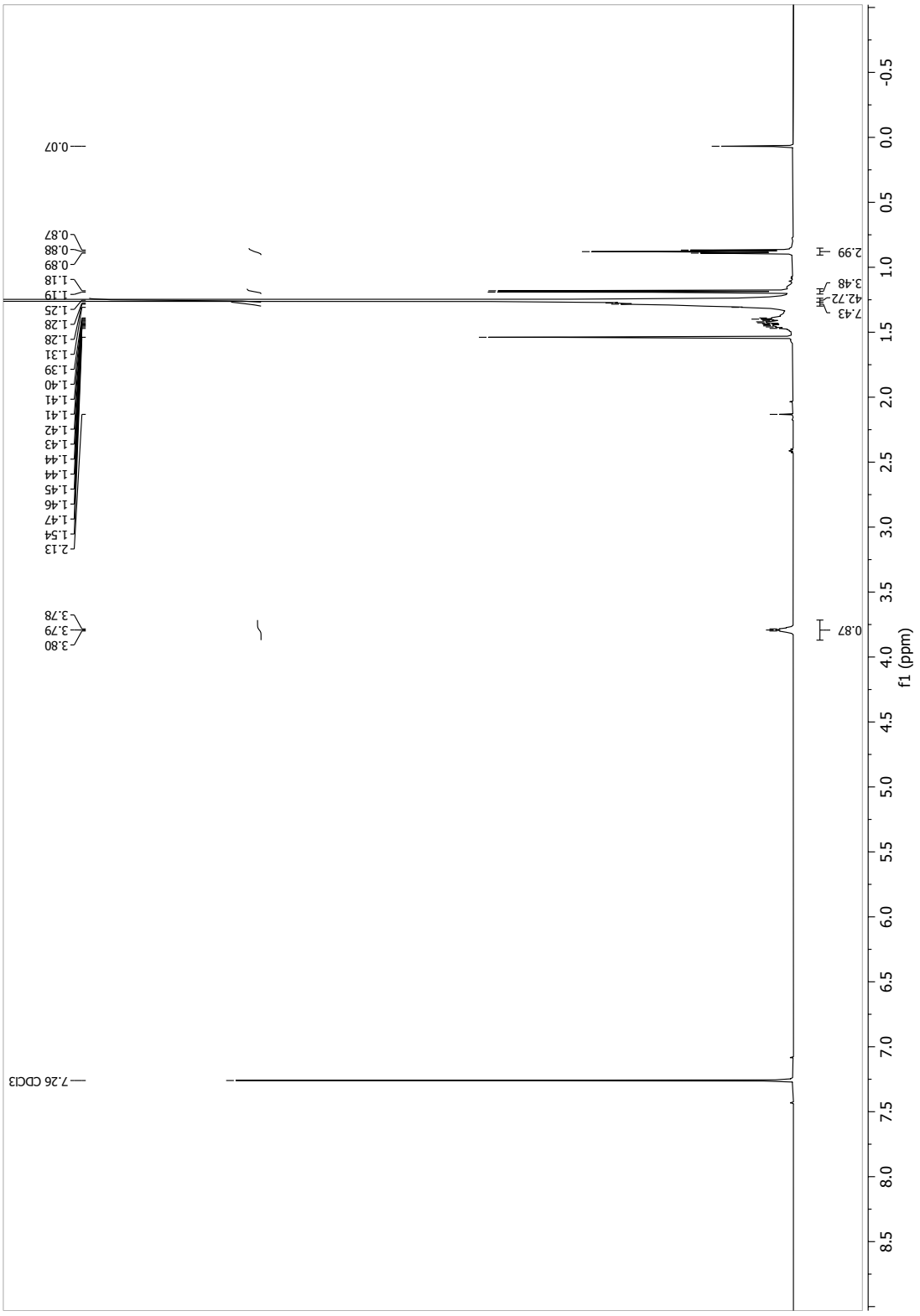

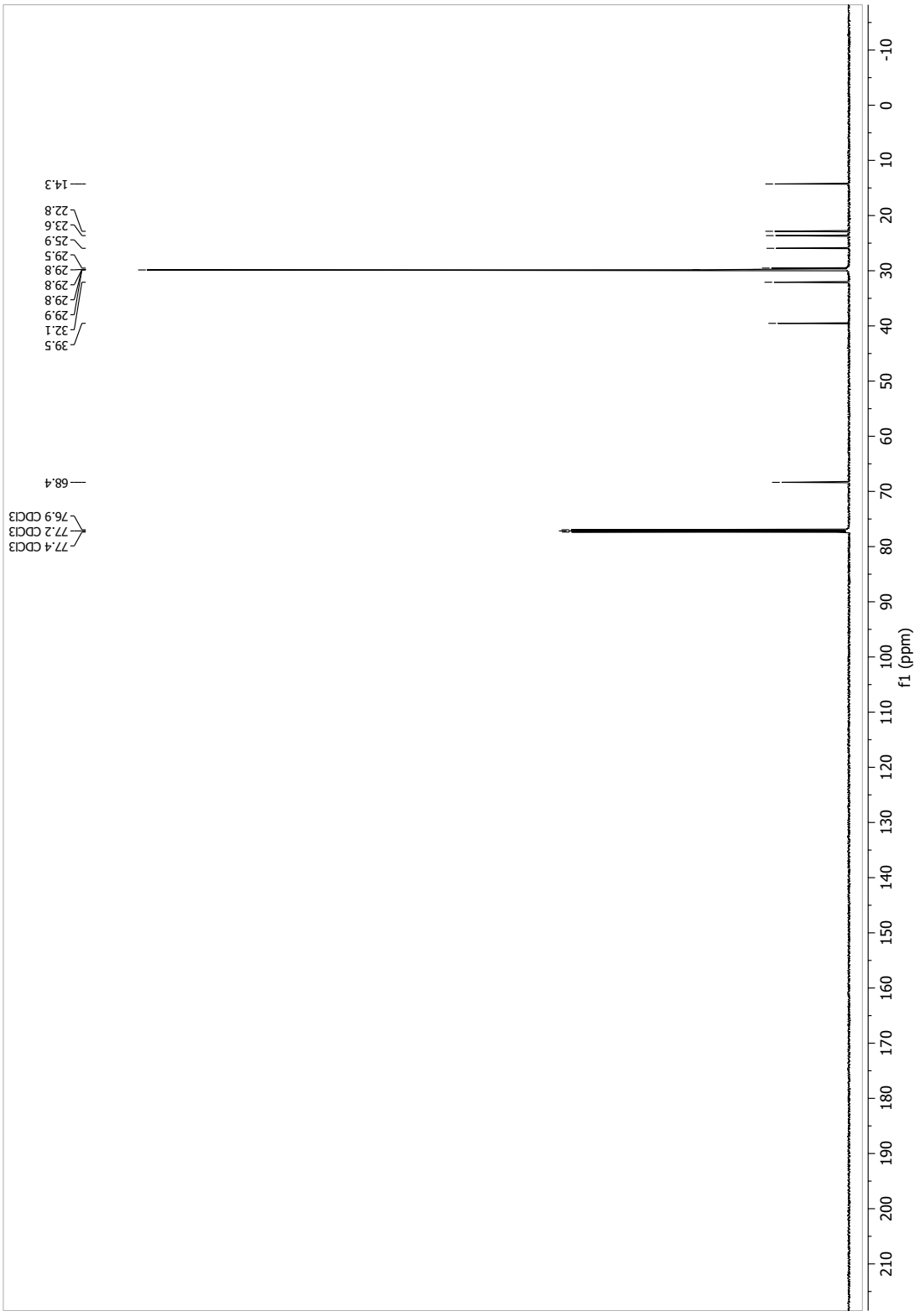
77.4 CDCl3
77.2 CDCl3
76.9 CDCl3
68.4
39.5
32.1
29.9
29.8
29.8
29.5
25.9
23.6
22.8
14.3
f1 (ppm)

13.1.19 [D_4]-(*R*)-pentacosan-2-ol (34b)

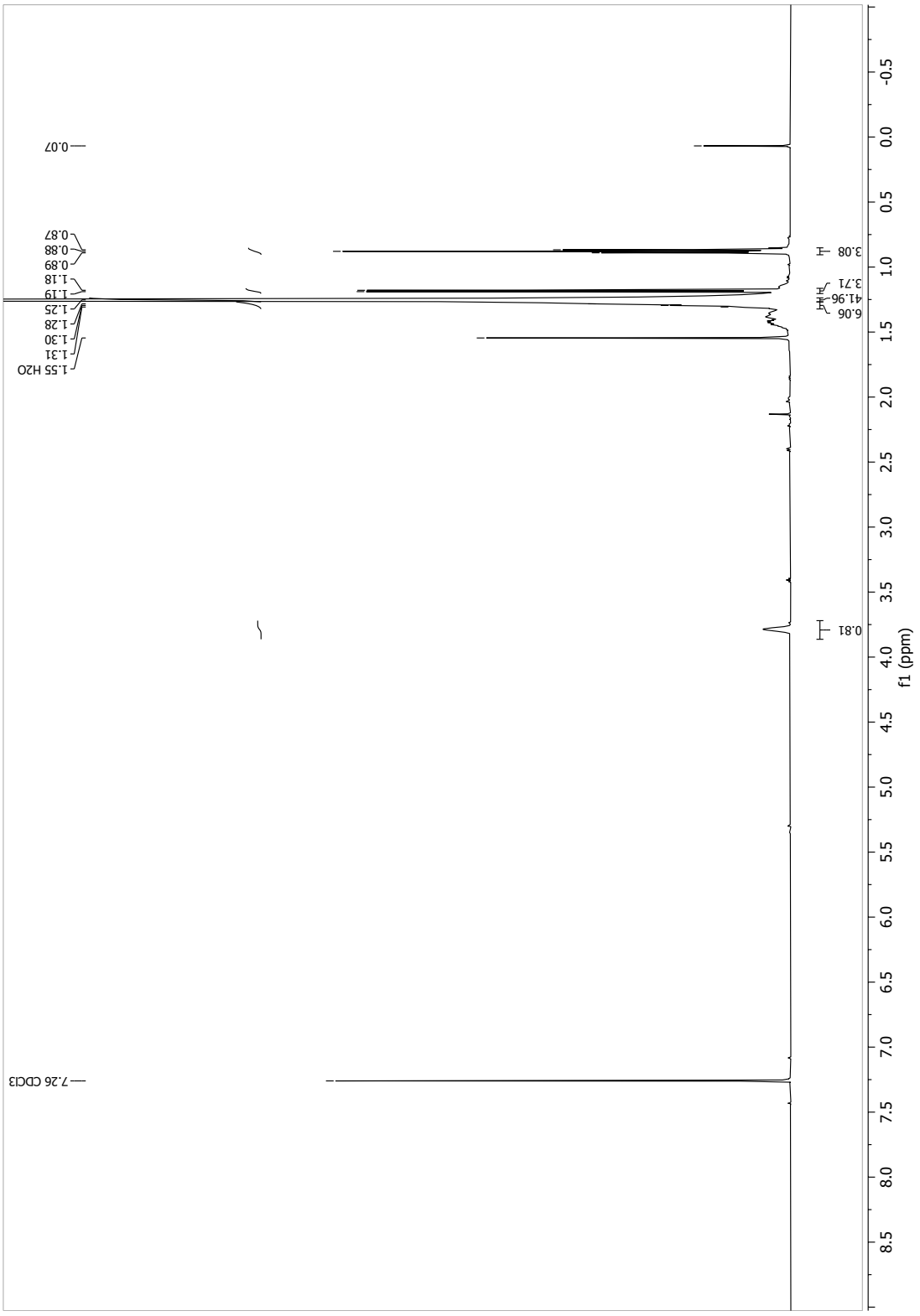

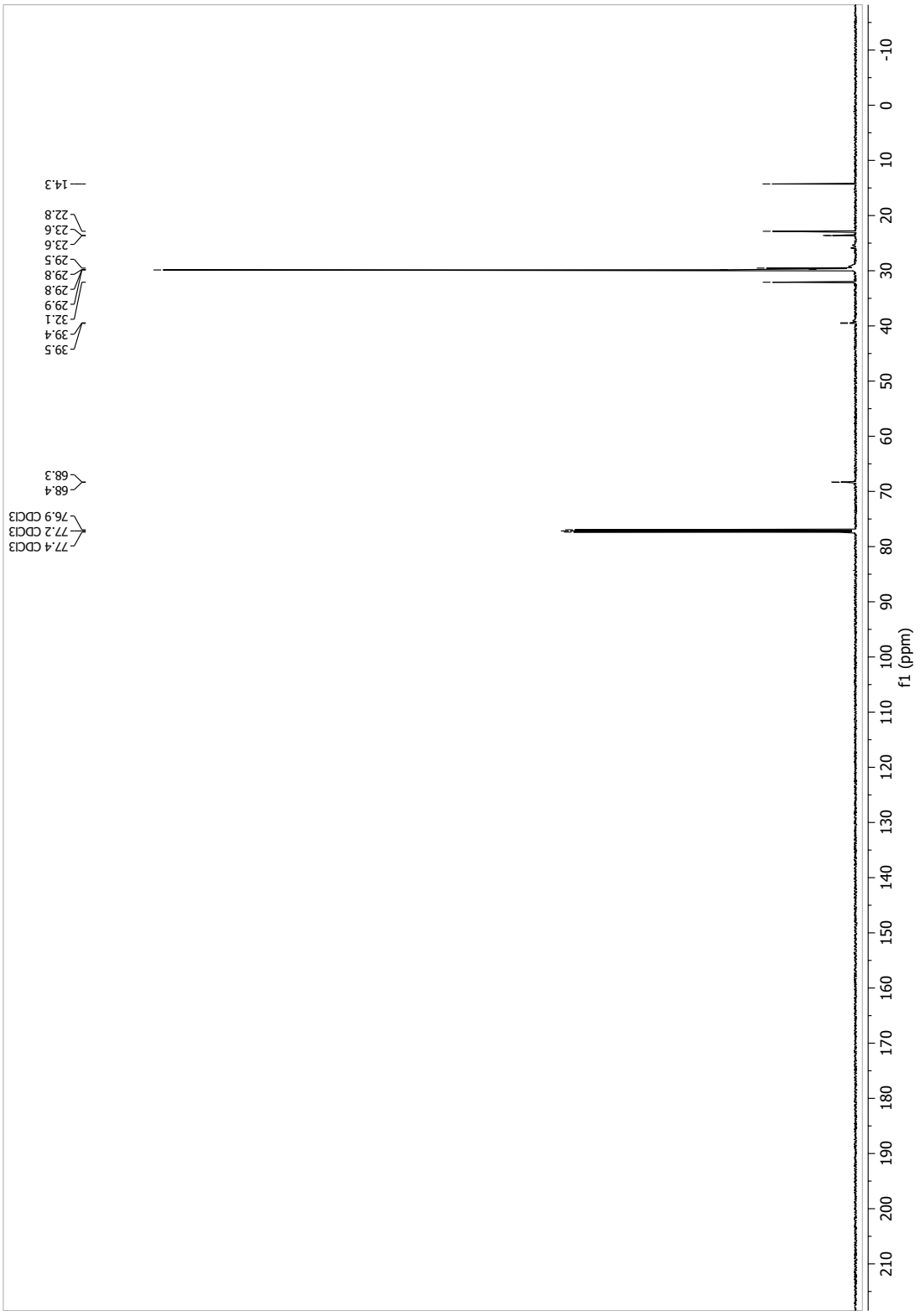
77.4 CDCl3
77.2 CDCl3
76.9 CDCl3
68.4
68.3
39.5
39.4
32.1
29.9
29.8
29.8
29.5
23.6
23.6
22.8
14.3
f1 (ppm)

13.1.20 15-Methylhexadecane-1,15-diol (46a)

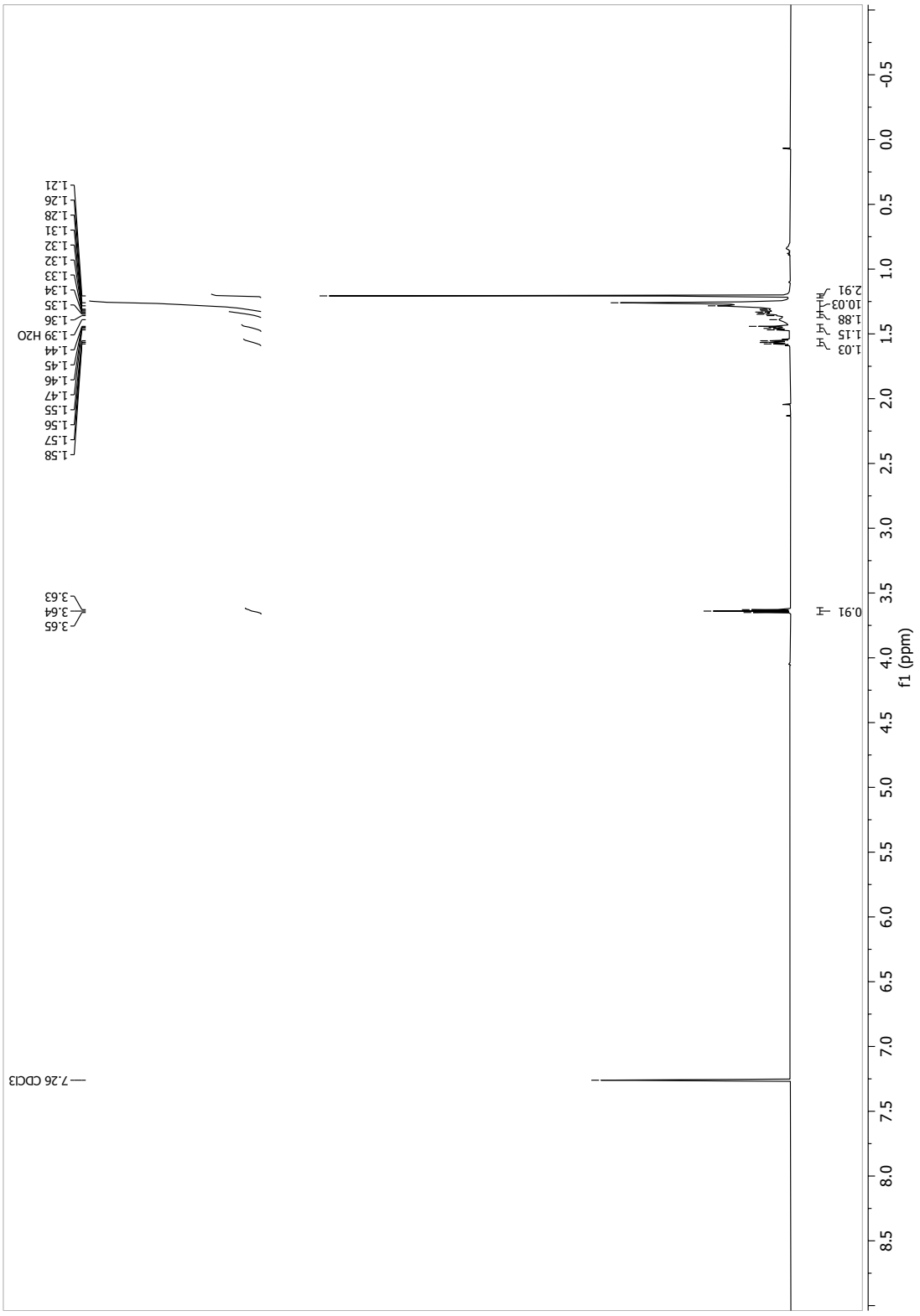

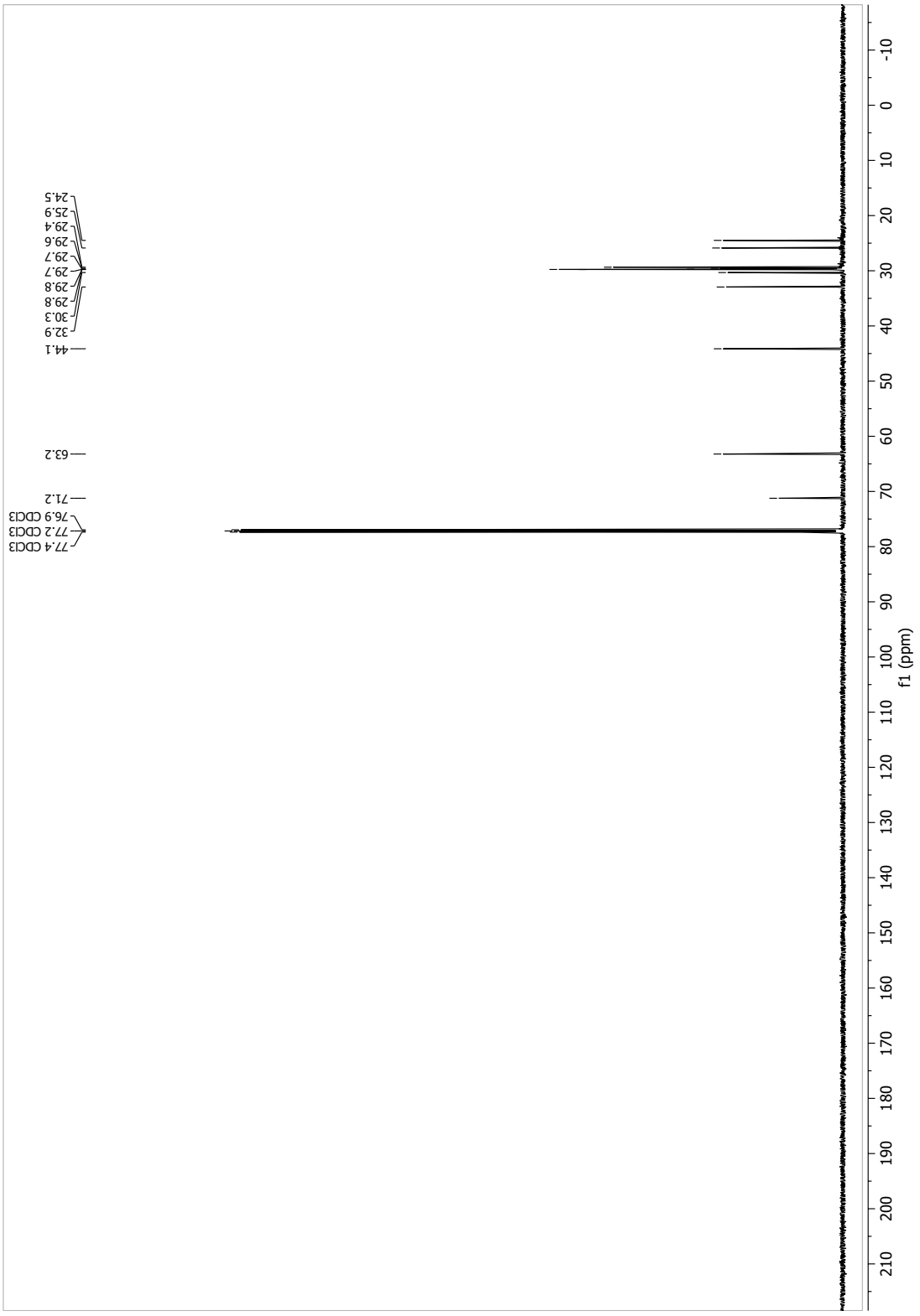
77.4 CDCl3
77.2 CDCl3
76.9 CDCl3
71.2
63.2
44.1
32.9
30.3
29.8
29.8
29.7
29.7
29.6
29.4
25.9
24.5
f1 (ppm)

13.1.21 15-Methylhexadecan-1-ol (47a)

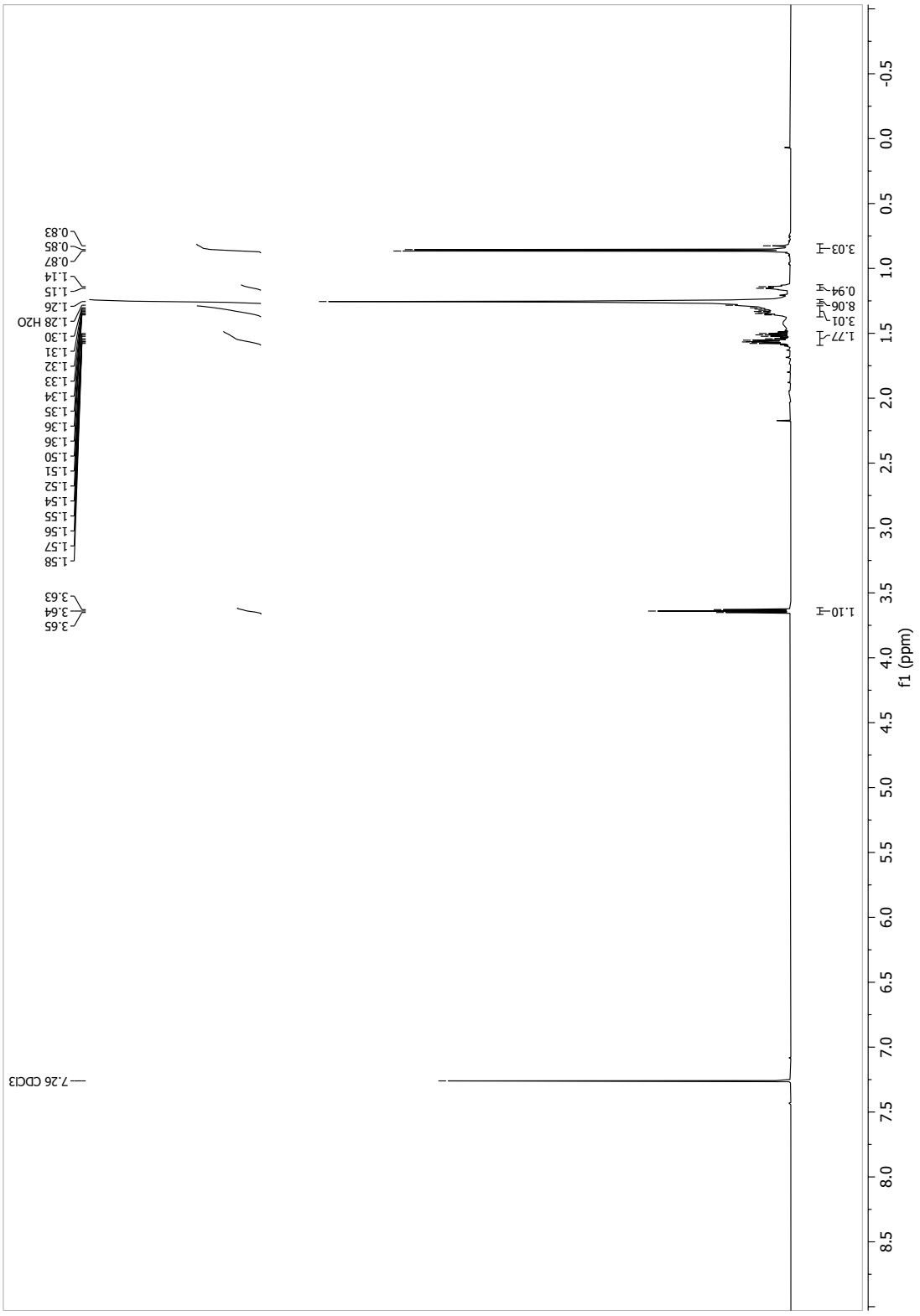

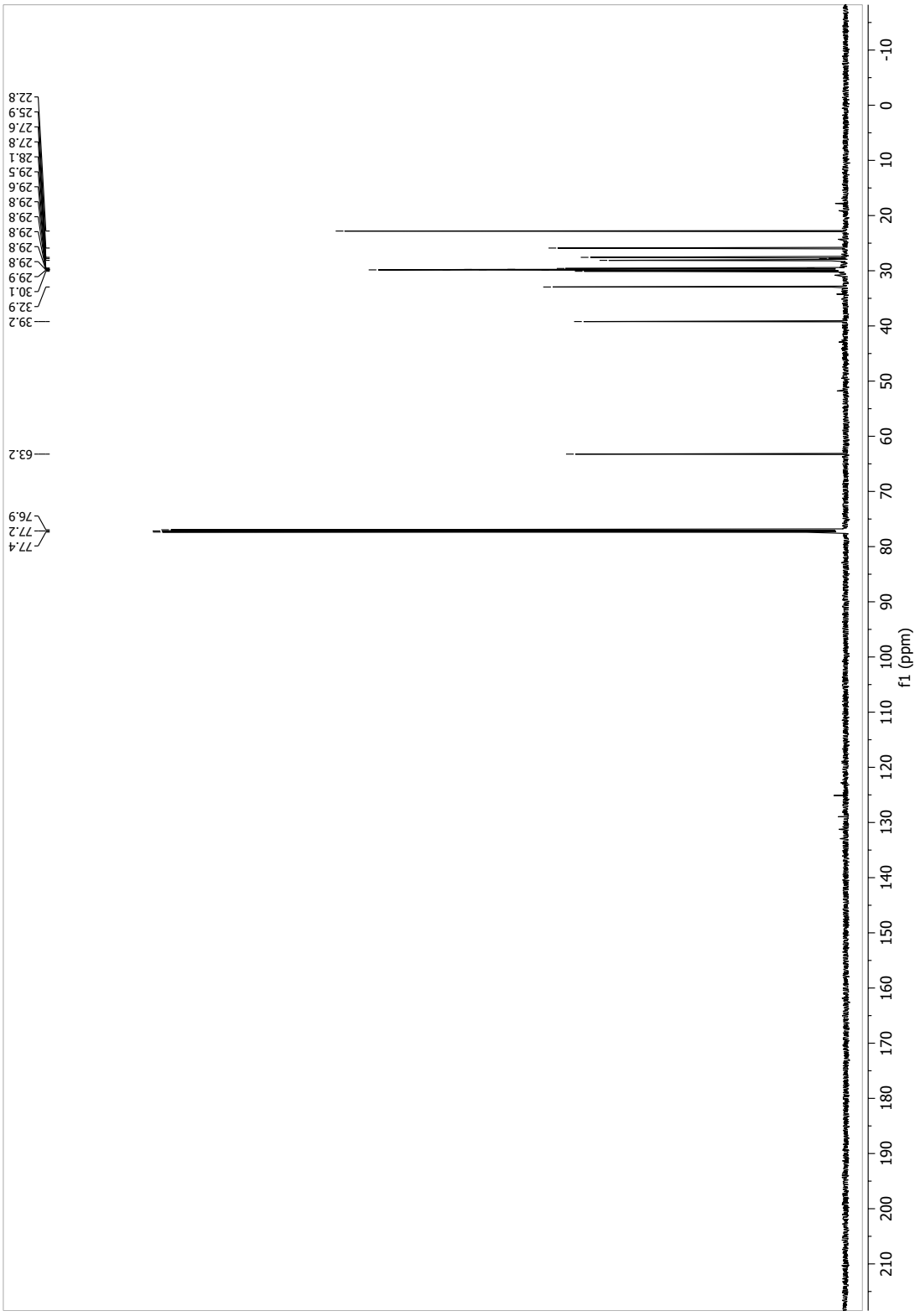
77.4
77.2
76.9
63.2
39.2
32.9
30.1
29.9
29.8
29.8
29.8
29.8
29.6
29.5
28.1
27.8
27.6
25.9
22.8
f1 (ppm)

13.1.22 1-Bromo-15-methylhexadecane (48)

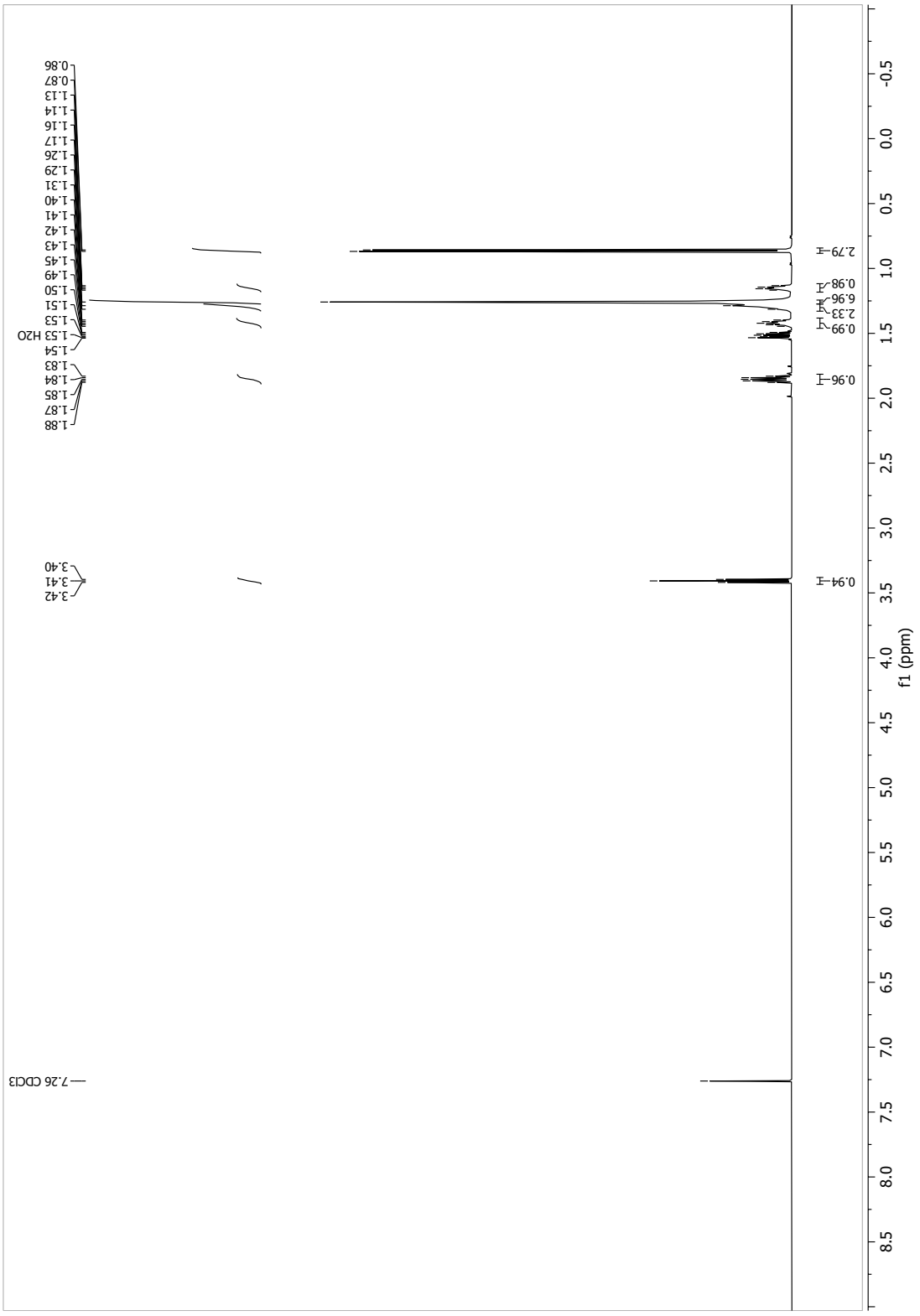

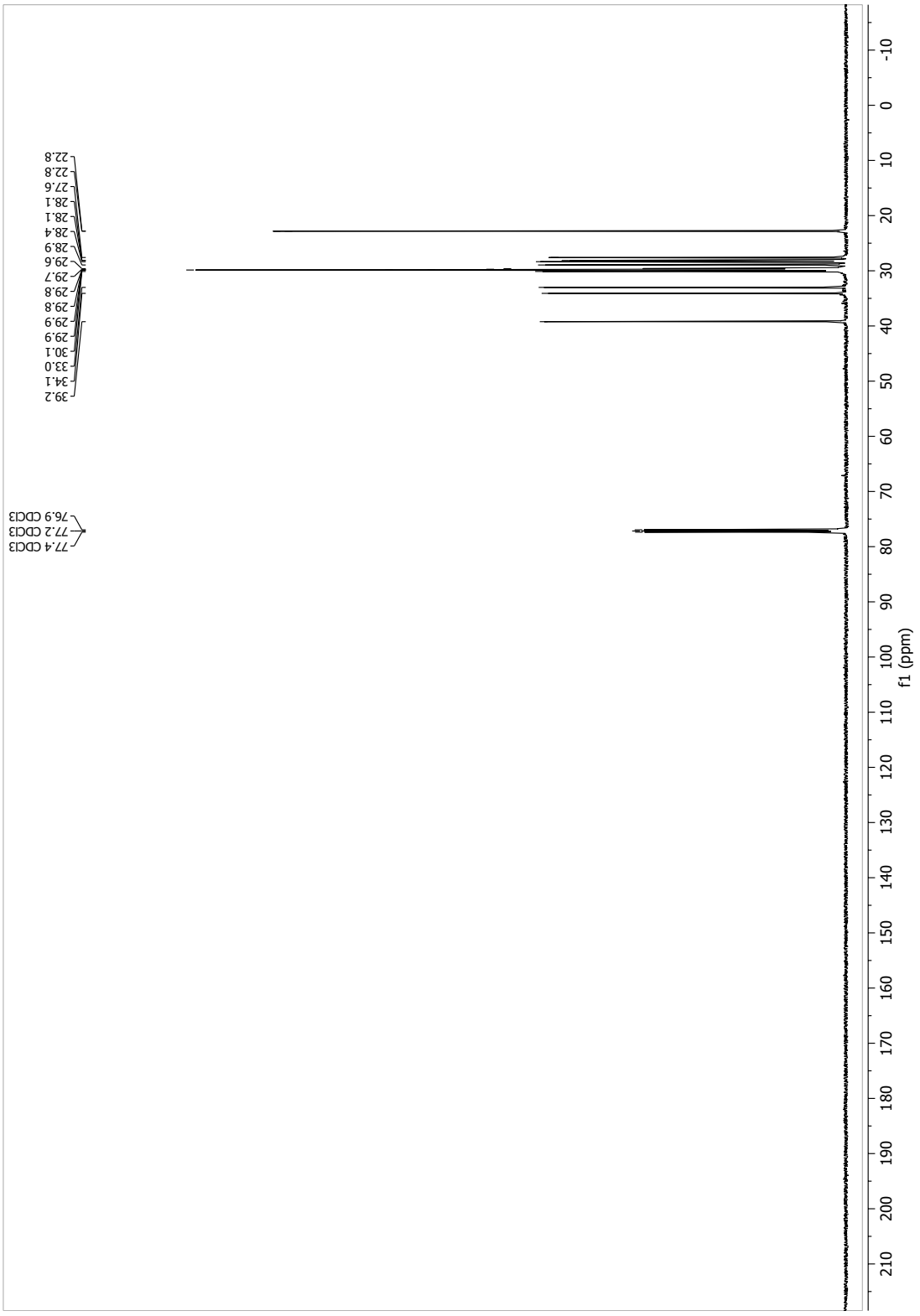
77.4 CDCl3
77.2 CDCl3
76.9 CDCl3
39.2
34.1
33.0
30.1
29.9
29.9
29.8
29.8
29.7
29.6
28.9
28.4
28.1
28.1
27.6
22.8
22.8
f1 (ppm)

13.1.23 2-((5-Bromopentyl)oxy)tetrahydro-2*H*-pyran (50)

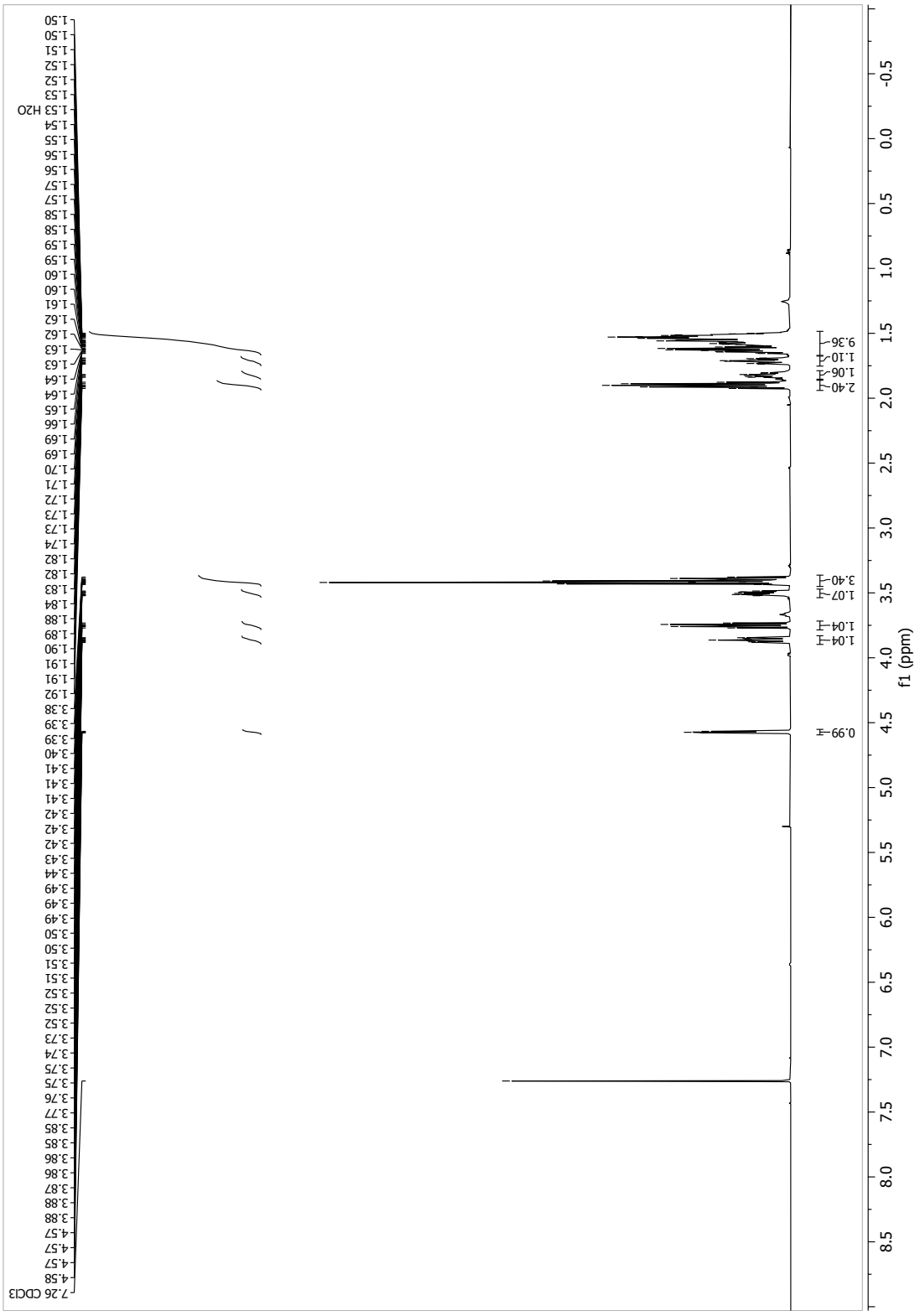

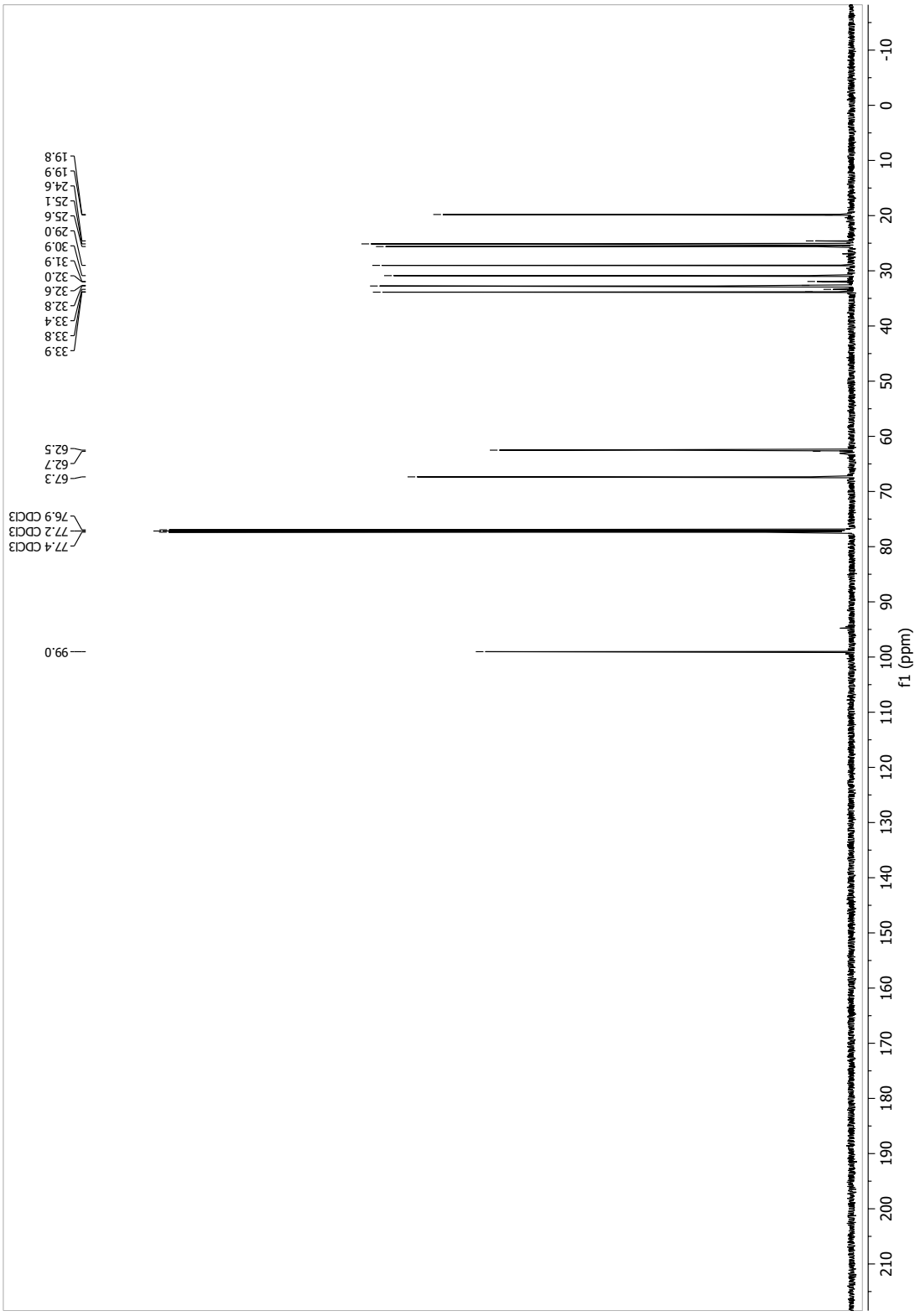
99.0
77.4 CDCl3
77.2 CDCl3
76.9 CDCl3
67.3
62.7
62.5
33.9
33.8
33.4
32.8
32.6
32.0
31.9
30.9
29.0
25.6
25.1
24.6
19.9
19.8
f1 (ppm)

13.1.24 2-((20-Methylhenicosyl)oxy)tetrahydro-2*H*-pyran (52)

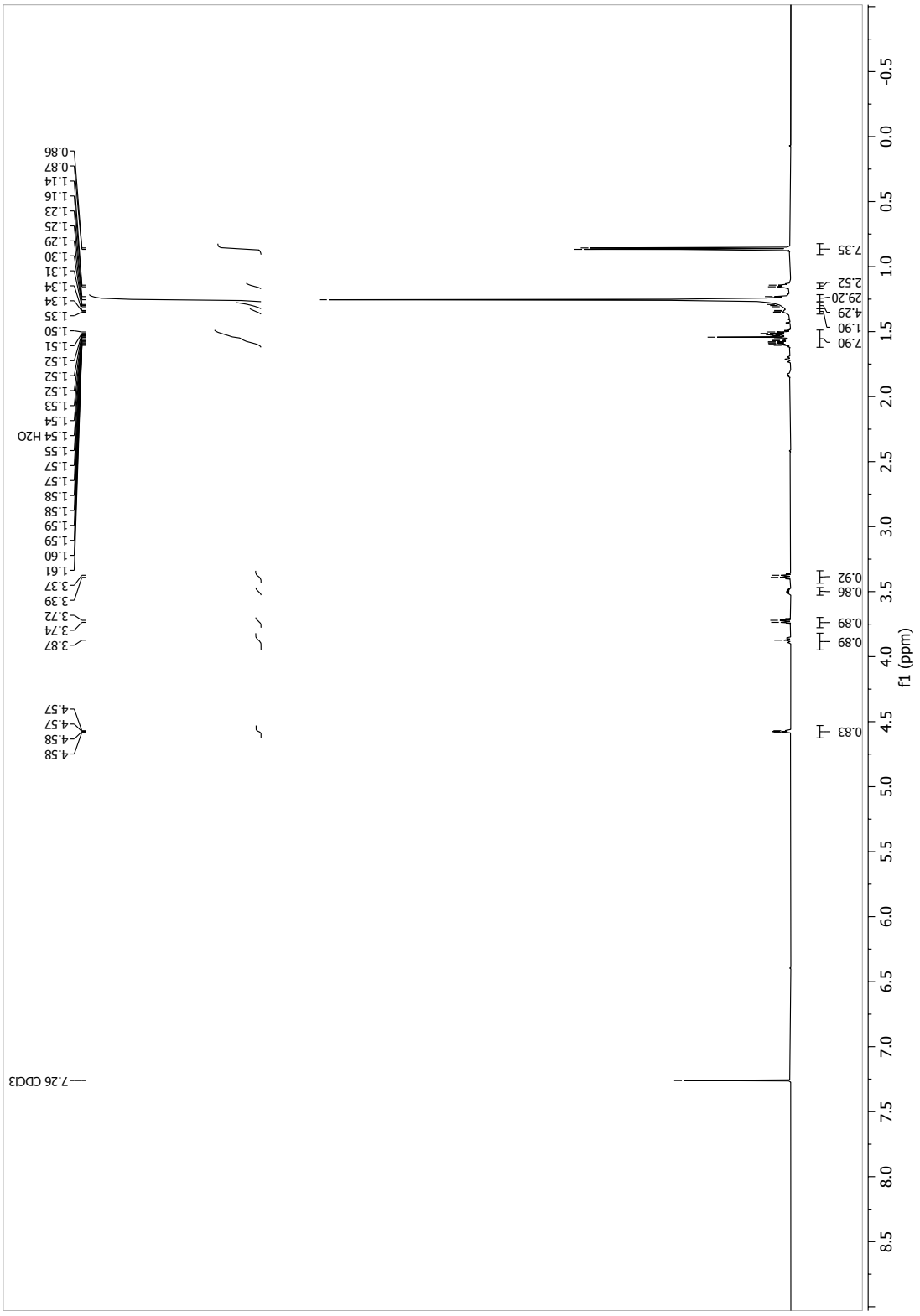

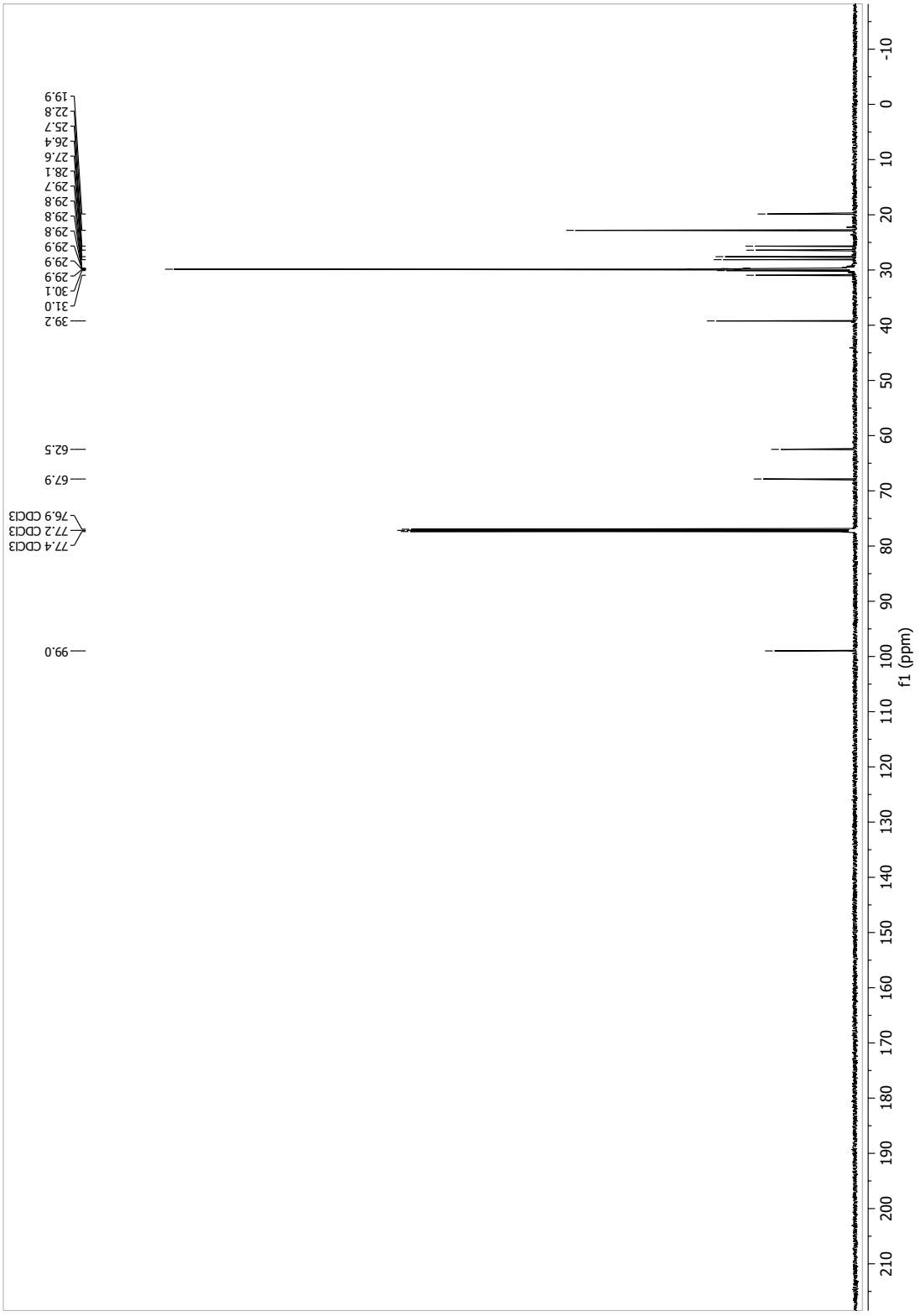
99.0
77.4 CDCl3
77.2 CDCl3
76.9 CDCl3
67.9
62.5
39.2
31.0
30.1
29.9
29.9
29.9
29.8
29.8
29.8
29.7
28.1
27.6
26.4
25.7
22.8
19.9
f1 (ppm)

13.1.25 1-Bromo-20-methylhenicosane (53)

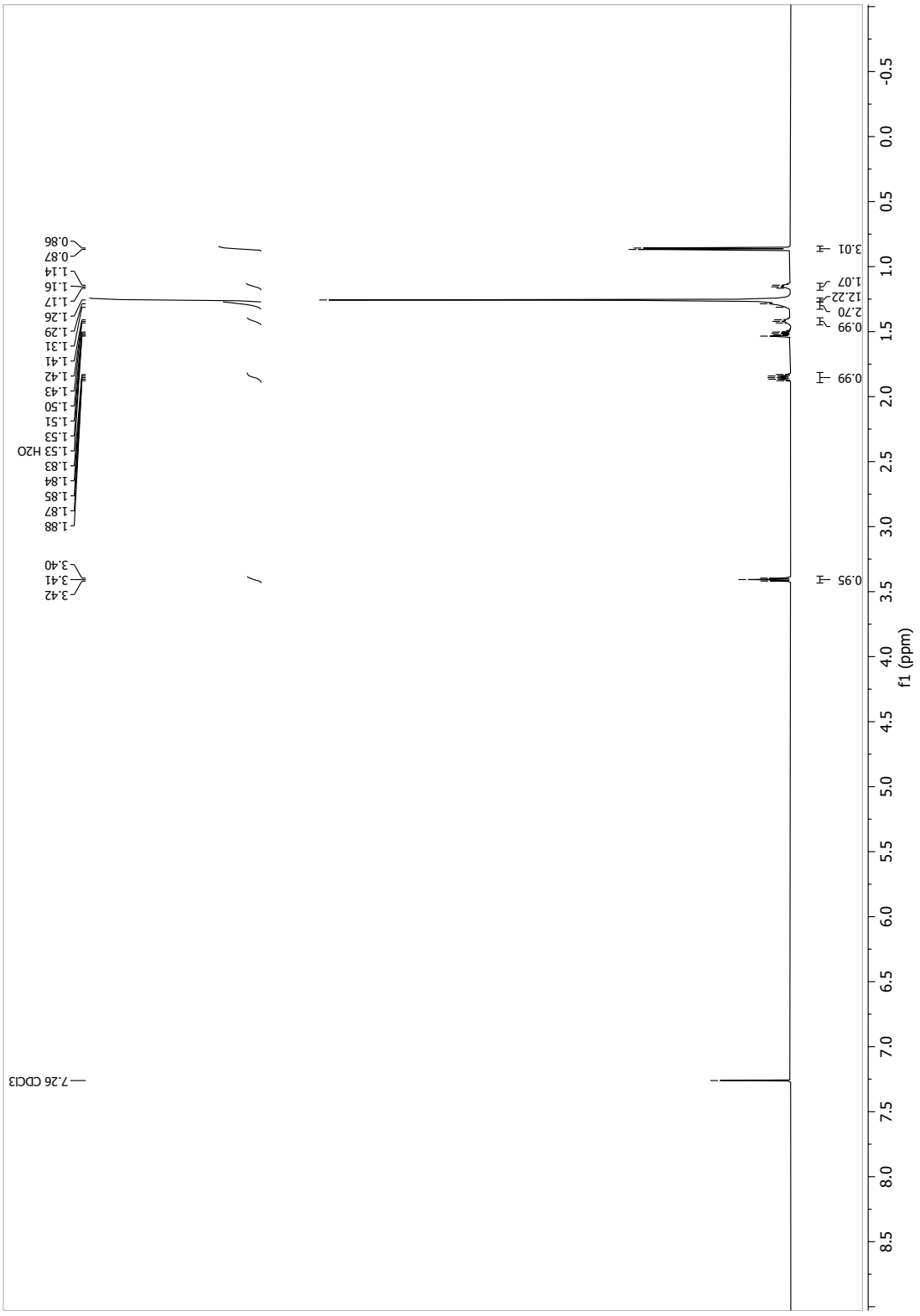

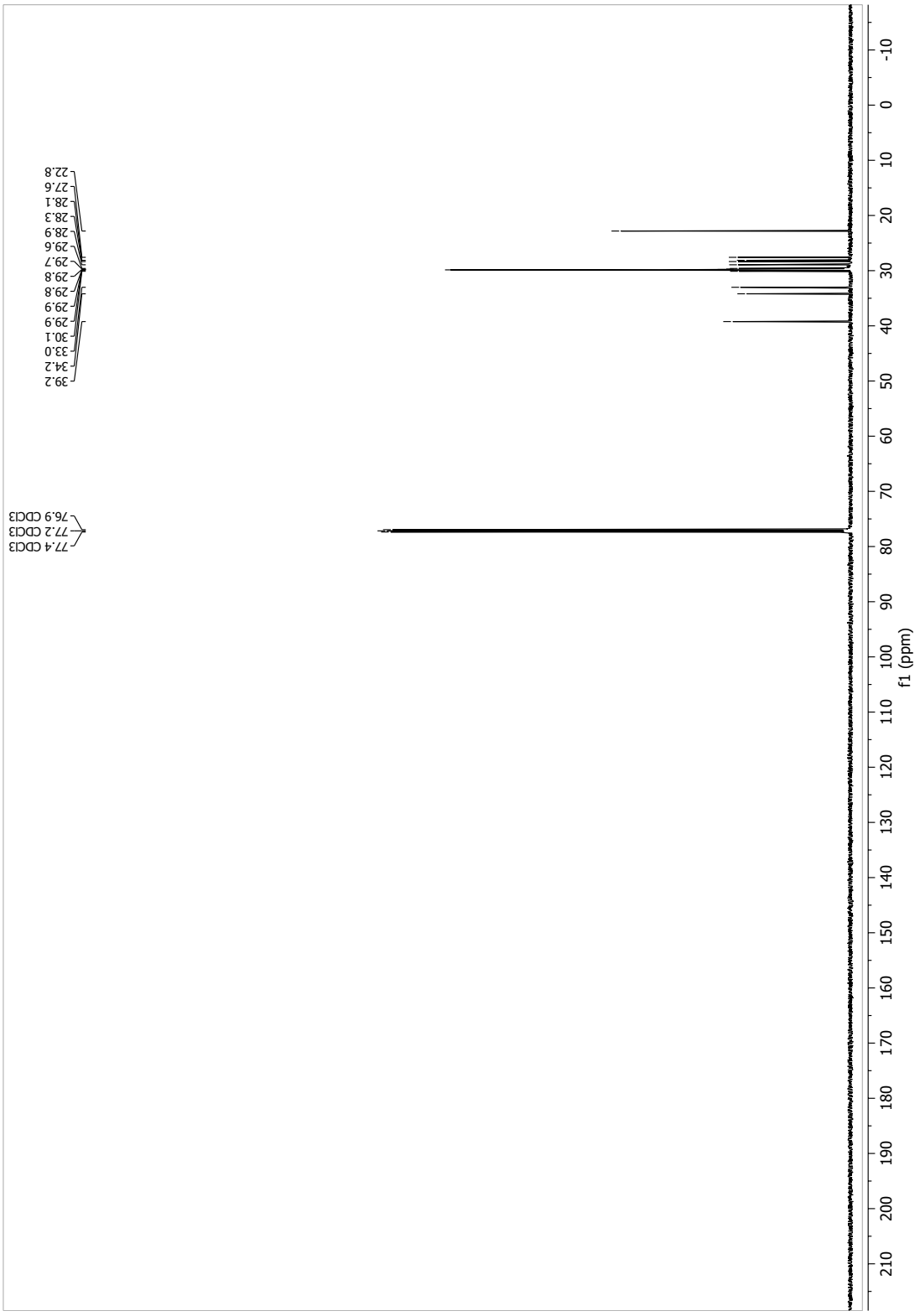
77.4 CDCl3
77.2 CDCl3
76.9 CDCl3
39.2
34.2
33.0
30.1
29.9
29.9
29.8
29.8
29.7
29.6
28.9
28.3
28.1
27.6
22.8
f1 (ppm)

13.1.27 (*R*)-*tert*-butyldimethyl((24-methylpentacos-3-yn-2-yl)oxy)silane (54)

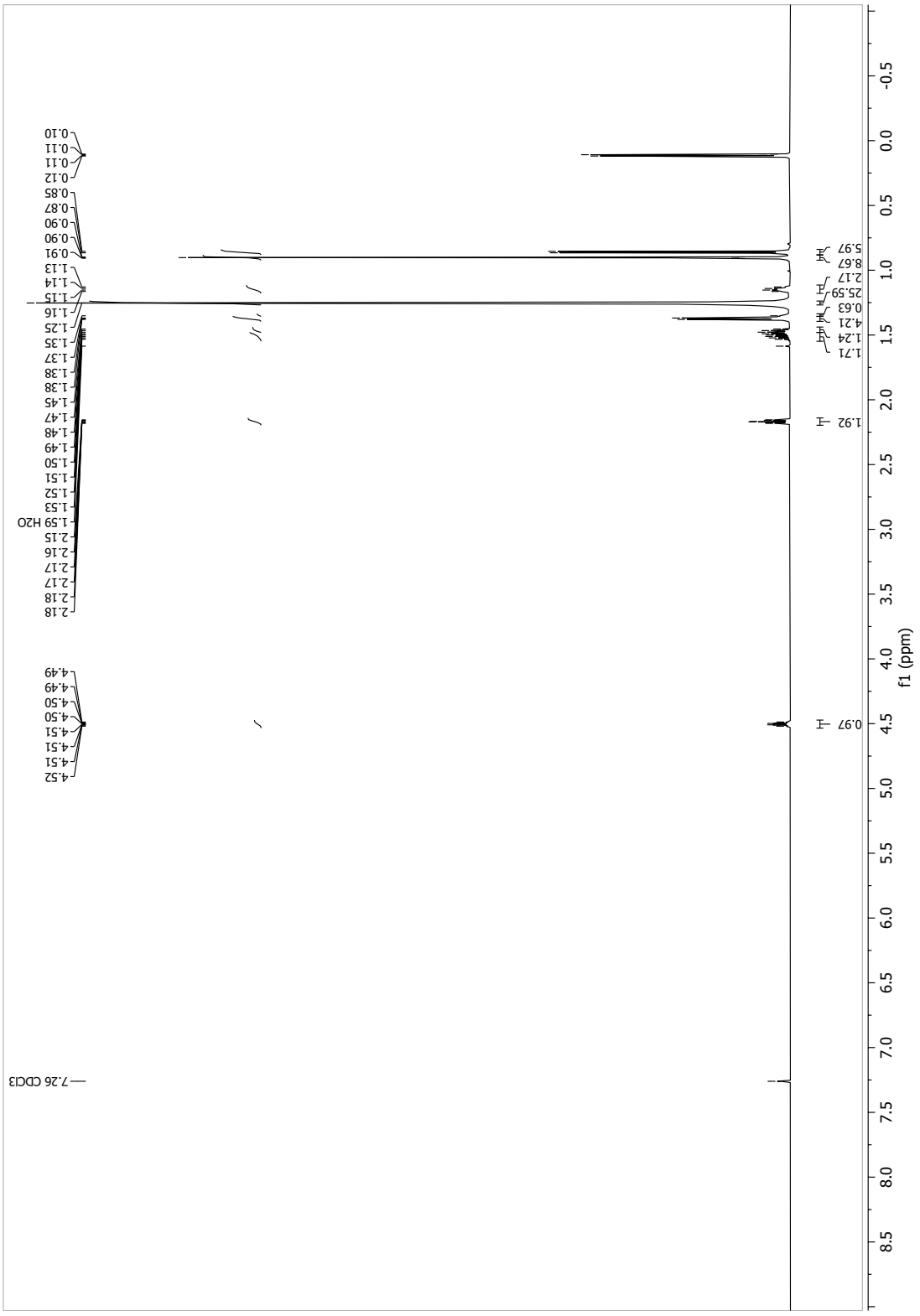

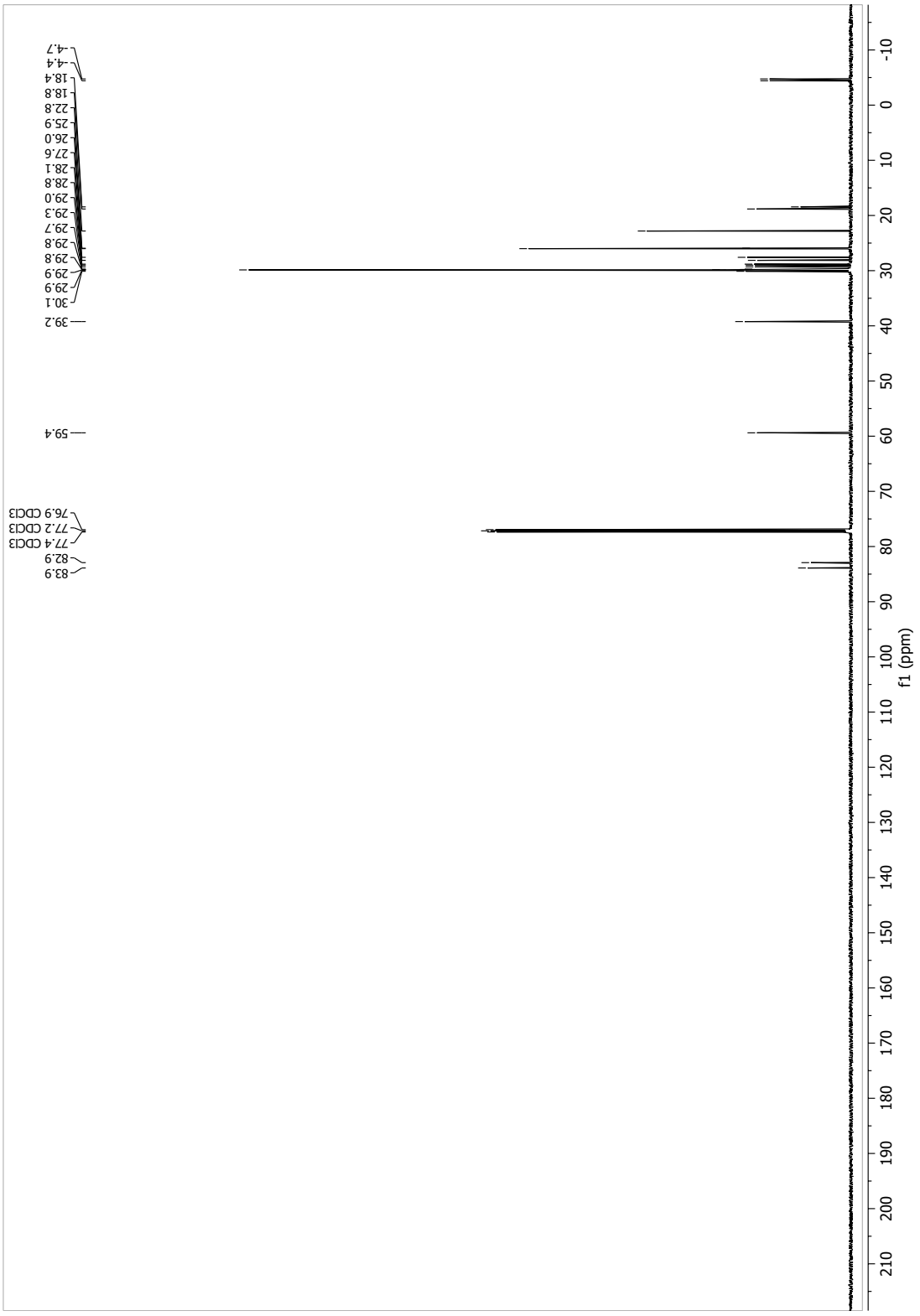
83.9
82.9
77.4 CDCl3
77.2 CDCl3
76.9 CDCl3
59.4
39.2
30.1
29.9
29.9
29.8
29.8
29.7
29.3
29.0
28.8
28.1
27.6
26.0
25.9
22.8
18.8
18.4
-4.4
-4.7
f1 (ppm)

13.1.28 (*R*)-*tert*-butyldimethyl((24-methylpentacosan-2-yl)oxy)silane (55a)

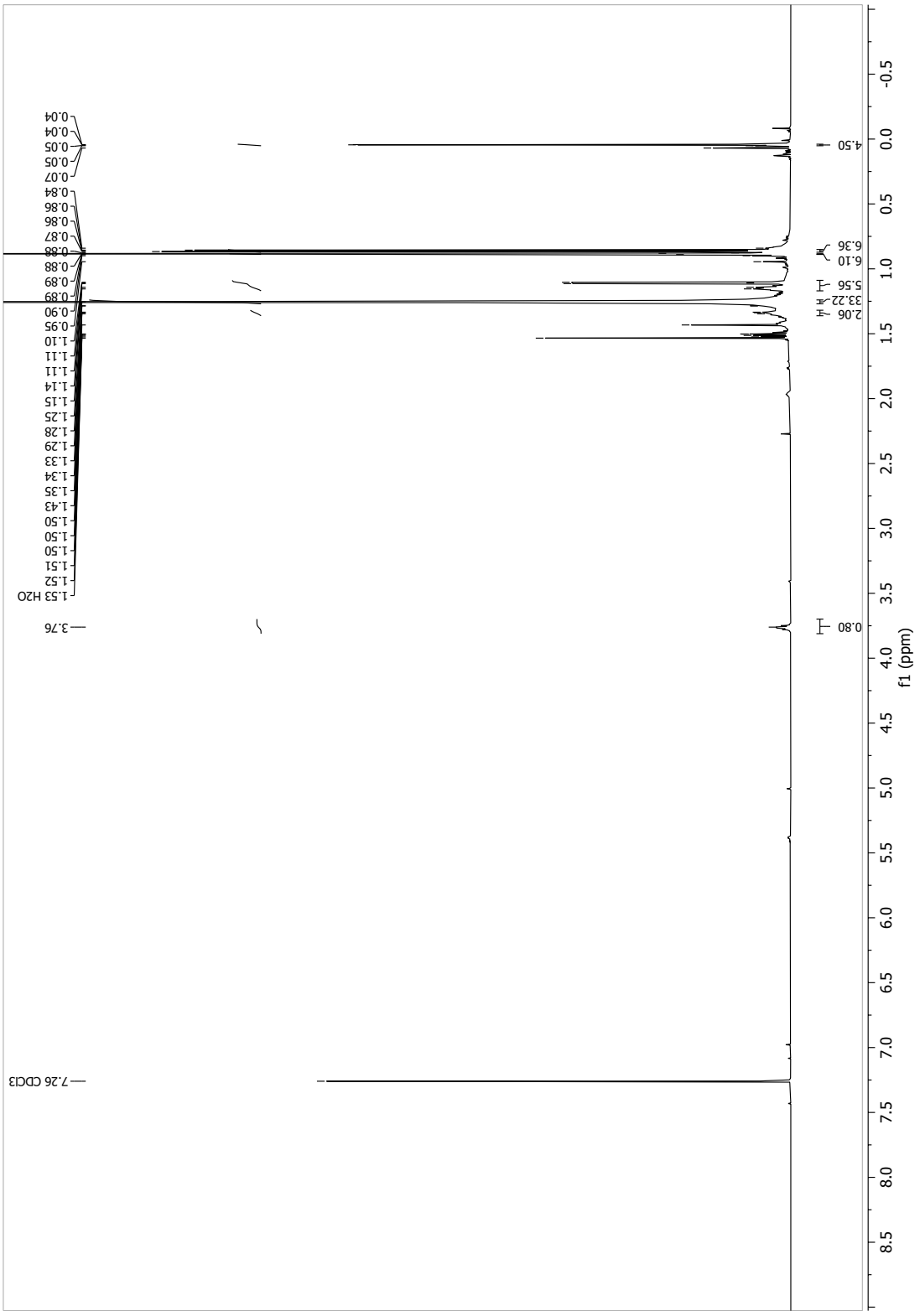

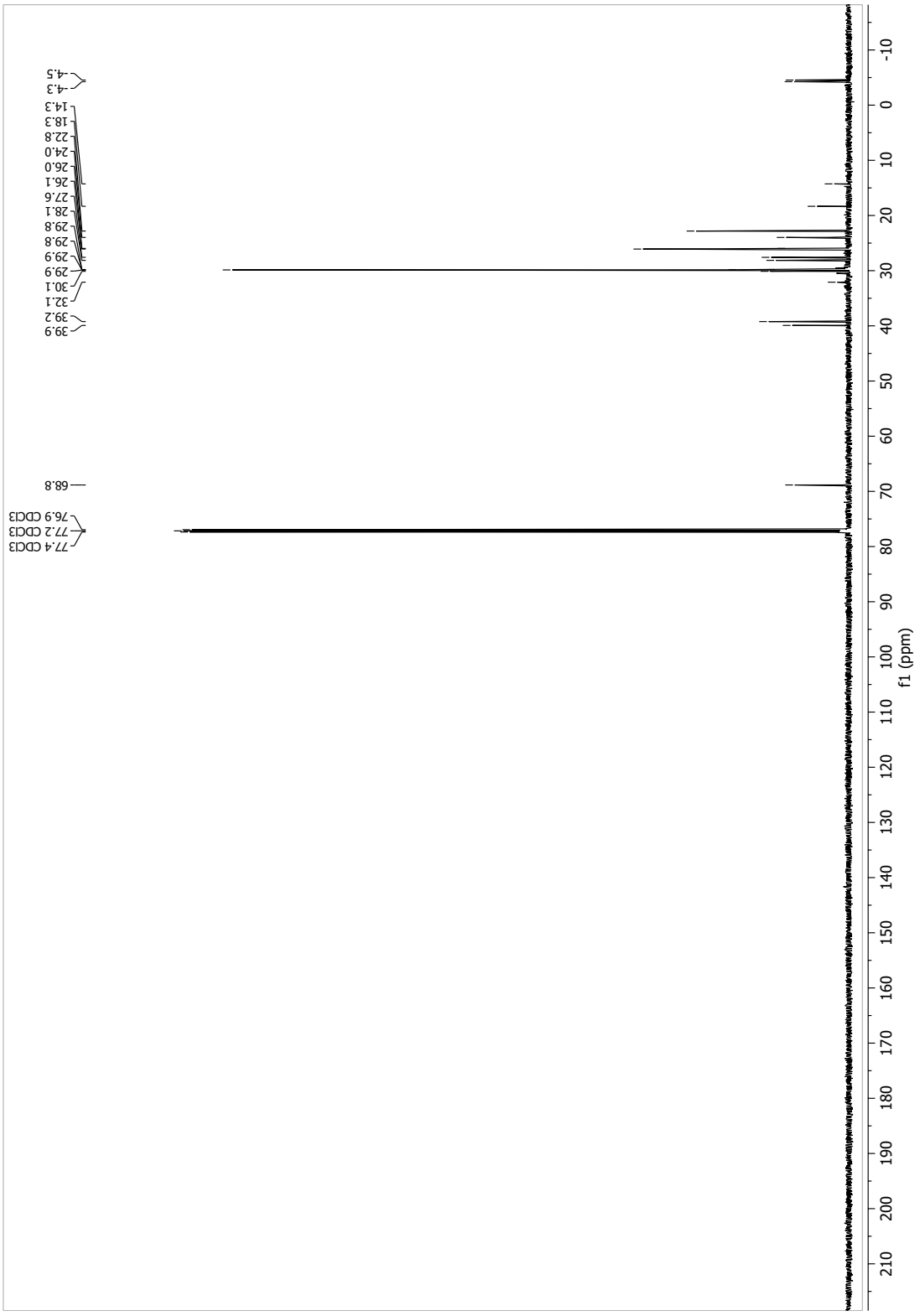
77.4 CDCl3
77.2 CDCl3
76.9 CDCl3
68.8
39.9
39.2
32.1
30.1
29.9
29.9
29.8
29.8
28.1
27.6
26.1
26.0
24.0
22.8
18.3
14.3
-4.3
-4.5
f1 (ppm)

13.1.29 [D_4]-(*R*)-*tert*-butyldimethyl((24-methylpentacosan-2-yl)oxy)silane (55b)

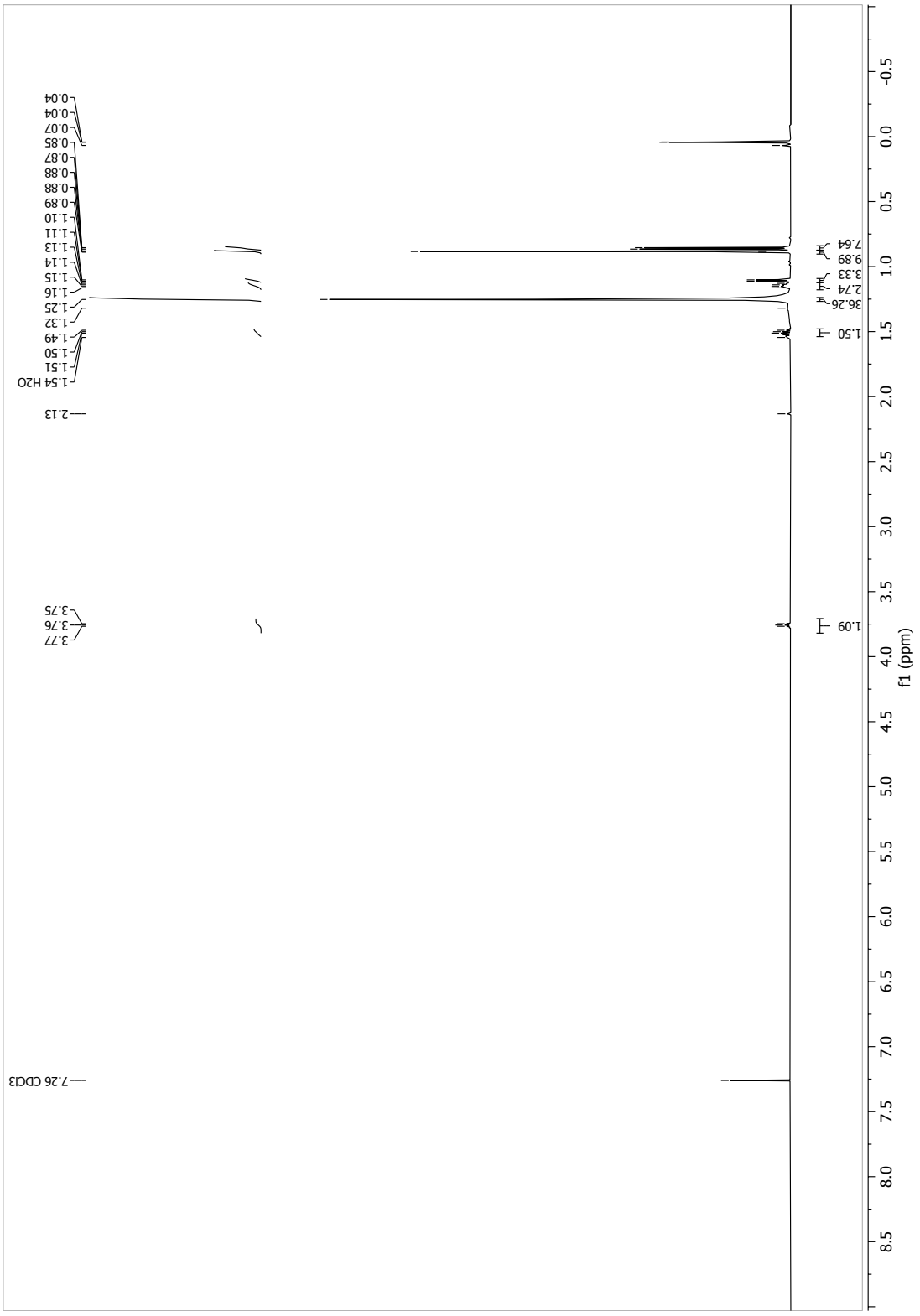

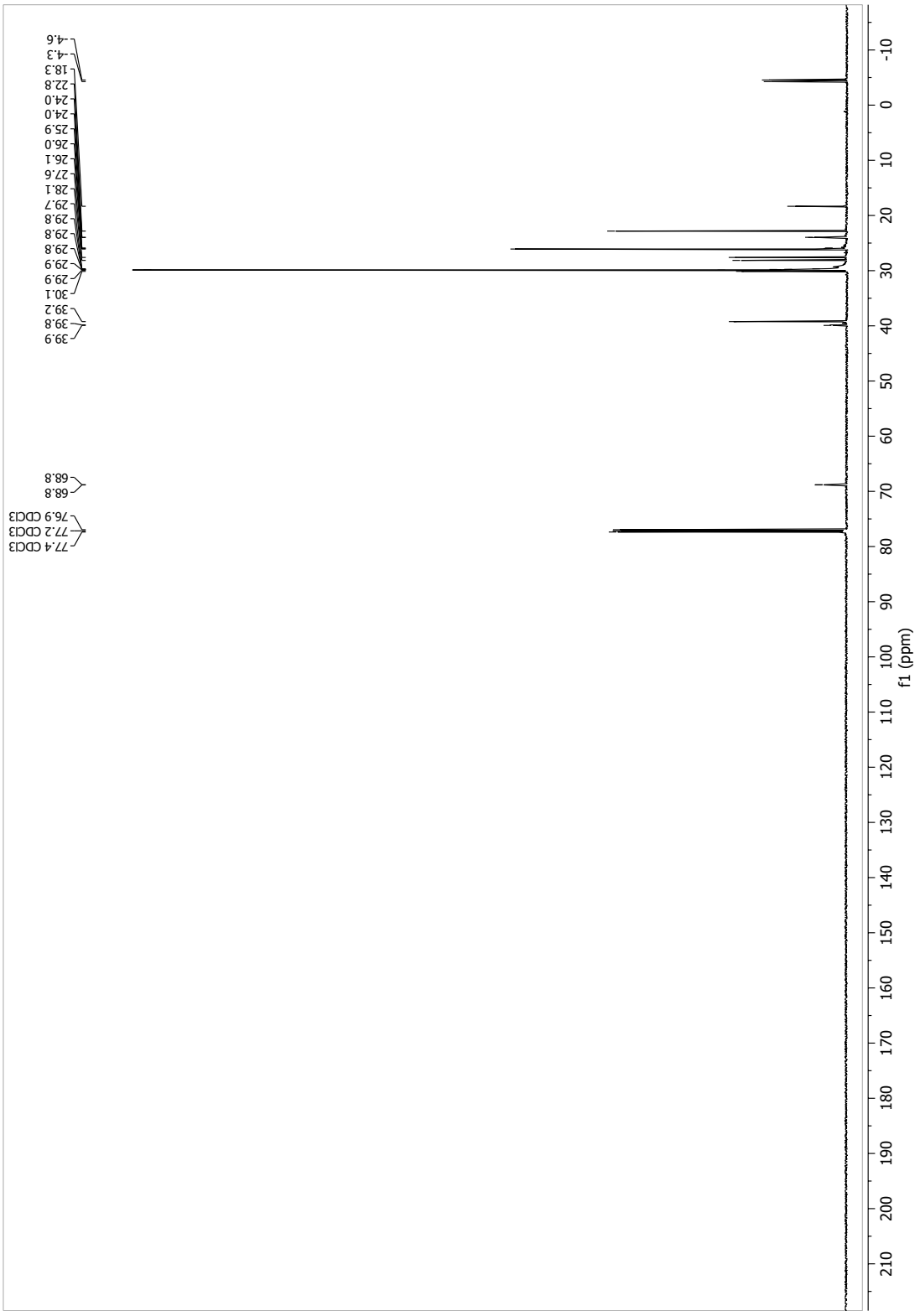
77.4 CDCl3
77.2 CDCl3
76.9 CDCl3
68.8
68.8
39.9
39.8
39.2
30.1
29.9
29.9
29.9
29.8
29.8
29.8
29.7
28.1
27.6
26.1
26.0
25.9
24.0
24.0
22.8
18.3
-4.3
-4.6
f1 (ppm)

13.1.30 (*R*)-24-Methylpentacosan-2-ol (44a)

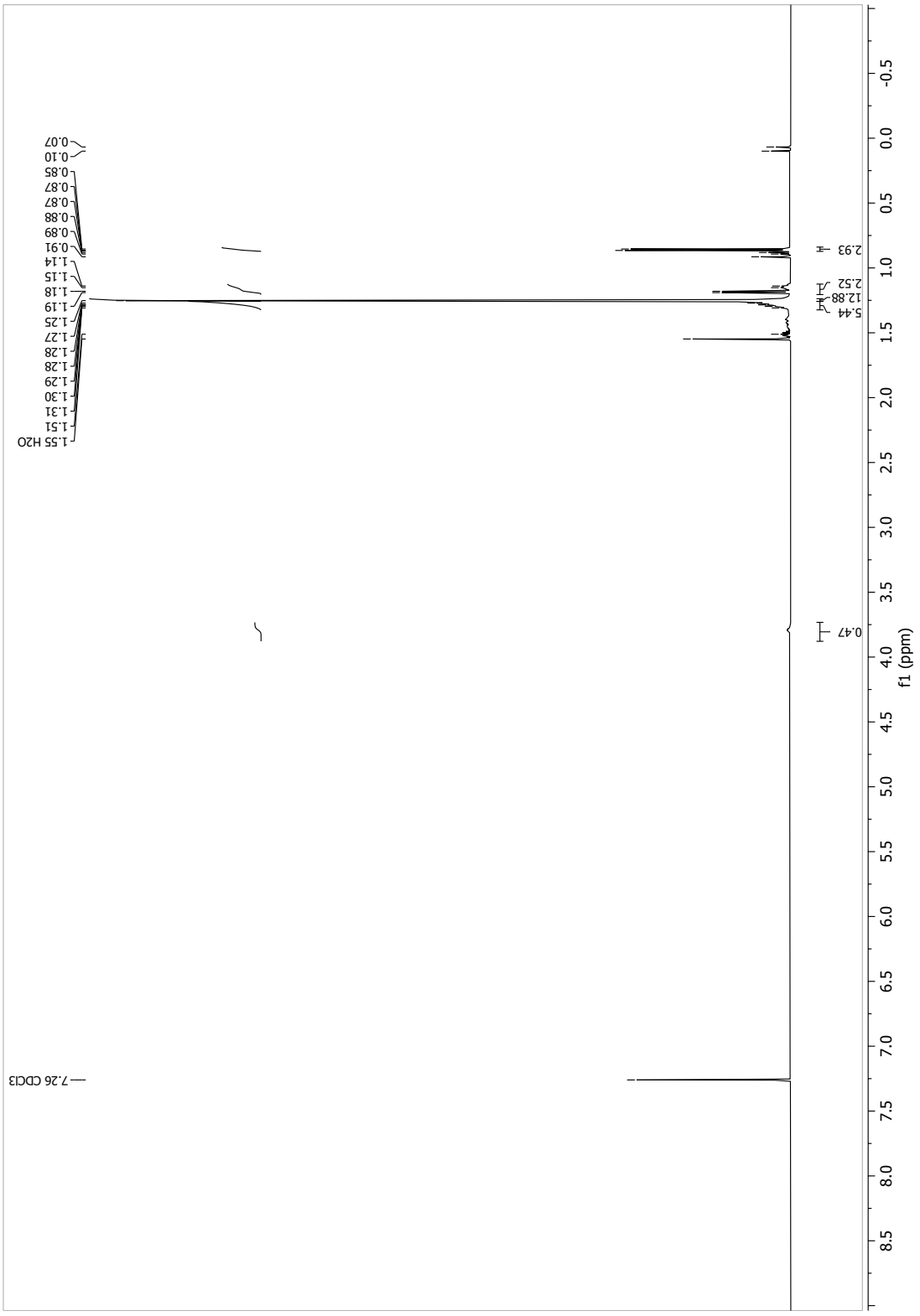

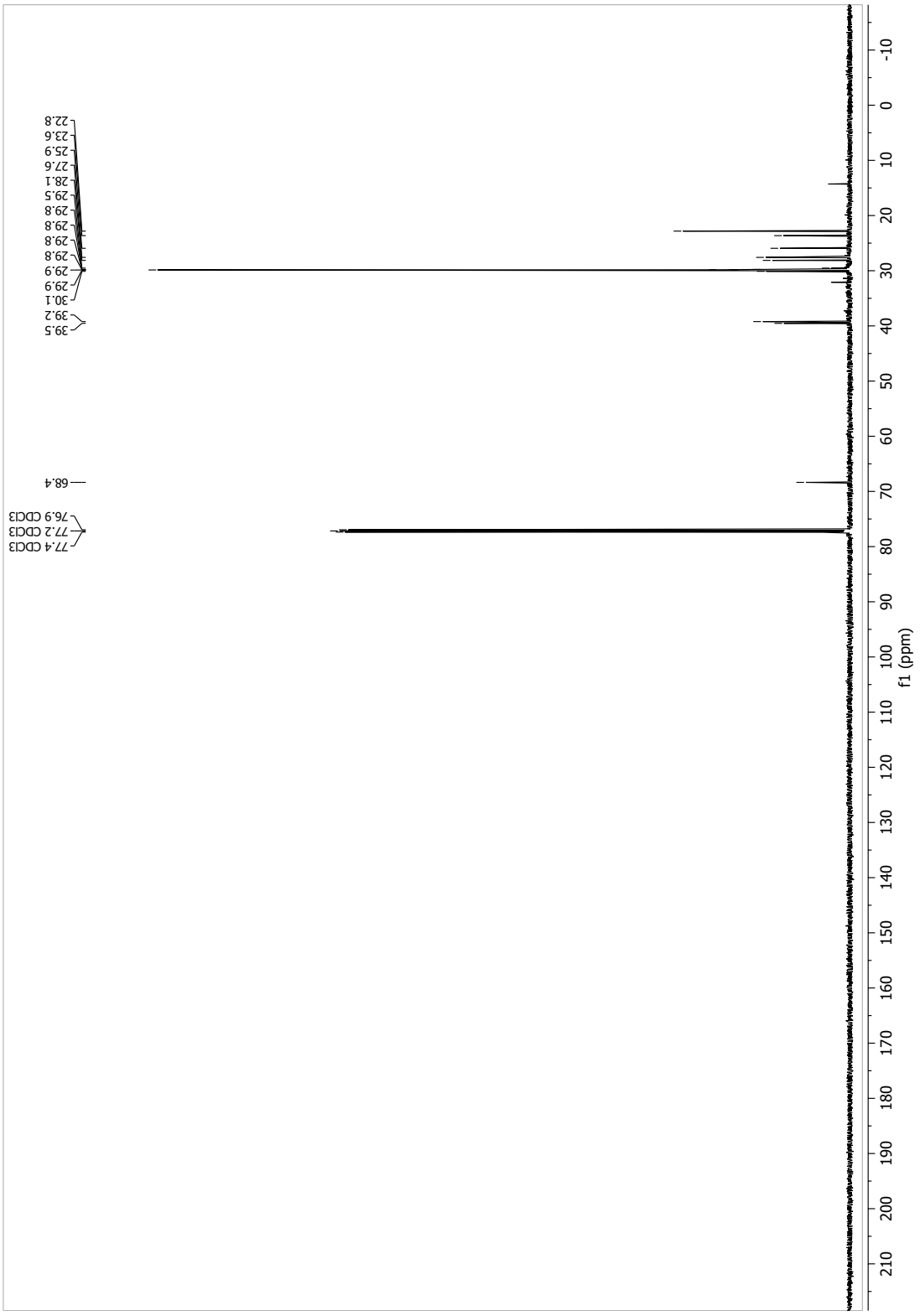
77.4 CDCl3
77.2 CDCl3
76.9 CDCl3
68.4
39.5
39.2
30.1
29.9
29.9
29.8
29.8
29.8
29.8
29.5
29.8
28.1
27.6
25.9
23.6
22.8
f1 (ppm)

13.1.31 [D_4]-(*R*)-24-methylpentacosan-2-ol (44b)

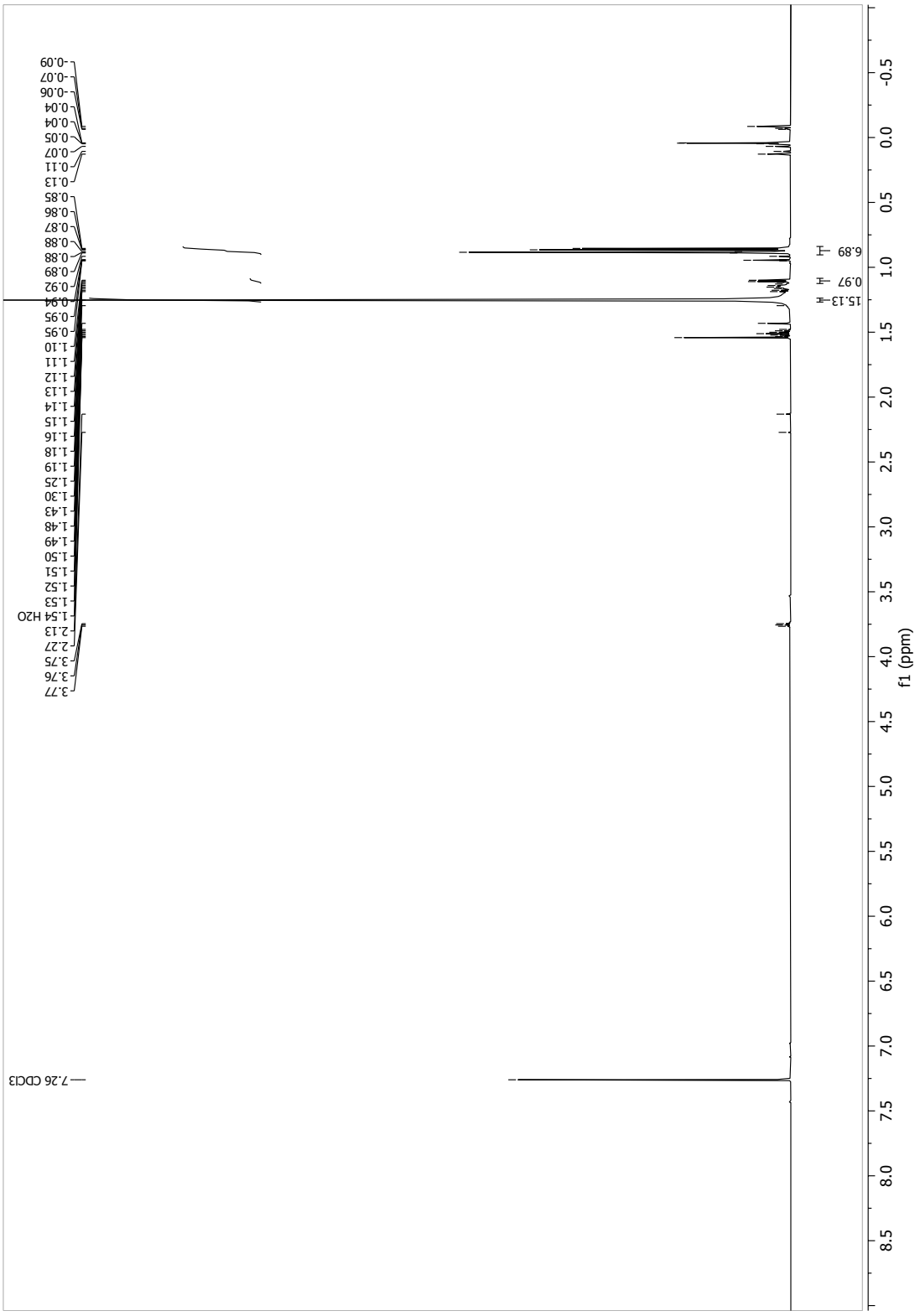

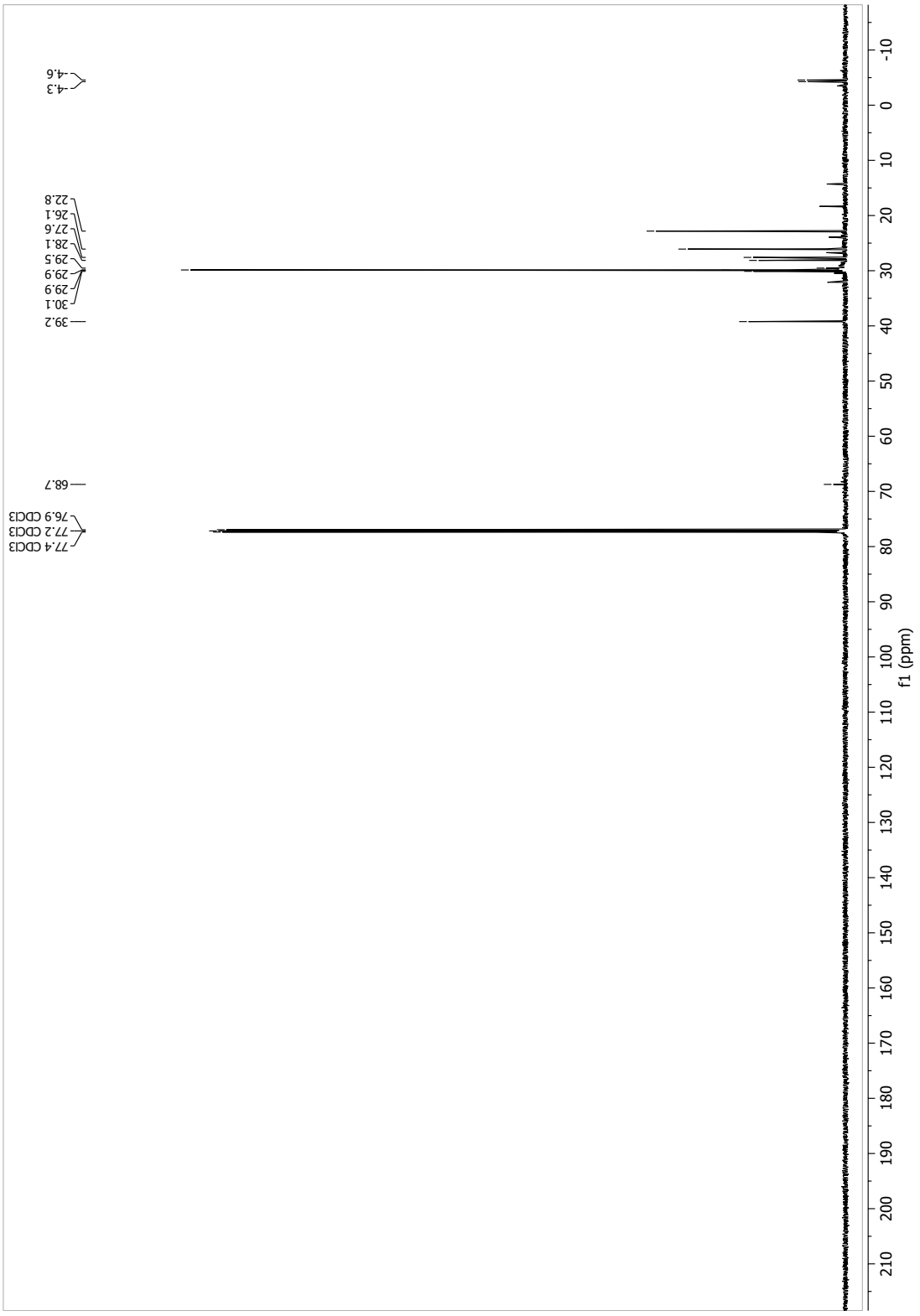
77.4 CDCl3
77.2 CDCl3
76.9 CDCl3
68.7
39.2
30.1
29.9
29.9
29.5
28.1
27.6
26.1
22.8
-4.3
-4.6
f1 (ppm)

13.1.32 2-(Undec-10-yn-1-yloxy)tetrahydro-2*H*-pyran (60)

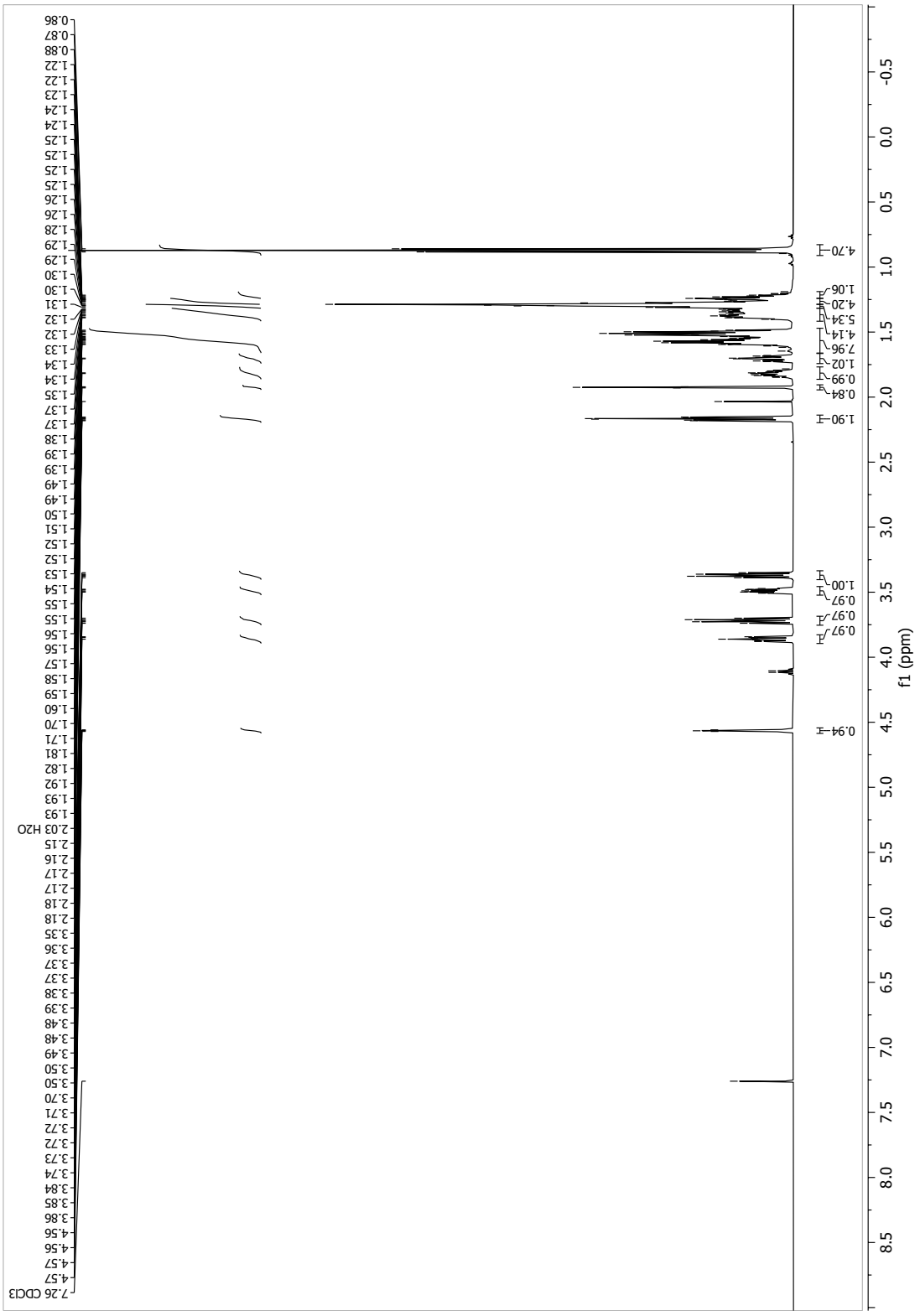

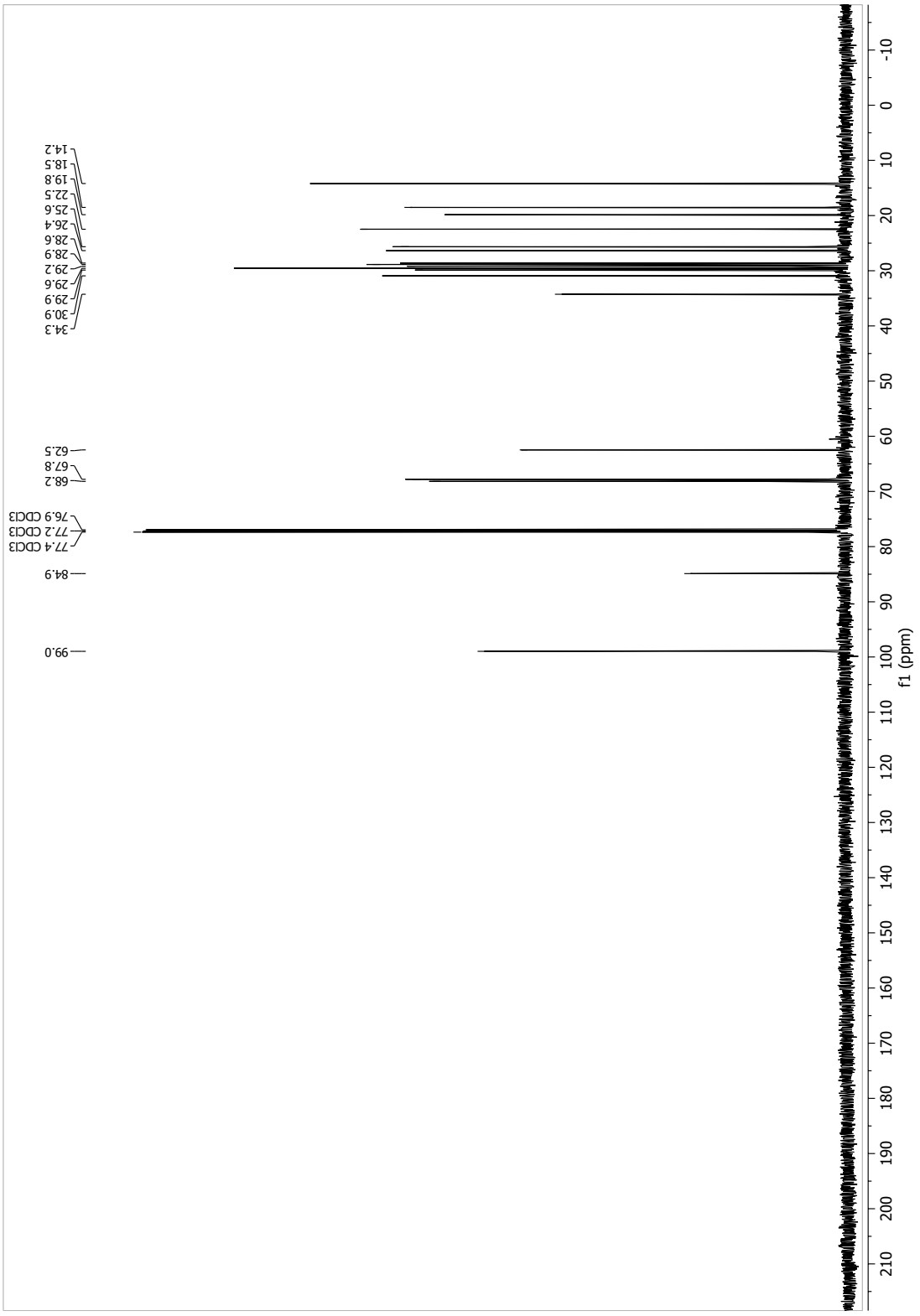
99.0
84.9
77.4 CDCl3
77.2 CDCl3
76.9 CDCl3
68.2
67.8
62.5
34.3
30.9
29.9
29.6
29.2
28.9
28.6
26.4
25.6
22.5
19.8
18.5
14.2
f1 (ppm)

13.1.33 2-(Heptacos-10-yn-1-yloxy)tetrahydro-2*H*-pyran (59)

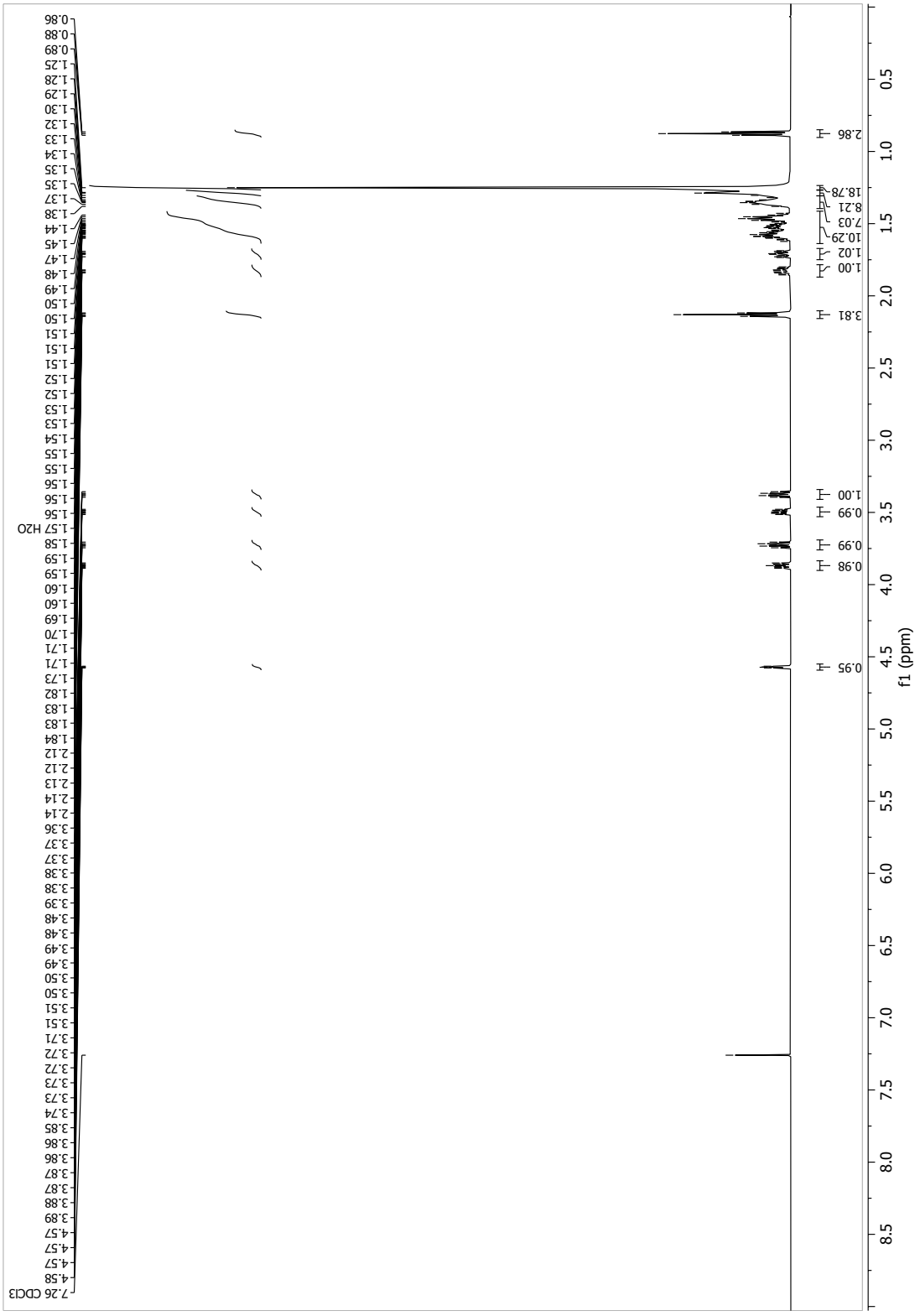

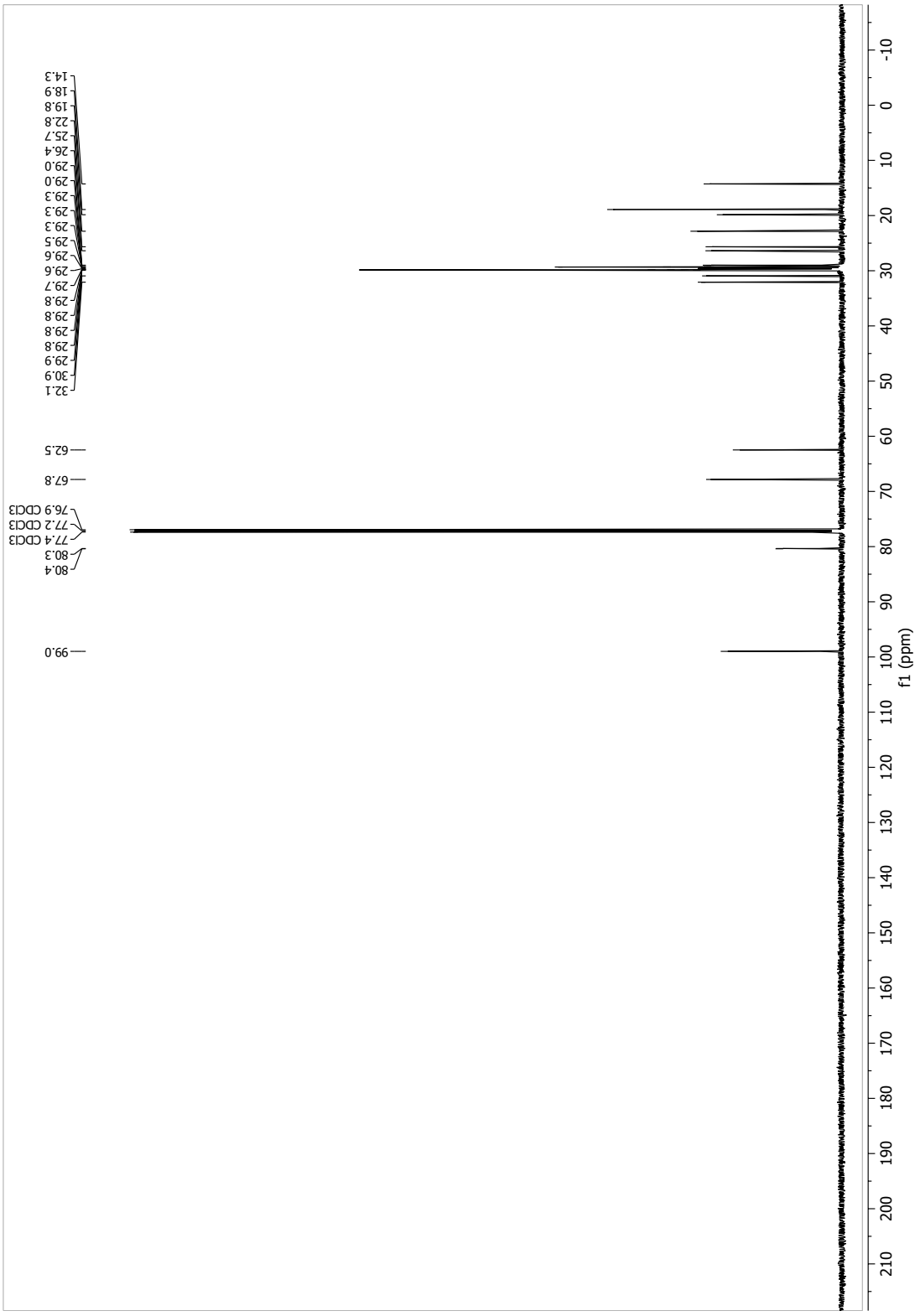
99.0
80.4
80.3
77.4 CDCl3
77.2 CDCl3
76.9 CDCl3
67.8
62.5
32.1
30.9
29.9
29.8
29.8
29.8
29.8
29.7
29.6
29.6
29.5
29.3
29.3
29.3
29.0
29.0
26.4
25.7
22.8
19.8
18.9
14.3
f1 (ppm)

13.1.34 2-(Heptacosyloxy)tetrahydro-2*H*-pyran (63)

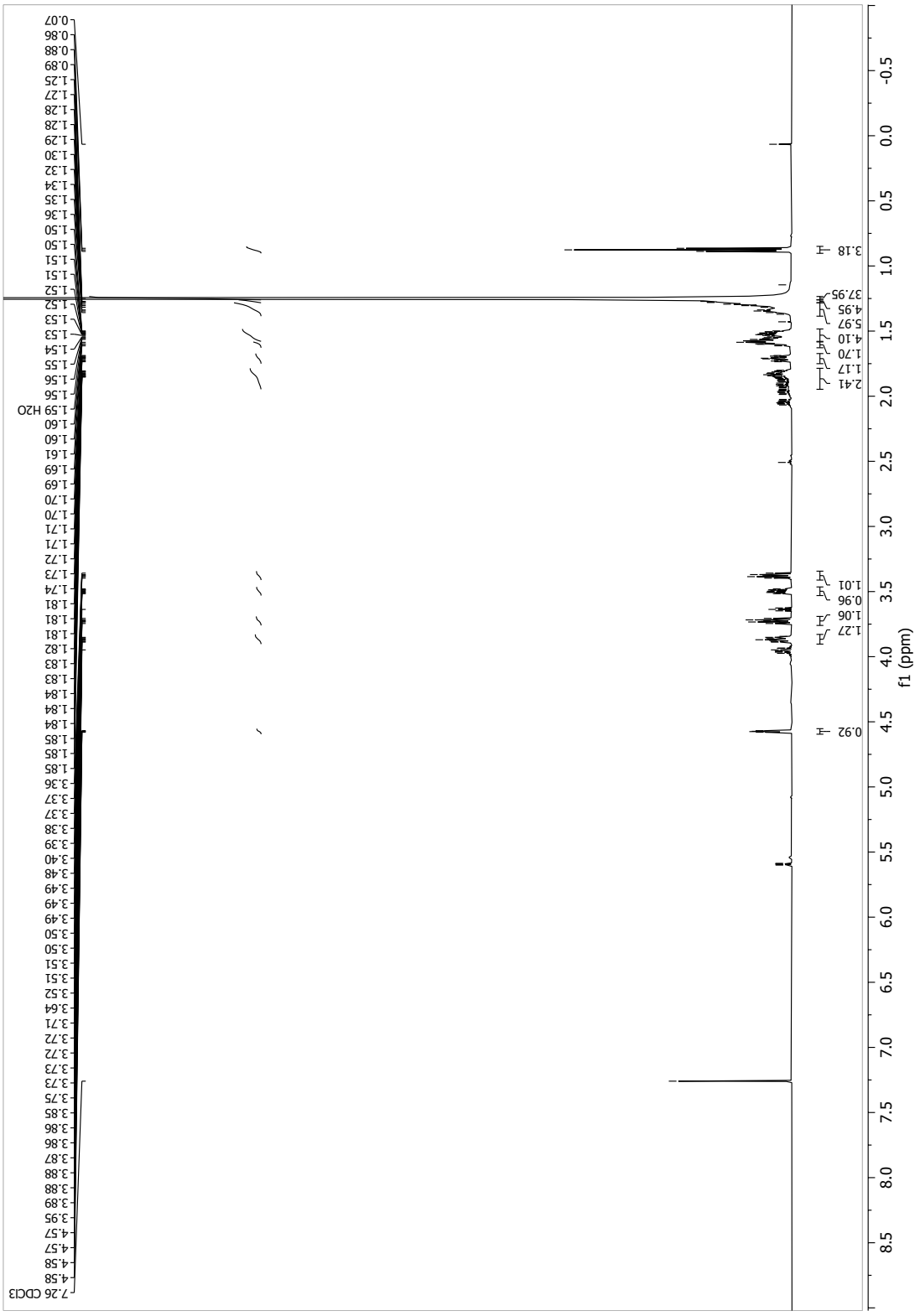

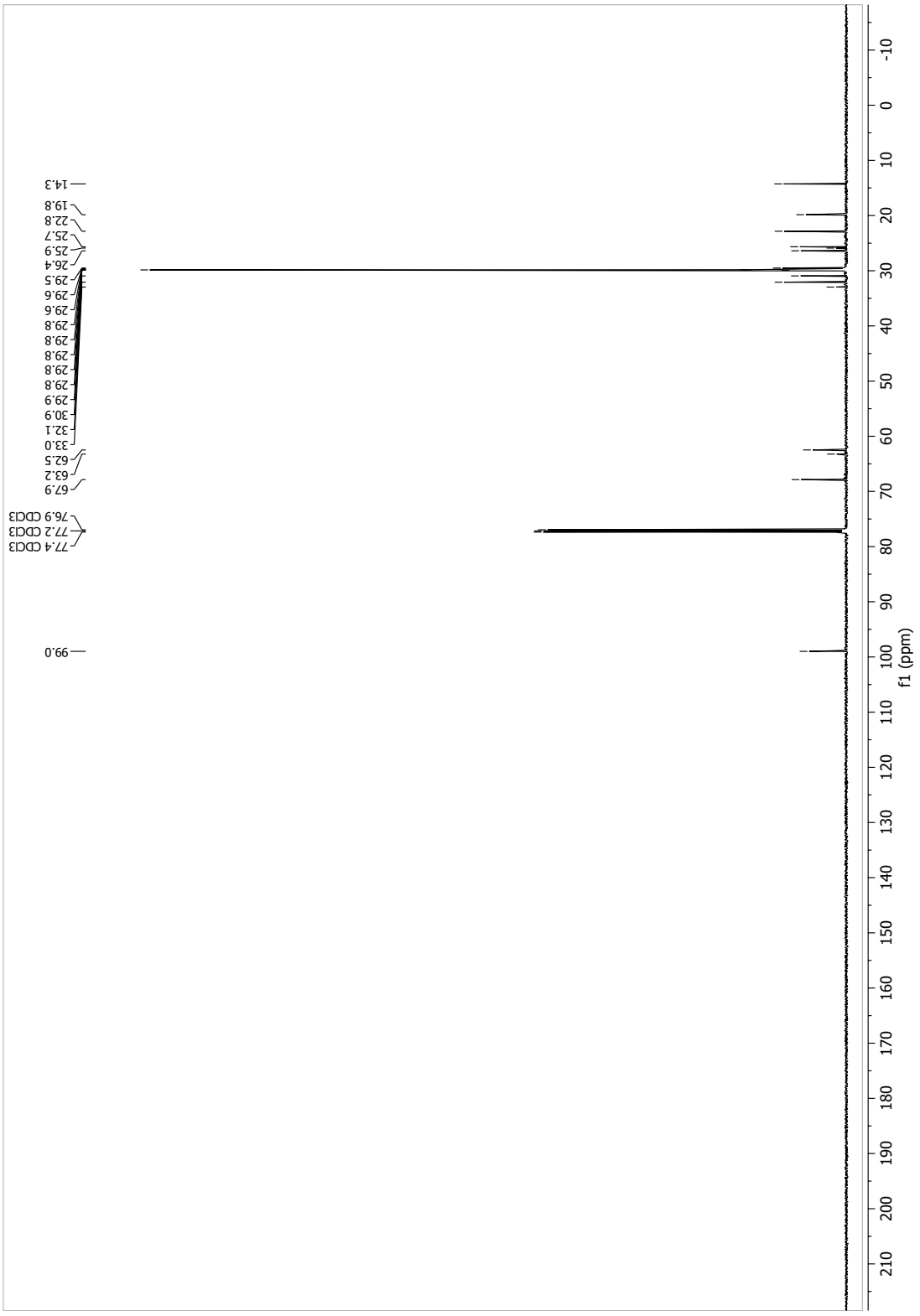
99.0
77.4 CDCl3
77.2 CDCl3
76.9 CDCl3
67.9
63.2
62.5
33.0
32.1
30.9
29.9
29.8
29.8
29.8
29.8
29.6
29.6
29.5
26.4
25.9
25.7
22.8
19.8
14.3
f1 (ppm)

13.1.35 1-Bromoheptacosane (64)

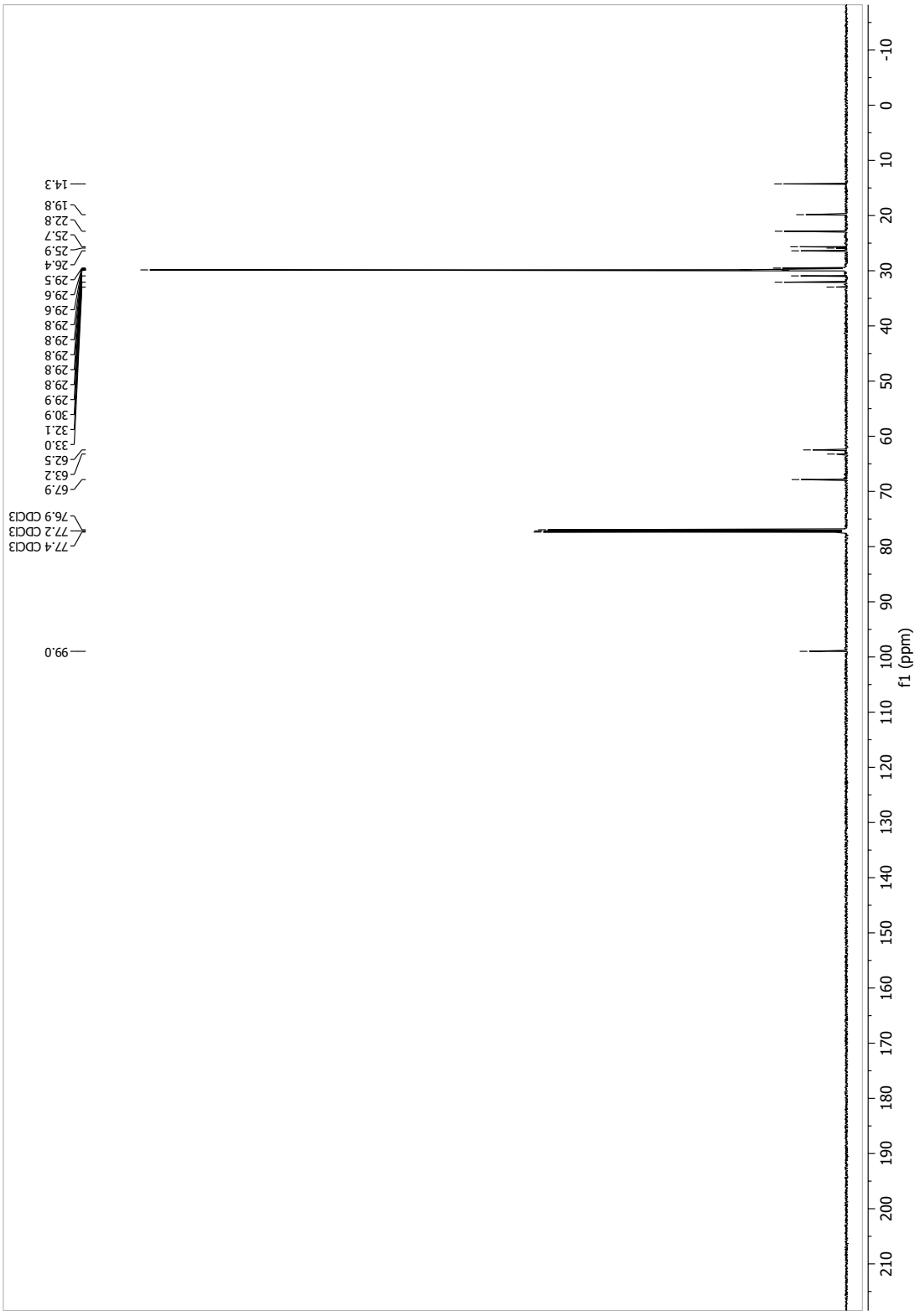

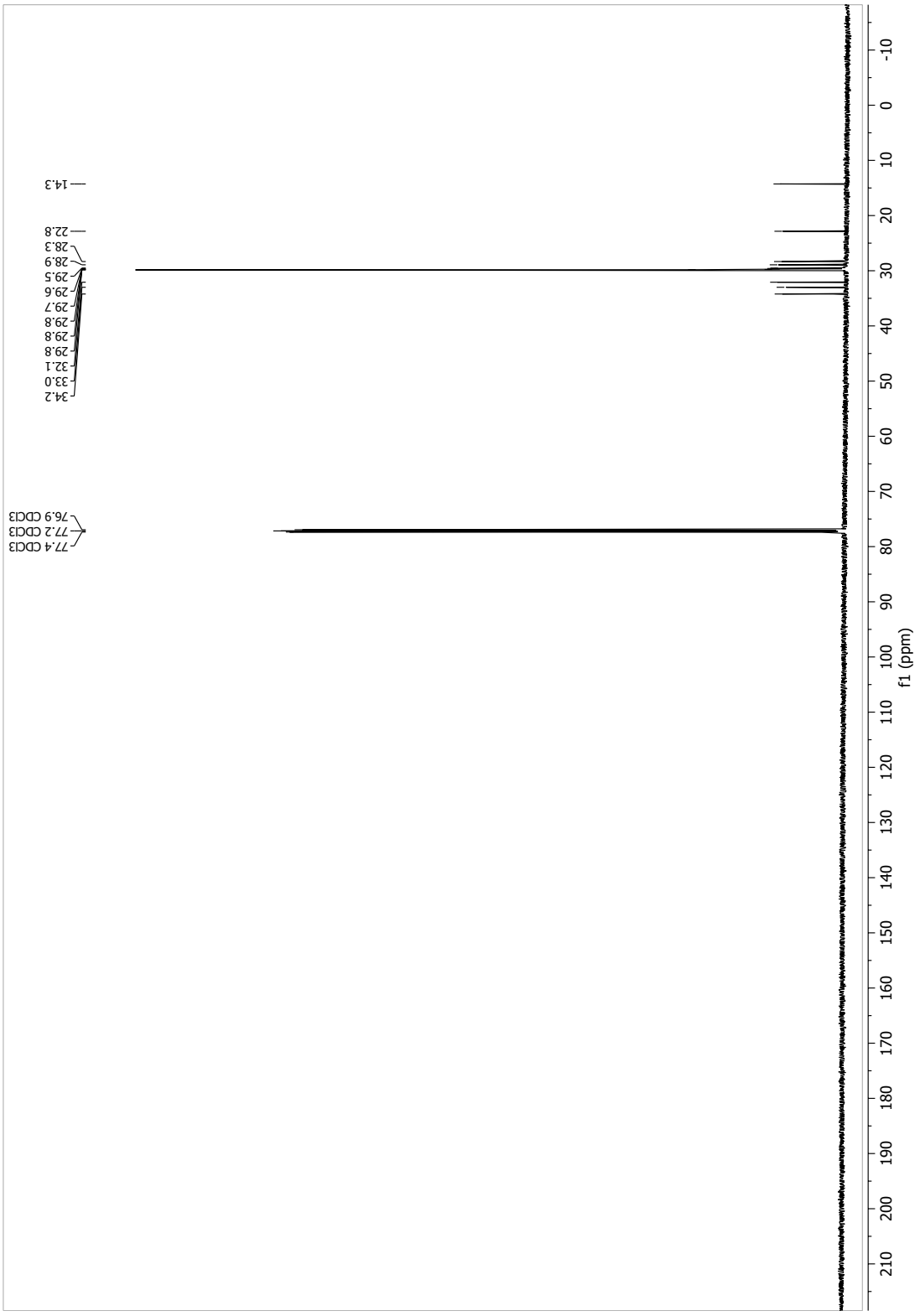
77.4 CDCl3
77.2 CDCl3
76.9 CDCl3
34.2
33.0
32.1
29.8
29.8
29.8
29.7
29.6
29.5
28.9
28.3
22.8
14.3
f1 (ppm)

13.1.36 (*R*)-*tert*-butyl(hentriacont-3-yn-2-yloxy)dimethylsilane (65)

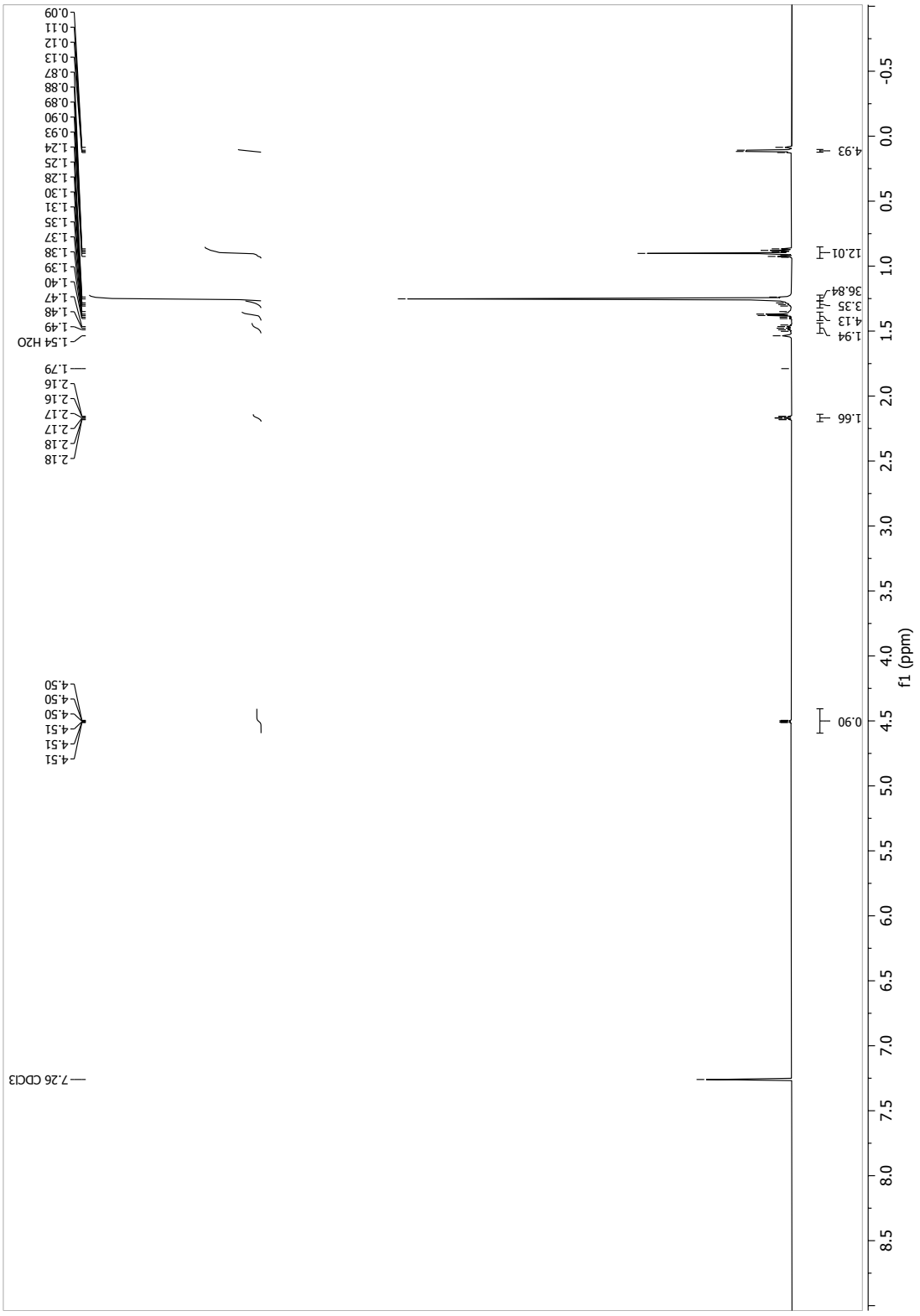

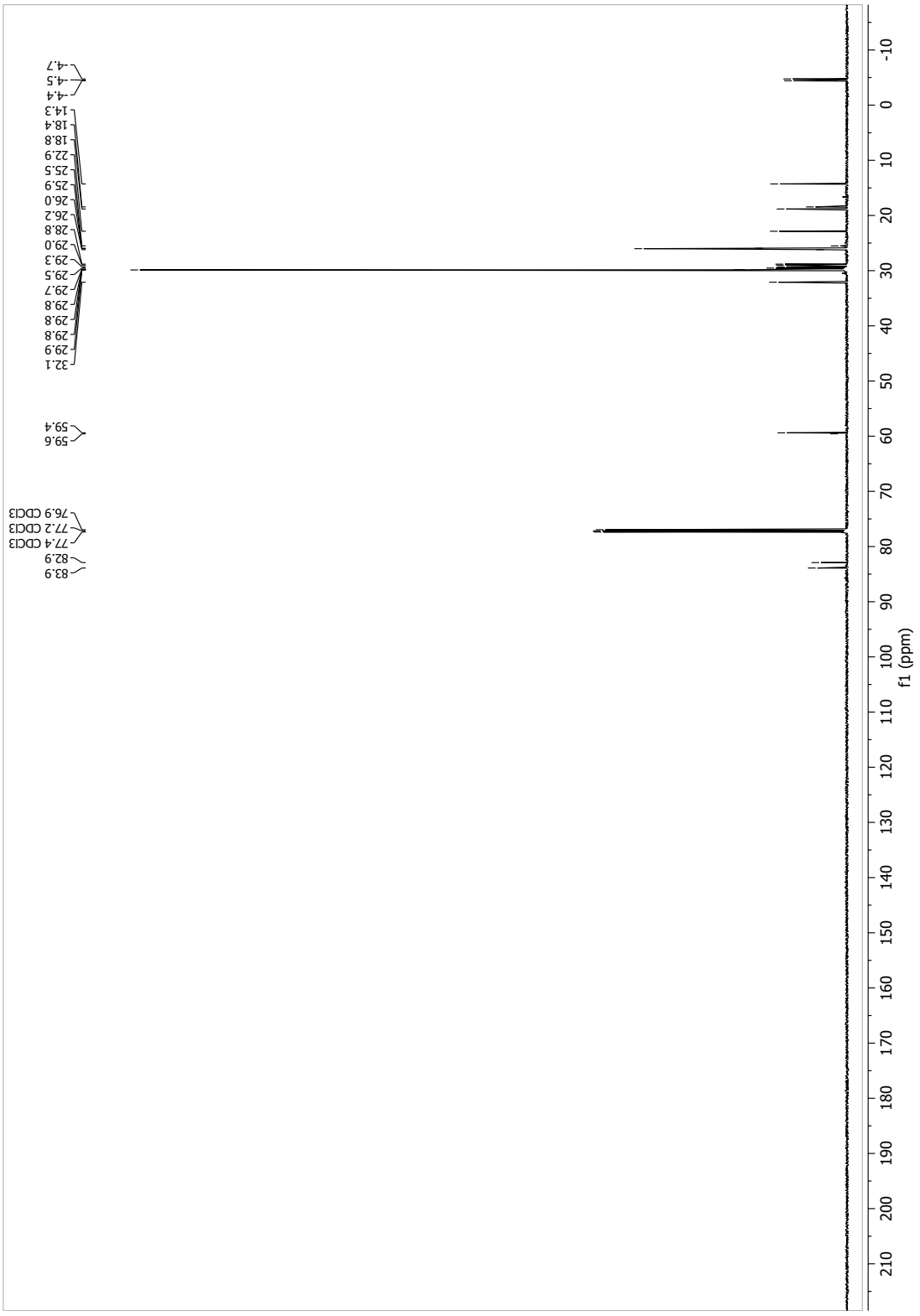
83.9
82.9
77.4 CDCl3
77.2 CDCl3
76.9 CDCl3
59.6
59.4
32.1
29.9
29.8
29.8
29.8
29.7
29.5
29.3
29.0
28.8
26.2
26.0
25.9
25.5
22.9
18.8
18.4
14.3
-4.4
-4.5
-4.7
f1 (ppm)

13.1.37 (*R*)-*tert*-butyl(hentriacontan-2-yloxy)dimethylsilane (66a)

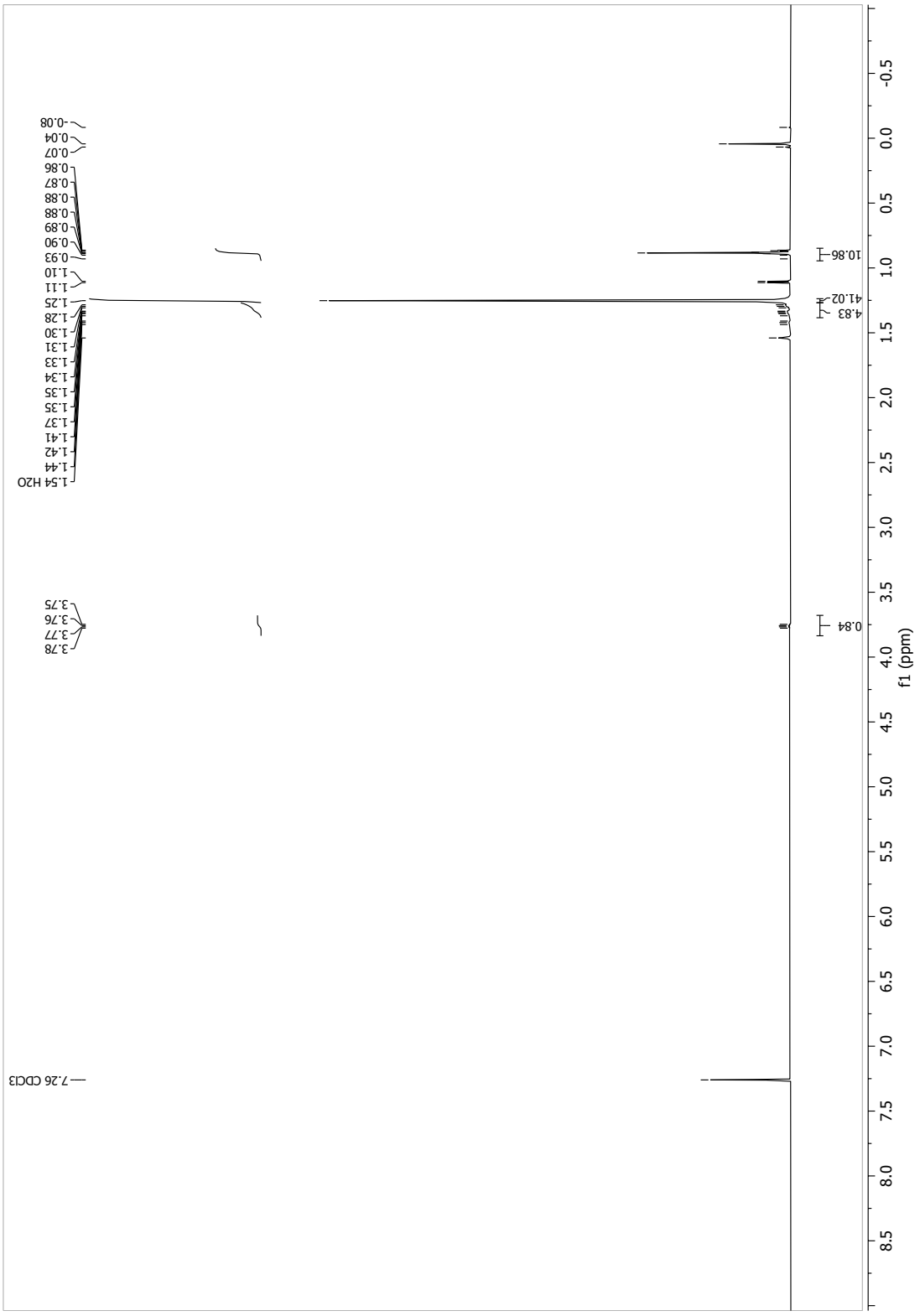

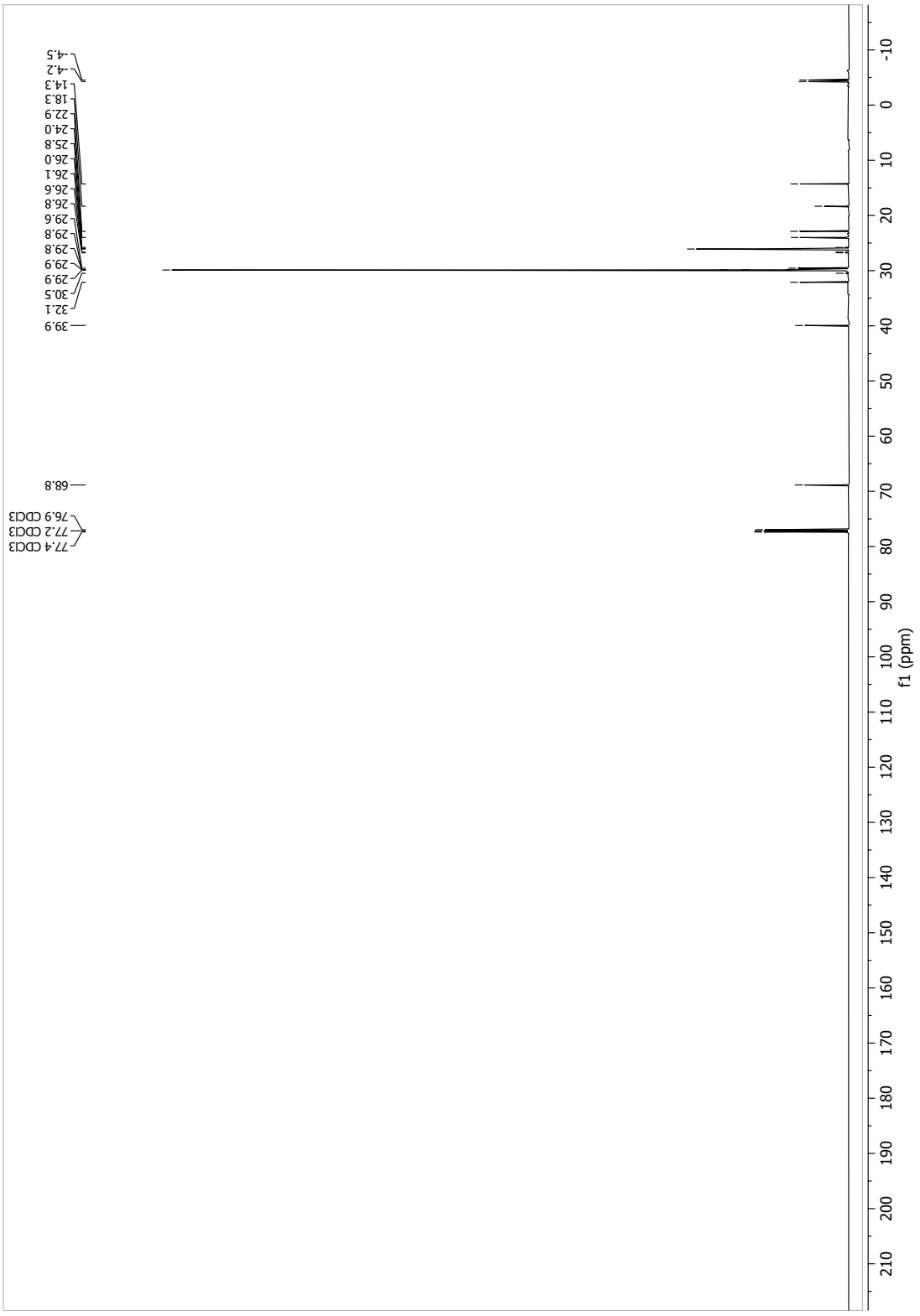
77.4 CDCl3
77.2 CDCl3
76.9 CDCl3
68.8
39.9
32.1
30.5
29.9
29.9
29.9
29.8
29.6
26.8
26.6
26.1
26.0
25.8
24.0
22.9
18.3
14.3
-4.2
-4.5
f1 (ppm)

13.1.38 [D_4]-(*R*)-*tert*-butyl(hentriacontan-2-yloxy)dimethylsilane (66b)

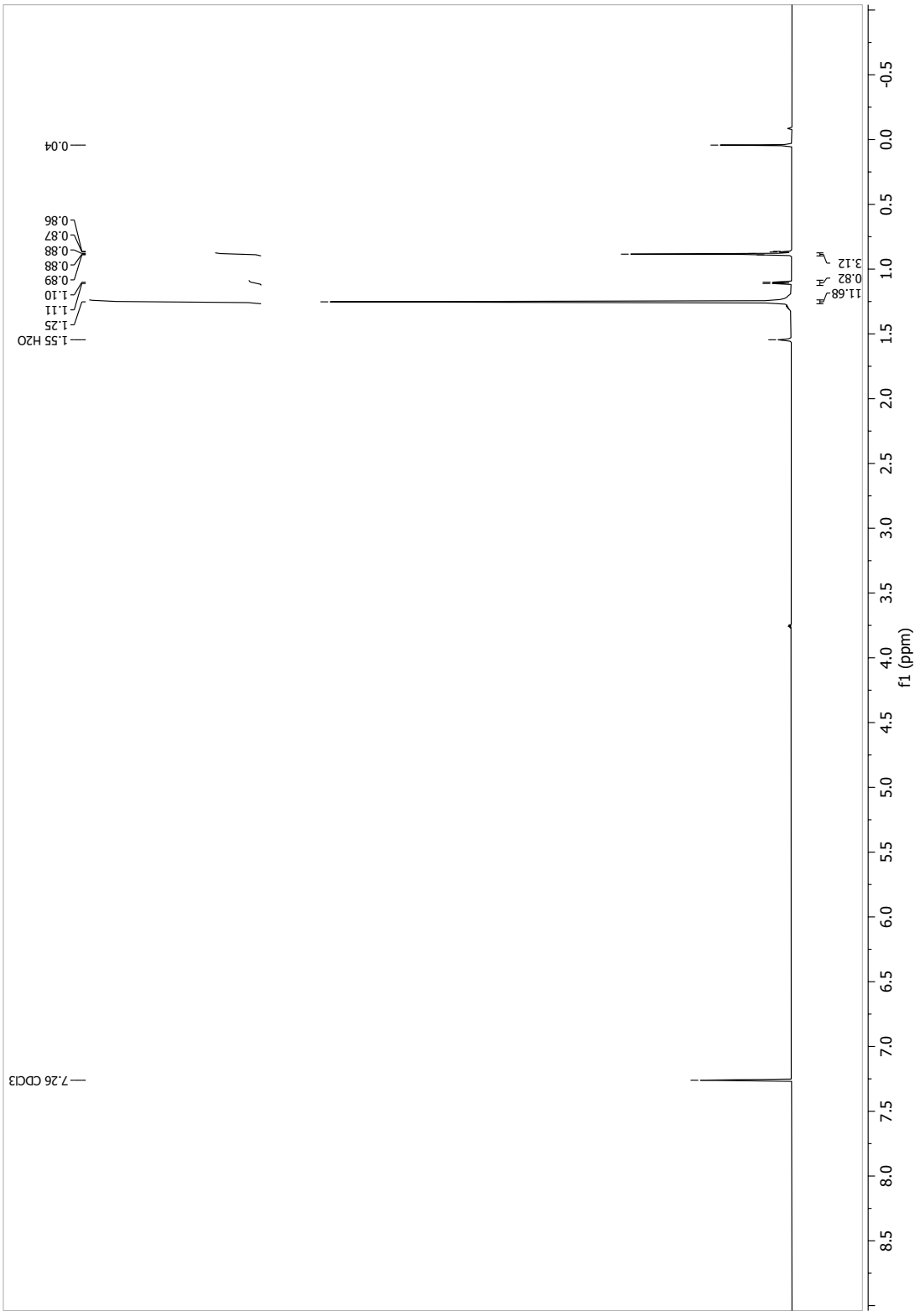

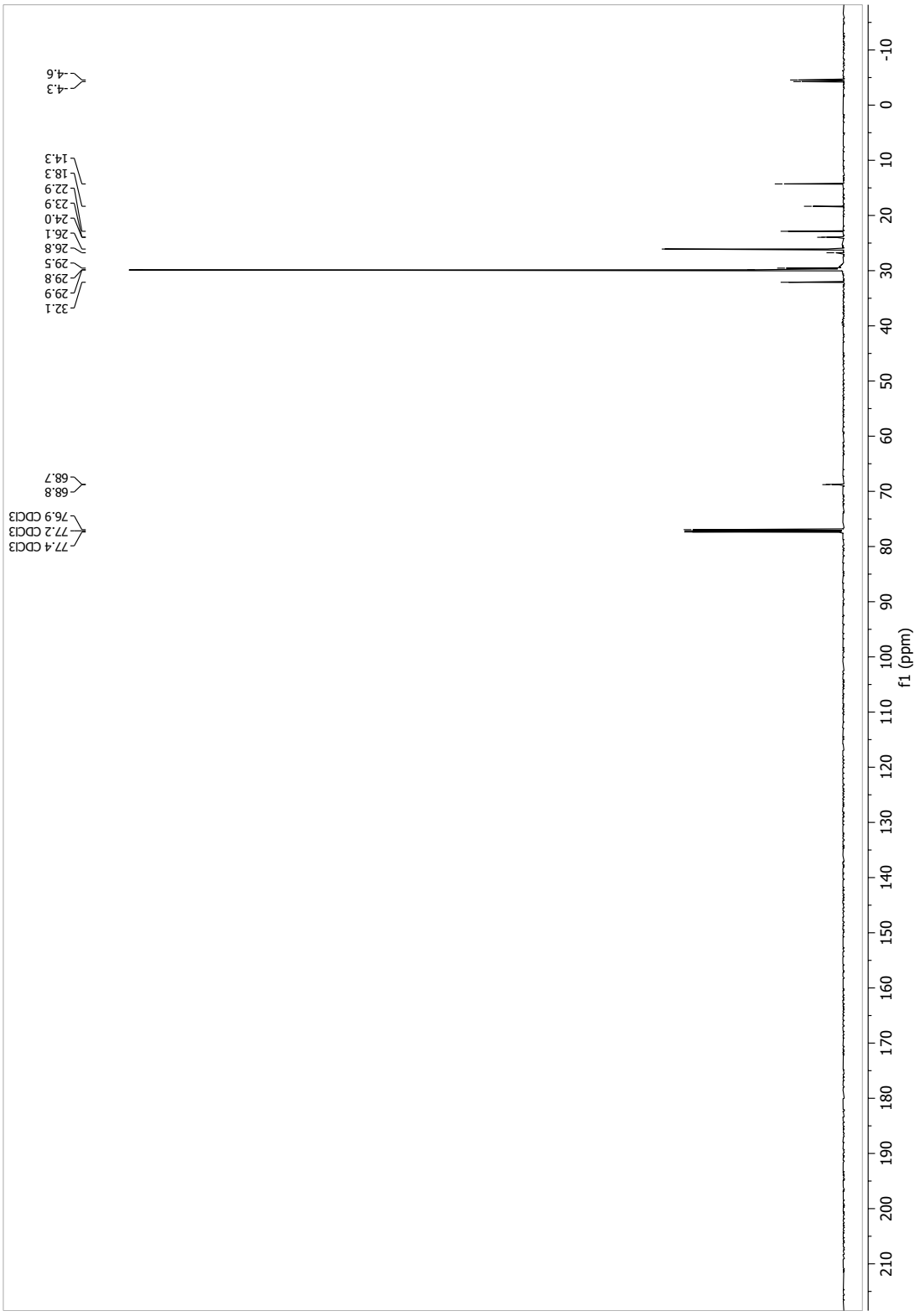
77.4 CDCl3
77.2 CDCl3
76.9 CDCl3
68.8
68.7
32.1
29.9
29.8
29.5
26.8
26.1
24.0
23.9
22.9
18.3
14.3
-4.3
-4.6
f1 (ppm)

13.1.39 (*R*)-Hentriacontan-2-ol (58a)

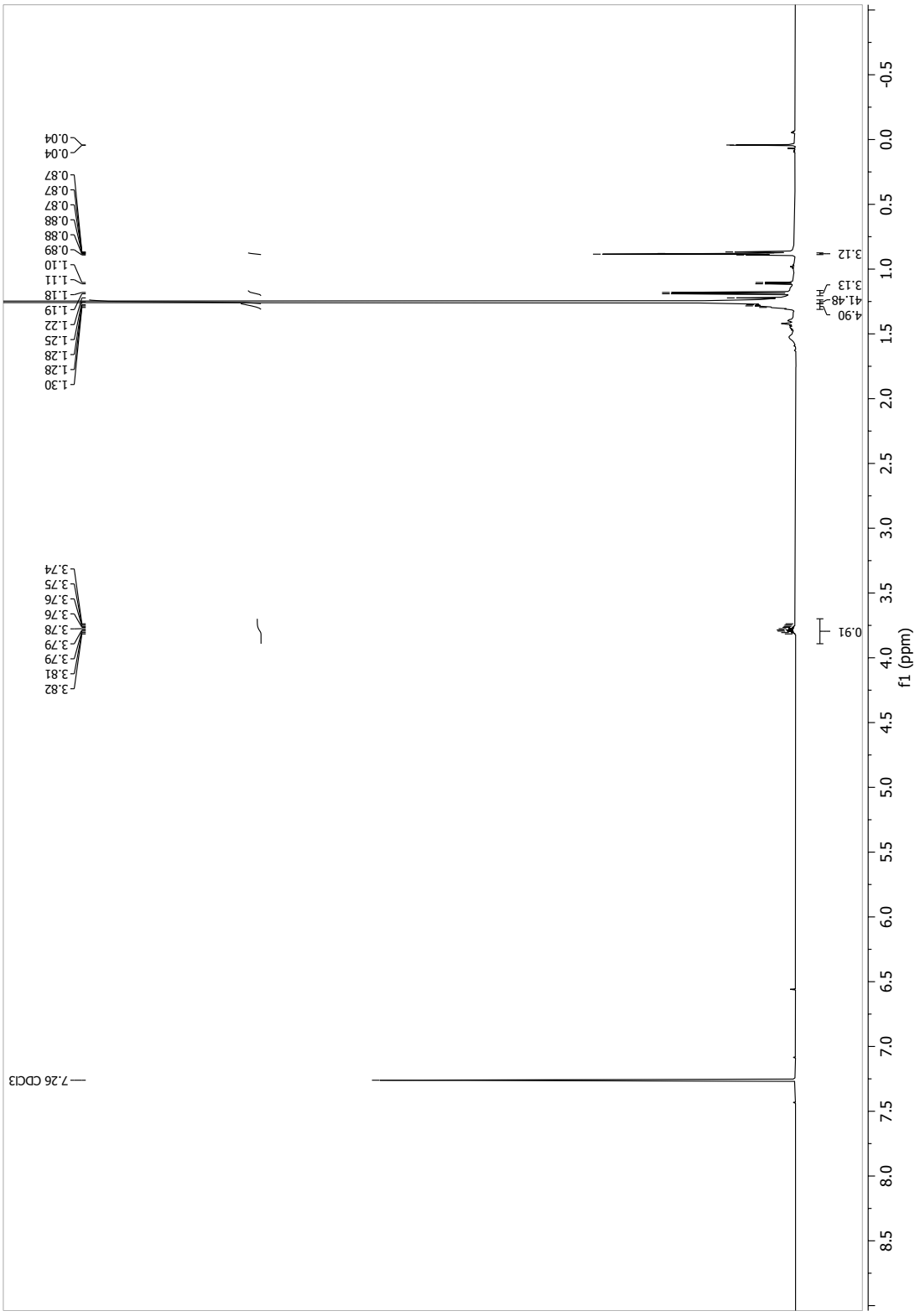

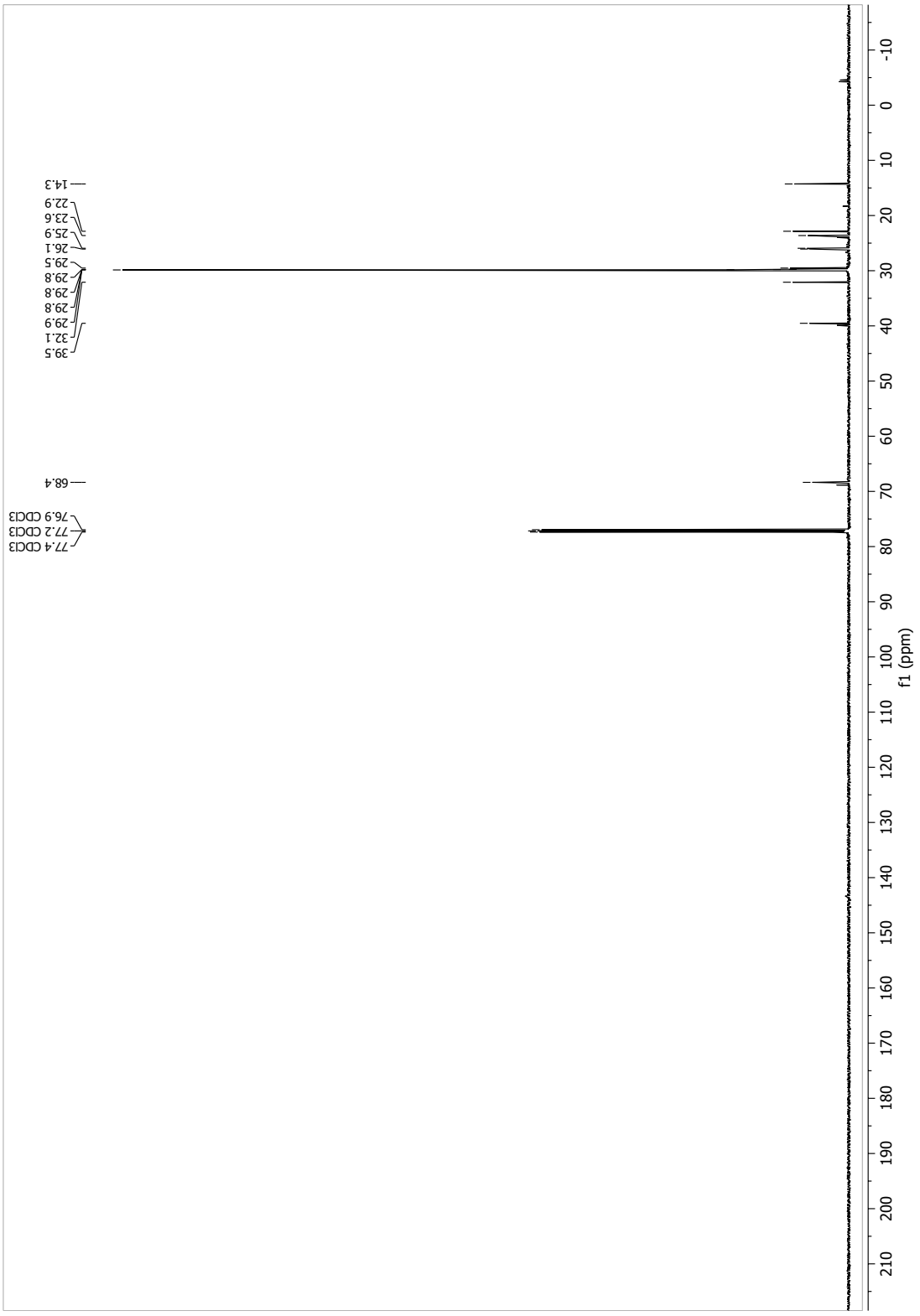
77.4 CDCl3
77.2 CDCl3
76.9 CDCl3
68.4
39.5
32.1
29.9
29.8
29.8
29.8
29.5
26.1
25.9
23.6
22.9
14.3
f1 (ppm)

13.1.40 [D_4]-(*R*)-hentriacontan-2-ol (58b)

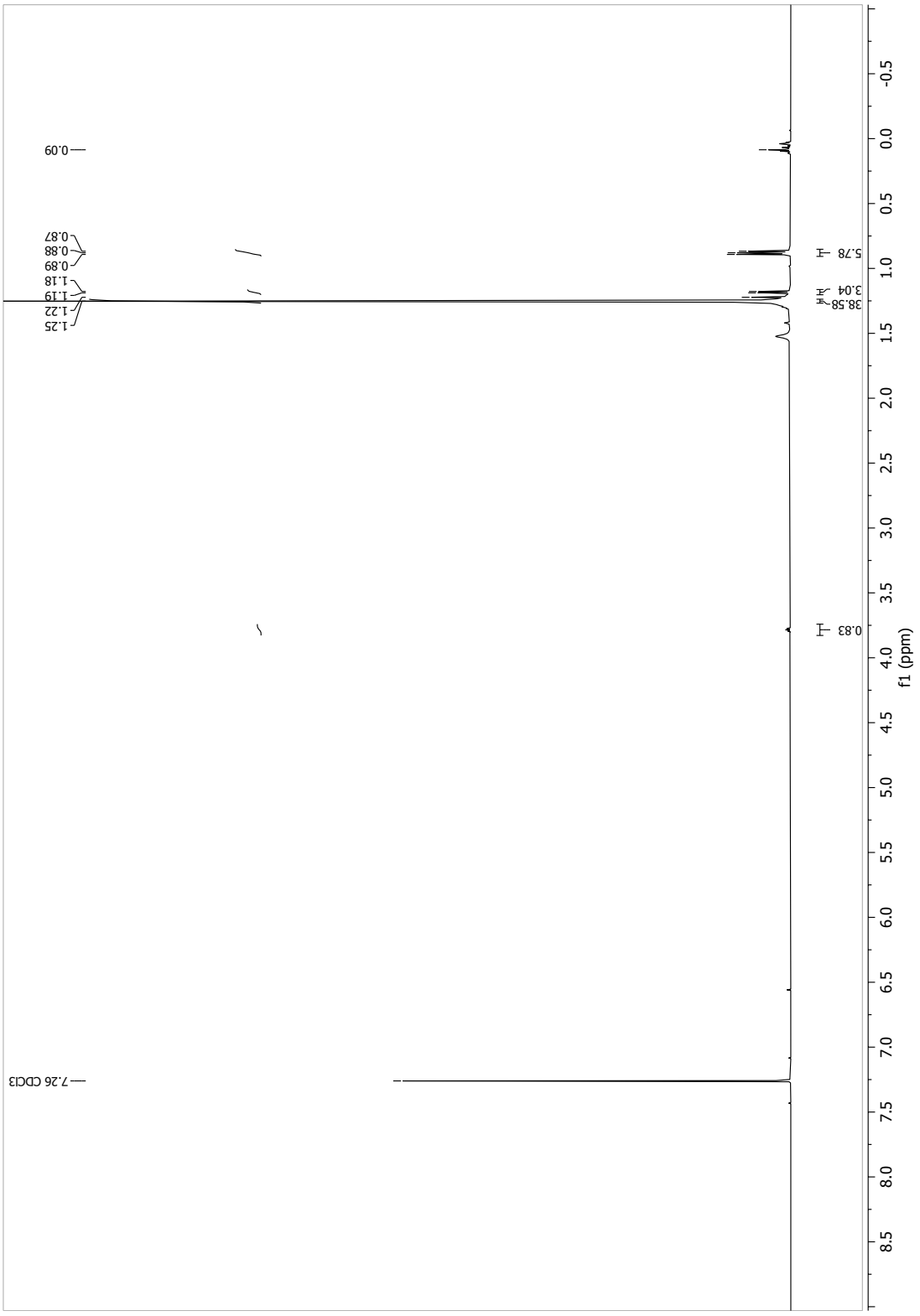

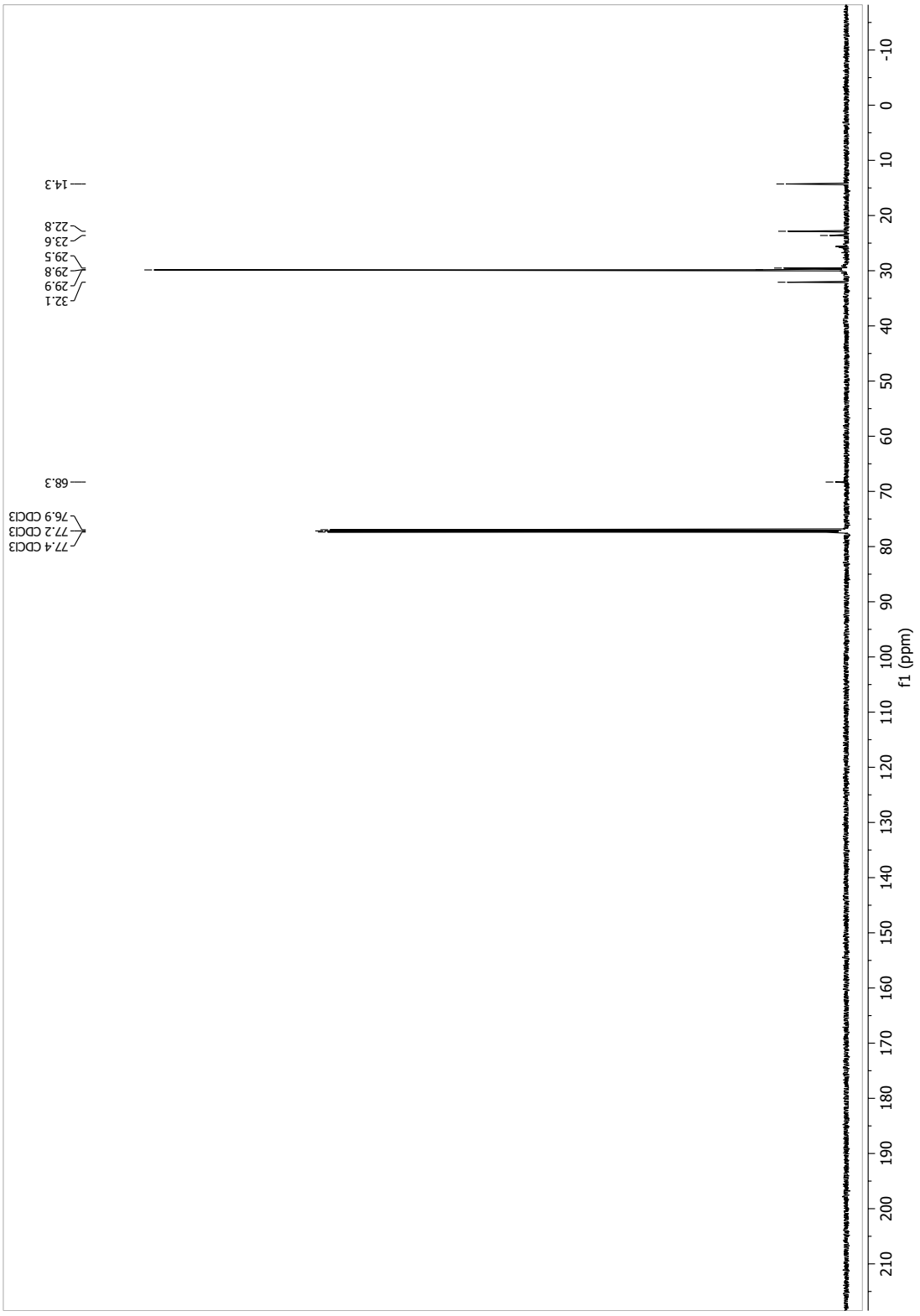
14.3
22.8
23.6
29.5
29.8
29.9
32.1
68.3
76.9 CDCl3
77.2 CDCl3
77.4 CDCl3
f1 (ppm)

13.1.41 *Tert*-butyldimethyl(prop-2-yn-1-yloxy)silane (72)

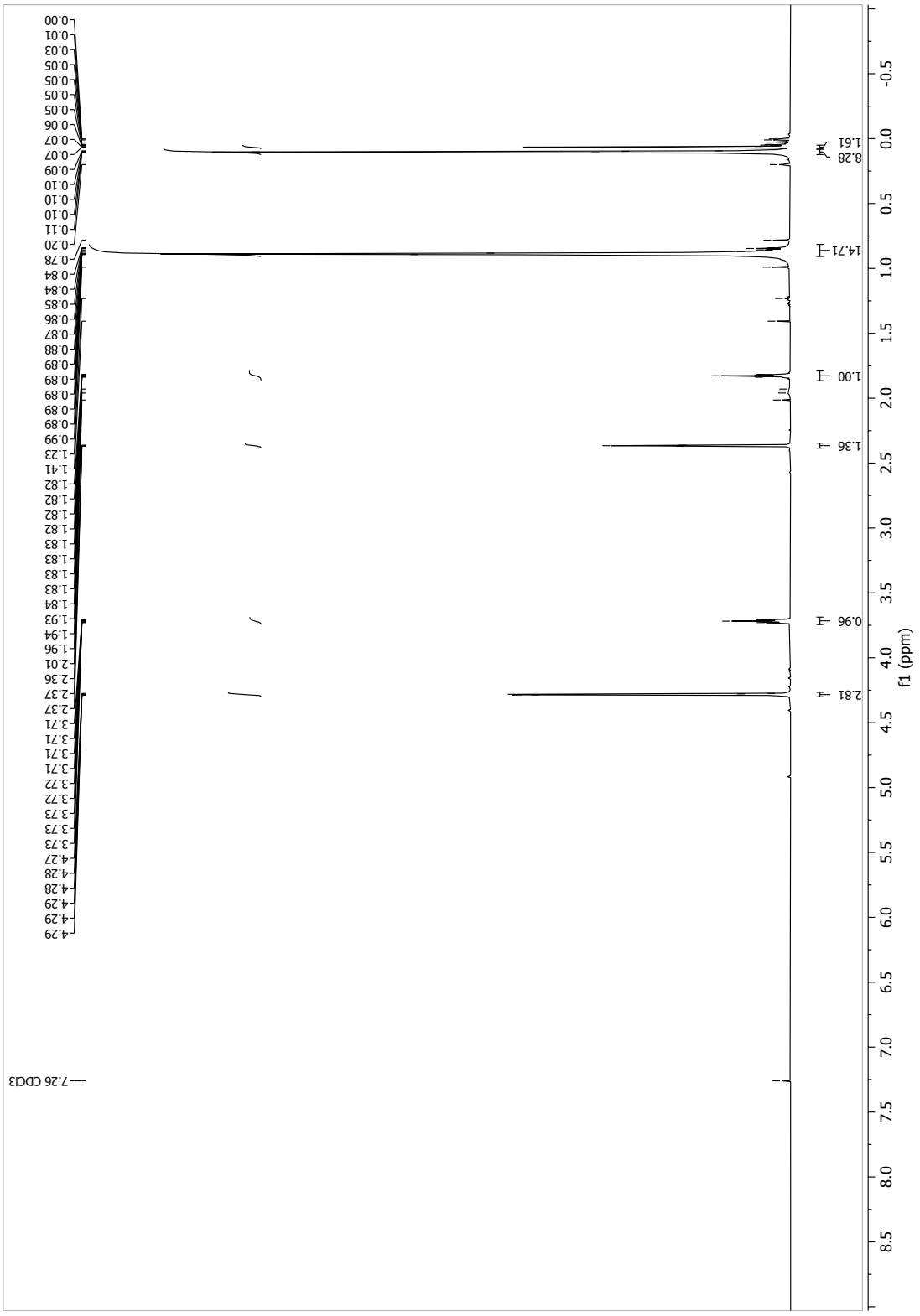

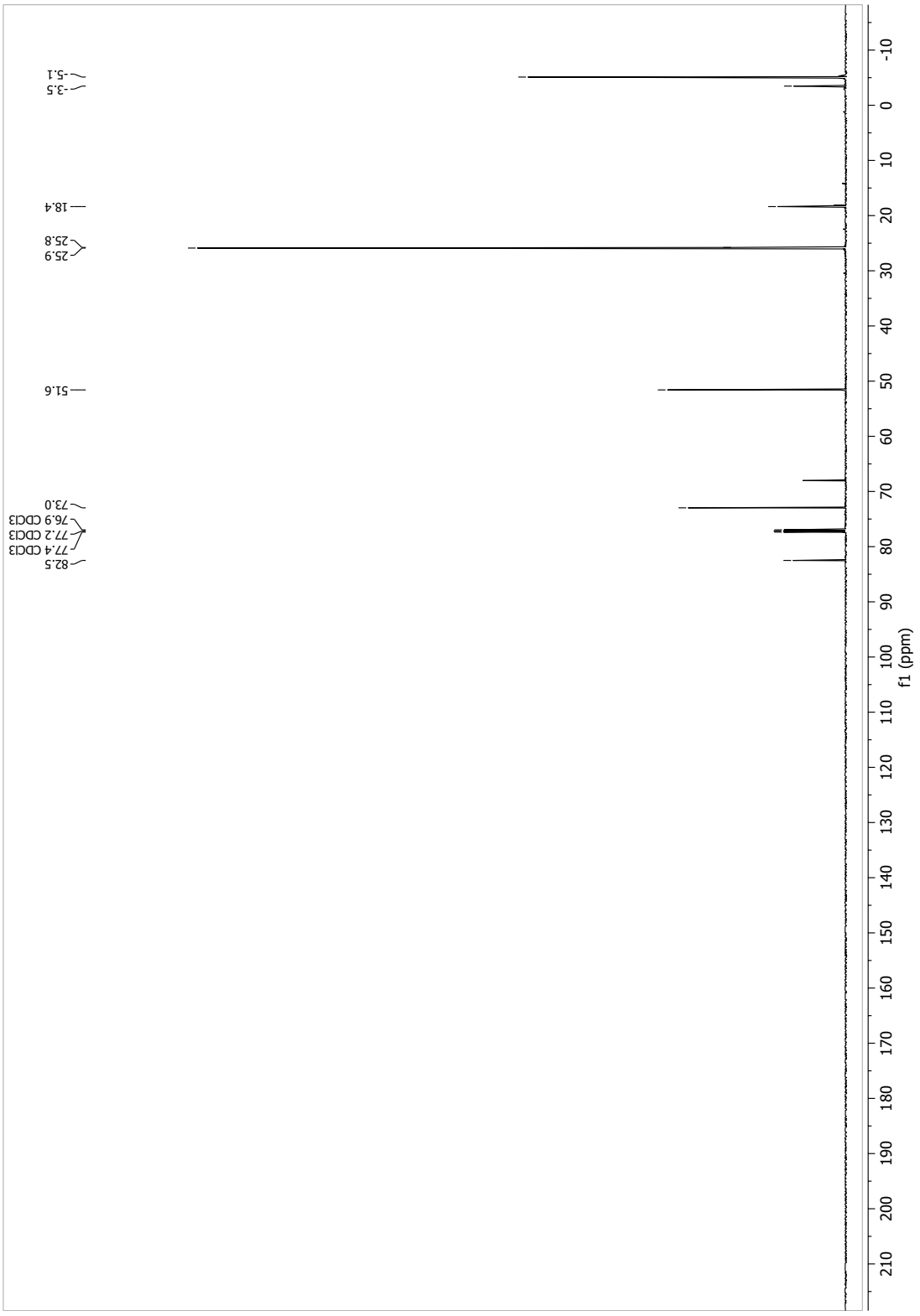
-5.1
-3.5
18.4
25.9
25.8
51.6
73.0
76.9 CDCl3
77.2 CDCl3
77.4 CDCl3
82.5
f1 (ppm)

13.1.42 *Tert*-butyl(henicos-2-yn-1-yloxy)dimethylsilane (74)

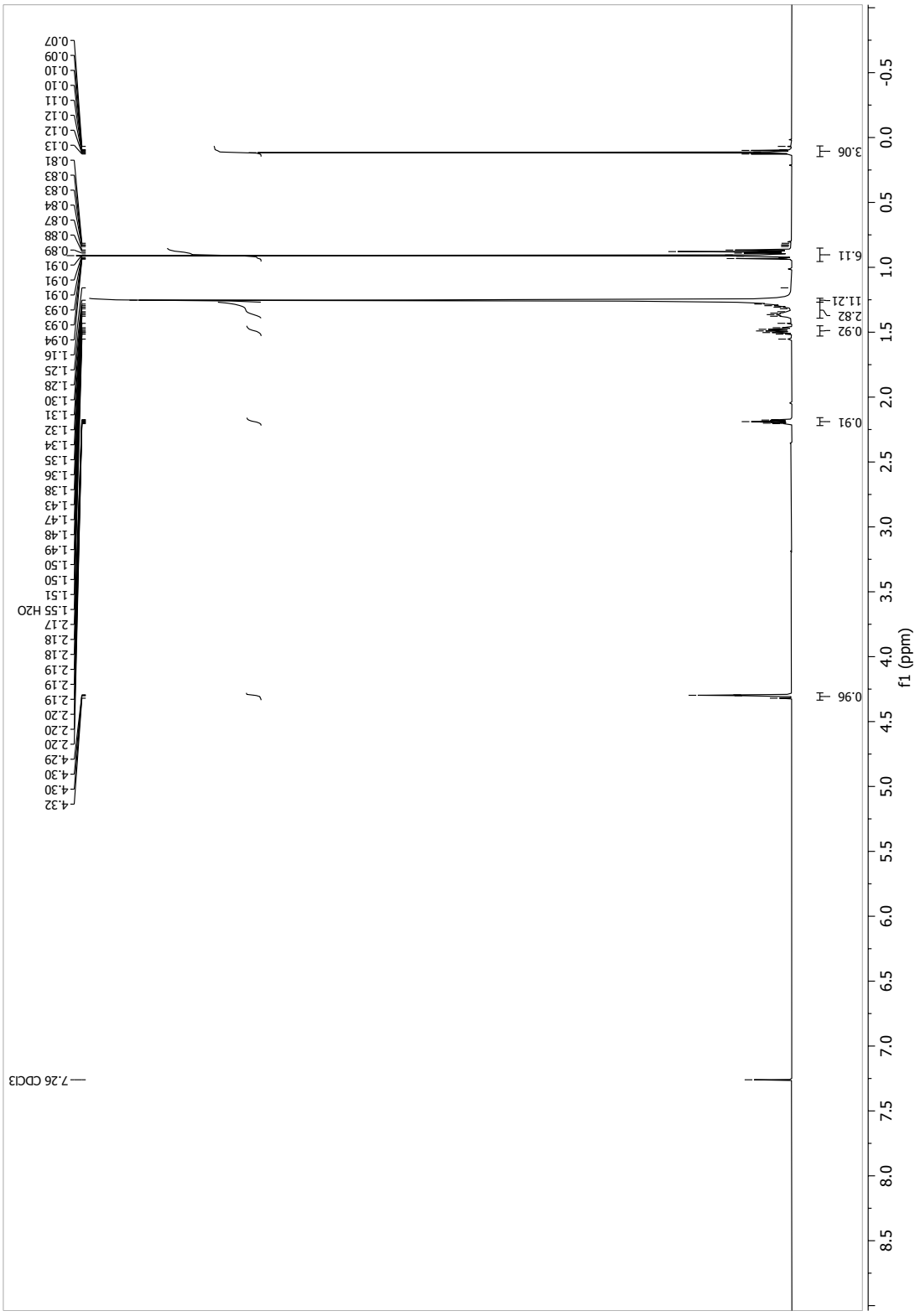

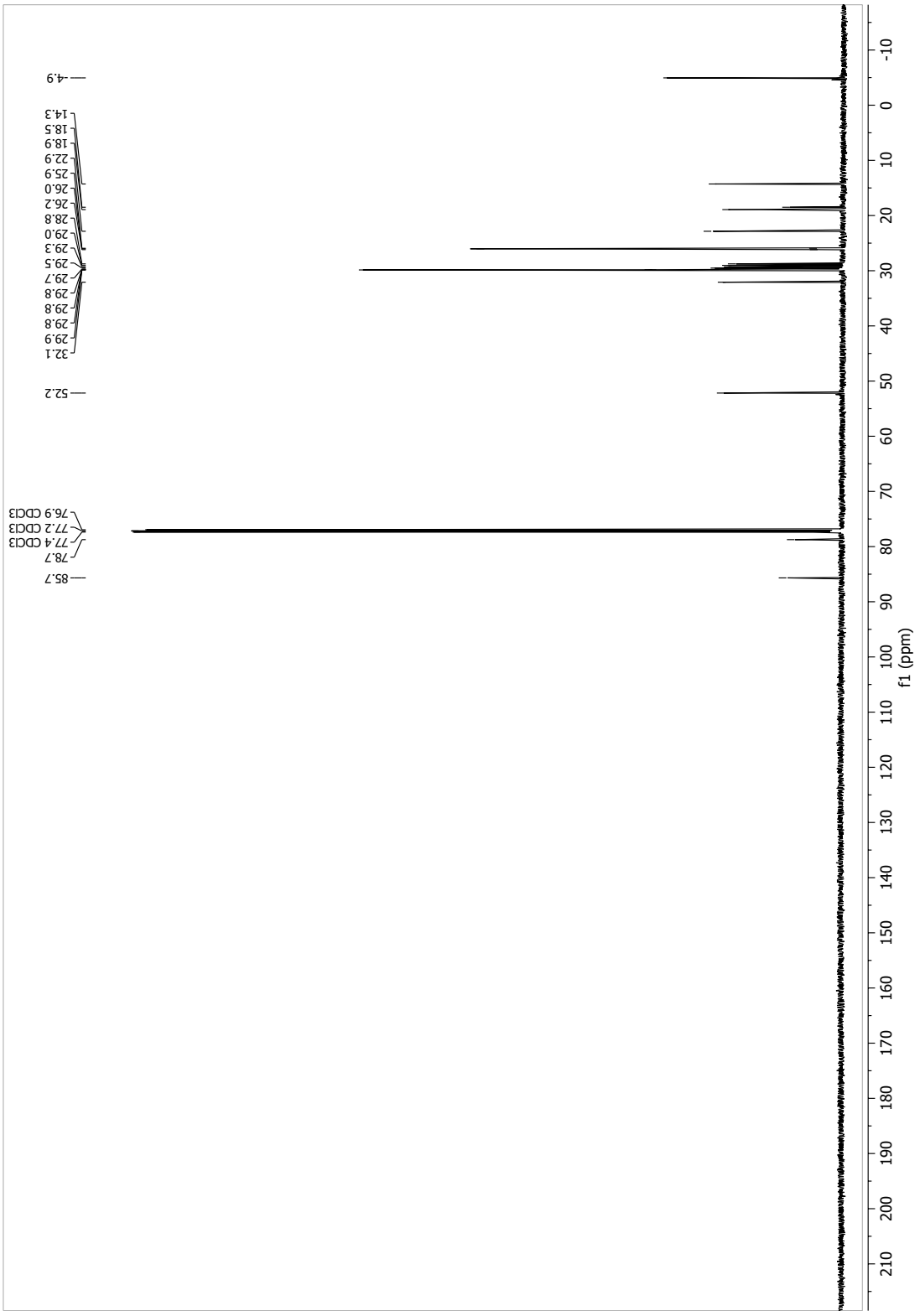
-4.9
14.3
18.5
18.9
22.9
25.9
26.0
26.2
28.8
29.0
29.3
29.5
29.7
29.8
29.8
29.8
29.9
32.1
52.2
76.9 CDCl3
77.2 CDCl3
77.4 CDCl3
78.7
85.7
f1 (ppm)

13.1.43 [D_4]-*tert*-butyl(henicosyloxy)dimethylsilane (75)

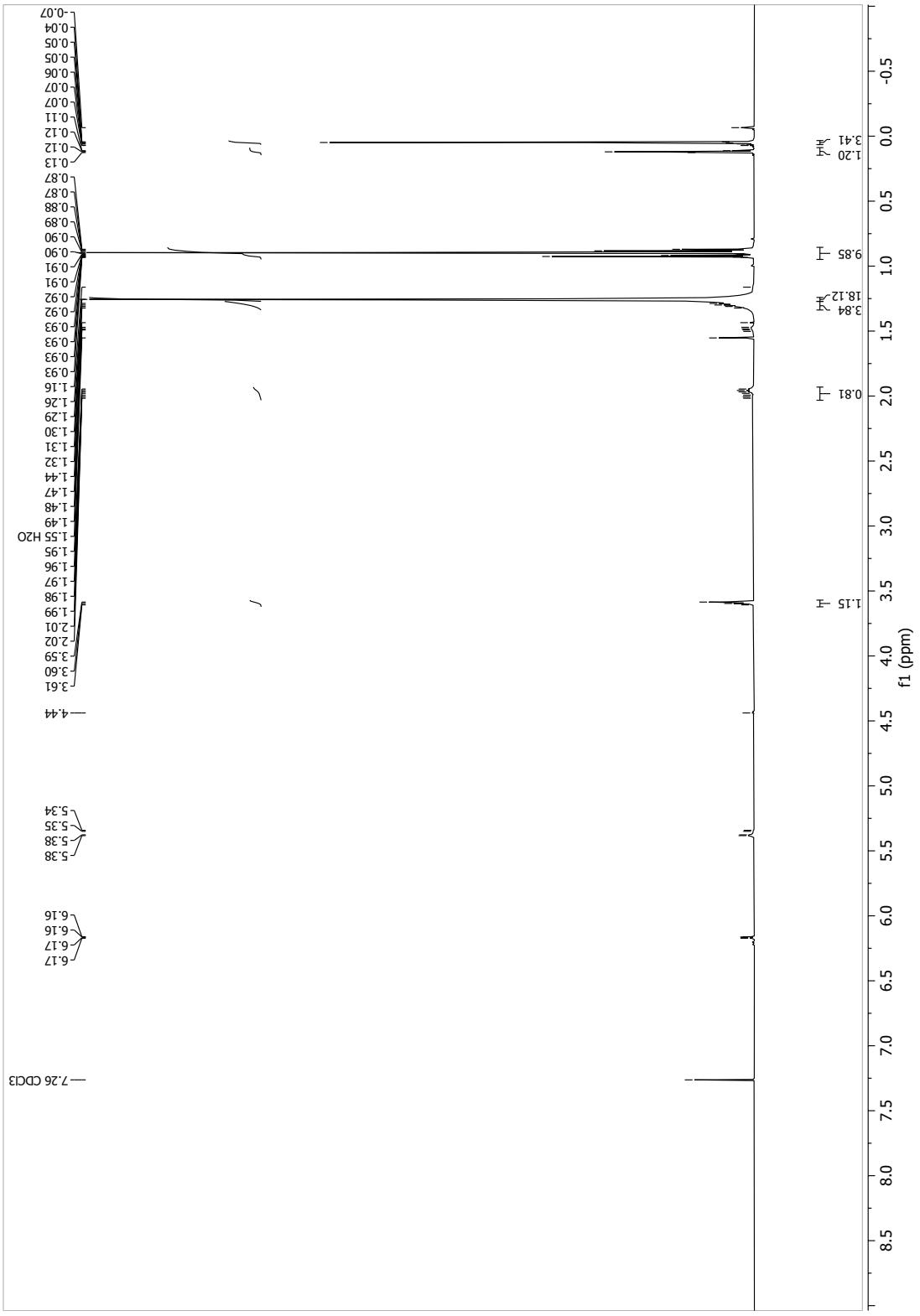

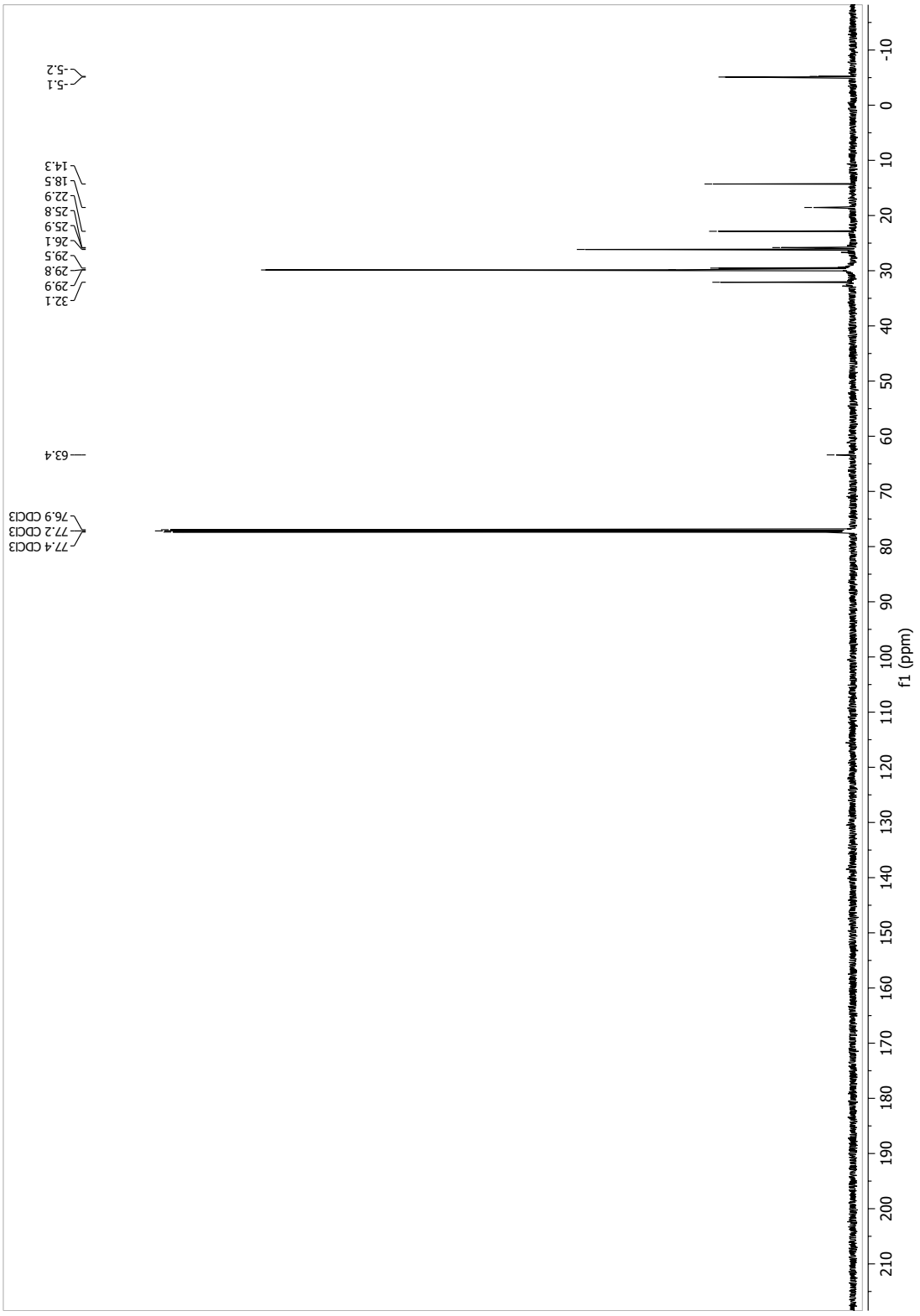
77.4 CDCl3
77.2 CDCl3
76.9 CDCl3
63.4
32.1
29.9
29.8
29.5
26.1
25.9
25.8
22.9
18.5
14.3
-5.1
-5.2
f1 (ppm)

13.1.44 [D_4]-henicosan-1-ol (68a)

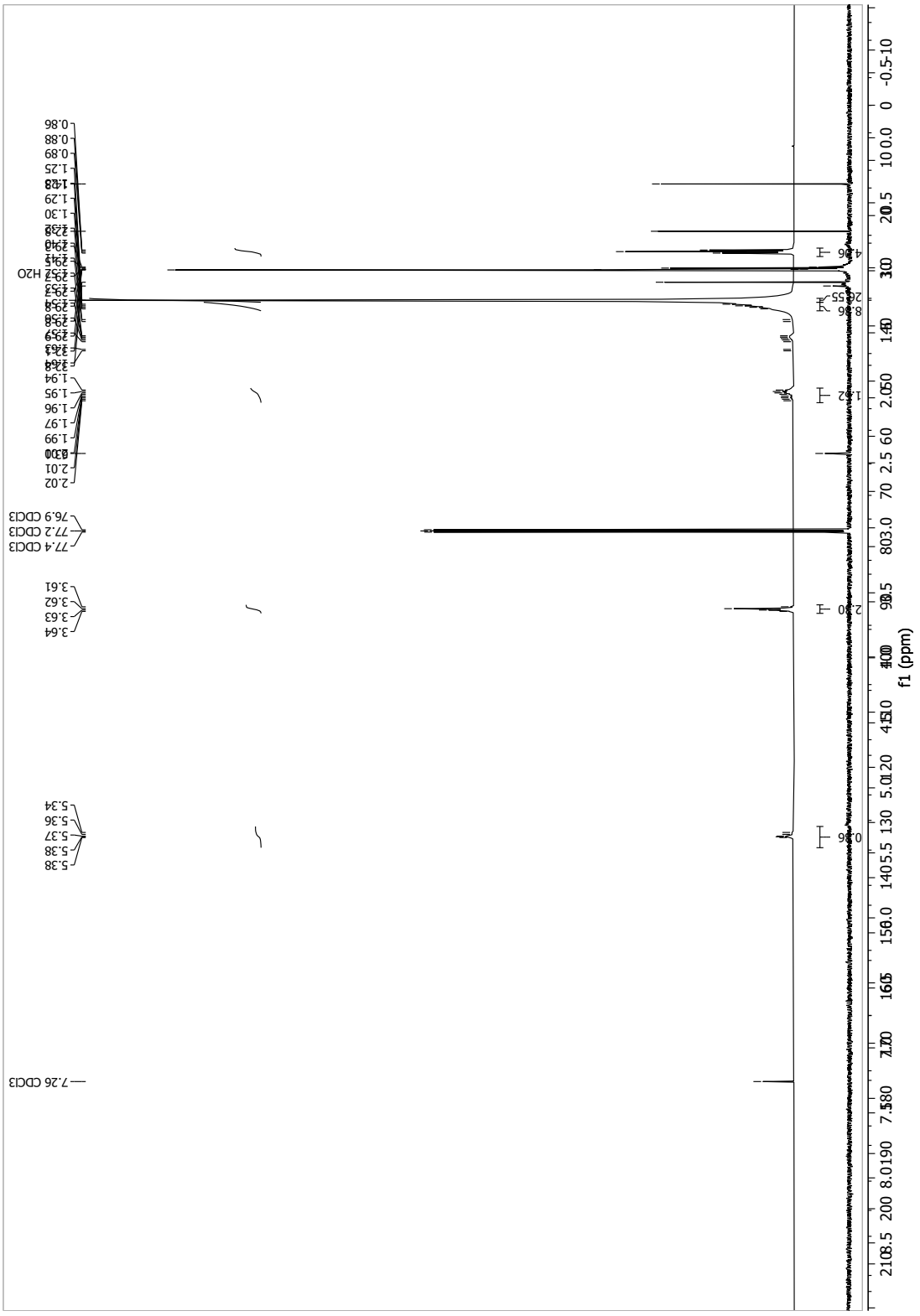

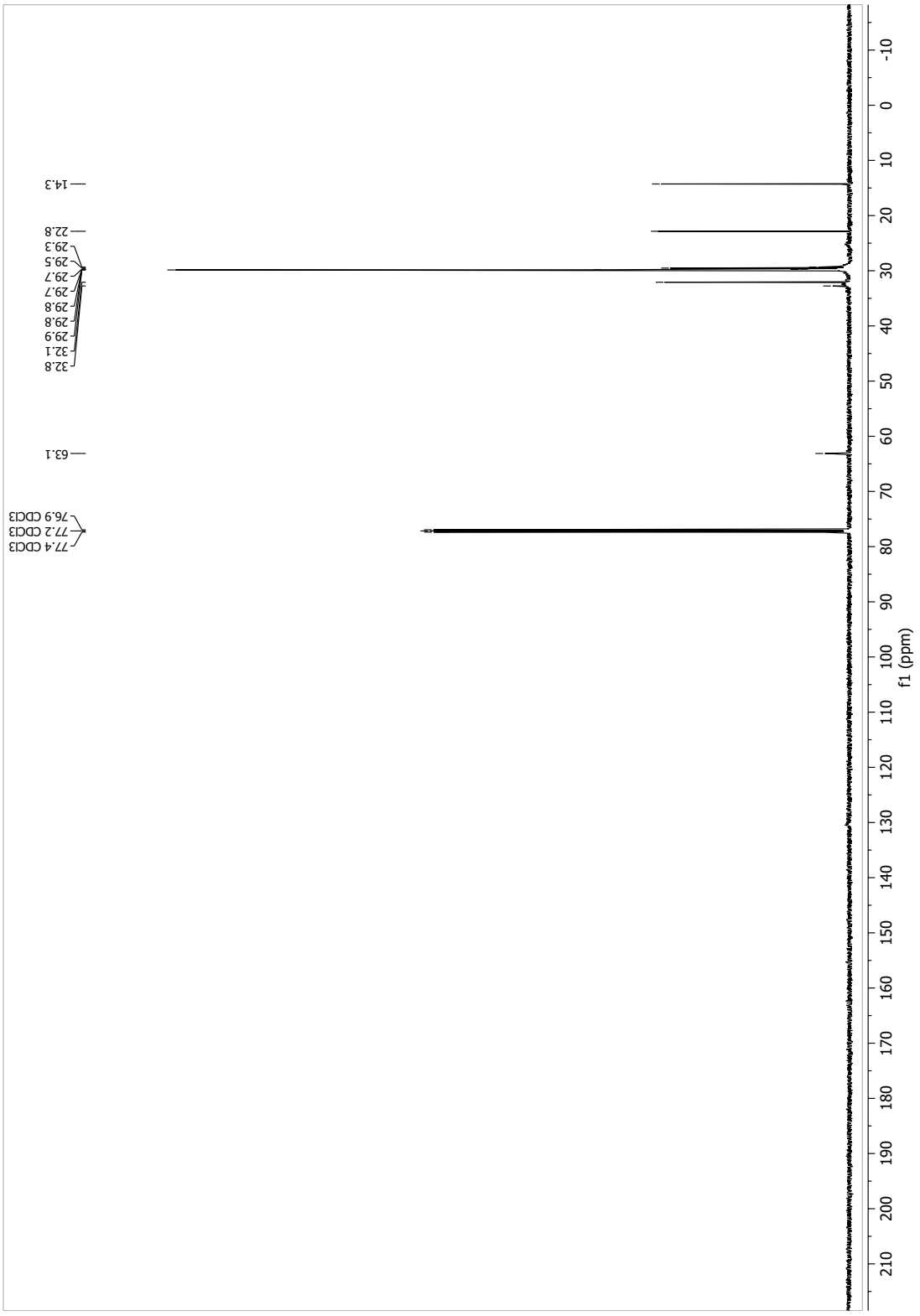
77.4 CDCl3
77.2 CDCl3
76.9 CDCl3
63.1
32.8
32.1
29.9
29.8
29.7
29.8
29.7
29.5
29.3
22.8
14.3
f1 (ppm)

13.1.45 Ethyl 2-acetyltridec-12-enoate (99)

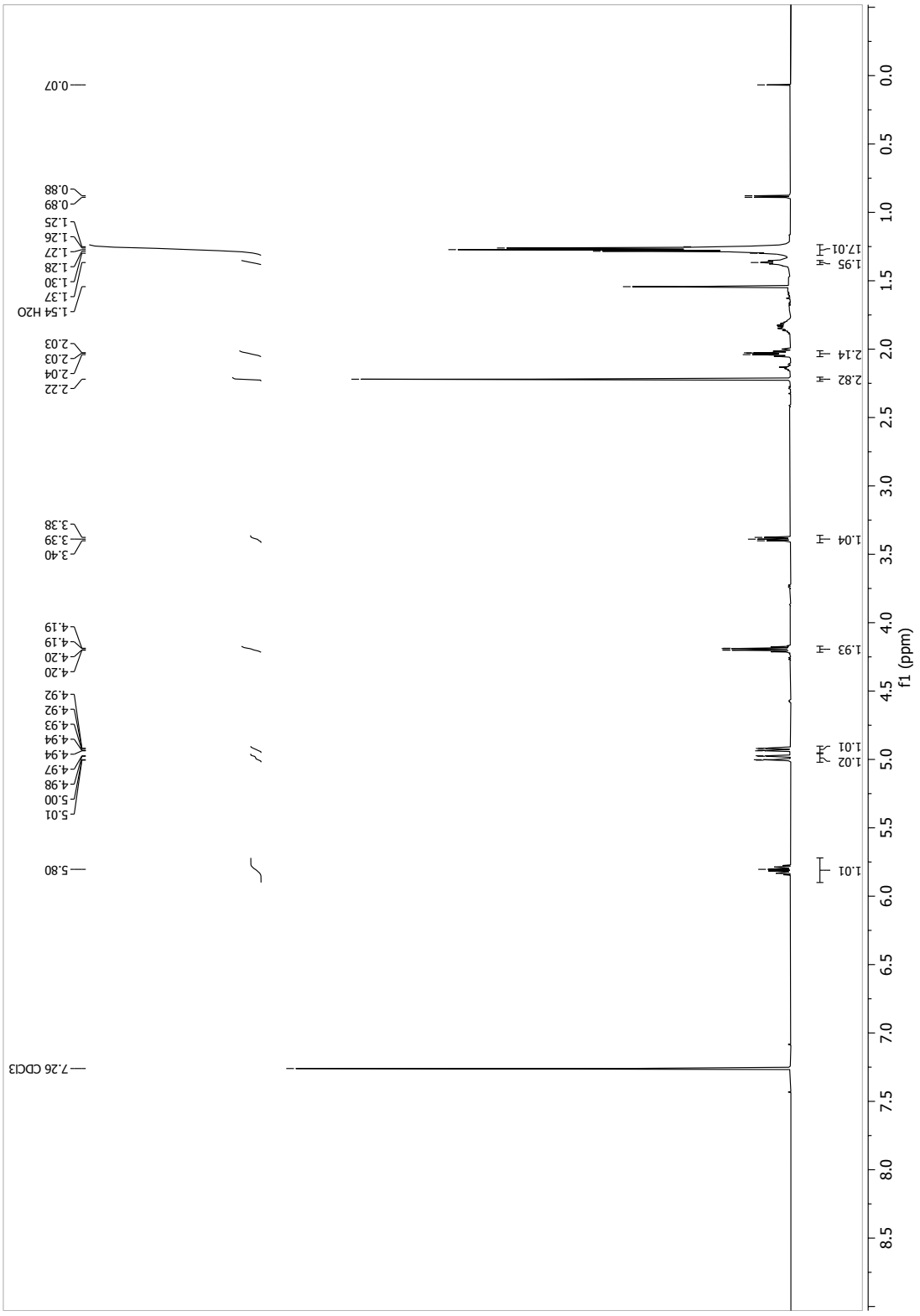

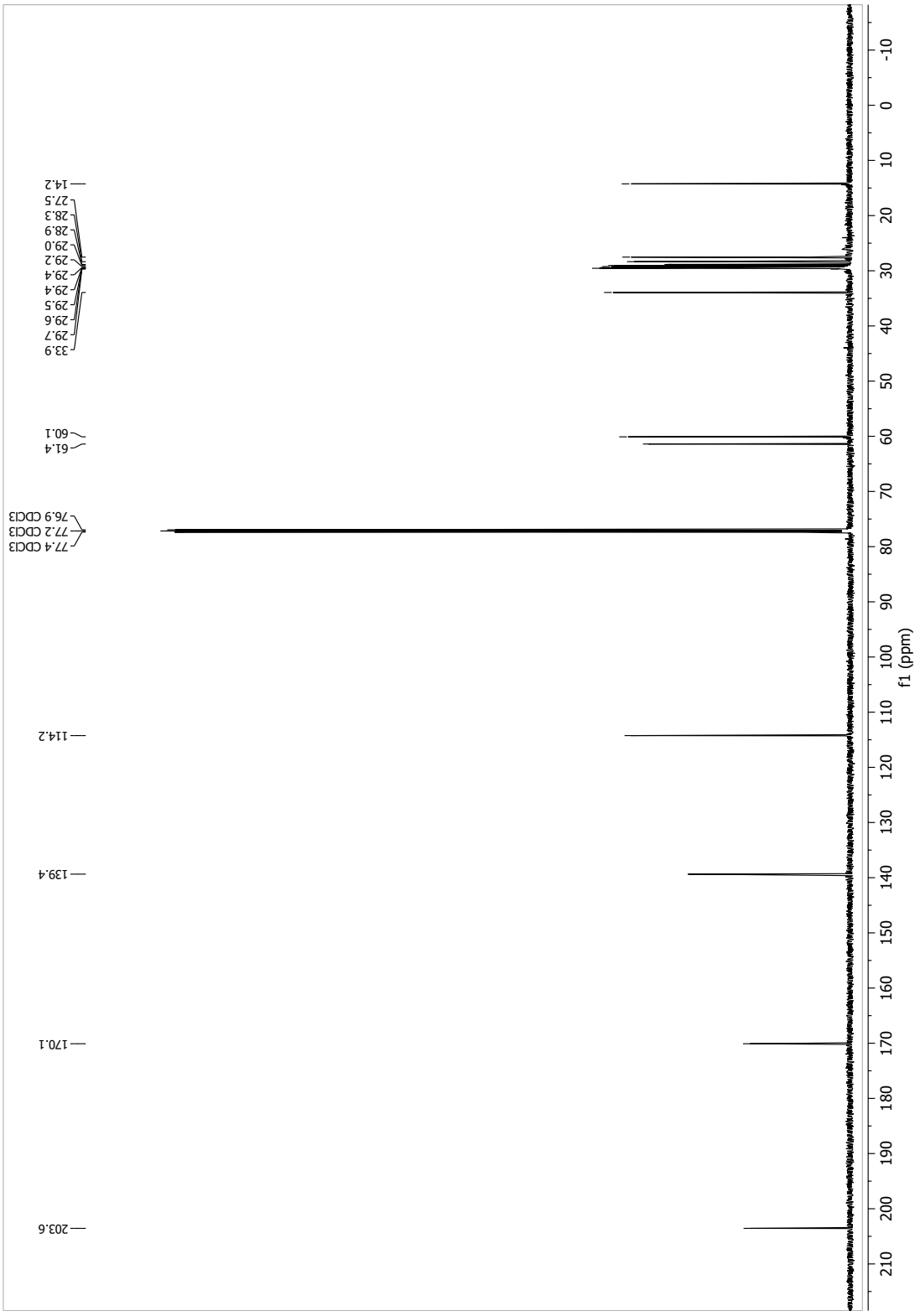
203.6
170.1
139.4
114.2
77.4 CDCl3
77.2 CDCl3
76.9 CDCl3
61.4
60.1
33.9
29.7
29.6
29.5
29.4
29.4
29.2
29.0
28.9
28.3
27.5
14.2
f1 (ppm)

13.1.46 Tetradec-13-en-2-one (94)

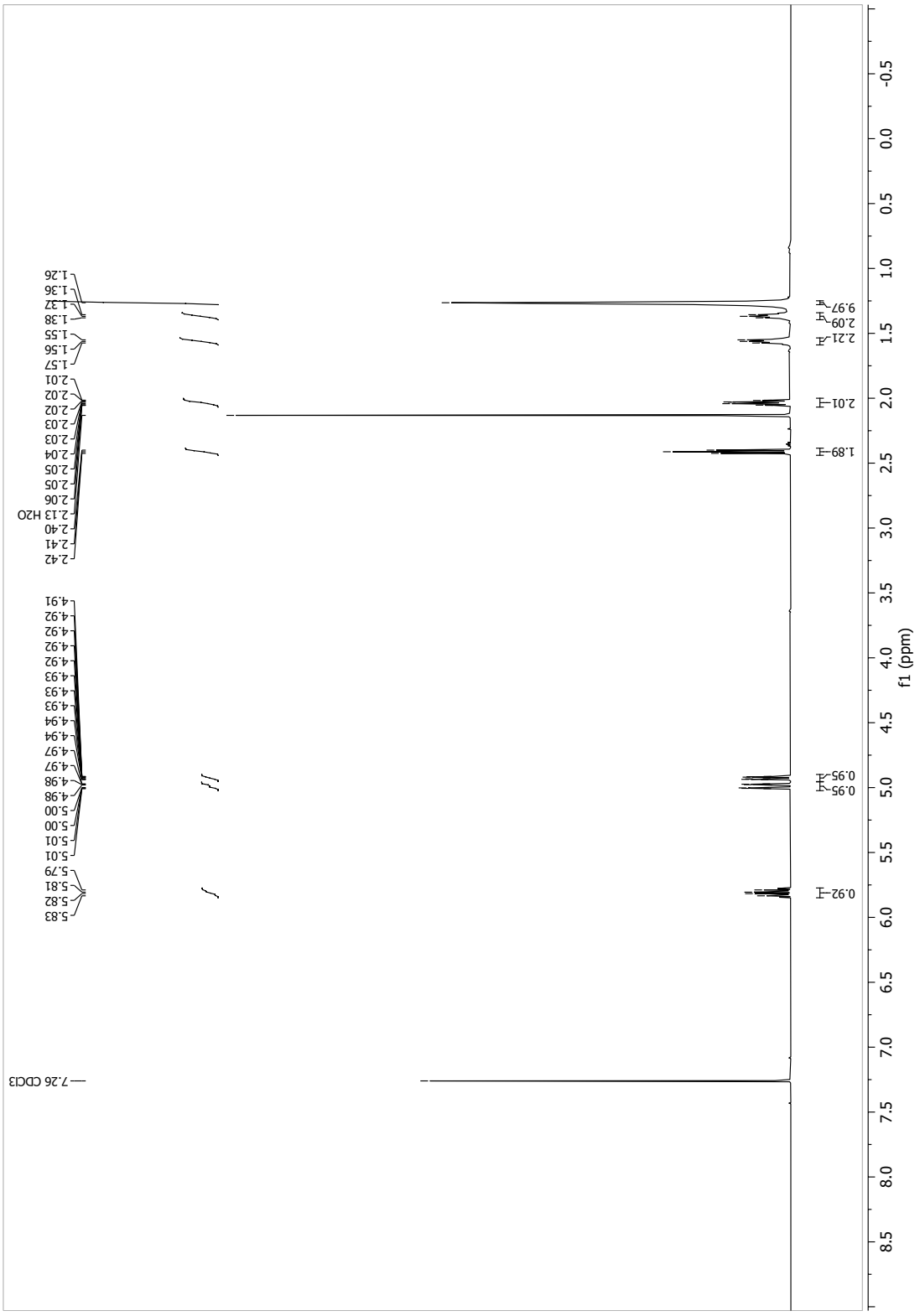

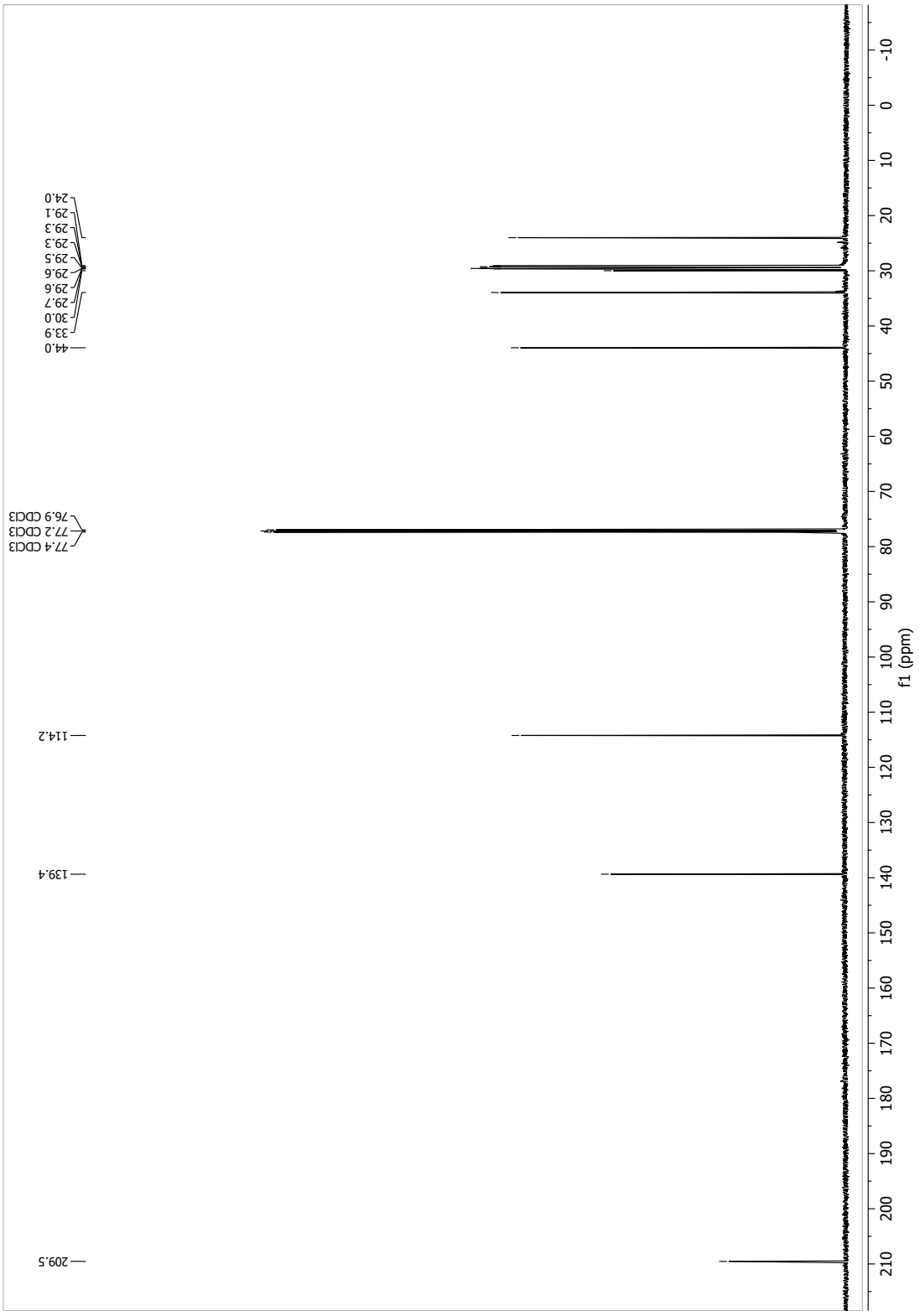
209.5
139.4
114.2
77.4 CDCl3
77.2 CDCl3
76.9 CDCl3
44.0
33.9
30.0
29.7
29.6
29.6
29.5
29.3
29.3
29.1
24.0
f1 (ppm)

13.1.47 Methyl 15-hydroxypentadecanoate (104)

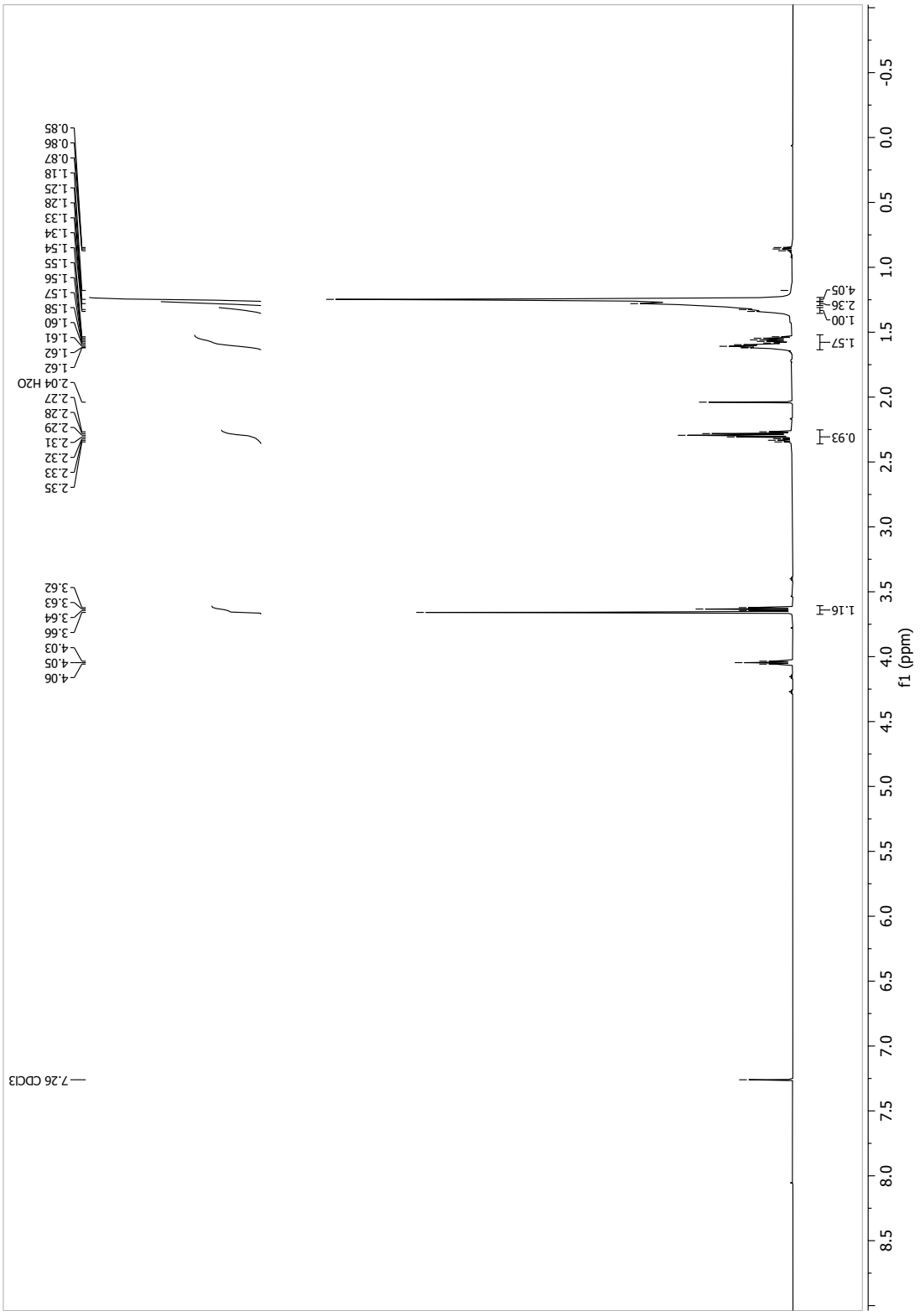

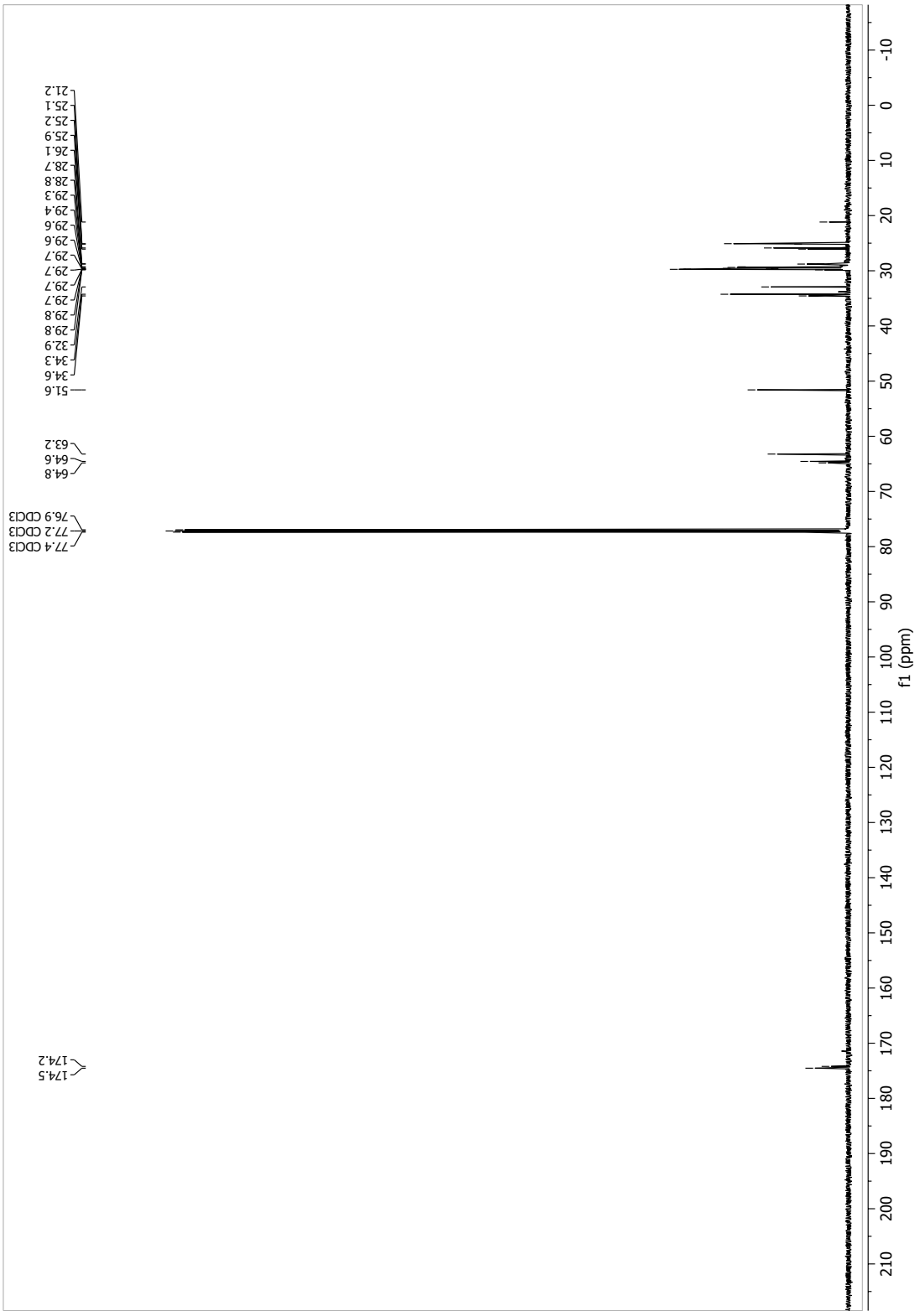
174.5
174.2
77.4 CDCl3
77.2 CDCl3
76.9 CDCl3
64.8
64.6
63.2
51.6
34.6
34.3
32.9
29.8
29.8
29.8
29.7
29.7
29.7
29.7
29.6
29.6
29.4
29.3
28.8
28.7
26.1
25.9
25.2
25.1
21.2
f1 (ppm)

13.1.48 Methyl 15-bromopentadecanoate (105)

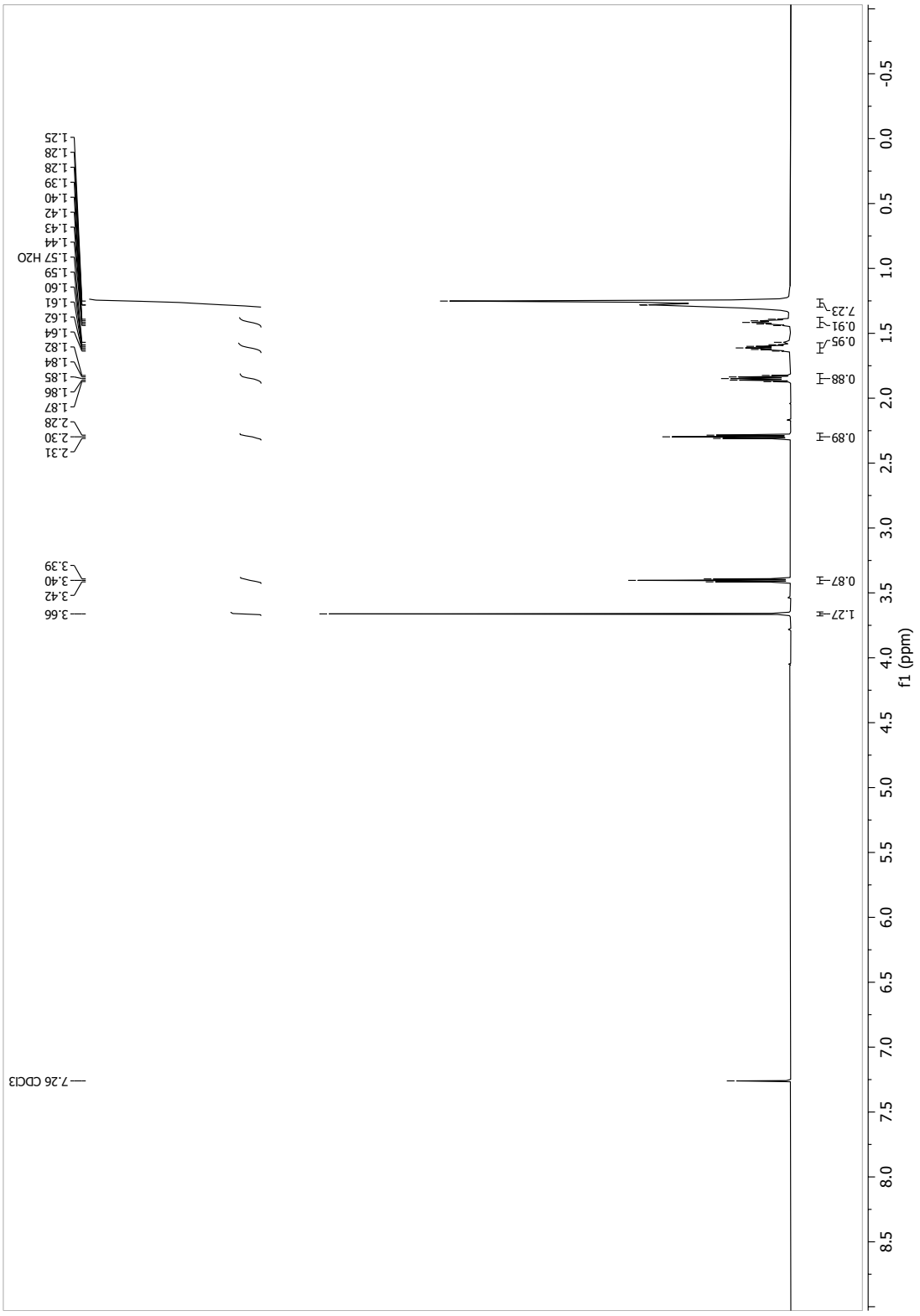

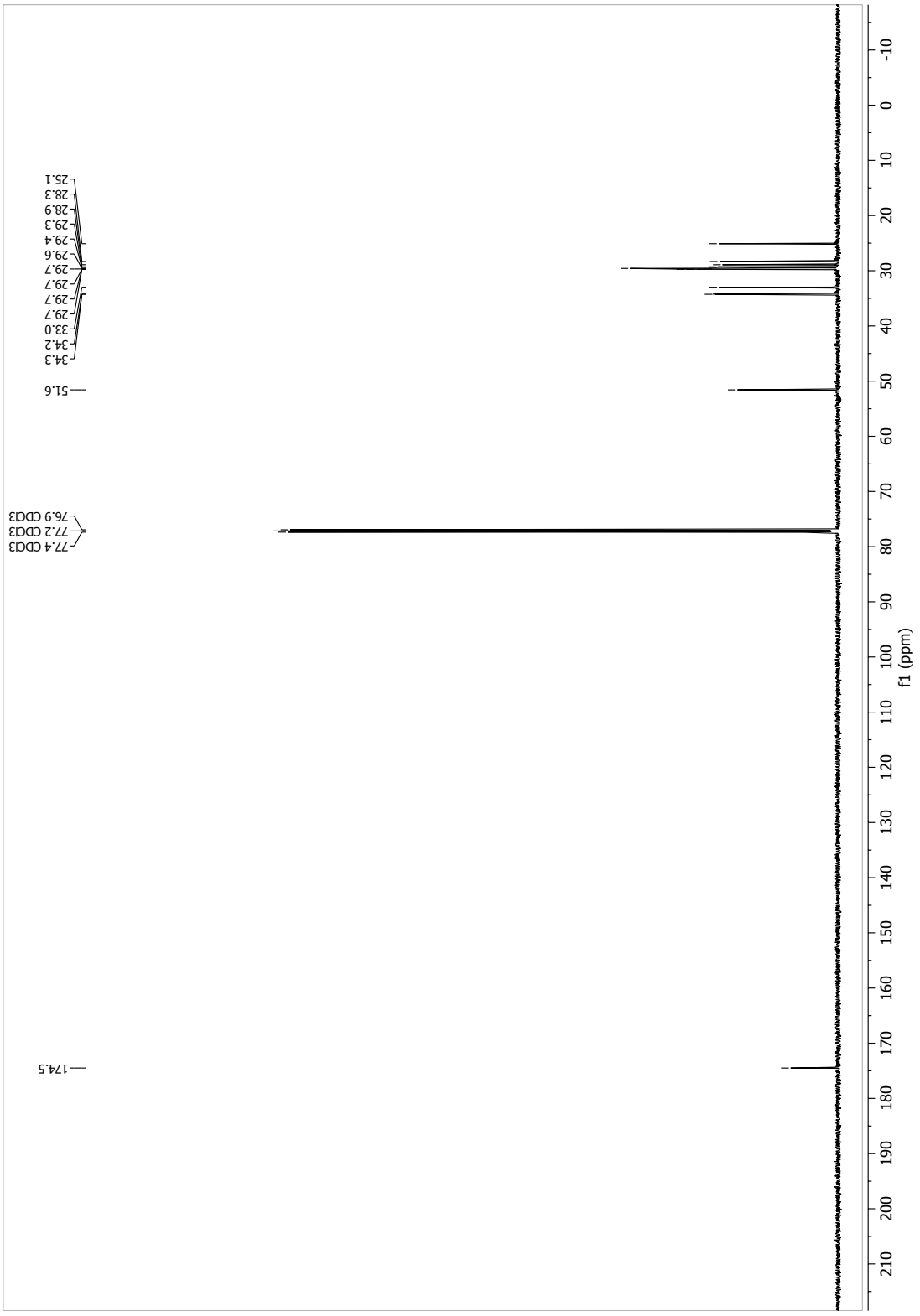
174.5
77.4 CDCl3
77.2 CDCl3
76.9 CDCl3
51.6
34.3
34.2
33.0
29.7
29.7
29.7
29.7
29.6
29.4
29.3
28.9
28.3
25.1
f1 (ppm)

13.1.49 Pentadec-14-enoic acid (106)

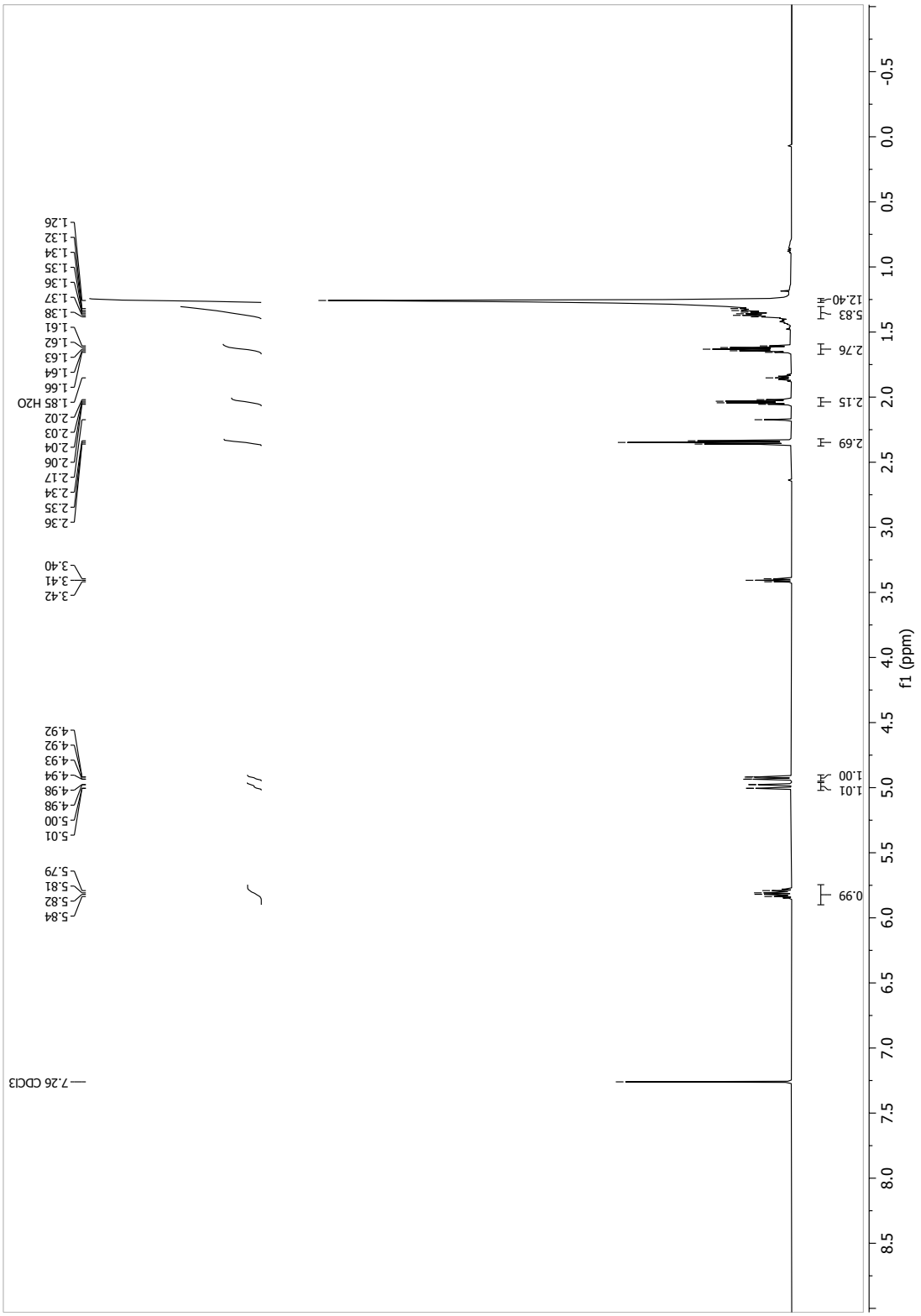

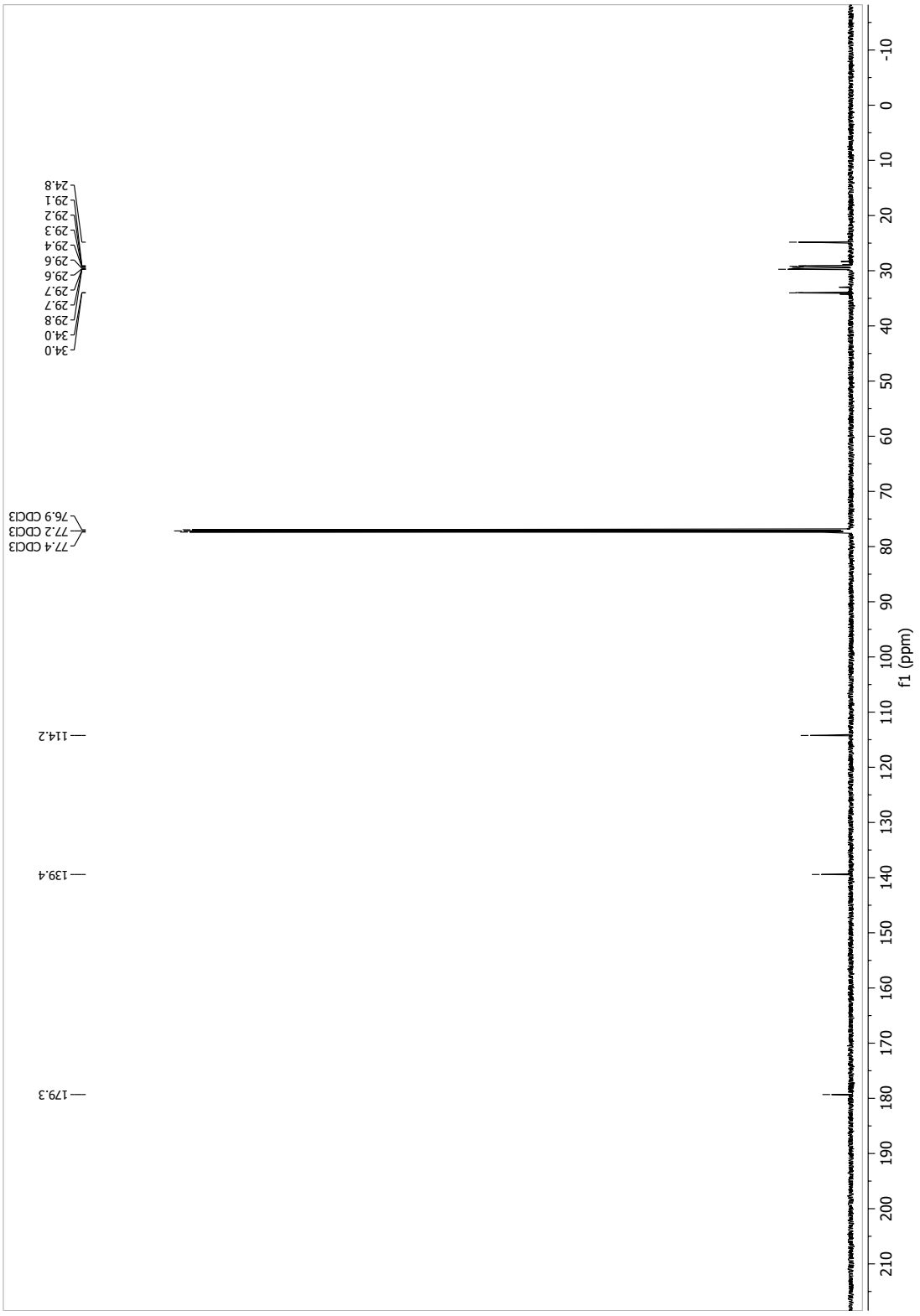
179.3
139.4
114.2
77.4 CDCl3
77.2 CDCl3
76.9 CDCl3
34.0
34.0
29.8
29.7
29.7
29.6
29.6
29.4
29.3
29.2
29.1
24.8
f1 (ppm)

13.1.50 Methyl pentadec-14-enoate (103)

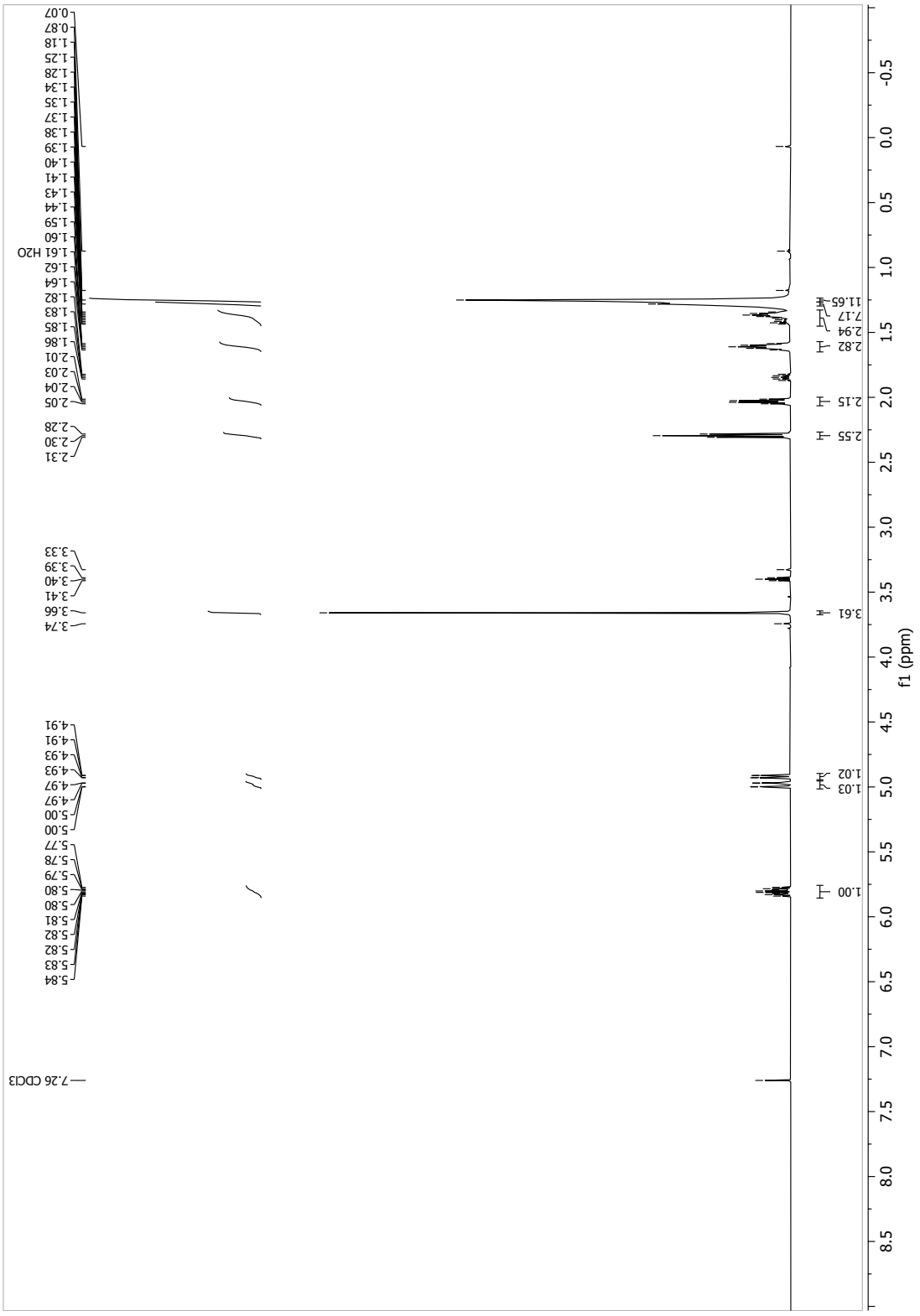

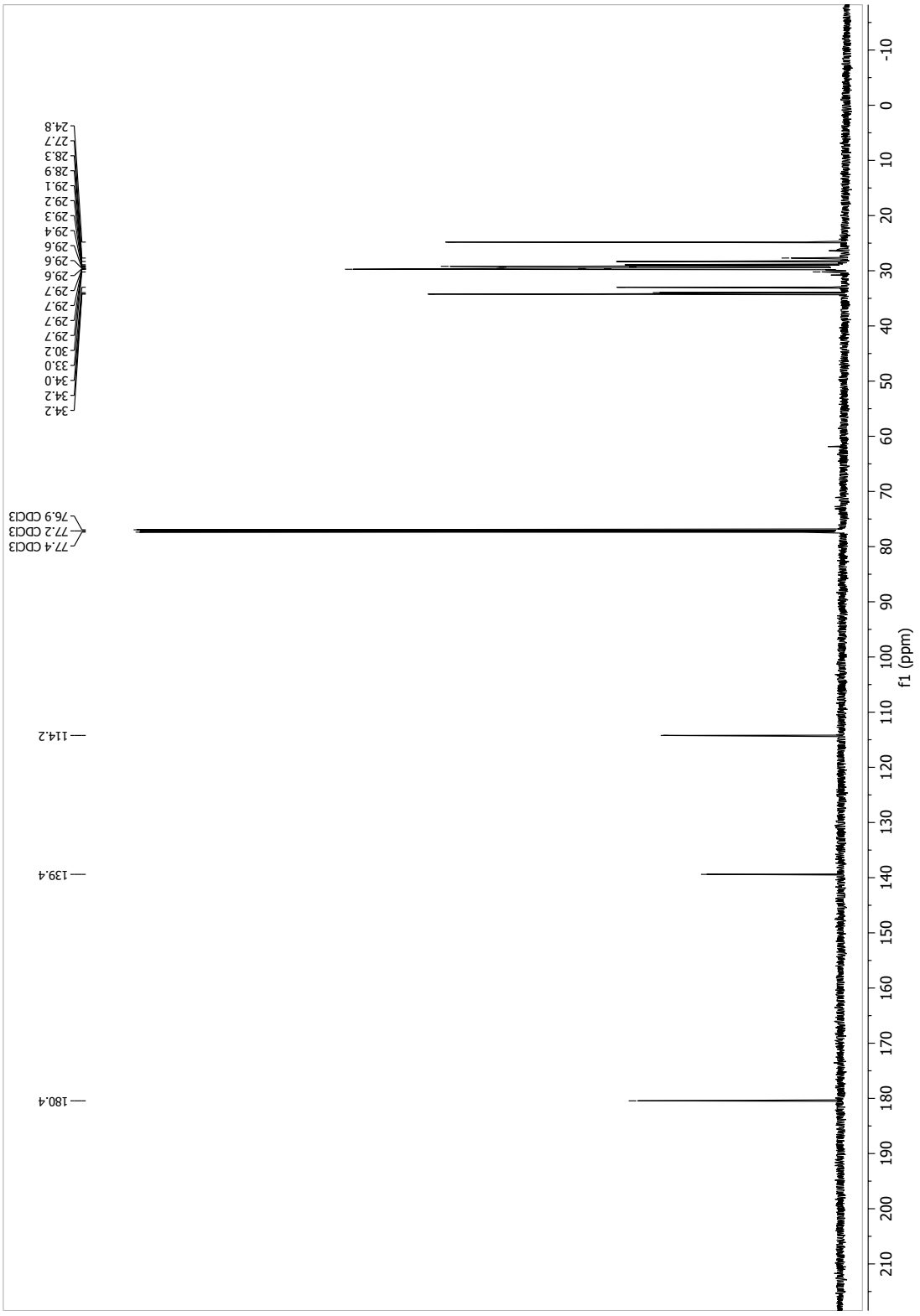
180.4
139.4
114.2
77.4 CDCl3
77.2 CDCl3
76.9 CDCl3
34.2
34.2
34.0
33.0
30.2
29.7
29.7
29.7
29.7
29.6
29.6
29.6
29.4
29.3
29.2
29.1
28.9
28.3
27.7
24.8
f1 (ppm)

13.1.51 [D_4]-(2*R*,3*R*,5*R*,6*S*)-2-(henicosyloxy)-6-methyltetrahydro-2*H*-pyran-3,5-diyl dibenzoate (70b)

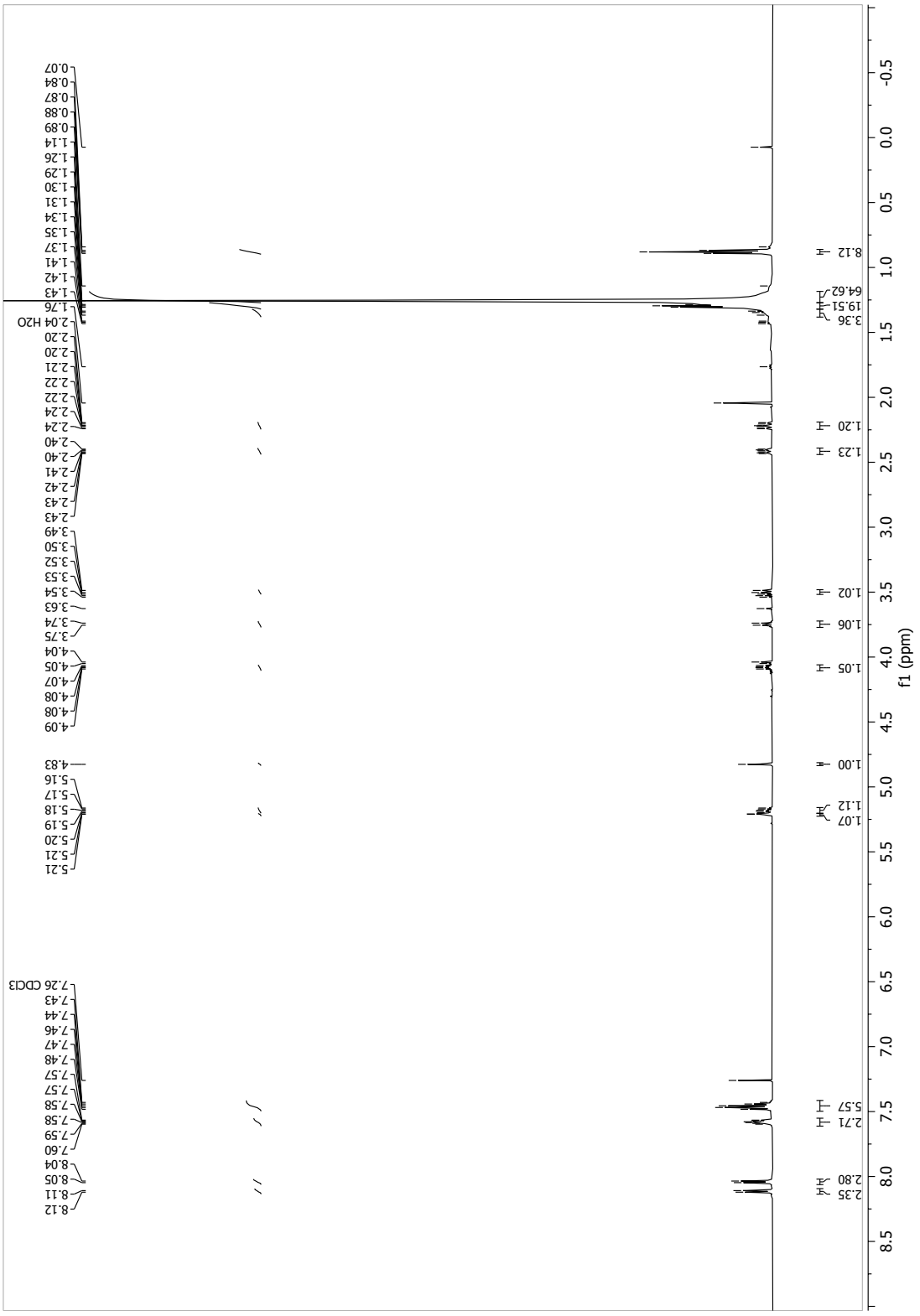

13.1.52 [D_4]-(2*S*,3*S*,5*S*,6*R*)-2-(henicosyloxy)-6-methyltetrahydro-2*H*-pyran-3,5-diol ([D_4]-asc-ωC21-H, 68b)

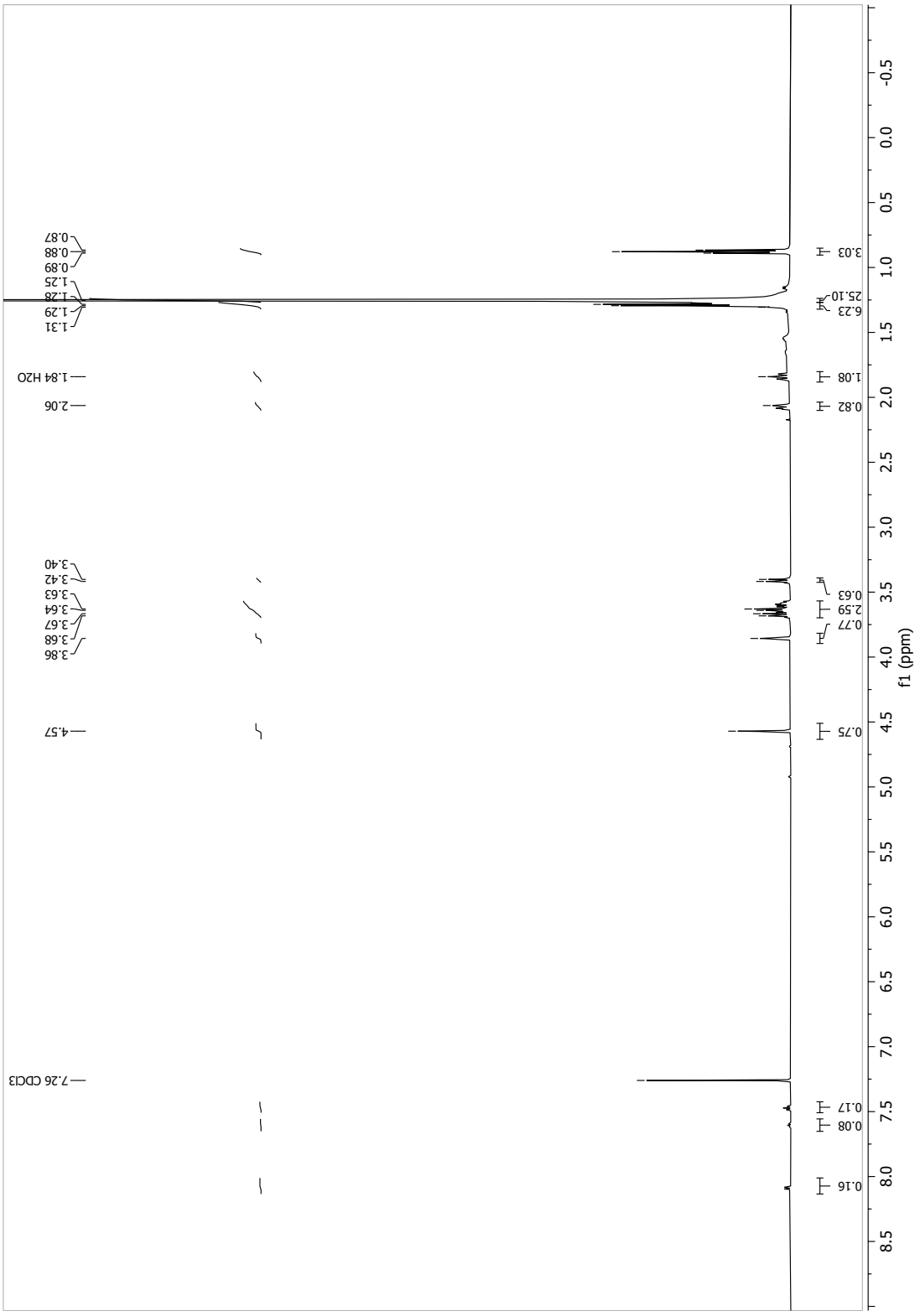

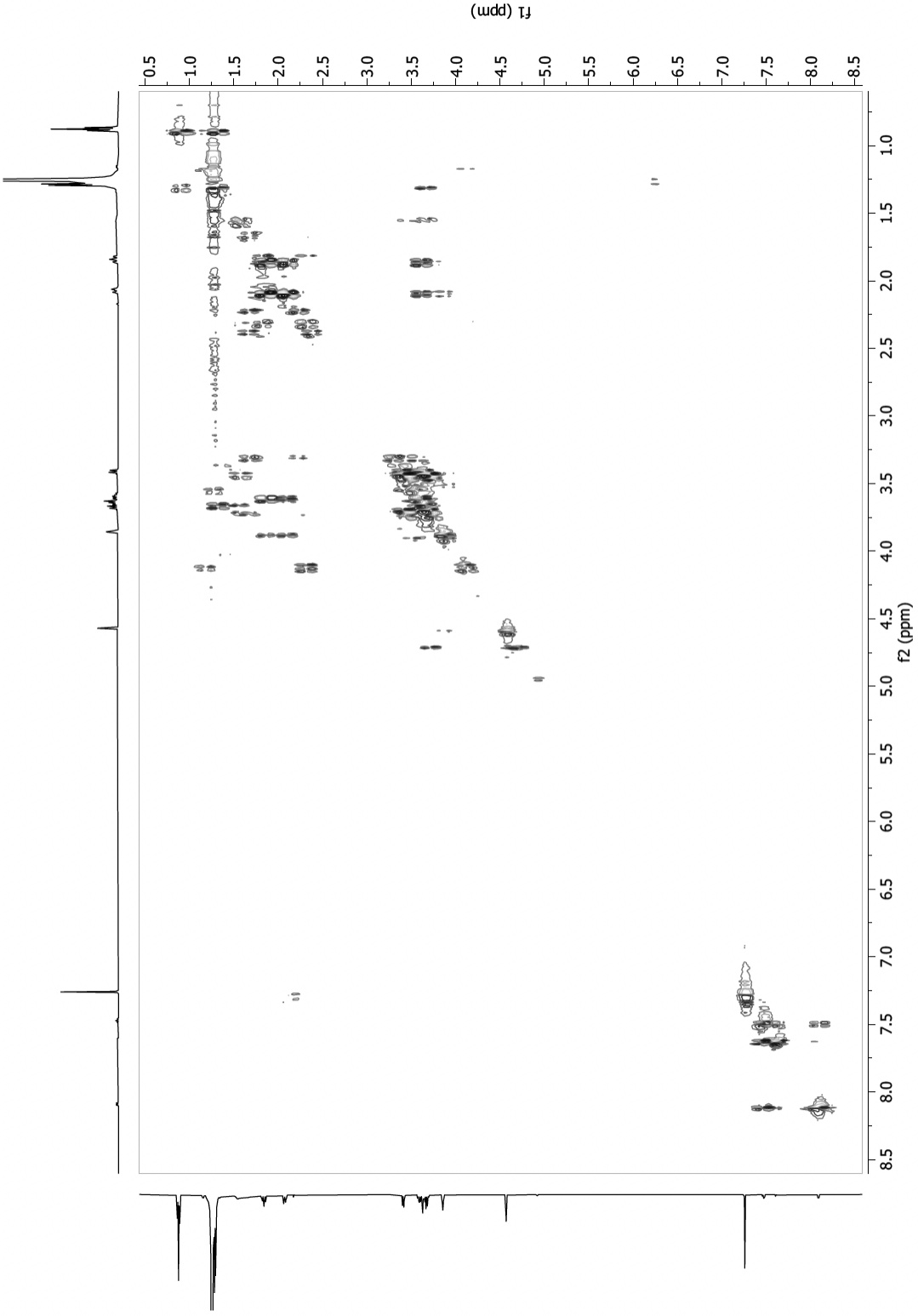
f1 (ppm)
f2 (ppm)

13.1.53 (2*R*,3*R*,5*R*,6*S*)-2-(henicosyloxy)-6-methyltetrahydro-2*H*-pyran-3,5-diyl dibenzoate (70a)

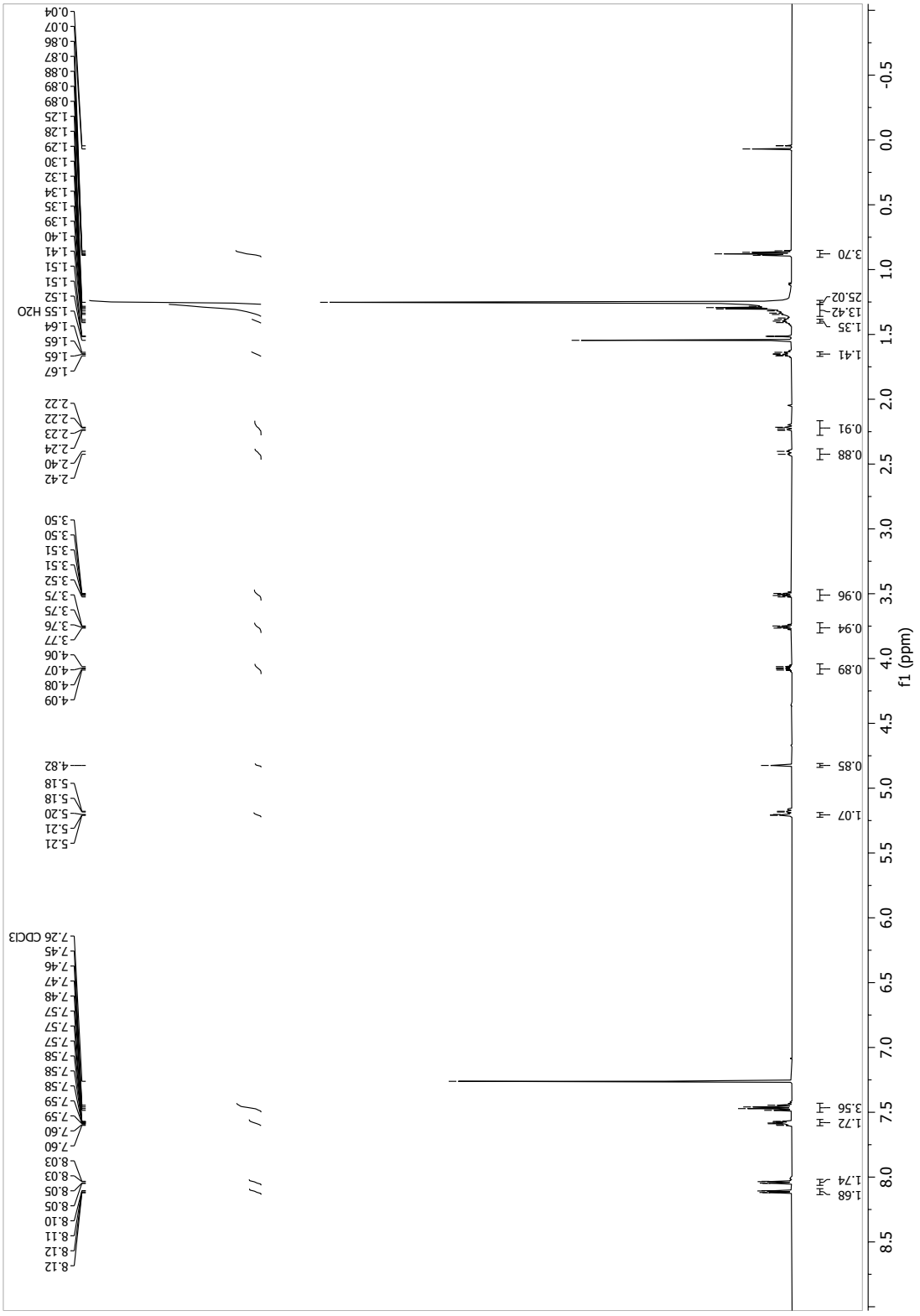

13.1.54 [D_4]-(2*R*,3*S*,5*S*,6*S*)-2-methyl-6-(((*R*)-pentacosan-2-yl)oxy)tetrahydro-2*H*-pyran-3,5-diyl dibenzoate (41b)

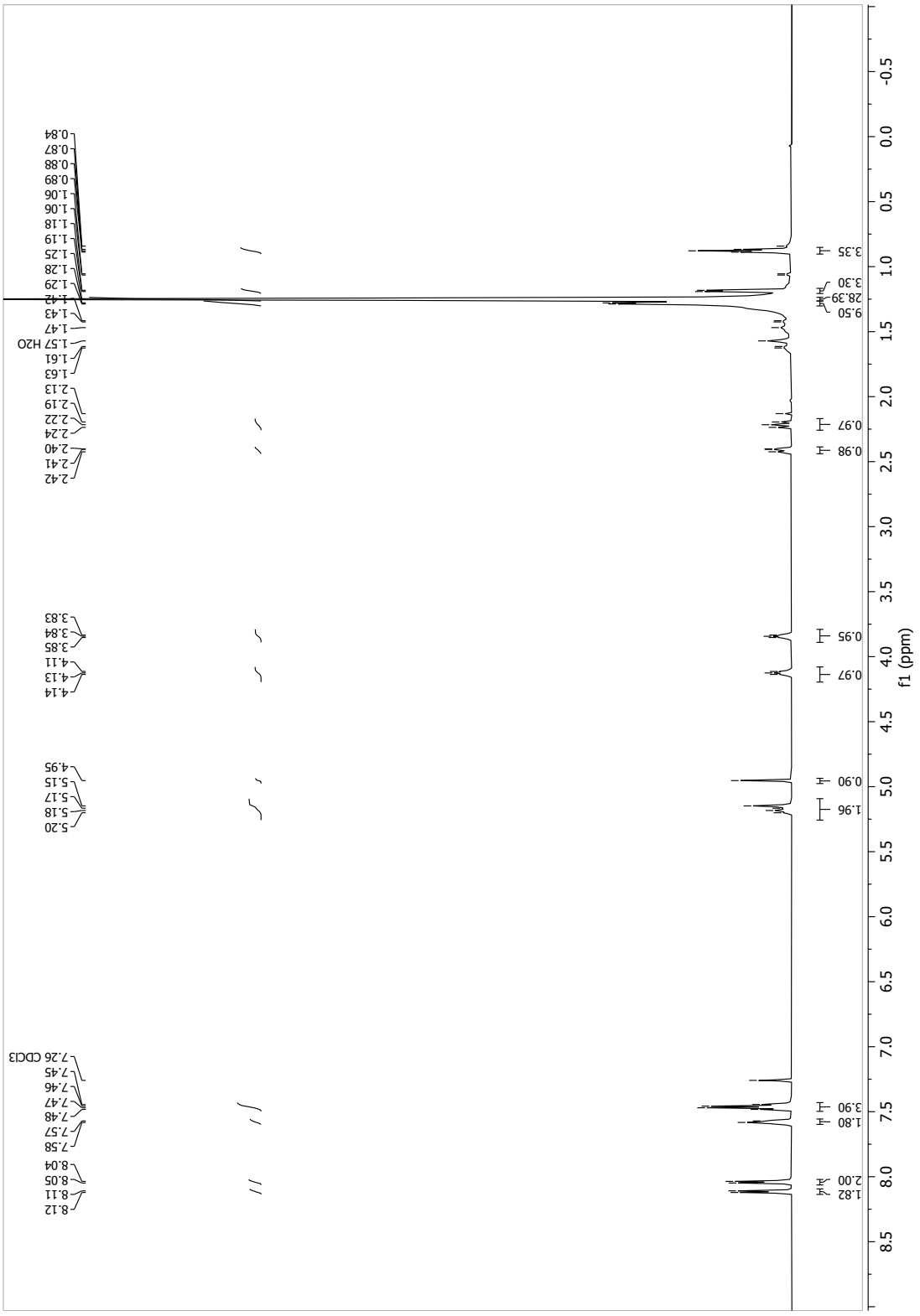

13.1.55 [D_4]-(2*S*,3*R*,5*R*,6*R*)-2-methyl-6-(((*R*)-pentacosan-2-yl)oxy)tetrahydro-2*H*-pyran-3,5-diol ([D_4]-asc-C25-H, 33b)

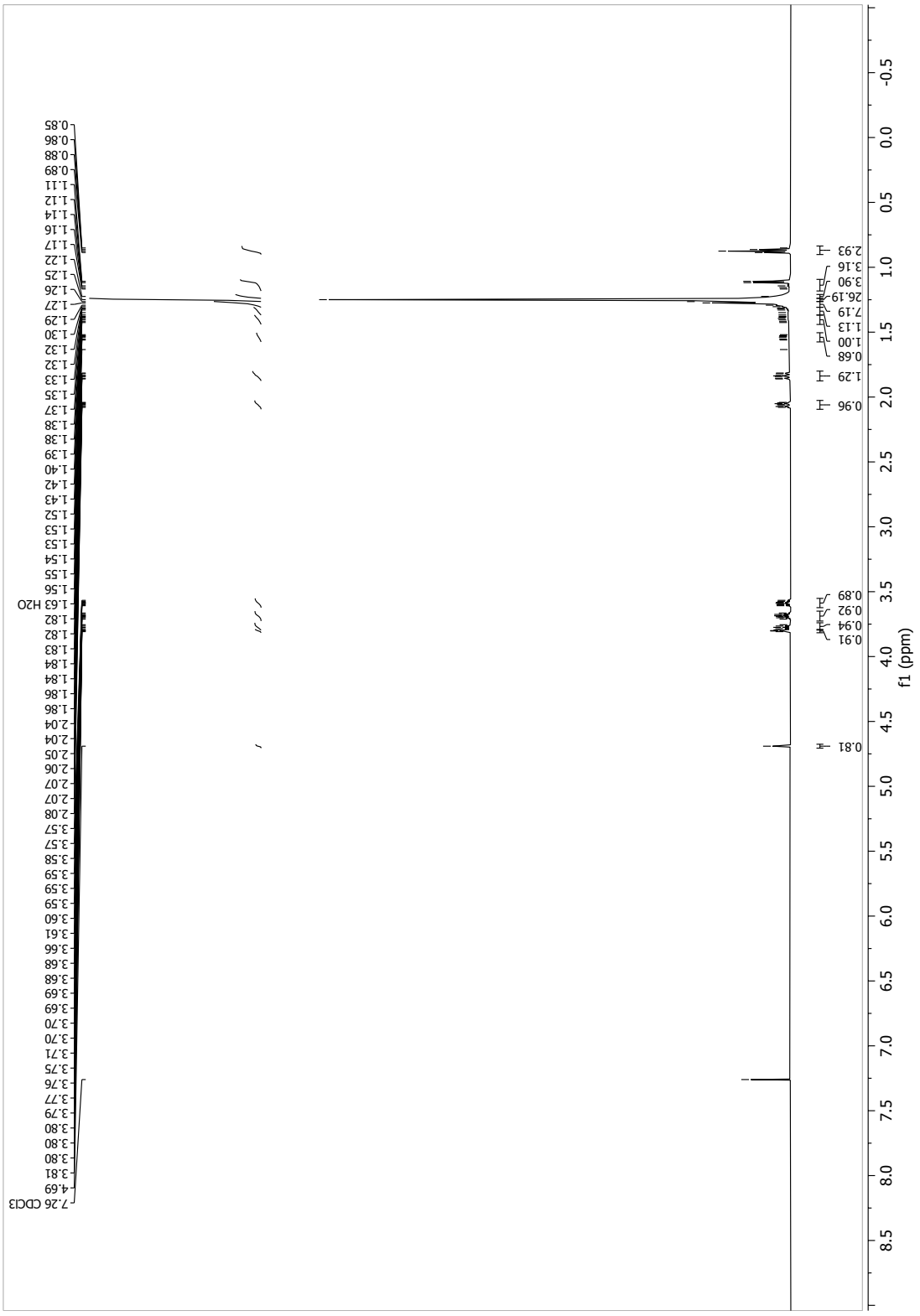

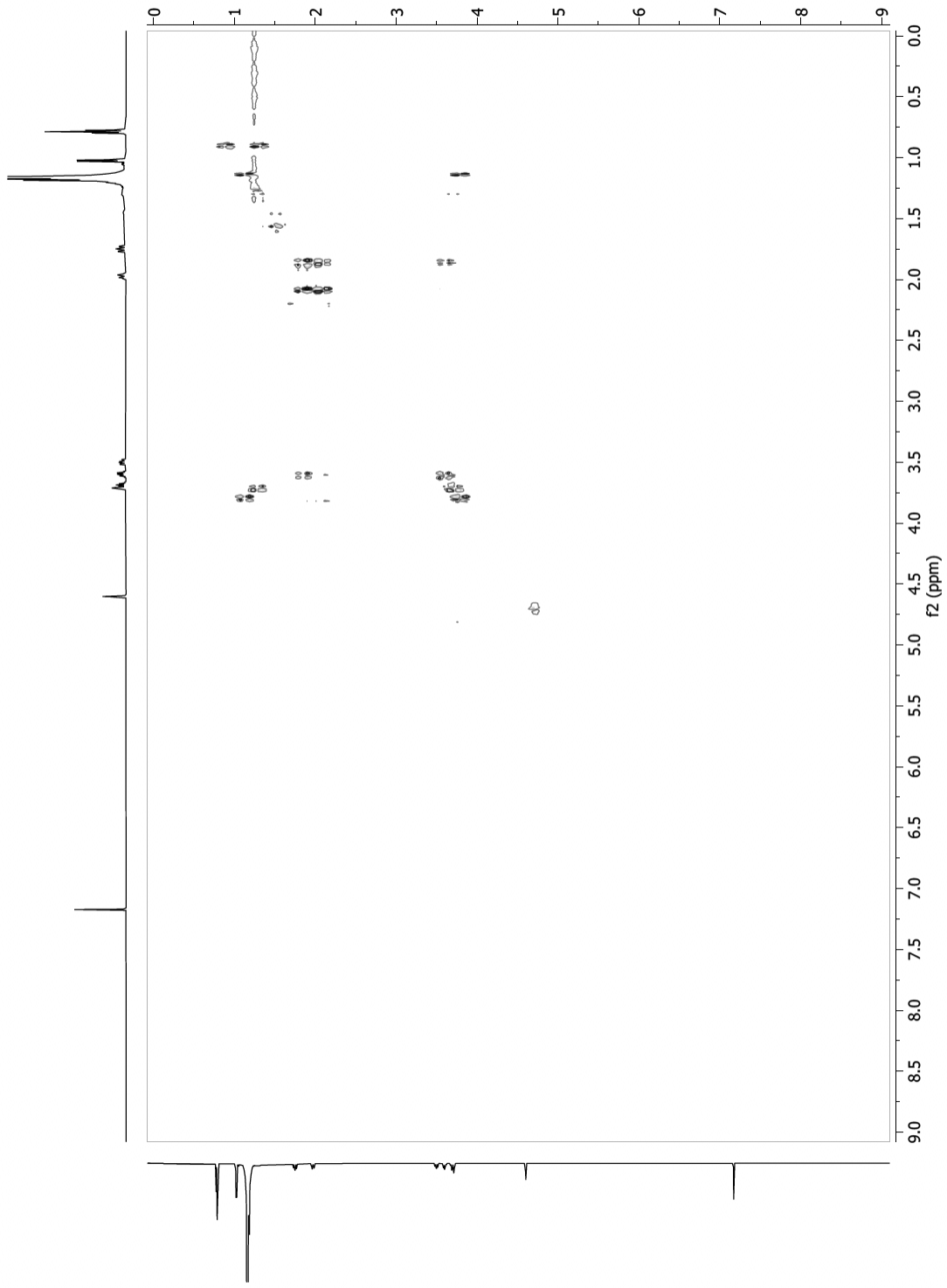
f1 (ppm)
f2 (ppm)

13.1.56 (2*R*,3*S*,5*S*,6*S*)-2-methyl-6-(((*R*)-pentacosan-2-yl)oxy)tetrahydro-2*H*-pyran-3,5-diyl dibenzoate (41a)

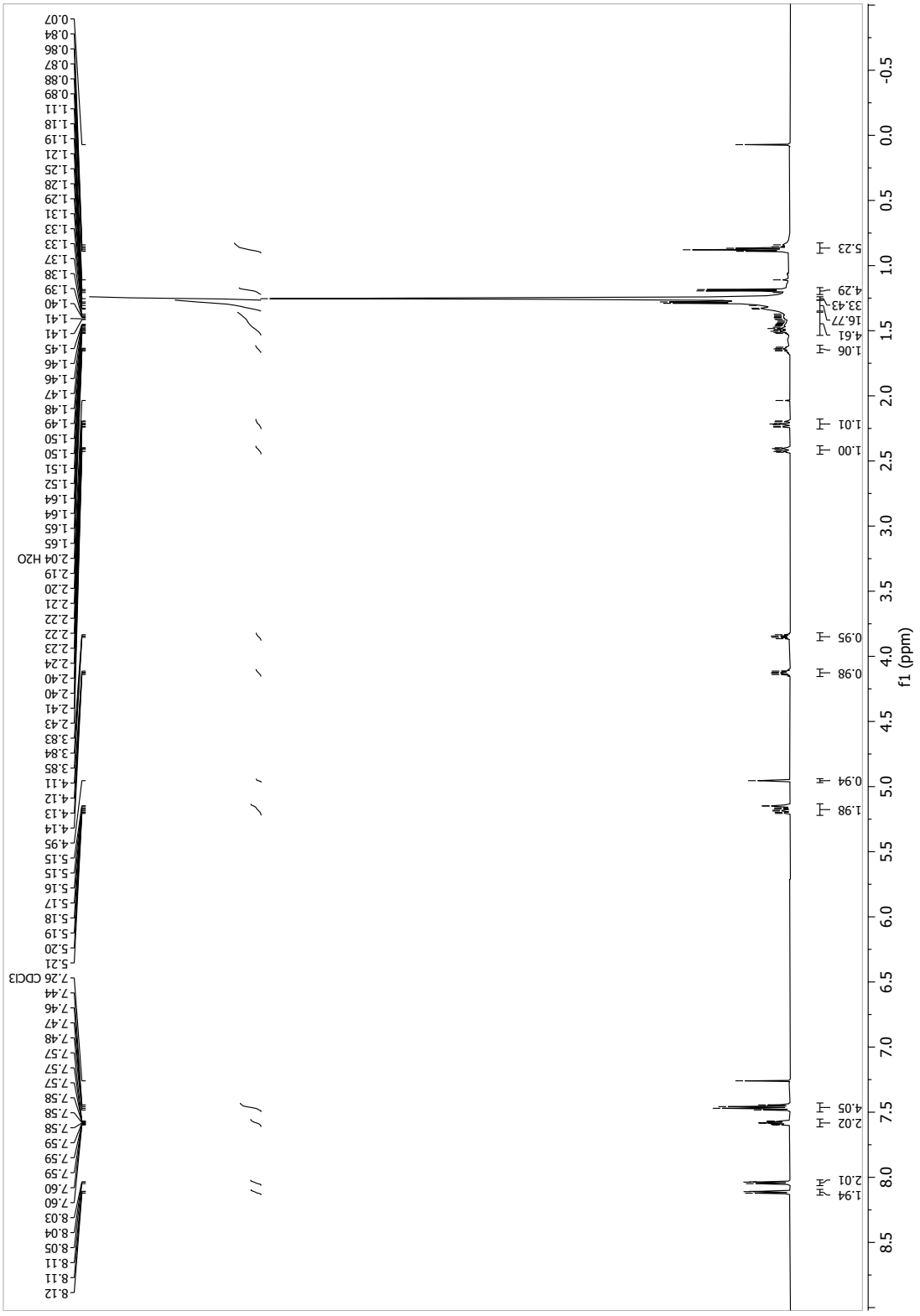

13.1.57 [D_4]-(2*S*,3*R*,5*R*,6*R*)-2-methyl-6-(((*R*)-24-methylpentacosan-2-yl)oxy)tetrahydro-2*H*-pyran-3,5-diyl dibenzoate (56b)

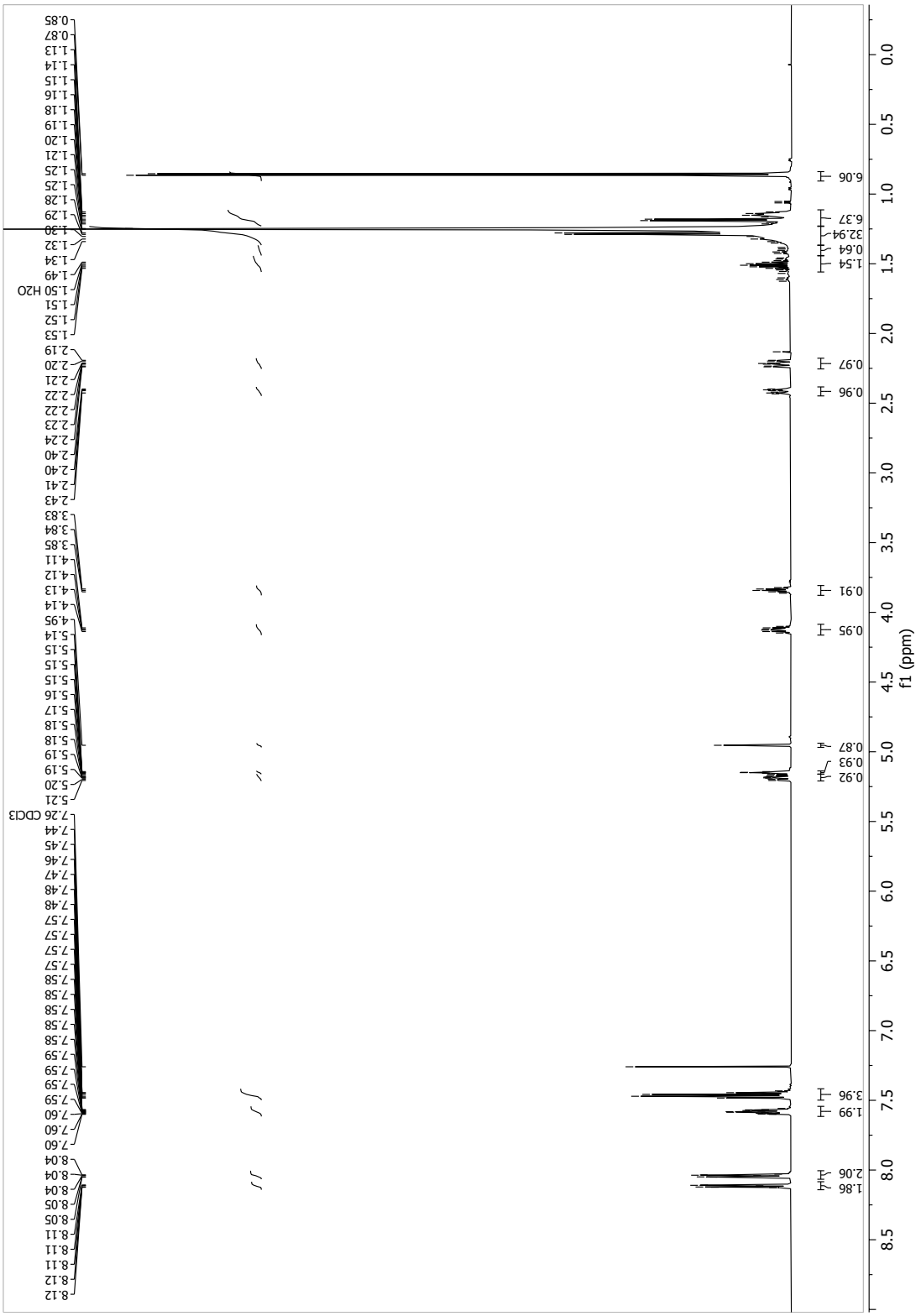

13.1.58 [D_4]-(2*S*,3*R*,5*R*,6*R*)-2-methyl-6-(((*R*)-24-methylpentacosan-2-yl)oxy)tetrahydro-2*H*-pyran-3,5-diol ([D_4]-asc-*i*C26-H, 43b)

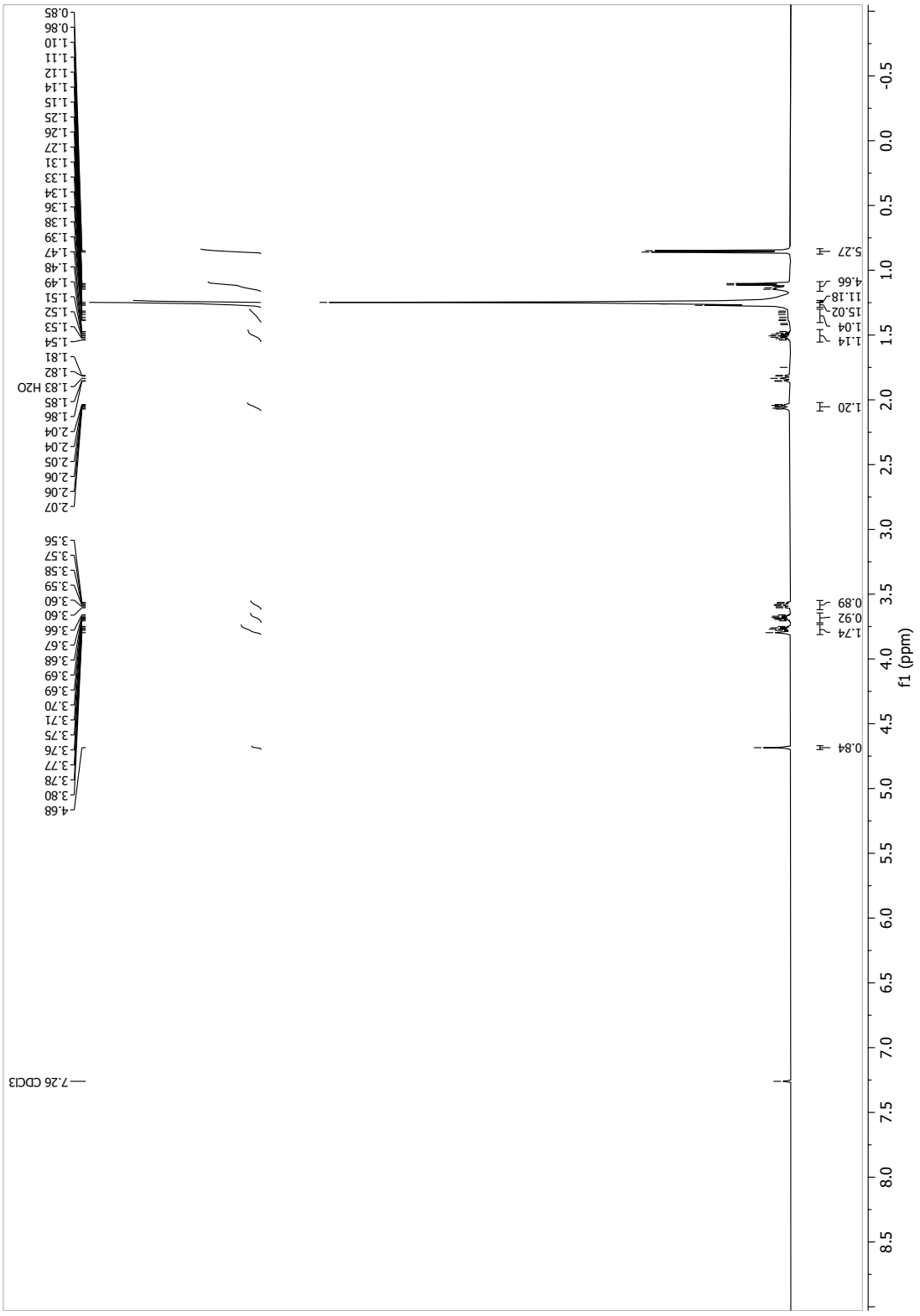

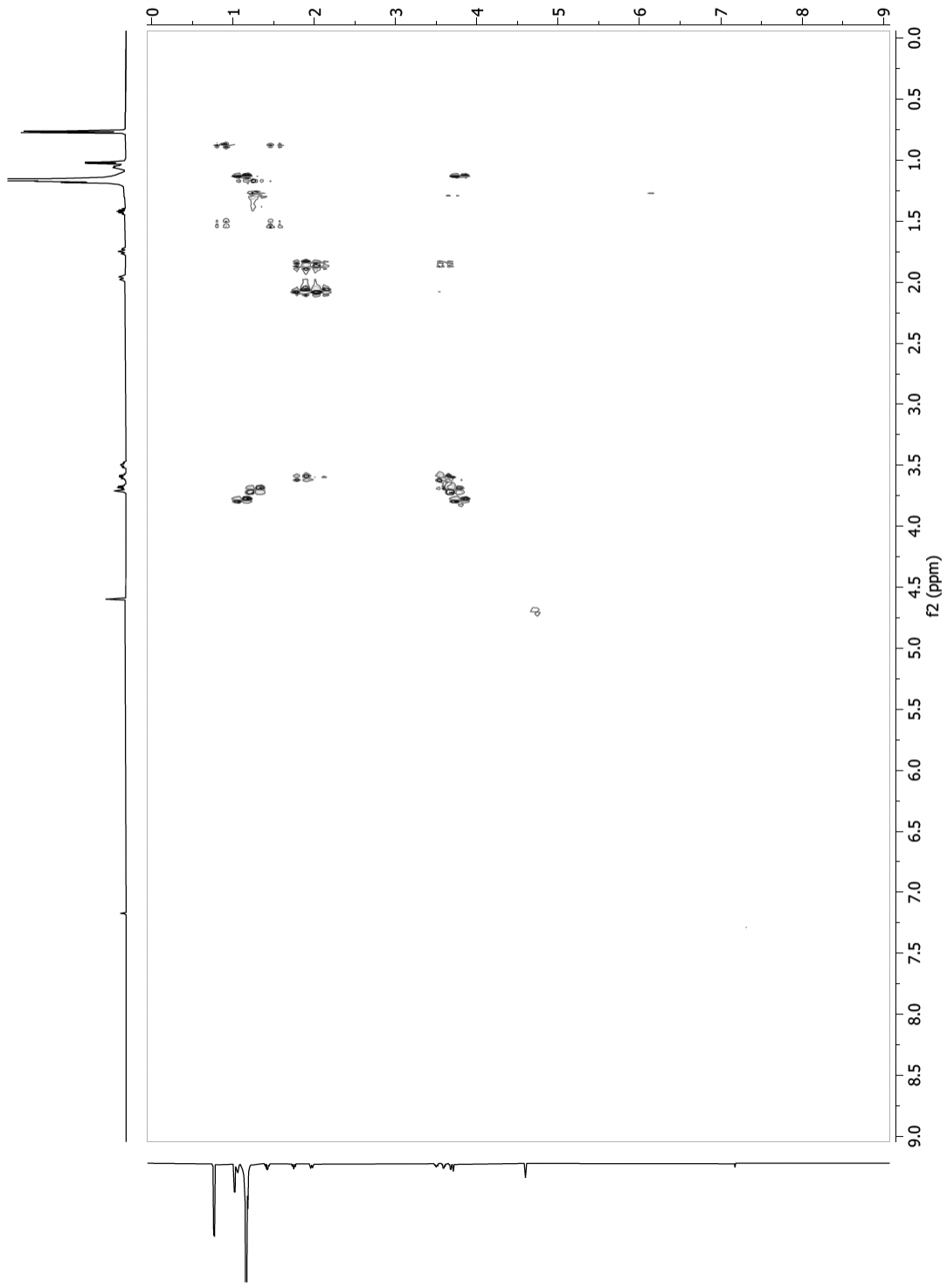
f1 (ppm)
f2 (ppm)

13.1.59 (2*S*,3*R*,5*R*,6*R*)-2-methyl-6-(((*R*)-24-methylpentacosan-2-yl)oxy)tetrahydro-2*H*-pyran-3,5-diyl dibenzoate (56a)

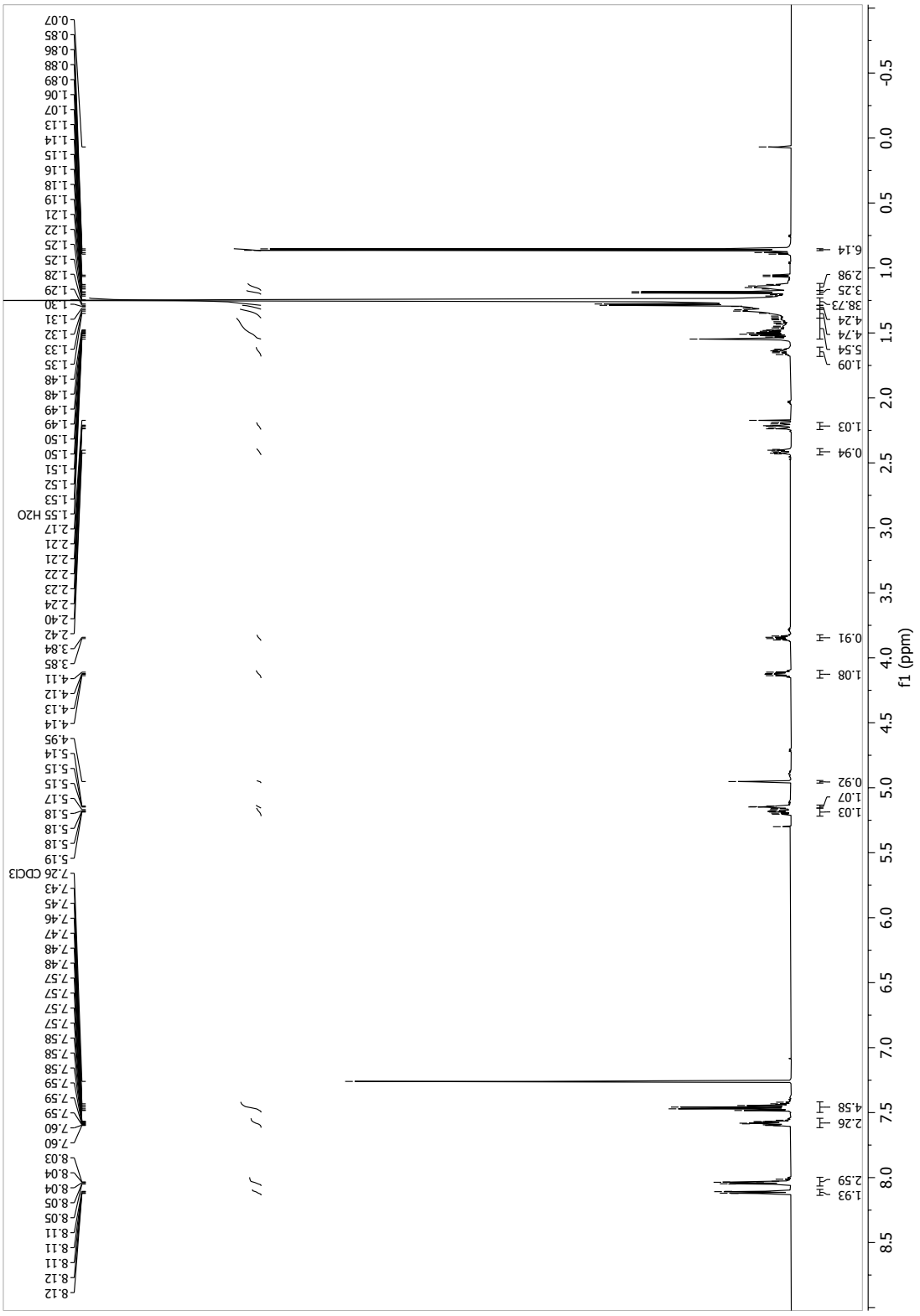

13.1.60 [D_4]-(2*R*,3*R*,5*R*,6*S*)-2-(((*R*)-hentriacontan-2-yl)oxy)-6-methyltetrahydro-2*H*-pyran-3,5-diyl dibenzoate (67b)

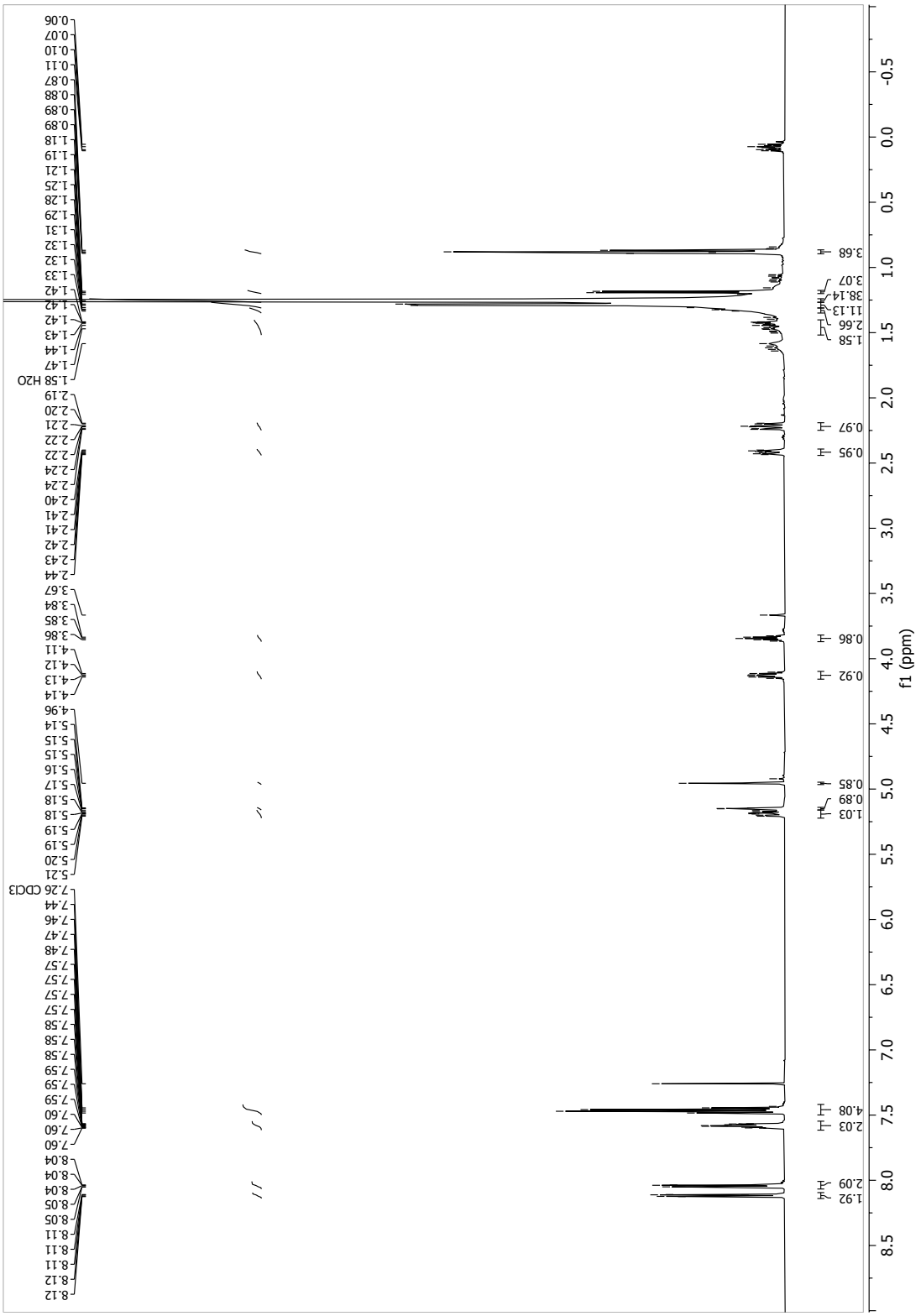

13.1.61 [D_4]-(2*R*,3*R*,5*R*,6*S*)-2-(((*R*)-hentriacontan-2-yl)oxy)-6-methyltetrahydro-2*H*-pyran-3,5-diol ([D_4]-asc-C31-H, 57b)

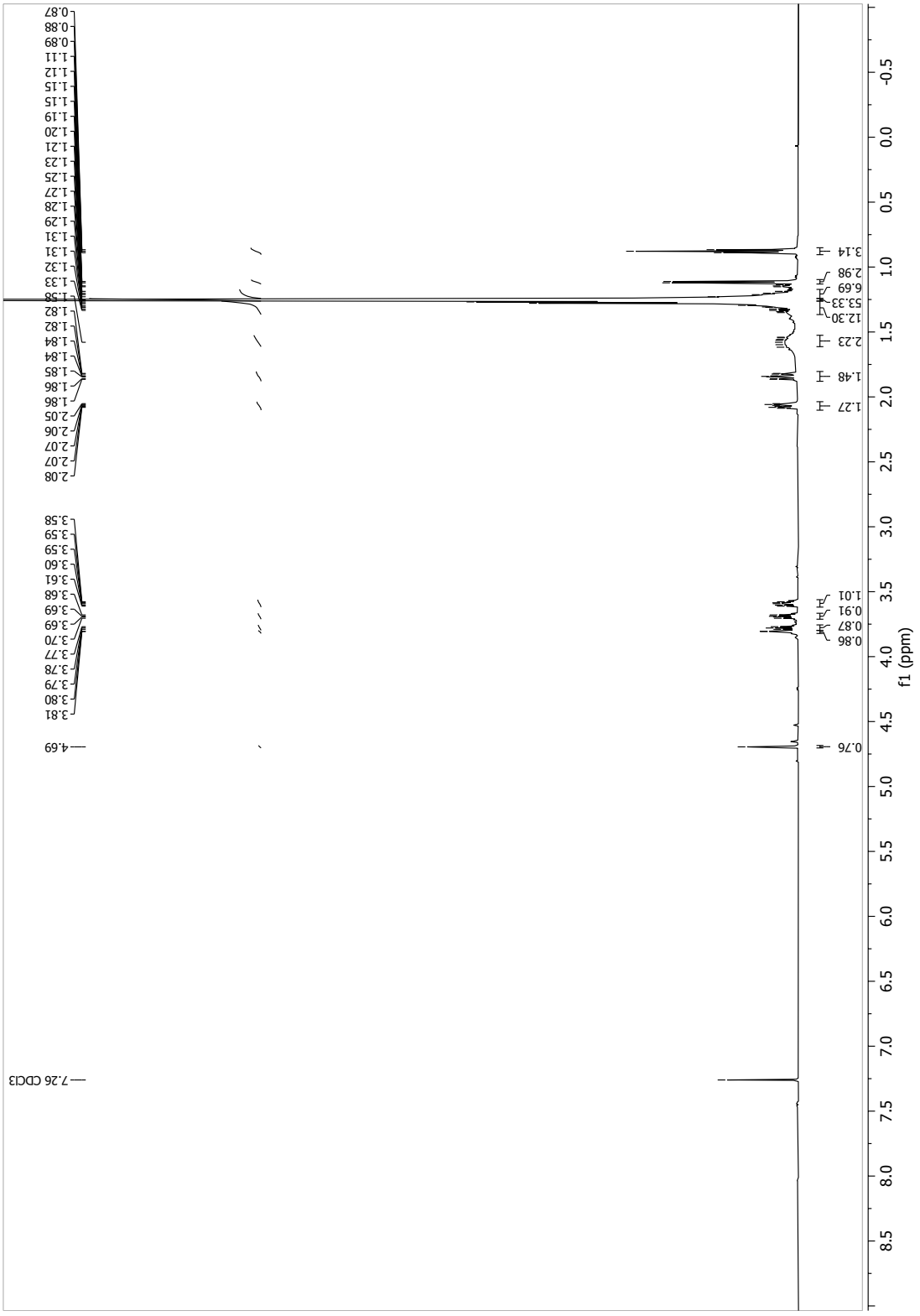

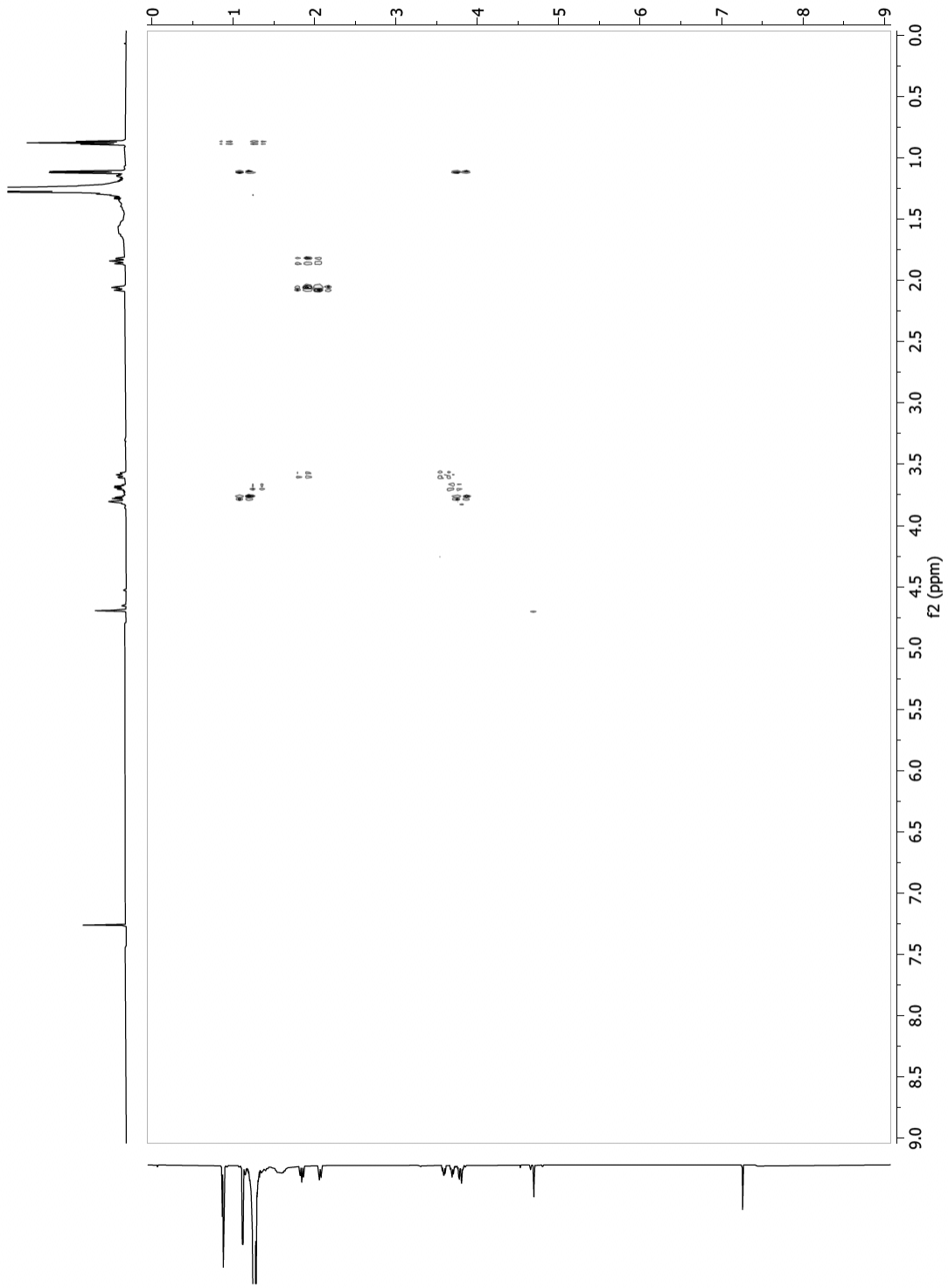
f1 (ppm)
f2 (ppm)

13.1.62 (2*R*,3*R*,5*R*,6*S*)-2-(((*R*)-hentriacontan-2-yl)oxy)-6-methyltetrahydro-2*H*-pyran-3,5-diyl dibenzoate (67a)

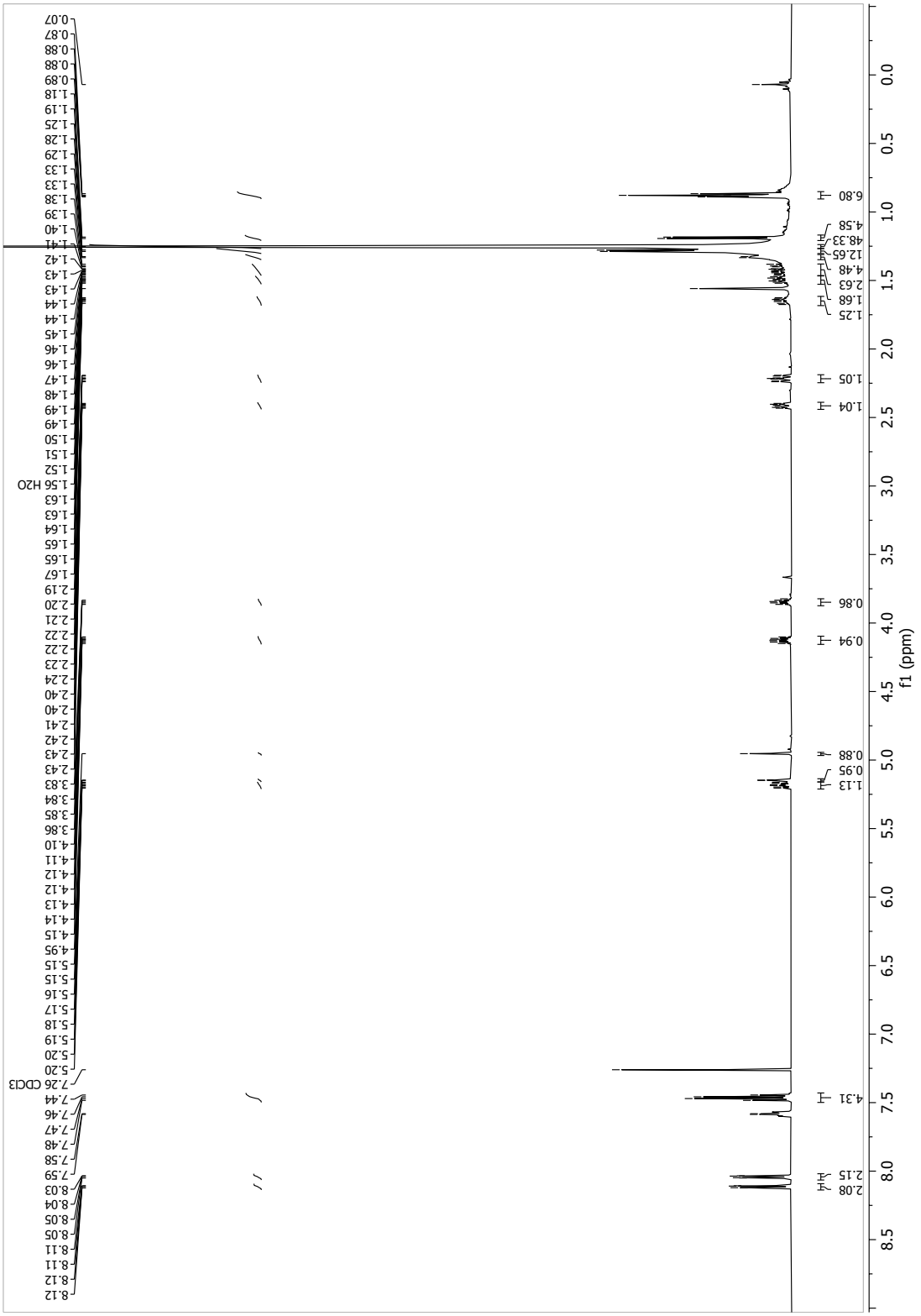

13.1.63 (2*R*,3*R*,5*R*,6*S*)-2-(((*R*)-5-(tert-butoxy)-5-oxopent-1-en-3-yl)oxy)-6-methyltetrahydro-2*H*-pyran-3,5-diyl dibenzoate (100)

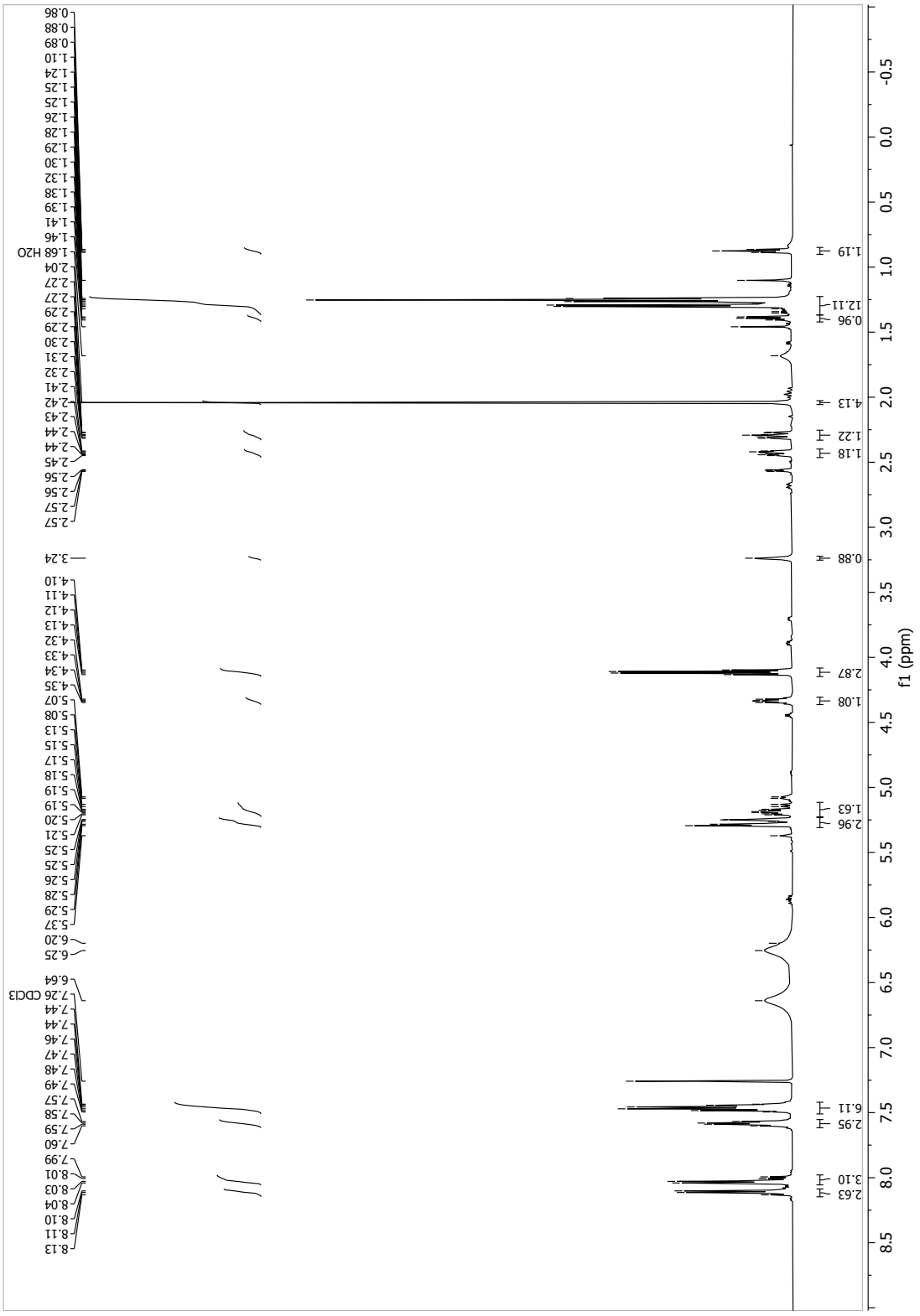

13.1.64 (2*R*,3*R*,5*R*,6*S*)-2-(((*R*)-5-methoxy-5-oxopent-1-en-3-yl)oxy)-6-methyltetrahydro-2*H*-pyran-3,5-diyl dibenzoate (108)

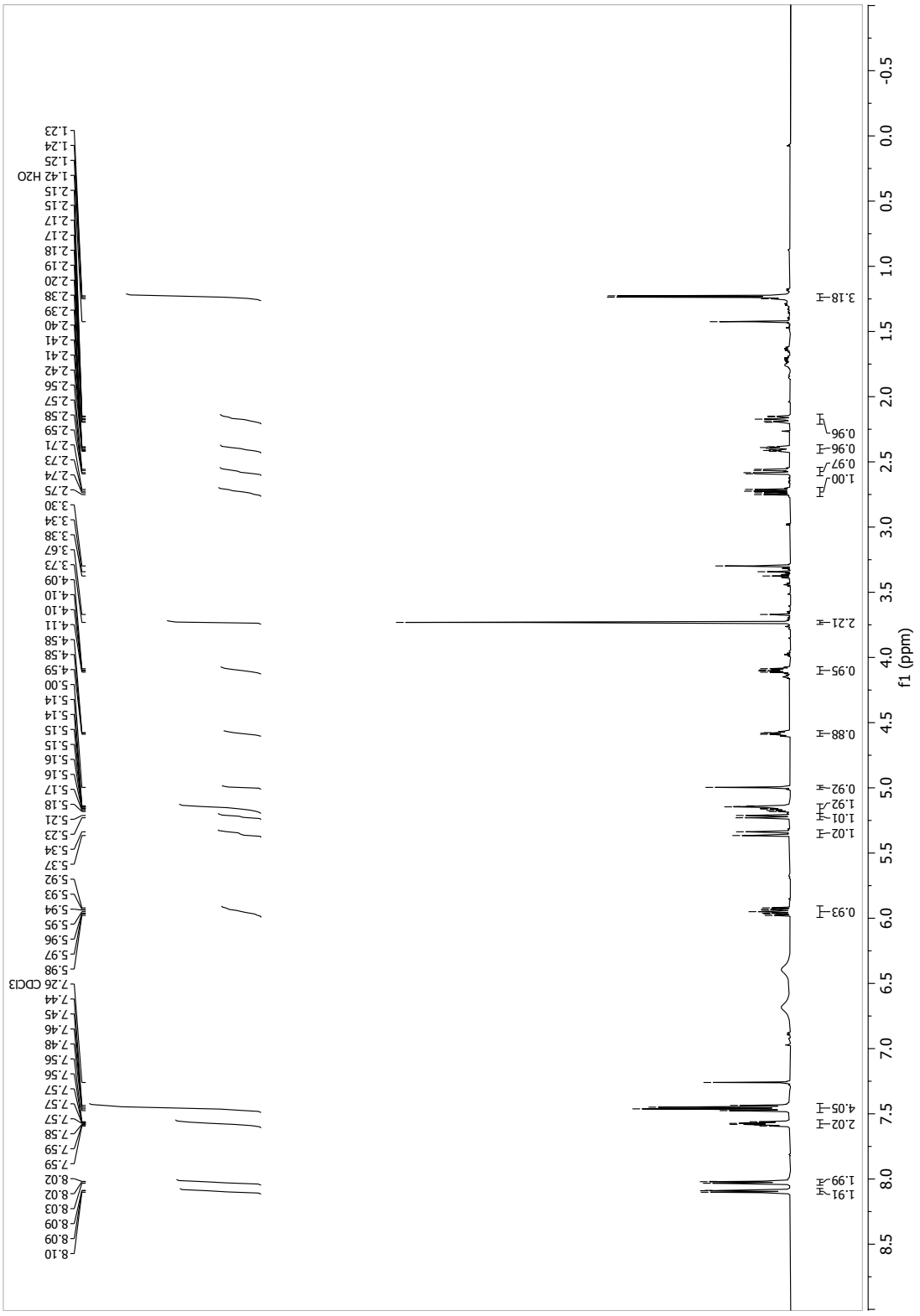

13.1.65 (2*R*,3*R*,5*R*,6*S*)-2-(((*R*,*E*)-1-(*tert*-butoxy)-1,16-dioxoheptadec-4-en-3-yl)oxy)-6-methyl tetrahydro-2*H*-pyran-3,5-diyl dibenzoate (101)

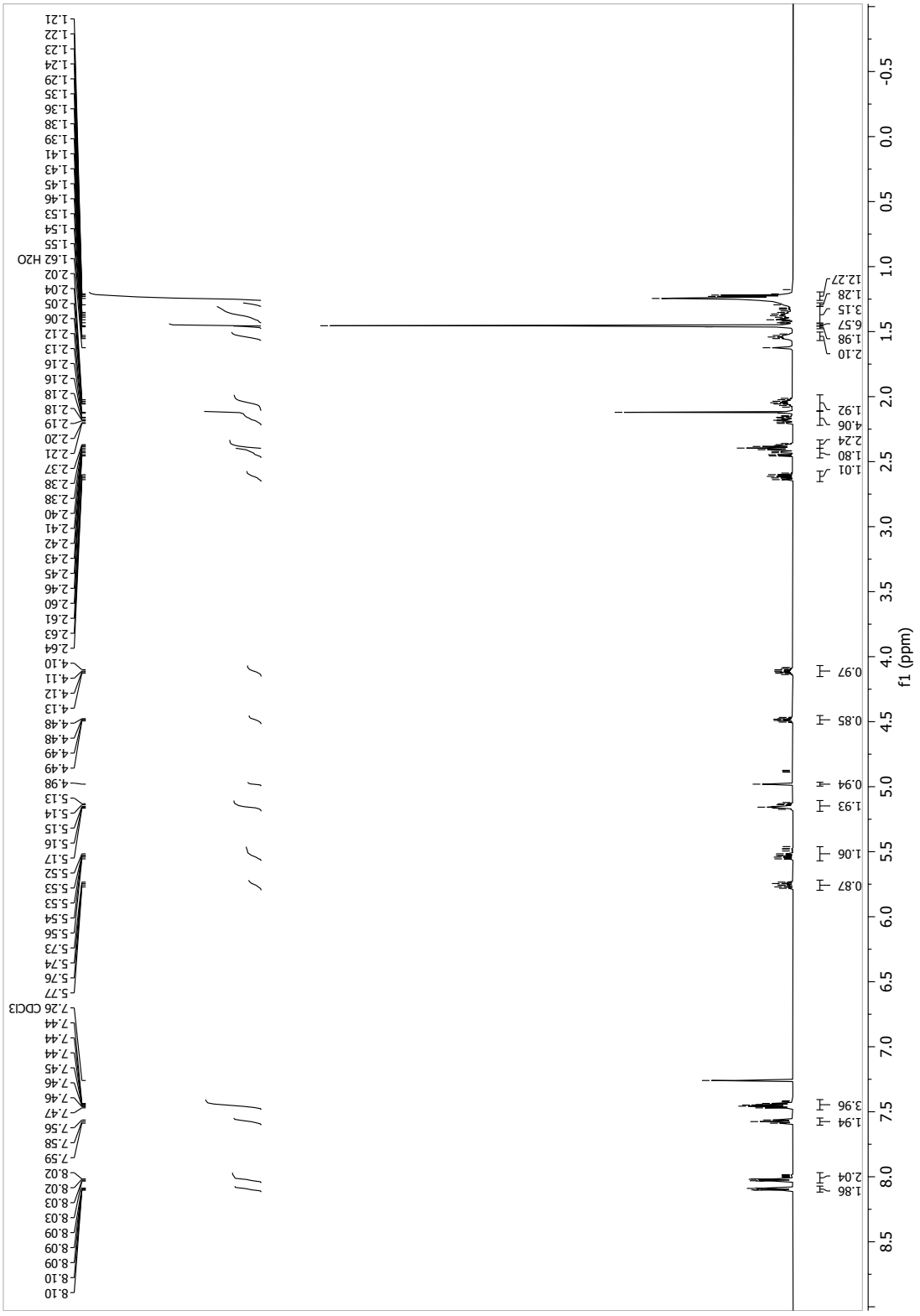

13.1.66 (2*R*,3*R*,5*R*,6*S*)-2-(((*S*)-1-(*tert*-butoxy)-1,16-dioxoheptadecan-3-yl)oxy)-6-methyltetrahydro -2*H*-pyran-3,5-diyl dibenzoate (102)

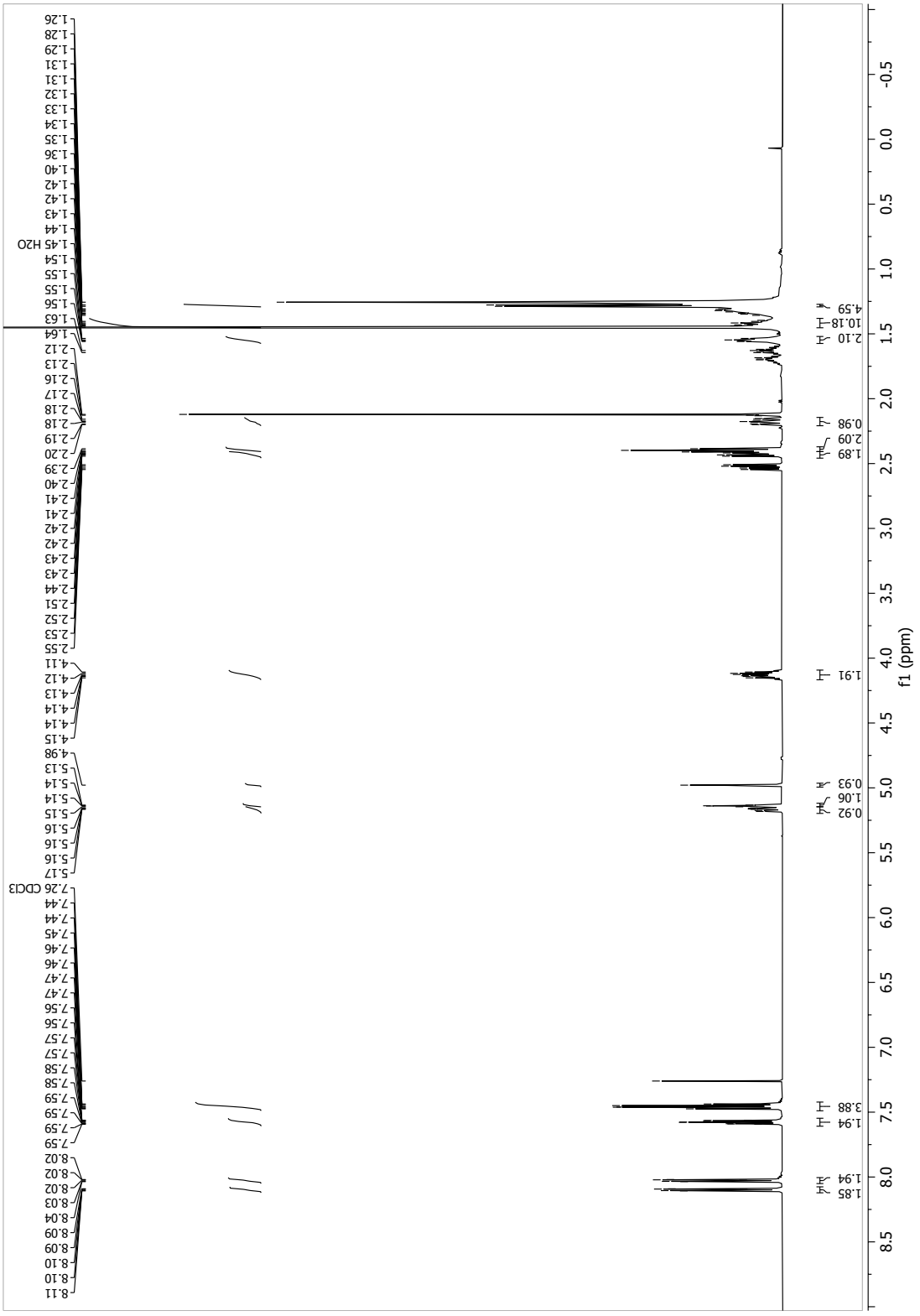

13.1.67 Dimethyl (*R*,*E*)-3-(((2*R*,3*R*,5*R*,6*S*)-3,5-bis(benzoyloxy)-6-methyltetrahydro-2*H*-pyran-2-yl)oxy)297ctadic-4-enedioate (109)

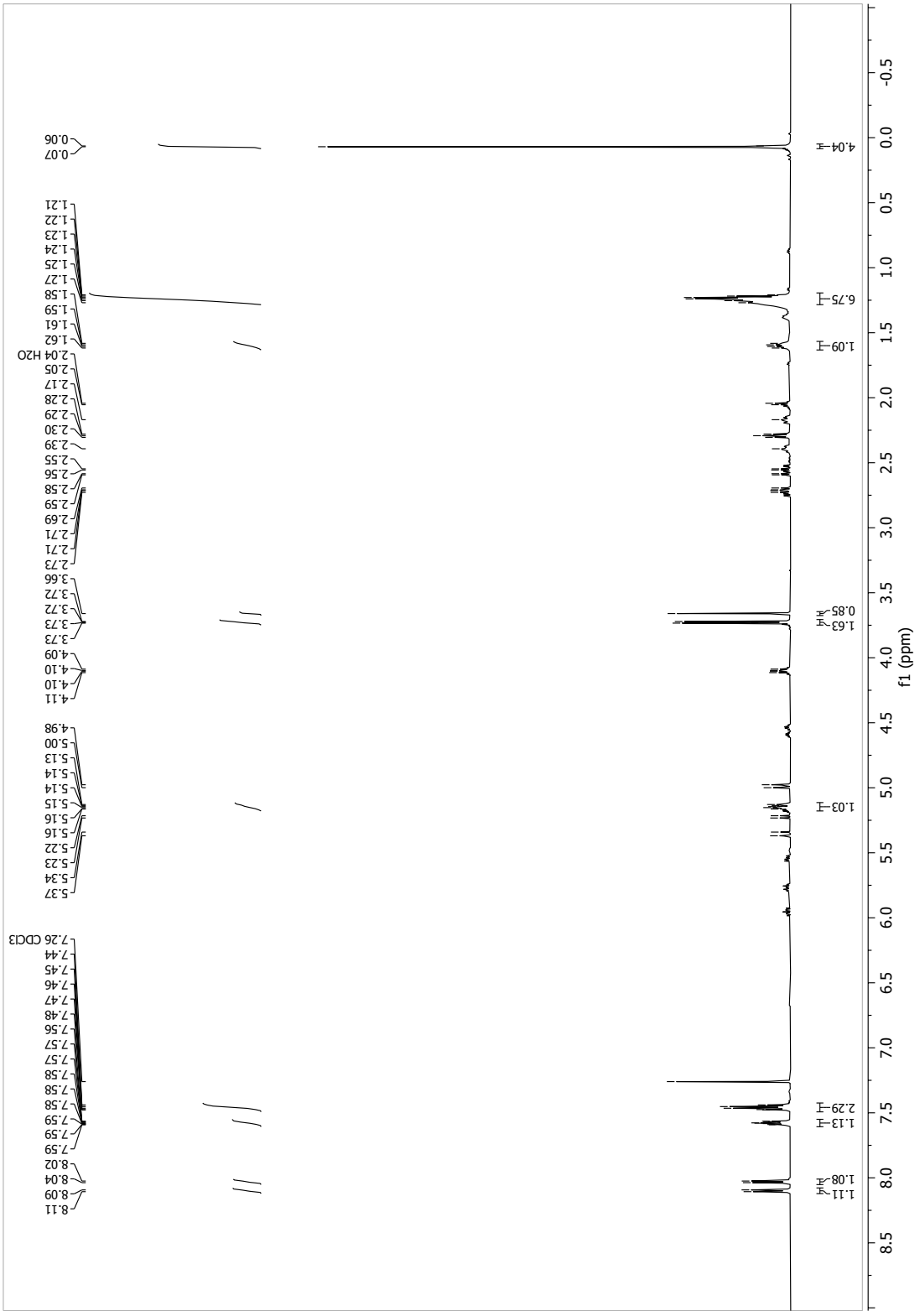

13.1.68 Dimethyl (*S*)-3-(((2*R*,3*R*,5*R*,6*S*)-3,5-bis(benzoyloxy)-6-methyltetrahydro-2*H*-pyran-2-yl)oxy)octadecanedioate (110)

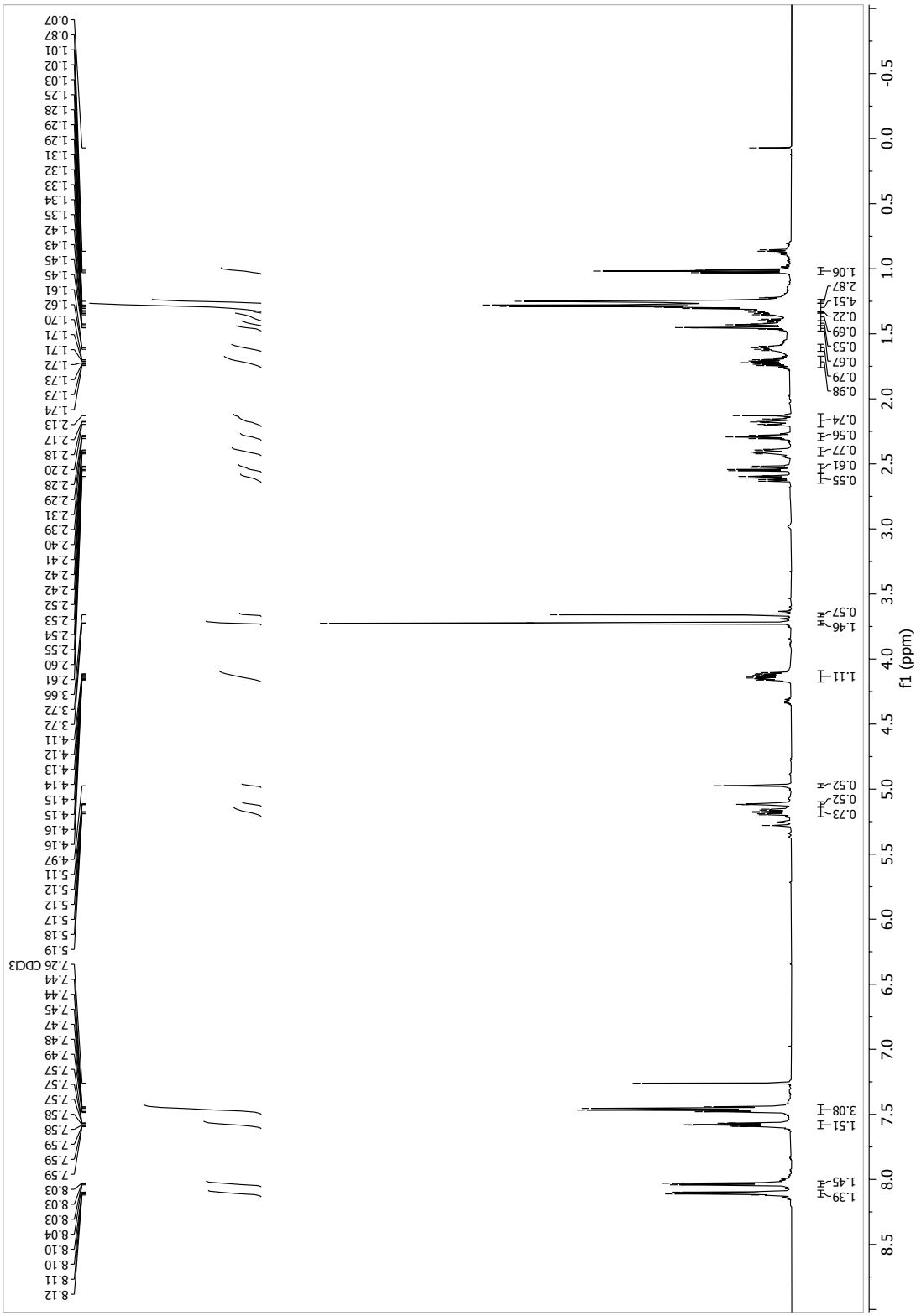

13.1.69 (2*S*,3*S*,5*S*,6*R*)-2-(henicosyloxy)-6-methyltetrahydro-2*H*-pyran-3,5-diol (asc-ωC21-H, 68a)

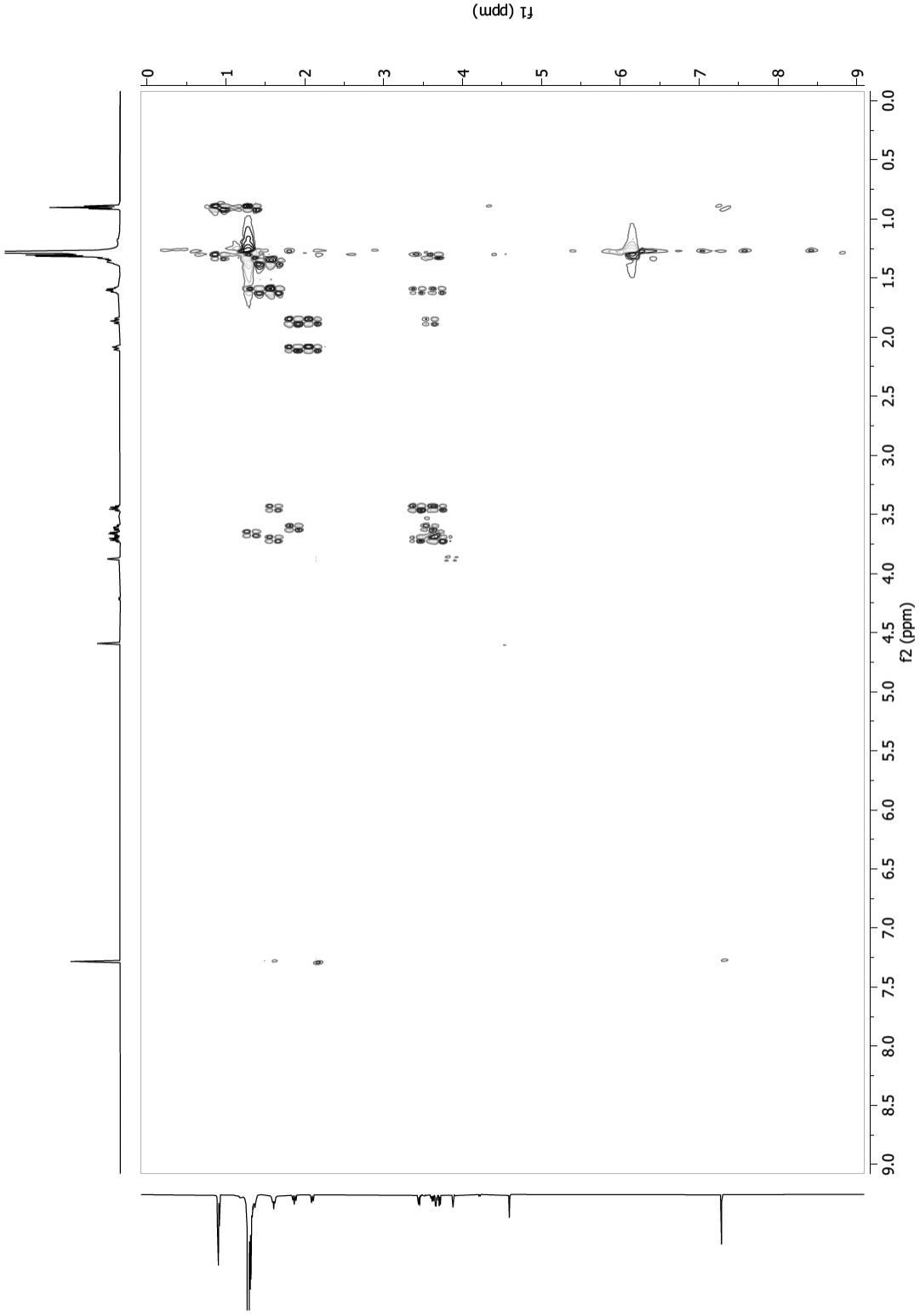

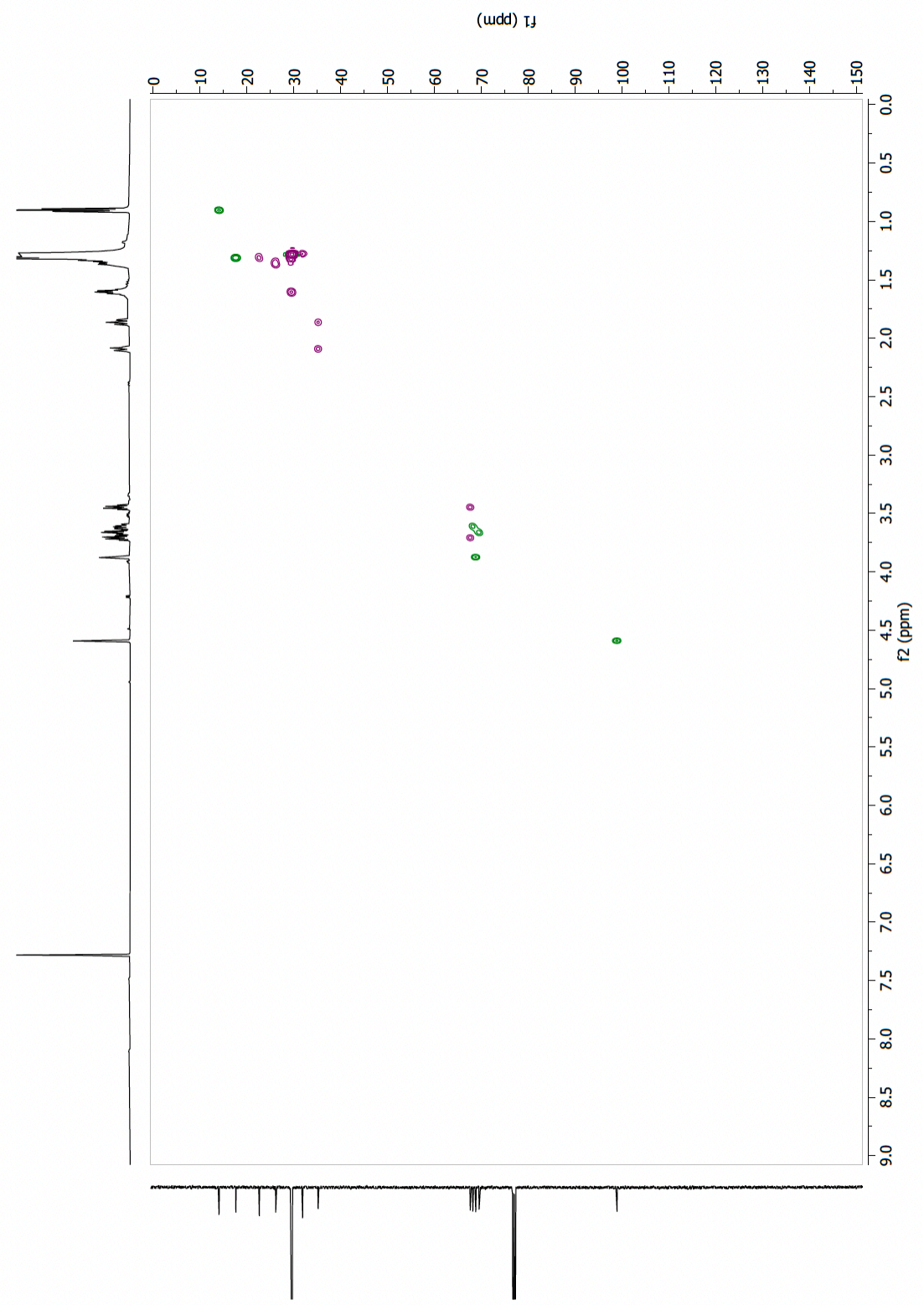
f1 (ppm)
f2 (ppm)

13.1.70 (2*S*,3*R*,5*R*,6*R*)-6-(henicosyloxy)-5-hydroxy-2-methyltetrahydro-2*H*-pyran-3-yl acetate (4-Ac-asc-ωC21-H, 80)

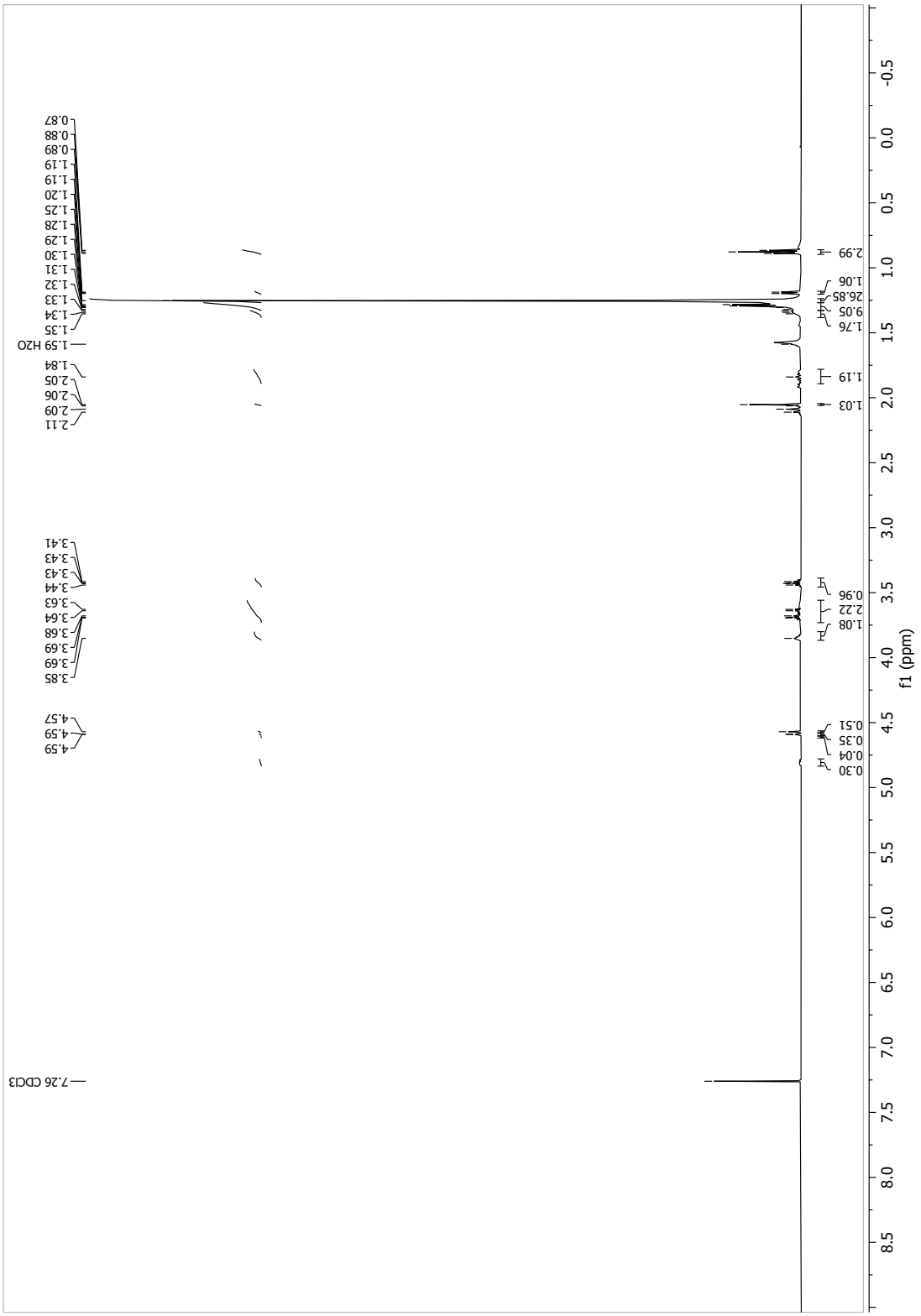

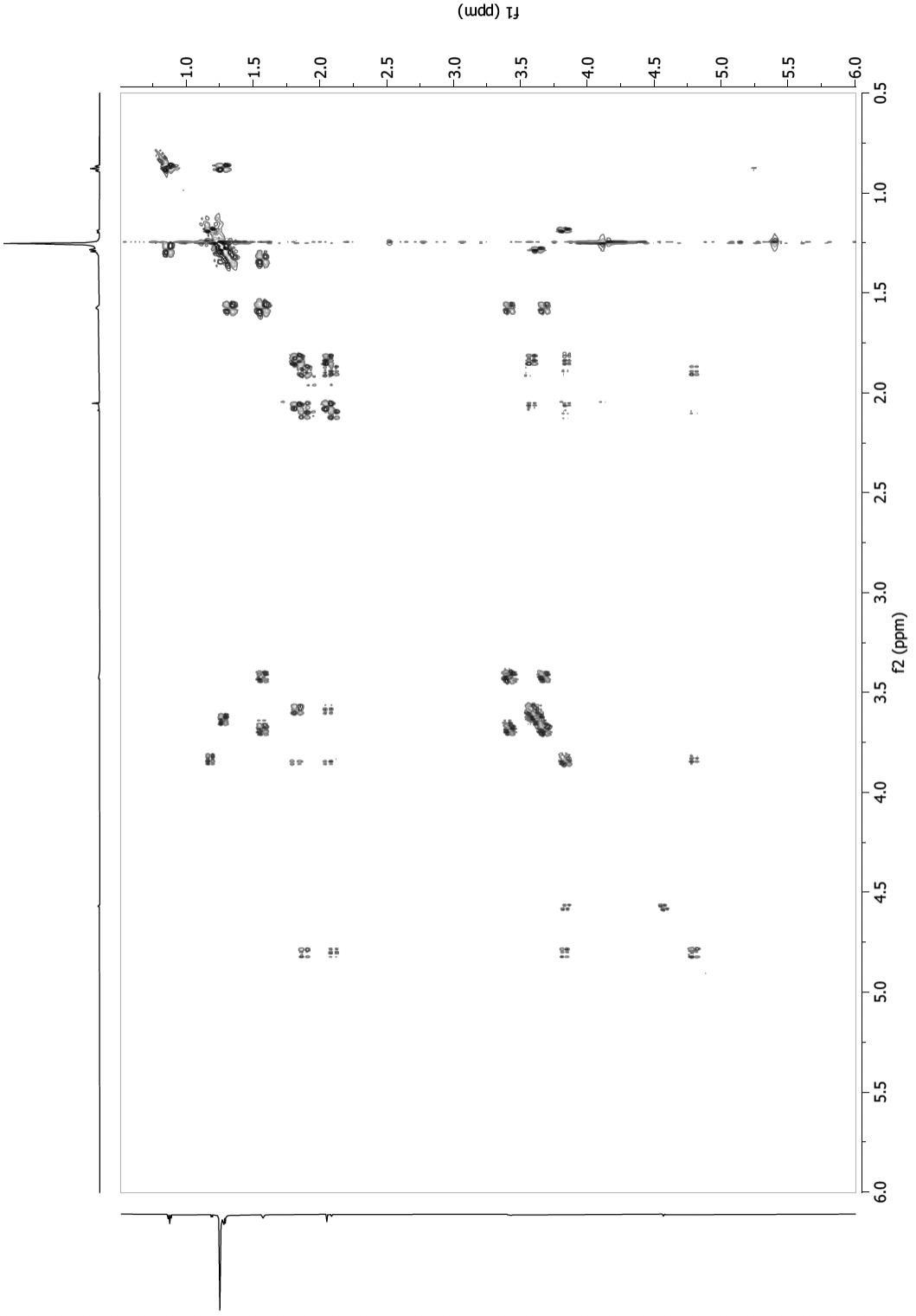
f1 (ppm)
1.0
1.5
2.0
2.5
3.0
3.5
4.0
4.5
5.0
5.5
6.0
f2 (ppm)
0.5
1.0
1.5
2.0
2.5
3.0
3.5
4.0
4.5
5.0
5.5
6.0

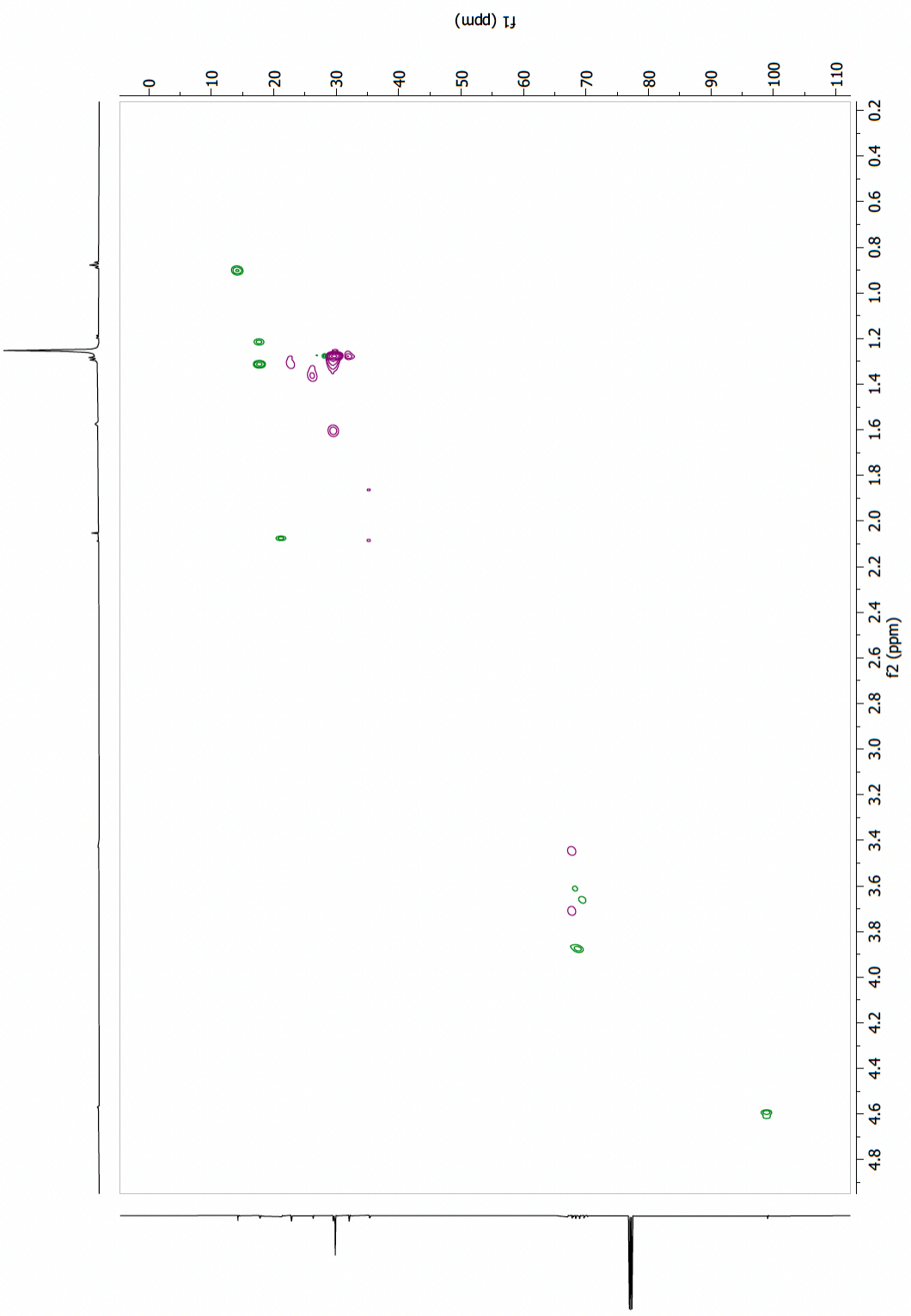
f1 (ppm)
0
10
20
30
40
50
60
70
80
90
100
110
f2 (ppm)
0.2
0.4
0.6
0.8
1.0
1.2
1.4
1.6
1.8
2.0
2.2
2.4
2.6
2.8
3.0
3.2
3.4
3.6
3.8
4.0
4.2
4.4
4.6
4.8

13.1.71 (2*R*,3*R*,5*R*,6*S*)-2-(henicosyloxy)-6-methyltetrahydro-2*H*-pyran-3,5-diyl diacetate (Ac2-asc-ωC21-H, 76)

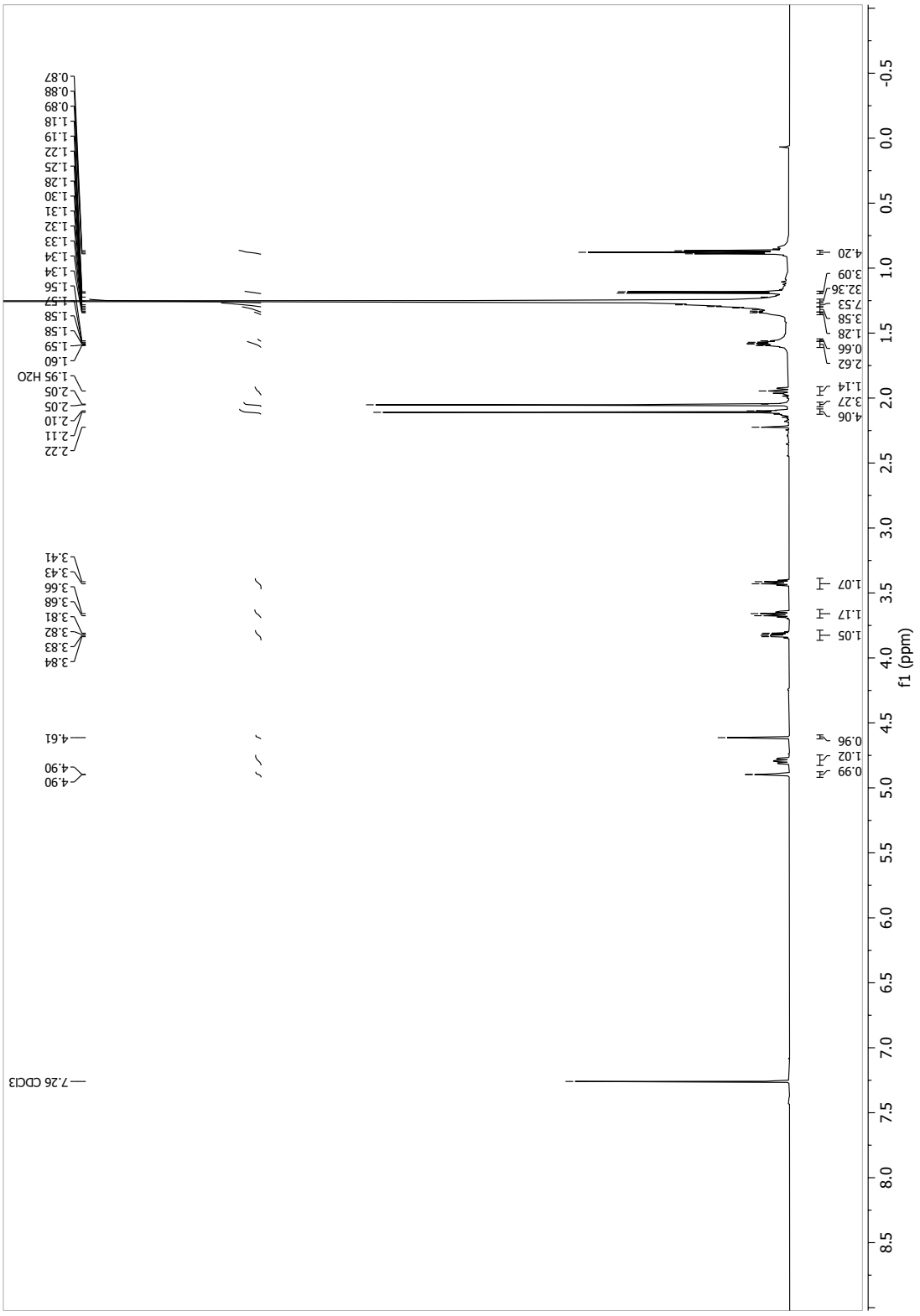

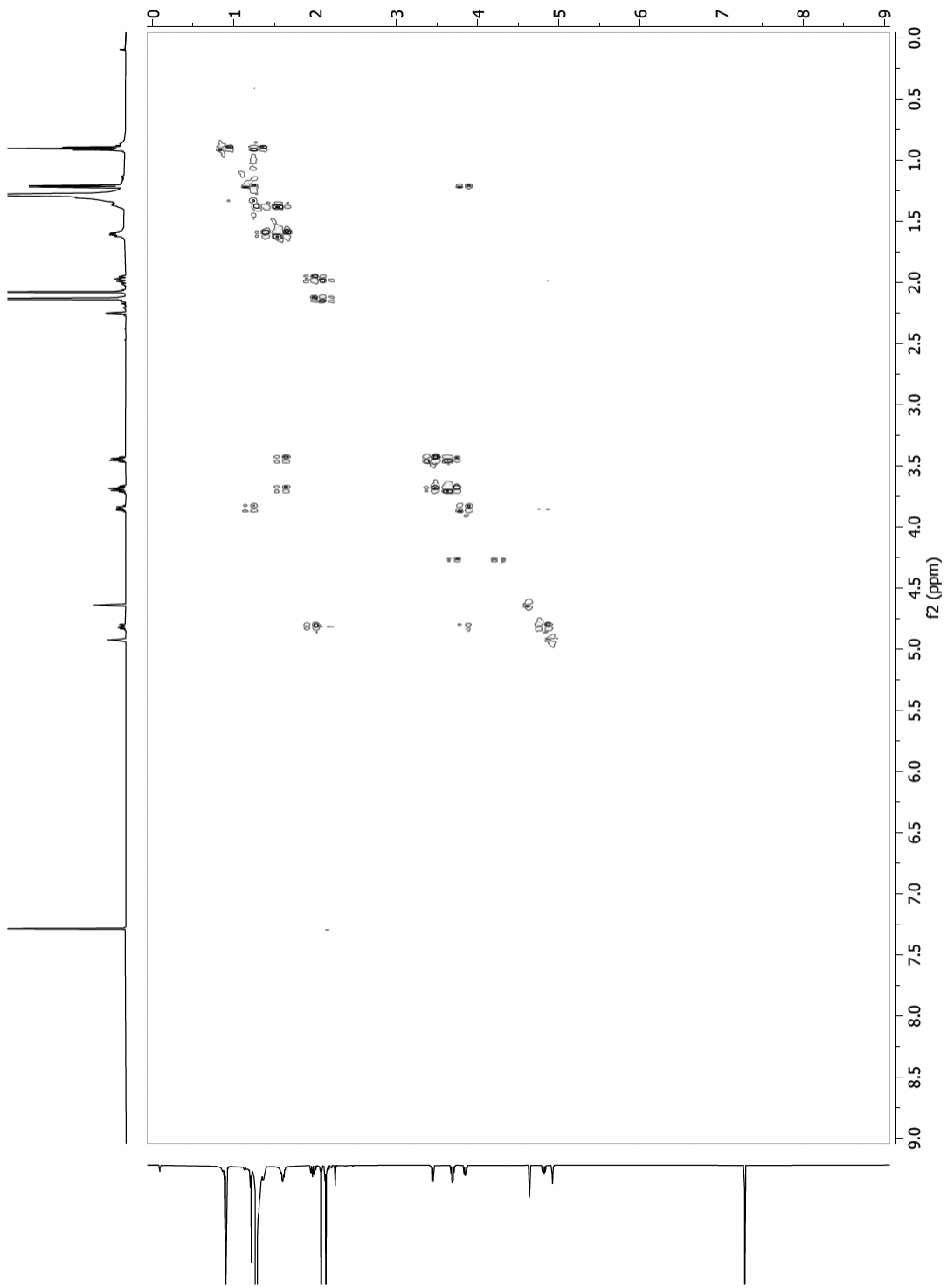
f1 (ppm)
f2 (ppm)

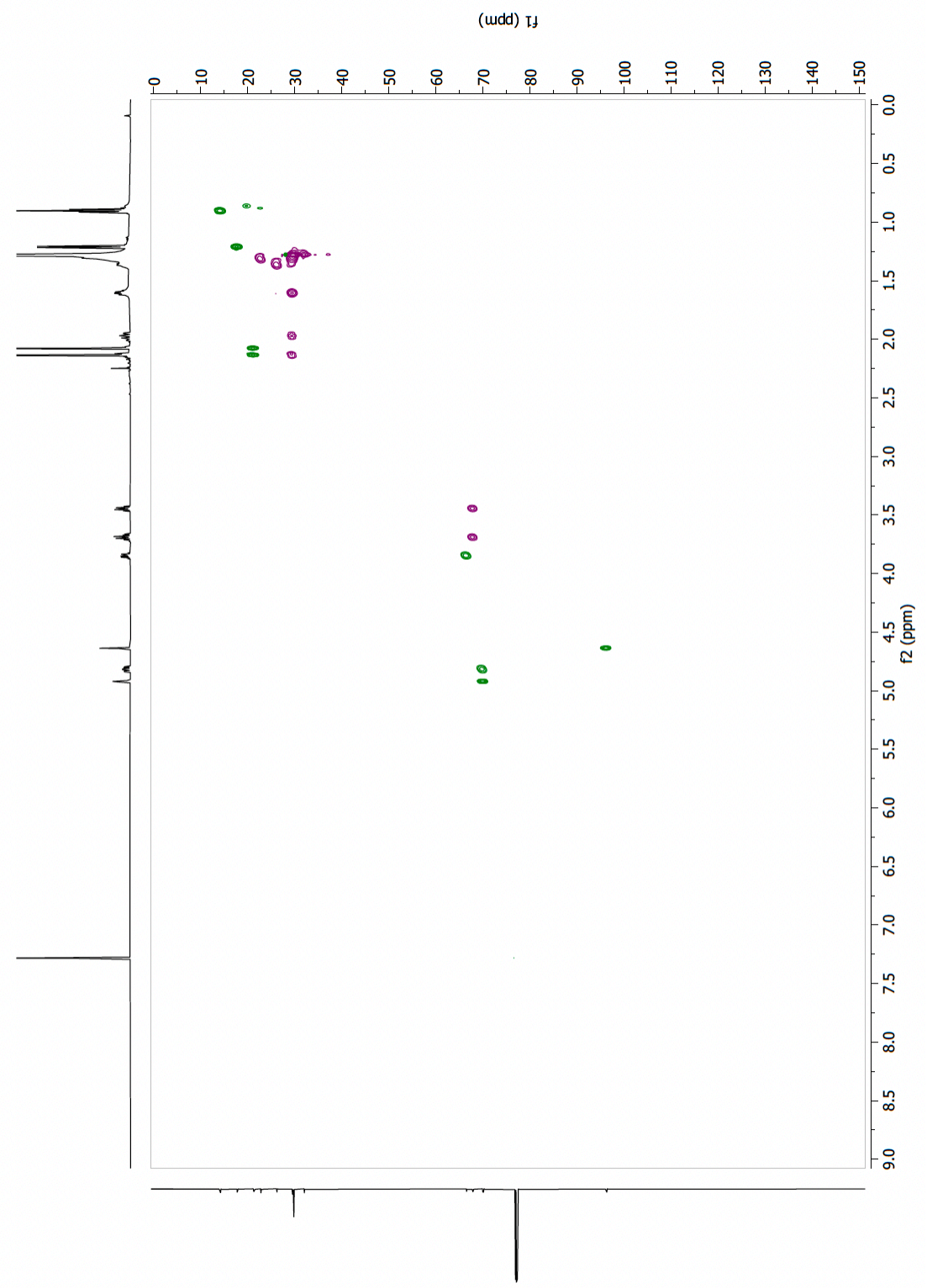
f1 (ppm)
0
10
20
30
40
50
60
70
80
90
100
110
120
130
140
150
f2 (ppm)
0.0
0.5
1.0
1.5
2.0
2.5
3.0
3.5
4.0
4.5
5.0
5.5
6.0
6.5
7.0
7.5
8.0
8.5
9.0

13.1.72 (2*S*,3*R*,5*R*,6*R*)-2-methyl-6-(((*R*)-pentacosan-2-yl)oxy)tetrahydro-2*H*-pyran-3,5-diol (asc-C25-H, 33a)

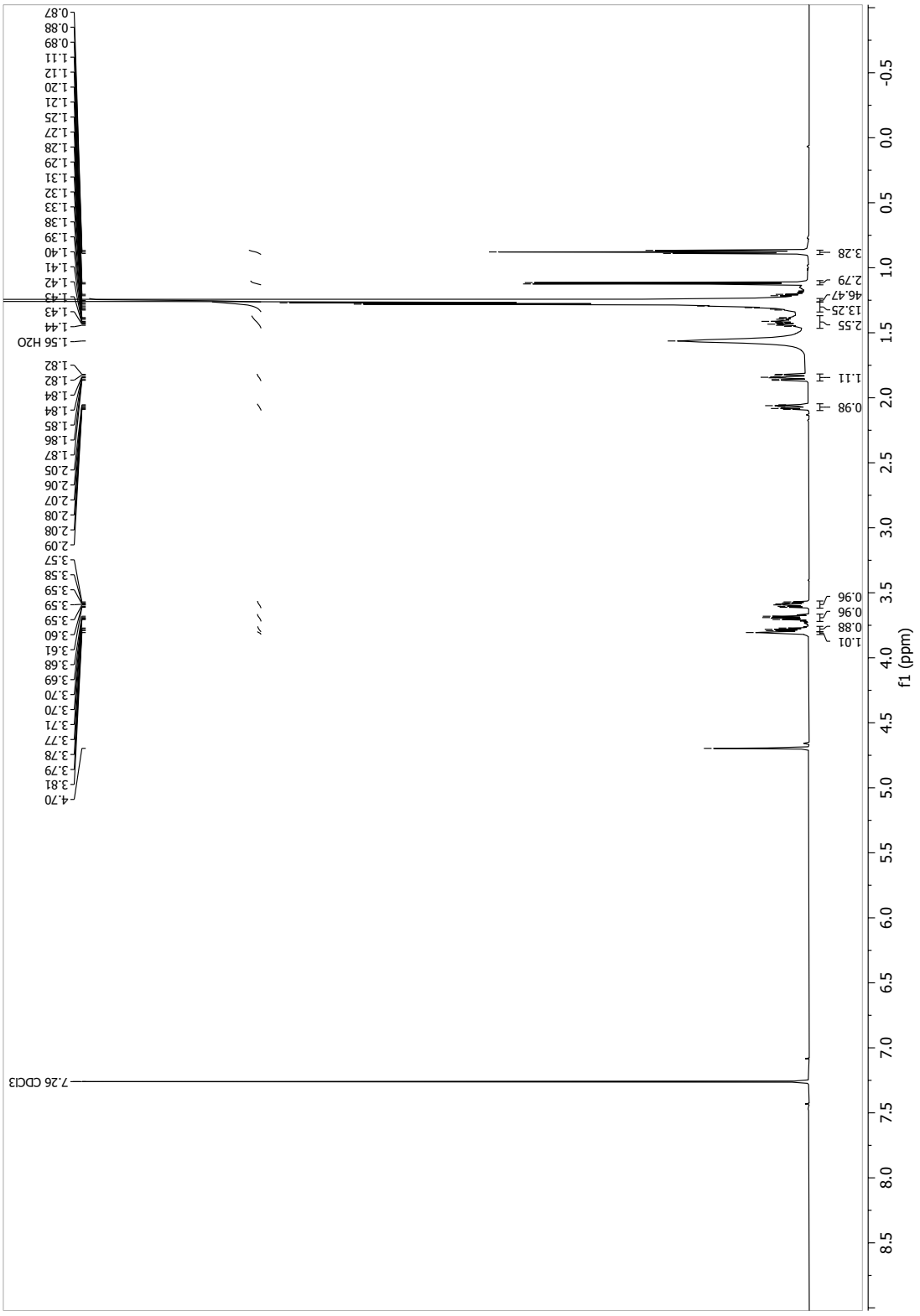

f1 (ppm)
f2 (ppm)

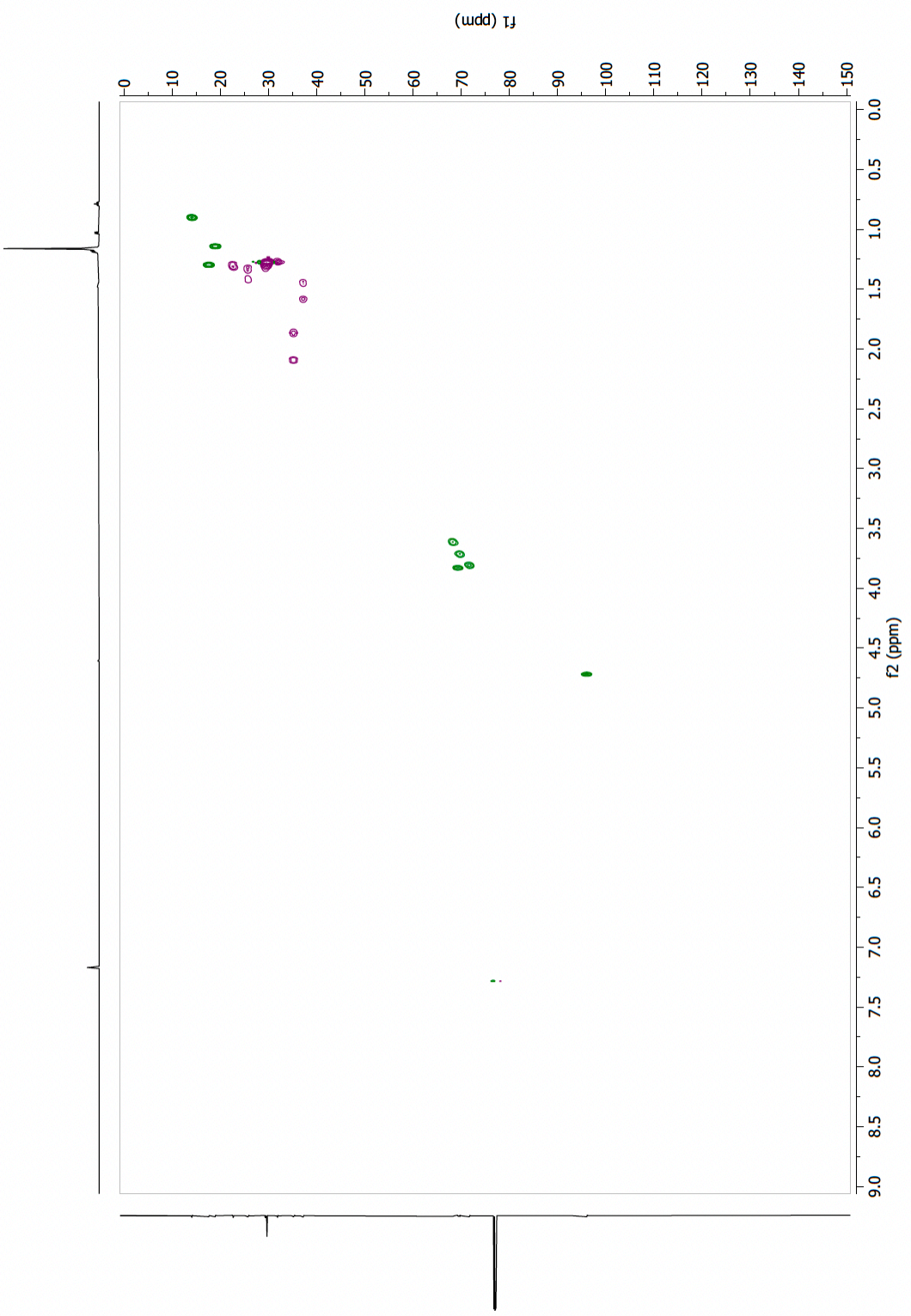
f1 (ppm)
0
10
20
30
40
50
60
70
80
90
100
110
120
130
140
150
f2 (ppm)
0.0
0.5
1.0
1.5
2.0
2.5
3.0
3.5
4.0
4.5
5.0
5.5
6.0
6.5
7.0
7.5
8.0
8.5
9.0

13.1.73 (2*S*,3*R*,5*R*,6*R*)-5-hydroxy-2-methyl-6-(((*R*)-pentacosan-2-yl)oxy)tetrahydro-2*H*-pyran-3-yl acetate (4-Ac-asc-C25-H, 81)

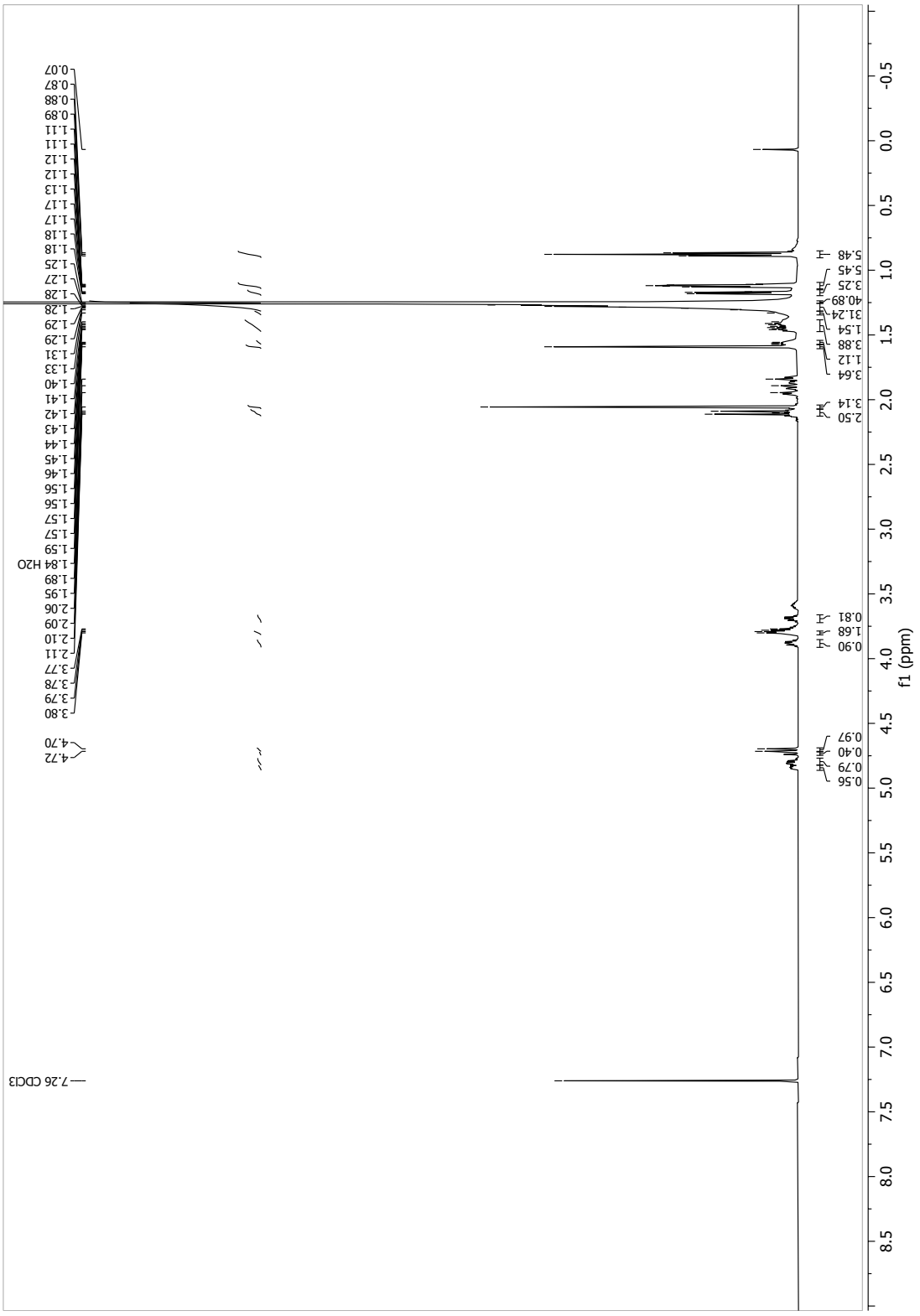

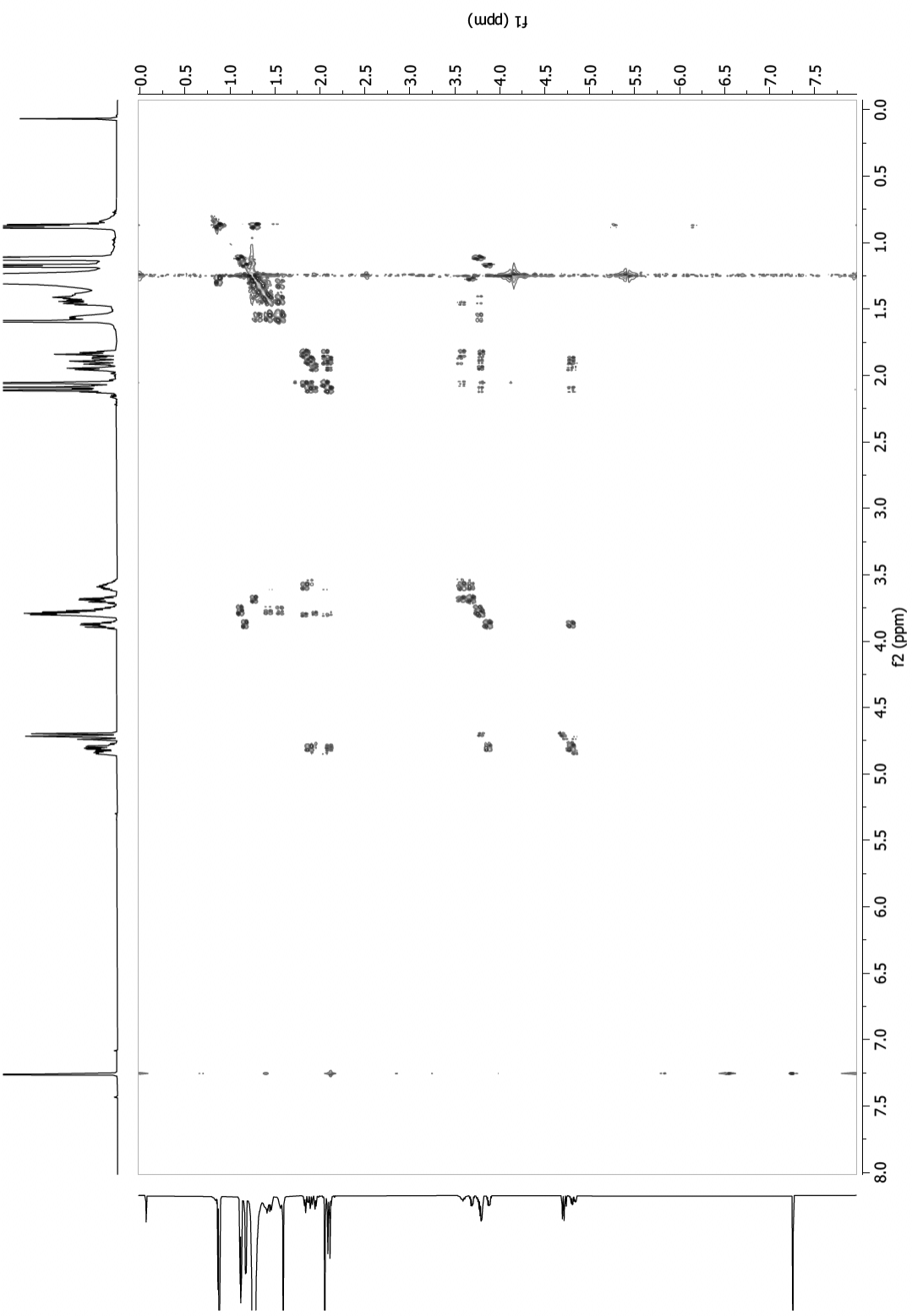
f1 (ppm)
0.0
0.5
1.0
1.5
2.0
2.5
3.0
3.5
4.0
4.5
5.0
5.5
6.0
6.5
7.0
7.5
8.0
f2 (ppm)

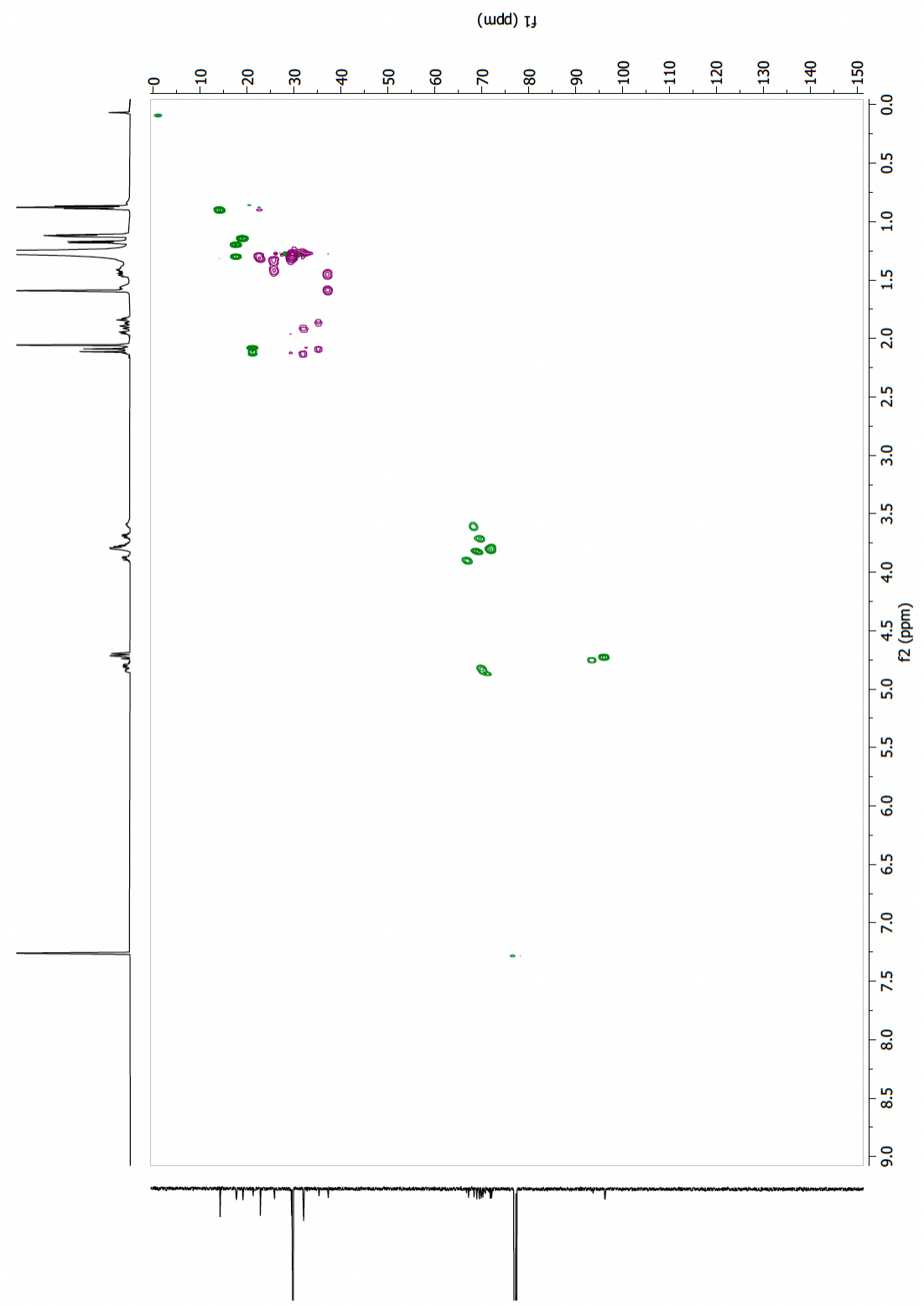
f1 (ppm)
0
10
20
30
40
50
60
70
80
90
100
110
120
130
140
150
f2 (ppm)
0.0
0.5
1.0
1.5
2.0
2.5
3.0
3.5
4.0
4.5
5.0
5.5
6.0
6.5
7.0
7.5
8.0
8.5
9.0

13.1.74 (2*S*,3*R*,5*R*,6*R*)-2-methyl-6-(((*R*)-pentacosan-2-yl)oxy)tetrahydro-2*H*-pyran-3,5-diyl (Ac2-asc-C25-H, 77)

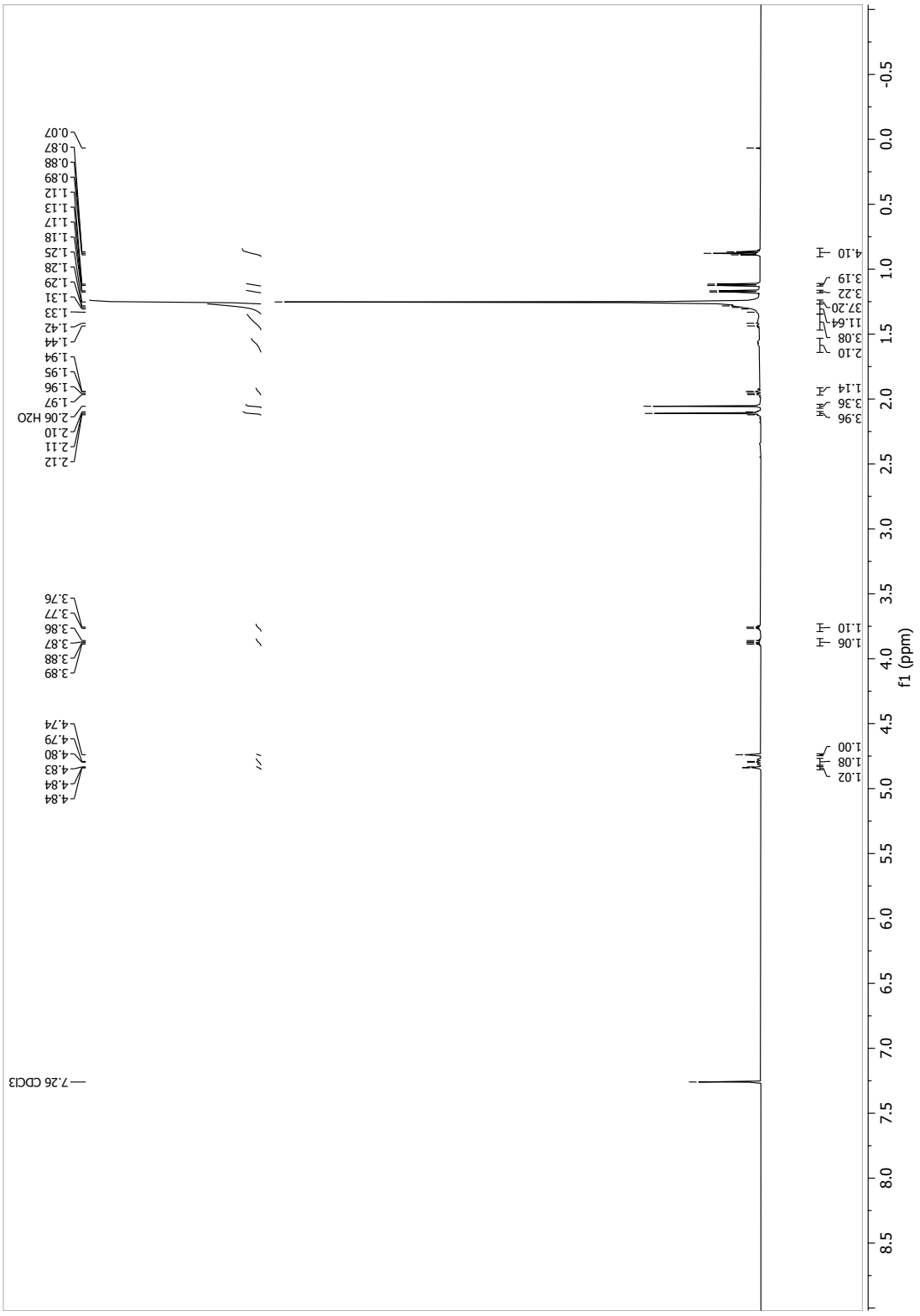

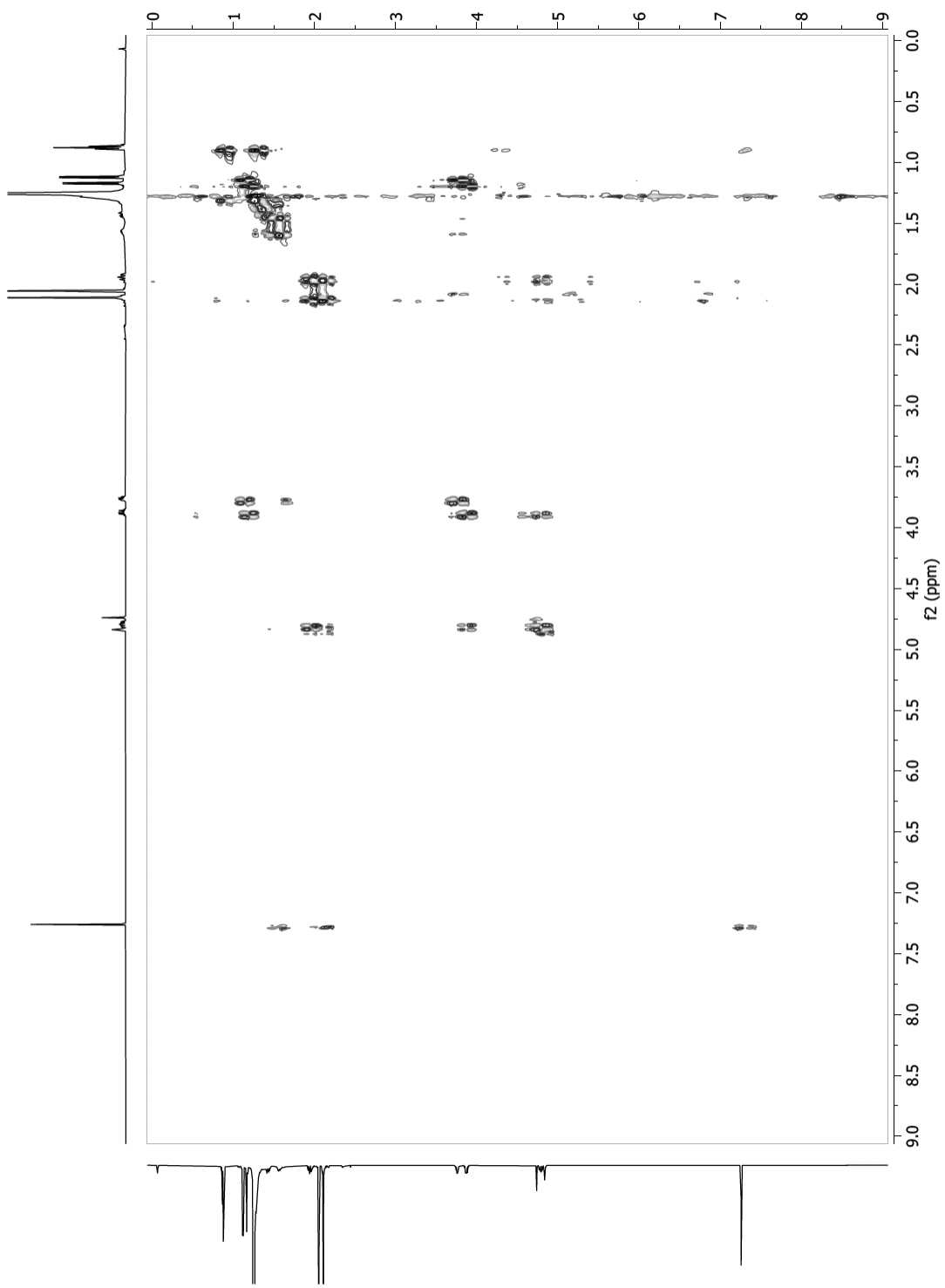
f1 (ppm)
f2 (ppm)

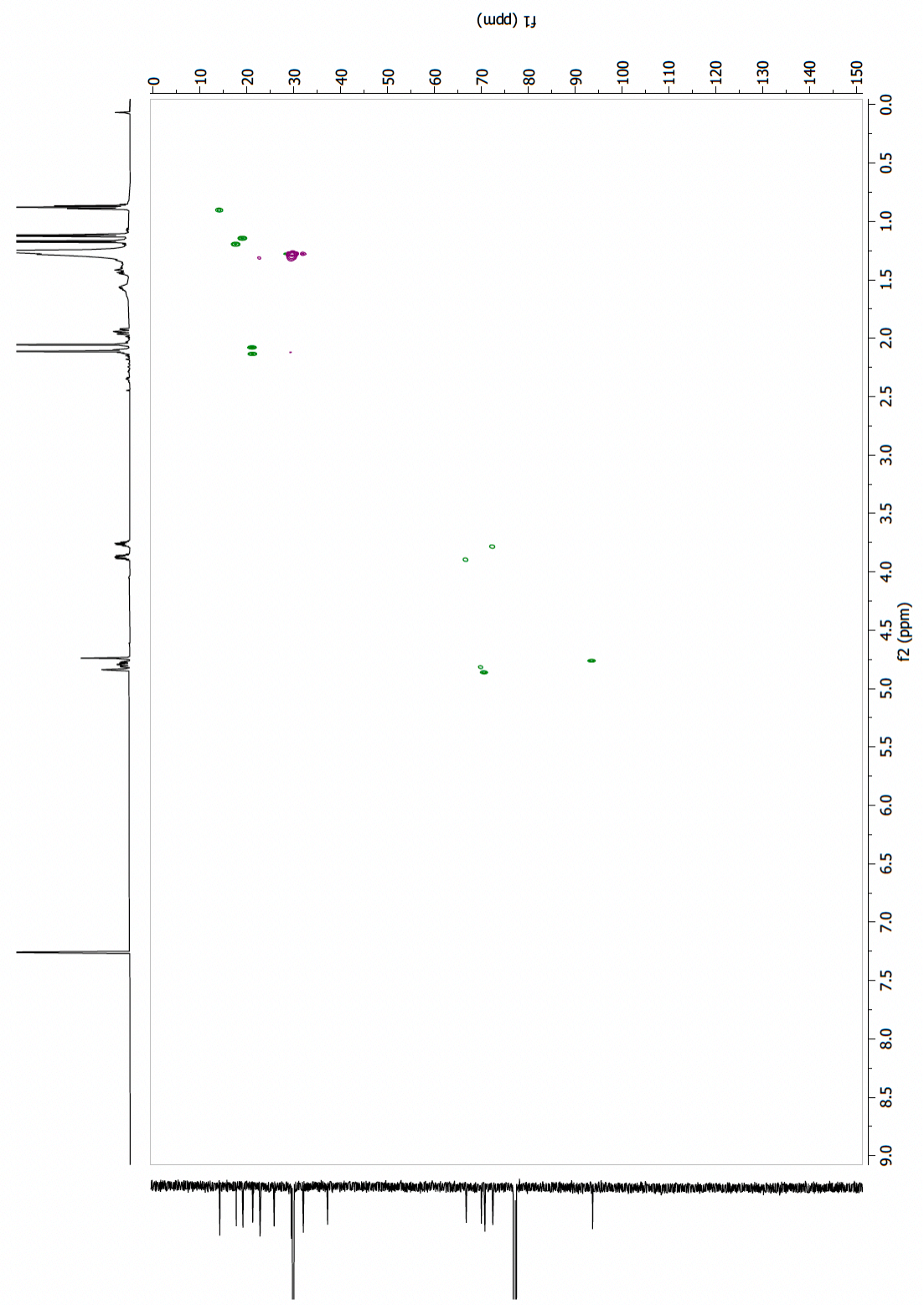
f1 (ppm)
0
10
20
30
40
50
60
70
80
90
100
110
120
130
140
150
f2 (ppm)
0.0
0.5
1.0
1.5
2.0
2.5
3.0
3.5
4.0
4.5
5.0
5.5
6.0
6.5
7.0
7.5
8.0
8.5
9.0

13.1.75 (2*S*,3*R*,5*R*,6*R*)-2-methyl-6-(((*R*)-24-methylpentacosan-2-yl)oxy)tetrahydro-2*H*-pyran-3,5-diol (asc-*i*C26-H, 43a)

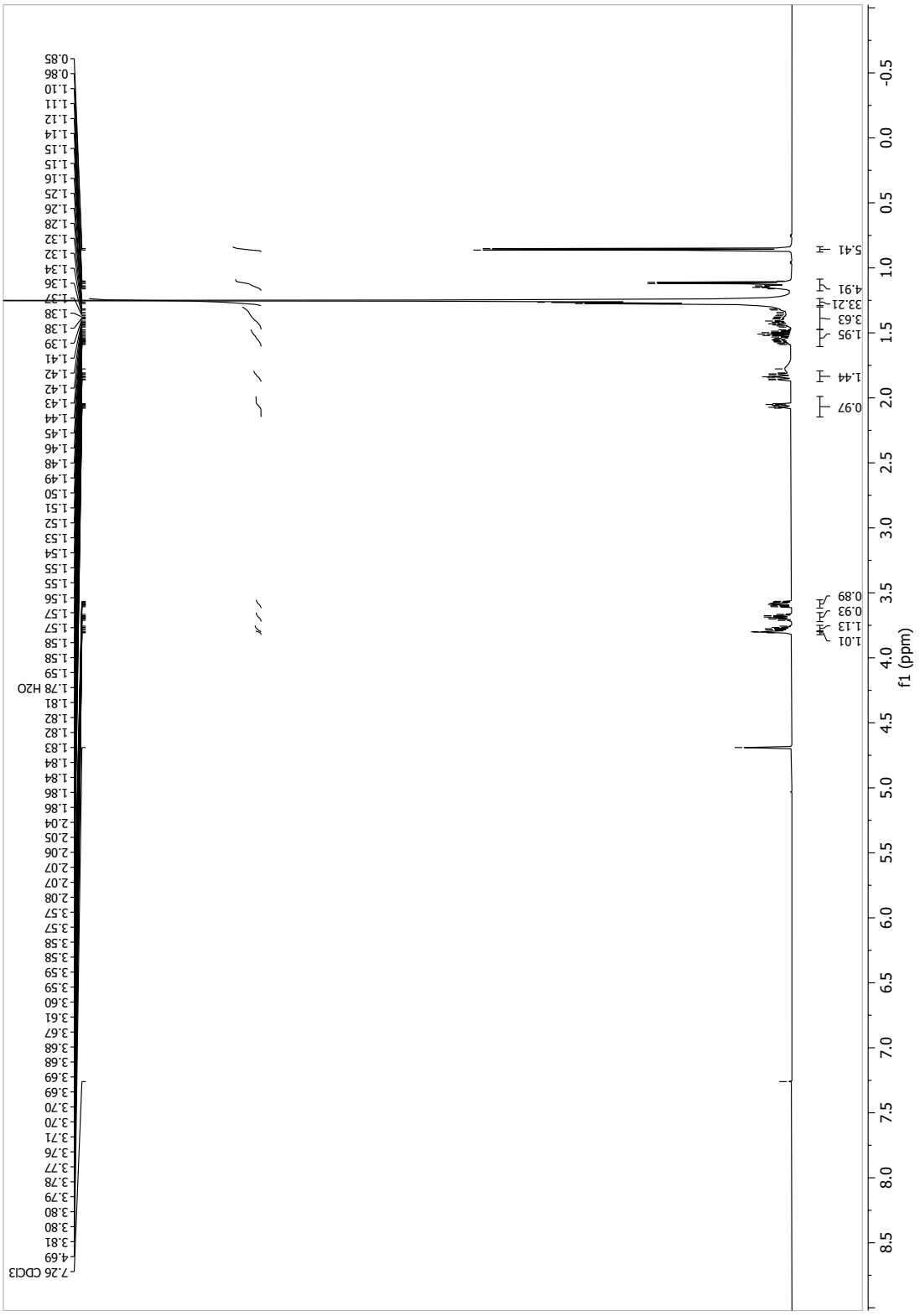

f1 (ppm)
0
1
2
3
4
5
6
7
8
9
f2 (ppm)
0.0
0.5
1.0
1.5
2.0
2.5
3.0
3.5
4.0
4.5
5.0
5.5
6.0
6.5
7.0
7.5
8.0
8.5
9.0

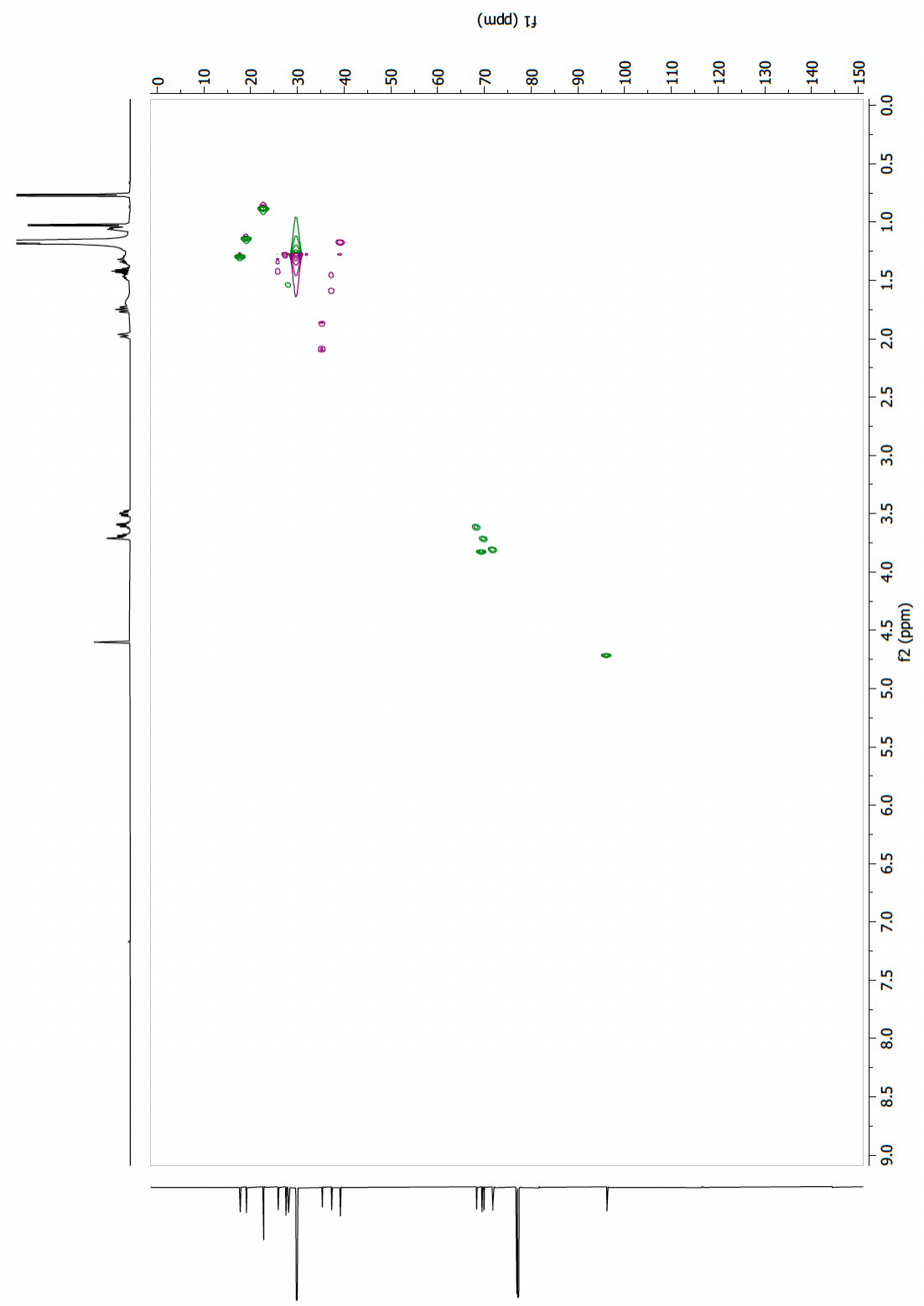
f1 (ppm)
0
10
20
30
40
50
60
70
80
90
100
110
120
130
140
150
f2 (ppm)
0.0
0.5
1.0
1.5
2.0
2.5
3.0
3.5
4.0
4.5
5.0
5.5
6.0
6.5
7.0
7.5
8.0
8.5
9.0

13.1.76 (2*S*,3*R*,5*R*,6*R*)-5-hydroxy-2-methyl-6-(((*R*)-24-methylpentacosan-2-yl)oxy)tetrahydro-2*H*-pyran-3-yl acetate (4-Ac-asc-*i*C26-H, 82)

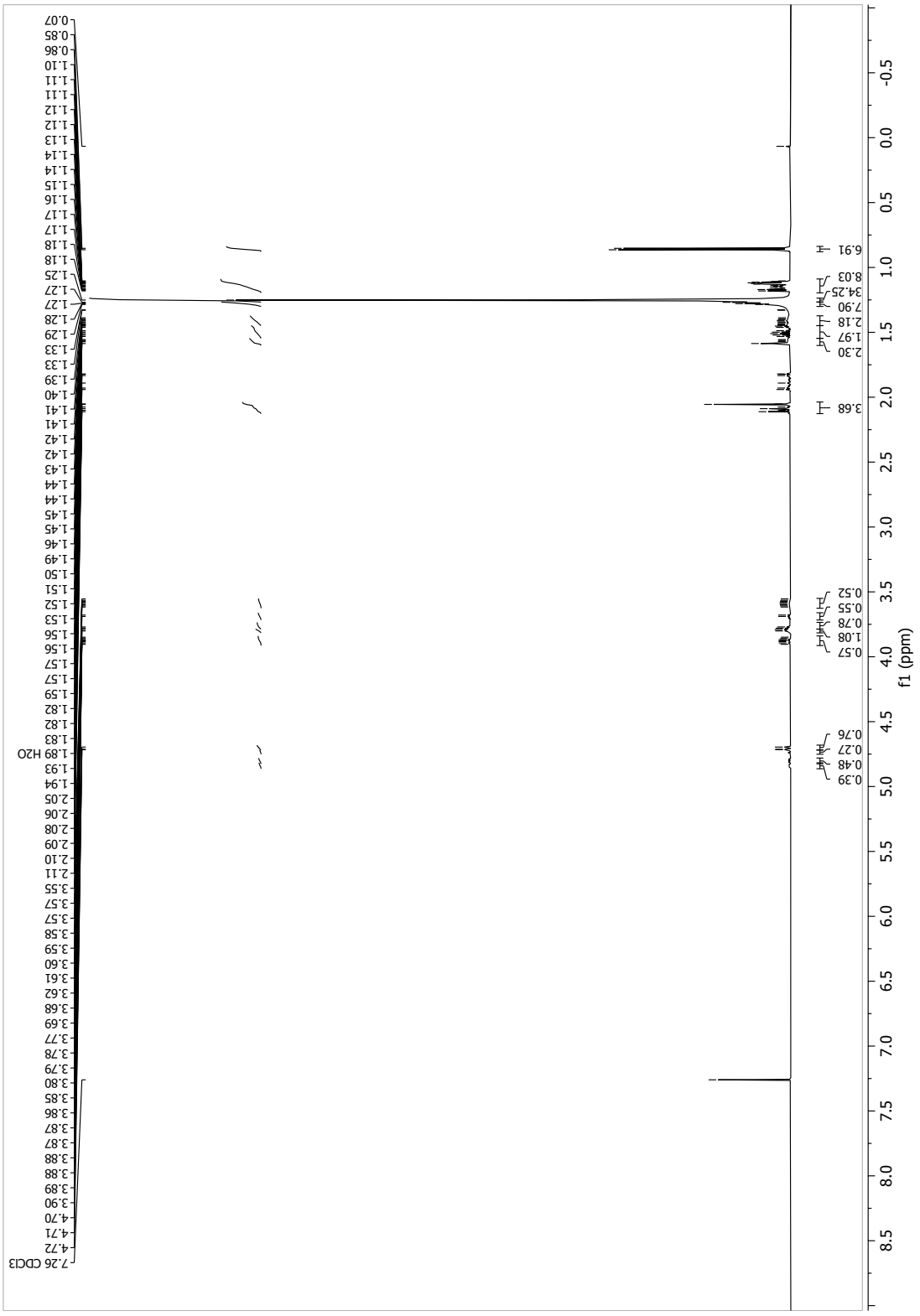

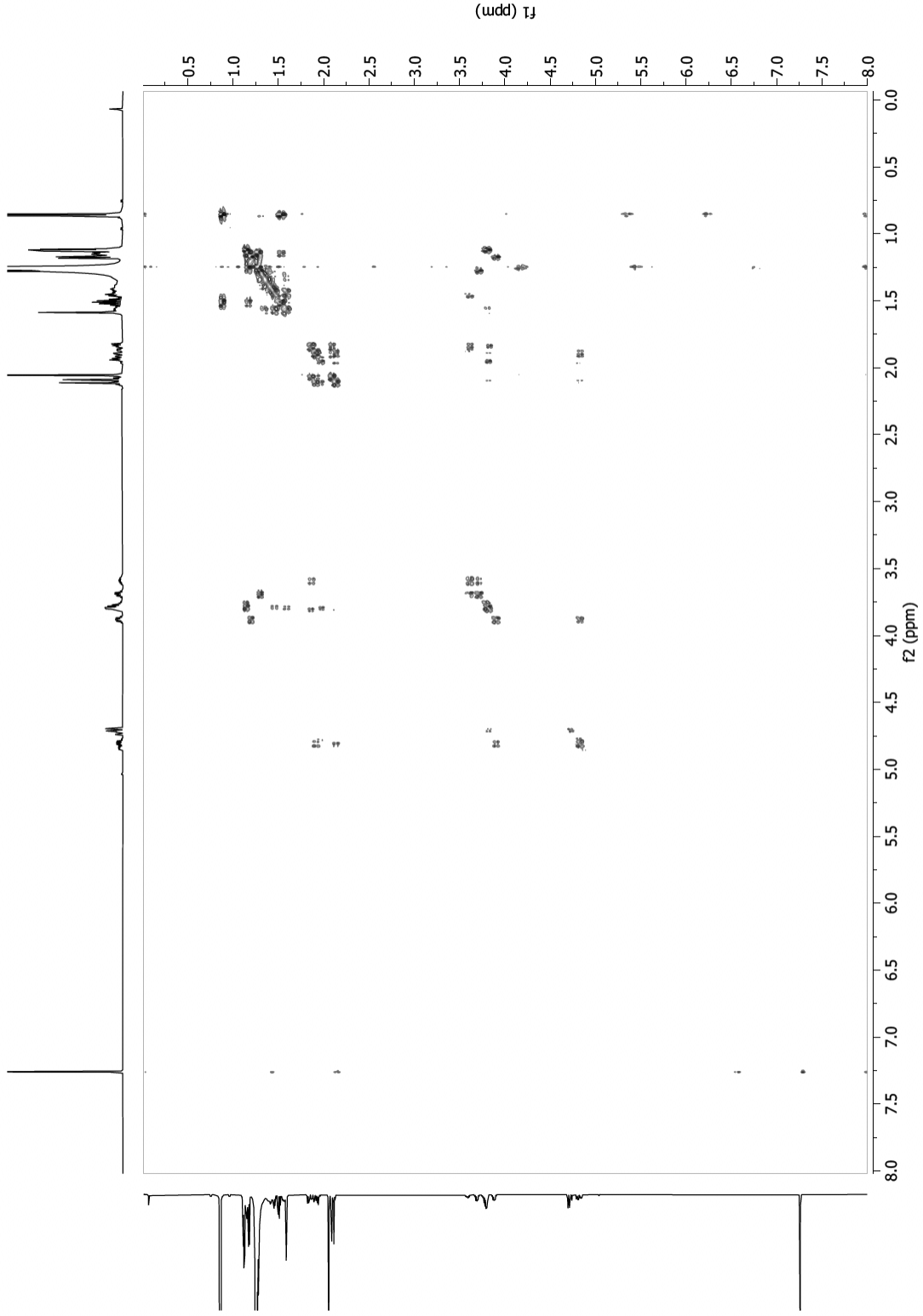
f1 (ppm)
0.5
1.0
1.5
2.0
2.5
3.0
3.5
4.0
4.5
5.0
5.5
6.0
6.5
7.0
7.5
8.0
f2 (ppm)
0.0
0.5
1.0
1.5
2.0
2.5
3.0
3.5
4.0
4.5
5.0
5.5
6.0
6.5
7.0
7.5
8.0

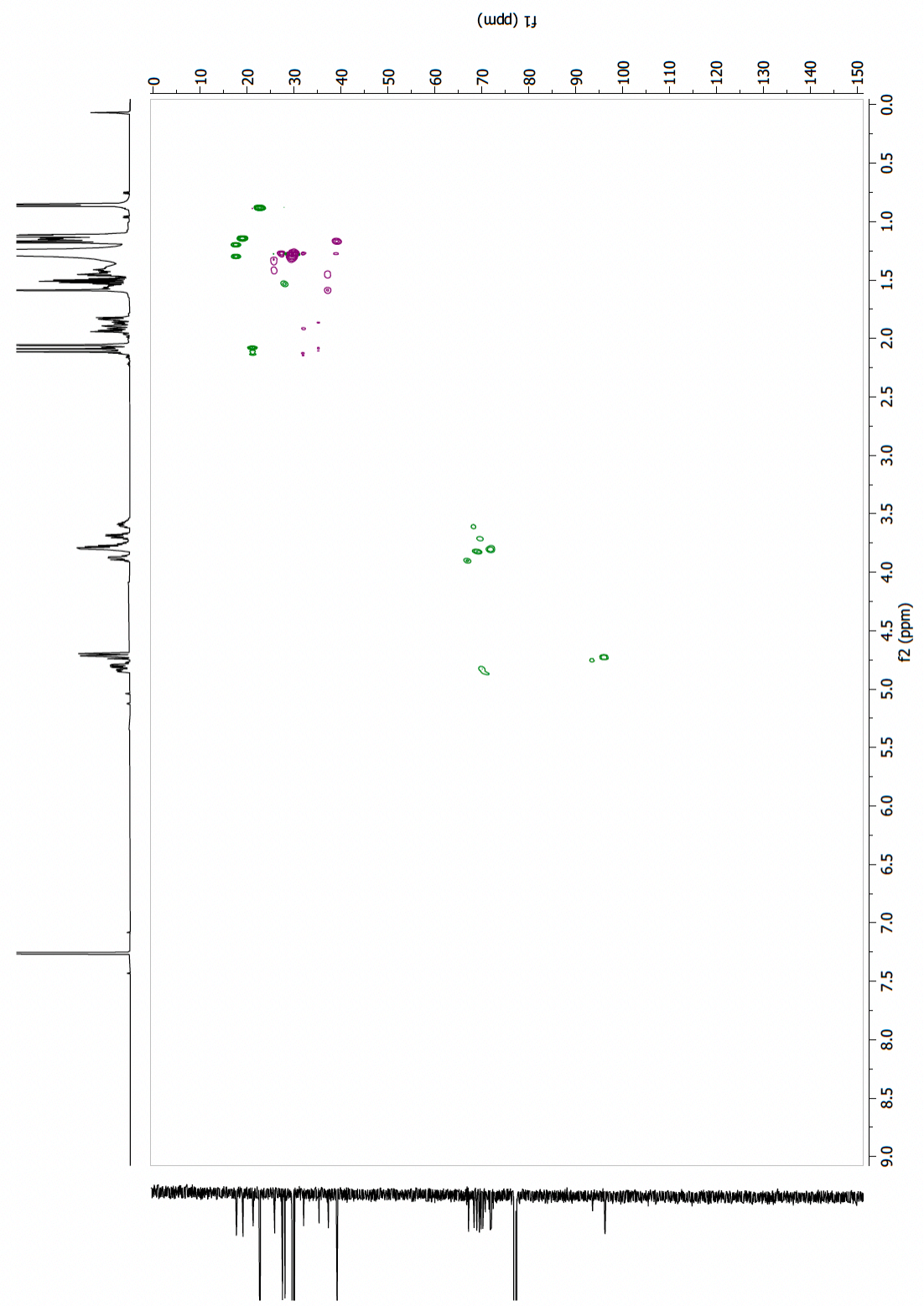
f1 (ppm)
0
10
20
30
40
50
60
70
80
90
100
110
120
130
140
150
f2 (ppm)
0.0
0.5
1.0
1.5
2.0
2.5
3.0
3.5
4.0
4.5
5.0
5.5
6.0
6.5
7.0
7.5
8.0
8.5
9.0

13.1.77 (2*S*,3*R*,5*R*,6*R*)-2-methyl-6-(((*R*)-24-methylpentacosan-2-yl)oxy)tetrahydro-2*H*-pyran-3,5-diyl diacetate (Ac2-asc-*i*C26-H, 78)

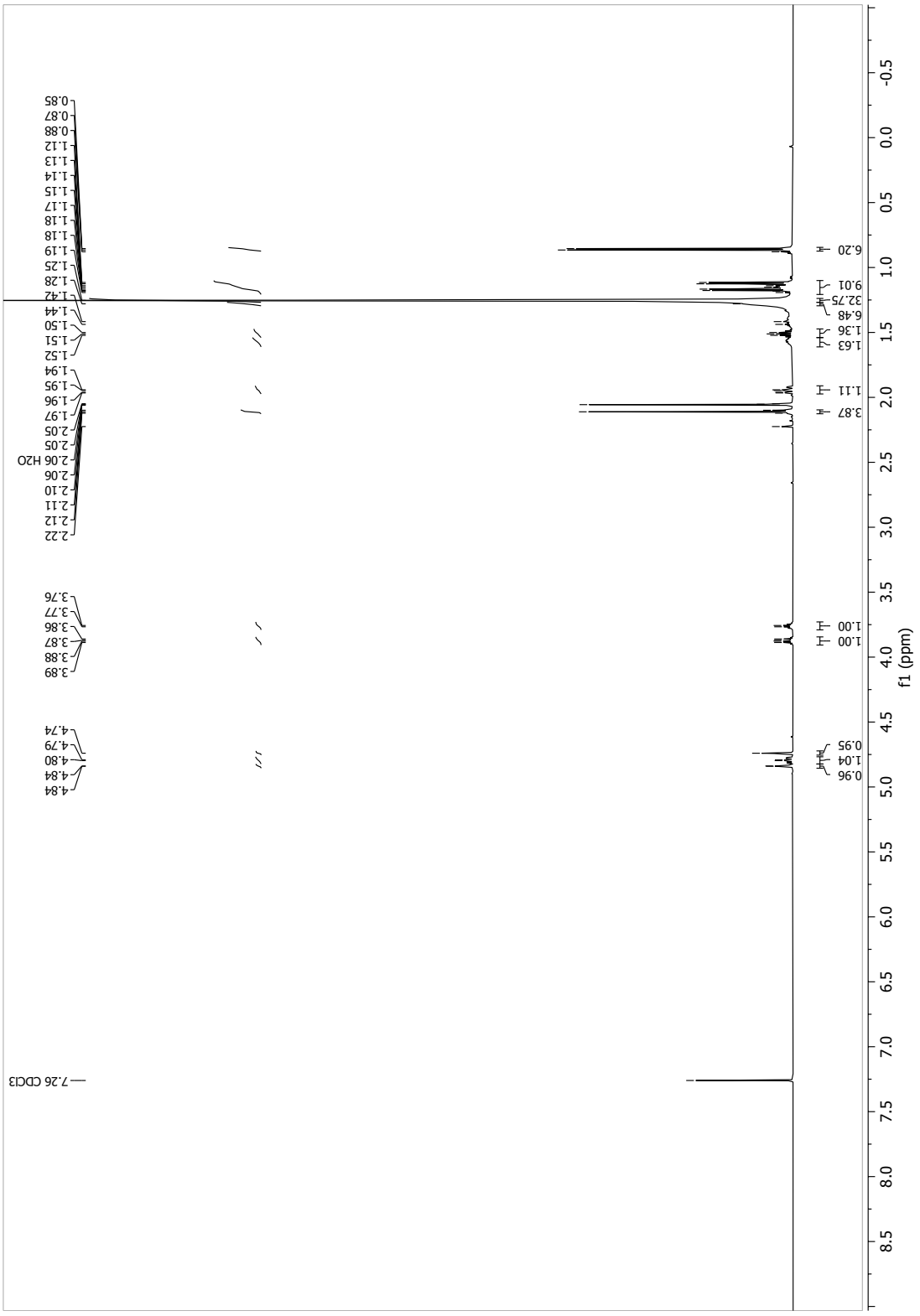

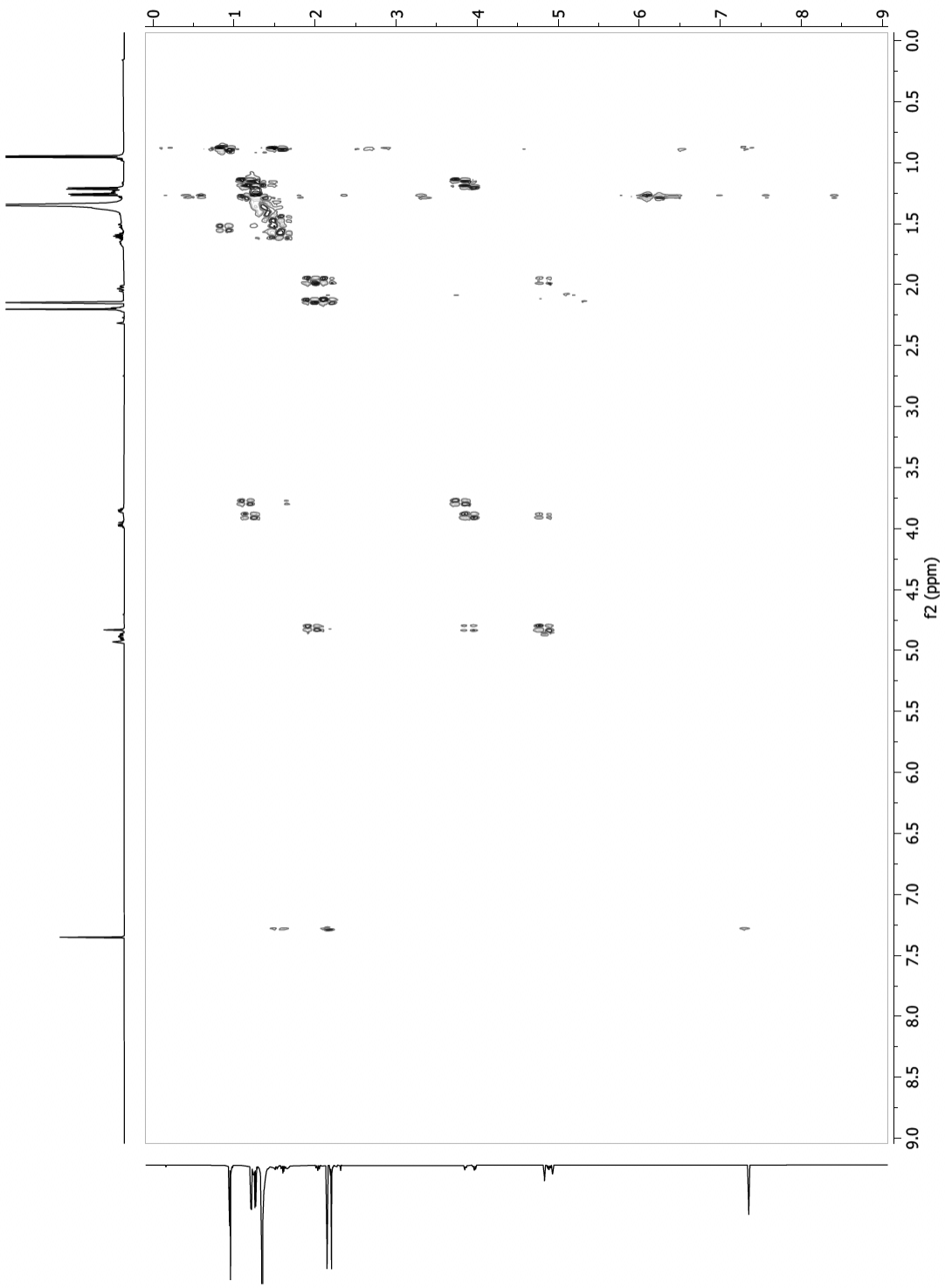
f1 (ppm)
f2 (ppm)

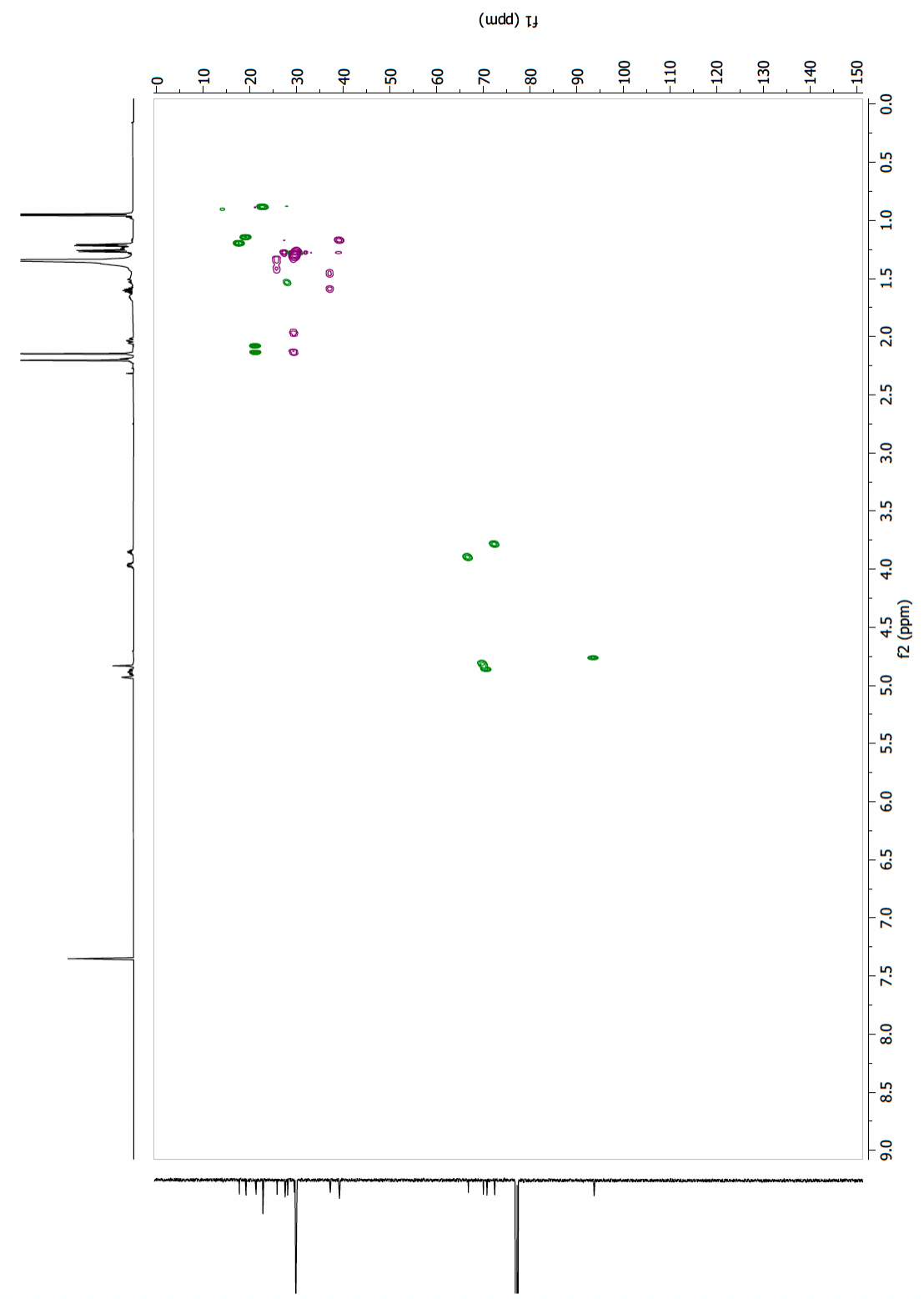
f1 (ppm)
0
10
20
30
40
50
60
70
80
90
100
110
120
130
140
150
f2 (ppm)
0.0
0.5
1.0
1.5
2.0
2.5
3.0
3.5
4.0
4.5
5.0
5.5
6.0
6.5
7.0
7.5
8.0
8.5
9.0

13.1.78 (2*R*,3*R*,5*R*,6*S*)-2-(((*R*)-hentriacontan-2-yl)oxy)-6-methyltetrahydro-2*H*-pyran-3,5-diol (asc-C31-H, 57a)

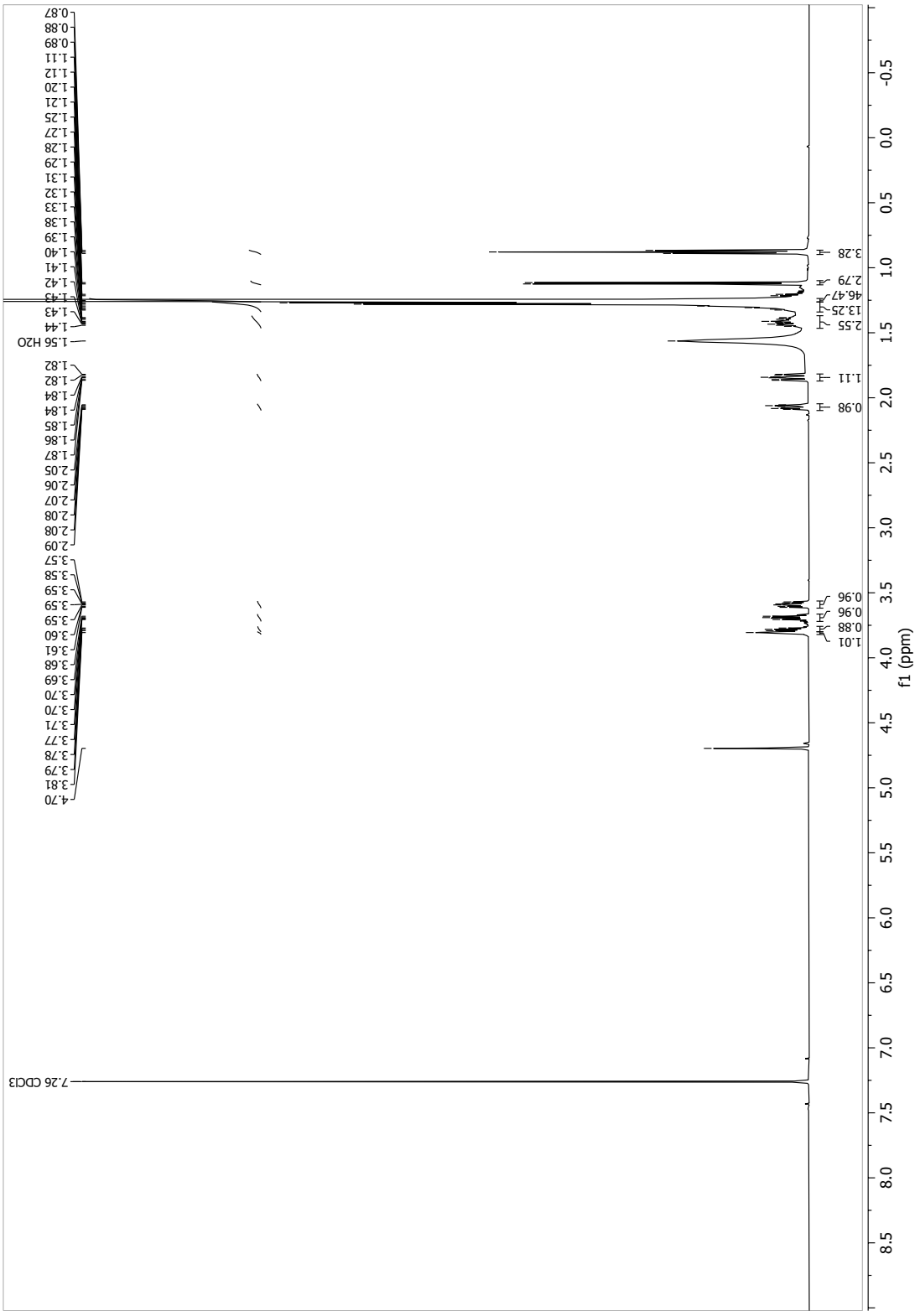

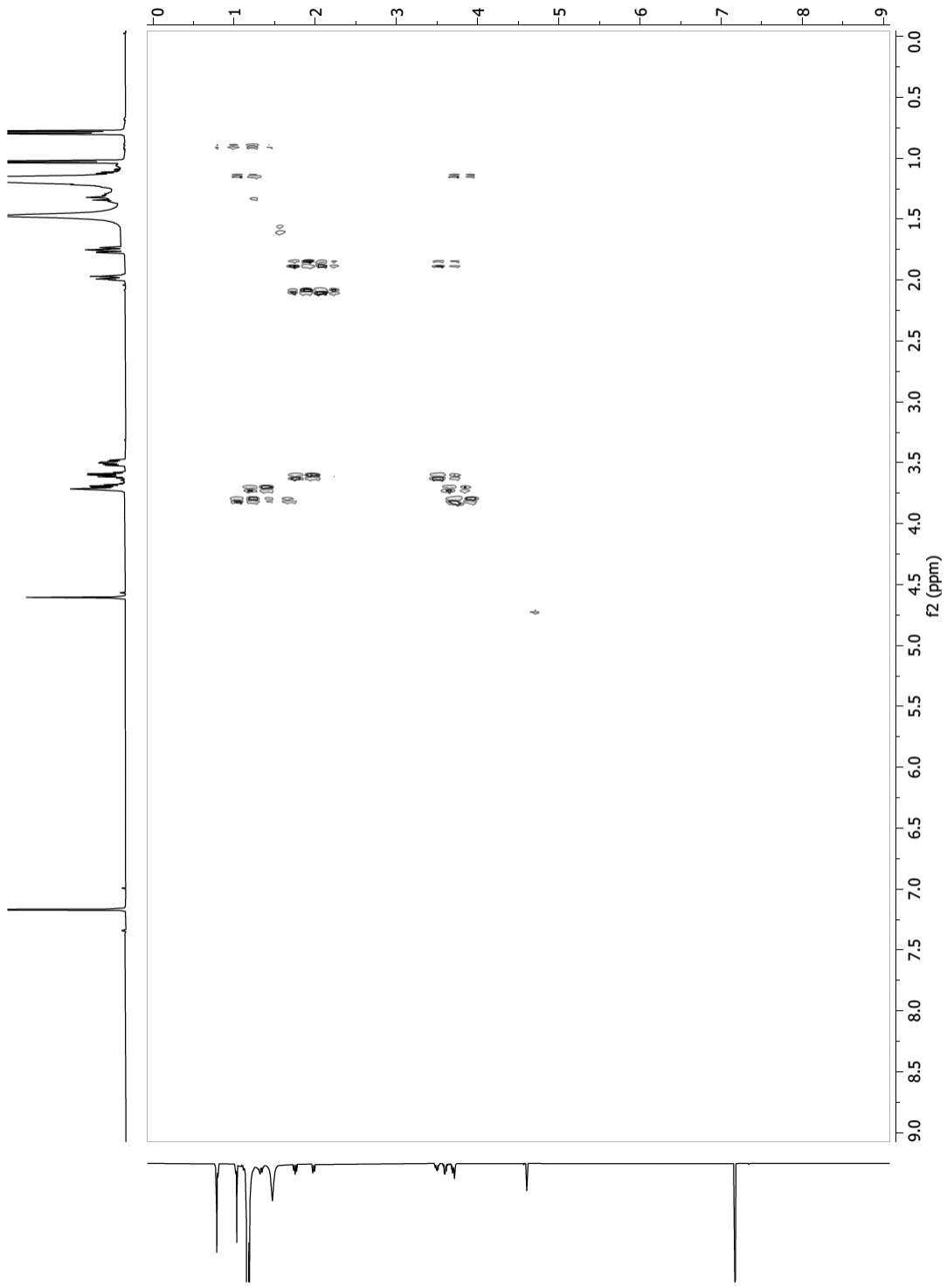
f1 (ppm)
f2 (ppm)

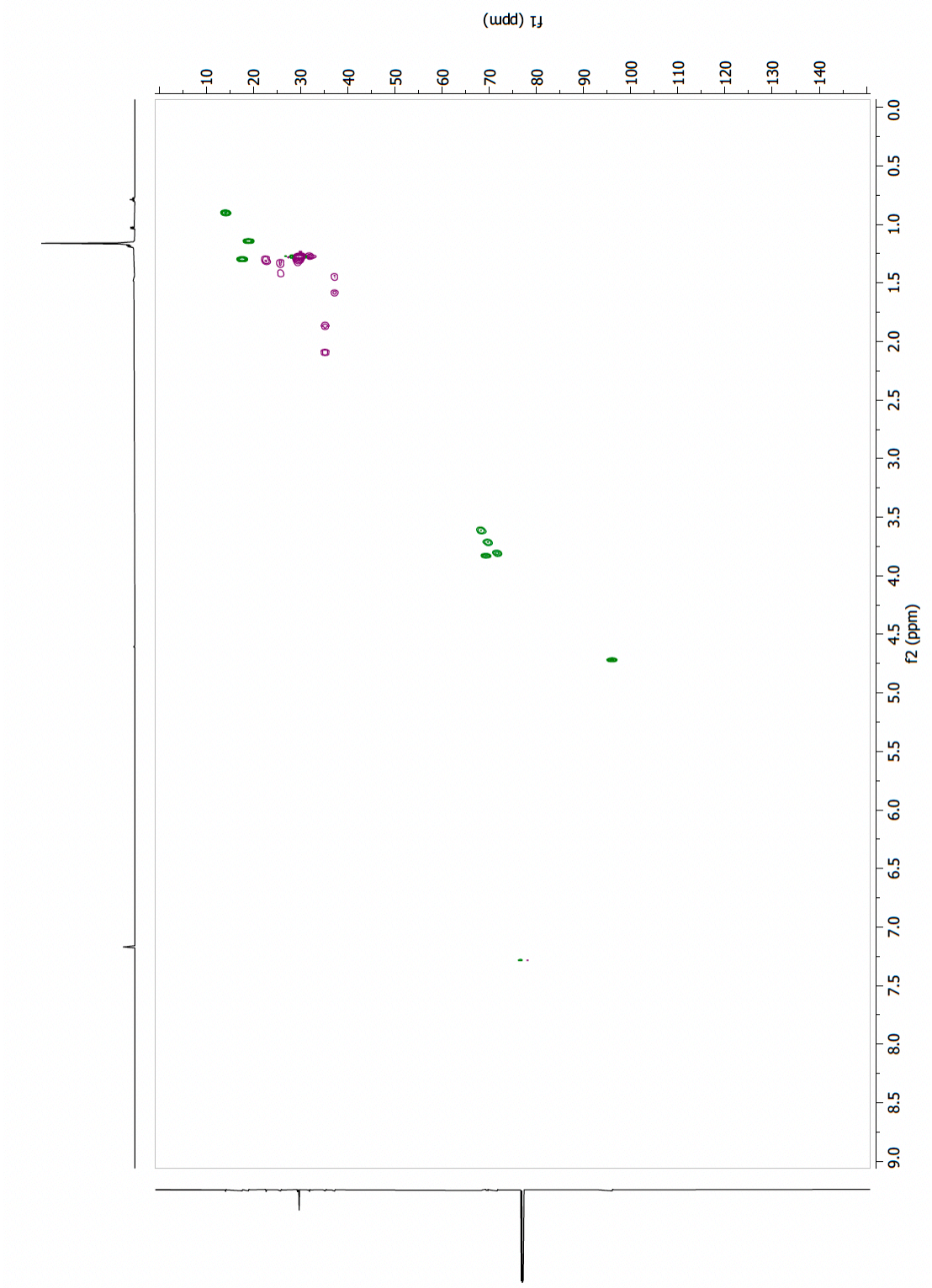
f1 (ppm)
10
20
30
40
50
60
70
80
90
100
110
120
130
140
f2 (ppm)
0.0
0.5
1.0
1.5
2.0
2.5
3.0
3.5
4.0
4.5
5.0
5.5
6.0
6.5
7.0
7.5
8.0
8.5
9.0

13.1.79 (2*S*,3*R*,5*R*,6*R*)-6-(((*R*)-hentriacontan-2-yl)oxy)-5-hydroxy-2-methyltetrahydro-2*H*-pyran-3-yl acetate (4-Ac-asc-C31-H, 83)

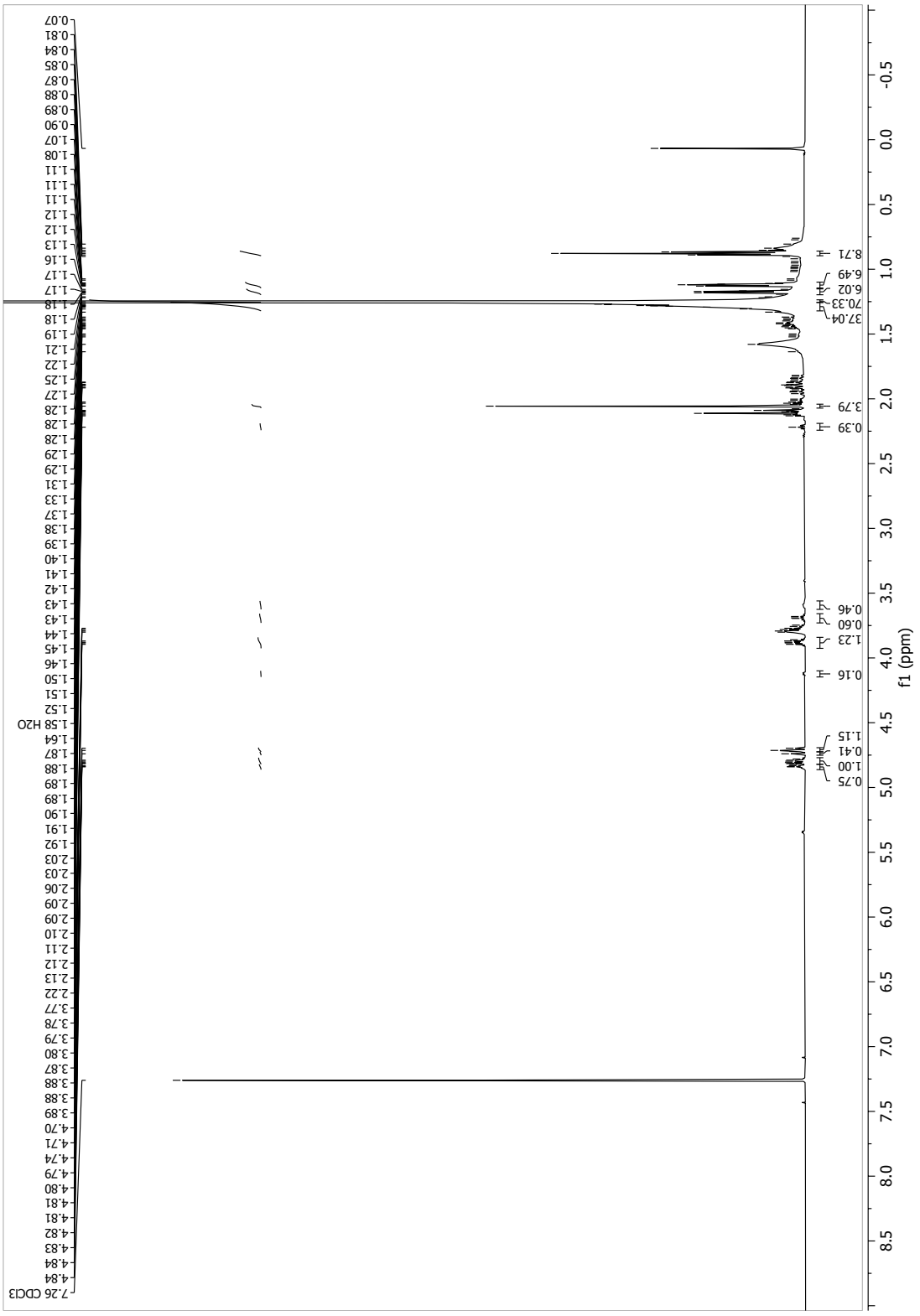

f1 (ppm)
f2 (ppm)

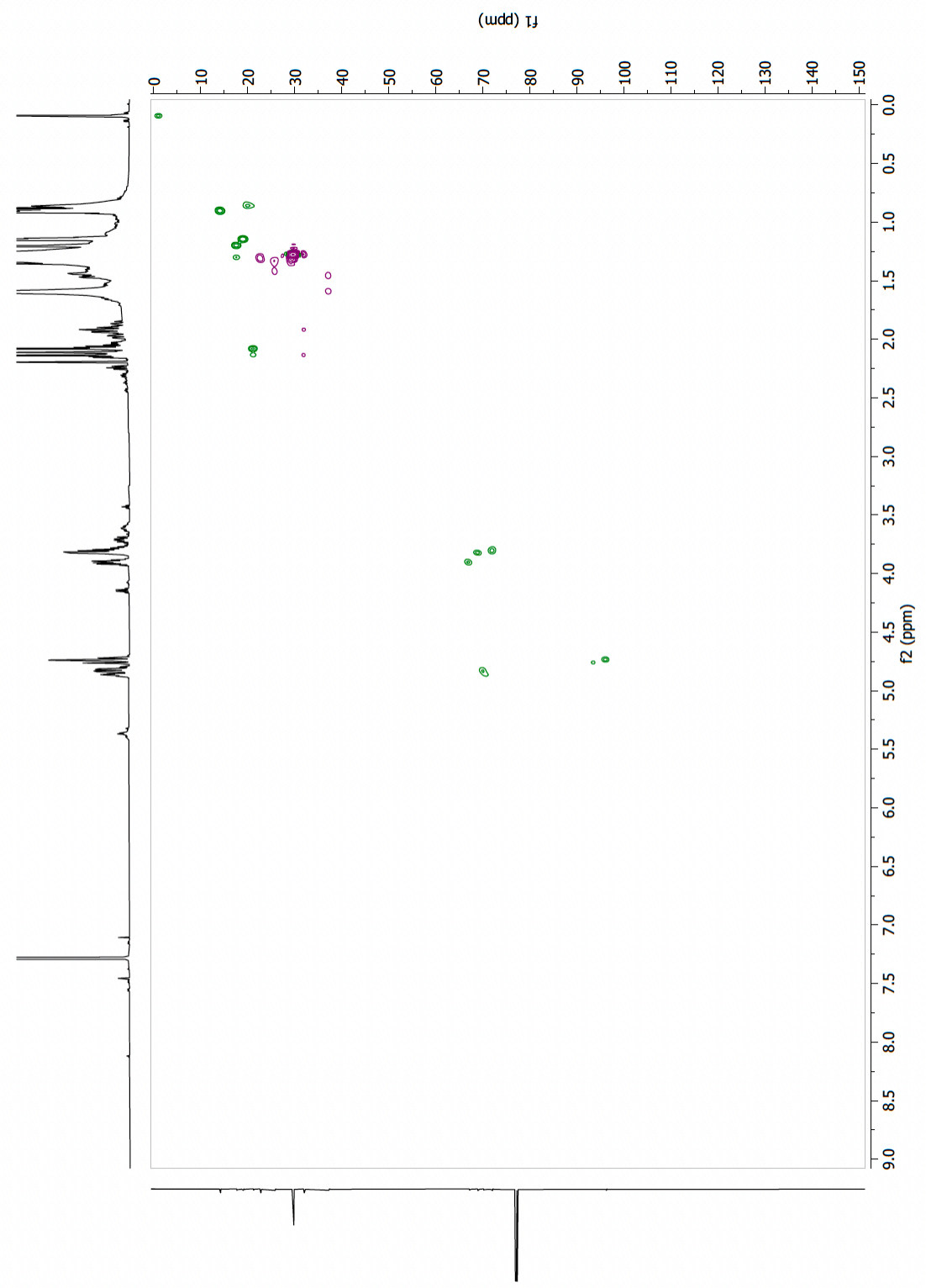
f1 (ppm)
0
10
20
30
40
50
60
70
80
90
100
110
120
130
140
150
f2 (ppm)
0.0
0.5
1.0
1.5
2.0
2.5
3.0
3.5
4.0
4.5
5.0
5.5
6.0
6.5
7.0
7.5
8.0
8.5
9.0

13.1.80 (2*R*,3*R*,5*R*,6*S*)-2-(((*R*)-hentriacontan-2-yl)oxy)-6-methyltetrahydro-2*H*-pyran-3,5-diyl diacetate (Ac2-asc-C31-H, 79)

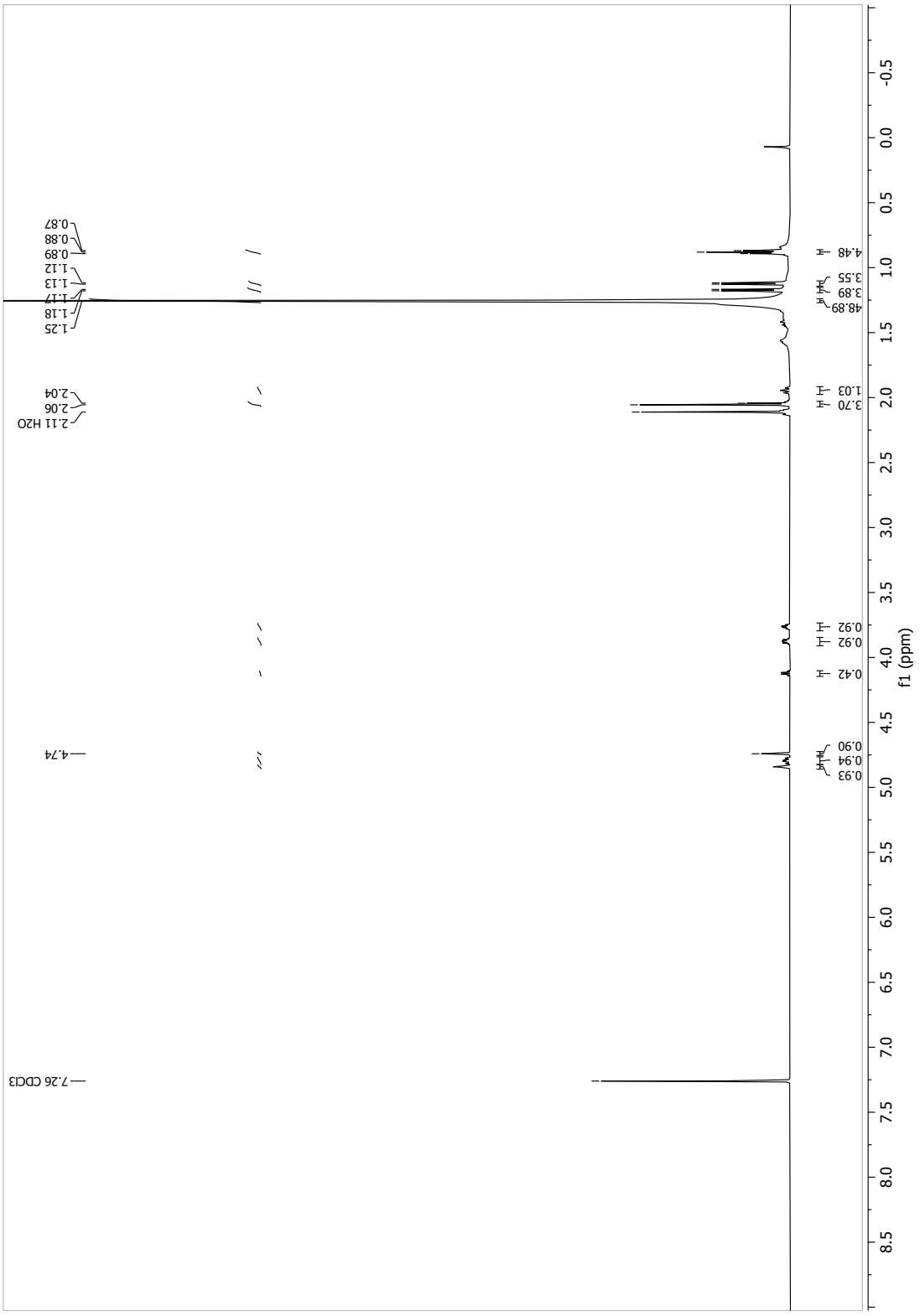

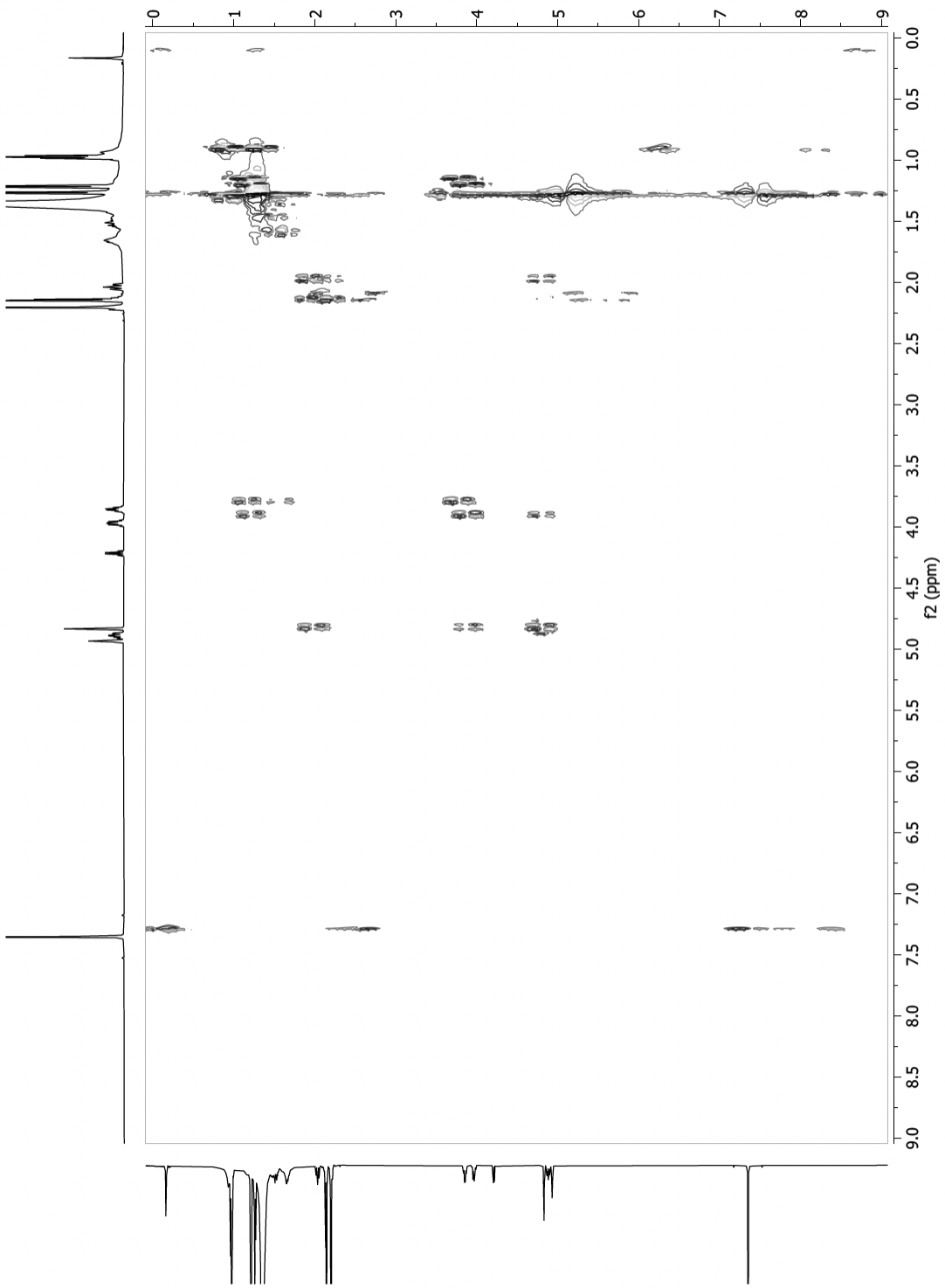
f1 (ppm)
f2 (ppm)

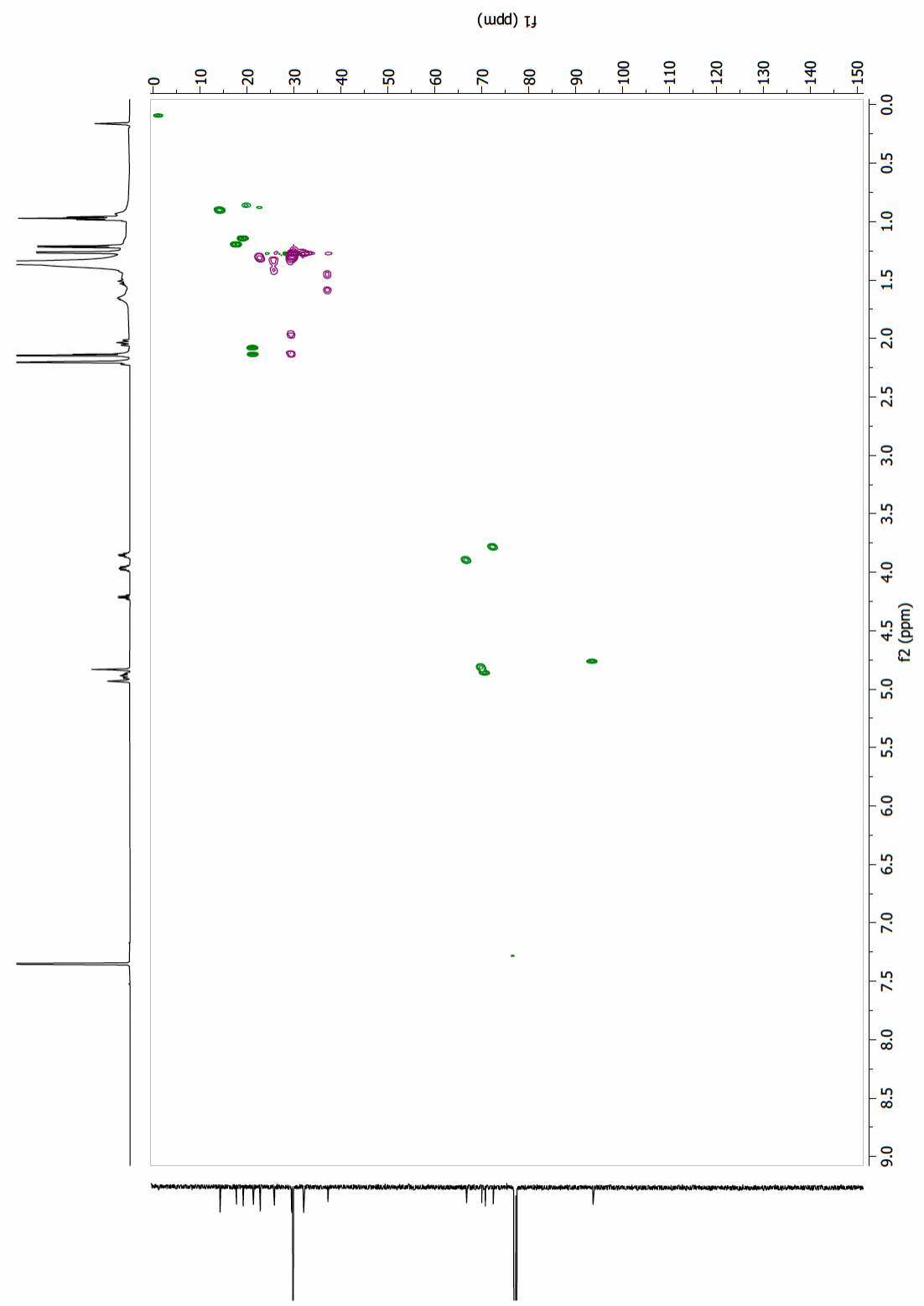
f1 (ppm)
0
10
20
30
40
50
60
70
80
90
100
110
120
130
140
150
f2 (ppm)
0.0
0.5
1.0
1.5
2.0
2.5
3.0
3.5
4.0
4.5
5.0
5.5
6.0
6.5
7.0
7.5
8.0
8.5
9.0

13.1.81 (*S*)-3-(((2*R*,3*R*,5*R*,6*S*)-3,5-dihydroxy-6-methyltetrahydro-2*H*-pyran-2-yl)oxy)-16-oxoheptadecanoic acid ((ω-COOH)-asc-C16-MK, 91)

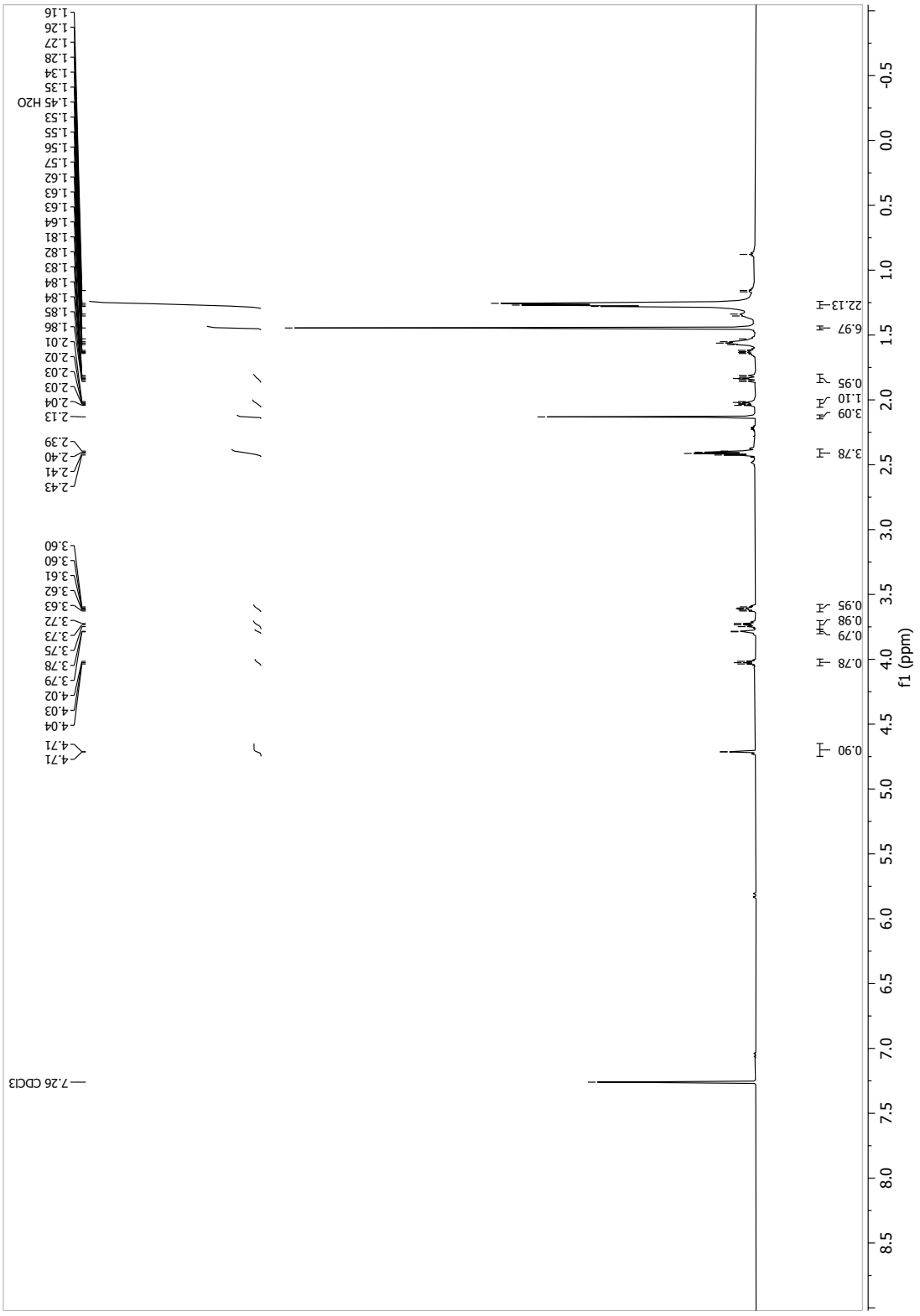

f1 (ppm)
0.5
1.0
1.5
2.0
2.5
3.0
3.5
4.0
4.5
5.0
5.5
6.0
6.5
7.0
7.5
0.0
0.5
1.0
1.5
2.0
2.5
3.0
3.5
4.0
4.5
5.0
5.5
6.0
6.5
7.0
7.5
8.0
f2 (ppm)

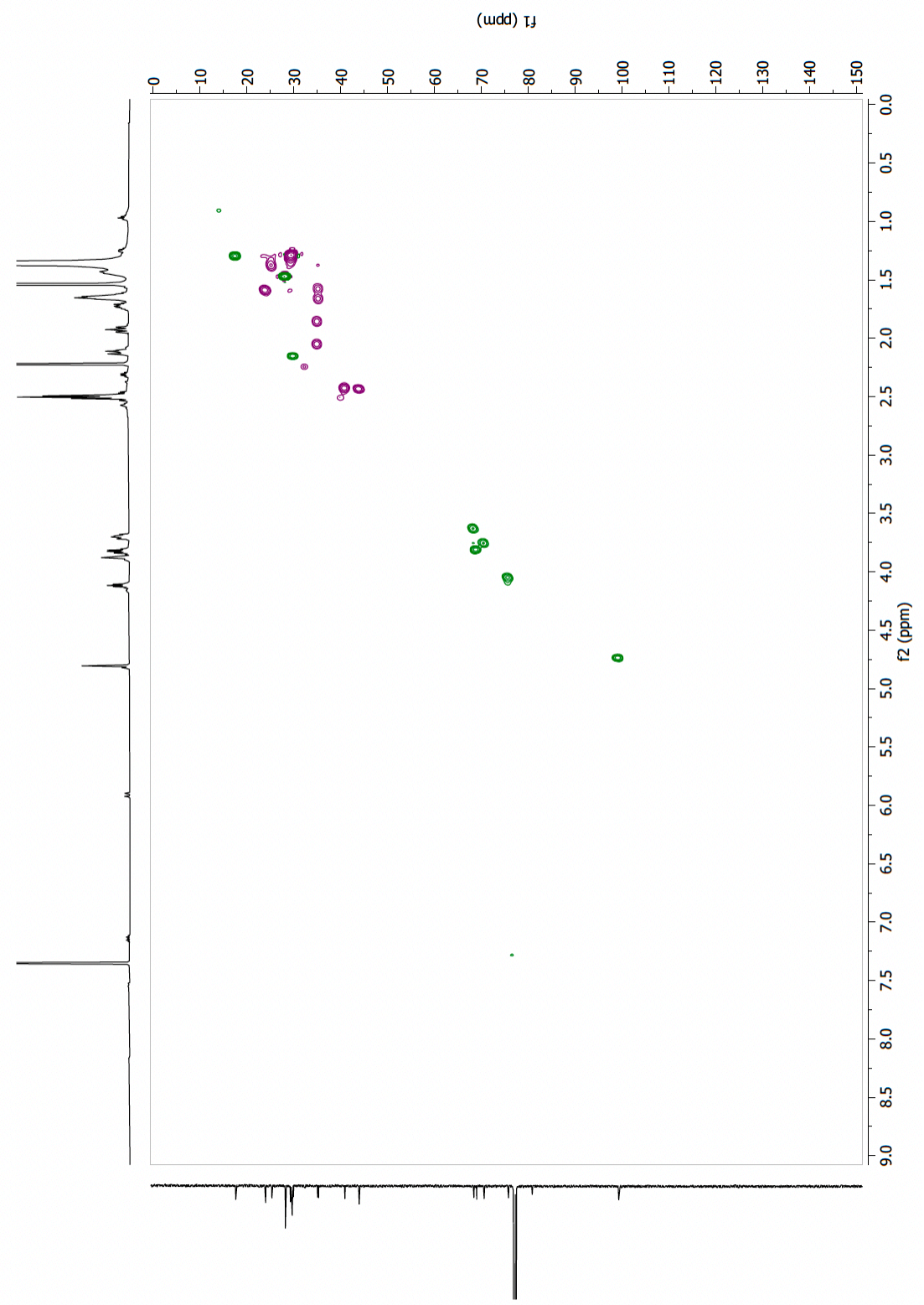
f1 (ppm)
0
10
20
30
40
50
60
70
80
90
100
110
120
130
140
150
f2 (ppm)
0.0
0.5
1.0
1.5
2.0
2.5
3.0
3.5
4.0
4.5
5.0
5.5
6.0
6.5
7.0
7.5
8.0
8.5
9.0

13.1.82 (*S*)-3-(((2*R*,3*R*,5*R*,6*S*)-3,5-dihydroxy-6-methyltetrahydro-2*H*-pyran-2-yl)oxy)octadecanedioic acid ((ω-COOH)-asc-C17, 92)

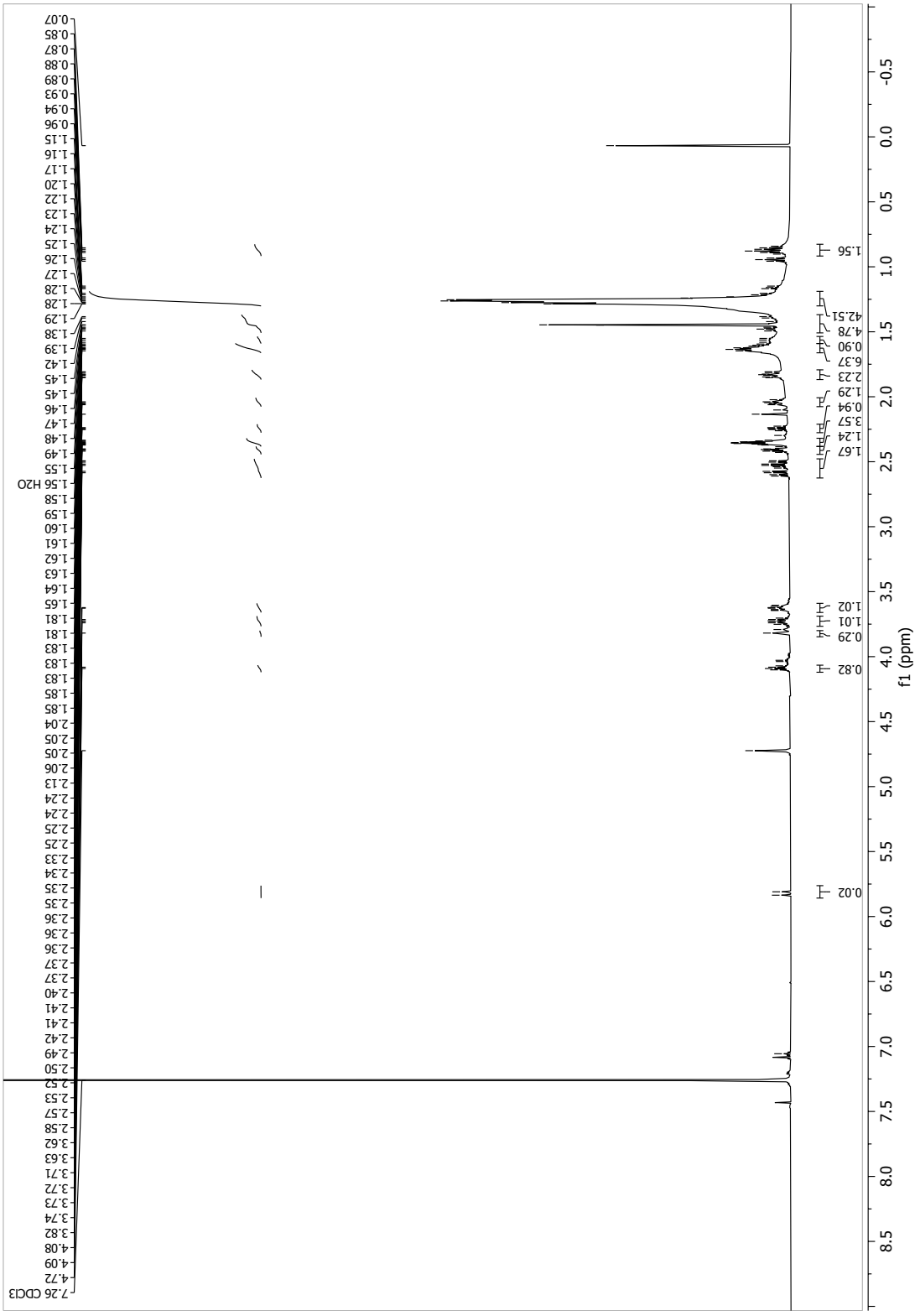

f1 (ppm)
0.5
1.0
1.5
2.0
2.5
3.0
3.5
4.0
4.5
5.0
5.5
6.0
6.5
7.0
f2 (ppm)
1.0
1.5
2.0
2.5
3.0
3.5
4.0
4.5
5.0
5.5
6.0
6.5
7.0

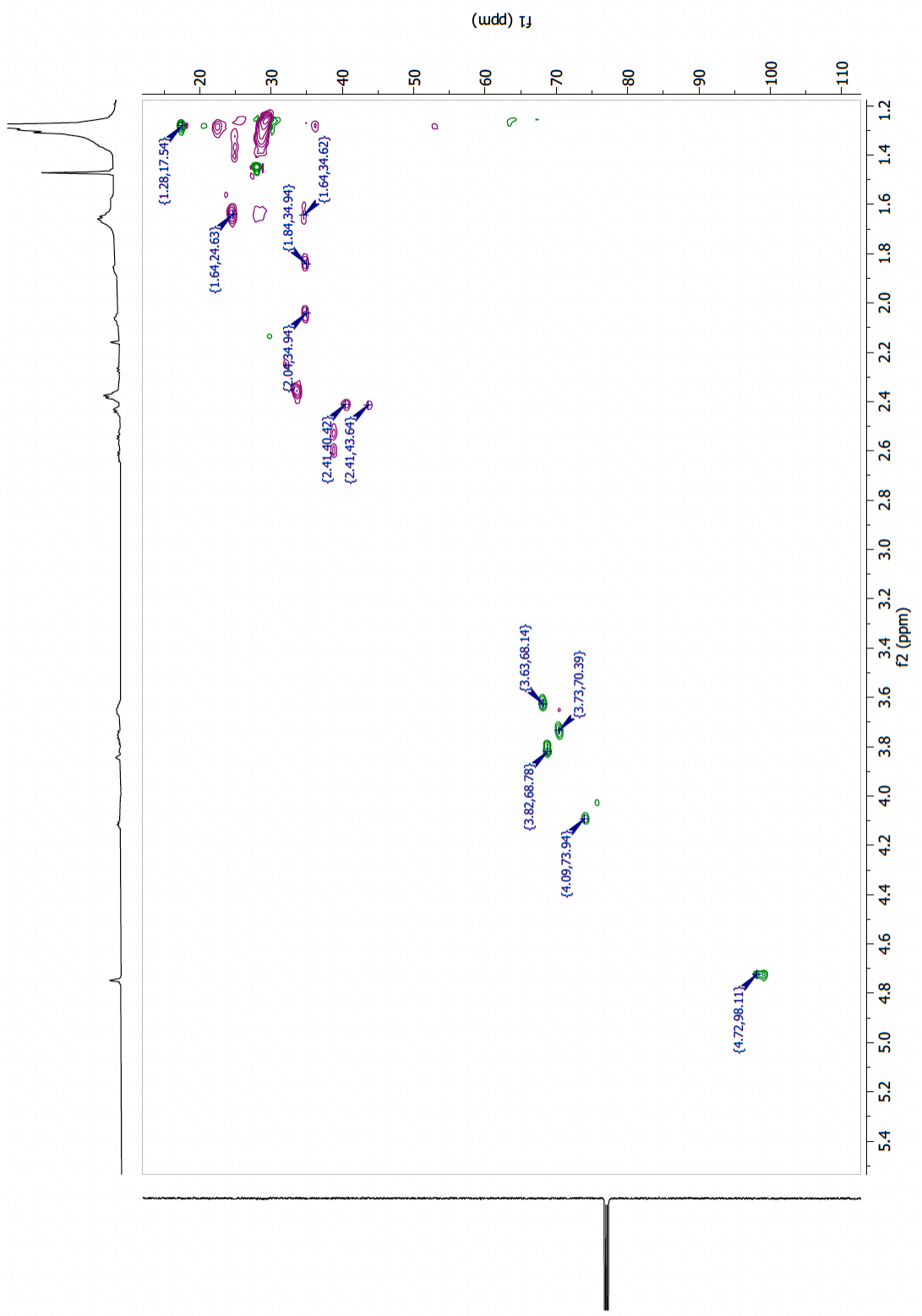
f1 (ppm)
f2 (ppm)
{1.28,17.54}
{1.64,24.63}
{1.84,34.94}
{1.64,34.62}
{2.04,34.94}
{2.41,40.42}
{2.41,43.64}
{3.63,68.14}
{3.73,70.39}
{3.82,68.78}
{4.09,73.94}
{4.72,98.11}

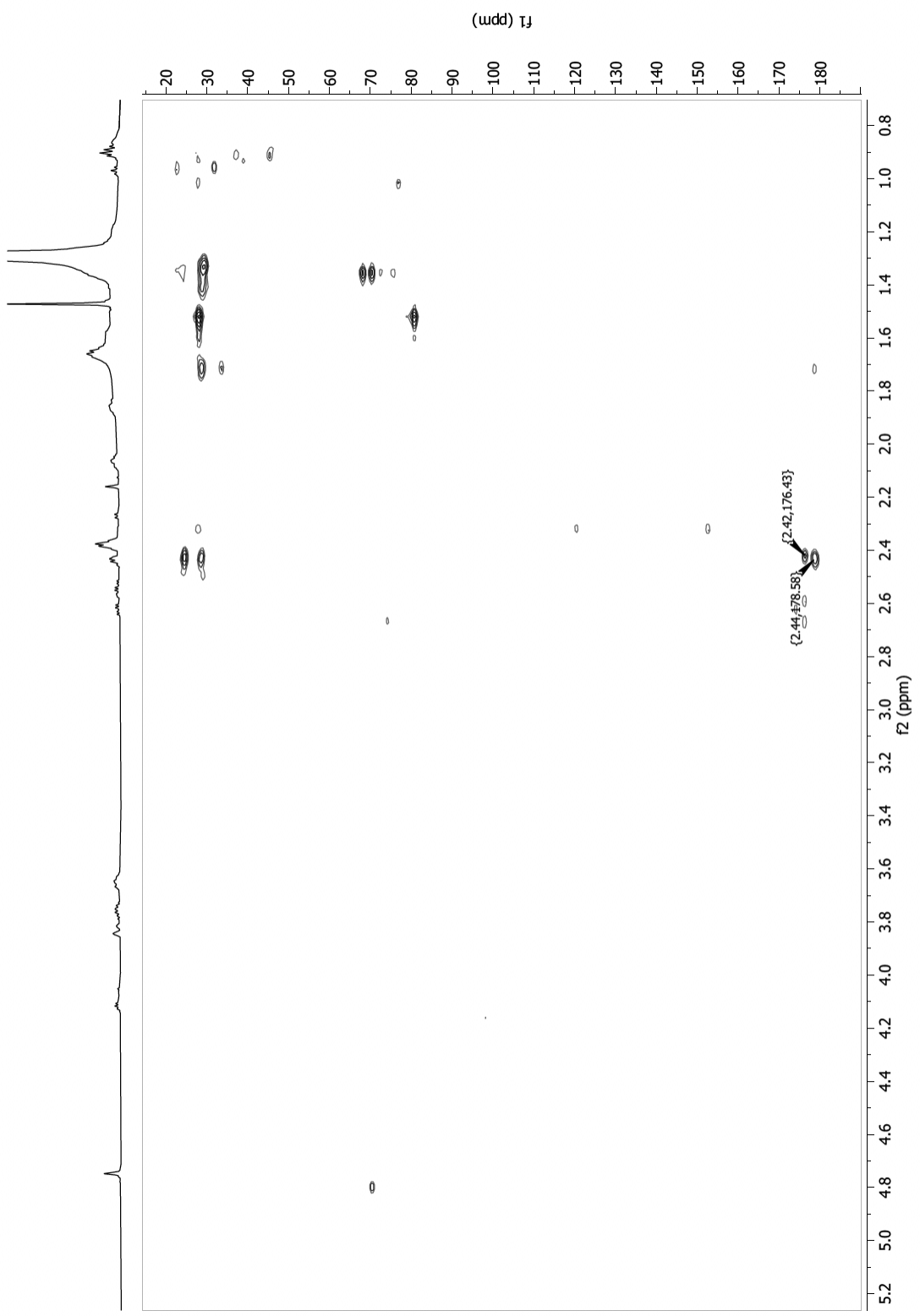
f1 (ppm)
20
30
40
50
60
70
80
90
100
110
120
130
140
150
160
170
180
f2 (ppm)
5.2
5.0
4.8
4.6
4.4
4.2
4.0
3.8
3.6
3.4
3.2
3.0
2.8
2.6
2.4
2.2
2.0
1.8
1.6
1.4
1.2
1.0
0.8
{2.42,176.43}
{2.44,178.58}

13.1.83 2-((11-Methyldodec-7-yn-1-yl)oxy)tetrahydro-2*H*-pyran (114)

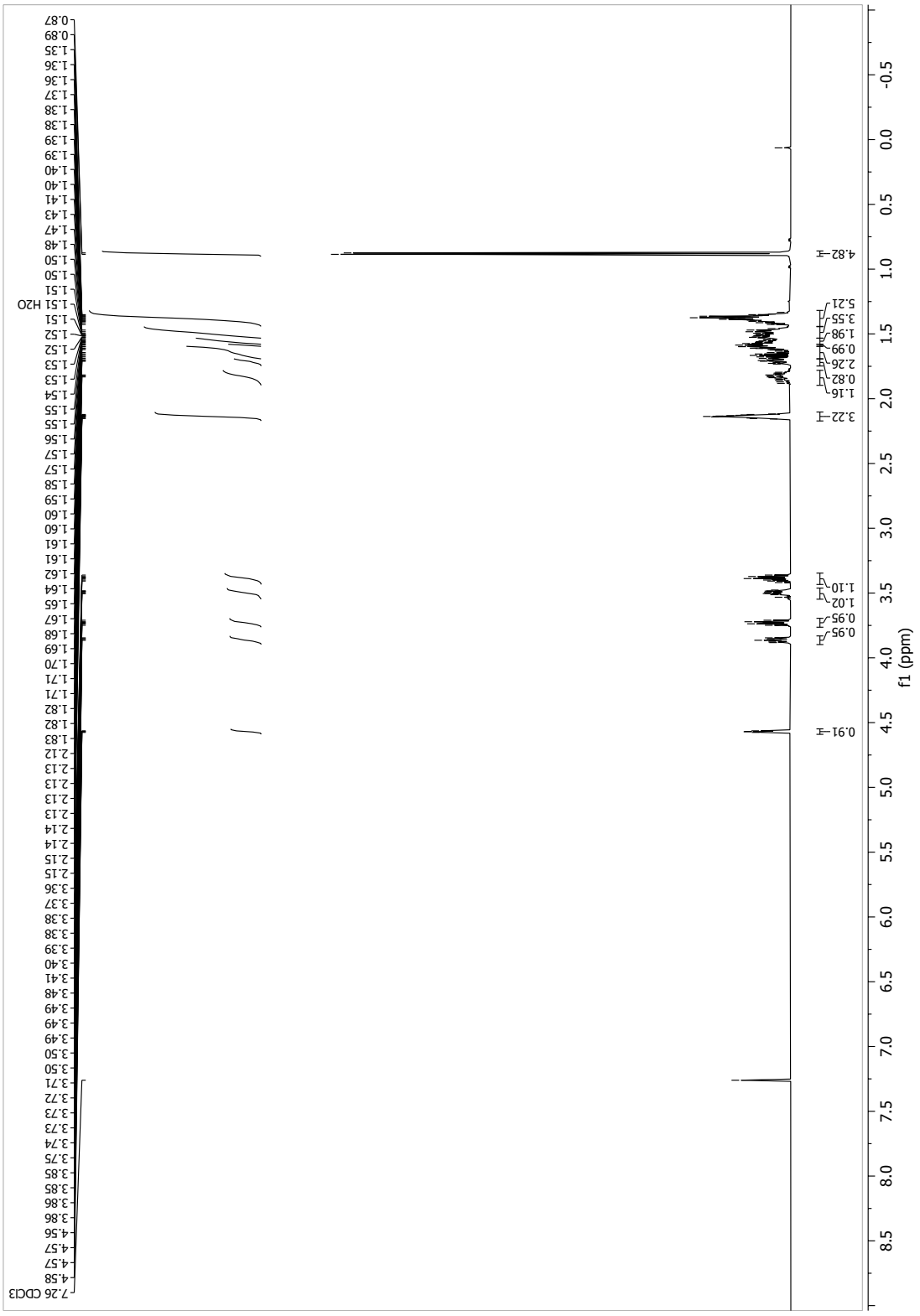

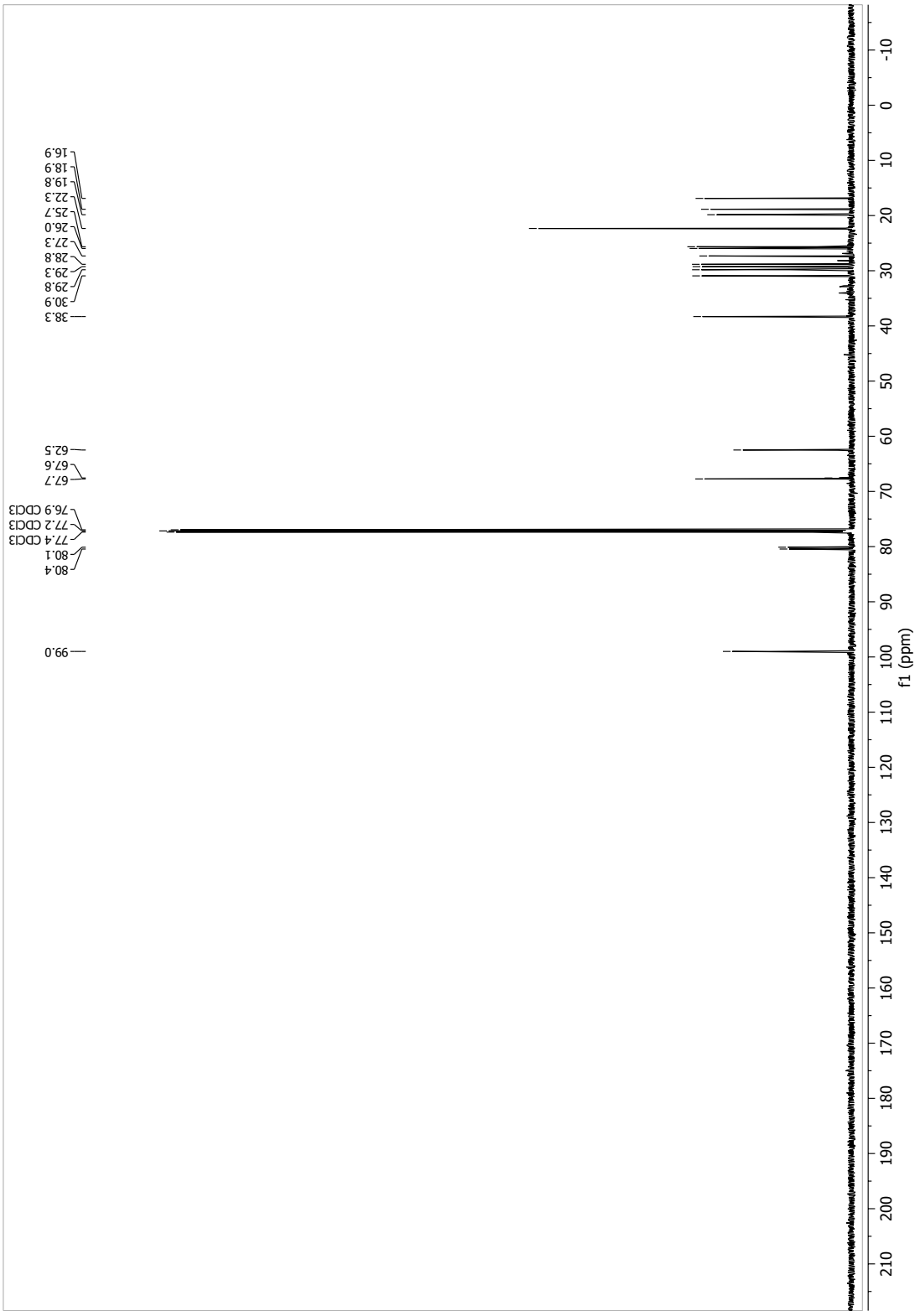
99.0
80.4
80.1
77.4 CDCl3
77.2 CDCl3
76.9 CDCl3
67.7
67.6
62.5
38.3
30.9
29.8
29.3
28.8
27.3
26.0
25.7
22.3
19.8
18.9
16.9
f1 (ppm)

13.1.84 2-((13-Methyltetradec-9-yn-1-yl)oxy)tetrahydro-2*H*-pyran (115)

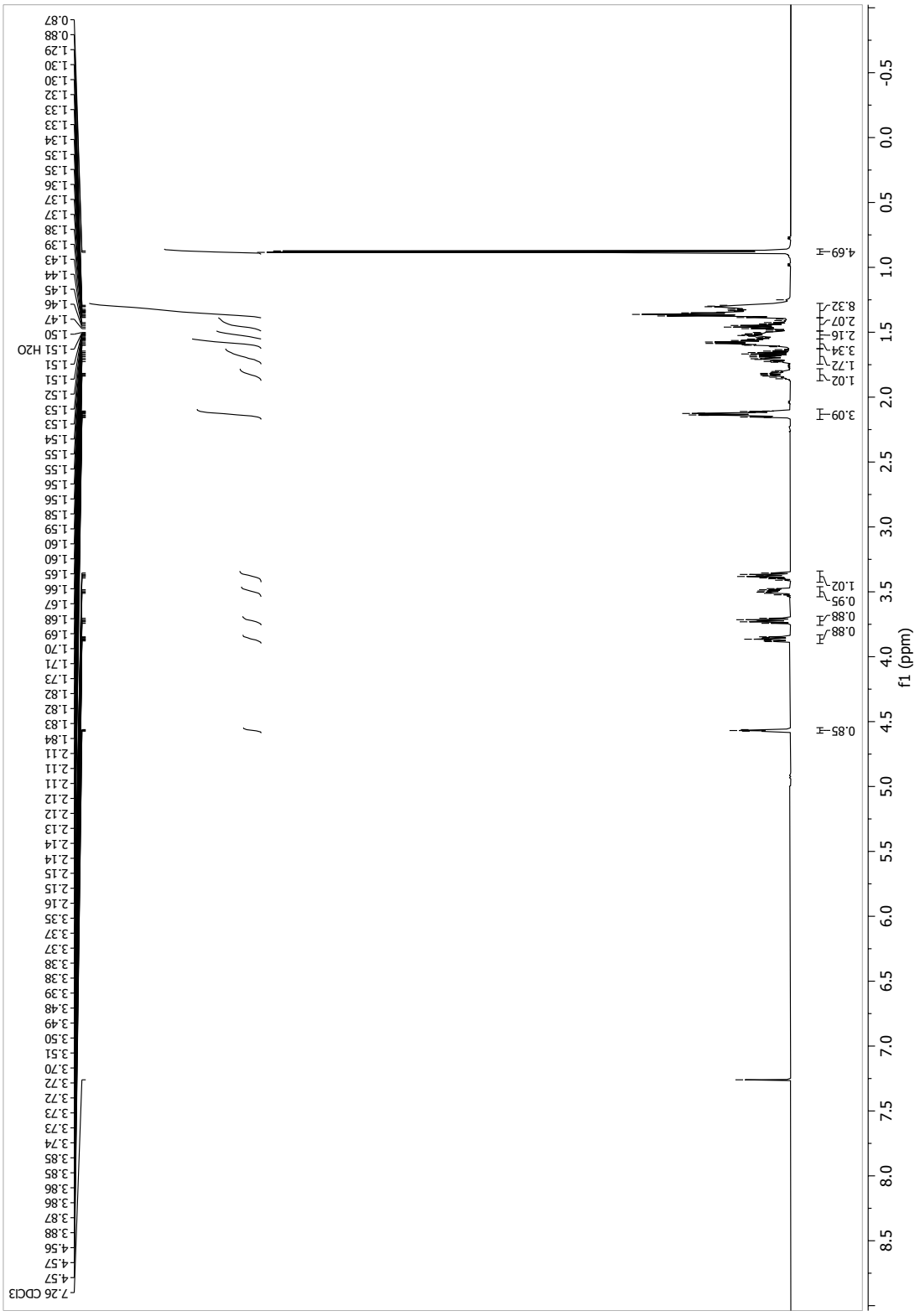

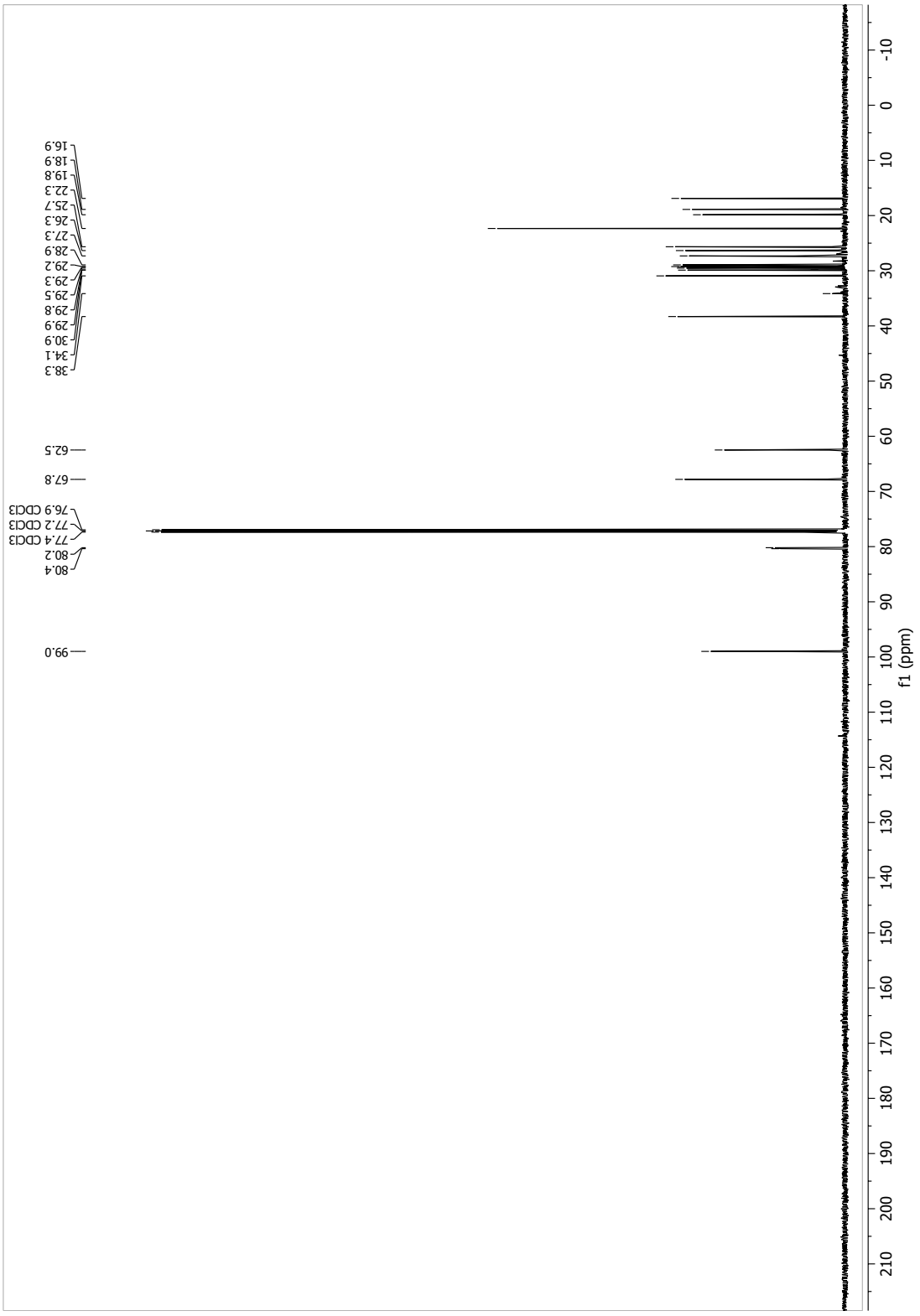
99.0
80.4
80.2
77.4 CDCl3
77.2 CDCl3
76.9 CDCl3
67.8
62.5
38.3
34.1
30.9
29.9
29.8
29.5
29.3
29.2
28.9
27.3
26.3
25.7
22.3
19.8
18.9
16.9
f1 (ppm)

13.1.85 11-Methyldodec-7-yn-1-ol (116)

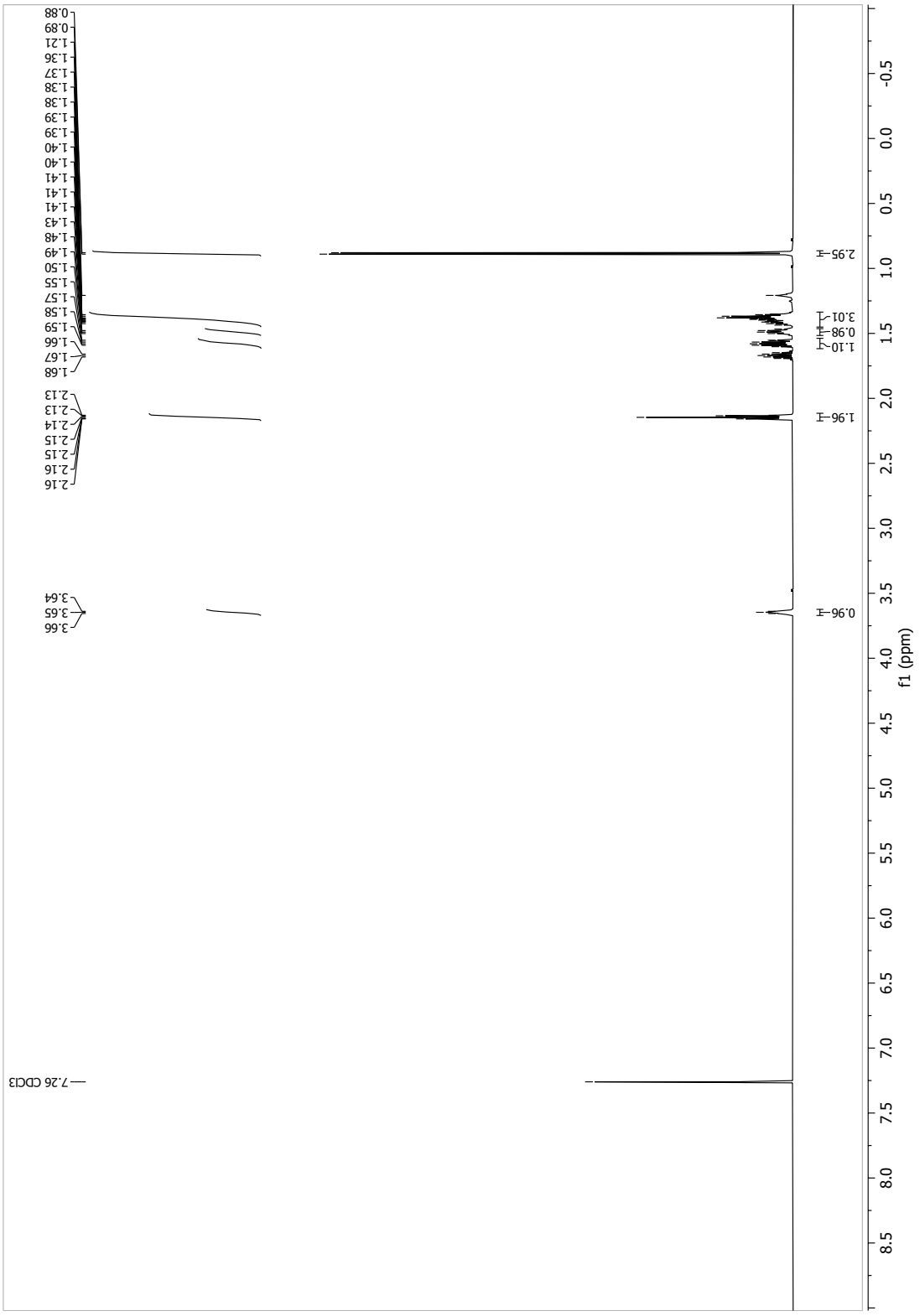

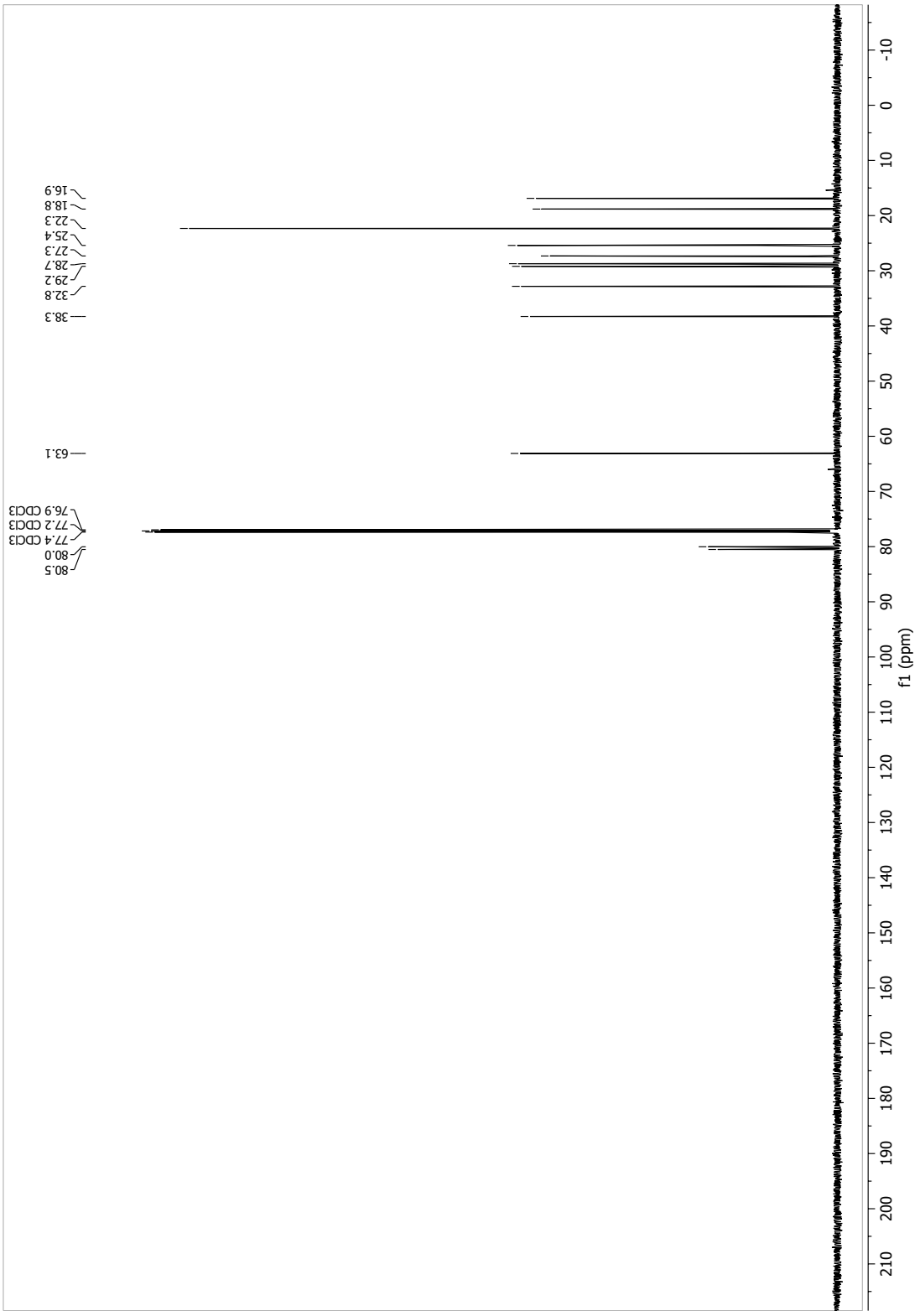
80.5
80.0
77.4 CDCl3
77.2 CDCl3
76.9 CDCl3
63.1
38.3
32.8
29.2
28.7
27.3
25.4
22.3
18.8
16.9
f1 (ppm)

13.1.86 13-Methyltetradec-9-yn-1-ol (117)

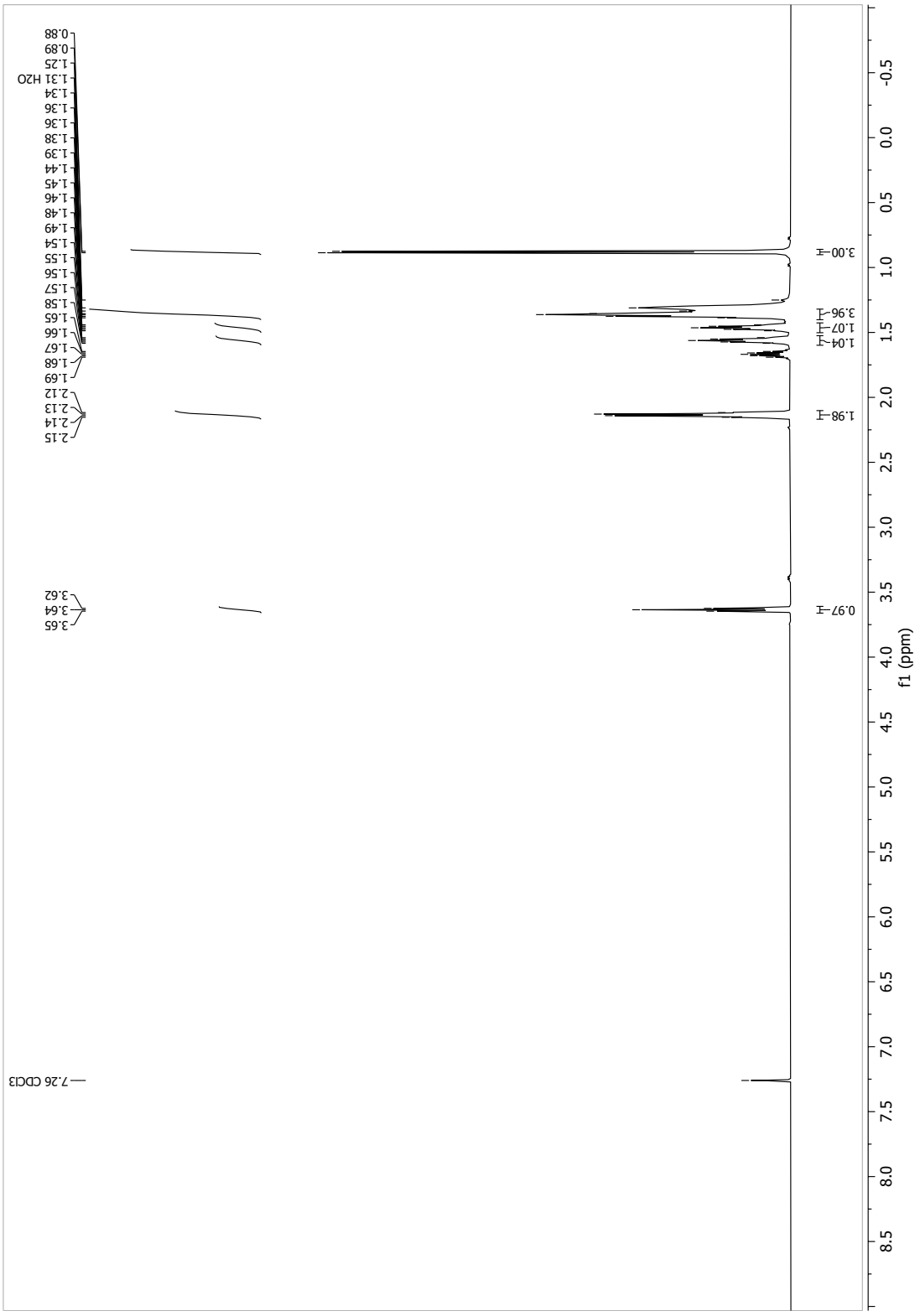

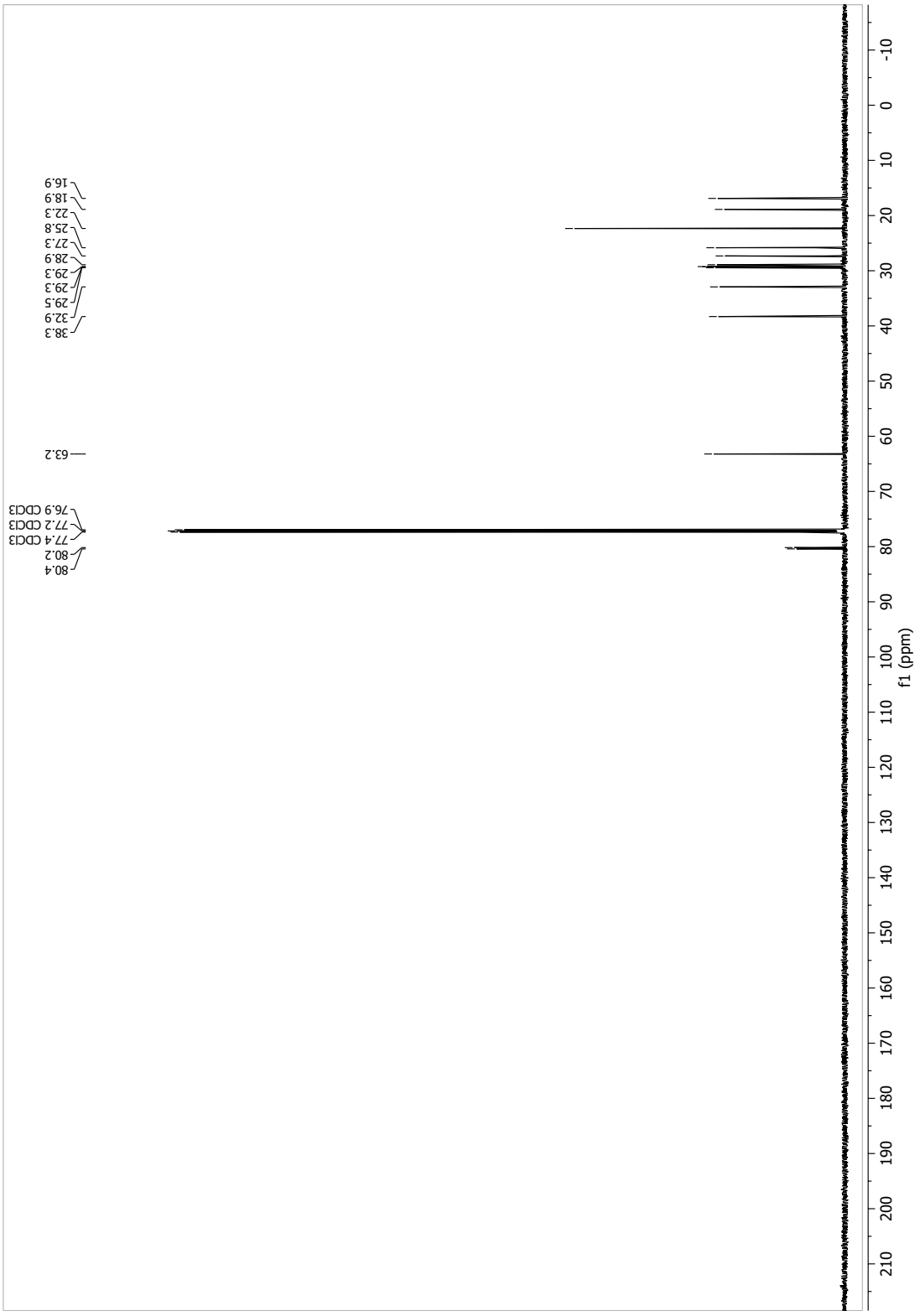
80.4
80.2
77.4 CDCl3
77.2 CDCl3
76.9 CDCl3
63.2
38.3
32.9
29.5
29.3
29.3
28.9
27.3
25.8
22.3
18.9
16.9
f1 (ppm)

13.1.87 11-Methyldodecan-1-ol (118a)

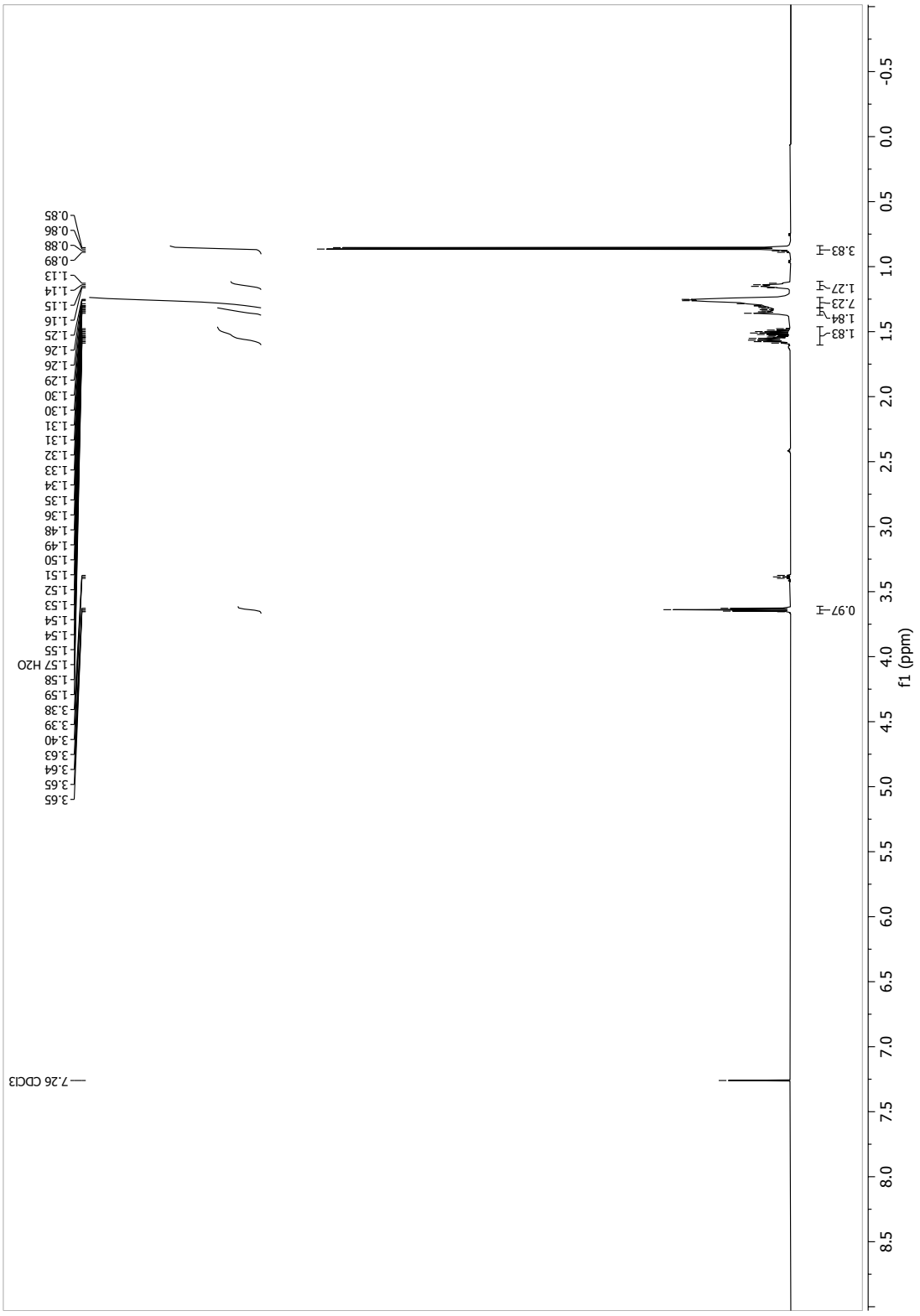

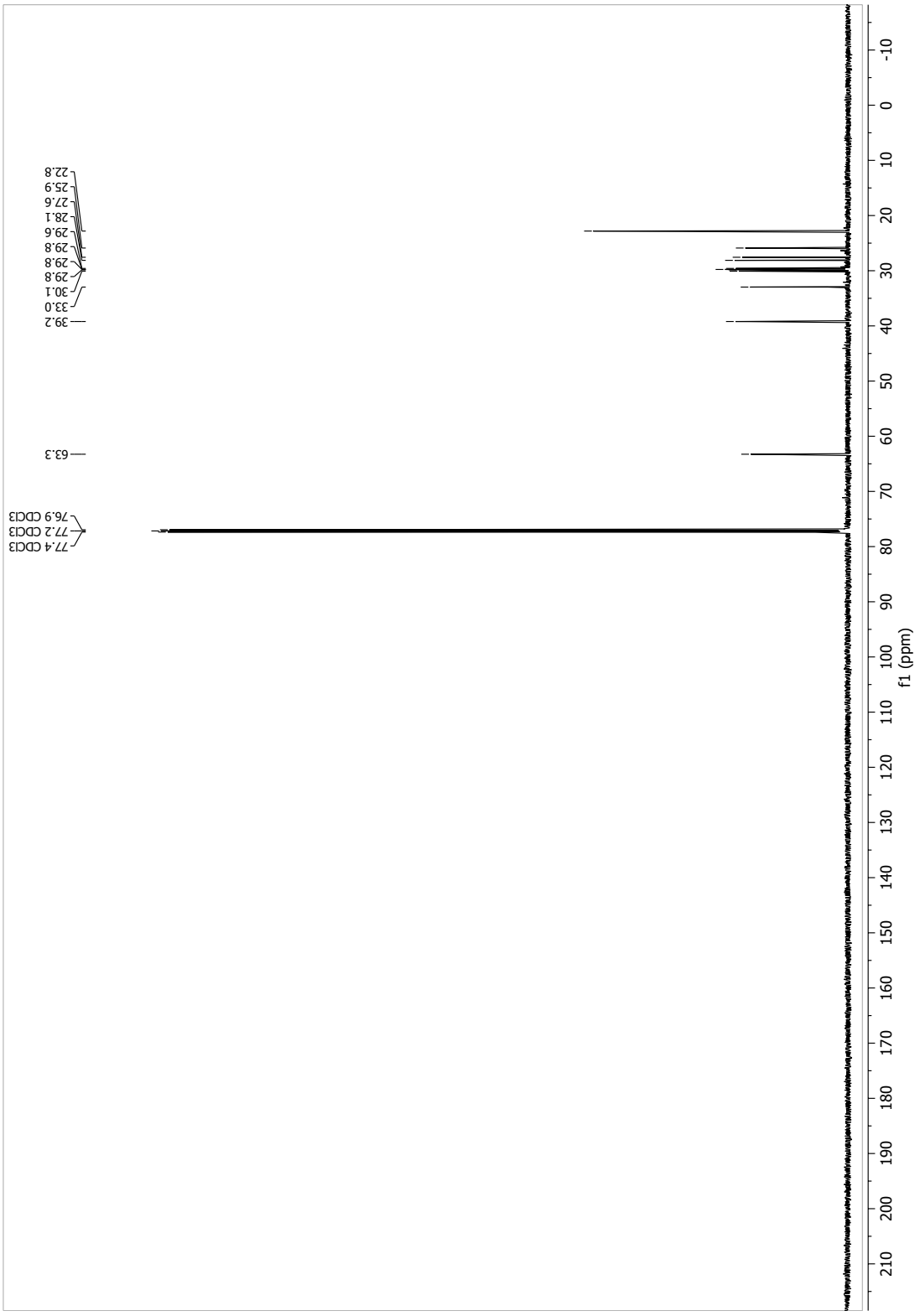
77.4 CDCl3
77.2 CDCl3
76.9 CDCl3
63.3
39.2
33.0
30.1
29.8
29.8
29.8
29.6
28.1
27.6
25.9
22.8
f1 (ppm)

13.1.88 [D_4]-11-methyldodecan-1-ol (118b)

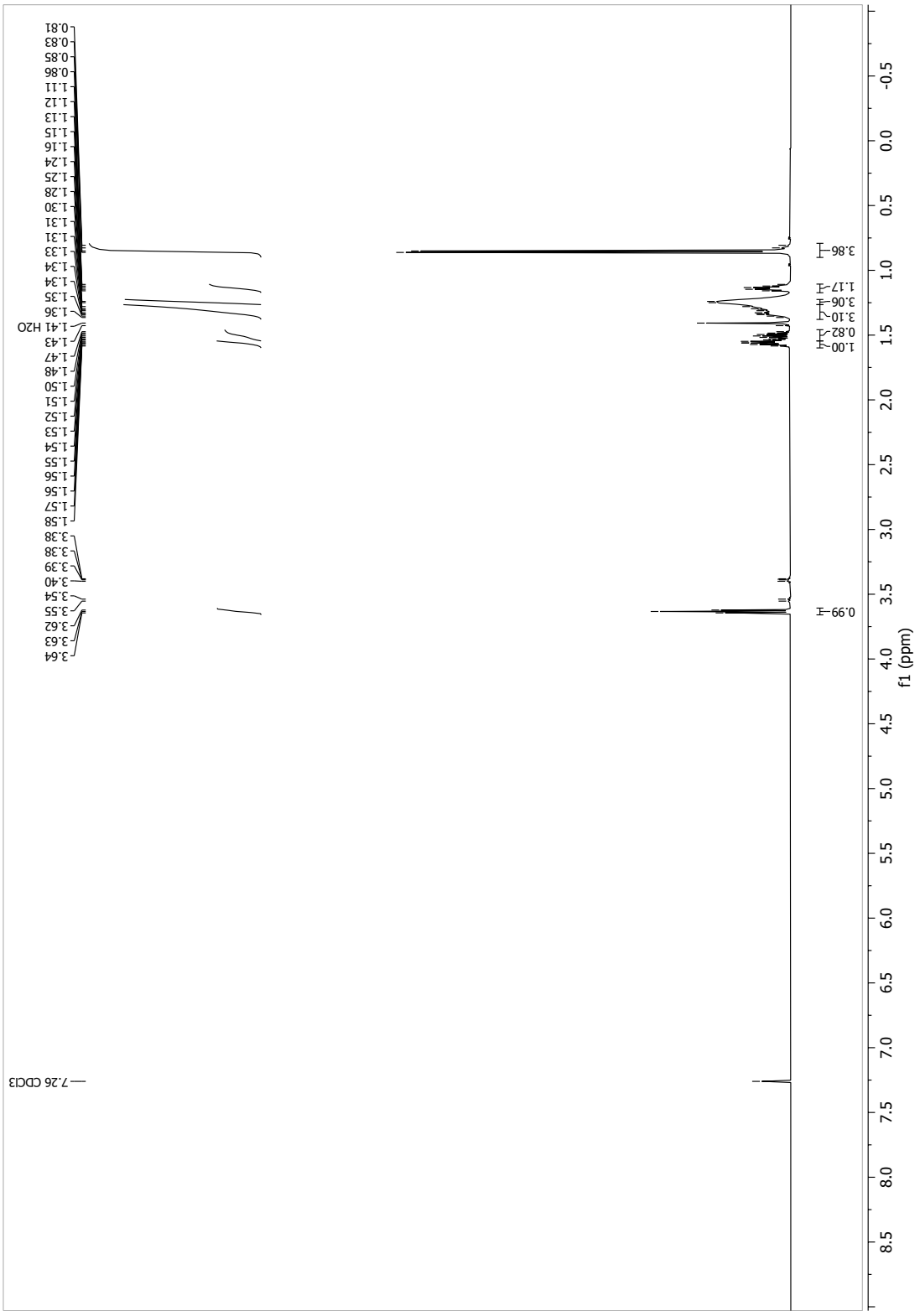

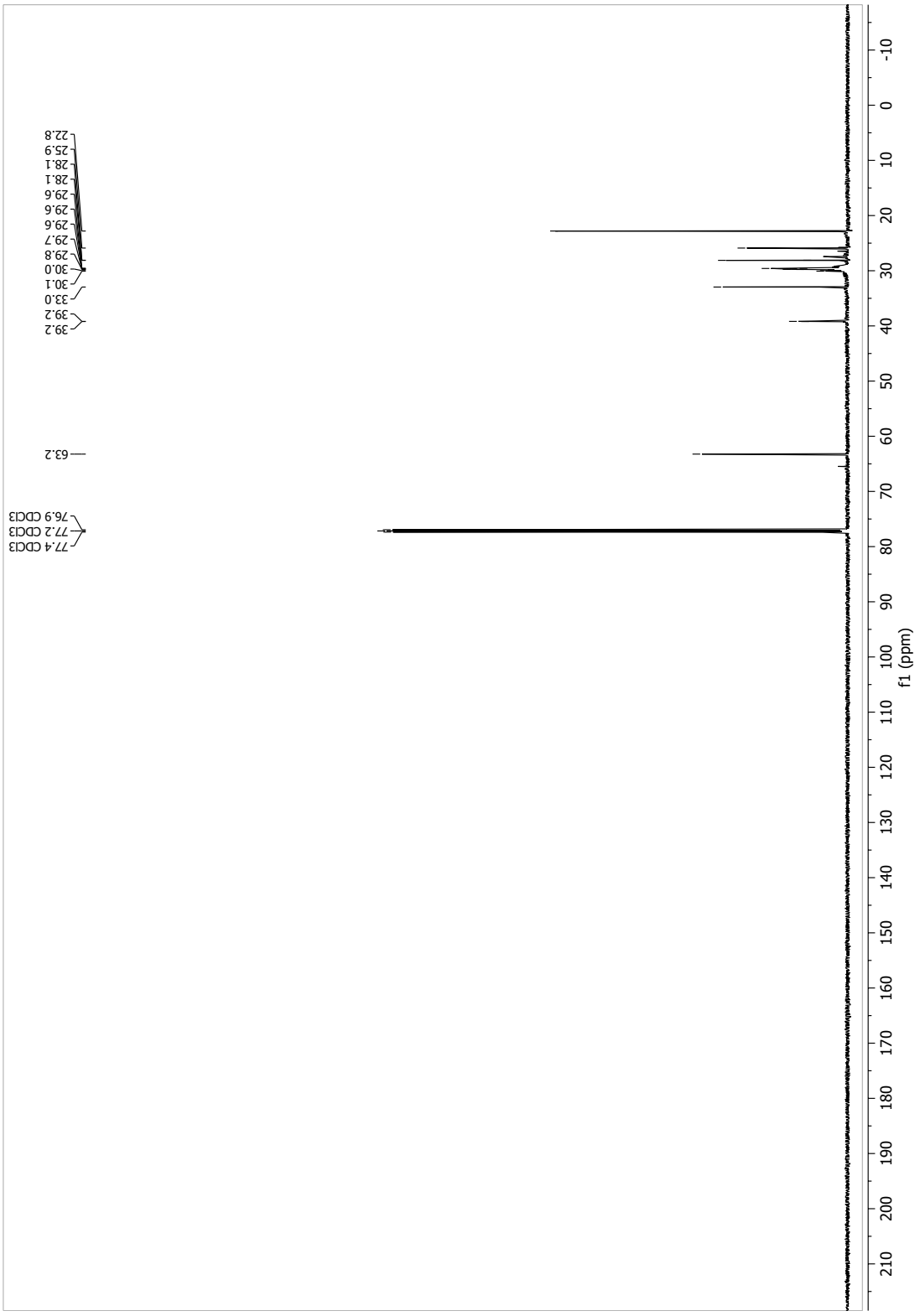
77.4 CDCl3
77.2 CDCl3
76.9 CDCl3
63.2
39.2
39.2
33.0
30.1
30.0
29.8
29.7
29.6
29.6
28.1
28.1
25.9
22.8
f1 (ppm)

13.1.89 13-Methyltetradecan-1-ol (119a)

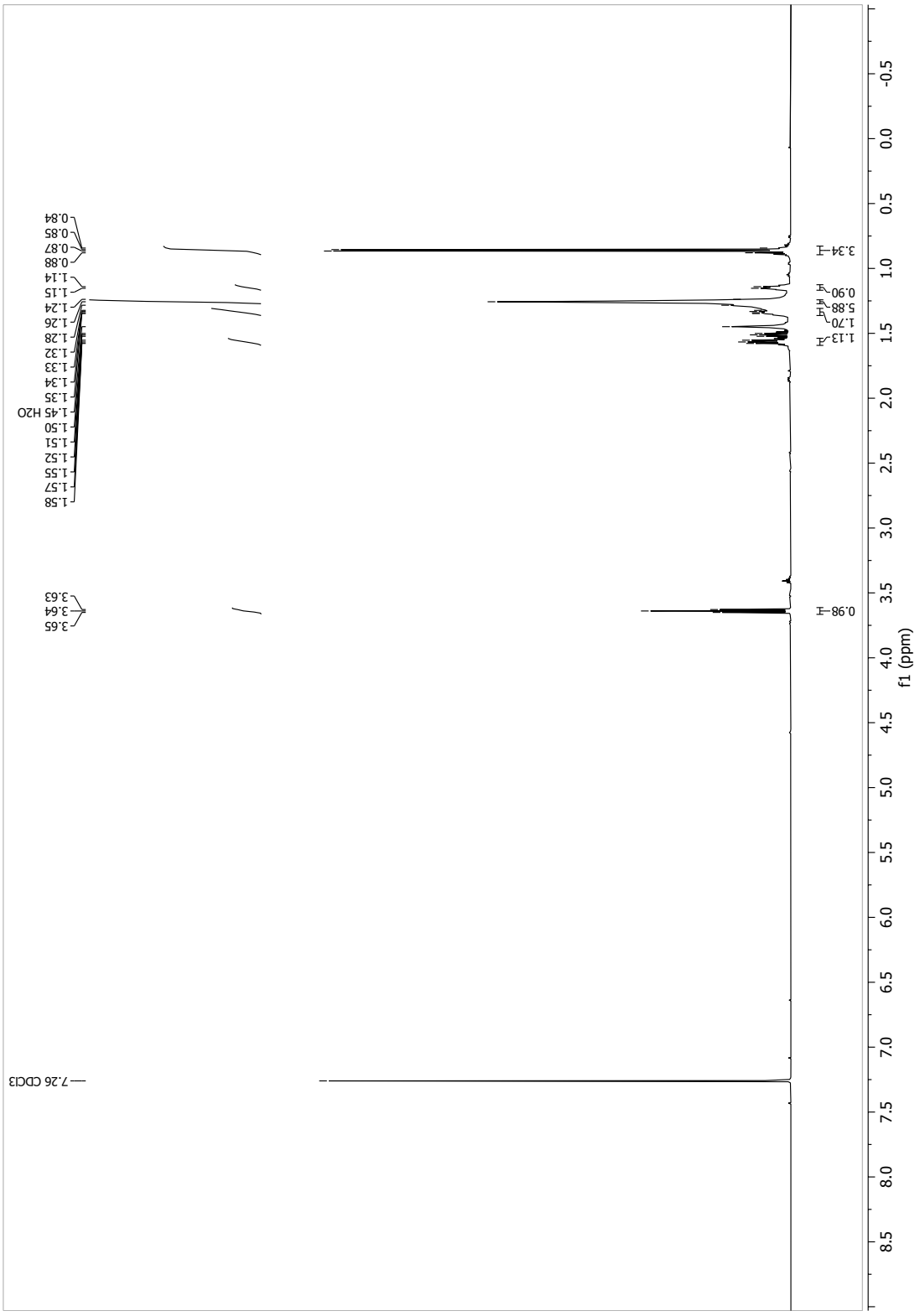

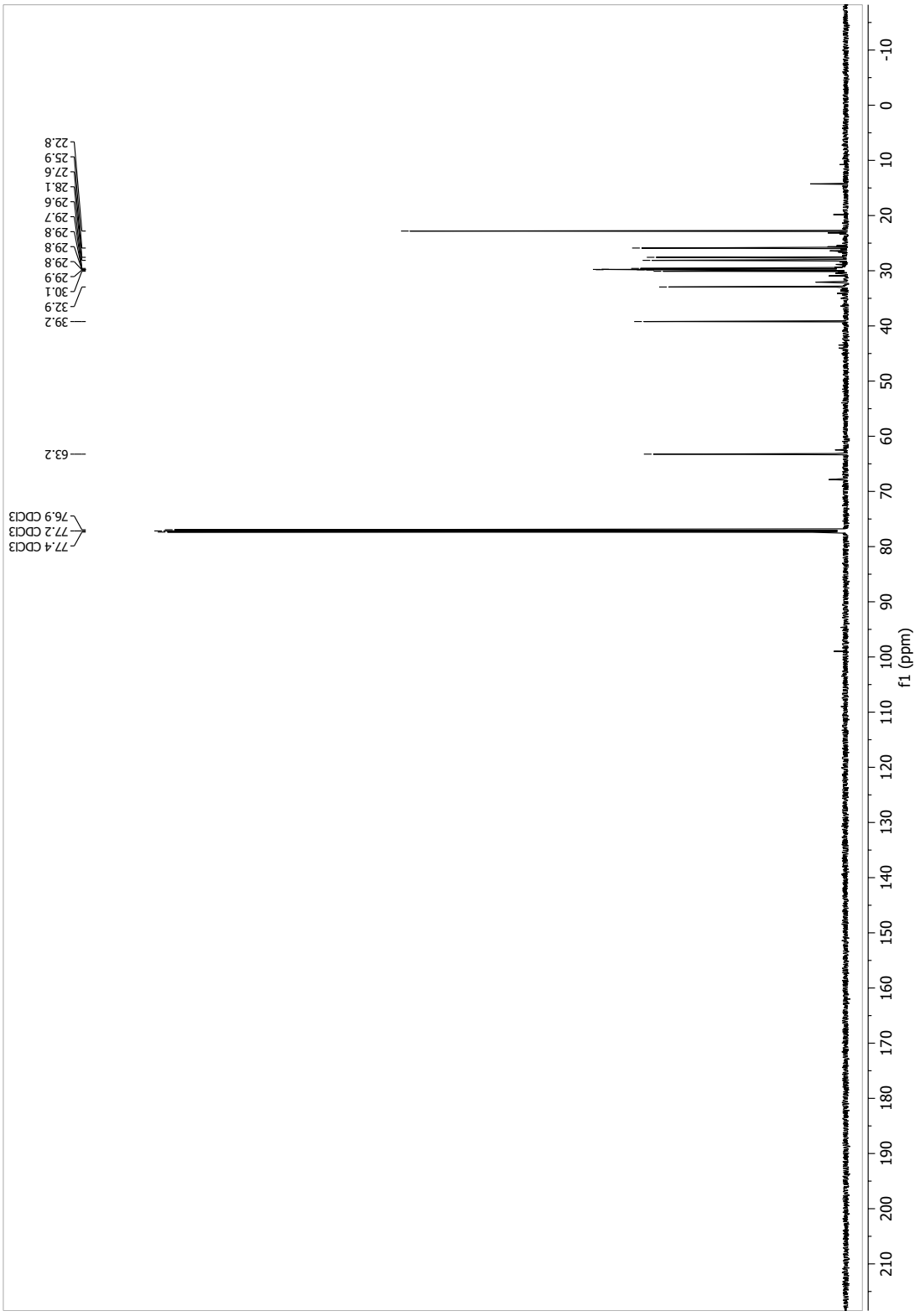
77.4 CDCl3
77.2 CDCl3
76.9 CDCl3
63.2
39.2
32.9
30.1
29.9
29.8
29.8
29.8
29.7
29.6
28.1
27.6
25.9
22.8
f1 (ppm)

13.1.90 [D_4]-13-methyltetradecan-1-ol (119b)

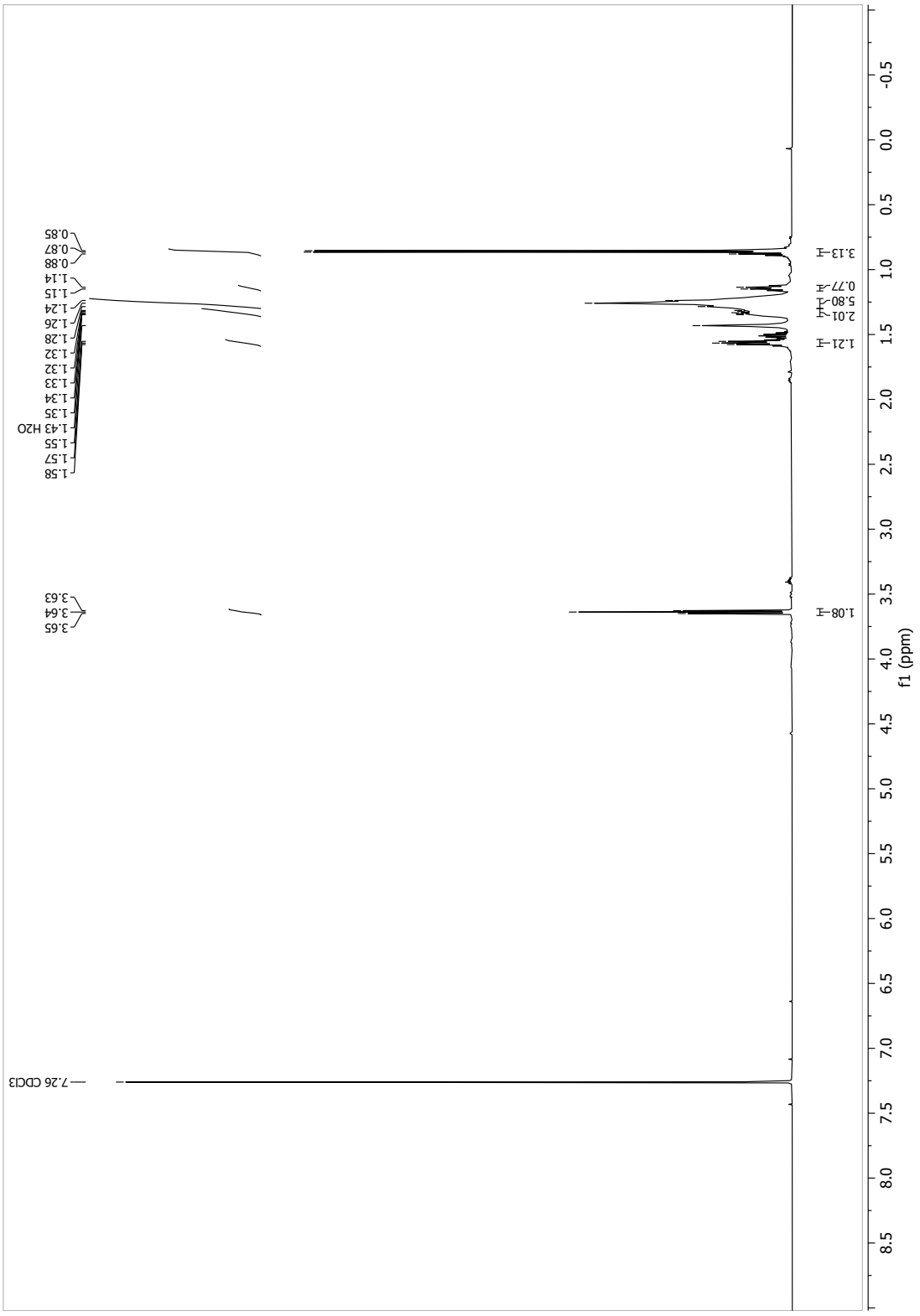

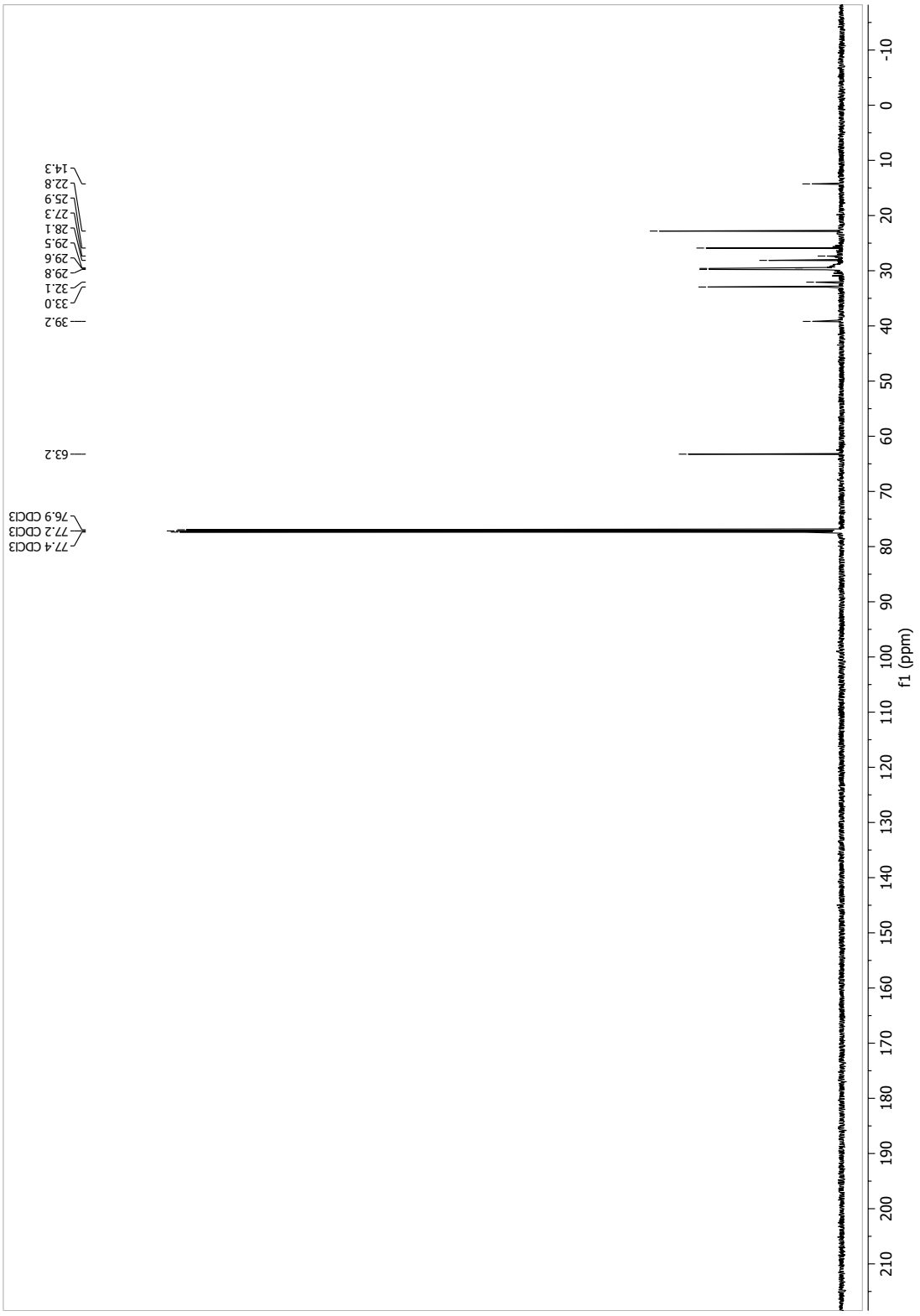
77.4 CDCl3
77.2 CDCl3
76.9 CDCl3
63.2
39.2
33.0
32.1
29.8
29.6
29.5
28.1
27.3
25.9
22.8
14.3
f1 (ppm)

13.1.91 11-Methyldodecanoic acid (*iso*C13, 16a), from route 1

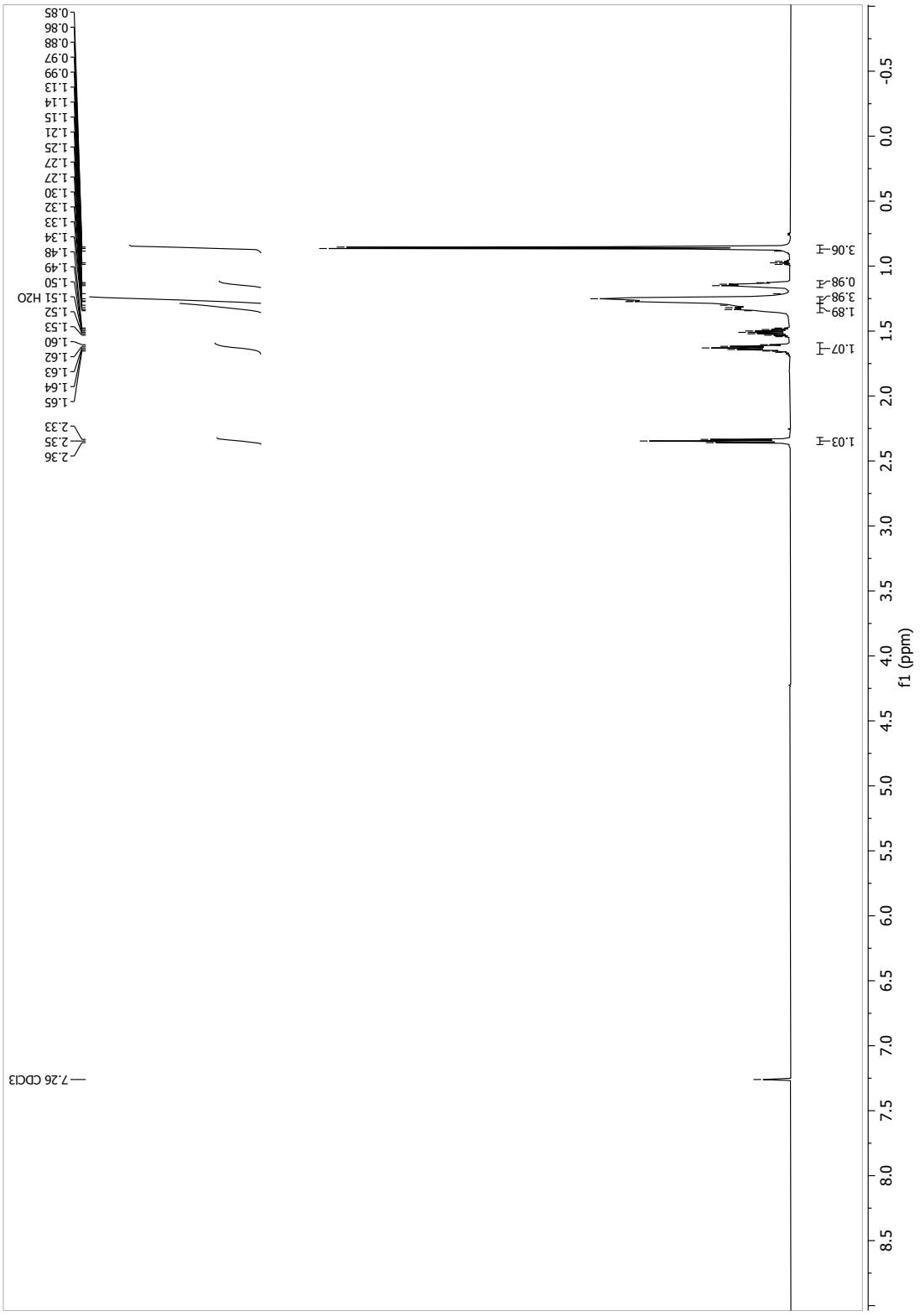

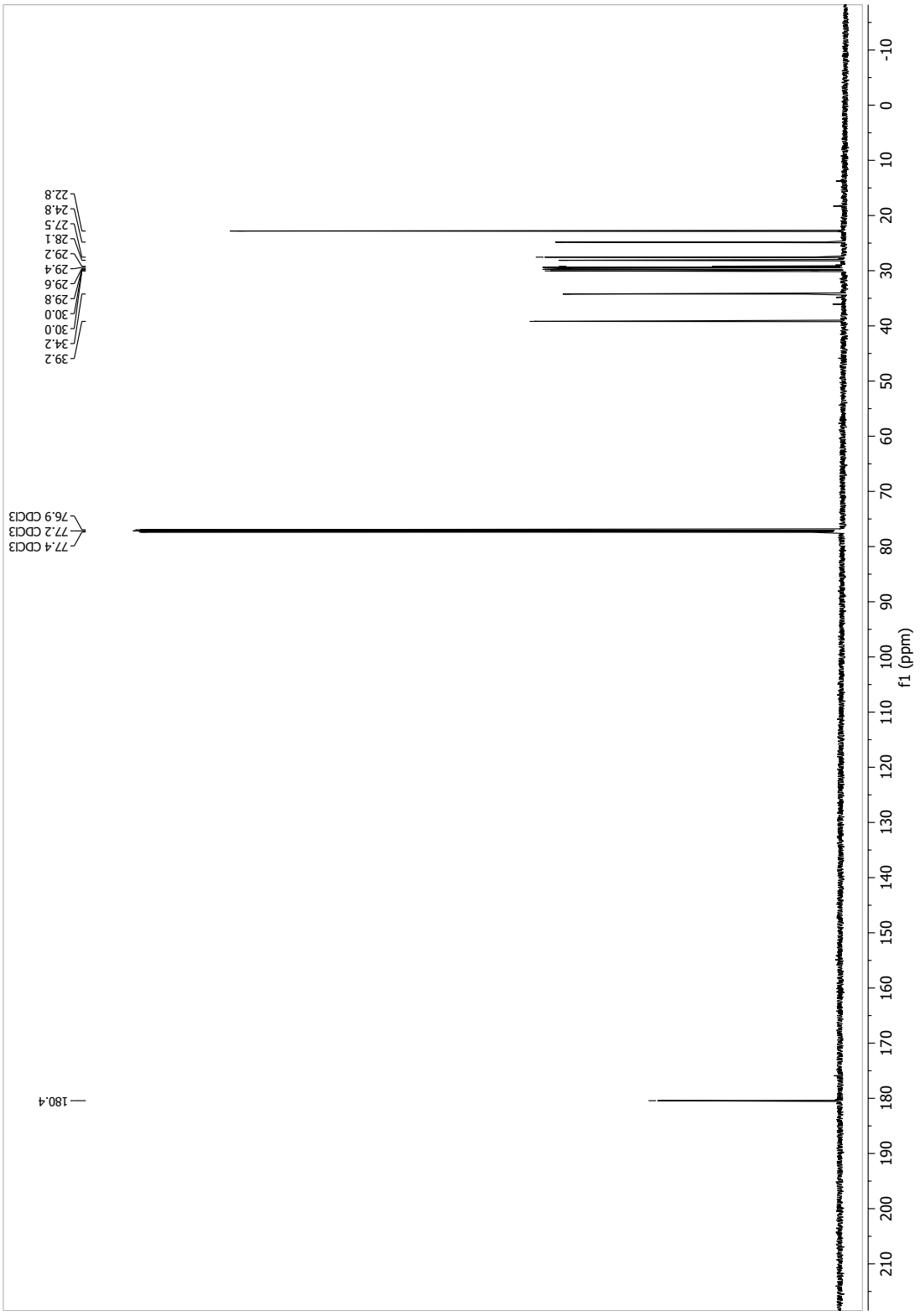
180.4
77.4 CDCl3
77.2 CDCl3
76.9 CDCl3
39.2
34.2
30.0
30.0
29.8
29.6
29.4
29.2
28.1
27.5
24.8
22.8
f1 (ppm)

13.1.92 [D_4]-11-methyldodecanoic acid ([D_4]-*iso*C13, 16b), from route 1

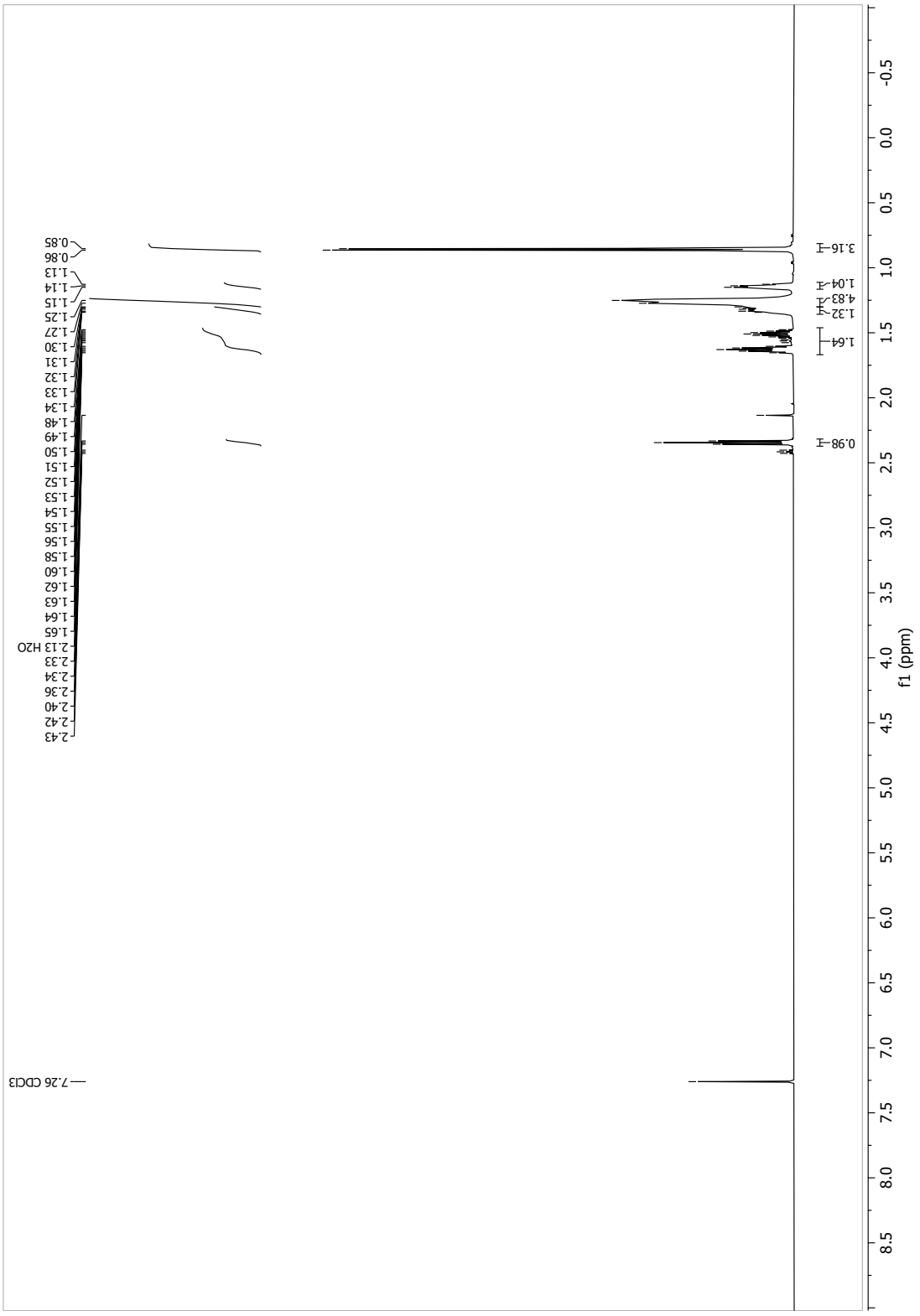

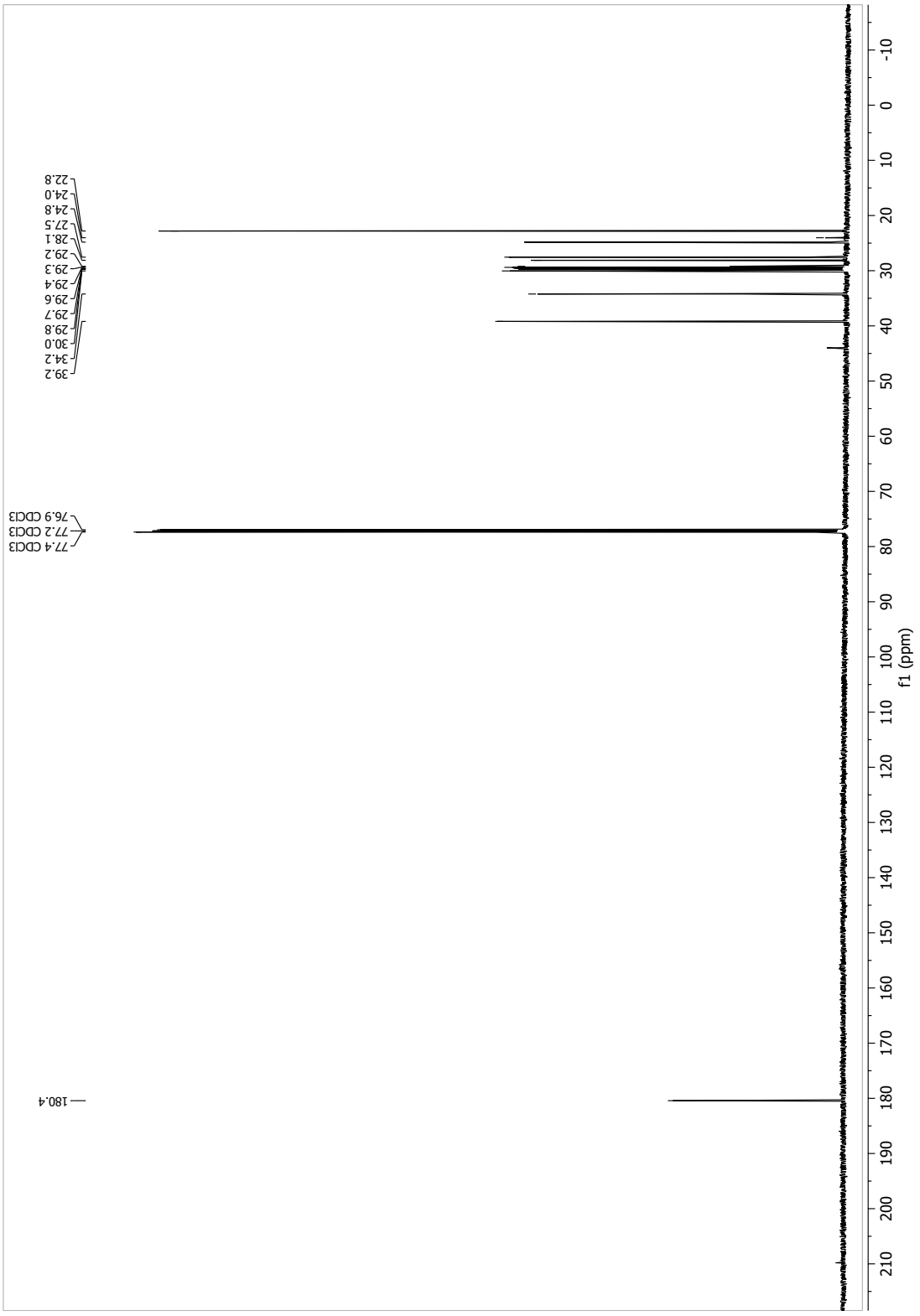
180.4
77.4 CDCl3
77.2 CDCl3
76.9 CDCl3
39.2
34.2
30.0
29.8
29.7
29.6
29.4
29.3
29.2
28.1
27.5
24.8
24.0
22.8
f1 (ppm)

13.1.93 13-Methyltetradecanoic acid (*iso*C15, 15a), from route 1

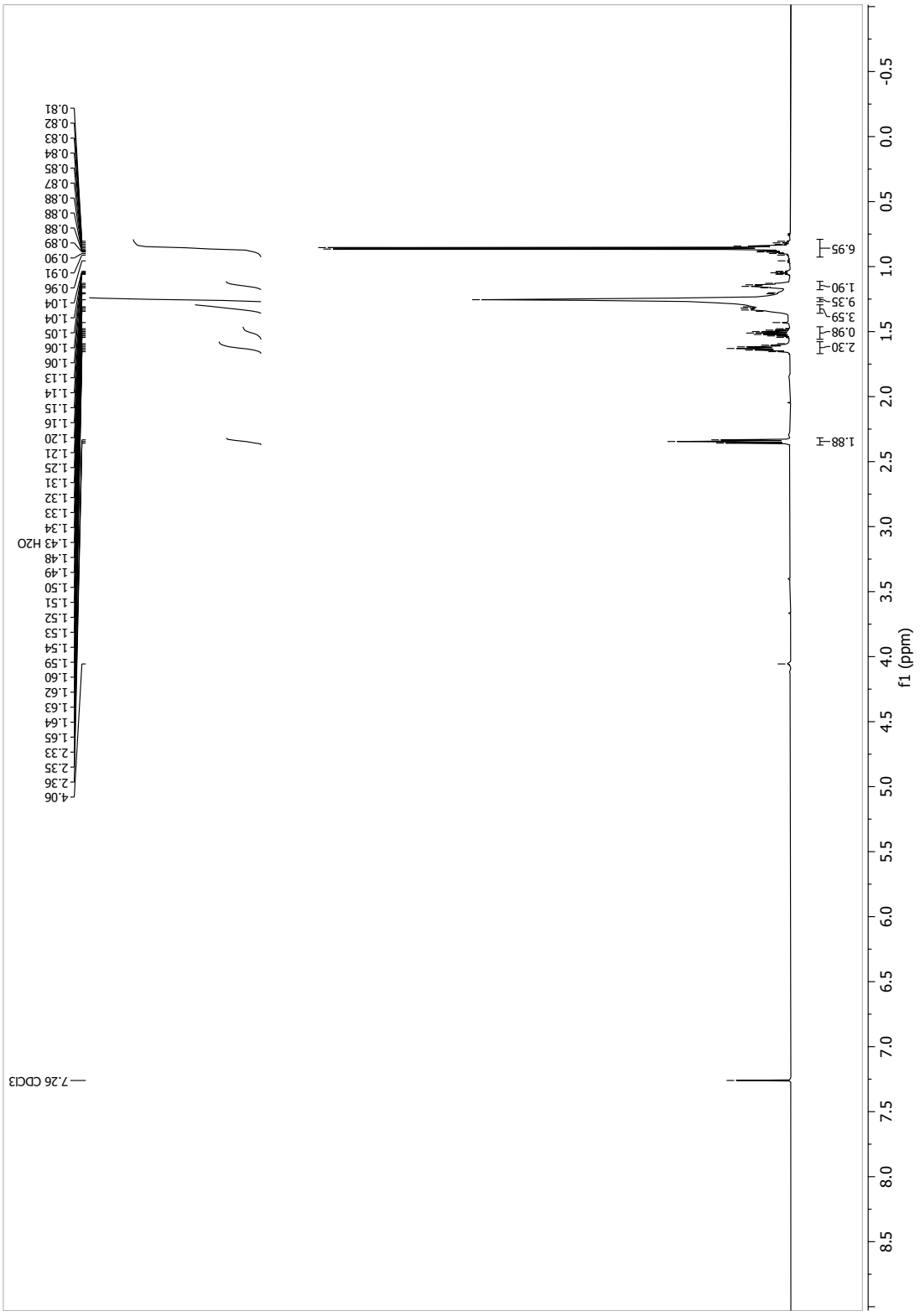

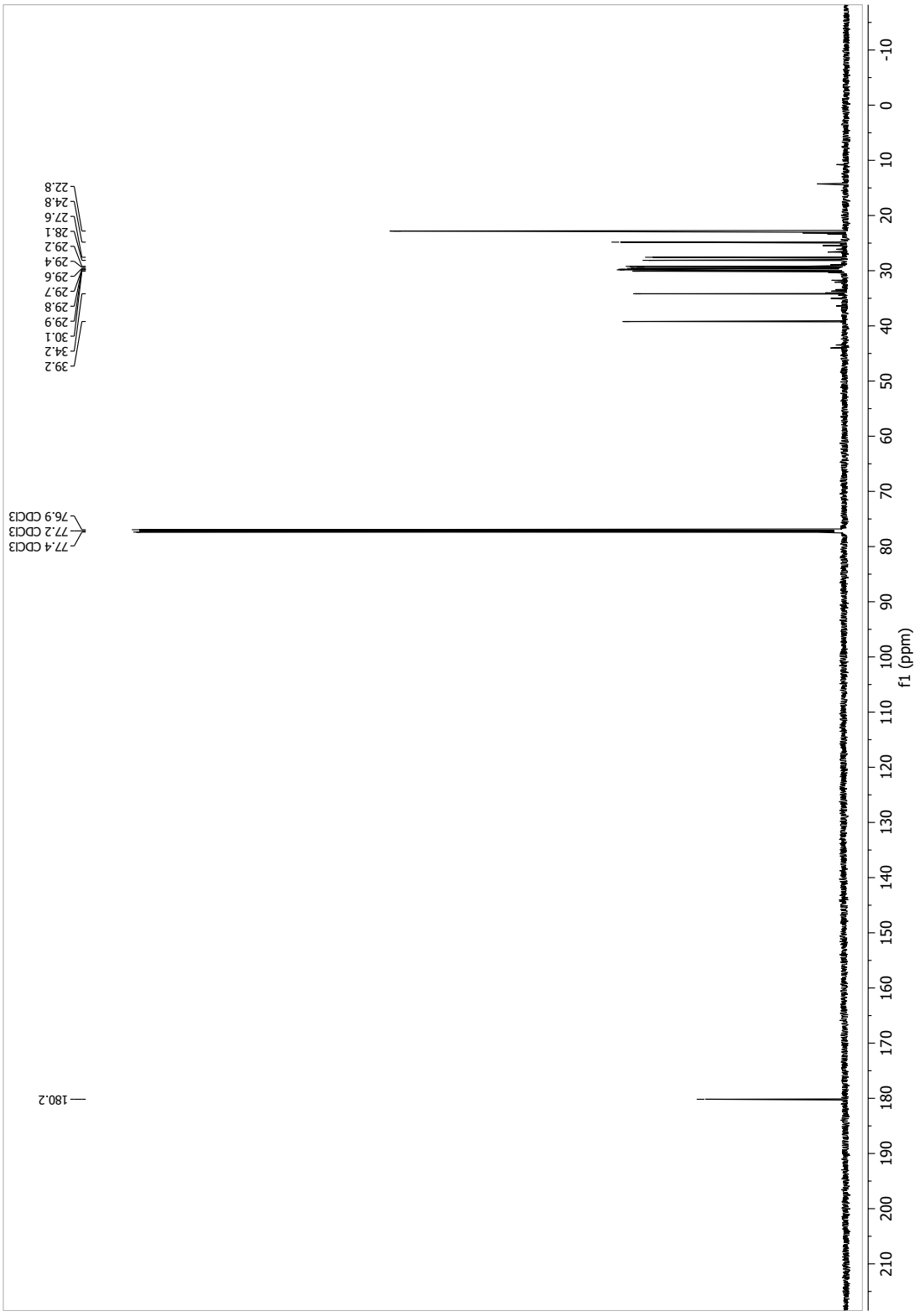
180.2
77.4 CDCl3
77.2 CDCl3
76.9 CDCl3
39.2
34.2
30.1
29.9
29.8
29.7
29.6
29.4
29.2
28.1
27.6
24.8
22.8
f1 (ppm)

13.1.94 [D_4]-13-Methyltetradecanoic acid ([D_4]-*iso*C15, 15b), from route 1

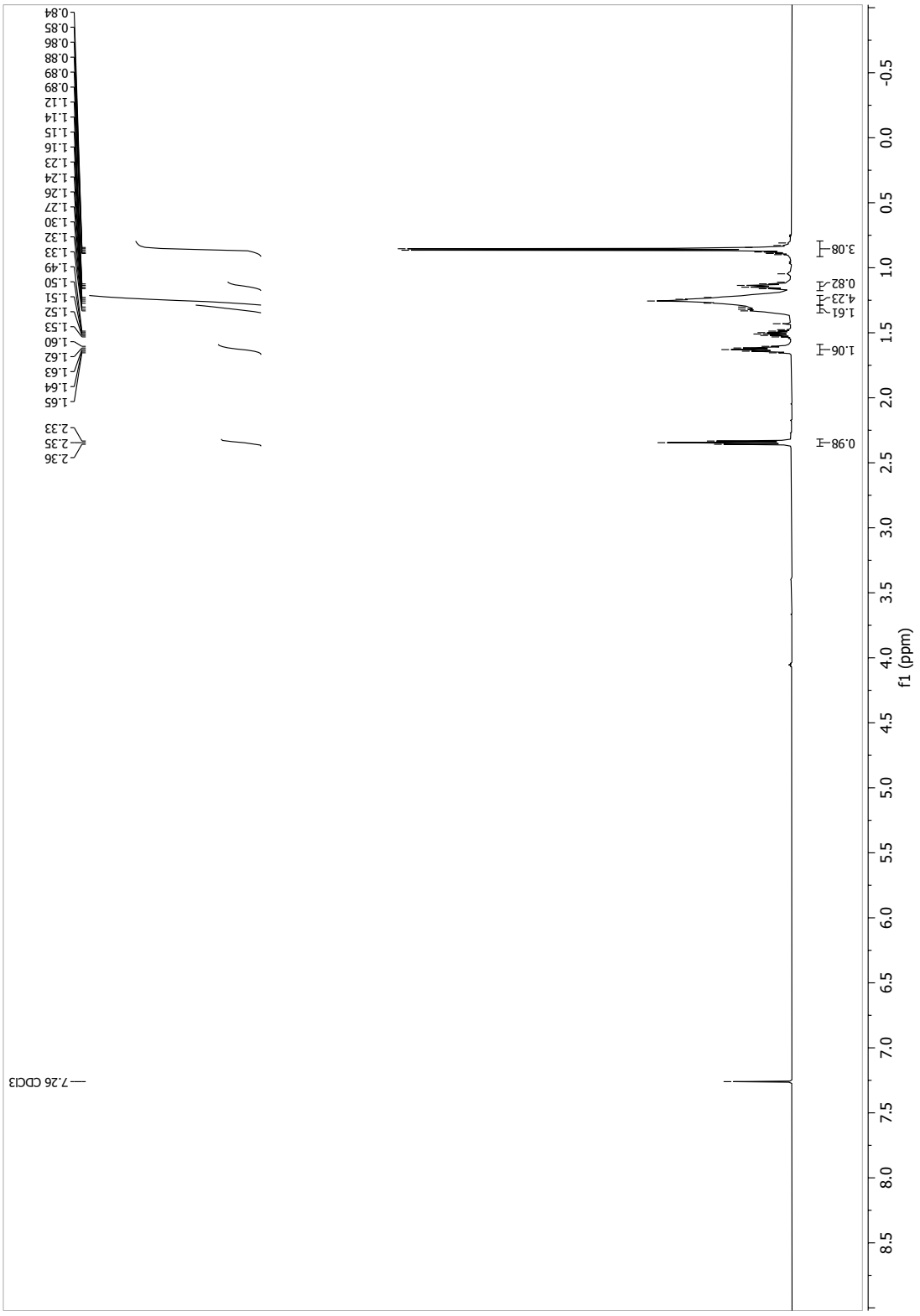

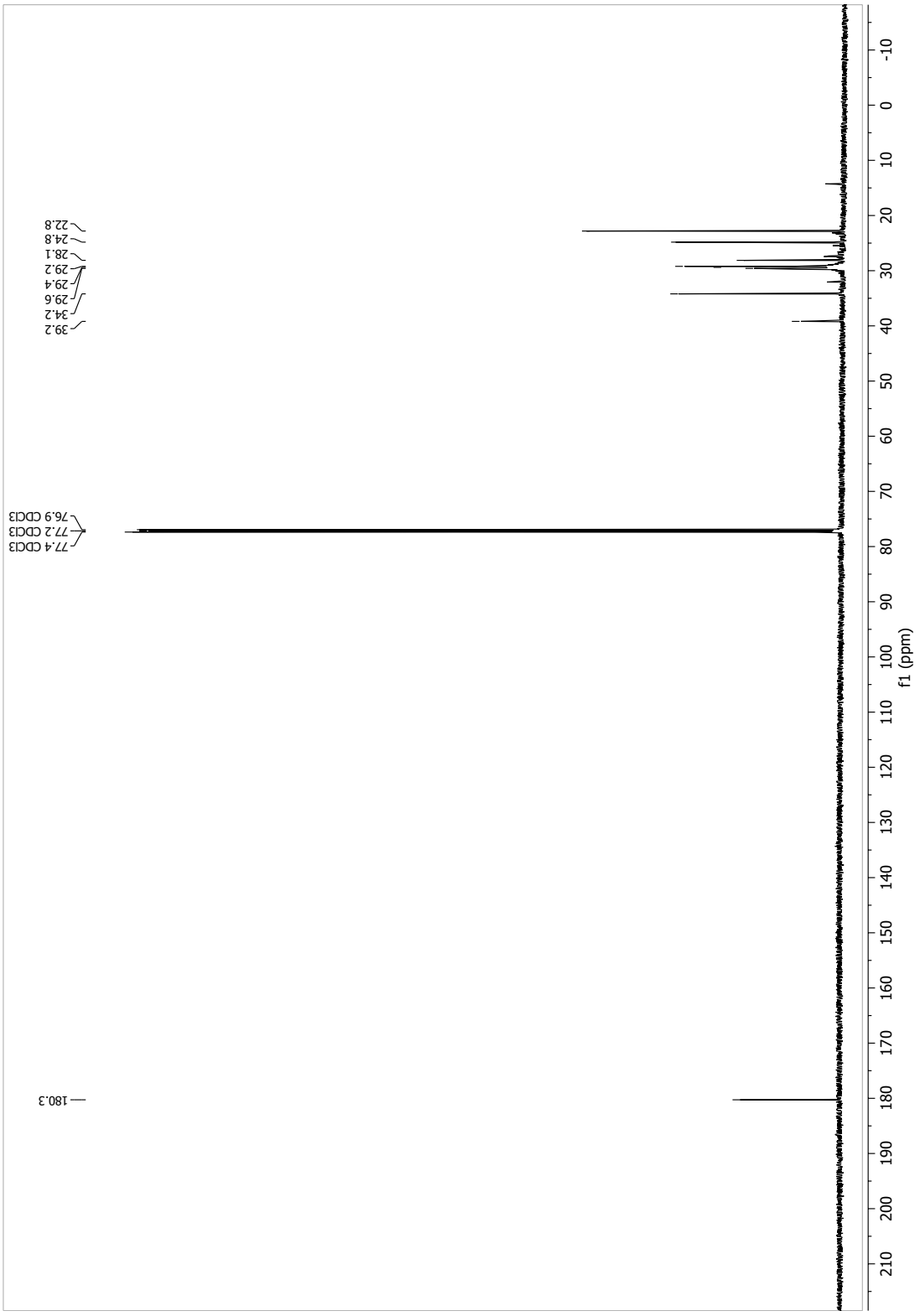
180.3
77.4 CDCl3
77.2 CDCl3
76.9 CDCl3
39.2
34.2
29.6
29.4
29.2
28.1
24.8
22.8
f1 (ppm)

13.1.95 2-Methyldodec-11-en-2-ol (121a)

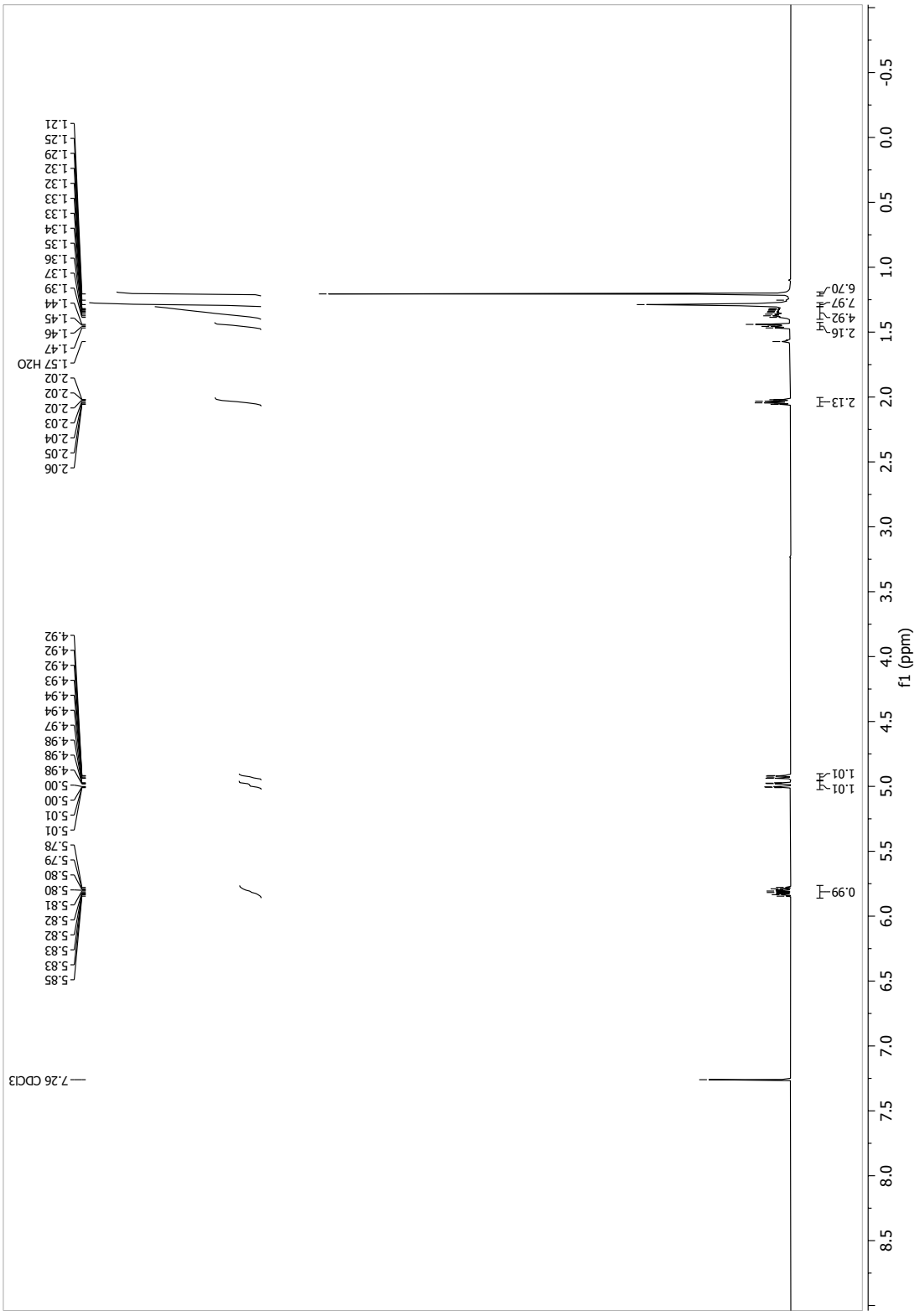

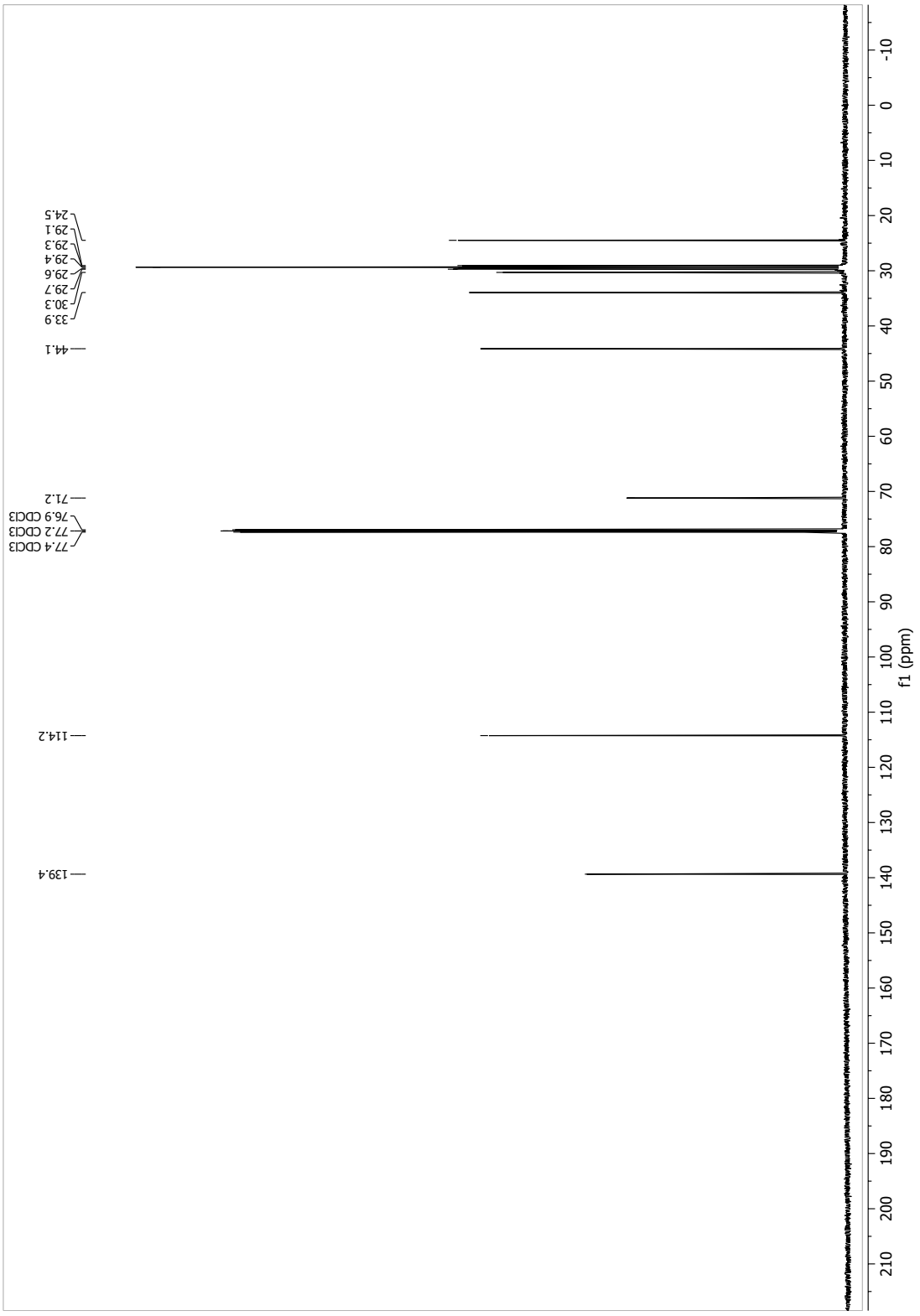
77.4 CDCl3
77.2 CDCl3
76.9 CDCl3
71.2
44.1
33.9
30.3
29.7
29.6
29.4
29.3
29.1
24.5
114.2
139.4
f1 (ppm)

13.1.96 [D_6]-2-methyldodec-11-en-2-ol (121c)

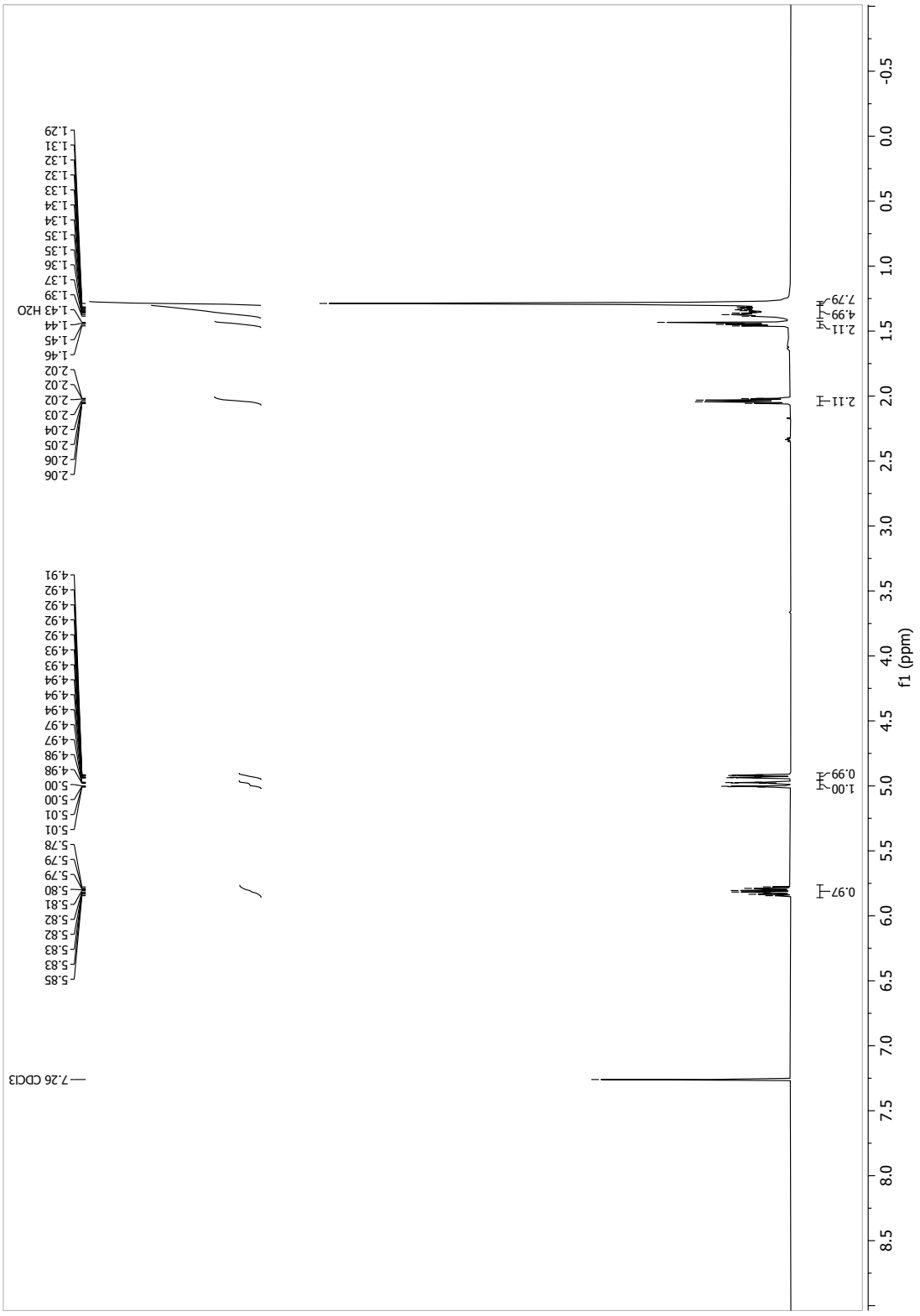

139.4
114.2
77.4 CDCl3
77.2 CDCl3
76.9 CDCl3
70.9
44.0
33.9
30.3
29.7
29.6
29.3
29.1
24.4
f1 (ppm)

13.1.97 11-Methyldodec-1-ene (122a)

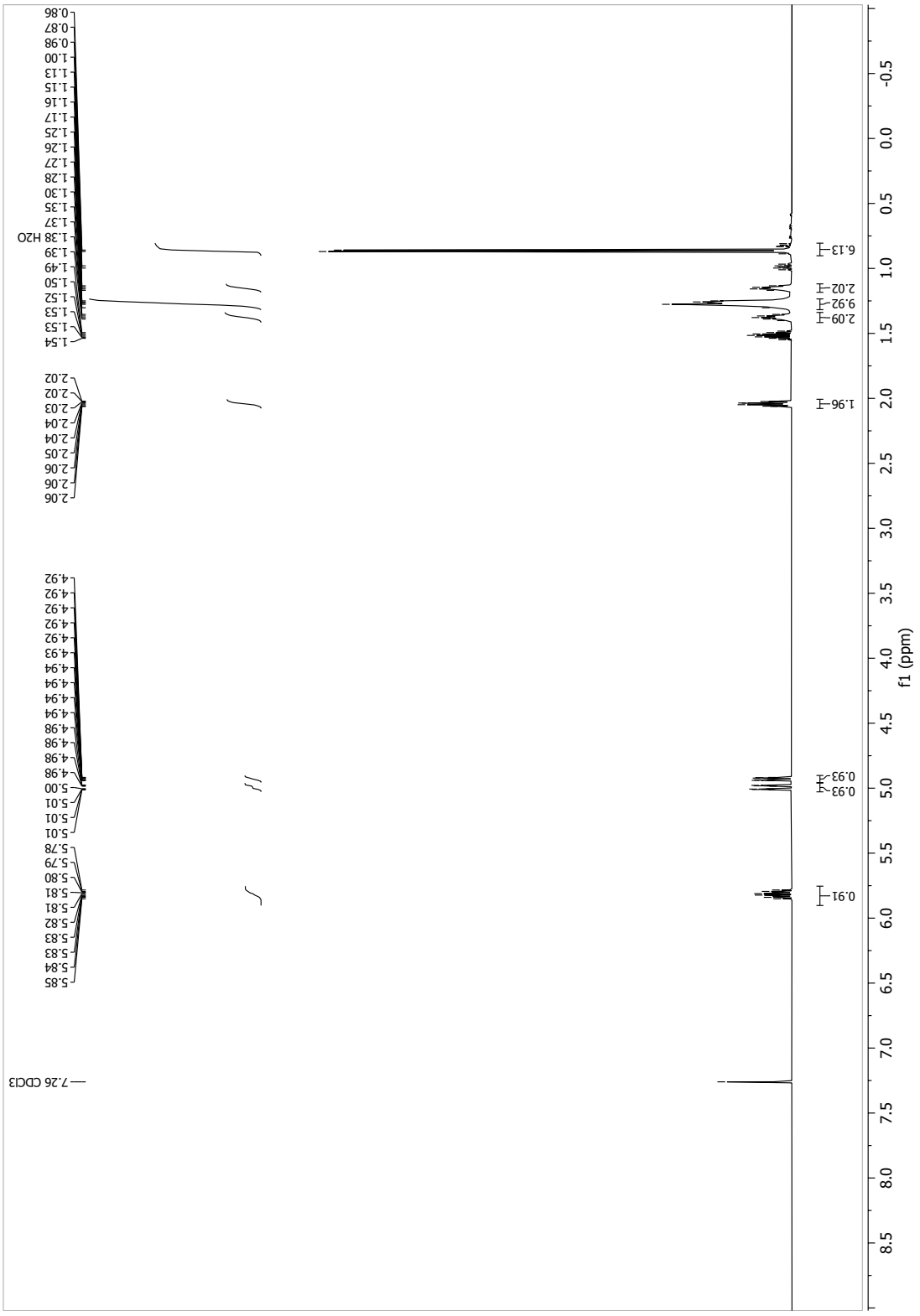

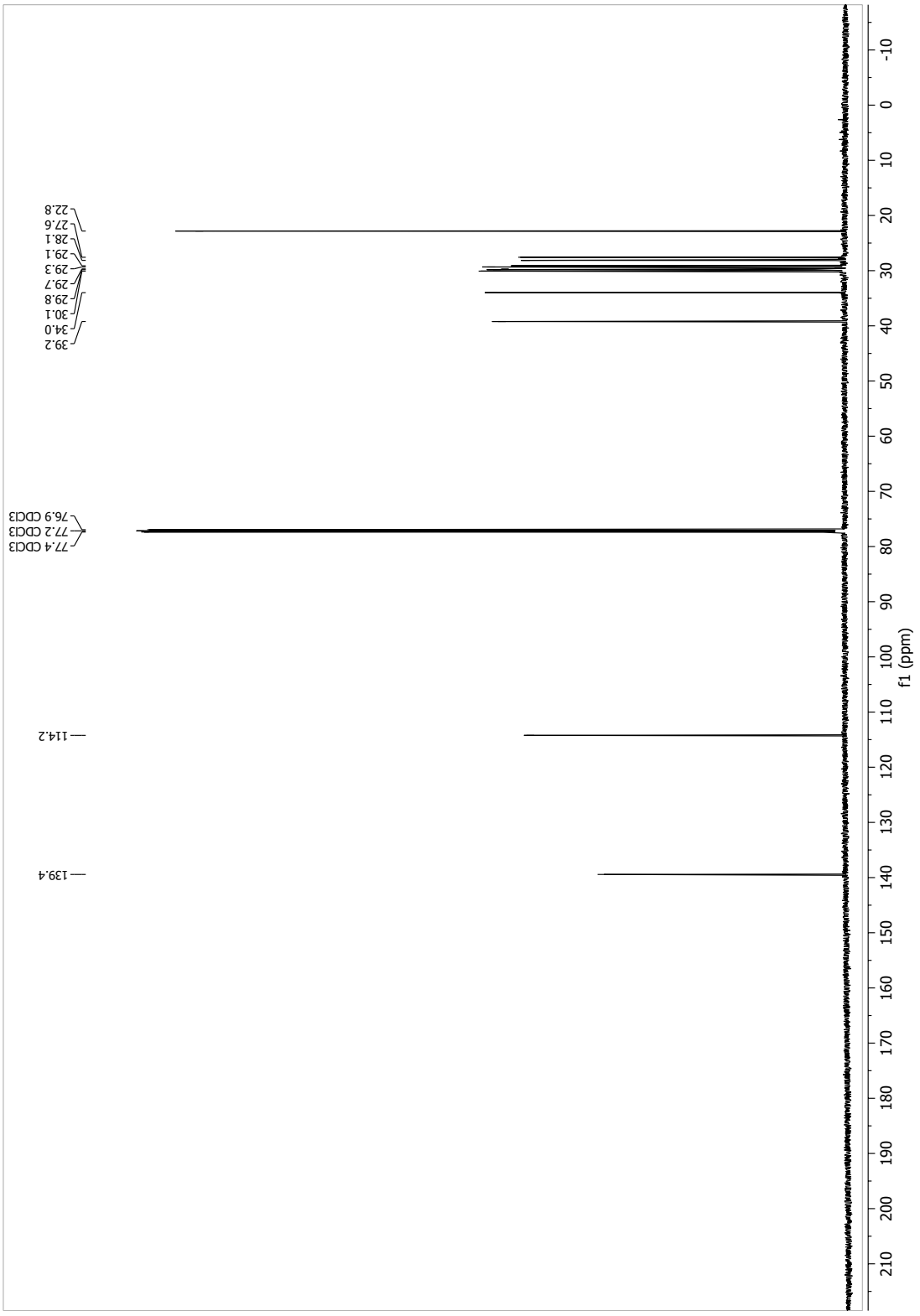
139.4
114.2
77.4 CDCl3
77.2 CDCl3
76.9 CDCl3
39.2
34.0
30.1
29.8
29.7
29.3
29.1
28.1
27.6
22.8
f1 (ppm)

13.1.98 [D_6]-11-methyldodec-1-ene (122c)

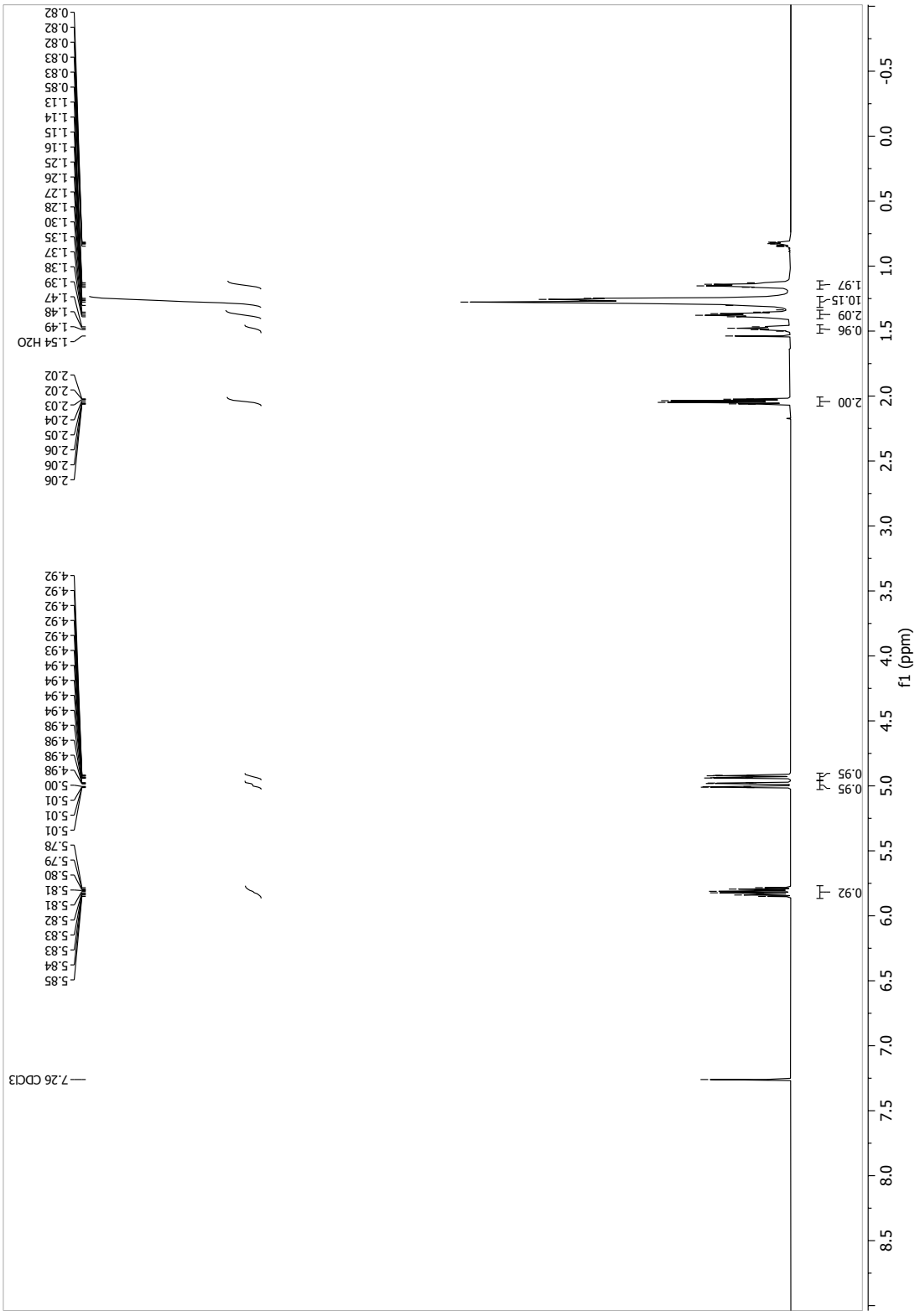

139.4
114.2
77.4 CDCl3
77.2 CDCl3
76.9 CDCl3
39.1
34.0
30.1
29.8
29.7
29.3
29.1
27.7
27.6
27.6
27.5
f1 (ppm)

13.1.99 11-Methyldodecan-1-ol (123a)

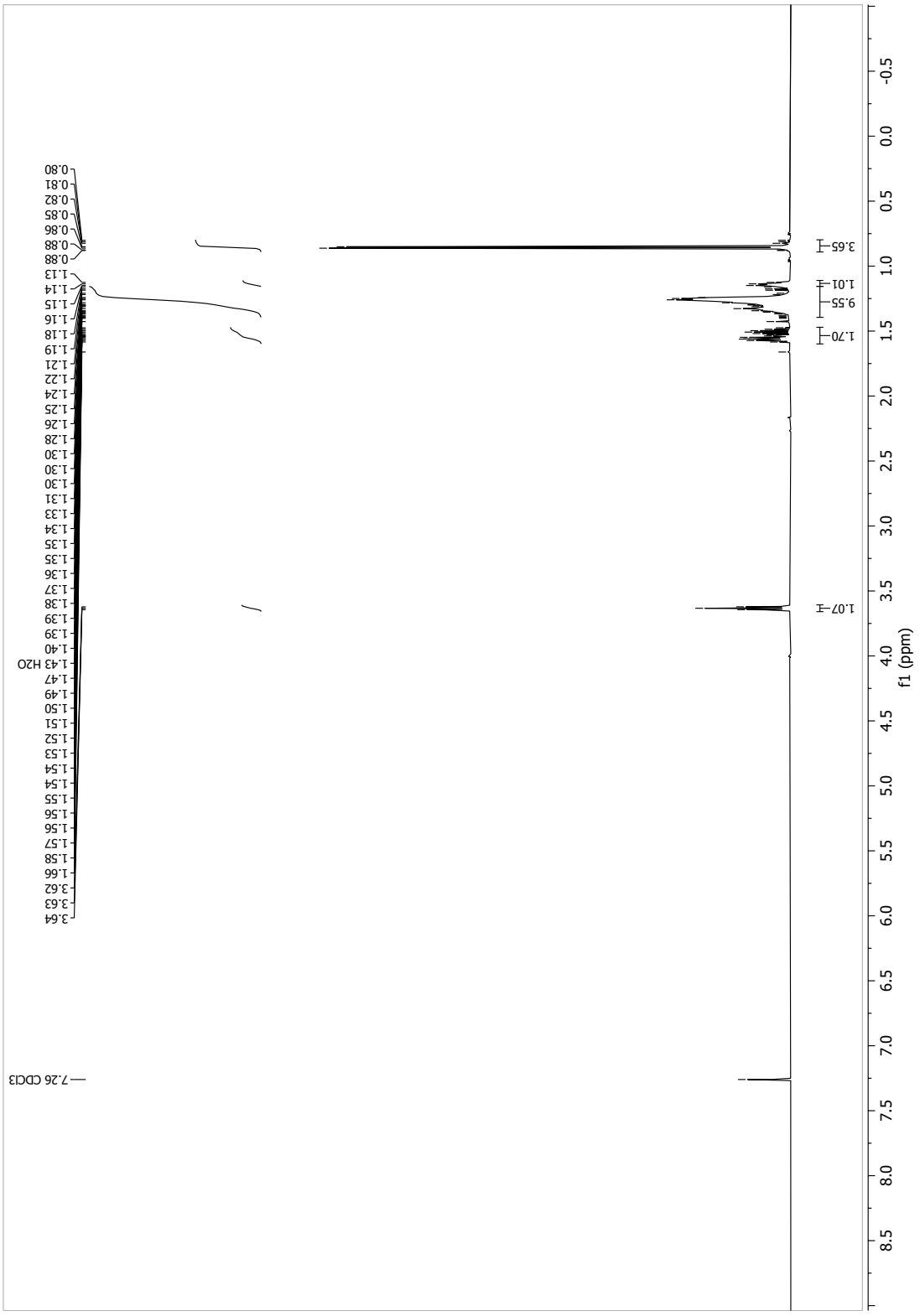

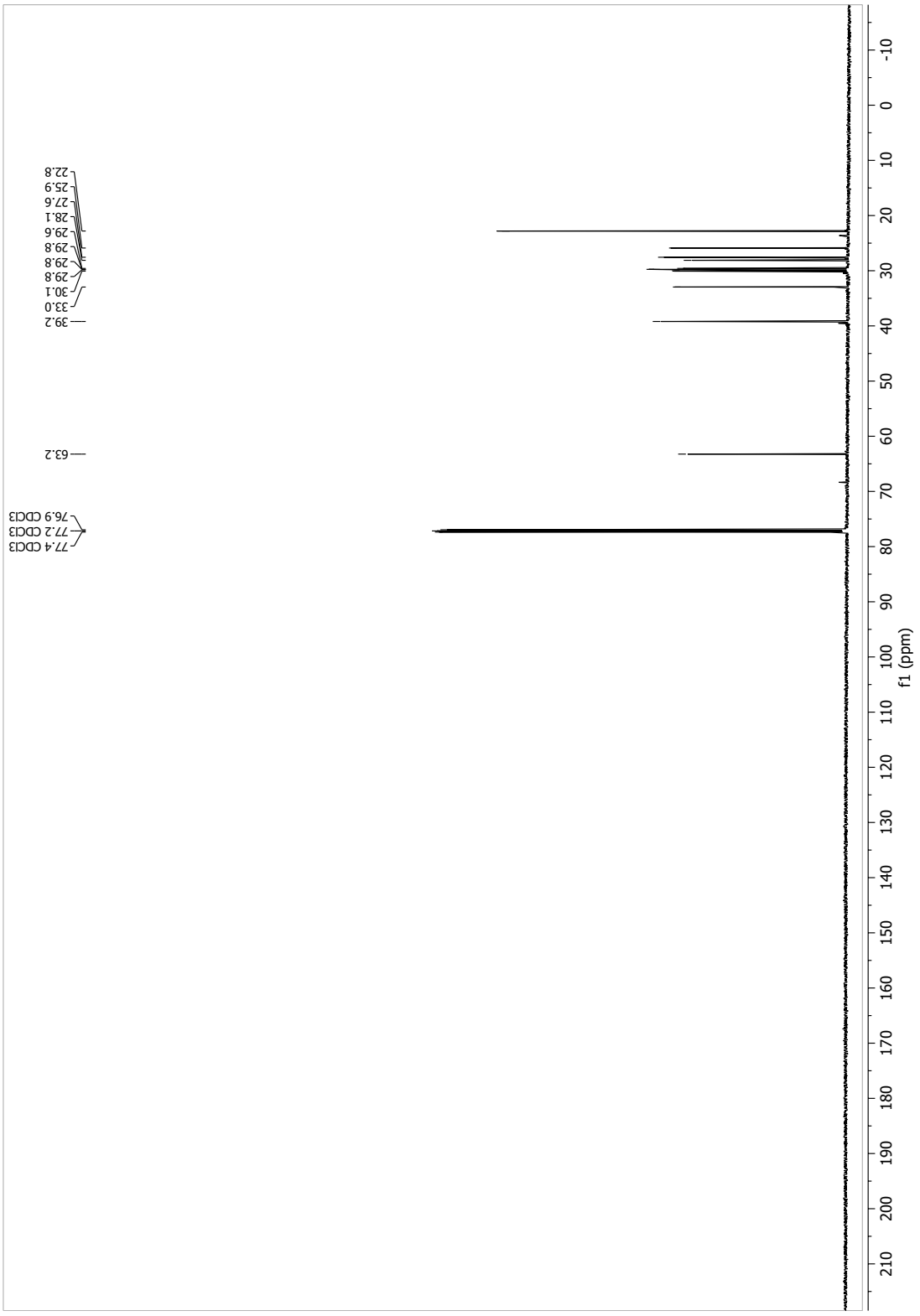
77.4 CDCl3
77.2 CDCl3
76.9 CDCl3
63.2
39.2
33.0
30.1
29.8
29.8
29.8
29.6
28.1
27.6
25.9
22.8
f1 (ppm)

13.1.100 [D_6]-11-methyldodecan-1-ol (123c)

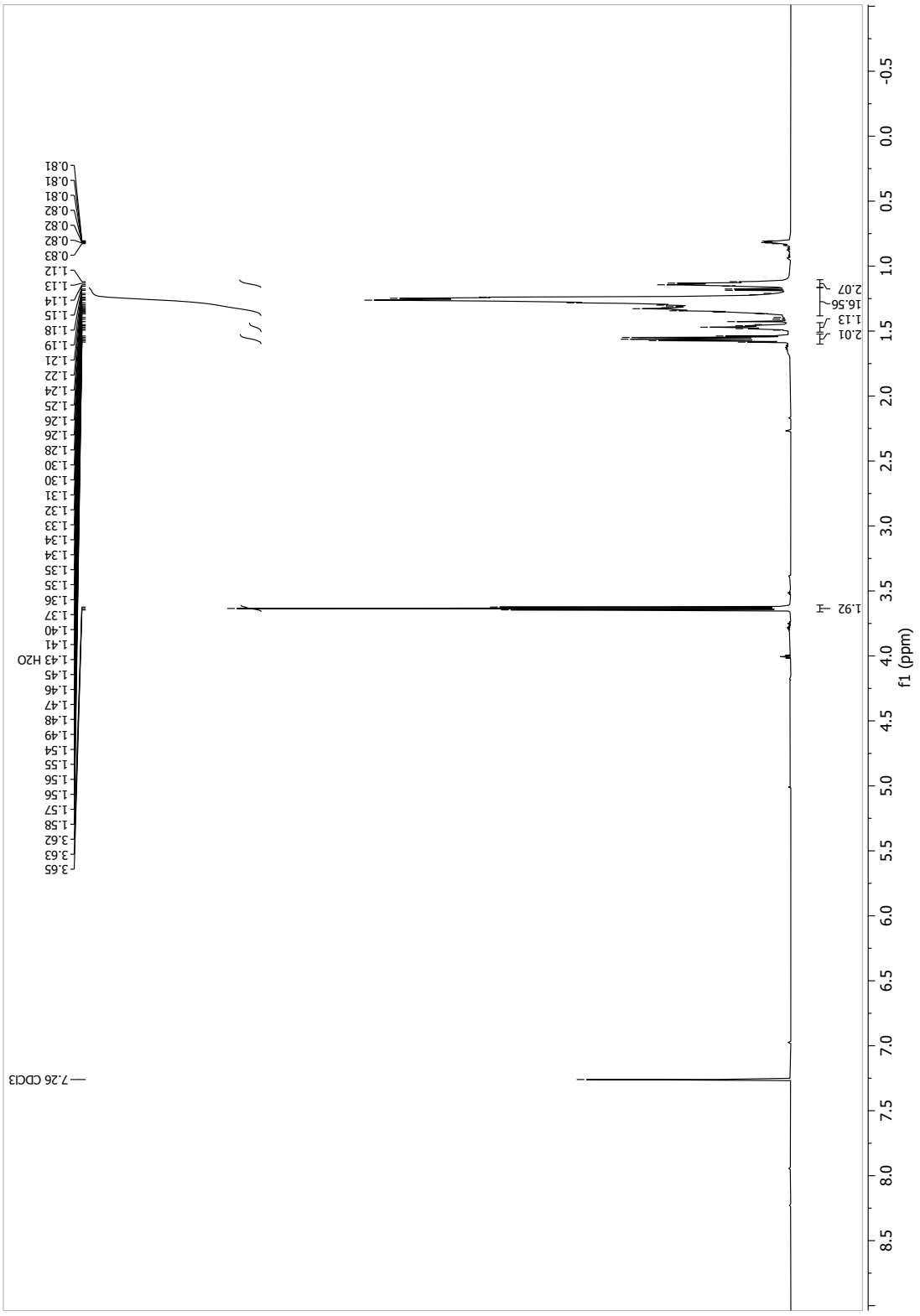

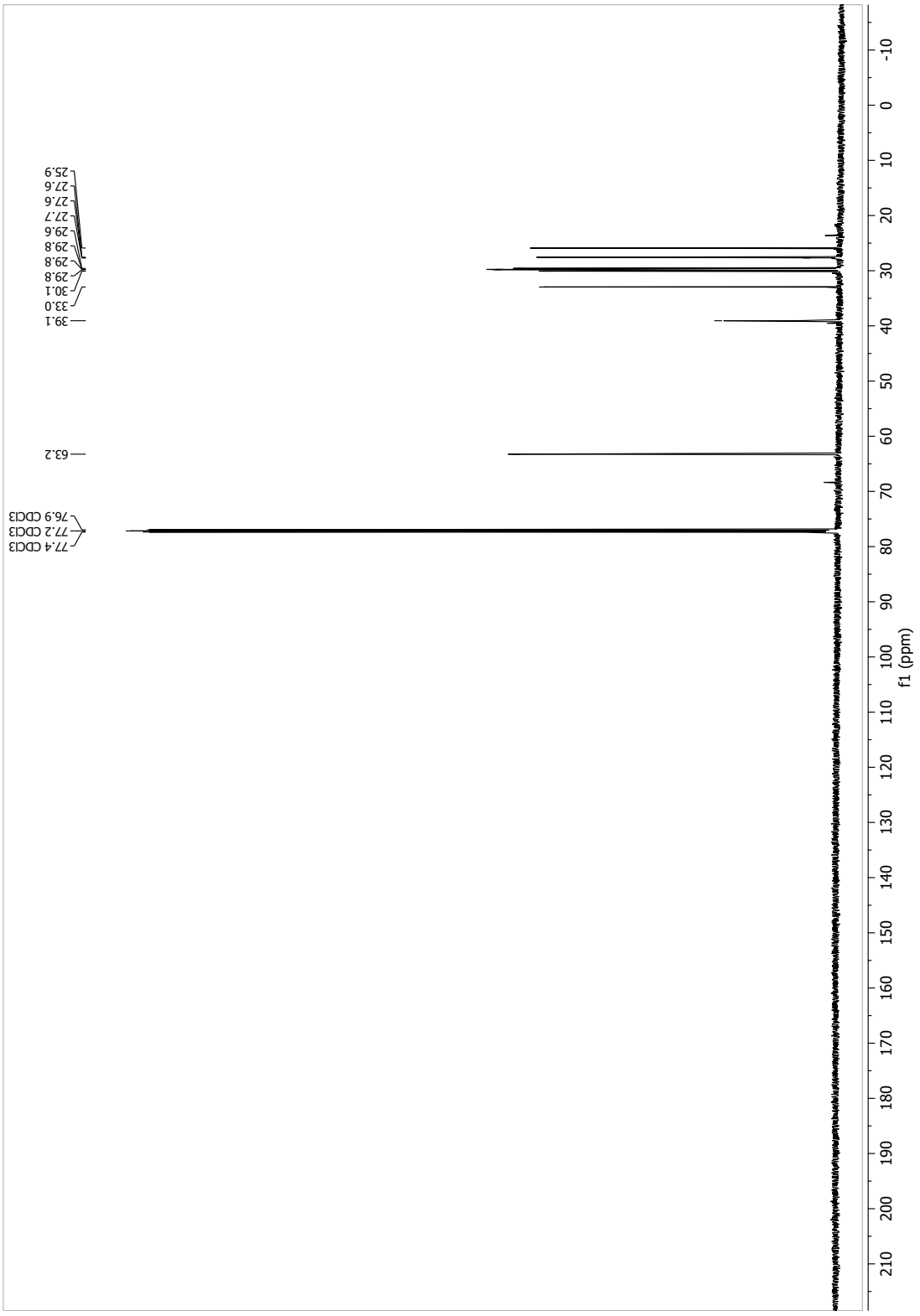
77.4 CDCl3
77.2 CDCl3
76.9 CDCl3
63.2
39.1
33.0
30.1
29.8
29.8
29.8
29.6
27.7
27.6
27.6
25.9
f1 (ppm)

13.1.101 11-Methyldodecanoic acid (*iso*C13, 16a), from route 2

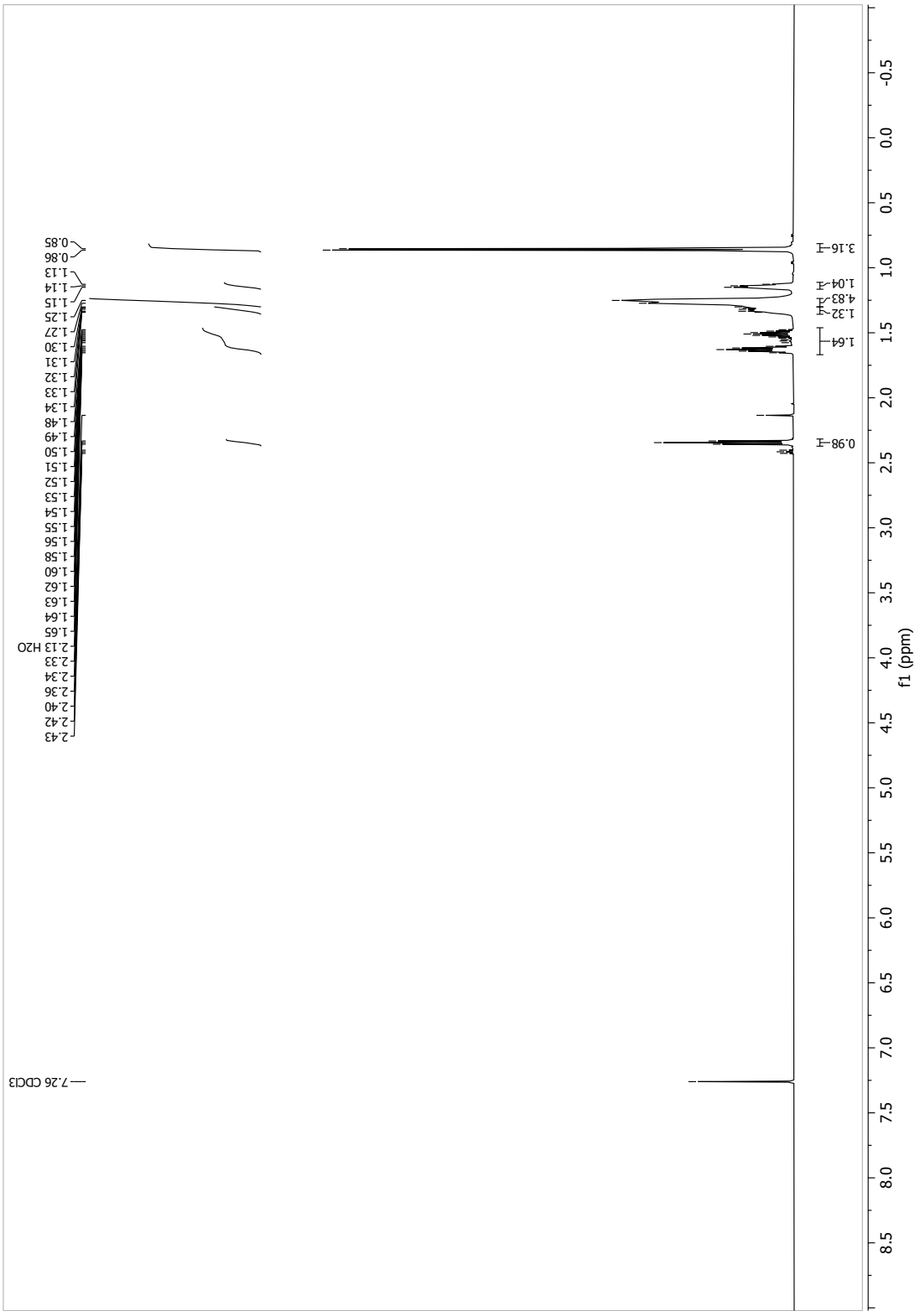

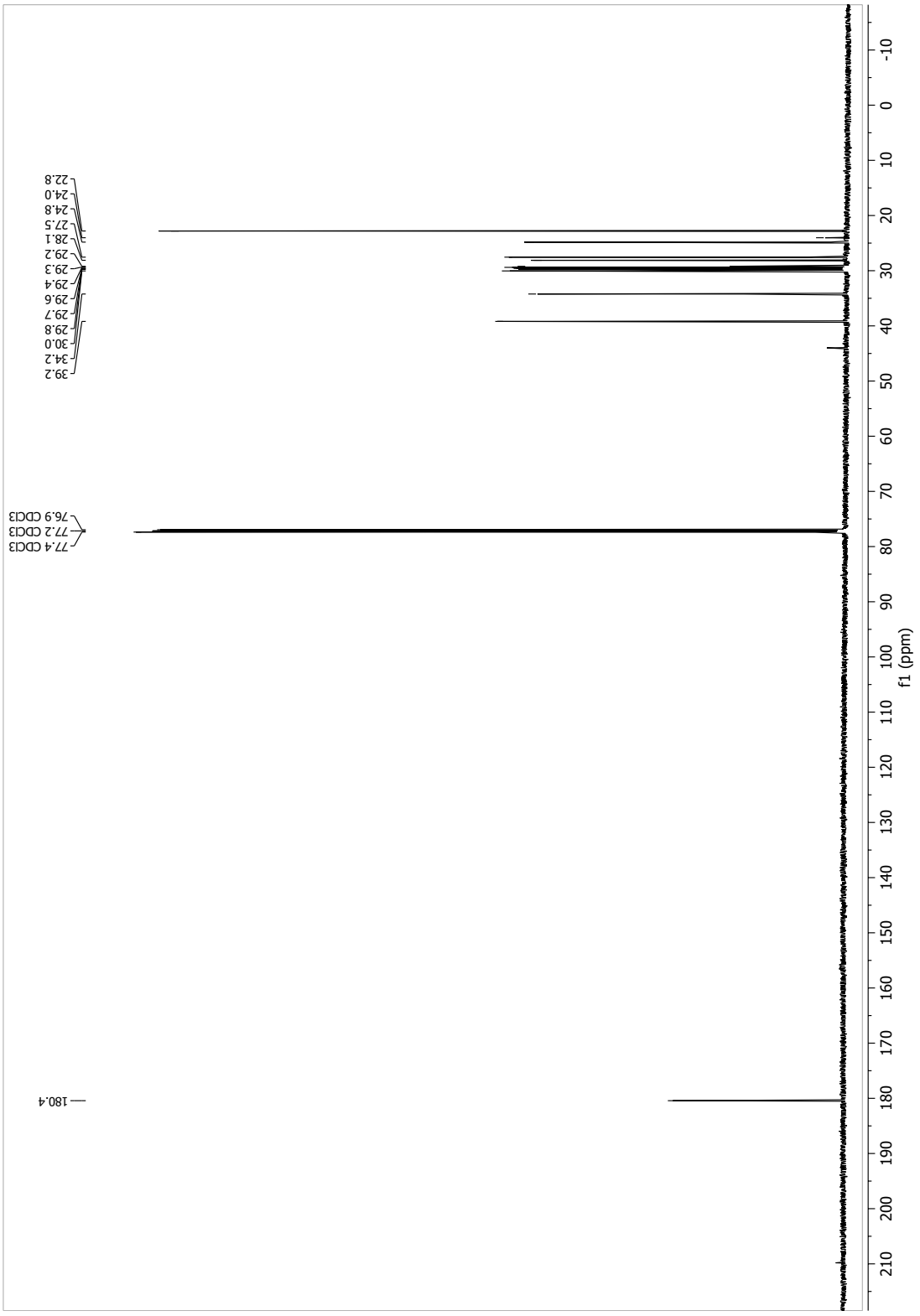
180.4
77.4 CDCl3
77.2 CDCl3
76.9 CDCl3
39.2
34.2
30.0
29.8
29.7
29.6
29.4
29.3
29.2
28.1
27.5
24.8
24.0
22.8
f1 (ppm)

13.1.102 [D_6]-11-methyldodecanoic acid ([D_6]-*iso*C13, 16c), from route 2

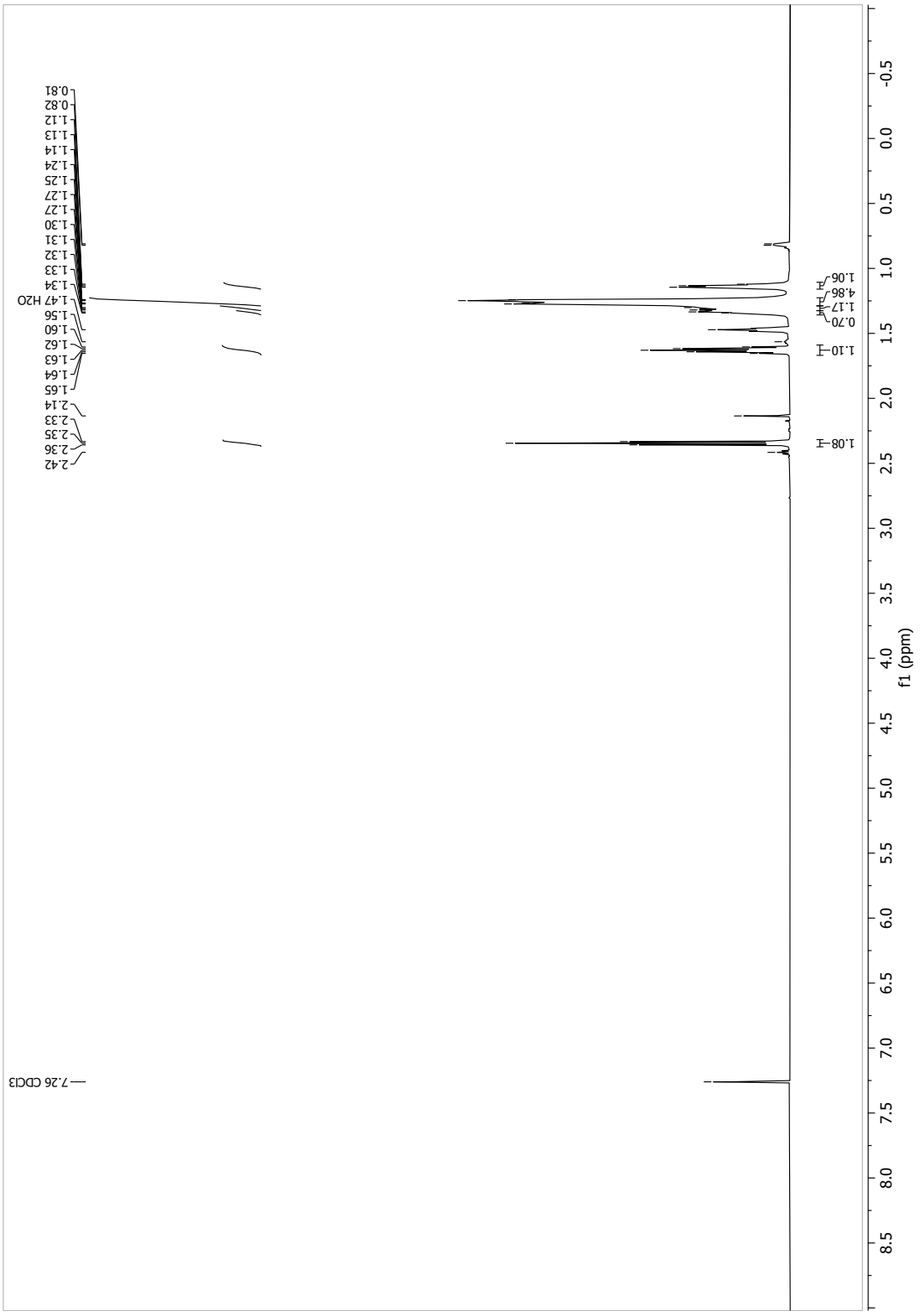

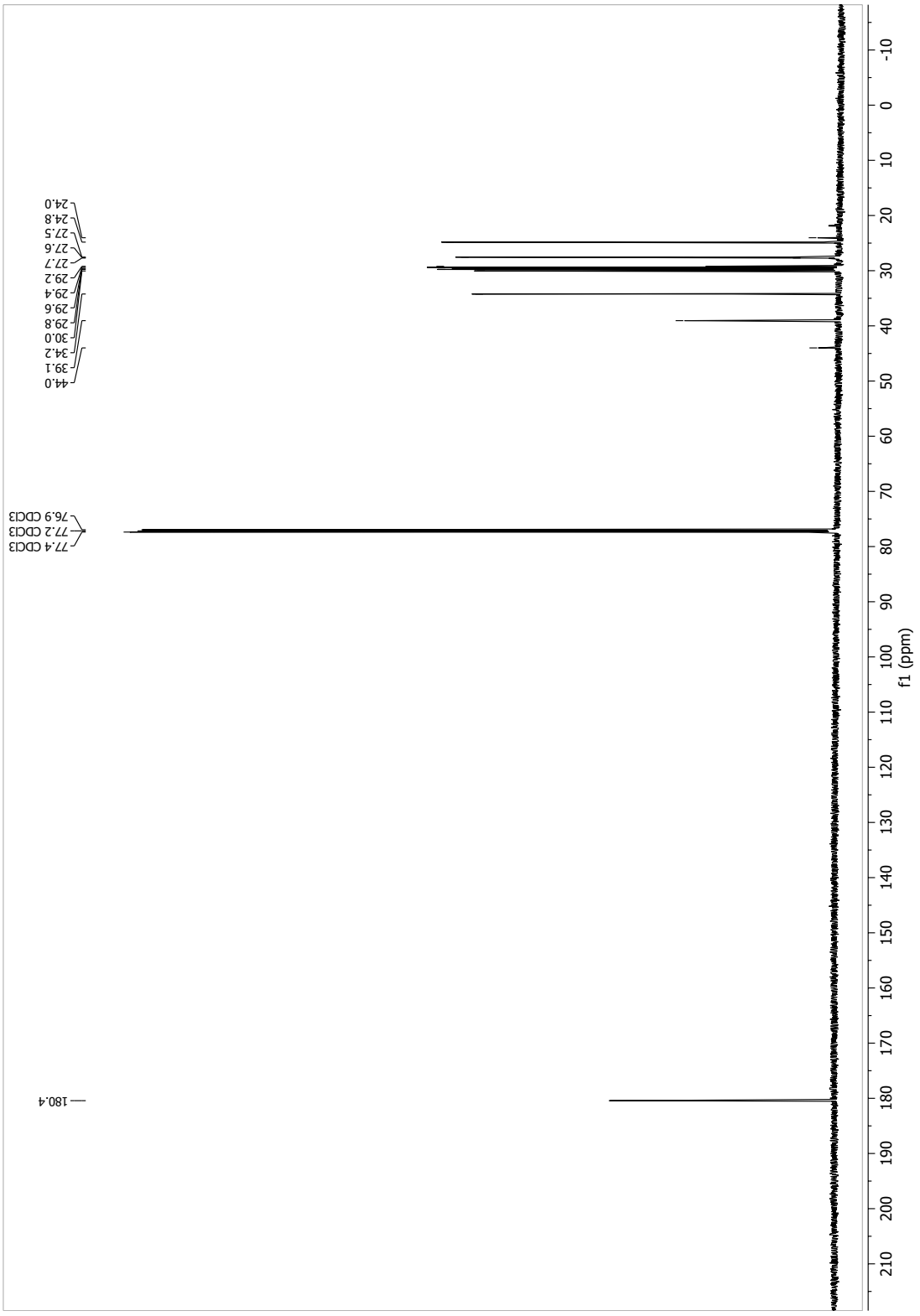
180.4
77.4 CDCl3
77.2 CDCl3
76.9 CDCl3
44.0
39.1
34.2
30.0
29.8
29.6
29.4
29.2
27.7
27.6
27.5
24.8
24.0
f1 (ppm)

13.1.103 1-Bromo-11-methyldodecane (124a)

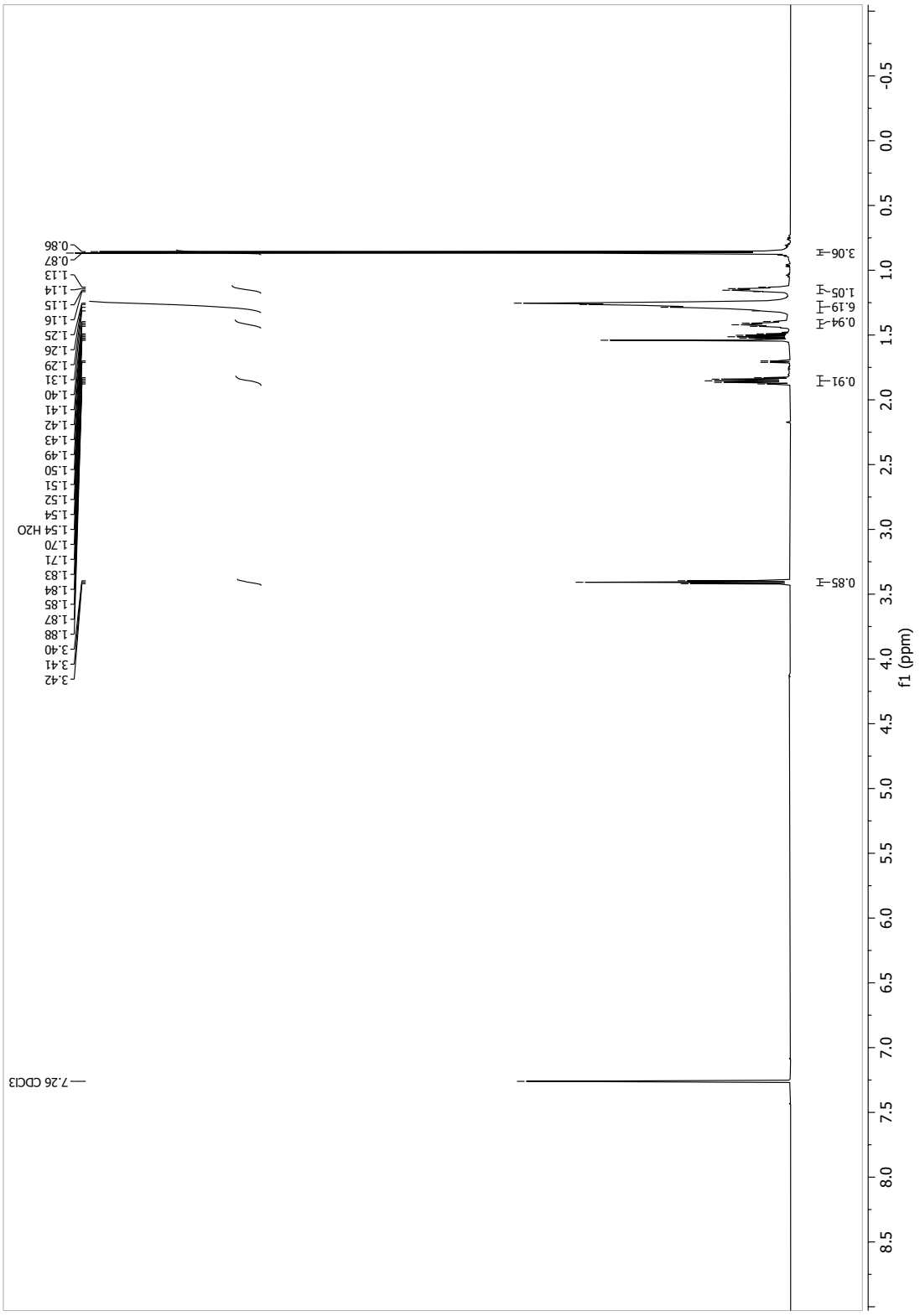

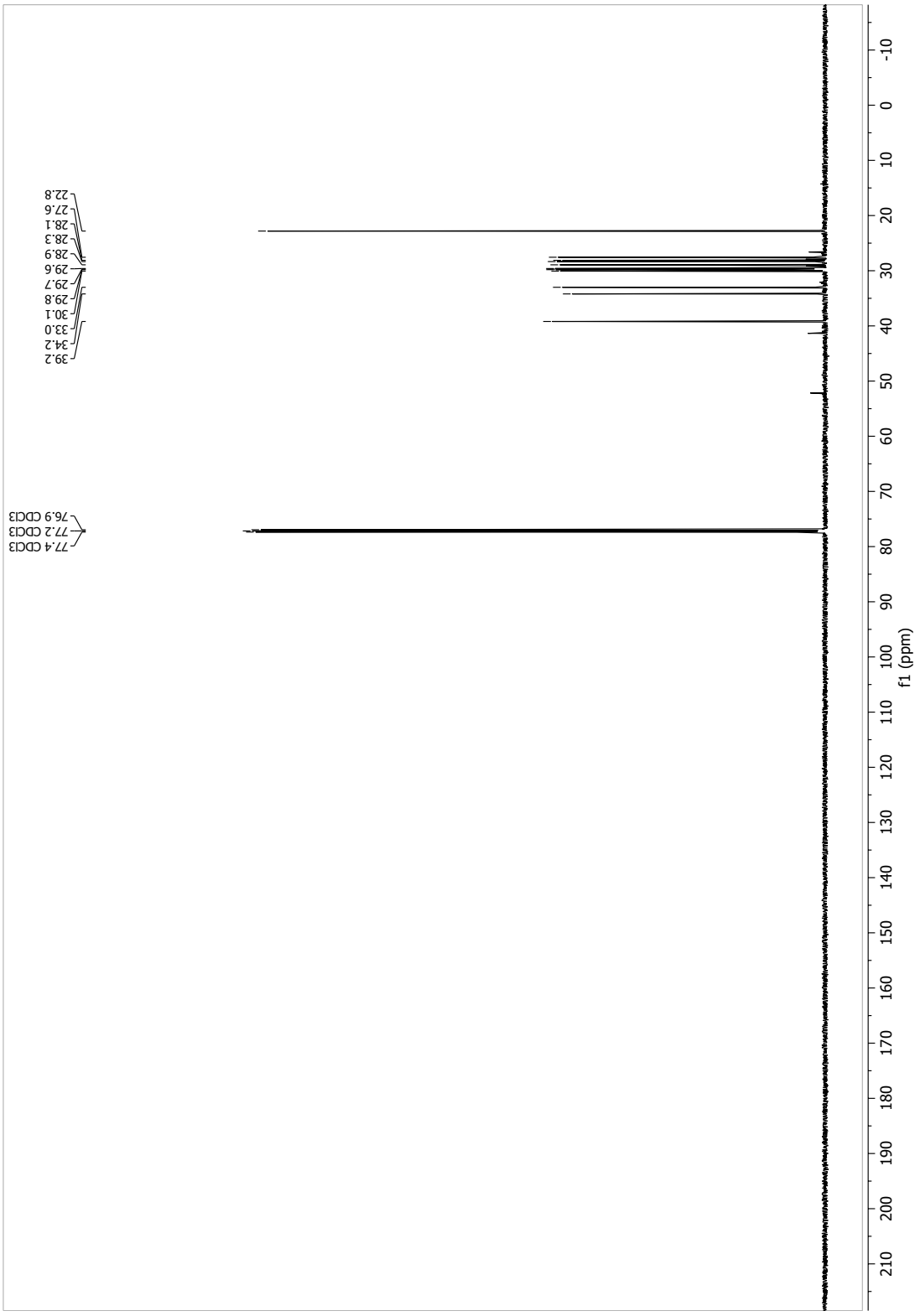
77.4 CDCl3
77.2 CDCl3
76.9 CDCl3
39.2
34.2
33.0
30.1
29.8
29.7
29.6
28.9
28.3
28.1
27.6
22.8
f1 (ppm)

13.1.104 [D_6]-1-bromo-11-methyldodecane (124c)

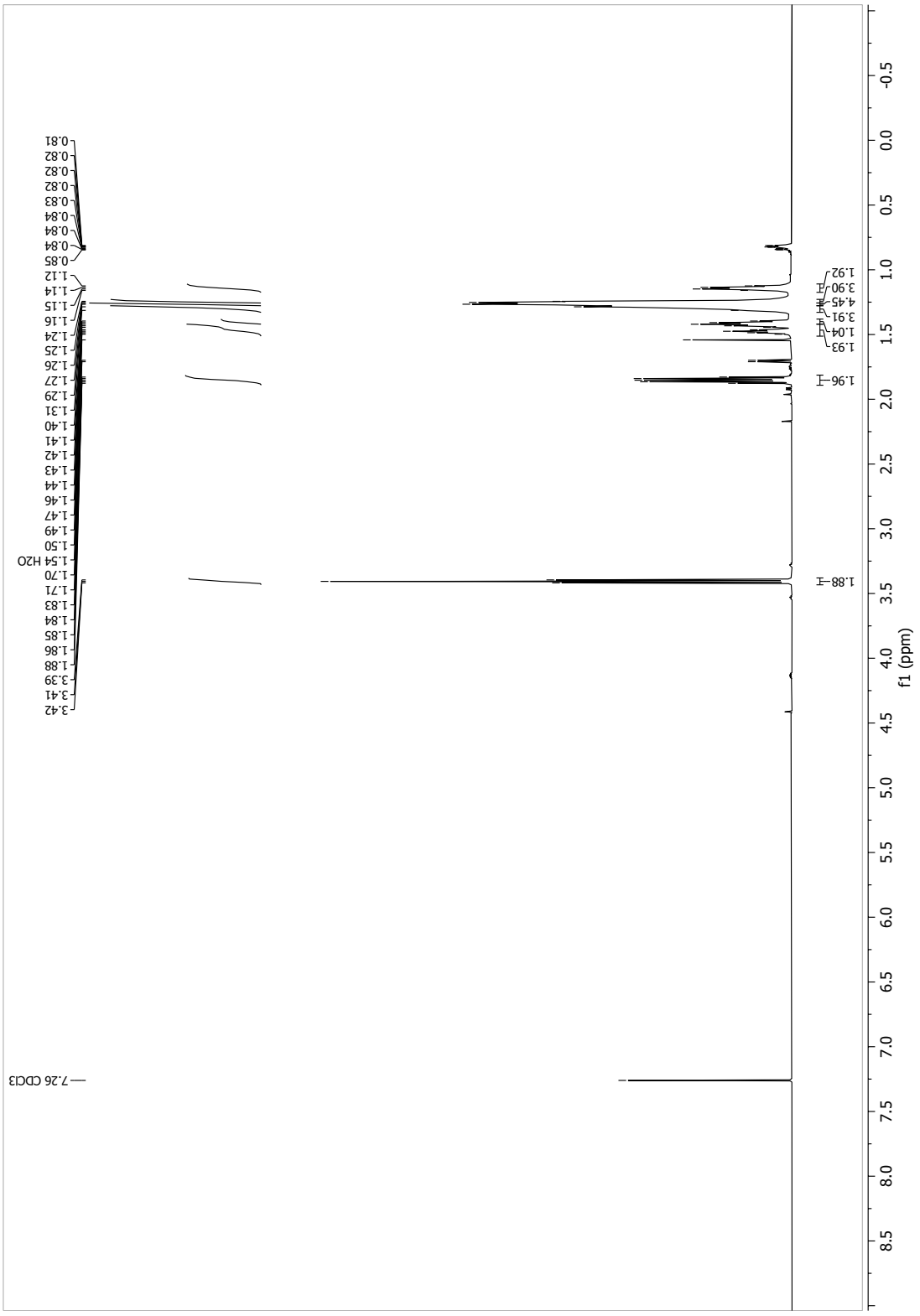

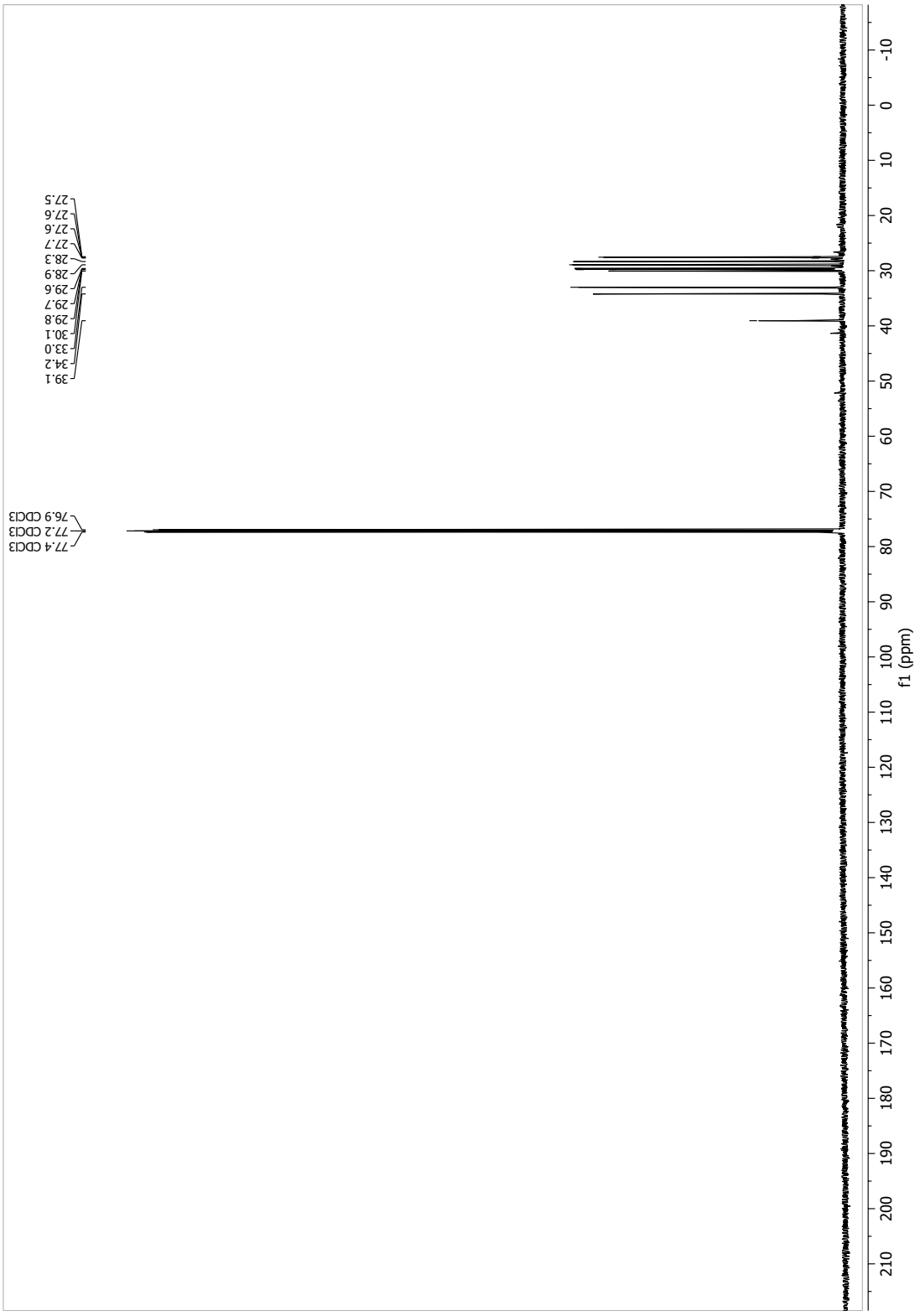
77.4 CDCl3
77.2 CDCl3
76.9 CDCl3
39.1
34.2
33.0
30.1
29.8
29.7
29.6
28.9
28.3
27.7
27.6
27.6
27.5
f1 (ppm)

13.1.105 13-Methyltetradec-1-ene (125a)

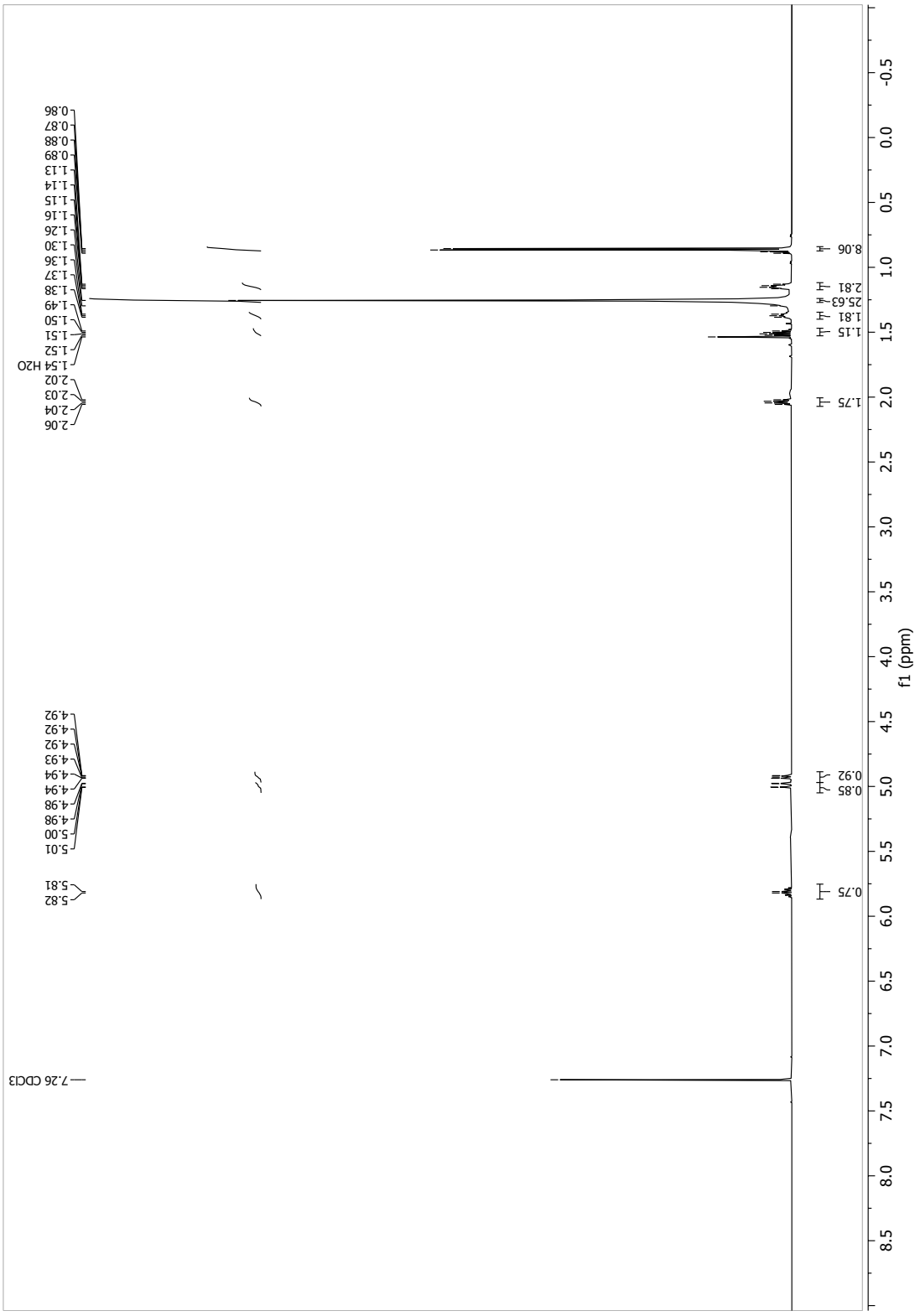

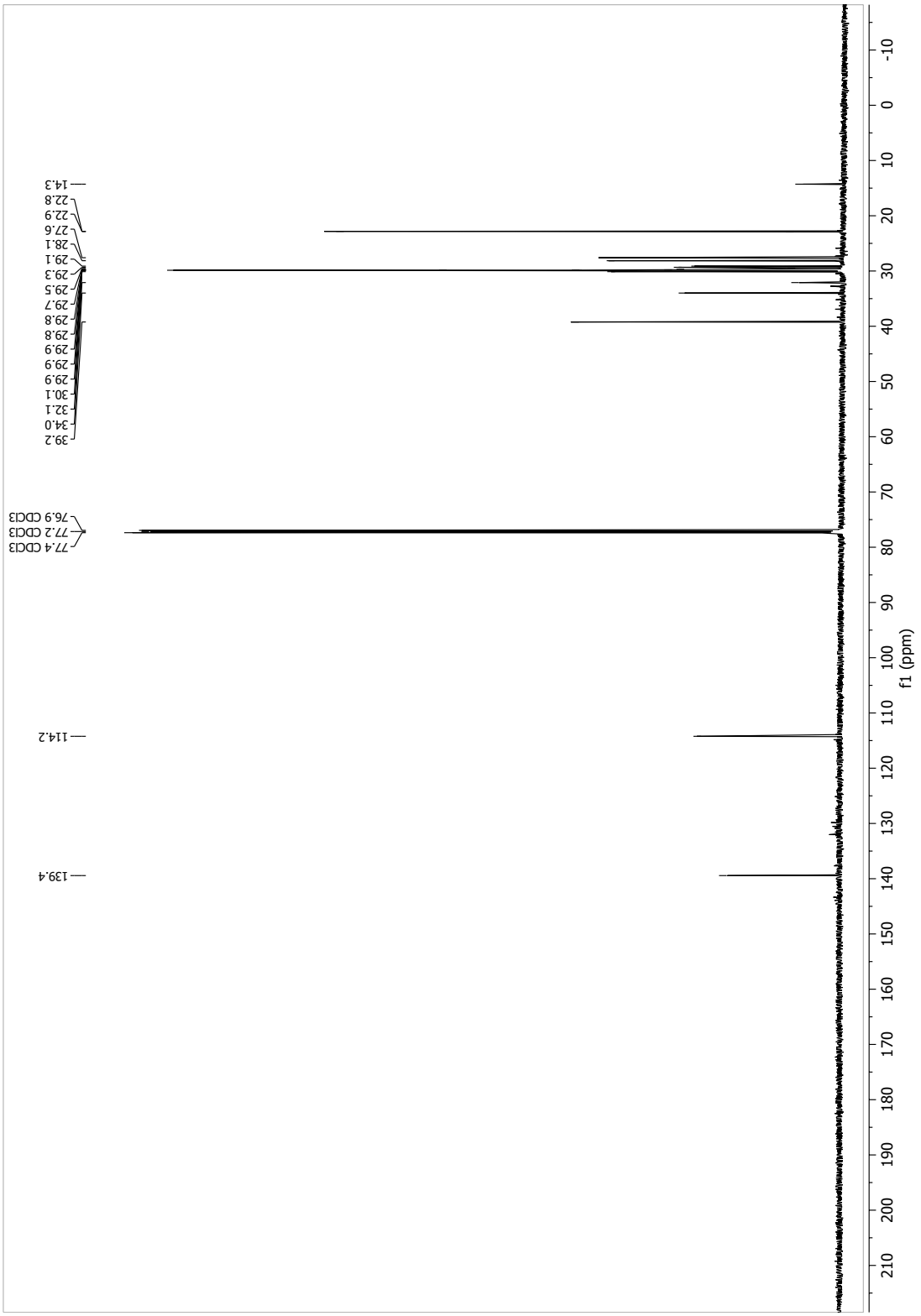
139.4
114.2
77.4 CDCl3
77.2 CDCl3
76.9 CDCl3
39.2
34.0
32.1
30.1
29.9
29.9
29.9
29.8
29.8
29.7
29.5
29.3
29.1
28.1
27.6
22.9
22.8
14.3
f1 (ppm)

13.1.106 [D_6]-13-methyltetradec-1-ene (125c)

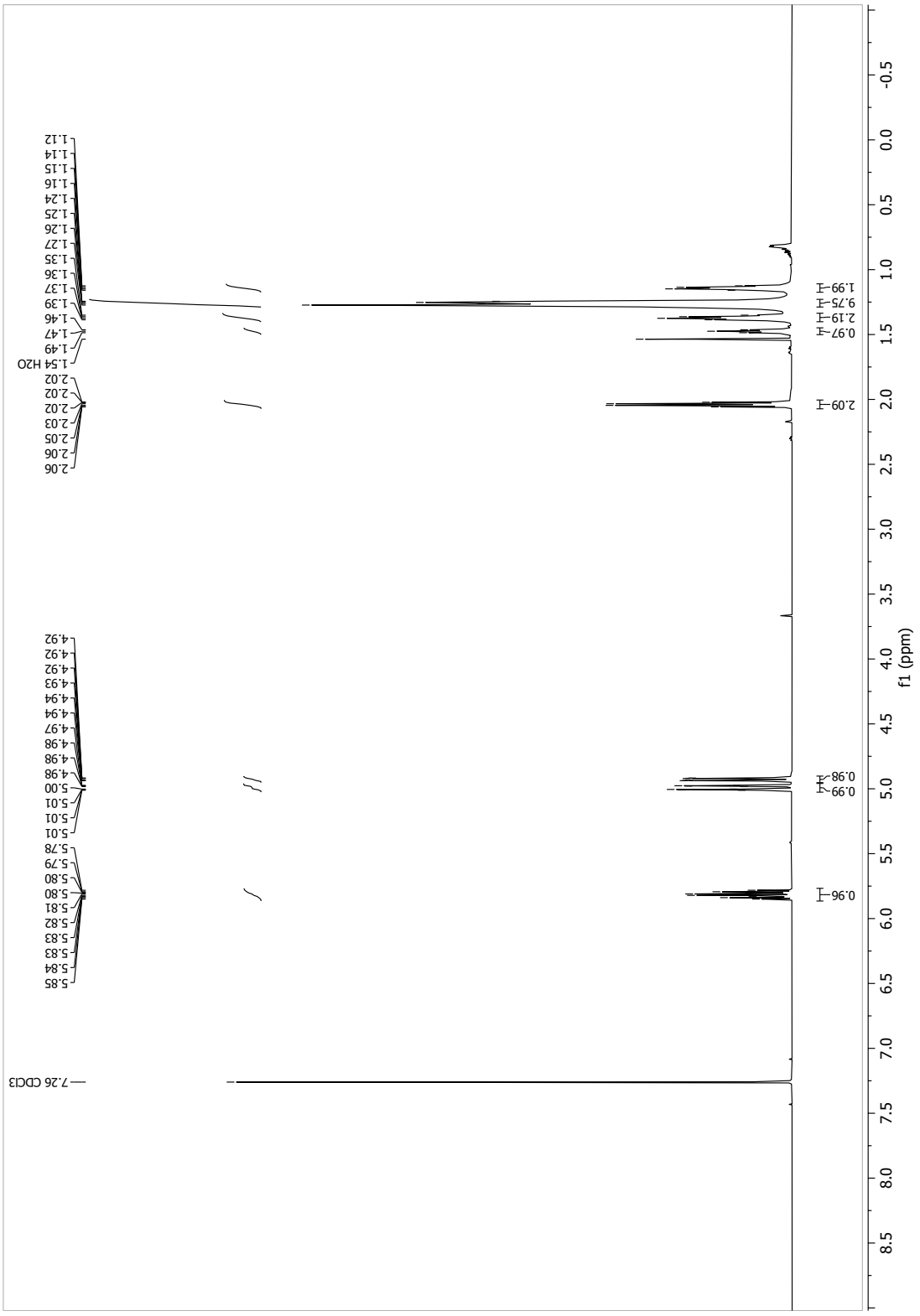

139.4
114.2
77.4 CDCl3
77.2 CDCl3
76.9 CDCl3
39.1
34.0
30.1
29.8
29.7
29.3
29.1
27.7
27.6
27.6
27.5
f1 (ppm)

13.1.107 13-Methyltetradecan-1-ol (126a)

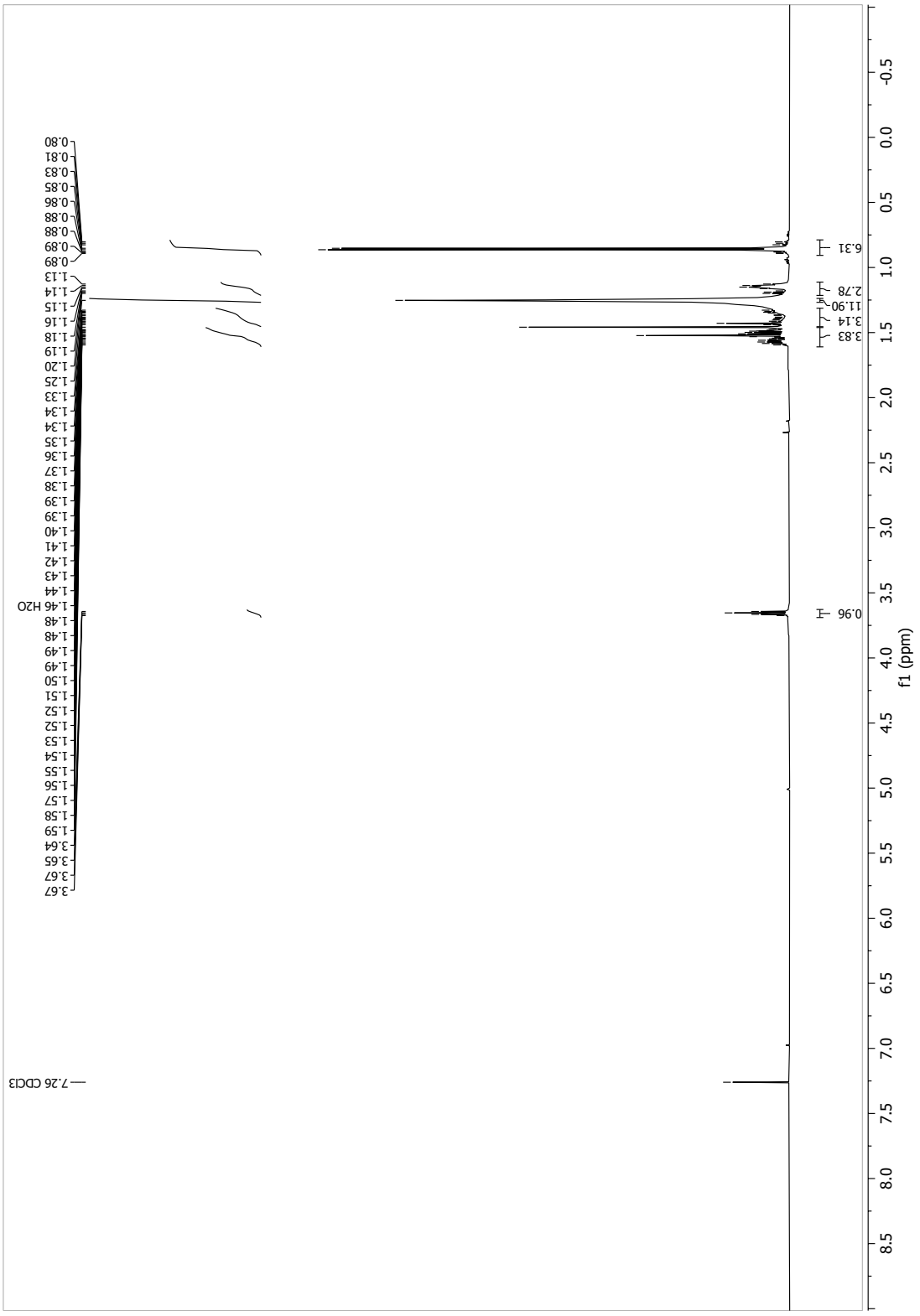

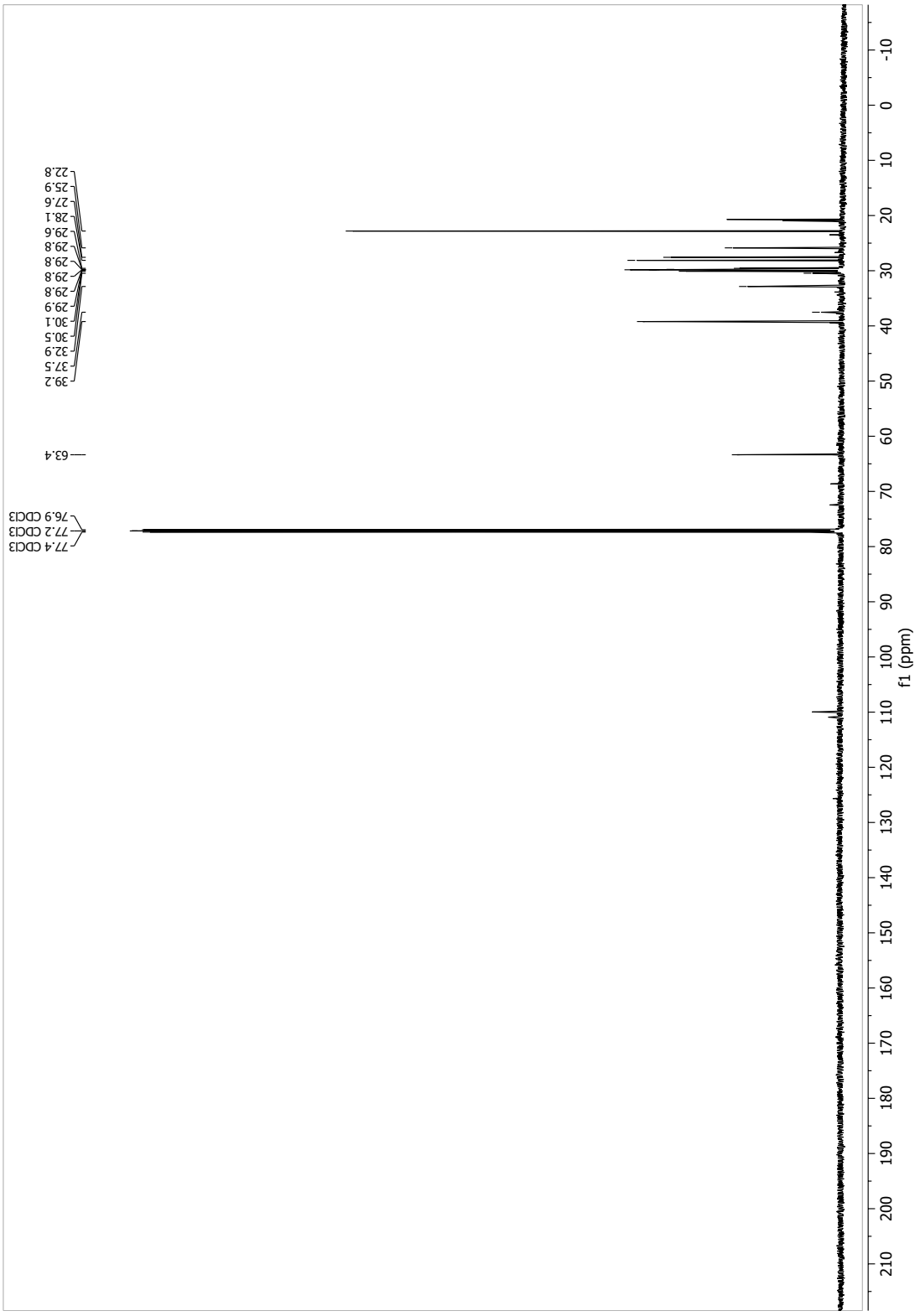
77.4 CDCl3
77.2 CDCl3
76.9 CDCl3
63.4
39.2
37.5
32.9
30.5
30.1
29.9
29.8
29.8
29.8
29.8
29.6
28.1
27.6
25.9
22.8
f1 (ppm)

13.1.108 [D_6]-13-methyltetradecan-1-ol (126c)

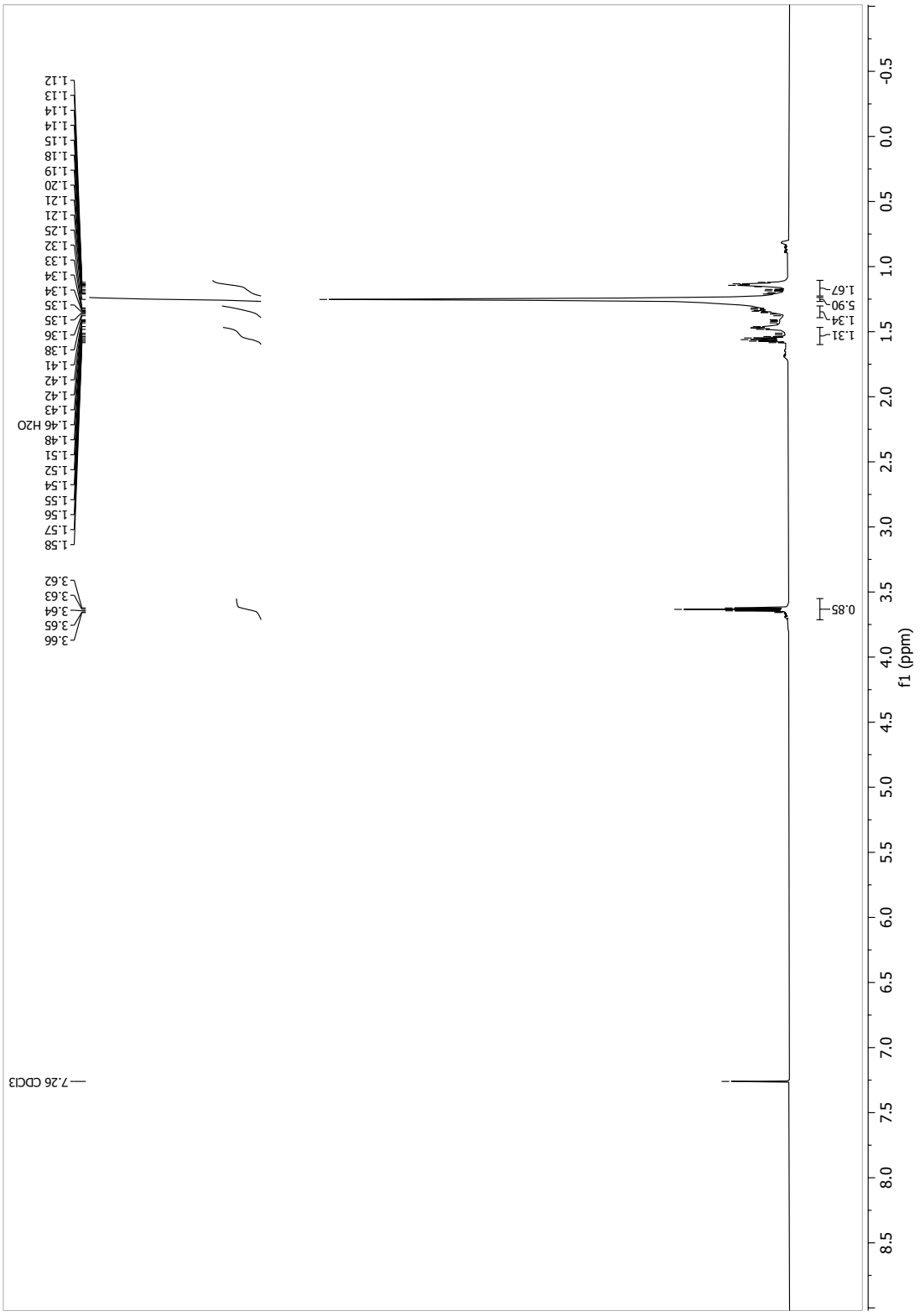

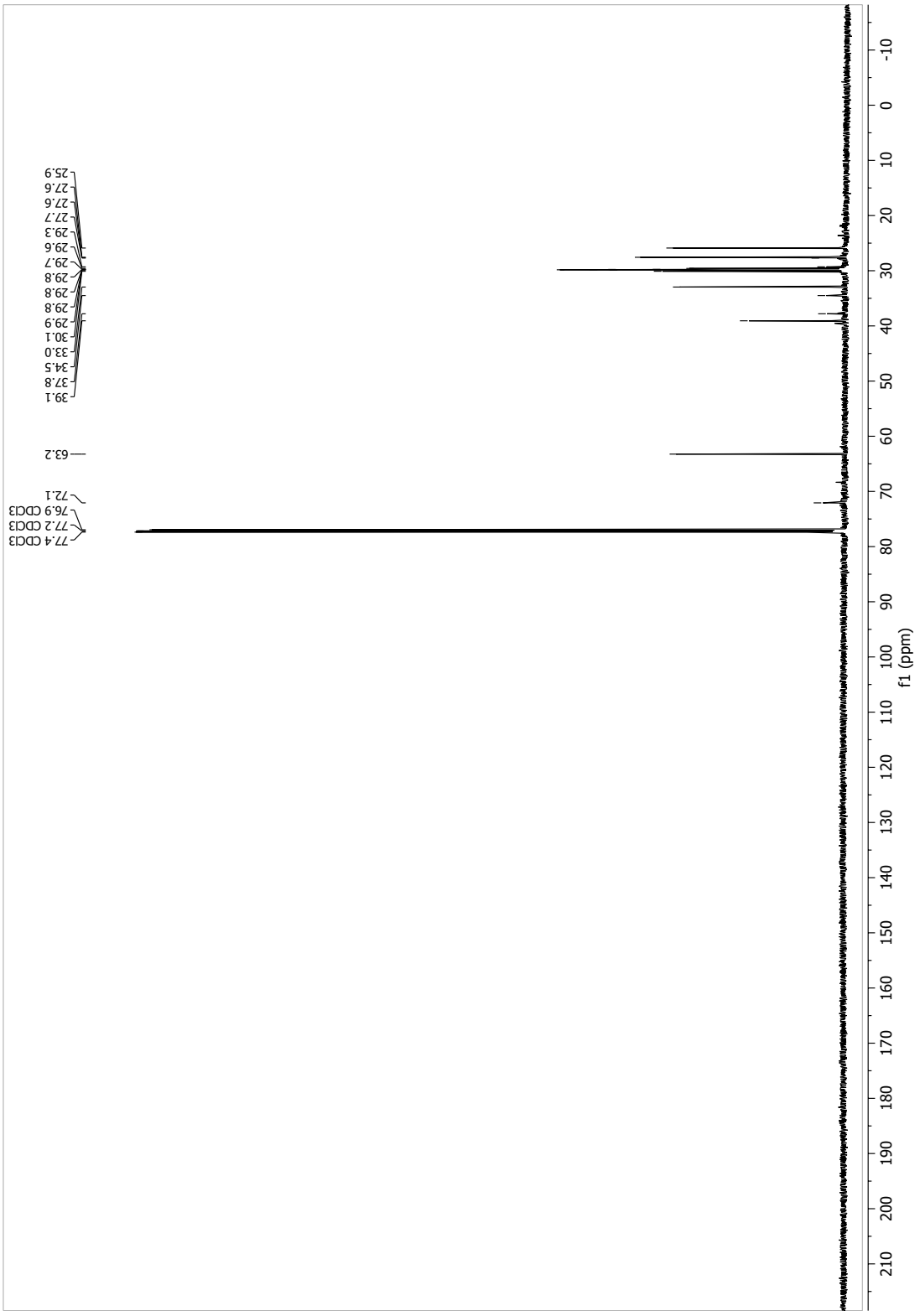
77.4 CDCl3
77.2 CDCl3
76.9 CDCl3
72.1
63.2
39.1
37.8
34.5
33.0
30.1
29.9
29.8
29.8
29.8
29.7
29.6
29.3
27.7
27.6
27.6
25.9
f1 (ppm)

13.1.109 13-Methyltetradecanoic acid (*iso*C15, 15a), from route 2

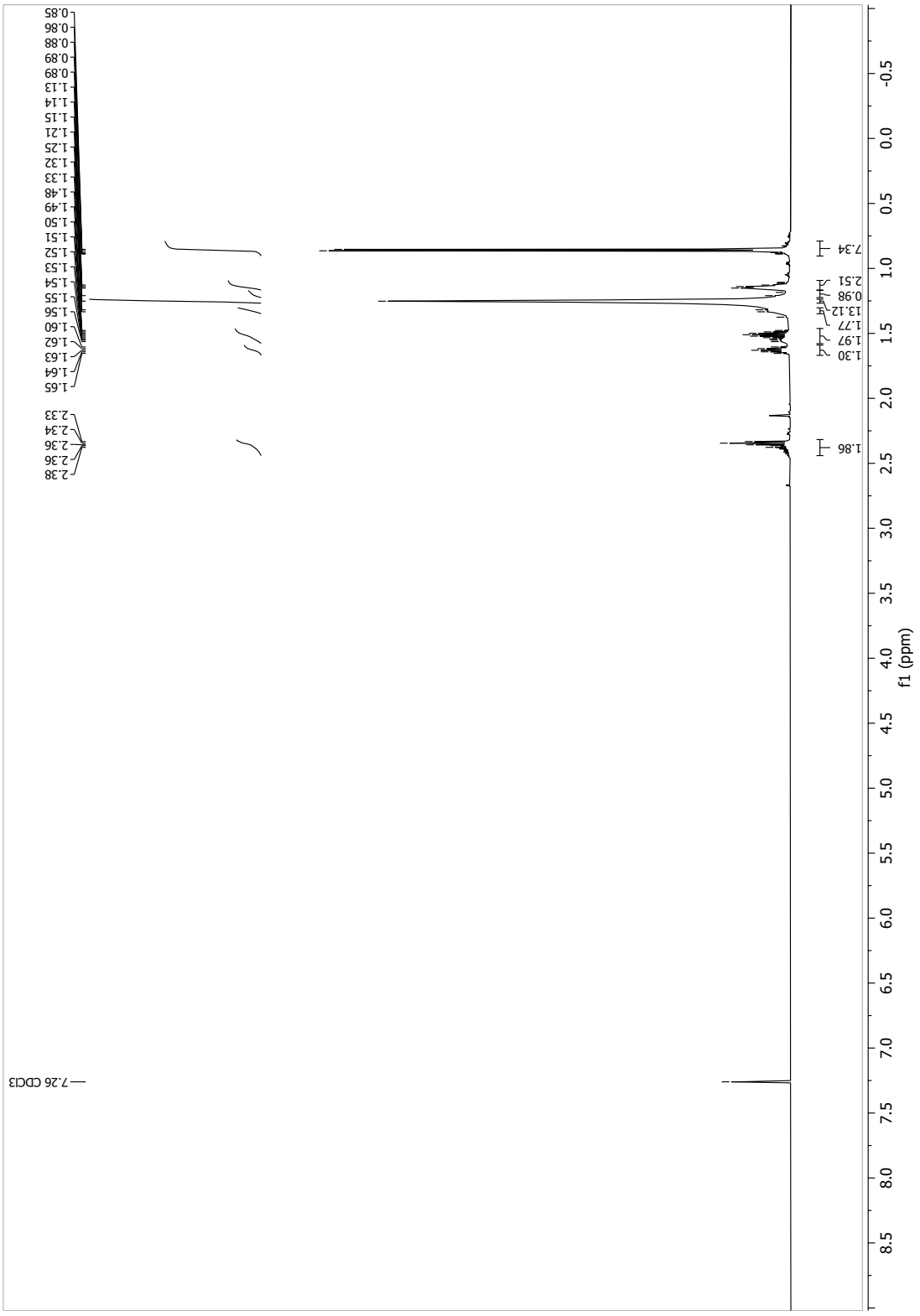

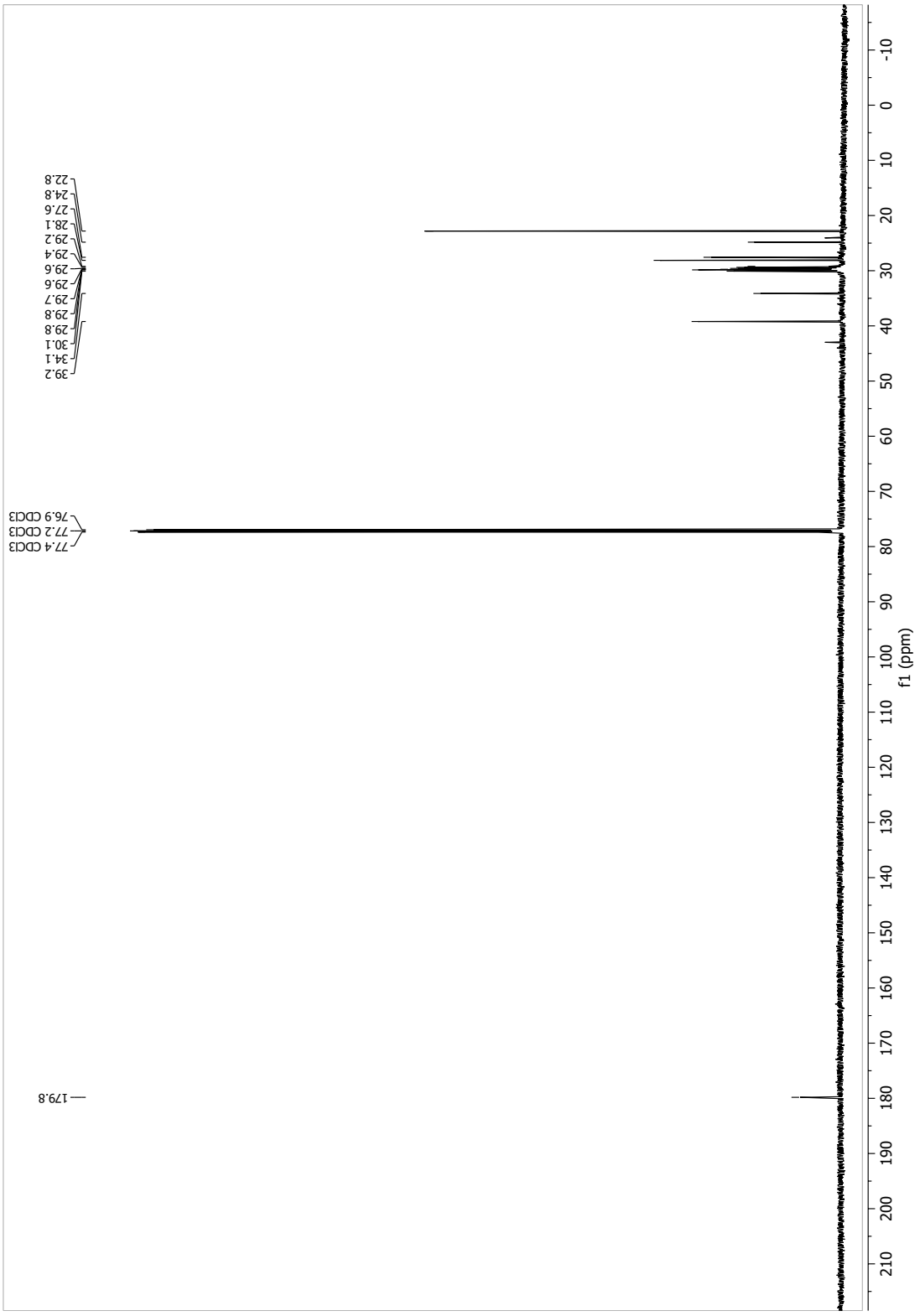
179.8
77.4 CDCl3
77.2 CDCl3
76.9 CDCl3
39.2
34.1
30.1
29.8
29.8
29.7
29.6
29.6
29.4
29.2
28.1
27.6
24.8
22.8
f1 (ppm)

13.1.110 [D_6]-13-methyltetradecanoic acid ([D_6]-*iso*C15, 15c), from route 2

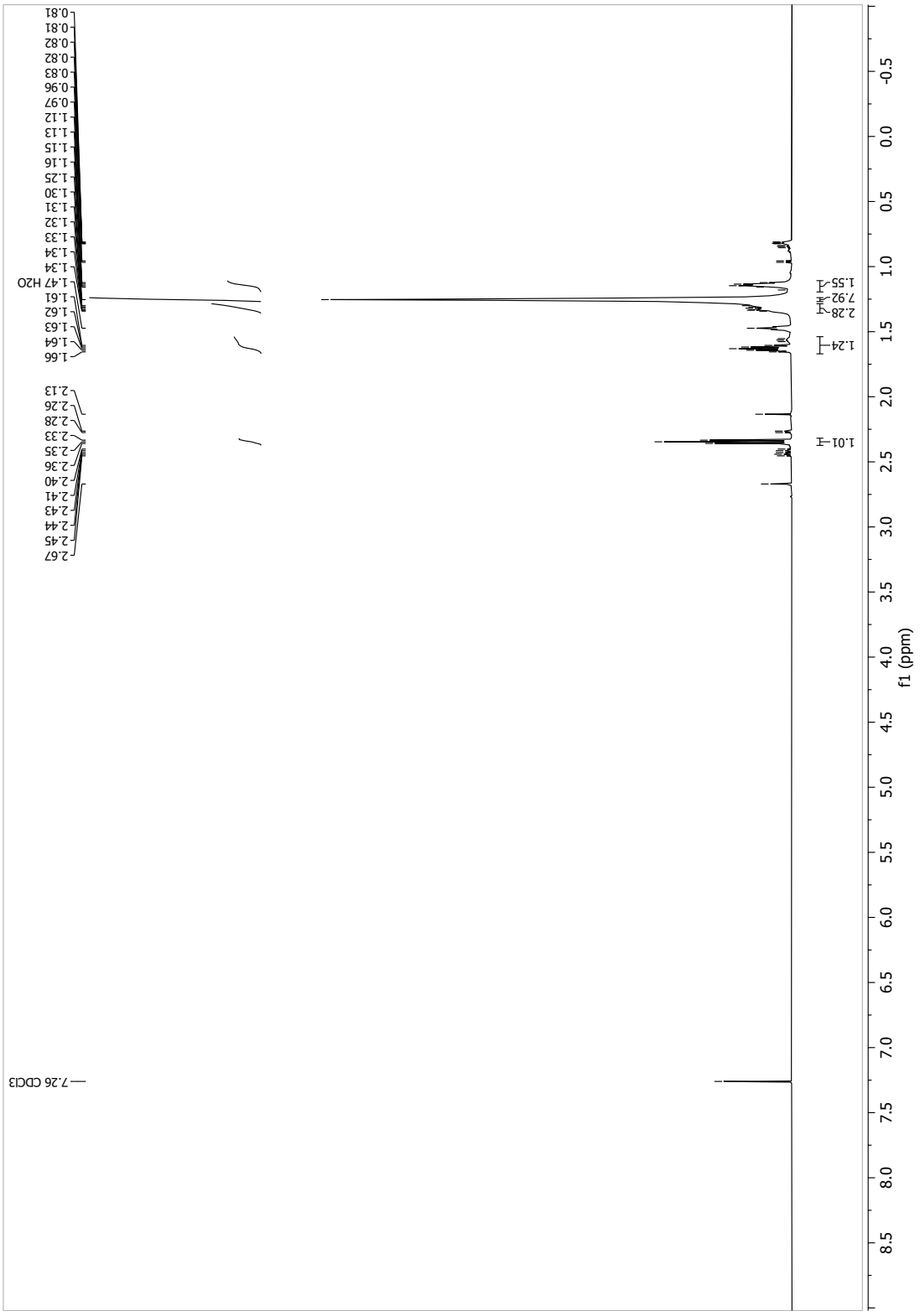

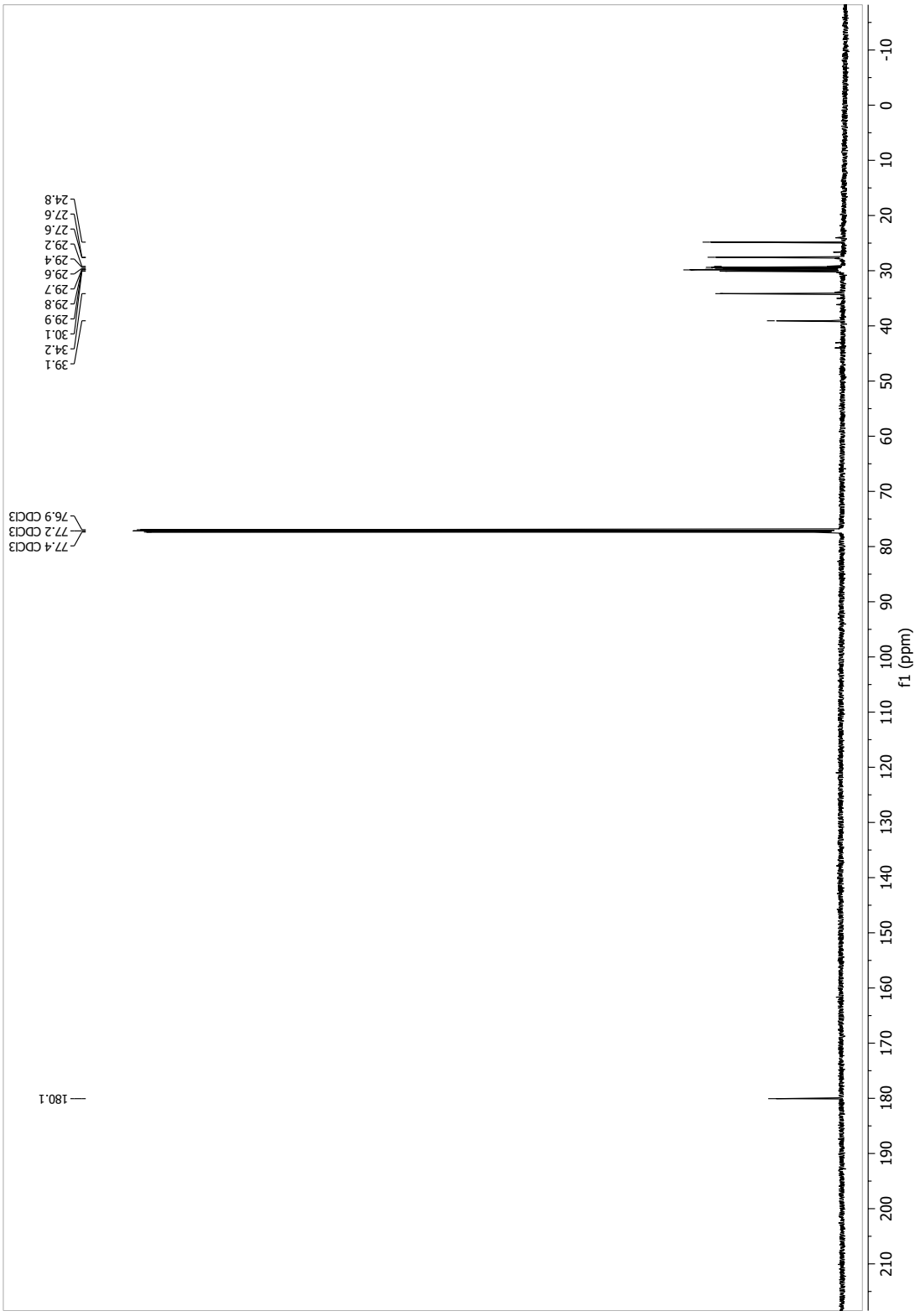
180.1
77.4 CDCl3
77.2 CDCl3
76.9 CDCl3
39.1
34.2
30.1
29.9
29.8
29.7
29.6
29.4
29.2
27.6
27.6
24.8
f1 (ppm)

13.1.111 [D_6]-15-methylhexadecan-1-ol (46c)

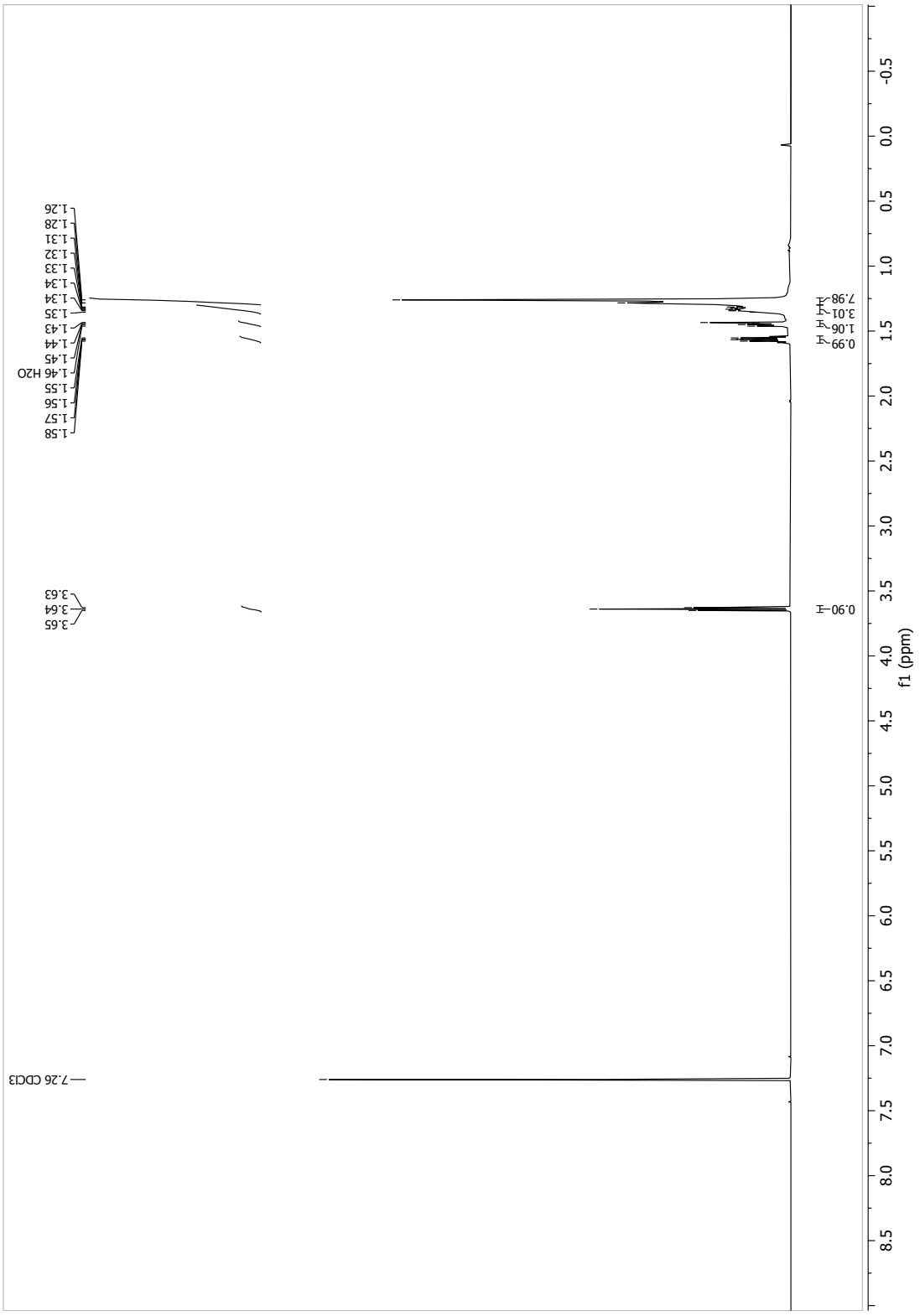

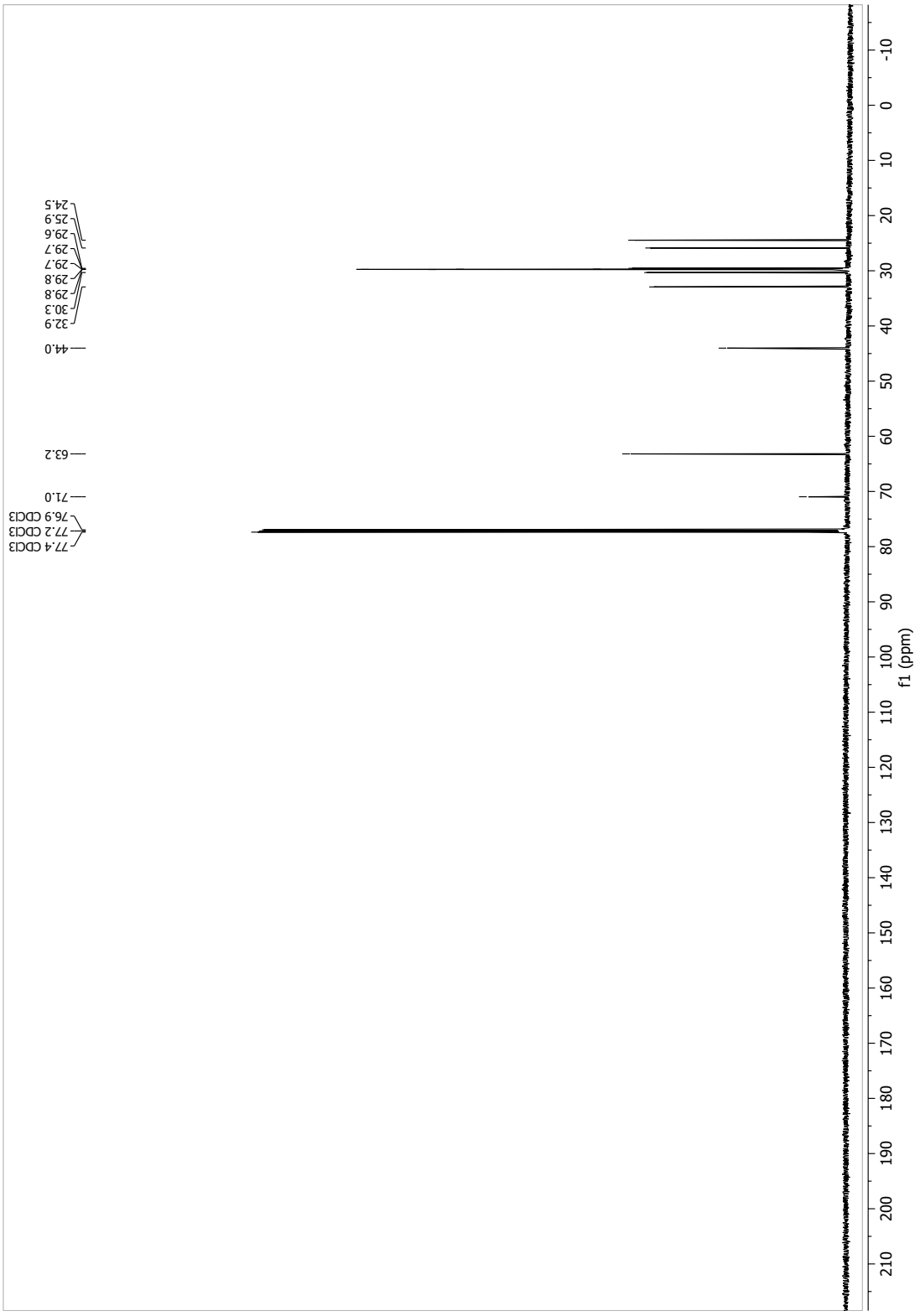
77.4 CDCl3
77.2 CDCl3
76.9 CDCl3
71.0
63.2
44.0
32.9
30.3
29.8
29.8
29.7
29.7
29.6
25.9
24.5
f1 (ppm)

13.1.112 [D_6]-15-methylhexadecan-1-ol (47c)

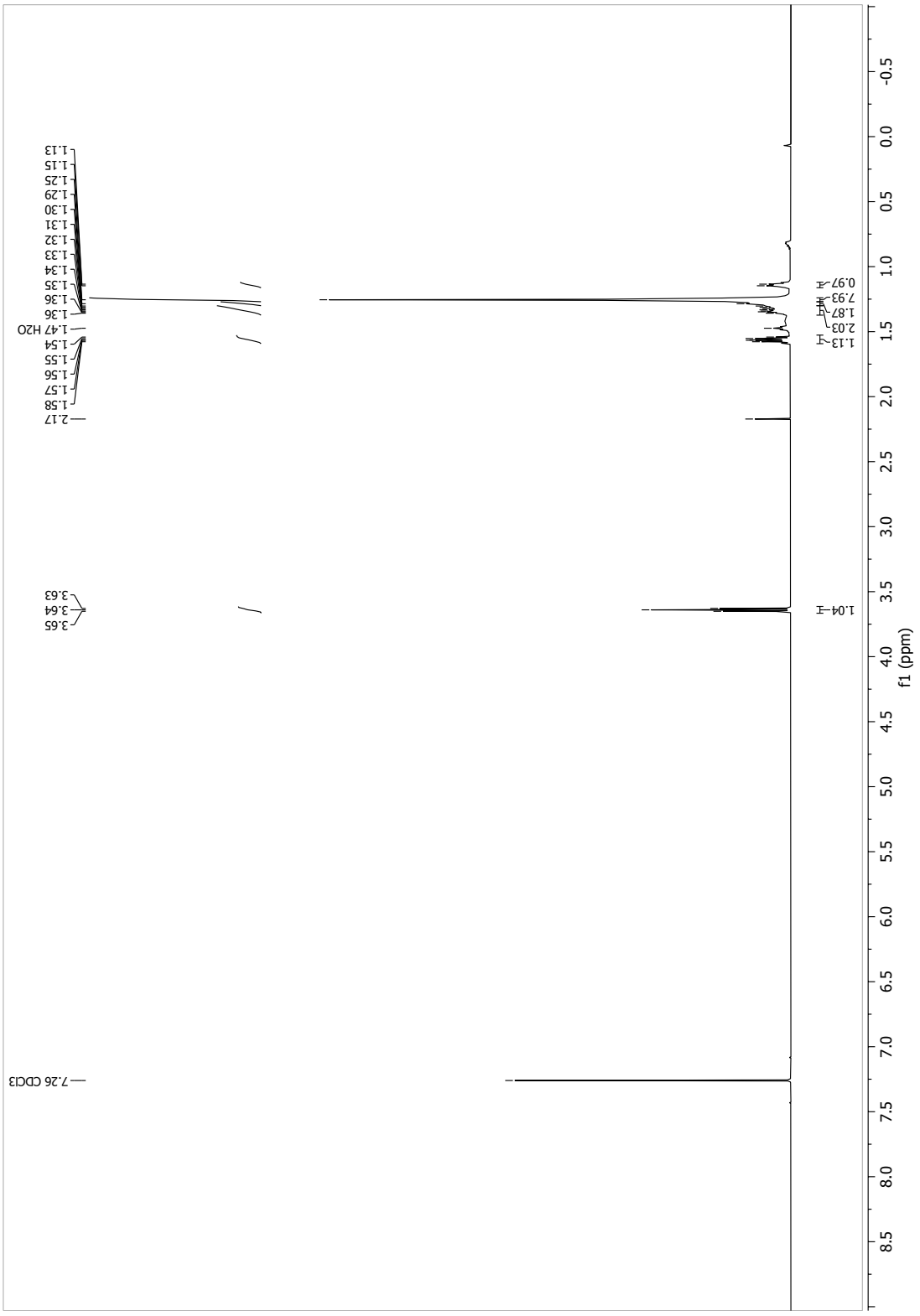

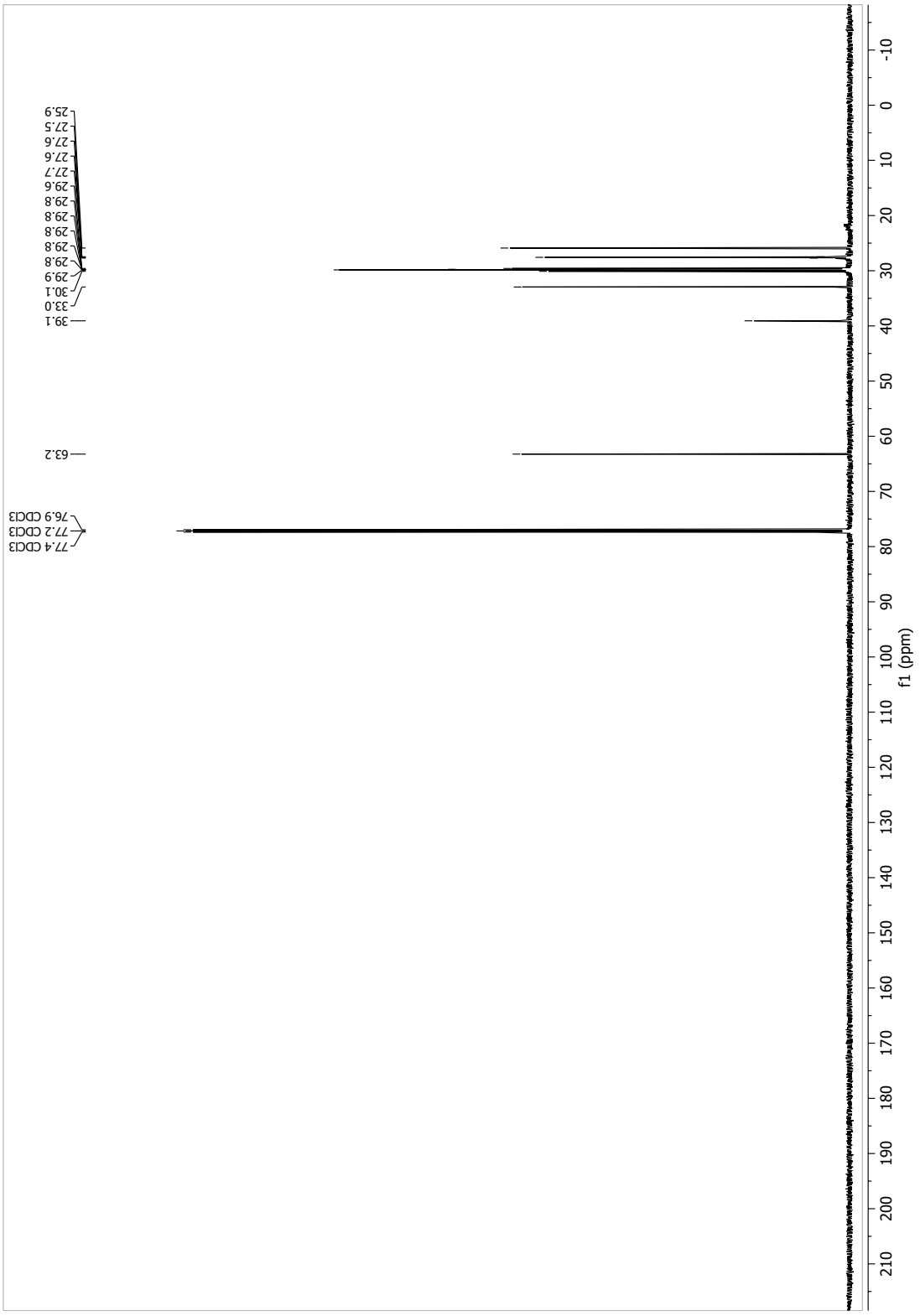
77.4 CDCl3
77.2 CDCl3
76.9 CDCl3
63.2
39.1
33.0
30.1
29.9
29.8
29.8
29.8
29.8
29.8
29.6
27.7
27.6
27.6
27.5
25.9
f1 (ppm)

13.1.113 15-Methylhexadecanoic acid (*iso*C17, 17a)

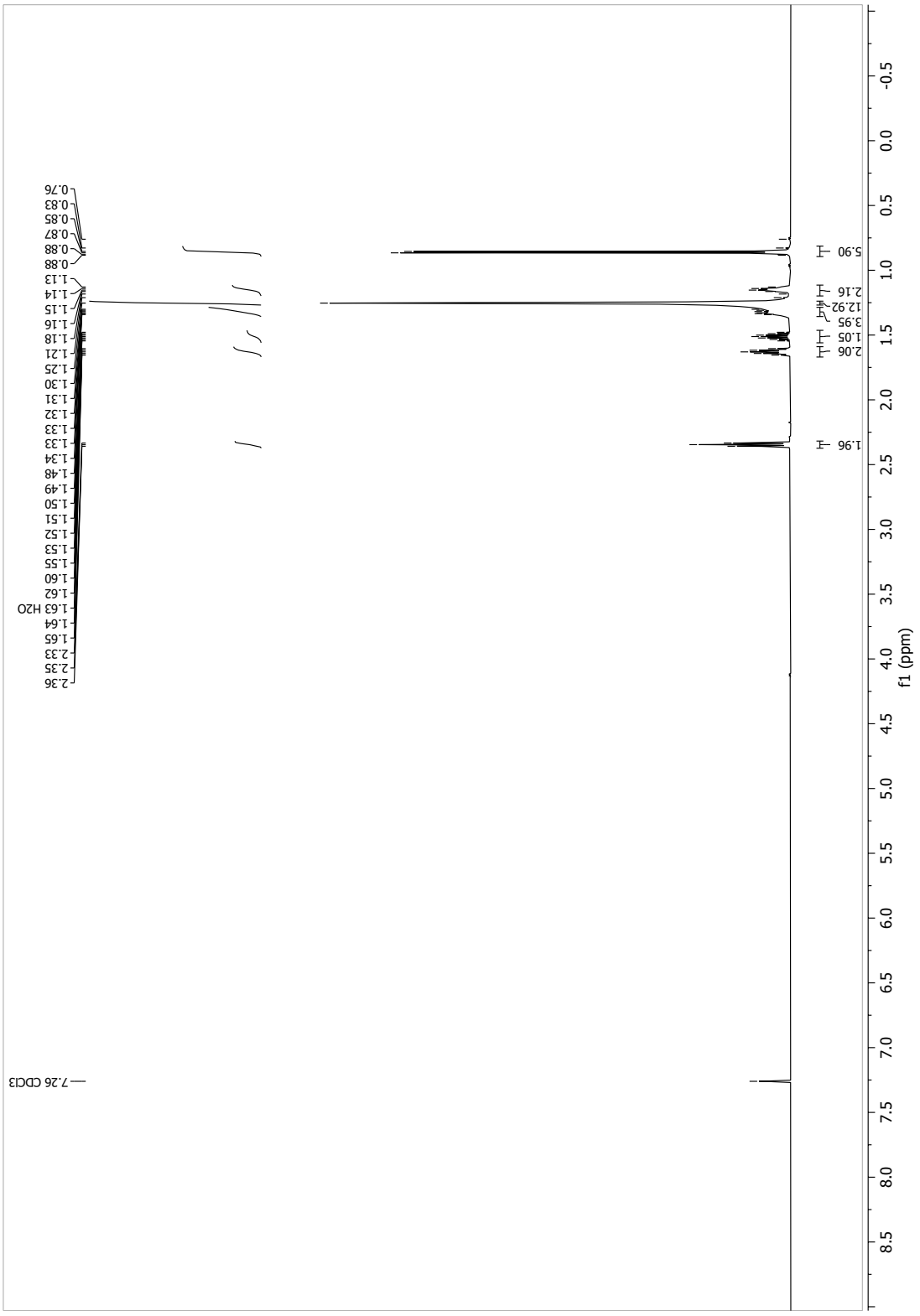

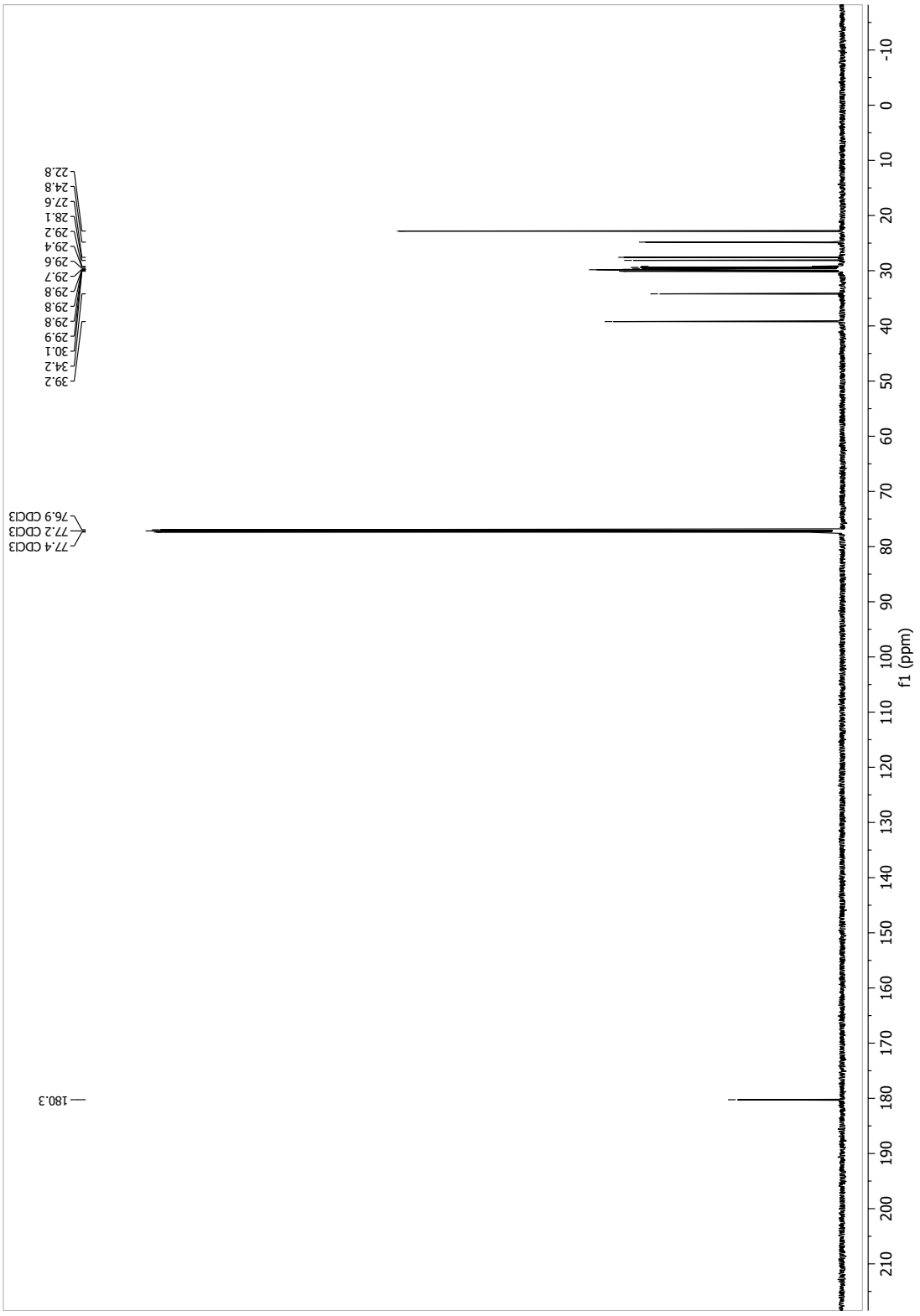
180.3
77.4 CDCl3
77.2 CDCl3
76.9 CDCl3
39.2
34.2
30.1
29.9
29.8
29.8
29.7
29.6
29.4
29.2
28.1
27.6
24.8
22.8
f1 (ppm)

13.1.114 [D_6]-15-methylhexadecanoic acid ([D_6]-*iso*C17, 17c)

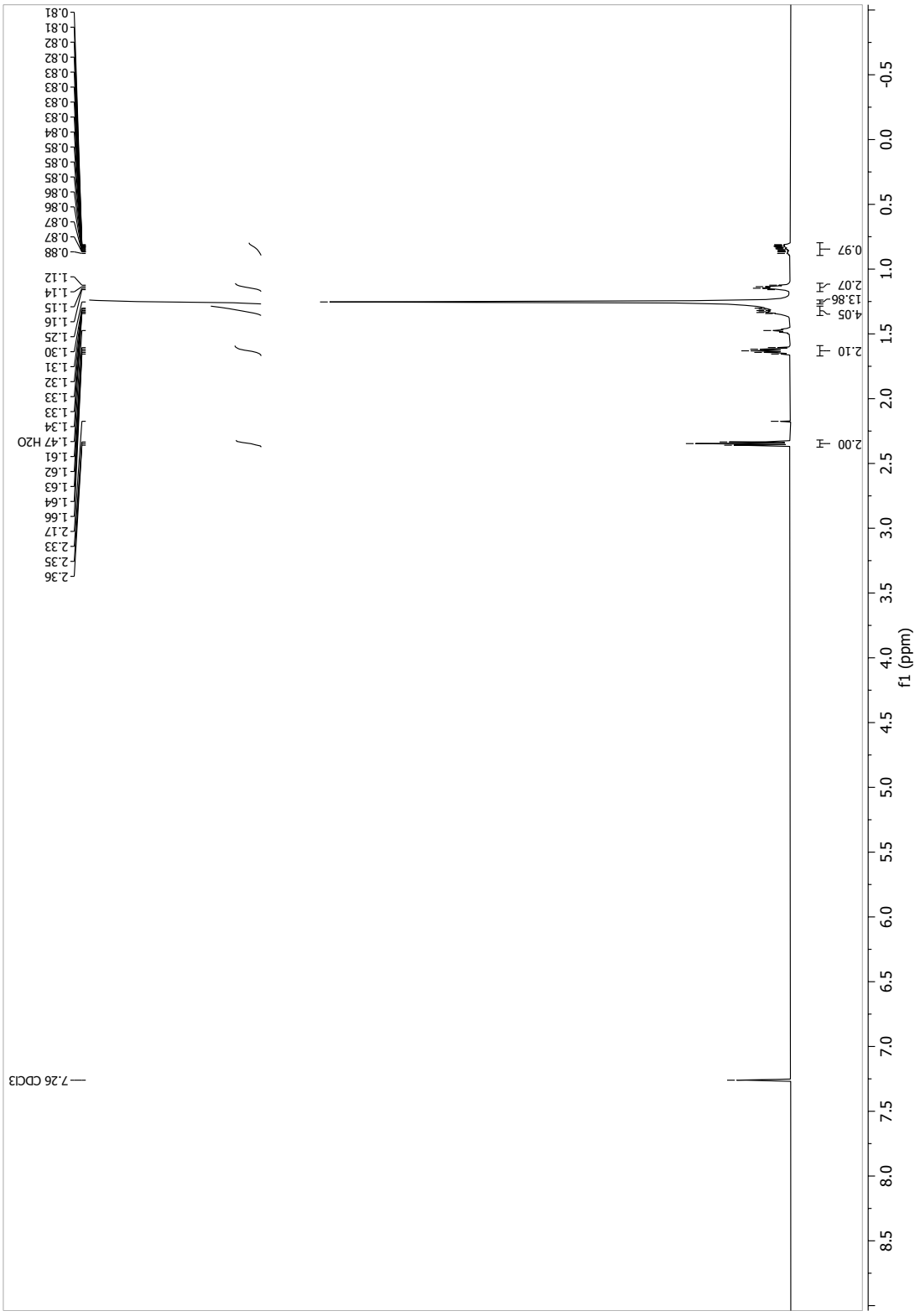

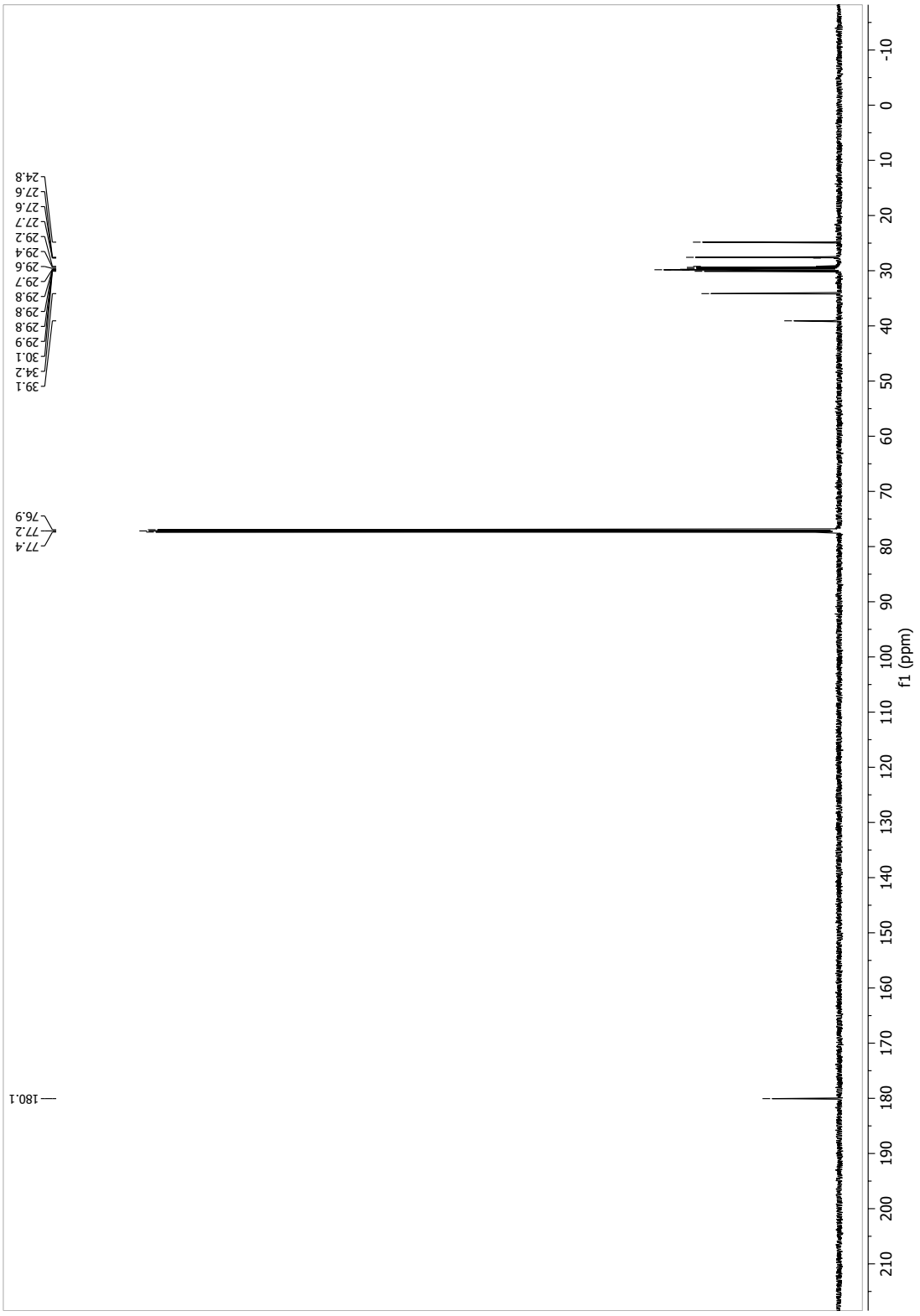
180.1
77.4
77.2
76.9
39.1
34.2
30.1
29.9
29.8
29.8
29.8
29.7
29.6
29.4
29.2
27.7
27.6
27.6
24.8
f1 (ppm)